frontiers | Research Topics

Land degradation pattern and ecosystem services

Edited by
Donatella Valente, Irene Petrosillo, Carlos Marcelo Scavuzzo and Thiru Selvan

Published in
Frontiers in Environmental Science

ISSN 1664-8714
ISBN 978-2-83251-808-3
DOI 10.3389/978-2-83251-808-3

About Frontiers

Frontiers is more than just an open access publisher of scholarly articles: it is a pioneering approach to the world of academia, radically improving the way scholarly research is managed. The grand vision of Frontiers is a world where all people have an equal opportunity to seek, share and generate knowledge. Frontiers provides immediate and permanent online open access to all its publications, but this alone is not enough to realize our grand goals.

Frontiers journal series

The Frontiers journal series is a multi-tier and interdisciplinary set of open-access, online journals, promising a paradigm shift from the current review, selection and dissemination processes in academic publishing. All Frontiers journals are driven by researchers for researchers; therefore, they constitute a service to the scholarly community. At the same time, the *Frontiers journal series* operates on a revolutionary invention, the tiered publishing system, initially addressing specific communities of scholars, and gradually climbing up to broader public understanding, thus serving the interests of the lay society, too.

Dedication to quality

Each Frontiers article is a landmark of the highest quality, thanks to genuinely collaborative interactions between authors and review editors, who include some of the world's best academicians. Research must be certified by peers before entering a stream of knowledge that may eventually reach the public - and shape society; therefore, Frontiers only applies the most rigorous and unbiased reviews. Frontiers revolutionizes research publishing by freely delivering the most outstanding research, evaluated with no bias from both the academic and social point of view. By applying the most advanced information technologies, Frontiers is catapulting scholarly publishing into a new generation.

What are Frontiers Research Topics?

Frontiers Research Topics are very popular trademarks of the *Frontiers journals series*: they are collections of at least ten articles, all centered on a particular subject. With their unique mix of varied contributions from Original Research to Review Articles, Frontiers Research Topics unify the most influential researchers, the latest key findings and historical advances in a hot research area.

Find out more on how to host your own Frontiers Research Topic or contribute to one as an author by contacting the Frontiers editorial office: frontiersin.org/about/contact

Land degradation pattern and ecosystem services

Topic editors
Donatella Valente — University of Salento, Italy
Irene Petrosillo — University of Salento, Italy
Carlos Marcelo Scavuzzo — National Space Activities Commission, Argentina
Thiru Selvan — Tripura University, India

Citation
Valente, D., Petrosillo, I., Scavuzzo, C. M., Selvan, T., eds. (2023). *Land degradation pattern and ecosystem services*. Lausanne: Frontiers Media SA. doi: 10.3389/978-2-83251-808-3

Table of contents

frontiers | Frontiers in Environmental Science

TYPE Editorial
PUBLISHED 16 February 2023
DOI 10.3389/fenvs.2023.1137768

Check for updates

OPEN ACCESS

EDITED AND REVIEWED BY
Abdelazim Negm,
Zagazig University, Egypt

*CORRESPONDENCE
Donatella Valente,
donatella.valente@unisalento.it

SPECIALTY SECTION
This article was submitted to Land Use Dynamics, a section of the journal Frontiers in Environmental Science

RECEIVED 04 January 2023
ACCEPTED 07 February 2023
PUBLISHED 16 February 2023

CITATION
Petrosillo I, Valente D, Scavuzzo CM and Selvan T (2023), Editorial: Land degradation pattern and ecosystem services.
Front. Environ. Sci. 11:1137768.
doi: 10.3389/fenvs.2023.1137768

Editorial: Land degradation pattern and ecosystem services

Irene Petrosillo[1,2], Donatella Valente[1]*, Carlos Marcelo Scavuzzo[3] and Thiru Selvan[4]

[1]Laboratory of Landscape Ecology, Department of Biological and Environmental Sciences and Technologies, University of Salento, Lecce, Italy, [2]NBFC, National Biodiversity Future Center, Palermo, Italy, [3]Institute of Advanced Space Studies Mario Gulich (IG), National Commission for Space Activities (CONAE), National University of Cordoba (UNC), Córdoba, Argentina, [4]Department of Forestry and Biodiversity, Tripura University, Agartala, India

KEYWORDS

land degradation susceptibility, monitoring tools, land degradation neutrality, land use/land cover change, ecosystem services supply and demand

Editorial on the Research Topic
Land degradation pattern and ecosystem services

Land constitutes one of the most vital natural resources and provides the basis for human livelihood and well-being through the provision of multiple ecosystem services. Globally, land degradation occurring due to unwarranted land use/land cover change (LULC) is continuing to affect the landscape multifunctionality potential, affecting the provision of ecosystem services from healthy ecosystems. Such land degradation has affected 3.2 billion people who are poor and marginalized, mainly in rural landscapes, with minimal adaptation options (Sena and Ebi, 2021). Since the Earth's land resources are finite, the sustainability of their use is the prerequisite to human well-being, as vital components for realizing sustainable development goals (SDGs) by 2030, in particular the SDG 15.3, focused on creating a world with zero net land degradation (UNDP, 2019; FAO, 2021). In this context, land use/land cover change (LUCC) is an important factor that can degrade land properties with consequences on the provision of ecosystem services. Severe soil degradation due to LULC can result in the loss in the provision of ecosystem services on a landscape scale, meaning that they are affected not only by local processes but also by landscape-level processes occurring in heterogeneous spaces. The articles included in this research topic have dealt with land degradation from different perspectives with the aim of exploring ways and means to optimize sustainable land use, management and recovery suitable to develop strategies against land degradation and to enhance the provision of ecosystem services.

The Research Topic has highlighted that some areas are more susceptible to land degradation than others (Figure 1), such as:

- Areas characterized by saline soils: analyzed in detail by Basak et al. that have presented a comprehensive review of the degradation of salt-affected soil both describing the causes and drivers for salinization as well as possible mechanism-oriented rehabilitation options. On the other side, Outbakat et al. have presented the possible environmental impacts of some saline soil rehabilitation options based on the use of Phosphogypsum and Gypsum that can cause heavy metal contamination.

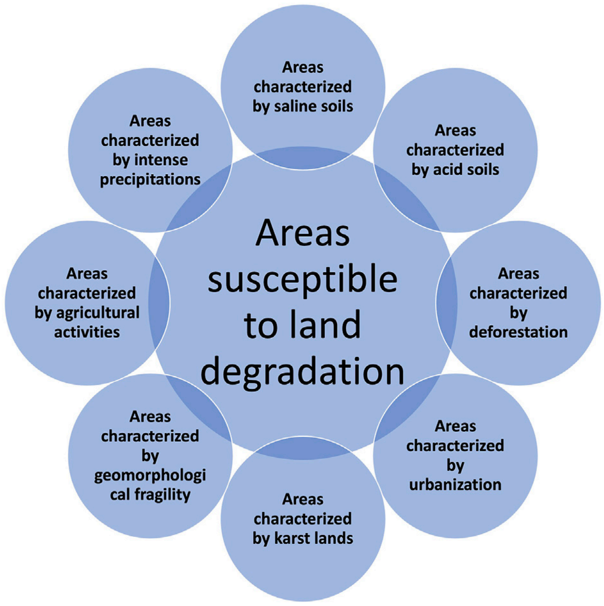

FIGURE 1
Conceptual map of the areas most susceptible to land degradation.

- Areas characterized by acid soils: where Ansari et al. have recommended a novel way to restore the soil quality and maximize crop productivity through legume green manuring and crop residue recycling in intensified cropping systems, with positive effects on supporting and regulating ecosystem services as well as on long-term productivity.
- Areas characterized by deforestation: Toro et al. have explored how socio-ecological drivers at the local scale can affect carbon dynamics across space and time in a Colombian region interested by deforestation and land use cover (LULC) changes during an armed conflict in the period 2009–2012. On the contrary, Kumar et al. have analyzed the effects of different forest management strategies in enhancing biodiversity conservation and soil carbon storage measured in terms of soil carbon density, which is one of the soil quality indicators.
- Areas characterized by urbanization: through an approach incorporating ecosystem services' supply and demand, Chen et al. have presented a novel perspective focused on ecosystem services to foster landscape optimization and conservation. The findings can have serious implications for coastal management and ecosystem sustainability.
- Areas characterized by karst lands: these are areas with great vulnerability to land degradation mainly related to land-use transformation. In this context, Liu et al. have identified priority areas for ecological restoration using transfer matrix, intensity and trajectory analysis. Their results can provide suitable insights for planning and decision making in karst regions.
- Areas characterized by geomorphological fragility: Li et al. have presented the possible mismatches between supply and demand of ecosystem services as a result of the complex interaction and comprehensive influence of multiple factors including socioeconomic development and natural factors. They found that anthropic factors were the most dominant factor influencing carbon storage, water and food provision whereas the major factor influencing soil conservation was geomorphology (i.e., mean slope) with consequences on land degradation.
- Areas characterized by agricultural activities: food supply is a crucial ecosystem services people worldwide depend on. However it depends on a good quality of soil. In this perspective, Panwar et al. have analyzed three crop management practices i) organic crop management, ii) inorganic crop management, and iii) integrated crop management, highlighting that towards organic approach (integrated application of organic amendments with a gradual reduction in mineral fertilizers) is better for keeping the rice–wheat system productive and sustainable in the long term. More in detail, Kumar et al. have focused their attention on soil C, which is severely depleted by anthropogenic activities. Also in this case, five prominent land use systems (LUS) (e.g., natural forest, natural grassland, maize-field-converted from the forest, plantation, and paddy crop) with different abilities to conserve soil organic carbon (SOC) and to emit C in the form of carbon dioxide (CO_2) have been tested. Research findings have suggested that SOC can be protected by adopting land use, namely forest soil protection, and by placing some areas under plantations.
- Areas characterized by intense precipitations: Van et al. have highlighted that soil erosion can be water-induced. In particular, they identify a two-stage process that begins with rain splash detaching soil particles from the topsoil surface and continues with surface runoff transporting the detached particles. A model based on the connections between rain intensity and kinetic energy has been developed and it was able to classify rainfall events into groups based on the magnitude of the mean rainfall intensity with different levels of soil erosion.

Degraded lands lose their ability to provide essential ecosystem services, including climate regulation, water regulation, biodiversity support, and carbon storage, potentially reducing supporting (e.g., primary production), provisioning (e.g., organic products), and regulation (e.g., carbon sequestration) services. Land degradation can be triggered by various factors, such as human activities and climatic factors with the spatial variability in soils, geomorphology, and topography impacting "vulnerability" to degradation. Improved understanding of landscape vulnerability to degradation and the evaluation of its drivers are essential to provide benchmarks and frameworks to decision-makers.

From a landscape perspective, land degradation can be seen as a loss of the ecological and economic resilience in terms of the adaptive capacity of the land system, intended as terrestrial social-ecological systems where human and environmental systems are strongly interrelated (Meyfroidt et al., 2022).

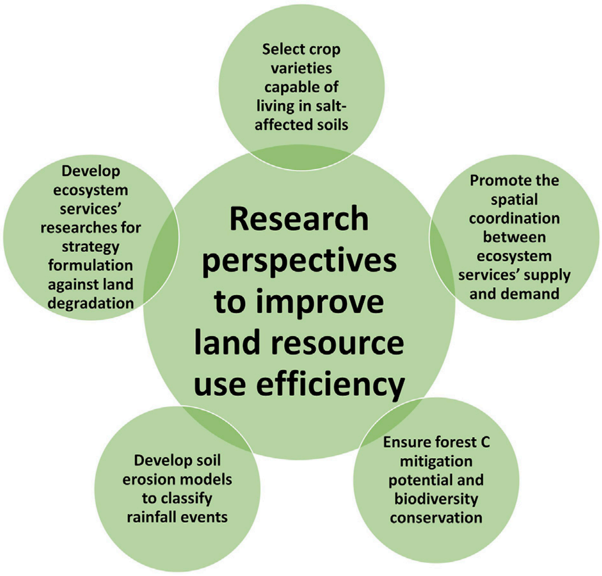

FIGURE 2
Research perspectives to improve land resource use efficiency.

The articles included in this Research Topic have presented several challenges and research perspectives to improve resource use efficiency, reduce environmental impact, increase productivity, and farm socio-economy (Figure 2):

- Improve the success of salt-affected soil by 1) selecting crop varieties capable of withstanding osmotic stress, water deficit, and toxicities of specific ions, 2) developing some formulations able to replace gypsum as an amendment for its content of heavy metals, 3) developing a soil quality index specific for salt-affected soils useful to assess the real-time impact of different management options on soil quality.
- Promote the spatial coordination between the supply and the demand of ecosystem services.
- Promote better coordination between local community and forest management agencies to ensure forest C mitigation potential and biodiversity conservation and to enhance C storage and soil functioning.
- Develop soil erosion models that employ the empirical connections between rain intensity and kinetic energy to classify rainfall events into groups based on the magnitude of the mean rainfall intensity with different levels of soil erosion at multiple geographical and temporal scales to develop more precise equations for calculating raindrop-induced soil erosion.
- Incorporate ecosystem services supply and demand perspectives for a complete and clear understanding of ecosystem evolution and ES dynamics and supports practical benefits for landscape optimization, ES management, and ecosystem conservation. However, further studies should be conducted to reveal the impacts of landscape structure on ES balance at different spatial scales and to practically support strategy formulation and implementation for combating land degradation.

Land degradation should be seen as an Research Topic interrelated with other environmental threats like climate change, biodiversity loss, food security, and the international attention is increasing year by year (Feng et al., 2022).

In setting planning strategies towards land degradation neutrality, the key principle to guide land use planning is the response hierarchy of 'Avoid > Reduce > Reverse land degradation' (Orr et al., 2017). This hierarchy highlights that the avoidance of land degradation is the most cost-effective strategy to deliver neutrality, while recovering from land degradation requires time and economic investments in replacing lost ecosystem services (Gibbons and Lindenmayer, 2007; Orr et al., 2017).

Novel instruments to assess and monitor land degradation are needed. Among others, remote-sensing data can play a leading role being a source for collecting information on the type, extent, and severity of land degradation (Prokop, 2020; de Oliveira et al., 2022).

Author contributions

Conceptualization IP, DV, and TS; Methodology IP, DV, CS, and TS; Formal Analysis IP, DV, and TS; Writing-Original draft preparation IP, DV, and TS; Writing-Review and Editing IP and DV; Visualization IP, DV, CS, and TS; Supervision IP, DV, CS, and TS. All authors have read and agreed with the published version of the manuscript.

Conflict of interest

The authors declare that the research was conducted in the absence of any commercial or financial relationships that could be construed as a potential conflict of interest.

Publisher's note

References

de Oliveira, M. L., dos Santos, C. A. C., de Oliveira, G., Silva, M. T., da Silva, B. B., Cunh, J. E. de B. L., et al. (2022). Remote sensing-based assessment of land degradation and drought impacts over terrestrial ecosystems in Northeastern Brazil. *Sci. Total Environ.* 835, 155490. doi:10.1016/j.scitotenv.2022.155490

FAO (2021). *De state of the world's land and water resources for food and agriculture*. Avaliable at: https://www.fao.org/3/cb7654en/cb7654en.pdf (accessed on 2022 December 27).

Feng, S., Zhao, W., Zhan, T., Yan, Y., and Pereira, P. (2022). Land degradation neutrality: A review of progress and perspectives. *Ecol. Indic.* 144, 109530. doi:10.1016/j.ecolind.2022.109530

Meyfroidt, P., de Bremond, A., Ryan, C. M., Archer, E., Aspinal, R., Chhabra, A., et al. (2022). Ten facts about land systems for sustainability. *P. Natl. Acad. Sci. U. S. A.* 119 (7), e2109217118. doi:10.1073/pnas.2109217118

Orr, A. L., Cowie, V. M., Castillo Sanchez, P., Chasek, N. D., Crossman, A., Erlewein, G., et al. (2017). *Scientific conceptual framework for land degradation neutrality, A report of the science-policy interface*. Bonn, Germany: United Nations Convention to Combat Desertification (UNCCD). Avaliable at: https://www.unccd.int/sites/default/files/documents/2017-08/LDN_CF_report_web-english.pdf (accessed on 2022 December 30).

Prokop, P. (2020). Remote sensing of severely degraded land: Detection of long-term land-use changes using high-resolution satellite images on the Meghalaya Plateau, northeast India. *Remote Sens. Appl. Soc. Environ.* 20, 100432. doi:10.1016/j.rsase.2020.100432

Sena, A., and Ebi, L. (2021). When land is under pressure health is under stress. *Int. J. Environ. Res. Public Health* 18 (1), 136. doi:10.3390/ijerph18010136

UNDP (2019). *Combatting land degradation: Securing a sustainable future*. New York, USA: United Nations Development Programme. Avaliable at: https://www.undp.org/publications/combatting-land-degradation-securing-sustainable-future (accessed on 2022 December 28).

frontiers | Frontiers in Environmental Science

TYPE Review
PUBLISHED 19 August 2022
DOI 10.3389/fenvs.2022.935785

OPEN ACCESS

EDITED BY
Donatella Valente,
University of Salento, Italy

REVIEWED BY
Mahmoud F. Seleiman,
King Saud University, Saudi Arabia
Swapan Talukdar,
Jamia Millia Islamia, India

*CORRESPONDENCE
Nirmalendu Basak,
nirmalendu.basak@icar.gov.in,
nirmalendubasak@rediffmail.com
Arvind Kumar Rai,
raiarvindkumar@gmail.com,
ak.rai@icar.gov.in
Parul Sundha,
parul.sundha@icar.gov.in

SPECIALTY SECTION
This article was submitted to Soil Processes,
a section of the journal
Frontiers in Environmental Science

RECEIVED 04 May 2022
ACCEPTED 11 July 2022
PUBLISHED 19 August 2022

CITATION
Basak N, Rai AK, Sundha P, Meena RL, Bedwal S, Yadav RK and Sharma PC (2022), Assessing soil quality for rehabilitation of salt-affected agroecosystem: A comprehensive review.
Front. Environ. Sci. 10:935785.
doi: 10.3389/fenvs.2022.935785

Assessing soil quality for rehabilitation of salt-affected agroecosystem: A comprehensive review

Nirmalendu Basak*, Arvind Kumar Rai*, Parul Sundha*, Rameshwar Lal Meena, Sandeep Bedwal, Rajender Kumar Yadav and Parbodh Chander Sharma

ICAR-Central Soil Salinity Research Institute, Karnal, India

One billion hectares of land worldwide is affected by several kinds of salinity and associated problems. The soil quality (SQ) in salt-affected soil (SAS) is impaired because of the presence of excess electrolytes, disproportionate Na and Ca in soil solution and exchange phase, rhythmic changes in the hydrological cycle, decreasing soil organic matter, poor vegetative cover, low soil biological activity, and crop residue return. Sodic and saline–sodic soils have the potential to provide alkaline reactions and soil physical constraints to regulate the soil attributes affecting SQ. Because of high spatial variability and rapid temporal changes, selection of simple, robust, low cost, and high-throughput master indicators for assessing SQ is very essential for monitoring the aggradation or degradation of SAS. Therefore, screening the master indicators for developing a minimum dataset for SQ assessment of SAS is an important issue for sustainable management of soil in these agro-ecologies. We captured the SQ indicators for SAS from several ecosystems of different countries and discussed the problems of parameterization for assessing SQ. Improved SQ for optimum soil functioning is needed for confirming agricultural productivity and food security around the globe. This review describes the causes and drivers for sodification/salinization and mechanism-oriented rehabilitation options such as the application of mineral gypsum, flue-gas–desulfurized gypsum, elemental S, acidified biochar, polymer, salt tolerance mechanisms, and other agro-techniques for improving the quality of SAS. Based on the SQ assessment, a suite of site-specific soil management practices are advocated for the greening of SAS and prosperity.

KEYWORDS

amendments, soil quality, soil quality indicators, salt-affected soil, salt tolerance mechanism, sustainable management

Introduction

The presence and abundance of soluble and precipitated salts are the primary cause of soil salinization, halting ecosystem functions and limiting crop growth and production (Seleiman et al., 2022). Rehabilitation of salt-affected soil (SAS) is a principal agenda in the present plans of developing countries and countries of arid–semi-arid regions to meet the food–feed–bioenergy need of the expanding population. Shortage of freshwater, erratic rain, increase in temperature, the incidence of drought, rise in evapotranspiration requirement of the crops, sea-level rise, intrusion of brackish water, ingression of sea–water, extension of irrigated farming in the canal command area, and dependency on wastewater for irrigation causes increase the salt load in the farmland (Al-Suhaibani et al., 2021; Alkharabsheh et al., 2021; Badawy et al., 2021). Furthermore, inappropriate drainage networks increase the risk of salinization/alkalization and cause deterioration of soil health (Kamra, 2021).

Based on the nature and stoichiometric dominance of electrolytes, SAS is categorized into saline, sodic, and saline–sodic soils. Saline soil has an electrolytic conductivity of the aqueous soil saturated paste extract (EC_e) higher than 4.0 dS m^{-1} at 25°C and the pH of the saturation paste (pH_s) less than 8.2 and ESP (exchangeable sodium percent) less than 15 or/and sodium adsorption ratio (SAR_e) of the same saturated paste extract <13.0 $mmol^{1/2}$ $L^{-1/2}$ (Abrol et al., 1998). Soil salinization occurs because of the existence of water-soluble salts in the soil; a rising flux of saline underground water; prolonged irrigation with saline, brackish, or wastewater; and drainage congestion and intrusion of saline seawater in the coastal areas (Singh, 1998; Eswar et al., 2021). The sodic soils are usually known as "alkali soils" carrying a disproportionately larger quantity of Na^+ than Ca^{2+} and Mg^{2+} in the soil solution and exchange phase. The soil reaction (pH_s) in this type of soil >8.2, ESP of greater than 15 or/and sodium adsorption ratio (SAR_e) of the saturated paste extract >13.0 $mmol^{1/2}$ $L^{-1/2}$ and variable electrolyte concentration. These soils are categorized as "saline–sodic" having pH_s of >8.5, ESP of >15%, SAR_e>13 $mmol^{1/2}$ $L^{-1/2}$, and EC_e of >4 dS m^{-1} at 25°C. Irrigation with sodic water (presence of carbonates and bicarbonates of Na) and a shallow sodic water table led to soil sodification (Choudhary et al., 2011; Sheoran et al., 2021). The unfavorable influence of different types of salts on soil properties creates limitations for crop production (Taha et al., 2020; Ding et al., 2021; Taha et al., 2021; Zain et al., 2021). Therefore, reclamation and strategic management are requisite for crop production (Rai et al., 2021c; Hopmans et al., 2021).

Soil health or soil quality is largely defined as "fitness for use" or "capacity of the soil to function" (Karlen et al., 1997). A modest attempt had been made for assessing the soil quality of agricultural soil (Masto et al., 2008a; Martins et al., 2017; Basak et al., 2021a). But only a few groups had attempted a comprehensive assessment of soil quality of salt-affected soils. Some discrete studies identified key soil quality indicators for addressing soil quality of saline and sodic soil (Mahajan et al., 2016, 2021b; Sione et al., 2017; Vasu et al., 2018; Yu et al., 2018). It is a well-established fact that reclamation and management of salt-affected soils are associated with a decline in ESP, EC_e, pH_s, and improved crop yield (Rai et al., 2022; Sheoran et al., 2022). But, the reclamation and management strategies in SAS had an influence on all soil processes influencing the physical, chemical, biological, and biochemical properties of soil (Mahajan et al., 2021b; Zhao et al., 2021). The relative response of different soil attributes depends upon the intrinsic soil properties, geological settings, hydrological cycle, and other pedogenic forces driving salinization and sodication (Jobbágy and Jackson, 2004). The nature and amount of the amendment needs are also governed by these factors. The amendments needed for bringing the same amount of change in soil quality to perform the desired function in vertisols are different from those of inceptisols at the same level of pH and ESP in the semi-arid region of the Indian Deccan Plateaus (Pal et al., 2006). Therefore, linking all the management and reclamation needs with the change in soil quality desired is an important aspect of the management of these soils. In the absence of a wholesome soil quality index, the imbalance in fertilization and other management practices not only reduces the use efficiency of applied nutrients but also increases the cost of cultivation. Overuse of some nutrients also acts as a non-point source of pollution in different components of the ecosystem. Soil salinity and use of poor quality groundwater (saline/sodic with high RSC; residual sodium carbonate) further aggravate the agrarian distress. Therefore, orienting the crop management decisions while keeping soil quality or soil health in focus is the first and foremost step needed to manage soils more efficiently and ensure profitability. Therefore, this study aimed to provide an overview of the global extent of salt-affected soils, strategies for successful rehabilitation, and approaches for soil quality assessment followed worldwide. The mechanism for salinity tolerance and agronomic measures for the management and their impact on soil quality are critically discussed. Furthermore, issues related to parameterization in salt-affected soils for developing a minimum dataset for describing the changes in soil attributes after the reclamation of salt-affected soils, soil quality assessment, and future research needs are also highlighted.

Materials and methods

This review was developed based on the published information on the extent, distribution, characteristics, development, rehabilitation strategies, salt-tolerance mechanisms in crop plants, and soil quality assessment as per the requirement of the hypothesis of the review. The information available from Google Scholar, Crossref, Google Scholar profile, Pubmed, ScienceDirect.com, Springer.com, Wiley Online

Library, CSIRO Publishing, FAO reports, and CSSRI database was retrieved using relevant keywords. Based on the comprehensive review of the available literature (n = 161), present state and key issues associated with the soil quality assessment of salt-affected soil were developed as envisaged in the hypotheses and objective of this review.

Results and discussion

Characterization and classification of salt-affected soils

Soluble salts of different nature and quantities are present in salt-affected soils. These salts are formed with a combination of cations (Na^+, Ca^{2+}, Mg^{2+}, and K^+) and anions [Cl^-, SO_4^{2-}, CO_3^{2-}, HCO_3^-, and SiO_x^{-n} as and minor quantity of $(H)_xPO_4^n$ and NO_3^-]. Considering the stoichiometric dominance of electrolytes and their nature, SAS are classified into saline, sodic, and saline–sodic.

Saline soils

Accumulation of soluble minerals from weathering of rocks and minerals, aeolian deposits, and evaporation of seawater in geological areas with drainage congestion are the reasons for soil salinization (Gupta and Mathur, 2011). Scarcity of rainfall, shift in precipitation patterns, high air temperature which led to intense evaporation, and shortage in surface irrigation water resources are the reasons for secondary salt accumulation in irrigated agriculture. Faulty irrigation management through border irrigation in the canal command area, imperfect drainage system, and excessive use of underground saline/alkali water without proper management also hastened soil salinity development (Cai et al., 2010). An extensive irrigation network had been developed in Indo-Gangetic Plain in India and Pakistan (Fishman, 2018; Hayat et al., 2020), China (Xu et al., 2013), Australia (Ranatunga et al., 2010), Egypt (Abdel-Fattah et al., 2020), and United States (Hansen et al., 2018) for creating the habitation settlement, crop productivity assurance, and increasing the livelihood security. Irrigation in some regions without giving due consideration to irrigability classification caused accumulation of the appreciable quantity of electrolytes (Na^+, Ca^{2+}, and Mg^{2+} salts) present in irrigation water in the root zone. Some proportions of electrolytes maintain soil permeability or prevent aggregate failure, loss in soil permeability, and drainage congestion (Quirk, 2001; Bennett et al., 2019). The poor vegetation cover and excess use of irrigation water and agricultural input alters the equilibrium of the underground water and causes exposure of soils to salts. Rise in mean air temperature causes an increase in evaporation demand as well as change and shifting in rainfall distribution. This phenomenon, in turn, increases/decreases water availability, drainage congestion or occurrence of flood, and land subsidence and soil erosion at coastal lines (Brammer, 2014). Sea level rise because of the melting of glacial snow and thermal expansion of seas are responsible for the inundation of adjacent coastlines (Eswar et al., 2021). The sea-level rise and terrestrial ingress of brackish water is the primary threat to global coastal ecosystems (Dasgupta et al., 2015). Heavy storm and/or surges influence the temporary inundation of low-lying coastal lines with brackish water. The recurring intrusion of seawater by land-use change from paddy rice to brackish aquaculture or shrimp farming is also responsible for soil salinization, build-up of acidity, and losses of organic C content, which increases the vulnerability of the rice ecosystem in coastal areas (Ali, 2006; Blankespoor et al., 2017). The climate change also drives soil salinization by promoting upward salt flux because of the increased temperature of the earth and seawater and changes in rainfall patterns (Wasko and Sharma, 2017; Seleiman and Kheir, 2018).

Sodic soils

Carbonate salts supplied through weathering of alkaline alumino–silicate minerals, shallow groundwater table, large evaporation demand, and aeolian deposition favor the build-up of these salts (Jobbágy et al., 2017). The Indus basin of India (Qadir et al., 2018; Sheoran et al., 2021), the vertisols (Shirale et al., 2018) of the Indian Deccan plateau, irrigated farming areas in Australia, Central Asia with Iraq, Iran, and the Aral Sea Basin (Raiesi and Kabiri, 2016), Nile and Niger valley in Egypt and Africa (Abdel-Fattah et al., 2020), and the irrigated basin of Argentina (Sione et al., 2017) showed the deposition of Na salts and prognosis of sodication (Figure 1). Sodic soil remains dispersed and deflocculated because of failure in aggregation. Clogging of pore space restricts air entry and lowers hydraulic conductivity (Bennett et al., 2019). Presence of Na^+ and CO_3^{2-}/HCO_3^- and poor microbial activity under alkaline soil pH conditions limits carbon supply and promotes its loss because of increased organic matter mobility (Datta et al., 2019; Basak et al., 2021a Deb et al., 2020). The precipitation of Ca^{2+} as amorphous $CaCO_3$ aggravated the Na^+-induced toxicity and nutritional deficiency of Ca^{2+} (Rai et al., 2021b). The disintegration of rocks is the primary source of $CaCO_3$ in the soil having poor aeration. The soluble Ca^{2+} and Mg^{2+} in the soil–water environment supplied from biochemical weathering and exchange process supply and prolonged water trajectory make sure the system is saturated with Ca^{2+}/Mg^{2+} upon HCO_3^- (Jobbágy et al., 2017). Contrarily, in short trajectories, the chance of HCO_3^- saturation may arise because of chemical weathering of calcareous rocks. Moreover, Na^+ selectivity in the sodic environment reinstates Ca in the solution and results in precipitation of $CaCO_3$. In an extreme alkaline condition (pH ~12.0), the hydrolysis of Na_2CO_3 (Bajwa and Swarup, 2012) and precipitation out of Ca^{2+} in $CaCO_3$ favor the existence of OH^- in soil–water solution. Therefore, a rise in the soil pH in calcareous sodic soils than in non-calcareous sodic

10.3389/fenvs.2022.935785

FIGURE 1
Salinity and sodicity: problem and threat (adopted from Falloon and Betts, 2010; Raiesi and Kabiri, 2016; Rengasamy, 2016; Liu et al., 2017; Sione et al., 2017; Mandal U. K. et al., 2019; Neubauer et al., 2019; Abdel-Fattah et al., 2020; Hayat et al., 2020; Mahajan et al., 2021a).

soil is rational because of the spontaneous release of OH^-. In one way, the presence of exchangeable Na and in another way the nonexistence of a good quantity of neutral soluble salts lead to development of extremely higher pH (Basak et al., 2015).

$$2NaHCO_3 \rightarrow Na_2CO_3 + CO_2 + H_2O,$$
$$Na_2CO_3 + 2HOH \rightarrow 2Na^+ + 2OH^- + H_2CO_3,$$
$$Na-\text{feldpars} + HOH \rightarrow H-\text{silicate clay} + NaOH.$$

Extent and impact of SAS

A significant land area (~932.2 Mha) of the Earth is affected with salinity (Rengasamy, 2006). The faulty irrigation practices further aggravated this problem, and 34.2 Mha of total irrigated area is affected by salinity (Mateo-Sagasta and Burke, 2011; Aquastat, 2016). Because of the dynamic nature of soil salinity/sodicity, more than hundred countries are affected by SAS distributed on all the continents. Central and southeastern Asian countries (China, India, Pakistan, Iran, and Iraq) and other Western countries (United States), a major part of Australia, Argentina, and some areas of Brazil from the Southern Hemisphere; Italy and Spain from Europe are the main spots of global soil salinization (Ghassemi et al., 1995; Aquastat, 2016). Soil salinization is extensively reported in some important river basins, namely, Aral Sea Basin in Central Asia, Indo-Gangetic Basin in India, Indus Basin in Pakistan, Euphrates Basin in Syria and Iraq, Yellow River Basin in China, San Joaquin Valley in California, and Murray–Darling Basin in Australia, and these are reported to have severe problems of salinization (Chang and Silva, 2014; Qadir et al., 2014). Salinity- and sodicity-induced land degradation and faulty agricultural practices promote the buildup of salinity and increase sodification and reduce crop productivity. Salinization dents nearly of US$ 31 million annual loss in agricultural productivity (FAO, 2015). The yield losses of major agricultural crops, namely, wheat, rice, sugarcane, and cotton are about 40, 45, 48, and 63 percent on SAS in the Indo-Gangetic Plain of India, respectively (Sharma et al., 2015). These losses in wheat and rice crops are 20–43 and 36–69 percent from SAS in the Indus Basin of Pakistan, respectively (Murtaza, 2013). Furthermore, in the United States, Egypt, Uzbekistan, and

Turkmenistan, the crop yield losses are 10, 30, 40, and 40 percent, respectively (Pitman et al., 2004). The monetary loss of agricultural production in India and Australia are ~2.0 and 1.3 billion US$, respectively. Long-time irrigation with high alkali water resulted in the build-up of sodicity with 14–16% loss in the grain yield of wheat and rice (Sheoran et al., 2021). The effect of salinity and presence of exchangeable Mg cause a yield loss of cotton in the Aral Sea Basin of southern Kazakhstan (Vyshpolsky et al., 2010). Depending on the type of land degradations and their intensity, the cultivated crop/cropping system followed, irrigation water quality, extension and congestion of the irrigation/drainage network, and available amendment use/management options available, and the saline areas of Kazakhstan, India, and Pakistan reported a wide variation in yield losses from 6 to 71, 40–63, and 36–69%, respectively. Because of inflation adjustment, the cost of salt-induced land degradation was US$ 441 ha^{-1} in 2013 (Qadir et al., 2014), and the aggregated total annual economic loss was US$ 30 billion (Shahid et al., 2018) at a global scale. Both yield penalty and need for additional investment of higher input multifaceted the economic costs for salt-affected lands. The crop yield losses are particularly detrimental at the farm level but often underestimated at the macro level (Mandal et al., 2018). India loses annually around 16.8 Mt of agricultural production because of salinity and associative constraints (Mandal S. et al., 2019). Five percent of the Earth's land area is salt-affected, and 75% of the cultivable area under irrigated agriculture is affected by salinity (Hopmans et al., 2021). For feeding the nine billion people by 2050, it is anticipated that crop production can be met by greening SAS soil with appropriate agro-techniques.

Plant adaptation strategies in the SAS ecosystem

Plants face primarily the osmotic stress when exposed to salinity (electrical conductivity, EC_e) and suboptimal soil water potential. Under these conditions, plants generate different osmolytes such as proline, simple carbohydrates, polyols, amino acids, and quaternary ammonium compounds such as betaine and glycine to increase the osmotic balance at the cytoplasmic scale and try to maintain cell turgidity (Seleiman et al., 2022). In this way, the plant metabolic activities are sustained, and their growth and productivity are maintained. By accumulating the simple and soluble carbohydrates, plants enhance their osmotic potential and alleviate osmotic stress (Sharp et al., 1990). In addition to water stress, roots also experienced toxicity of Na^+ in severe salinity; therefore, plants need acclimatization under such conditions. When Na^+ is absorbed by roots, the plants can either exclude Na^+ from the cytoplasm or move it to the inactive metabolic sites such as vacuoles. The K^+/Na^+ antiporter present at the vacuolar surface plays a major role in separating Na^+ and consequently lowering the Na^+ concentration in the cytoplasm (Liang et al., 2018). The tolerant plants generate an antioxidant mechanism by biosynthesis of various enzymes, namely, superoxide dismutase and catalase. Several reports proved that the antioxidant guard mechanism copes with the oxidative damage during salinity stress in crops (Noctor and Foyer, 1998).

Soil quality of salt-affected soils: Problems in parameterization

Huge spatial and temporal variations of soil are a challenge for estimating some soil properties of SAS for soil quality assessment. Alkalinity usually affect soil physical properties with poor soil water permeability. Massive soil structure and hard crust on the surface layer hinder seedling emergence and poor plant establishment. Greater osmotic potential of saline soils because of the abundance of soluble and quasi-soluble electrolytes largely affect soil–plant water relation, and plants face severe water stress due to physiological unavailability of water (Wong et al., 2010). Impaired biogeochemical cycling of essential nutrients, namely, excess losses of N, mysterious behavior of soil P (Sundha et al., 2017), and an antagonism relation between Cl^- and $H_2PO_4^-$, Cl^- and NO_3^-, Cl^-, and SO_4^{2-} and Na^+ and K^+ (Rai et al., 2021b; Sundha et al., 2022) are the major issues associated with the nutrition of plant under SAS. Furthermore, increased ionic strength also affects nutrient elements present on soil colloids. Deficiency of Ca and excess of Na affect K nutrition; the toxic appearance of HCO_3^- and CO_3^{2-} in alkali soil also decreases the solubility and availability of Zn and Fe. Many sodic areas also exhibit severe soil erosion, which promotes the loss of soil organic matter (Wong et al., 2010; Datta et al., 2019; Deb et al., 2021; Basak et al., 2021b). The extended periods of submergence because of poor soil permeability also affect soil biological properties (Wong et al., 2010). The researcher mostly specified most of the time to analyze physical features and climatic factors associated with specific salt-affected soils. Therefore, special attention is needed while selecting analytical techniques (Table 1) for estimating physical, chemical, and biological attributes of these soils (USSL, 1954; Bhargava, 2003; Basak, 2014).

Soil quality assessment of SAS

Soil quality is measured for making an inventory of the health status of soils and assessing the impacts of human perturbations on them. Such assessment should be carried out with respect to undisturbed pristine or virgin sites. However, it is difficult to find such sites (as a reference level) for comparison to capture possible degradation or aggradation caused by anthropogenic perturbation. Therefore, a relative assessment of the quality of soils with varying anthropogenic stresses is performed for screening and subsequent adoption of less/non-damaging types for upkeeping health (Basak

TABLE 1 Critical issues associated with quality data generation at a usual soil science laboratory for analyses of parameters of salt-affected soil.

Soil attribute	Significance for soil function	Method employed for analysis	Important consideration for SAS
Soil physical attribute			
Bulk density	Leaching, productivity, and erosivity	Undisturbed soil clods disturb soil analysis	Preference should be for *in situ* undisturbed soil method
Hydraulic conductivity	Water relations and aeration	Guelph permeameter, constant head method with disturbed soil samples	Falling head method is recommended with undisturbed samples for sodic or saline–sodic soil because of poor permeability
Soil texture	Soil water relation, nutrient availability, and soil erosion	International pipette method	For saline and saline–sodic soil excess electrolytes need to wash out (<40 μS cm^{-1}) to promote dispersion of soil particles Bhargava, (2003)
Aggregate analysis	Physical stability and support aeration and water relation	By wet sieving	*In situ* undisturbed soil is a good representative
Soil chemical attribute			
Soil pH and electrical conductivity (EC)	Chemical environment of the rhizosphere	Soil pH of saturation paste (pH_s) and EC of saturation paste extract instead of soil pH and EC in soil: water mixture of 1:2	This process truly expresses the soil chemical environment and available soil water content to crop growth. Additionally, these corrected expressions can categorize the problematic soils from normal soil USSL, (1954)
Soil organic C and soil organic matter	Food web in soil and determinant of soil health	Analysis of SOM/SOC through Walkey and Black wet oxidation method corrected for recover factor	Oxidizable organic C is poorly correlated with the total organic C of soil. The very labile C is a better representative of available N. Very labile C determination is less expensive and environment-friendly Majumder et al. (2008)
Soil total C	C concentration in soil	Elemental analyzer	Enough precaution needed because of small sample handling
Soil available P	P supply to the plant	Olsen's and Bray's and Kurtz method for neutral to alkaline and acidic soils, respectively	Very sensitive to silicate contamination; use of itched glass recommended to avoid contamination
Cation exchange capacity	Nutrient retention, buffering capacity, filtration of water, Sanyal et al. (2012)	Leaching and centrifugation method Bhargava, (2003)	Proper washing of soluble salts is requisite to minimize error in results of salt-affected soils Tucker, (1985)
Presence of toxic substance	Soil biological activity and food chain contamination	Extractable and proximate analysis	AAS and ICPES facilities are necessary for detection of extent and intensity of pollutant
Soil biological attribute			
Soil microbial biomass C	Microbial catalytic potential and repository for nutrient; an early indicator of management effect on soil properties	Chloroform fumigation and extraction method	Time-consuming and laborious, possibility of generating a spurious dataset; correction factor needed to convert extracted carbon flux to MBC Vance et al. (1987)
Soil respiration	Microbial activity	Laboratory incubation	Suffers from large spatio-temporal variability
Soil enzymes	Extracellular decomposition of complex organic compounds	Individual methodology are described for determining some assay values of soil enzyme	Determination is very costly Each enzyme represent specific soil function

et al., 2021a). Screening of the indicator constitutes an important part of soil quality assessment. Indicators are of two types—one, inherent indicators—these are native and quasi-permanent and undergo little changes; and the other, dynamic indicators—these reflect/capture the signatures of perturbations to which soils are subjected. They are selected based on several principles, as indicated in Figure 2 (Mandal et al., 2016).

Formulation of minimum datasets

After generating the database on identified indicators for soils subjected to different management practices, a critical statement needs to be made as to the aggrading or degrading influence of the practices on their (soils) quality (Masto et al., 2008b). Often, it is difficult to assess the soil quality using

FIGURE 2
Criteria for soil quality indicator selection modified from Mandal et al. (2016)

individual indicators, unless the databases are judged for their influence on the functional goal of soil. Accordingly, the databases are screened through several parametric and nonparametric statistical tests based on their influence on goal variables to formulate a minimum dataset (MDS) of indicators (Masto et al., 2008b). Subsequently, the databases for different indicators screened are validated with goal variables or with expected functions through statistical tools, namely, simple correlation, multiple regression, principal component analysis (PCA), and discriminant analysis (DA) to indicate their (indicators) representation in the variability of goal functions. The whole process of the formulation of MDS has elegantly been described by earlier researchers (Andrews and Carroll, 2001; Andrews et al., 2004; Basak et al., 2016) (Figure 3). Many researchers in India also screened out master indicators for different soil types and cropping systems for assessment of soil health as a function of biological productivity/sustainable yield only (Table 2); few of them have assessed soil quality using management goals, namely, productivity, environmental protection, specify targeted soil threats, and/or ecosystem services by capturing identified distinguishing minimum datasets of indicators (Bhaduri et al., 2014; Bhaduri and Purakayastha, 2014; Bünemann et al., 2018). These indicators varied significantly even within a soil type or production system. Similarly, variation was apparent in screened master indicators for salt-affected soil across the globe (Table 2). Therefore, the selection of methods for measuring indicators assumes significance to minimize the variation within a soil type or production system and measure soil functionality and their integration to capture informative soil quality indices (Lehmann et al., 2020). A few desirable features of methods for measuring indicators are 1) high throughput, 2) ease of use, 3) storage, 4) potential reference material, 5) achievability, 6)

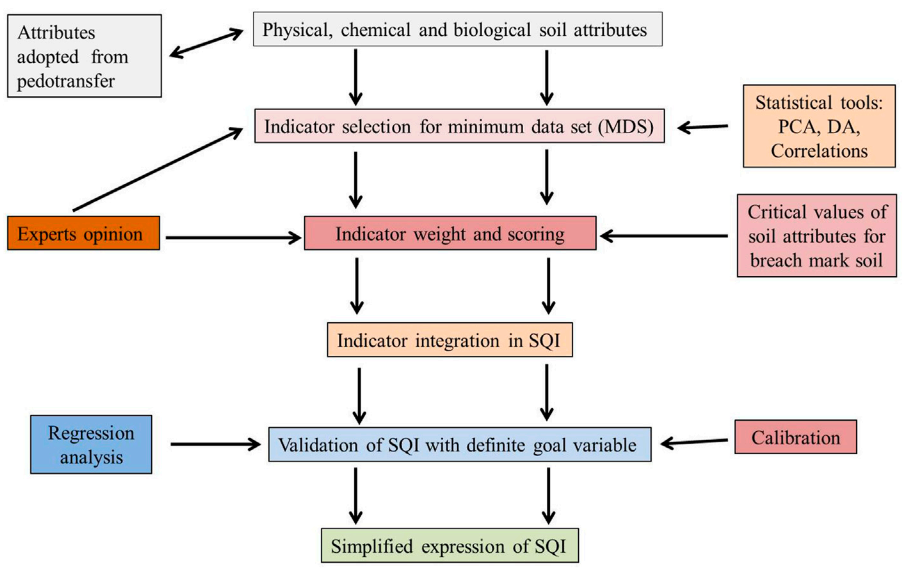

FIGURE 3
Schematic diagram showing all the processes, namely, indicator selection, minimum dataset formation, interpretation, and integration involved for calculation of soil quality index (modified from Andrews et al., 2004)

TABLE 2 Soil quality assessment in salt-affected soils; figures in parenthesis are the number of attributes used.

Agroecology and region	Country	Method used	Variability explained (%)	Selected soil quality indicator	Reference
Alkaline soil, semi-arid region	China	Principal component analysis and expert opinion (EO)	86 (22)	Invertage, N/P ratio, dissolve soil organic carbon (SOC), sodium adsorption ratio, very labile C	Yu et al. (2018)
Semi-arid environment under different tillage	Iran	PCA	89 (16)	C and N mineralization, alkaline phosphatase, urease, microbial biomass C, and $CaCO_3$ content	Raiesi and Kabiri, (2016)
Vertisols under sodic water irrigation	Argentina	Regression analysis and EO		Aggregate stability, water percolation, SOC, exchangeable sodium percent (ESP), pH, and electrical conductivity (EC_e)	Sione et al. (2017)
Semi-arid Deccan plateau	India	PCA and EO	86 (24)	Clay, pH, $CaCO_3$, ESP, exchangeable magnesium, and saturated hydraulic conductivity	Vasu et al. (2018)
Saline soil in Indo-Gangetic Plain	India	PCA and EO	62–67 (15)	α-glucosidase activity, microbial biomass C (MBC), EC_e, $KMnO_4$– oxidizable N, MBC: MBN, and urease activity	Soni et al. (2021)
Sunderbans delta	India	PCA and EO	84 (23)	MBC, EC_e, soil moisture content, and pH	Mitran et al. (2021)
Sodic soil, Indo-Gangetic Plain	India	PCA	73 (23)	EC_e, SAR, DTPA extractable Cu, SOC, hot water–soluble B and Olsen's P	Barman et al. (2021)
Coastal saline soil	India	PCA	82 (18)	Soil $pH_{1:2.5}$, $EC_{1:2.5}$, DTPA extractable Fe, Zn, Cu, hot water–soluble B, basal soil respiration, and urease	Mahajan et al. (2021b)

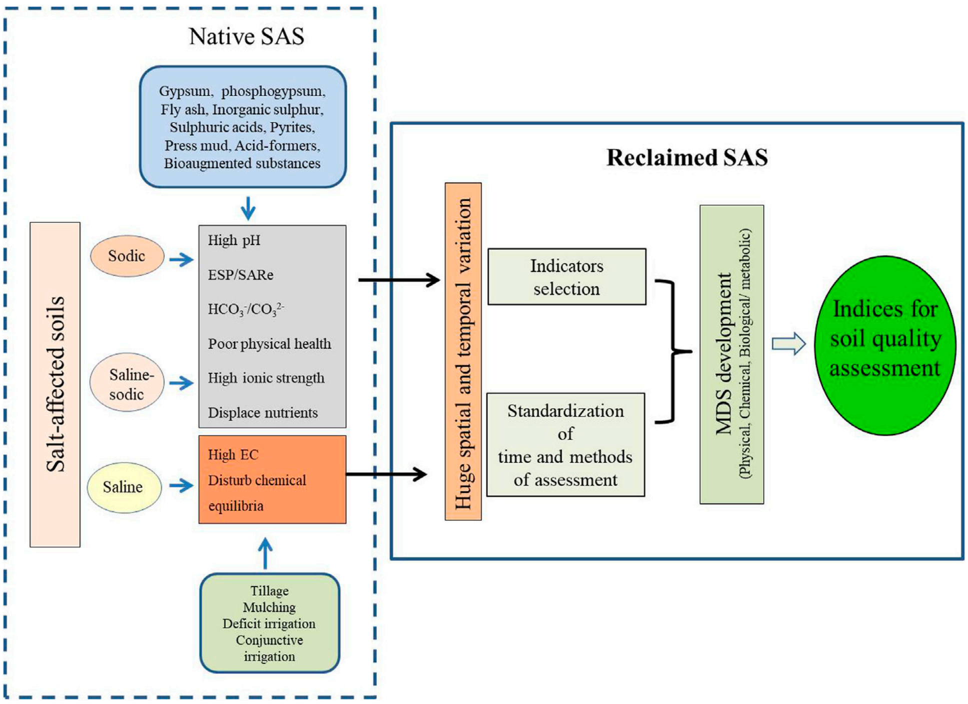

FIGURE 4
A comprehensive framework for developing soil quality indices.

deployment status, 7) sample collection, 8) international comparisons, 9) how much soil, 10) infrastructure, 11) cost—hardware/labor, and 12) multi-parametric in nature among the screened indicators even for a similar production system raised at different geographical sites (Mandal et al., 2016). One of the major tasks for researchers is to work on finding commonality in indicators for different soil types and production systems. This will facilitate development of easy and inexpensive methods for common master indicators and their inclusion in routine analysis in soil testing laboratories for assessment of soil health. Studies assessing the quality of soils to meet other ecosystem services have hardly been conducted in India, although its role and capability for providing water security (NO_3, As, or F pollution), waste recycling, biodiversity, environmental protection, and climate change abatement are in urgent demand for assessment. A modest beginning can be made with the existing long-term experiments where along with biological productivity, biological diversity, carbon budgeting, and crop quality may be included as goal variables (Bhaduri et al., 2014).

Calculation of soil quality index

Screened soil quality indicators for a production system highlighting the aggradation or degradation effect through multidimensional trends (positive, negative, or no change) and intensity (degree) are converted into an index. These indicators are combined together (Figure 3) into a combinable index (soil quality index) for getting a unique value for describing aggradations or degradation in soils owing to specific management practices. To combine the indicators, sometimes different weights are given to them based on personal judgment or values of the coefficients of determinations of multiple regression, principal component analysis (PCA), and discriminant analysis (DA) associated with those indicators during screening through different statistical methods in the form of a weighted additive or simple additive (Andrews and Carroll, 2001; de Lima et al., 2008; Mukherjee and Lal, 2014). The soil quality index (SQI) is developed for soils under different management practices and cropping systems in a large number of long-term fertility experiments in India by several researchers (Basak et al., 2021a; Figure 4). Recently, Soni et al. (2021) assessed the SQI for saline soils under tillage, mulching, and deficit saline water irrigation.

Soil quality improvement under different rehabilitation approaches for SAS

Improving soil quality of sodic soils—impact of gypsum and alternate reclamation technology

Sodic soil reclamation was initiated by applying inorganic substances, namely, gypsum, phosphogypsum, fly ash, inorganic sulfur, sulfuric acids, pyrites, aluminum chloride, sugar industry byproduct press mud and acid formers, and bioaugmented substances with gypsum (CSSRI, 2006; Hafez et al., 2015; Rai et al., 2021a). If irrigation water is safe for soil and crops, then soil sodicity reclamation is principally a single-time investment for sustaining production (Rai et al., 2021b). Usually, 3–4 years are required after the adoption of reclamation technology for rice-based cropping systems to reach their productivity potential because of the gradual replacement of a large amount of Na^+ from soil colloids by Ca^{2+} during the progress of reclamation (Abrol and Bhumbla, 1979; Zhang et al., 2021). When sodicity is a consequence of water-born alkalinity, then recurring applications of amendments are advocated to overcome water-born sodicity (residual alkalinity) and maintain soil quality and sustainable crop yield (Singh et al. 2019; Sheoran et al., 2021). The application of organic materials such as city waste compost, gypsum enrich compost, sulfur-rich compost, and the byproduct of sugarcane industry press mud in conjunction with gypsum improves crop yield by decreasing soil pH and ESP because of decrease in the precipitation of Ca and greater removal of Na in drainage waters (Grigg et al., 2006; Choudhary et al., 2011; Sundha et al., 2020). Calcareous sodic soils are recommended for reclamation through the application of elemental sulfur (Ganjegunte et al., 2018). On-farm and participatory research experiments conducted in the CSSRI and other national laboratories reported improvement in soil quality upon reclamation (Supplementary Table S1). The rice–wheat system in the sodic area ($pH_{1:2}$ 8.7) of western India maintained optimum yield by addition of 100 and 150 percent of the recommended doses of fertilizer (RDF) with necessary improvement in $pH_{1:2}$, $EC_{1:2}$, SOC, Olsen's P, NH_4OAc extractable K, and DTPA extractable Zn and Mn (Swarup and Yaduvanshi, 2000). Application of N @120 and P @ 26 kg ha^{-1} + FYM/press mud/gypsum improved SOC and sustained wheat yield in sodic soil ($pH_{1:2}$) when irrigated with sodic water (RSC 8.5 me L^{-1}; SAR of 8.8) in sodic areas of northwestern India (Yaduvanshi and Sharma 2008; Yaduvanshi and Swarup, 2005). Reclamation of soil declined soil $pH_{1:2}$ and SAR_e and improved SOC, and increased the uptake of $KMnO_4$–N, Olsen's P, and NH_4OAc extractable K. The results from the participatory experiments carried out at 10 locations in the central Indo-Gangetic plain showed a reduced level of sodicity (as decrement in ESP, SAR_e, and soil $pH_{1:2}$ and $EC_{1:2}$Singh) and increased SOC and improved soil porosity, void ratio, and saturated hydraulic conductivity because of green manuring in the rice–wheat cropping system (Singh et al., 2014), although the phosphogypsum (PG) application is questionable because of the presence of heavy metals (Mishra et al., 2019). However, the application of PG was associated with declined soil $pH_{1:2}$, $EC_{1:2}$, ESP, and SAR_e and improved soil fertility (increased Olsen's P, NH_4OAc extractable K, and DTPA extractable Fe, Mn, Zn, Cu etc.), soil physical quality (reducing water-dispersible clay and bulk density; and improving infiltration, aggregate ratio, mean weight diameter and aggregate associated C), and improved rice yield (Nayak et al., 2013). Recently, Yu et al. (2014) claimed the neutralization of soil sodicity and improvement of soil physical properties such as an increase in hydraulic conductivity and soil porosity reduce by the application of flue gas desulphurization gypsum (FGDG). Acidified biochar produced from rice straw and dicer wood chips facilitate the losses of Na and reduce the EC and SAR_e (Sadegh-Zadeh et al., 2018).

Improving soil quality of saline soil: impact of agronomic practices and engineering measures

Reduce tillage, deficit irrigation, mulching, adoption of low water requiring crops, and cultivation of salt-tolerant varieties for water-saving and minimizing salt load in applied irrigation events are strategies for productive utilization of saline soils (Singh, 2009; Li et al., 2019; Seleiman et al., 2019). Deficit irrigation (DI) with available saline water is adopted to check frequent drought and sustain crop production (Jiang et al., 2012; Nagaz et al., 2012). Paddy straw mulch and efficient water management had the potential for restoring soil health, checking evaporation, and improving crop productivity (Purakayastha et al., 2019; Soni et al., 2021) (Supplementary Table S2). These practices permit water to move more quickly into and through the soil profile, increasing salt leaching and inhibiting salt build-up in surface soil (Grigg et al., 2006; Yuan et al., 2019; Zhang et al., 2021). Therefore, the DI and mulching synergized with the climate and soil of a geographical area can be a nature-based solution working within the limits of the existing natural resources (Visser et al., 2019; Soni et al., 2021). Zero tillage is also effective in increasing soil fertility, building soil organic carbon, restoring soil structure, and leading to a reduction in soil evaporation and salinity (Wang et al., 2014). Several researchers report that salinity has an undesirable effect on soil microbial biomass C, N, and basal soil respiration (BSR), whereas it has a positive effect on metabolic quotient (qCO_2) (Tripathi et al., 2006; Egamberdieva et al., 2011; Iwai et al., 2012; Mahajan et al., 2016). Salinity-induced stress might have reduced the positive respiratory activities of the microorganisms (Tripathi et al., 2007; Iwai et al., 2012). The toxic effect of the dominant cation Na^+ slows down the growth of soil microorganisms and MBC rather than the C input (Rietz and Haynes, 2003; Egamberdieva et al., 2011; Mavi and Marschner, 2013). In general, larger soil enzyme activities were noted with low electrolyte concentration and vice versa. Organic amendments in association with microflora increase mineralization, with an associated increase in CO_2 release and, consequently, soil aeration, apparently due to increased enzymatic activities. Such an increase in mineralization improves the soil fertility and crop productivity in saline soil. Leaching accomplished by ponding water in the well-leveled field with good quality water (annual rain, river, or underground) is the reasonable choice to remove excess salts and electrolytes in soils below the root zone in the soil profile. The amount of salts leached from soils depends on the amount and quality of irrigation water and soil texture. Surface flushing with water is advocated to wash surface-deposited salts (Nayak et al., 2008). This practice is recommended for soil with low permeability, and soil is prone to crust formation. Scarping of loaded salts is followed to manage marginal landholding affected by salinity; however, recurring removal of salts is recommended to attain desired change in soil salinity for productive use. Proper leveling, zero (minimum) tillage, mulching, conjunctive use of saline water in cyclic or mixing mode with good quality water, light and frequent application of saline irrigation for reduction of cumulative water deficit, irrigating with best available water at sensitive crop stages (germination and seeding emerging stages), pre-sowing irrigation for Kharif (summer) crop, improving water use efficiency practice by pressurized drip/sprinkler irrigation which facilitates the washing of root zone salinity, and sustaining crop production are the promising options for fruitful utilization of SAS and saline water (Soni et al., 2021; Garg et al., 2022; Rai et al., 2022). Exogenous application of plant growth regulators (salicylic acid, thio-urea, and potassium nitrate) alleviated sodicity stress of both soil and water-born sodicity by triggering physiological parameters of the rice (Singh et al., 2022). The use of bio-drainage is advocated to manage waterlogged saline soils by physiological transpiration of water (Dagar et al., 2016).

Underground or surface drainage is a long-term solution for lowering the water table and leaching of salts and providing a favorable salt balance in surface soil. A perforated corrugated PVC pipe protected with synthetic filter consistently established in the proper plan below the rooting depth to reduce poor quality water table and remove excess salts and water by gravitational action or pressurized pump. Ingress of brackish water and seawater tides can be checked by building tall and well-made earthen banks. Building of pond and water harvesting unit conserves seasonal rain and utilization of it for irrigation of dry season crops and leaching of salts. The farm pond technology delivers the scope for crop diversification, round-the-year cropping, and integrated farming because of improved irrigation facilities, checking of salinity, and improved drainage conditions (Chinchmalatpure et al., 2015).

Conclusion and future research direction

Soil salinity and sodicity are the major issues impacting crop production on ~1 billion hectares of land distributed in arid and semi-arid regions worldwide. These soils are broadly categorized into saline, sodic, and saline–sodic depending upon the dominance of soluble (chloride/sulfate) and/or alkaline salts (carbonate/bicarbonates) of Na, K, Ca, and Mg. The disproportionate presences of salts in these soils reduce the choice of the crop and incur the annual productivity loss equivalent to 31 million US dollars. Application of Ca-bearing salts, pyrites, and other organic amendments and engineering and agronomic approaches are successful in the rehabilitation of these soils. The success of rehabilitation of SAS can be further enhanced by selecting crop varieties capable of withstanding osmotic stress, water deficit, and toxicities of specific ions. The soil quality indices developed for different stages of the rehabilitation of salt-affected soils act as a tool for monitoring the real-time progress of the management process adopted in these soils. The screening of the inherent and dynamic indicators capturing the signature of the soil perturbations constitutes an important part of soil quality assessment. Different studies had identified the bulk density, hydraulic conductivity, pH, electrical conductivity, exchangeable sodium percent, microbial biomass C, and soil enzymes, which are the master indicators for soil quality assessment. The spatial and temporal variations of salt-affected areas are the major problems for the selection of master indicators of soil. A developed soil quality index for the SAS soil will enable the functionaries to assess the real-time impact of management options for different soil functions. It also enables the farmers to select site-specific and goal-specific management plans for improved resource use efficiency, reduced environmental impact, increased productivity, and farm economy. The soil quality–based management plan can be a tool for policy planners for monitoring the progress of land reclamation, soil health management, and environmental protection. Recent development in material science has the potential to develop some formulations such as polymers, nano-materials, acidified biochars, elemental sulfur, sulfuric acid generator, and flue-gas-desulphurization gypsum (FGDG), having the potential for replacing gypsum as an amendment. In the future, scientifically managed city waste compost can also supplement the sodic soil reclamation program. Moreover, future application of these alternatives for sustainable and profitable use in salt-affected soils would not be practicable unless efficacy and efficiency in sodic soil reclamation are established and low-cost methods for the production are not devised.

Author contributions

NB: conceptualization, framework development, and preparation of the manuscript; AKR: conceptualization, framework development, and preparation of the draft; PS: collection and organization of the database, preparation of the manuscript; RM: collection and organization of the database, preparation of the manuscript; SB: collection and organization of the database, review and editing; RKY: resources, review, and editing; PCS: resources, review, and editing.

Funding

This work was supported by the Indian Council of Agricultural Research, New Delhi (India).

Acknowledgments

This work is a part of the CSSRI project “Developing soil quality indices for sodic soil under different reclamation strategies (NRMACSSRISIL201801700969)”. The authors thank the Director, CSSRI, Karnal (Haryana) for the financial support.

Conflict of interest

The authors declare that the research was conducted in the absence of any commercial or financial relationships that could be construed as a potential conflict of interest.

Publisher’s note

All claims expressed in this article are solely those of the authors and do not necessarily represent those of their affiliated organizations, or those of the publisher, the editors, and the reviewers. Any product that may be evaluated in this article, or claim that may be made by its manufacturer, is not guaranteed or endorsed by the publisher.

Supplementary material

The Supplementary Material for this article can be found online at: https://www.frontiersin.org/articles/10.3389/fenvs.2022.935785/full#supplementary-material

References

Abdel-Fattah, M. K., Abd-Elmabod, S. K., Aldosari, A. A., Elrys, A. S., and Mohamed, E. S. (2020). Multivariate analysis for assessing irrigation water quality: A case study of the bahr mouise canal, eastern nile delta. *Water* 12, 2537. doi:10.3390/w12092537

Abrol, I. P., and Bhumbla, D. R. (1979). Crop responses to differential gypsum applications in a highly sodic soil and the tolerance of several crops to exchangeable sodium under field conditions. *Soil Sci.* 127, 79–85. doi:10.1097/00010694-197902000-00004

Abrol, I. P., Yadav, J. S. P., and Massoud, F. I. (1998). *Salt-affected soils and their management*. FAO: Rome, Italy.

Al-Suhaibani, N., Seleiman, M. F., El-Hendawy, S., Abdella, K., Alotaibi, M., Alderfasi, A., et al. (2021). Integrative effects of treated wastewater and synthetic fertilizers on productivity, energy characteristics, and elements uptake of potential energy crops in an arid agro-ecosystem. *Agronomy* 11, 2250. doi:10.3390/agronomy11112250

Ali, A. M. S. (2006). Rice to shrimp: Land use/land cover changes and soil degradation in Southwestern Bangladesh. *Land Use Policy* 23, 421–435. doi:10.1016/j.landusepol.2005.02.001

Alkharabsheh, H. M., Seleiman, M. F., Hewedy, O. A., Battaglia, M. L., Jalal, R. S., Alhammad, B. A., et al. (2021). Field crop responses and management strategies to mitigate soil salinity in modern agriculture: A review. *Agronomy* 11, 2299. doi:10.3390/agronomy11112299

Andrews, S. S., and Carroll, C. R. (2001). Designing a soil quality assessment tool for sustainable agroecosystem management. *Ecol. Appl.* 11, 1573–1585. doi:10.1890/1051-0761(2001)011[1573:DASQAT]2.0.CO;2

Andrews, S. S., Karlen, D. L., and Cambardella, C. A. (2004). The soil management assessment framework. *Soil Sci. Soc. Am. J.* 68, 1945–1962. doi:10.2136/sssaj2004.1945

Aquastat (2016). *FAO's information system on water and agriculture*. Rome, Italy: Food and Agricultural Organization (FAO).

Badawy, S. A., Zayed, B. A., Bassiouni, S. M. A., Mahdi, A. H. A., Majrashi, A., Ali, E. F., et al. (2021). Influence of nano silicon and nano selenium on root characters, growth, ion selectivity, yield, and yield components of Rice (Oryza sativa L.) under salinity conditions, Plants (Basel). *Plants* 10, 1657. doi:10.3390/plants10081657

Bajwa, M. S., and Swarup, A. (2012). "Soil salinity and alkalinity," in *Fundamentals of soil science*. N. N. Goswami, R. K. Rattan, G. Dev, G. Narayansamy, and D. K. Das. New Delhi, 329–339.

Barman, A., Sheoran, P., Yadav, R. K., Abhishek, R., Sharma, R., Prajapat, K., et al. (2021). Soil spatial variability characterization: Delineating index-based management zones in salt-affected agroecosystem of India. *J. Environ. Manag.* 296, 113243. doi:10.1016/j.jenvman.2021.113243

Basak, N., Chaudhuri, S. K., and Sharma, D. K. (2015). Influence of water quality on exchange phase-solution phase behavior of texturally different salt-affected soils. *J. Indian Socie. Soil Scie*. 64, 365. doi:10.5958/0974-0228.2015.00048.1

Basak, N., Datta, A., Mitran, T., Roy, S. S., Saha, B., Biswas, S., et al. (2016). Assessing soil-quality indices for subtropical rice-based cropping systems in India. *Soil Res.* 54, 20. doi:10.1071/SR14245

Basak, N., Mandal, B., Rai, A. K., and Basak, P. (2021a). Soil quality and productivity improvement: Indian story. *Proc. Indian Natl. Sci. Acad.* 87, 2–10. doi:10.1007/s43538-021-00007-8

Basak, N., Sheoran, P., Sharma, R., Yadav, R. K., Singh, R. K., Kumar, S., et al. (2021b). Gypsum and pressmud amelioration improve soil organic carbon storage and stability in sodic agroecosystems. *Land Degrad. Dev.* 32, 4430–4444. doi:10.1002/ldr.4047

Basak, R. K. (2014). *Soil testing and recommenation*. second Ludhiana, India: Kalyani Publishers.

Bennett, J. M., Marchuk, A., Marchuk, S., and Raine, S. R. (2019). Towards predicting the soil-specific threshold electrolyte concentration of soil as a reduction in saturated hydraulic conductivity: The role of clay net negative charge. *Geoderma* 337, 122–131. doi:10.1016/j.geoderma.2018.08.030

Bhaduri, D., and Purakayastha, T. J. (2014). Long-term tillage, water and nutrient management in rice–wheat cropping system: Assessment and response of soil quality. *Soil Tillage Res.* 144, 83–95. doi:10.1016/j.still.2014.07.007

Bhaduri, D., Purakayastha, T. J., Patra, A. K., and Chakraborty, D. (2014). Evaluating soil quality under a long-term integrated tillage–water–nutrient experiment with intensive rice–wheat rotation in a semi-arid Inceptisol, India. *Environ. Monit. Assess.* 186, 2535–2547. doi:10.1007/s10661-013-3558-8

Bhargava, G. P. (2003). *Training manual for undertaking studies on Genesis of sodic/alkali soils*. Karnal 132001: Central Soil salinity Resarch Institute.

Blankespoor, B., Dasgupta, S., and Lange, G.-M. (2017). Mangroves as a protection from storm surges in a changing climate. *Ambio* 46, 478–491. doi:10.1007/s13280-016-0838-x

Brammer, H. (2014). Bangladesh's dynamic coastal regions and sea-level rise. *Clim. Risk Manag.* 1, 51–62. doi:10.1016/j.crm.2013.10.001

Bünemann, E. K., Bongiorno, G., Bai, Z., Creamer, R. E., De Deyn, G., de Goede, R., et al. (2018). Soil quality – a critical review. *Soil Biol. Biochem.* 120, 105–125. doi:10.1016/j.soilbio.2018.01.030

Cai, X., Sharma, B. R., Matin, M. A., Sharma, D., and Gunasinghe, S. (2010). *An assessment of crop water productivity in the Indus and ganges river basins: Current status and scope for Improvement 140*. IMWI Research Report. Columbo, Srilanka.

Chang, A. C., and Silva, D. B. (2014). "Prologue BT - salinity and drainage in san Joaquin Valley, California: Science, technology, and policy," in, eds. A. C. Chang and D. Brawer Silva (Dordrecht: Springer Netherlands), 1–6. doi:10.1007/978-94-007-6851-2_1

Chinchmalatpure, A. R., Ali, S., Kulshrestra, N., Singh, R. K., Bundela, D. S., Kumar, P., et al. (2015). *Intellectual property management and commercialization of ICAR-CSSRI technologies for management of salt-affected and waterlogged soils of India*. Haryana: ICAR-Central Soil Salinity Research Institute.

Choudhary, O. P., Ghuman, B. S., Bijay-SinghThuy, N., and Buresh, R. J. (2011). Effects of long-term use of sodic water irrigation, amendments and crop residues on soil properties and crop yields in rice–wheat cropping system in a calcareous soil. *Field Crops Res.* 121, 363–372. doi:10.1016/j.fcr.2011.01.004

CSSRI (2006). *CSSRI: A journey to excellence (1969-2006)*. Karnal 132 001, India: Central Soil Salinity Research Institute.

Dagar, J. C., Lal, K., Ram, J., Kumar, M., Chaudhari, S. K., Yadav, R. K., et al. (2016). Eucalyptus geometry in agroforestry on waterlogged saline soils influences plant and soil traits in North-West India. *Agric. Ecosyst. Environ.* 233, 33–42. doi:10.1016/j.agee.2016.08.025

Dasgupta, S., Hossain, M. M., Huq, M., and Wheeler, D. (2015). Climate change and soil salinity: The case of coastal Bangladesh. *Ambio* 44, 815–826. doi:10.1007/s13280-015-0681-5

Datta, A., Setia, R., Barman, A., Guo, Y., and Basak, N. (2019). "Carbon dynamics in salt-affected soils," in *Research developments in saline agriculture*. Editors J. Dagar and R. Yadav (Singapore: Springer).

de Lima, A. C. R., Hoogmoed, W., and Brussaard, L. (2008). Soil quality assessment in rice production systems: Establishing a minimum data set. *J. Environ. Qual.* 37, 623–630. doi:10.2134/jeq2006.0280

Deb, S., Mandal, B., and Bhadoria, P. B. S. (2020). Influence of sea water ingression on carbon sequestration in soils under coastal agro-ecosystems of eastern India. *Agric. Res.* 9, 622–630. doi:10.1007/s40003-020-00456-5

Ding, Z., Kheir, A. M. S., Ali, O. A. M., Hafez, E. M., ElShamey, E. A., Zhou, Z., et al. (2021). A vermicompost and deep tillage system to improve saline-sodic soil quality and wheat productivity. *J. Environ. Manag.* 277, 111388. doi:10.1016/j.jenvman.2020.111388

Egamberdieva, D., Kucharova, Z., Davranov, K., Berg, G., Makarova, N., Azarova, T., et al. (2011). Bacteria able to control foot and root rot and to promote growth of cucumber in salinated soils. *Biol. Fertil. Soils* 47, 197–205. doi:10.1007/s00374-010-0523-3

Eswar, D., Karuppusamy, R., and Chellamuthu, S. (2021). Drivers of soil salinity and their correlation with climate change. *Curr. Opin. Environ. Sustain.* 50, 310–318. doi:10.1016/j.cosust.2020.10.015

Falloon, P., and Betts, R. (2010). Climate impacts on European agriculture and water management in the context of adaptation and mitigation—the importance of an integrated approach. *Sci. Total Environ.* 408, 5667–5687. doi:10.1016/j.scitotenv.2009.05.002

FAO, I. (2015). *Status of the world's soil resources – main report*. Rome, Italy: Food and Agriculture Organization of the United Nations and Intergovernmental Technical Panel on Soils.

Fishman, R. (2018). Groundwater depletion limits the scope for adaptation to increased rainfall variability in India. *Clim. Change* 147, 195–209. doi:10.1007/s10584-018-2146-x

Ganjegunte, G. K., Clark, J. A., Parajulee, M. N., Enciso, J., and Kumar, S. (2018). Salinity management in pima cotton fields using sulfur burner. *Agrosyst. Geosci. Environ.* 1, 1–10. doi:10.2134/age2018.04.0006

Garg, N., Choudhary, O. P., Thaman, S., Sharma, V., Singh, H., Vashistha, M., et al. (2022). Effects of irrigation water quality and NPK-fertigation levels on plant growth, yield and tuber size of potatoes in a sandy loam alluvial soil of semi-arid region of Indian Punjab. *Agric. Water Manag.* 266, 107604. doi:10.1016/j.agwat.2022.107604

Ghassemi, F., Jakeman, A. J., and Nix, H. A. (1995). *Stalinization of land and water resources: Human causes, extent, management and case studies*. Wallingford, UK: CABI.

Grigg, A. H., Sheridan, G. J., Pearce, A. B., and Mulligan, D. R. (2006). The effect of organic mulch amendments on the physical and chemical properties and revegetation success of a saline-sodic minespoil from central Queensland, Australia. *Soil Res.* 44, 97. doi:10.1071/sr05047

Gupta, R. N., and Mathur, A. (2011). "Origin, distribution and classificatinof the salt-affeted soils of India," in *Bulletin of the Indian society of soil science*. Editors R. Rattan and A. K. Singh (New Delhi, India: Indian Society of Soil Science), 1–28.

Hafez, E. M., Hassan, W. H. A. E., Gaafar, I. A., and Seleiman, M. F. (2015). Effect of gypsum application and irrigation intervals on clay saline-sodic soil characterization, rice water use efficiency, growth, and yield. *J. Agric. Sci. (Tor).* 7, 208. doi:10.5539/jas.v7n12p208

Hansen, J. A., Jurgens, B. C., and Fram, M. S. (2018). Quantifying anthropogenic contributions to century-scale groundwater salinity changes, San Joaquin Valley, California, USA. *Sci. Total Environ.* 642, 125–136. doi:10.1016/j.scitotenv.2018.05.333

Hayat, K., Bundschuh, J., Jan, F., Menhas, S., Hayat, S., Haq, F., et al. (2020). Combating soil salinity with combining saline agriculture and phytomanagement with salt-accumulating plants. *Crit. Rev. Environ. Sci. Technol.* 50, 1085–1115. doi:10.1080/10643389.2019.1646087

Hopmans, J. W., Qureshi, A. S., Kisekka, I., Munns, R., Grattan, S. R., Rengasamy, P., et al. (2021). "Chapter One - critical knowledge gaps and research priorities in global soil salinity," in, ed. A. Sparks (Academic Press), 1–191. doi:10.1016/bs.agron.2021.03.001

Iwai, C. B., Oo, A. N., and Topark-ngarm, B. (2012). Soil property and microbial activity in natural salt affected soils in an alternating wet–dry tropical climate. *Geoderma* 190, 144–152. doi:10.1016/j.geoderma.2012.05.001

Jiang, J., Huo, Z., Feng, S., and Zhang, C. (2012). Effect of irrigation amount and water salinity on water consumption and water productivity of spring wheat in Northwest China. *Field Crops Res.* 137, 78–88. doi:10.1016/j.fcr.2012.08.019

Jobbágy, E. G., and Jackson, R. B. (2004). Groundwater use and salinization with grassland afforestation. *Glob. Chang. Biol.* 10, 1299–1312. doi:10.1111/j.1365-2486.2004.00806.x

Jobbágy, E. G., Tóth, T., Nosetto, M. D., and Earman, S. (2017). On the fundamental causes of high environmental alkalinity (ph ≥ 9): An assessment of its drivers and global distribution. *Land Degrad. Dev.* 28, 1973–1981. doi:10.1002/ldr.2718

Kamra, S. K. (2021). "Subsurface drainage for saline and waterlogged alluvial soils," in *Managing salt affected soils for sustainable agricultue*. Editors P. S. Minhas, R. K. Yadav, and P. C. Sharma (New Delhi, India: Indian Council of Agricultural Research ICAR), 346–366.

Karlen, D. L., Mausbach, M. J., Doran, J. W., Cline, R. G., Harris, R. F., Schuman, G. E., et al. (1997). Soil quality: A concept, definition, and framework for evaluation (A guest editorial). *Soil Sci. Soc. Am. J.* 61, 4–10. doi:10.2136/sssaj1997.03615995006100010001x

Lehmann, J., Bossio, D. A., Kögel-Knabner, I., and Rillig, M. C. (2020). The concept and future prospects of soil health. *Nat. Rev. Earth Environ.* 1, 544–553. doi:10.1038/s43017-020-0080-8

Li, J., Gao, Y., Zhang, X., Tian, P., Li, J., Tian, Y., et al. (2019). Comprehensive comparison of different saline water irrigation strategies for tomato production: Soil properties, plant growth, fruit yield and fruit quality. *Agric. Water Manag.* 213, 521–533. doi:10.1016/j.agwat.2018.11.003

Liang, W., Ma, X., Wan, P., and Liu, L. (2018). Plant salt-tolerance mechanism: A review. *Biochem. Biophysical Res. Commun.* 495, 286–291. doi:10.1016/j.bbrc.2017.11.043

Liu, X., Ren, Y., Gao, C., Yan, Z., and Li, Q. (2017). Compensation effect of winter wheat grain yield reduction under straw mulching in wide-precision planting in the North China Plain. *Sci. Rep.* 7, 213. doi:10.1038/s41598-017-00391-6

Mahajan, G. R., Das, B., Manivannan, S., Manjunath, B. L., Verma, R. R., Desai, S., et al. (2021a). Soil and water conservation measures improve soil carbon sequestration and soil quality under cashews. *Int. J. Sediment Res.* 36, 190–206. doi:10.1016/j.ijsrc.2020.07.009

Mahajan, G. R., Das, B., Morajkar, S., Desai, A., Murgaokar, D., Patel, K. P., et al. (2021b). Comparison of soil quality indexing methods for salt-affected soils of Indian coastal region. *Environ. Earth Sci.* 80, 725. doi:10.1007/s12665-021-09922-x

Mahajan, G. R., Manjunath, B. L., Latare, A. M., D'Souza, R., Vishwakarma, S., Singh, N. P., et al. (2016). Microbial and enzyme activities and carbon stock in unique coastal acid saline soils of Goa. *Proc. Natl. Acad. Sci. India Sect. B. Biol. Sci.* 86, 961–971. doi:10.1007/s40011-015-0552-7

Majumder, B., Mandal, B., Bandyopadhyay, P. K., Gangopadhyay, A., Mani, P. K., Kundu, A. L., et al. (2008). Organic amendments influence soil organic carbon pools and rice-wheat productivity. *Soil Sci. Soc. Am. J.* 72, 775–785. doi:10.2136/sssaj2006.0378

Mandal, B., Basak, N., Singha, R. S., and Biswas, S. (2016). "Soil health measurement techniques," in *Soil health: Concept* (New Delhi: Status and Monitoringonitoring), 1–98.

Mandal, S., Mandal, U. K., Lama, T. D., Burman, D., and Sharma, P. C. (2019). Economic analysis of farm-level agricultural risks in coastal region of West Bengal in India. *J. Soil Salin. Water Qual.* 11, 269–279.

Mandal, U. K., Burman, D., Bhardwaj, A. K., Nayak, D. B., Samui, A., Mullick, S., et al. (2019). Waterlogging and coastal salinity management through land shaping and cropping intensification in climatically vulnerable Indian Sundarbans. *Agric. Water Manag.* 216, 12–26. doi:10.1016/j.agwat.2019.01.012

Mandal, S., Raju, R., Kumar, A., Kumar, P., and Sharma, P. C. (2018). Current status of research, technology response and policy needs of salt-affected soils in India -A review. *J. Indian Soc. Coast. Agric. Res.* 36, 40–53.

Martins, A. P., Denardin, L. G. de O., Borin, J. B. M., Carlos, F. S., Barros, T., Ozório, D. V. B., et al. (2017). Short-term impacts on soil-quality assessment in alternative land uses of traditional paddy fields in southern Brazil. *Land Degrad. Dev.* 28, 534–542. doi:10.1002/ldr.2640

Masto, R. E., Chhonkar, P. K., Purakayastha, T. J., Patra, A. K., and Singh, D. (2008a). Soil quality indices for evaluation of long-term land use and soil management practices in semi-arid sub-tropical India. *Land Degrad. Dev.* 19, 516–529. doi:10.1002/ldr.857

Masto, R. E., Chhonkar, P. K., Singh, D., and Patra, A. K. (2008b). Alternative soil quality indices for evaluating the effect of intensive cropping, fertilisation and manuring for 31 years in the semi-arid soils of India. *Environ. Monit. Assess.* 136, 419–435. doi:10.1007/s10661-007-9697-z

Mateo-Sagasta, J., and Burke, J. (2011). *Agriculture and water quality interactions: A global overview" (solaw background thematic report-T R08*. Rome, Italy: Food and Agricultural Organization (FAO).

Mavi, M. S., and Marschner, P. (2013). Salinity affects the response of soil microbial activity and biomass to addition of carbon and nitrogen. *Soil Res.* 51, 68. doi:10.1071/SR12191

Meena, M. D., Joshi, P. K., Narjary, B., Sheoran, P., Jat, H. S., Chinchmalatpure, A. R., et al. (2016). Effects of municipal solid waste compost, rice-straw compost and mineral fertilisers on biological and chemical properties of a saline soil and yields in a mustard–pearl millet cropping system. *Soil Res.* 54, 958. doi:10.1071/SR15342

Mishra, V. K., Jha, S. K., Damodaran, T., Singh, Y. P., Srivastava, S., Sharma, D. K., et al. (2019). Feasibility of coal combustion fly ash alone and in combination with gypsum and green manure for reclamation of degraded sodic soils of the indo-gangetic plains: A mechanism evaluation. *Land Degrad. Dev.* 30, 1300–1312. doi:10.1002/ldr.3308

Mitran, T., Basak, N., Mani, P. K., Tamang, A., Singh, D. K., Biswas, S., et al. (2021). Improving crop productivity and soil quality through soil management practices in coastal saline agro-ecosystem. *J. Soil Sci. Plant Nutr.* 21, 3514–3529. doi:10.1007/s42729-021-00624-8

Mukherjee, A., and Lal, R. (2014). Comparison of soil quality index using three methods. *Plos One* 9 (8), e105981. doi:10.1371/journal.pone.0105981

Murtaza, G. (2013). *Economic aspects of growing rice and wheat crops on salt-affected soils in the Indus Basin of Pakistan*. Faisalabad, Pakistan: Institute of Soil and Environmental Sciences, University of Agriculture. (unpublished data).

Nagaz, K., Masmoudi, M. M., and Mechlia, N. Ben (2012). Impacts of irrigation regimes with saline water on carrot productivity and soil salinity. *J. Saudi Soc. Agric. Sci.* 11, 19–27. doi:10.1016/j.jssas.2011.06.001

Nayak, A. K., Mishra, V. K., Sharma, D. K., Jha, S. K., Singh, C. S., Shahabuddin, M., et al. (2013). Efficiency of phosphogypsum and mined gypsum in reclamation and productivity of rice–wheat cropping system in sodic soil. *Commun. Soil Sci. Plant Analysis* 44, 909–921. doi:10.1080/00103624.2012.747601

Nayak, A. K., Sharma, D. K., Mishra, V. K., Minhas, P. S., and Verma, C. L. (2008). Reclamation of saline-sodic soil under a rice–wheat system by horizontal surface flushing. *Soil Use Manag.* 24, 337–343. doi:10.1111/j.1475-2743.2008.00162.x

Neubauer, S. C., Piehler, M. F., Smyth, A. R., and Franklin, R. B. (2019). Saltwater intrusion modifies microbial community structure and decreases denitrification in tidal freshwater marshes. *Ecosystems* 22, 912–928. doi:10.1007/s10021-018-0312-7

Noctor, G., and Foyer, C. H. (1998). Ascorbate and glutathione: Keeping active oxygen under control. *Annu. Rev. Plant Physiol. Plant Mol. Biol.* 49, 249–279. doi:10.1146/annurev.arplant.49.1.249

Oades, J. M. (1988). The retention of organic matter in soils. *Biogeochemistry* 5, 35–70. doi:10.1007/BF02180317

Pal, D. K., Bhattacharyya, T., Ray, S. K., Chandran, P., Srivastava, P., Durge, S. L., et al. (2006). Significance of soil modifiers (Ca-zeolites and gypsum) in naturally degraded Vertisols of the Peninsular India in redefining the sodic soils. *Geoderma* 136, 210–228. doi:10.1016/j.geoderma.2006.03.020

Pitman, A. J., Narisma, G. T., Pielke, ., R. A., Sr, and Holbrook, N. J. (2004). Impact of land cover change on the climate of southwest Western Australia. *J. Geophys. Res.* 109, D18109. doi:10.1029/2003JD004347

Purakayastha, T. J., Pathak, H., Kumari, S., Biswas, S., Chakrabarty, B., Padaria, R. N., et al. (2019). Soil health card development for efficient soil management in Haryana, India. *Soil Tillage Res.* 191, 294–305. doi:10.1016/j.still.2018.12.024

Qadir, M., Quillérou, E., Nangia, V., Murtaza, G., Singh, M., Thomas, R. J., et al. (2014). Economics of salt-induced land degradation and restoration. *Nat. Resour. Forum* 38, 282–295. doi:10.1111/1477-8947.12054

Qadir, M., Schubert, S., Oster, J. D., Sposito, G., Minhas, P. S., Cheraghi, S. A. M., et al. (2018). High-magnesium waters and soils: Emerging environmental and food security constraints. *Sci. Total Environ.* 642, 1108–1117. doi:10.1016/j.scitotenv.2018.06.090

Quirk, J. P. (2001). The significance of the threshold and turbidity concentrations in relation to sodicity and microstructure. *Soil Res.* 39, 1185. doi:10.1071/SR00050

Rai, A. K., Basak, N., Soni, P. G., Kumar, S., Sundha, P., Narjary, B., et al. (2022). Bioenergy sorghum as balancing feedback loop for intensification of cropping system in salt-affected soils of the semi–arid region: Energetics, biomass quality and soil properties. *Eur. J. Agron.* 134, 126452. doi:10.1016/j.eja.2021.126452

Rai, A. K., Basak, N., and Sundha, P. (2021a). "Alternate amendments for reclamation of alkali soils," in *Managing salt-affected soil for sustainable agriculture*. Editors P. C. S. P. S. Minhas and R. K. Yadav (New Delhi, India: New Delhi: Indian Council of Agricultural Research ICAR), 332–345.

Rai, A. K., Basak, N., and Sundha, P. (2021b). "Chemistry of salt-affected soils," in *Managing salt-affected soils for sustainable agriculture*. Editors P. C. S. P. S. Minhas and R. K. Yadav (New Delhi: Indian Council of Agricultural Research ICAR).

Rai, A. K., Basak, N., and Sundha, P. (2021c). "Saline and sodic ecosystems in the changing world," in *Soil science: Fundamentals to recent advances*. Editors B. A. A. Rakshit, S. Singh, and P. Abhilash (Singapore: Springer), 175–190. doi:10.1007/978-981-16-0917-6_9

Raiesi, F., and Kabiri, V. (2016). Identification of soil quality indicators for assessing the effect of different tillage practices through a soil quality index in a semi-arid environment. *Ecol. Indic.* 71, 198–207. doi:10.1016/j.ecolind.2016.06.061

Ranatunga, K., Nation, E. R., and Barodien, G. (2010). Potential use of saline groundwater for irrigation in the Murray hydrogeological basin of Australia. *Environ. Model. Softw.* 25, 1188–1196. doi:10.1016/j.envsoft.2010.03.028

Rengasamy, P. (2016). Soil chemistry factors confounding crop salinity tolerance—A review. *Agronomy* 6, 53. doi:10.3390/agronomy6040053

Rengasamy, P. (2006). World salinization with emphasis on Australia. *J. Exp. Bot.* 57, 1017–1023. doi:10.1093/jxb/erj108

USSL (1954). "Diagnosis and improvement of saline and alkali soils,". Editor L. A. Richards (Washington, DC: USDA Handbook).

Rietz, D. N., and Haynes, R. J. (2003). Effects of irrigation-induced salinity and sodicity on soil microbial activity. *Soil Biol. Biochem.* 35, 845–854. doi:10.1016/S0038-0717(03)00125-1

Sadegh-Zadeh, F., Parichehreh, M., Jalili, B., and Bahmanyar, M. A. (2018). Rehabilitation of calcareous saline-sodic soil by means of biochars and acidified biochars. *Land Degrad. Dev.* 29, 3262–3271. doi:10.1002/ldr.3079

Sanyal, S. K., Poonia, S. R., and Baruah, T. C. (2012). *Soil colloids and ion exchange in soil*. New DelhiNew Delhi: Indian Society of Soil Science India.

Seleiman, M. F., Aslam, M. T., Alhammad, B. A., Hassan, M. U., Maqbool, R., Chattha, M. U., et al. (2022). Salinity stress in wheat: Effects, mechanisms and management strategies. *Phyt. J. Exp. Bot.* 91. doi:10.32604/phyton.2022.017365

Seleiman, M. F., Kheir, A. M. S., Al-Dhumri, S., Alghamdi, A. G., Omar, E.-S. H., Aboelsoud, H. M., et al. (2019). Exploring optimal tillage improved soil characteristics and productivity of wheat irrigated with different water qualities. *Agronomy* 9, 233. doi:10.3390/agronomy9050233

Seleiman, M. F., and Kheir, A. M. S. (2018). Saline soil properties, quality and productivity of wheat grown with bagasse ash and thiourea in different climatic zones. *Chemosphere* 193, 538–546. doi:10.1016/j.chemosphere.2017.11.053

Shahid, S. A., Zaman, M., and Heng, L. (2018). *Soil salinity: Historical perspectives and a world overview of the problem BT - guideline for salinity assessment, mitigation and adaptation using nuclear and related techniques*. Cham: Springer International Publishing.

Sharma, D. K., ThimmappaChinchmalatpure, K. A. R., Mandal, A. K., Yadav, R. K., Chaudhury, S. K., Kumar, S., et al. (2015). *Assessment of production and monetary losses from salt-affected soils in India*. Haryana, India: Technical Bulletin. Karnal.

Sharp, R. E., Hsiao, T. C., and Silk, W. K. (1990). Growth of the maize primary root at low water potentials 1: II. Role of growth and deposition of hexose and potassium in osmotic adjustment. *Plant Physiol.* 93, 1337–1346. doi:10.1104/pp.93.4.1337

Sheoran, P., Basak, N., Kumar, A., Yadav, R. K., Singh, R., Sharma, R., et al. (2021). Ameliorants and salt tolerant varieties improve rice-wheat production in soils undergoing sodification with alkali water irrigation in Indo–Gangetic Plains of India. *Agric. Water Manag.* 243, 106492. doi:10.1016/j.agwat.2020.106492

Sheoran, P., Sharma, R., Kumar, A., Singh, R. K., Barman, A., Prajapat, K., et al. (2022). Climate resilient integrated soil–crop management (CRISCM) for salt affected wheat agri–food production systems. *Sci. Total Environ.* 837, 155843. doi:10.1016/j.scitotenv.2022.155843

Shirale, A. O., Kharche, V. K., Wakode, R. R., Meena, B. P., Das, H., Gore, R. P., et al. (2018). Influence of gypsum and organic amendments on soil properties and crop productivity in degraded black soils of central India. *Commun. Soil Sci. Plant Analysis* 49, 2418–2428. doi:10.1080/00103624.2018.1510952

Singh, R., Yaduvanshi, N. P. S., Singh, K. N., Kumar, S., Mishra, V. K., Singh, Y. P., et al. (2014). Bio-chemical amelioration effects on physico-chemical dynamics of sodic soils under rice (*Oryza sativa*) – wheat (*Triticum aestivum*) cropping system. *Indian J. Agric. Sci.* 84, 349–355.

Singh, A., Bali, A., Kumar, A., Yadav, R. K., and Minhas, P. S. (2022). Foliar spraying of potassium nitrate, salicylic acid, and thio-urea effects on growth, physiological processes, and yield of sodicity-stressed paddy (Oryza sativa l.) with alkali water irrigation. *J. Plant Growth Regul.* 41, 1989–1998. doi:10.1007/s00344-022-10575-8

Singh, G. (2009). Salinity-related desertification and management strategies: Indian experience. *Land Degrad. Dev.* 20, 367–385. doi:10.1002/ldr.933

Singh, O. P. (1998). "Salinity and waterlogging problems in irrigation commands," in, eds. N. K. Tyagi and P. S. Minhas (Karnal (Haryana), India.: *Agricultural salinity management in India*. Centreal Soil Salinity Research Institute).

Singh, R. K., Singh, A., and Sharma, P. C. (2019). *Successful adaptations in salt affected agroecosystems of India*. Karnal (Haryana), India: ICAR-Central Soil Salinity Research Institute.

Singh, R., Yaduvanshi, N. P. S., Singh, K. N., Kumar, S., Mishra, V. K., Singh, Y. P., et al. (2014). Bio-chemical amelioration effects on physico-chemical dynamics of sodic soils under rice (Oryza sativa) –wheat (*Triticum aestivum*) cropping system. *Indian J. Agric. Sci.* 84, 349–355.

Singh, R. K., Singh, A., and Sharma, P. C. (2019). *Successful adaptations in salt affected agroecosystems of India*. Karnal (Haryana), India: ICAR-Central Soil Salinity Research Institute.

Sione, S. M. J., Wilson, M. G., Lado, M., and González, A. P. (2017). Evaluation of soil degradation produced by rice crop systems in a Vertisol, using a soil quality index. *Catena* 150, 79–86. doi:10.1016/j.catena.2016.11.011

Soni, P. G., Basak, N., Rai, A. K., Sundha, P., Narjary, B., Kumar, P., et al. (2021). Deficit saline water irrigation under reduced tillage and residue mulch improves soil health in sorghum-wheat cropping system in semi-arid region. *Sci. Rep.* 11, 1880. doi:10.1038/s41598-020-80364-4

Sundha, P., Basak, N., Rai, A. K., Yadav, R. K., Sharma, P. C., Sharma, D. K., et al. (2020). Can conjunctive use of gypsum, city waste composts and marginal quality water rehabilitate saline-sodic soils? *Soil Tillage Res.* 200, 104608. doi:10.1016/j.still.2020.104608

Sundha, P., Basak, N., Rai, A., Yadav, R., Sharma, D., and Sharma, P. (2017). N and P Release pattern in saline-sodic soil amended with gypsum and municipal solid waste compost. *J. Soil Salin. Water Qual.* 9, 145–155.

Sundha, P., Rai, A. K., Basak, N., Yadav, R. K., and Sharma, P. C. (2022). P solubility and release kinetics in the leachate of saline–sodic soil: Effect of reclamation strategies and water quality. *Soil Tillage Res.* 222, 105440. doi:10.1016/j.still.2022.105440

Swarup, A., and Yaduvanshi, N. P. S. (2000). Effects of integrated nutrient management on soil properties and yield of rice in alkali soils. *J. Indian Soc. Soil Sci.* 48, 279–282.

Taha, S. R., Seleiman, M. F., Alhammad, B. A., Alkahtani, J., Alwahibi, M. S., Mahdi, A. H. A., et al. (2021). Activated yeast extract enhances growth, anatomical structure, and productivity of lupinus termis l. plants under actual salinity conditions. *Agronomy* 11, 74. doi:10.3390/agronomy11010074

Taha, S. R., Seleiman, M. F., Alotaibi, M., Alhammad, B. A., Rady, M. M., Mahdi, H. A., et al. (2020). Exogenous potassium treatments elevate salt tolerance and performances of Glycine max L. by boosting antioxidant defense system under actual saline field conditions. *Agronomy* 10, 1741. doi:10.3390/agronomy10111741

Tripathi, S., Chakraborty, A., Chakrabarti, K., and Bandyopadhyay, B. K. (2007). Enzyme activities and microbial biomass in coastal soils of India. *Soil Biol. Biochem.* 39, 2840–2848. doi:10.1016/j.soilbio.2007.05.027

Tripathi, S., Kumari, S., Chakraborty, A., Gupta, A., Chakrabarti, K., Bandyapadhyay, B. K., et al. (2006). Microbial biomass and its activities in salt-affected coastal soils. *Biol. Fertil. Soils* 42, 273–277. doi:10.1007/s00374-005-0037-6

Tucker, B. M. (1985). The partitioning of exchangeable magnesium, calcium and sodium in relation to their effects on the dispersion of Australian clay subsoils. *Soil Res.* 23, 405. doi:10.1071/SR9850405

Vance, E. D., Brookes, P. C., and Jenkinson, D. S. (1987). Microbial biomass measurements in forest soils: The use of the chloroform fumigation-incubation method in strongly acid soils. *Soil Biol. Biochem.* 19, 697–702. doi:10.1016/0038-0717(87)90051-4

Vasu, D., Tiwary, P., Chandran, P., Singh, S. K., Ray, S. K., Butte, P., et al. (2018). A conceptual model of natural land degradation based on regressive pedogenesis in semiarid tropical environments. *Land Degrad. Dev.* 29, 2554–2567. doi:10.1002/ldr.3000

Visser, S., Keesstra, S., Maas, G., de Cleen, M., and Molenaar, C. (2019). Soil as a basis to create enabling conditions for transitions towards sustainable land management as a key to achieve the SDGs by 2030. *Sustainability* 11, 6792. doi:10.3390/su11236792

Vyshpolsky, F., Mukhamedjanov, K., Bekbaev, U., Ibatullin, S., Yuldashev, T., Noble, A. D., et al. (2010). Optimizing the rate and timing of phosphogypsum application to magnesium-affected soils for crop yield and water productivity enhancement. *Agric. Water Manag.* 97, 1277–1286. doi:10.1016/j.agwat.2010.02.020

Wang, Q., Lu, C., Li, H., He, J., Sarker, K. K., Rasaily, R. G., et al. (2014). The effects of no-tillage with subsoiling on soil properties and maize yield: 12-Year experiment on alkaline soils of northeast China. *Soil Tillage Res.* 137, 43–49. doi:10.1016/j.still.2013.11.006

Wasko, C., and Sharma, A. (2017). Global assessment of flood and storm extremes with increased temperatures. *Sci. Rep.* 7, 7945. doi:10.1038/s41598-017-08481-1

Wong, V. N. L., Greene, R. S. B., Dalal, R. C., and Murphy, B. W. (2010). Soil carbon dynamics in saline and sodic soils: A review. *Soil Use Manag.* 26, 2–11. doi:10.1111/j.1475-2743.2009.00251.x

Xu, X., Huang, G., Sun, C., Pereira, L. S., Ramos, T. B., Huang, Q., et al. (2013). Assessing the effects of water table depth on water use, soil salinity and wheat yield: Searching for a target depth for irrigated areas in the upper Yellow River basin. *Agric. Water Manag.* 125, 46–60. doi:10.1016/j.agwat.2013.04.004

Yaduvanshi, N. P. S., and Swarup, A. (2005). Effect of continuous use of sodic irrigation water with and without gypsum, farmyard manure, pressmud and fertilizer on soil properties and yields of rice and wheat in a long term experiment. *Nutr. Cycl. Agroecosyst.* 73, 111–118. doi:10.1007/s10705-005-3361-1

Yaduvanshi, N. P. S., and Sharma, D. R. (2008). Tillage and residual organic manures/chemical amendment effects on soil organic matter and yield of wheat under sodic water irrigation. *Soil Tillage Res.* 98, 11–16. doi:10.1016/j.still.2007.09.010

Yu, H., Yang, P., Lin, H., Ren, S., and He, X. (2014). Effects of sodic soil reclamation using flue gas desulphurization gypsum on soil pore characteristics, bulk density, and saturated hydraulic conductivity. *Soil Sci. Soc. Am. J.* 78, 1201–1213. doi:10.2136/sssaj2013.08.0352

Yu, P., Liu, S., Zhang, L., Li, Q., and Zhou, D. (2018). Selecting the minimum data set and quantitative soil quality indexing of alkaline soils under different land uses in northeastern China. *Sci. Total Environ.* 616, 564–571. doi:10.1016/j.scitotenv.2017.10.301

Yuan, C., Feng, S., Huo, Z., and Ji, Q. (2019). Effects of deficit irrigation with saline water on soil water-salt distribution and water use efficiency of maize for seed production in arid Northwest China. *Agric. Water Manag.* 212, 424–432. doi:10.1016/j.agwat.2018.09.019

Zain, D., Seleiman, M., Khan, I., Chattha, M. U., Ali, E. F., Alhammad, B., et al. (2021). Glycine-betaine induced salinity tolerance in maize by regulating the physiological attributes, antioxidant defense system and ionic homeostasis. *Not. Bot. Horti Agrobot. Cluj. Napoca.* 49, 12248. doi:10.15835/nbha49112248

Zhang, W., Zhao, Y., Wang, S., Li, Y., Zhuo, Y., Liu, J., et al. (2021). Soil salinity and sodicity changes after a one-time application of flue gas desulphurization gypsum to paddy fields. *Land Degrad. Dev.* 32, 4193–4202. doi:10.1002/ldr.4025

Zhao, Y.-G., Wang, S.-J., Liu, J., Zhuo, Y.-Q., Li, Y., Zhang, W.-C., et al. (2021). Fertility and biochemical activity in sodic soils 17 years after reclamation with flue gas desulfurization gypsum. *J. Integr. Agric.* 20, 3312–3322. doi:10.1016/S2095-3119(20)63446-3

frontiers | Frontiers in Environmental Science

TYPE Original Research
PUBLISHED 06 September 2022
DOI 10.3389/fenvs.2022.940349

Soil quality restoration and yield stabilization in acidic soils of northeastern Himalayas: Five years impact of green manuring and crop residue management

Meraj A. Ansari[1,2]*, Subhash Babu[3]*, Jairam Choudhary[2], Natesan Ravisankar[2] and Azad S. Panwar[2]

[1]ICAR Research Complex for NEH Region, Manipur Centre, Lamphelpat, India, [2]ICAR- Indian Institute of Farming System Research, Modipuram, Meerut, India, [3]Division of Agronomy, ICAR- Indian Agricultural Research Institute, New Delhi, India

Check for updates

OPEN ACCESS

EDITED BY
Thiru Selvan,
Tripura University, India

REVIEWED BY
Mengyang You,
Chinese Academy of Sciences (CAS), China
Sanjeev Kumar Chaudhary,
Regional Horticultural Research Sub Station Bhaderwah, India

*CORRESPONDENCE
Meraj A. Ansari,
merajiari@gmail.com
Subhash Babu,
subhiari@gmail.com

SPECIALTY SECTION
This article was submitted to Land Use Dynamics,
a section of the journal
Frontiers in Environmental Science

RECEIVED 10 May 2022
ACCEPTED 25 July 2022
PUBLISHED 06 September 2022

CITATION
Ansari MA, Babu S, Choudhary J, Ravisankar N and Panwar AS (2022), Soil quality restoration and yield stabilization in acidic soils of northeastern Himalayas: Five years impact of green manuring and crop residue management.
Front. Environ. Sci. 10:940349.
doi: 10.3389/fenvs.2022.940349

Soil quality restoration and crop productivity maximization are the global challenge to feed the galloping population. The task is much more daunting in a risk-prone, fragile, and low productive hilly region due to the depletion of supporting and regulating ecosystem services. A five-year long-term (2012–2017) field experiment was conducted to stabilize the yield and soil quality through legume green manuring and crop residue recycling in intensified cropping systems in the Eastern Himalayan region of India. Four treatments involving three green manures [green gram (*Vigna radiata*); cowpea (*Vigna unguiculata*); *Sesbania* (*Sesbania aculeata*) along with control (no-green manure)], three cropping systems [groundnut (*Arachis hypogaea*)—pea (*Pisum sativum*); maize (*Zea mays*)—pea, and maize + groundnut–pea] and two levels of residue management practices [residue removal and residue retention] were evaluated in three times replicated split–split plot design. Among the green manure options, *Sesbania* exerted a significant positive impact on the soil organic carbon (SOC) stock, available micro- (Fe, Mn, Zn, and Cu), and macronutrients (N, P and K) in surface (0–0.15 m) and subsurface (0.15–0.45 m) soils. The improvement in soil enzymatic activities (acid phosphatase, alkaline phosphatase, dehydrogenase, beta-glucosidase, and aryl sulfatase activity) ($p < 0.05$) in *Sesbania*-treated soil was +28.1% to +38.9% in surface and +18.3% to +27.3% in subsurface soils over non-green manure. *Sesbania*-treated soils also exhibited higher soil quality index (SQI) and stratification ratio (SR) of available soil nutrients and enzymes over non-green manured soils. Among the cropping systems, groundnut intercropped with maize followed by peas (MGP) with *in situ* residue retention increased ($p < 0.05$) the available soil macro- and micronutrients, SOC stock, soil enzymes, SR, and SQI in comparison to other cropping systems. *Sesbania* green manuring and residue retention improved the yield sustainability by +19% and +11% in the MGP system over non-green manuring and residue removal, respectively. Therefore, *Sesbania* green manuring in the MGP cropping system along with residue retention is recommended for stabilizing the

soil quality through enhancing supporting and regulating ecosystem services and maintaining long-term productivity in the fragile Eastern Himalayan ecosystem of India.

KEYWORDS

crop residue management, nutrient storage, soil enzymatic activities, stratification ratio, soil quality index, sustainability index

Introduction

Land degradation, irrational population growth, and urbanization are threatening the food security and ecosystem services of agroecology in many countries (Yadav et al., 2021). Factors associated with land degradation are mainly on account of over reliance of agri-food production systems on agrochemicals, accelerating the losses of regulating and supporting ecosystem services and deteriorating the environmental sustainability, which foster the challenges for achieving United Nations sustainable development goals (SDGs). Yield stagnation has become a major hurdle for food security and zero hunger (SDG–2). Similarly, reduction in soil ecosystem services and fertility is mainly caused by nutrient mining, soil erosion, imbalanced fertilization, poor nutrient recycling (residue recycling), lack of soil restoration practices, mono-cropping systems, etc. (Singh et al., 2021). It has become a challenge to address SDG–3 (good health and well-being) and SDG–15 (life on land). Eastern Himalayan Region of India, a habitat for ~50 million populace, is suffering from poor farm productivity due to the tremendous pressure of land degradation (Singh et al., 2021). Large-scale adoption of mono-cropping generally results in yield stagnation (Babu et al., 2020; Ansari et al., 2022a), low farm income, and poor resource utilization (Sarkar et al., 2018). Therefore, soil quality stabilization has emerged as a major challenge to sustain soil fertility without reduction in crop productivity (Babu et al., 2020). In the hilly ecosystem of the North Eastern Himalayan (NEH) region, where the annual rainfall is high, cultivation along the steep slopes often results in the loss of soil organic carbon (SOC), nutrients, and soil binding agents. This causes a decline in soil aggregation and structural degeneration leading to soil erosion and environmental degradation (Choudhury et al., 2022).

Aluminum-induced soil acidity, intermittent moisture stress and soil degradation in the upland, and reduction of soil productive capacity are some of the major notable causes of low crop production in the Indian Himalayas (Meena et al., 2018). In acid soils, the reduction of H^+ by organic anions to H_2O and CO_2 during the mineralization of organic manure increases the soil pH (Buragohain et al., 2017). Because of oxidation, Fe and Mn consume protons generated during the breakdown of organic matter and reduction of organic compounds may cause the soil pH to rise (Meena et al., 2018). Green manuring using legumes is easily decomposable and offers the extra benefit of fixing atmospheric N. Soil carbon storage, nutrient availability, biological aspects of soil, and yield stability could be possible only through sustainable management practices. Maintaining agronomic productivity and SOC levels is difficult in intensive cereal-based monoculture with minimal nutritional supplementation and poor soil management practices (Ansari et al., 2021; Ravisankar et al., 2022). In many parts of the world, the sequential cereal-based cropping systems with pulses in sole or inter-cropping considerably increase soil quality and productivity (Wander et al., 2019). Crop residue recycling and green manuring are used to improve and sustain the soil through long-term stabilization of SOC stock, soil biological properties including soil microbial biomass carbon (SMBC) and soil enzymatic activities, and soil chemical properties (macro- and micronutrients) (Yuan and Yue, 2012).

Therefore, the integration of fast-growing legumes with high nitrogen-fixing fecundity in cereal-based cropping systems as green manure has been considered a substitute and sustainable approach for restoring soil fertility and system productivity. Incorporation of crops at the active vegetative stage in soil could amplify the soil nutrient supplying capacity to the succeeding crops (Yadav et al., 2021). Nutrient pumping from deeper soil horizons to the furrow soil layer improves the crop yield after cultivation or incorporation of green manure crops (Stagnari et al., 2017). Green manures improved ecosystem services like soil physical properties, water holding capacity, which helps in reducing the soil moisture loss, improving soil organic matter and microbial activity, and also results in cooling effect (Melero et al., 2006). Green manuring also increased the quantity and quality of soil organic matter, thereby a suitable alternative to restore the quality of poor/degraded soils (Meena et al., 2018). The fast-growing, deep-rooted, high nitrogen-fixing, and low lignin-containing crops like *Sesbania* and cowpea are efficient in capturing and recycling nutrients (Das et al., 2021).

Hence, there is a need to explore the spatial and temporal intensification in existing cropping systems with fast growing legumes without compromising the land productivity and food security. Due to population pressure and land scarcity, small and marginal growers do not prefer the cultivation of green manures; hence, there is a need to sandwich short duration crops within the existing cropping systems. The probability of integrating green manures into the system becomes necessary when nutrient mining imbalances the soil quality stabilization due to inadequate management practices. The potential niche available in these cropping systems would be degraded due to the non-incorporation of legumes in the cereal rotation system (Amede and Taboge, 2007; Das et al., 2018). Therefore, biomass recycling becomes important to regulate and stabilize the soil quality with the improvement of soil biological (soil enzymatic activities), physical, and chemical properties (macro- and micronutrients).

Storage and stabilization of soil carbon, nutrients, and soil biological properties in subsurface soil are equally important as in surface soil. The presence of more than 60% of the maize vegetative roots in the 0.2–0.6 m soil layer indicated that subsurface soil interacts greatly with ground vegetation (Zhang et al., 2014). As a result, it is critical to understand the impact of long-term vegetation regeneration on changes in SOC stock and available macro- and micronutrients in the subsoil. In this respect, the stratification ratio (SR) is a very important criterion to evaluate the stabilization of soil properties in the subsoil. SR is the ratio of a surface layer property to a deeper layer property. Good soil quality is indicated by high SR values. The SR is extensively used as a farmland soil quality indicator (Peregrina et al., 2014).

However, systematic research on green manuring coupled with crop residue retention and its effect on ecosystem service restoration viz., SOC storage, soil enzymatic activities, and available nutrients in surface and subsurface soils, is limited especially in the regions where soil acidity is the major phenomenon in farming. We hypothesized that green manuring along with crop residue retention in groundnut intercropped with maize systems could improve the crop productivity as a result of improvement in ecosystem services. Further, studies on SRs are lacking, and evidence for using SRs to determine soil quality in the subsoil under manuring and residue recycling is needed. Therefore, to test the hypothesis, a field experiment was executed for five consecutive years (2012–2017) to assess the effect of legume green manuring and crop residue recycling in three different cropping systems involving combination cereal and legumes. We studied their effect on the vertical distribution of SOC storage, soil microbial enzymes, and nutrients and developed the soil quality stabilization indices like soil quality index (SQI) and SR. The findings of the study will help researchers and policy planners in the designing of ecosystem supportive policy for improving agronomic productivity while stabilizing soil quality in fragile hill ecosystem of the Eastern Himalayas.

Materials and methods

Description of the site, soil characteristics, and weather

The study site was in the Himalayan foothills of the Indian State of Manipur located in North Eastern Himalayan (NEH) region. Soils of these regions are mainly formed from sedimentary rocks, with parent materials from the Disang (Eocene) and Barail (Oligocene) groups of sandstone and shale (Ansari et al., 2022b). The sloping hill agriculture limits the cultivable land to 2.23 M ha (<12% of the total geographical area of Manipur) confined only to the intermontane valleys. Soil quality and crop productivity of hill ecosystem of NEH region are declining due to the burning of vegetation under jhum/shifting cultivation and it has become a challenge to fulfill the food requirement of the burgeoning population (Ansari et al., 2020). Rainfed paddy-based crop intensification in the lowlands was popularized to meet immediate food demand from limited farm lands. In the hill ecosystem, sole rainfed cereals (primarily rice and maize) are grown as mono-cropping throughout the rainy season (April to October), with only a minor periodic replenishment of plant nutrients from external organic or inorganic sources, typifying the region's subsistence farming (Ansari et al., 2021).

Field study was conducted with fixed plots for five continuous years (2012–2017) at Langol Hill Research Farm (24°49' N latitude, 93°55' E longitude, and 786 m above MSL altitude) of the ICAR (Indian Council of Agricultural Research) Research Complex for NEH Region, Manipur Centre, Imphal, India. The climate of the study site is subtropical humid with the average minimum and maximum temperatures during the 5 years' study period ranging between 14.8°C and 16.2°C and 26.8°C and 28.5°C, respectively. The mean monthly minimum and maximum relative humidities varied between 57.8–64% and 84.2–90.3%, respectively (Supplementary Figure S1). During the experimental period, the study area received an average annual rainfall of 1,545.5 mm. The soil of the experimental site was sandy clay loam in texture. Depth-wise information of different soil parameters (0–0.45 m) at the initiation of the study is given in Supplementary Table S1.

Treatment details and experimental design

The field experiment was conducted with three green manuring crops, viz., 1) GGM: green gram (Vigna radiata); 2) CGM: cowpea (*Vigna unguiculata*); 3) SGM: *Sesbania* (*Sesbania* aculeata); 4) control (NGM: no green manuring); and three cropping systems viz., 1) [groundnut (*Arachis hypogaea*)—pea (*Pisum sativum*) (GP); 2) maize (Zea mays)—pea (MP) and 3) maize + groundnut—pea (MGP)] involving two levels of residue management practices [residue removal (R-) and residue retention (R+)]. Green manuring, cropping systems, and residue management treatments were imposed as main plots, sub plots, and sub–sub plots, respectively, in a split–split plot design and replicated thrice. The dimensions of the main plots, sub plots, and sub–sub plots for each replication were 50.4 m × 12.6 m, 4.2 m × 12.6 m, and 4.2 m × 6.3 m, respectively.

Crop management

The main *Kharif* crops, i.e., maize (cv. HQPM–5) and groundnut (cv. ICGS–76), were manually sown as sole and intercrops during the month of June every year. Field for succeeding main crops (maize/groundnut) was prepared by two ploughings with power tiller followed by one planking. In residue retention plots, all the above-ground crop residues were retained in the field. For this, maize, groundnut, and pea crops were harvested, and above-ground residues were retained in the field after collecting their economic part. In the residue removal plots, residues of maize, groundnut, and pea were removed completely. Before sowing of the main crop in each of three cropping systems, three green manuring crops were sown in the respective plots by broadcasting after single ploughing and planking during the first week of April (65–70 days before sowing of main crops) with the pre-monsoon showers. Green manuring crops were chopped and incorporated 60 days after sowing and before field preparation for succeeding main crops in the respective plots. To compare the effect of green manuring on cropping system performance, and soil properties (soil nutrients and enzymes), one treatment without any green manuring crop was also maintained.

A spacing (row to row and plant to plant) of 60 cm × 30 cm for maize and 30 cm × 10 cm for groundnut was adopted under sole cropping. In maize + groundnut intercropping, one row of groundnut was sown between two rows of maize (60 cm) with 10 cm plant to plant distance. Maize and groundnut were harvested during the last week of October till the first week of November. During the winter season, pea "Rachna" was sown under zero tillage in all the plots during the 2nd week of November and harvested during the 3rd week of February. The recommended dose of fertilizers (RDF) [20–40–40 kg N—P_2O_5—K_2O ha^{-1}] was applied as a basal dose in groundnut. In sole cropping of maize and intercropping (maize + groundnut), the RDF was applied at 100–60–40 kg N–P_2O_5–K_2O ha^{-1}. In maize (sole and intercropping), 50% nitrogen and full dose of phosphorus and potassic fertilizers were applied as basal, and the remaining nitrogen (50%) was top-dressed in two equal splits at 30 and 55 days after sowing. The source of fertilizer N, P_2O_5, and K_2O was urea (46% N), single super phosphate (16% P_2O_5), and muriate of potash (60% K_2O), respectively. The experiment was conducted under rainfed conditions.

Soil sampling and analysis

Initial soil properties of experimental field were assessed before the commencement of the experiment (Supplementary Table S1). After completion of the experiment, soil samples were taken from three different depths (L_1: 0–0.15 m, L_2: 0.15–0.30 m, and L_3: 0.30–0.45 m) using a bucket augur during the post-monsoon period (March 2017) from each plot. Three random spots in each plot were sampled, which were then composited to provide a representative soil sample. For the SMBC determination, fresh soil from each sample was kept at 4°C. For examination, the remaining soils were air-dried, crushed, and passed through a 2.0 mm mesh sieve. After oven drying at 105 ± 1°C, soil bulk density (ρb) was determined *in situ* using the core method (5.15 cm height and 4.7 cm diameter) (Blake and Hartge, 1986). Soil pH was determined using a 1:2.5 soil: water suspension (pH meter; Eutech pH 700-Eutech Instruments, Singapore). The available N (Av. N) was determined using the $KMnO_4$ oxidation method (Subbiah and Asija, 1956), and the SOC content was determined using the $K_2Cr_2O_7$ wet oxidation method (Walkley and Black, 1934). The available P (Av. P) was extracted using the Bray-1 reagent. The available K (Av. K) in soil extracted with neutral normal NH_4OAc solution was determined using a flame photometer (ESICO-1382, India). The chloroform fumigation extraction method (Vance et al., 1987) was used to determine the SMBC. Modified universal buffer (MUB, pH 6.5 and 11) and p-nitrophenyl phosphate disodium salt (0.025 M) as a substrate were used to estimate the acid (ACP) and alkaline phosphatase (ALK) activity (Tabatabai and Bremmer, 1969). The activity of the β-glucosidase enzyme (GLU) was determined by using the Eivazi and Tabatabai's (1988) method. Arylsulfatase activity (ARY) was measured with sodium acetate buffer and p-nitrophenyl sulfate (0.025 M) as a substrate (Tabatabai and Bremner, 1970). Soil dehydrogenase activity (DHY) was estimated by the method of Casida et al. (1964). A UV-VIS spectrophotometer (Spectroquant ® Prove 300, Germany) was used to measure the soil enzymatic activities. Lindsay and Norvell (1978) approach was used to estimate the available micronutrients (Fe, Mn, Zn, Cu) in soil. In a 10 g soil sample, 20 ml of 0.005 mol L^{-1} DTPA (diethylenetriamine pentaacetic acid) + 0.1 mol L^{-1} TEA (triethanolamine) + 0.01 mol L^{-1} $CaCl_2$ (at pH 7.30) were added (Sarkar et al., 2018; Choudhury et al., 2021). The solution was centrifuged and filtered through Whatman No. 42 filter paper after being shaken for 2 hours at room temperature. DTPA-extractable micronutrient (available Fe, Mn, Zn, and Cu) concentrations were then determined using an atomic absorption spectrophotometer (AAS) on clear aliquots (Model Perkin Elmer A Analyst 200). For the determination of the total micro- and macro (P, K)-nutrients in plant tissues, 1 g of plant samples was ashed in a muffle furnace at 550°C for 3 h and subsequently extracted with 2 N HCl. The extract, after suitable dilution, was analyzed for Fe, Mn, Zn, and Cu using AAS; P (Vanadomolybdate yellow color method; Jackson, 1973) and K (Flame photometer). The total nitrogen concentration of plant tissues was determined by micro-Kjeldahl digestion and distillation (Nelson and Sommers, 1973). The total macro- (N, P, K) and micro (Fe, Mn, Zn, Cu)-nutrients added through green manuring/crop residues (maize/groundnut/pea) during 5 years

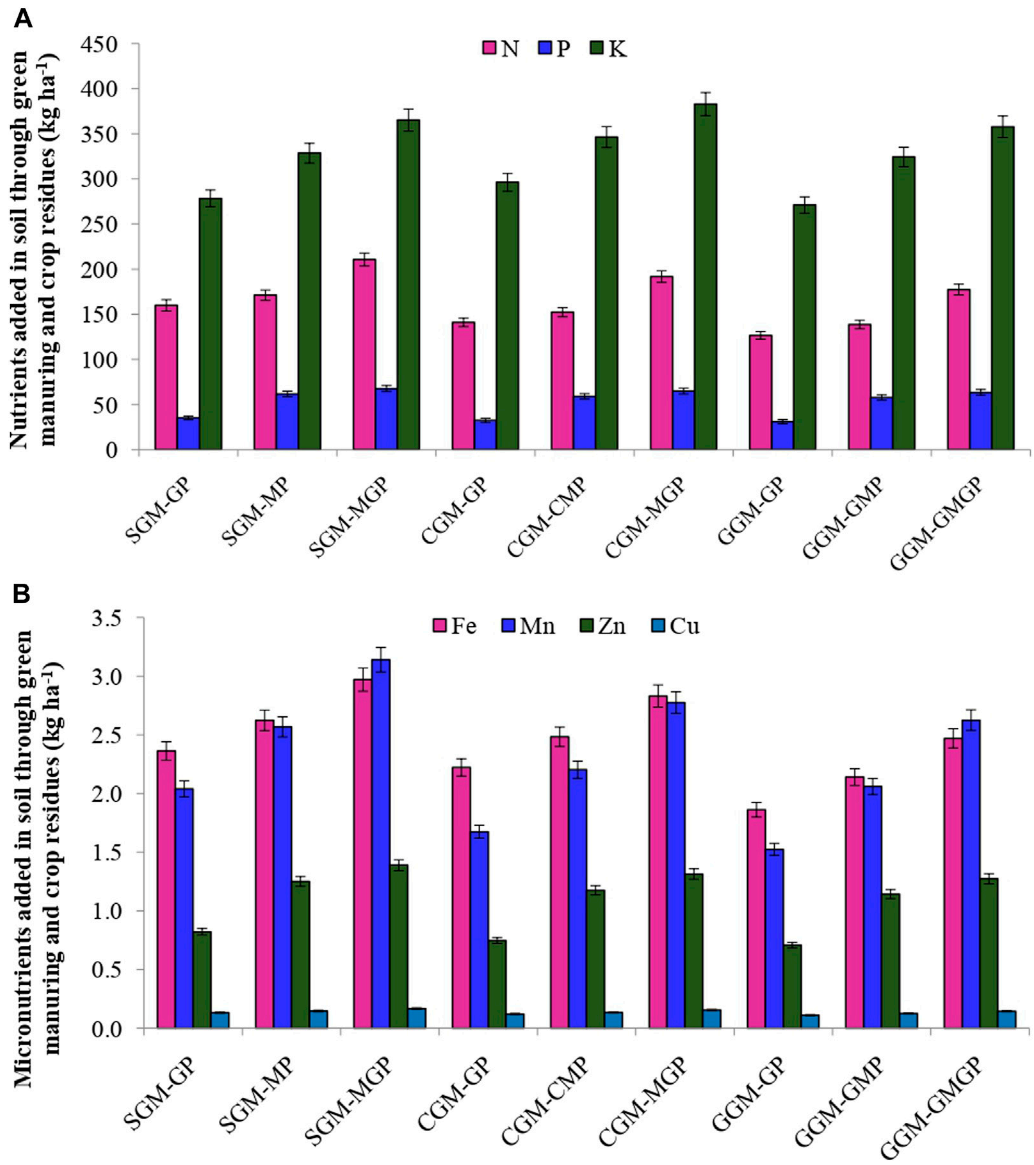

FIGURE 1
Nutrient input **(A)** macronutrients (N, P, K: Available nitrogen, phosphorus, and potassium, respectively), **(B)** micronutrients (Fe, Mn, Zn, Cu; DTPA-extractable soil micronutrients iron, manganese, zinc, and copper, years of experimentation. GGm: greengram green manuring, CGM: cowpea green manuring, SGM: sesbania green manuring, GP: groundnut–pea, MP: maize + groundnut–pea. Vertical bar (both way) represents the standard error of mean ($p<0.05$).

(2012–2017) of the respective treatments are presented in Figure.1.

Soil quality index

The SQI was calculated for each farming system using the approach given by Banerjee et al. (2015). To summarize, all of the soil indicators studied (physical, chemical, and biological) were treated with principal component analysis (PCA) to reduce dimensionality while maintaining the most variation in the dataset. The largest variability was explained by the first PC, and the remainder of the residual variability was explained by the remaining PCs. Based on factor loading values, the essential underlying variables for each PC were discovered. Under each PC, the variables with absolute values less than 20% of the maximum weighted factor were kept. The correlation matrix was used to verify the inter-linkage of the extracted variables under respective PCs, and the most prominent variables from each PC were chosen for SQI development. After homothetic translation of each value within a mutual scale ranging from 0.1 to 1.0, the weighted addition for the final computation of SQI for each cropping system was computed individually.

Stratification ratio

SR is the value of a soil parameter at the overlying layer divided by the value at the underneath layer (L_1/L_2 and L_1/L_3) (Qua et al., 2020). The SR allows comparing the wide range of diversity of soils on the same assessment scale through internal normalization procedure by accounting for inherent soil differences. The SR of soil nutrients and soil enzymes are efficient indicators of soil quality, and its increase is related to the rate and amount of soil improvement through their addition (Franzluebbers, 2002).

Computation of sustainability index

Sustainability yield index was computed by using Eq. 1

$$Sustainability\ yield\ index\ (SYI) = \frac{(y - \sigma)}{ymax} \quad (1)$$

where y, σ, and ymax represent the average yield of a treatment over the years, standard deviation, and observed maximum yield over the years.

Data analysis

Using the PROC GLM procedure in SAS version 9.2, the data generated from soil analysis and measuring grain yield were processed for analysis of variance (ANOVA) in a split–split plot design to test the statistical significance among the treatments (green manuring, cropping system, and residue management). LSD of the mean was computed based on Duncan's multiple range test (DMRT) ($p < 0.05$) by using SAS 9.2 (SAS Institute, Cary, North Carolina, United States). In DMRT, the values in a column that are followed by a similar letter in lowercase are not significantly different at the $p < 0.05$ level of significance. Principal component analysis (PCA) was used to reduce dimensionality while maintaining the most variation in the examined dataset by analyzing data on soil quality indicators (SOC stock, macro- and micro-nutrients, and soil enzymes) from various treatments. Variables with factor loadings and PCs with multiple eigen values were judged to be variables that best described system attributes. Therefore, PCs with eigen values more than 1.0 were considered for further analysis as these PCs were considered more informative than the others (Kaiser, 1960). The first PC explained maximum variability, and the rest of the PCs explained the remaining lion share for the residual variability (Supplementary Table S2). The NCSS 2020 programme was used to create the 3D surface plots.

Results

Soil enzymatic activities

Green manuring had a significant positive effect on soil enzymatic activities. Maximum and significant improvement of the enzymatic activities was recorded under SGM compared to that in other green manures and NGM treatment. SGM harbored 28.3%–38.9%, 16.4%–27.5%, and 18.2%–27.9% more enzymatic activities in 0–0.15 m, 0.15–0.30 m, and 0.30–0.45 m soil layers, respectively, as compared to NGM treatment (Table 1). As shown in Table 1, soil enzymes acid phosphatase (ACP), alkaline phosphatase (ALK), dehydrogenase (DHY), beta-glucosidase (GLU), and arylsulfatase (ARY) activities were improved by 16.0%–28.3%, 16.0%–28.3%, 20.6%–31.3%, 12.5%–28.1%, and 19.7%–38.9%, respectively, in 0–0.15 m soil layer over NGM treatment. Higher enzymatic activities were recorded in the topsoil layer (0–0.15 m) than in subsurface soil (0.15–0.45 m). The relative increase in the topsoil layer being almost twice as compared to the subsurface soil layer (Table 1).

MGP cropping system significantly improved the soil enzymes acid phosphatase, alkaline phosphatase, dehydrogenase, beta-glucosidase, and arylsulfatase activity by 13.5%–21.8%, 9.1%–13.6%, 12.9%–14.6%, 2.6%–14.7%, and 1–7.8%, respectively, in surface (0–0.15 m) soil layer compared to GP and MP systems. On an average, the highest soil enzymes in the subsurface (0.15–0.45 m) soil layer were also recorded in the MGP (ACP: 21.0 μ mol pNP g^{-1} of soil h^{-1}, ALK: 21.0 μg g^{-1} of soil h^{-1}, DHY: 32.7 μg TPF g^{-1} of soil h^{-1}, GLU: 3.0 μg g^{-1} of soil h^{-1} and ARY: 67.7 μg pNP g^{-1} of soil h^{-1}) cropping system. The enzymatic activities decreased in the subsurface soil layer, as compared to the surface soil layer (Table 1).

The residue retention-mediated soil enzymatic activities (ACP, ALK, DHY, GLU, and ARY) were significantly ($p <$ 0.05) higher in the surface (12.6%–31.5%) and subsurface soils (6.1%–16.8%) (Table 1).

Nutrient storage

The highest macronutrient (available N, P, and K) storage was recorded in SGM in the surface layer as compared to other green manuring treatments. The similar trend was also found in the subsurface layer under SGM over the remaining green manures. Green manuring (*Sesbania*, cowpea, and greengram) increased the available N, P, and K significantly by 16.6%–29.9%, 15.4%–31.5%, and 16.3%–26.0%, respectively, in 0–0.15 m soil layer as compared to NGM. Similarly, macronutrients (available

TABLE 1 Effect of green manuring, cropping systems, and residue management on soil enzymes in different soil depths after 5 years of experimentation.

Treatment	0–0.15 m					0.15–0.30 m					0.30–0.45 m				
	ACP	ALK	DHY	GLU	ARY	ACP	ALK	DHY	GLU	ARY	ACP	ALK	DHY	GLU	ARY
Green manuring (GM)															
NGM	21.9	21.9	35.0	3.2	88.2	19.5	19.5	30.8	2.8	66.6	14.9	14.9	23.6	2.2	48.7
GGM	25.4	25.4	42.2	3.6	105.6	21.1	21.1	35.4	3.1	74.4	16.4	16.4	27.1	2.3	55.8
CGM	27.3	27.3	44.0	4.0	116.1	22.0	22.0	36.7	3.3	80.1	17.3	17.4	27.5	2.5	59.9
SGM	28.1	28.1	45.9	4.1	122.5	22.7	22.7	38.3	3.4	84.9	18.1	18.0	29.0	2.6	62.3
LSD ($p < 0.05$)	4.3	4.0	4.2	0.5	6.7	2.1	1.8	3.4	0.4	3.5	2.1	2.2	2.6	0.2	3.5
Cropping system (CS)															
GP	25.1	25.3	40.2	3.8	110.0	21.1	21.1	34.3	3.2	78.3	16.1	16.2	26.0	2.5	57.7
MP	23.4	24.3	39.6	3.4	103.1	19.4	19.4	34.6	2.9	73.6	15.4	15.4	26.2	2.2	54.7
MGP	28.5	27.6	45.4	3.9	111.1	23.4	23.5	37.0	3.4	77.6	18.5	18.5	28.3	2.6	57.7
LSD ($p < 0.05$)	3.1	2.5	4.0	0.4	4.8	1.5	2.0	2.3	0.3	4.0	2.2	2.0	2.0	0.2	3.1
Residue management (RM)															
R-	23.4	22.2	38.7	3.4	101.7	19.7	19.7	33.7	3.0	73.9	15.4	15.4	25.7	2.3	55.2
R+	28.0	29.2	44.9	4.0	114.5	23.0	23.0	36.9	3.4	79.1	18.0	18.0	28.0	2.5	58.1
LSD ($p < 0.05$)	1.0	1.1	1.5	0.2	2.7	1.3	1.2	2.5	0.1	1.9	1.1	1.3	1.1	0.1	2.4
Interaction															
GM*CS	ns	ns	ns	ns	ns	ns	ns	ns	0.6	ns	ns	ns	ns	ns	ns
GM* RM	ns	ns	ns	0.4	5.3	ns	ns	ns	0.2	3.8	ns	ns	ns	0.3	4.8
CS* RM	ns	ns	ns	0.8	ns	ns	ns	ns	0.8	11.7	ns	ns	ns	0.6	8.5
GM*CS* RM	ns	ns	ns	ns	17.6	ns	ns	ns	0.7	16.5	ns	ns	ns	0.9	ns

NGM, no green manuring; GGM, greengram green manuring; CGM, cowpea green manuring; SGM, *sesbania* green manuring; GP, groundnut–pea; MP, maize–pea; MGP, maize + groundnut-pea; R-, residue removal; R+, residue retention; ns, non-significant ($p > 0.05$). ACP, Acid phosphatase (μ mol pNP g^{-1} of soil h^{-1}); ALK, alkaline phosphatase (μg g^{-1} of soil h^{-1}); DHY, dehydrogenase (μg TPF g^{-1} of soil h^{-1}); GLU, beta glucosidase (μg g^{-1} of soil h^{-1}); ARY, arylsulfatase activity (μg pNP g^{-1} of soil h^{-1}).

N, P, and K) also increased significantly by 12.4%–22.7%, 9.9%–24.8%, and 11.1%–19.4% in 0.15–0.30 m soil layer as well as by 11.3%–21.5%, 10.4%–23.9%, and 13.6%–20.8% in 0.30–0.45 m soil layer compared to non-green manuring (Table 2). SGM highly improved the micronutrient (available Fe, Mn, Zn, and Cu) storage in the surface soil layer (0–0.15 m) as compared to the other green manuring tested. These changes manifested the highest in the top soil layers as compared to the subsurface soil layers. The available Fe, Mn, Zn, and Cu storage increased by 11.8%–27.1%, 8.45–25.3, 21.1–36.8, and 9.5%–28.8%, respectively, in 0–0.15 m soil layer over the NGM treatment. However, it decreased in the subsequent soil layers (0.15–0.30 and 0.30–0.45 m) compared to the topsoil layer (0–0.15 m) (Table 3).

Averaged over 5 years, the maize + groundnut–pea and groundnut–pea cropping system increased the available N by 9.4%–9.6% and 5.7%–5.9% in 0–0.15 and 0.15–0.30 m soil layers, respectively, over the maize–pea cropping system, while the non-significant difference was recorded in 0.30–0.45 m soil layer. There was no significant improvement of available P and K in all three soil layers (Table 2). The available Fe concentration increased significantly more in the surface (0–0.15 m) soil layer in maize + groundnut–pea and maize–pea (by 8.7% and 7.1%, respectively) than groundnut–pea cropping system, while the maize + groundnut–pea system significantly influenced the available Fe concentration only in 0.15–0.30 m soil layers (by 3.8%) over groundnut–pea system. The remaining micronutrients (available Mn, Zn, and Cu) did not significantly differ due to the cropping systems in the surface and subsurface (0.15–0.45 m) soil layers (Table 3).

Residue retention resulted in significantly higher ($p < 0.05$) available N, P, and K concentrations in surface soil (0–0.15 m) by 9.4%, 13.9%, and 8.3%, respectively, over residue removal. Notably, residue retention had also higher ($p < 0.05$) available N, P, and K concentrations in subsurface soil (0.15–0.45 m: 6.5%, 9.7%, 5.4%, respectively) as compared to residue removal after 5 years of experimentation. Similarly, residue retention had significantly higher micronutrient concentration (available Fe, Mn, Zn, and Cu) over residue removal and increased by 10.1%, 22.1%, 11.4%, and 13.0% in surface soils and by 6.4%, 9.5%, 10.9%, and 5.1% in subsurface soils. The surface soil (0–0.15 m) had significantly higher available micronutrient concentration than the subsoil layers, and it decreased linearly with an increase in soil depth (Table 3).

TABLE 2 Effect of green manuring, cropping systems, and residue management on the nutrient storage of available N, P, and K in different soil depths after 5 years of experimentation.

Treatment	0–0.15 m			0.15–0.30 m			0.30–0.45 m		
	N	P	K	N	P	K	N	P	K
Green manuring (GM)									
NGM	222.7	14.3	93.3	210.8	12.1	83.8	177.6	9.6	69.1
GGM	259.6	16.5	108.5	236.9	13.3	93.1	197.6	10.6	78.5
CGM	287.7	18.2	116.2	257.4	14.7	99.7	215.7	11.9	83.0
SGM	289.3	18.8	117.6	258.7	15.1	100.1	215.4	11.9	83.5
LSD (p < 0.05)	18.5	1.4	10.4	17.6	1.3	9.9	17.4	1.7	9.6
Cropping system (CS)									
GP	272.4	16.4	104.9	245.2	13.4	90.3	203.6	10.7	75.3
MP	249.1	17.0	110.3	232.0	14.0	95.5	197.2	11.1	79.5
MGP	273.0	17.4	111.5	245.7	14.0	96.7	203.9	11.1	80.7
LSD (p < 0.05)	13.2	ns	ns	12.2	ns	ns	ns	ns	ns
Residue management (RM)									
R-	253.0	15.8	104.5	233.9	13.1	91.4	194.8	10.5	76.7
R+	276.7	18.0	113.2	248.0	14.4	97.0	208.3	11.5	80.3
LSD (p < 0.05)	7.7	0.5	2.4	6.5	0.2	2.3	6.5	0.3	2.7
Interaction (p < 0.05)									
GM*CS	ns	ns	ns	ns	ns	ns	ns	ns	ns
GM* RM	15.4	ns	ns	13.1	ns	ns	13.1	ns	ns
CS* RM	ns	ns	ns	ns	ns	ns	ns	ns	ns
GM*CS* RM	43.8	ns	ns	ns	ns	ns	ns	ns	ns

NGM, no green manuring; GGM, greengram green manuring; CGM, cowpea green manuring; SGM, *sesbania* green manuring; GP, groundnut–pea; MP, maize–pea; MGP, maize + groundnut-pea; R-, residue removal; R+, residue retention; ns, non-significant (p > 0.05). N, available nitrogen (kg ha^{-1}); P, available phosphorus (kg ha^{-1}); K, available potassium (kg ha^{-1}).

SOC stock

The highest SOC stock was recorded in SGM (18.7, 14.6, and 10.9 Mg ha^{-1}, respectively, in L_1, L_2, and L_3 layers) compared to the remaining green manuring practices. Green manuring compared with no green manuring significantly increased the SOC stock by 15%–33.6%, 13.3%–29.2%, and 8.4%–14.7%, respectively, in L_1, L_2, and L_3 soil layers (Table 3). MGP and MP increased the SOC stock by 5.4%–7.5%, 3.8%–4.7%, and 2.9%–3.8% in the L_1, L_2, and L_3 soil layers over the GP cropping system, respectively. SOC stock was increased by 18.4% to 12.1% in surface and subsurface soils, respectively, due to residue retention over residue removal (Table 3).

Stratification ratio

Among the green manuring treatments, the highest SR1 was recorded in *Sesbania* followed by cowpea and greengram. Notably, the SR2 of available N, P, and K between the surface (L_1) to bottom-most layer (L_3) was higher in *Sesbania* followed by cowpea and greengram (Figure 2). The highest SR of micronutrients (SR1: 1.14–1.24) and SR2 (1.28–1.67) was recorded in *Sesbania* green manuring followed by cowpea > green gram green manuring treatment (Figure 2). Green manuring (*Sesbania* > cowpea > greengram) increased (p < 0.05) the SR1 and SR2 on an average by 8.71>8.14>8.71% and 6.15>7.44>8.32%, respectively, over the NGM treatment. However, across the green manuring treatments (*Sesbania* > cowpea > greengram), ARY was highly (SR1: 1.42 to 1.45, SR2: 1.91–1.99) stratified enzyme than the ALK > ACP > DHY > GLU (Figure 2). SR in the cropping system did not differ significantly; however, higher SR1 and SR2 of available macro- and micronutrients as well as soil enzymes were recorded in the MGP cropping system (Supplementary Figure S2).

The SR was significantly (p < 0.05) influenced by residue retention. The estimated SR1 of available N (+3.1%), P (+3.7%), and K (+2.0%) were higher (p < 0.05) in residue retention than in the residue removal treatment. Similarly, the estimated SR2 of available N, P, and K were higher (1.33, 1.59, and 1.41) in residue retention as compared to residue removal (1.31, 1.53, and 1.37), respectively (Figure 3). The SR1 estimated for micronutrients (available Fe, Mn, Zn, and Cu) were higher (+3.6% to +6.2%) in residue retention than in the residue removal. SR2 of available micronutrients increased most for the Mn (+8.7%) followed by Cu > Fe > Zn in residue retention than in the residue removal

TABLE 3 Effect of green manuring, cropping systems, and residue management on micronutrients and soil organic C storage in different soil depths after 5 years of experimentation.

Treatment	0–0.15 m				0.15–0.30 m				0.30–0.45 m				SOC stock		
	Fe	Mn	Zn	Cu	Fe	Mn	Zn	Cu	Fe	Mn	Zn	Cu	0-0.15 m	0.15-0.30 m	0.30-0.45 m
Green manuring (GM)															
NGM	88.9	21.3	3.8	2.1	113.1	84.8	18.5	3.5	74.1	13.6	2.6	1.8	14.0	11.3	9.5
GGM	99.4	23.1	4.6	2.3	119.8	93.1	19.1	4.0	79.5	14.4	3.1	1.9	16.1	12.8	10.3
CGM	108.3	25.2	5.0	2.6	120.7	99.7	20.7	4.3	86.0	15.6	3.4	2.1	17.7	13.9	11.0
SGM	113.0	26.7	5.2	2.7	122.4	100.1	21.7	4.5	86.5	16.2	3.5	2.2	18.7	14.6	10.9
LSD (p < 0.05)	4.2	3.6	0.5	0.3	4.5	9.6	2.9	0.5	6.4	3.0	0.5	0.2	1.16	0.49	0.45
Cropping system (CS)															
GP	97.1	22.9	4.4	2.4	116.9	90.5	18.9	3.8	78.3	14.4	2.9	1.9	15.9	12.8	10.2
MP	104.5	24.6	4.8	2.4	118.8	95.8	20.6	4.2	82.5	15.1	3.2	2.0	16.8	13.3	10.6
MGP	105.5	24.8	4.8	2.5	121.3	97.0	20.7	4.2	83.7	15.2	3.3	2.1	17.1	13.4	10.5
LSD (p < 0.05)	4.3	ns	ns	ns	3.3	ns	ns	ns	ns	ns	ns	ns	0.59	0.37	0.24
Residue management (RM)															
R-	97.5	21.7	4.4	2.3	114.3	91.6	18.6	4.0	79.7	14.0	3.0	1.9	15.2	12.4	9.8
R+	107.3	26.5	4.9	2.6	123.7	97.2	21.4	4.2	83.3	15.8	3.2	2.0	18.0	13.9	11.0
LSD (p < 0.05)	2.7	0.8	0.1	0.1	2.5	2.7	1.3	0.1	3.2	1.0	0.1	0.1	0.45	0.32	0.27
Interaction															
GM*CS	ns	ns	ns	ns	ns	ns	ns	ns	ns	ns	ns	ns	ns	ns	ns
GM* RM	ns	ns	0.2	ns	ns	ns	0.2	ns	ns	ns	ns	ns	ns	ns	0.55
CS* RM	ns	ns	ns	ns	ns	ns	ns	ns	ns	ns	ns	ns	ns	ns	2.10
GM*CS* RM	ns	ns	ns	ns	ns	ns	ns	ns	ns	ns	ns	ns	ns	ns	ns

NGM, no green manuring; GGM, greengram green manuring; CGM, cowpea green manuring; SGM, *sesbania* green manuring; GP, groundnut–pea; MP, maize–pea; MGP, maize + groundnut-pea; R-, residue removal; R+, residue retention; ns, non-significant (p < 0.05). Fe, Mn, Zn, Cu; DTPA- extractable soil micronutrients (ppm) iron, manganese, zinc, and copper, respectively; SOC, stock, soil organic carbon stock (Mg ha^{-1}).

treatment. Similarly, SR1 and SR2 of soil enzymes (ACP, ALK, DHY, GLU, and ARY) increased by 2.2%–6.1% and 1.8%–8.2%, respectively, in residue retention than in the residue removal treatment (Figure 3).

Soil quality index

For deriving SQI, available macronutrients (N, P, and K), micronutrients (Fe, Mn, Zn, and Cu), and soil enzyme (ACP, ALK, DHY, GLU, and ARY) datasets were subjected to PCA analysis. In Figure 4 and Supplementary Table S2, the first and second PCs explained 76.48% and 8.82% of variability with eigen values of 11.47 and 1.32, respectively. Therefore, the eigen values of two PCs were ≥1, which explained 85.30% of the cumulative variability. The highly weighted factors were explained (>0.8) with all the variables in the first principal component (PC-1) except GLU, which has less than 0.8 factor loading (0.714). SOC stock has shown a strong positive correlation with other soil quality indicators and it was retained in PC-1 as minimum dataset (MDS). In the PC-2, GLU (0.539) was selected with the highest loading factor. Thus, SOC and GLU were selected as MDS for the calculation of SQI. The maximum improvement of the SQI was recorded under SGM in surface (SQIs: 0.547) and subsurface (SQIss: 0.525) followed by CGM and GGM as compared to no green manuring treatment (SQIs: 0.403 and SQIss: 0.422). The maximum SQI in surface (SQIs: 0.521) and subsurface (SQIss: 0.500) soil was recorded in the MGP cropping system as compared to MP and GP systems. Similarly, residue retention significantly increased the SQI by 15.7% and 8.1%, respectively, in surface and subsurface soil over residue removal treatment (Figure 5).

The surface plot analysis revealed a strong positive relationship between SQIs and SQIss with maize grain yield in sole cropping (r =0.9612** and 0.9902**, p < 0.01) as well as intercropping (r =0.8673 and 0.8461, p < 0.01); pod yield of groundnut in sole cropping (r =0.8991** and 0.8893**, p < 0.01) as well as intercropping (r =0.8797**, p < 0.01) (Figure 6). Grain yield of pea was also strongly correlated with SQIs and SQIss (r =0.8739** and 0.8732, p < 0.01). The favorable relationship between soil parameters and grain/pod yield has a significant impact on maize/groundnut/pea system productivity.

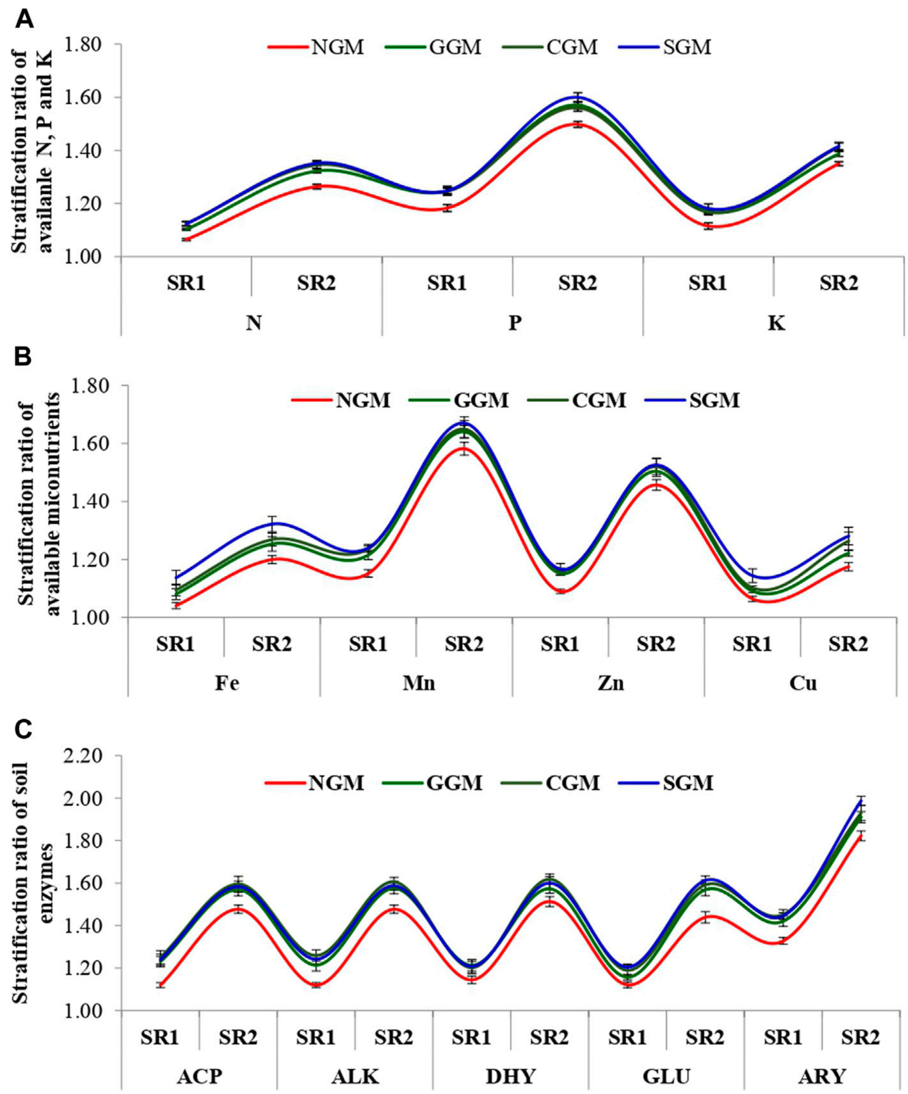

FIGURE 2
Stratification rations of **(A)** available N, P, and K **(B)**. Micronutrients Fe, Mn, Zn, and Cu **(C)**. Soil enzymes as influenced by green manuring after five years of experimentation. NGM: No green manuring, GGM: greengram green manuring, CGM: cowpea green manuring, SGM: sesbania green manuring, R-: residue stratification ratio (ratio of 0.15–0.30 and 0.30–0.45 m soil depth) ACP: Acid phosphates (ug TPF g^{-1} of soil h^{-1}), ALK: Alkaline phosphates (ug g^{-1} of soil h^{-1}), DHY: Dehydrogenase (ug TPF g^{-1} of soil h^{-1}), GLU: beta glucosidase (ug g^{-1} of soil h^{-1}), ARY: arylsulfatase activity (ug pNp g^{-1} of soil h^{-1}) vertical bar (both way) represents the standard error of mean ($p < 0.05$).

Sustainability yield index

Among the green manuring treatments, SYI was significantly ($p < 0.05$) higher in *Sesbania* green manuring (0.80) followed by cowpea (0.74) and green gram green manuring (0.73) as compared to non-green manuring (0.67) treatment. Similarly, groundnut intercropped with maize followed by pea cropping system observed the highest ($p < 0.05$) SYI (0.787) followed by groundnut–pea (0.74) and maize–pea (0.67) cropping systems. Residue retention resulted in significantly higher ($p < 0.05$) SYI (0.78) as compared to residue removal (0.70) treatment (Figure 7).

Discussion

Soil enzymes, nutrients, and C stock

Ecologically viable agricultural management practices are crucial in maintaining supporting and regulating ecosystem services (Baveye et al., 2016; Singh et al., 2021). Soil quality is a set of specific soil parameters that are important for long-term agricultural production and ecosystem health (vegetation and soil) (Karlen et al., 2001). In tropical and subtropical soils, biomass addition, either through green manuring (leguminous) or crop residue retention in

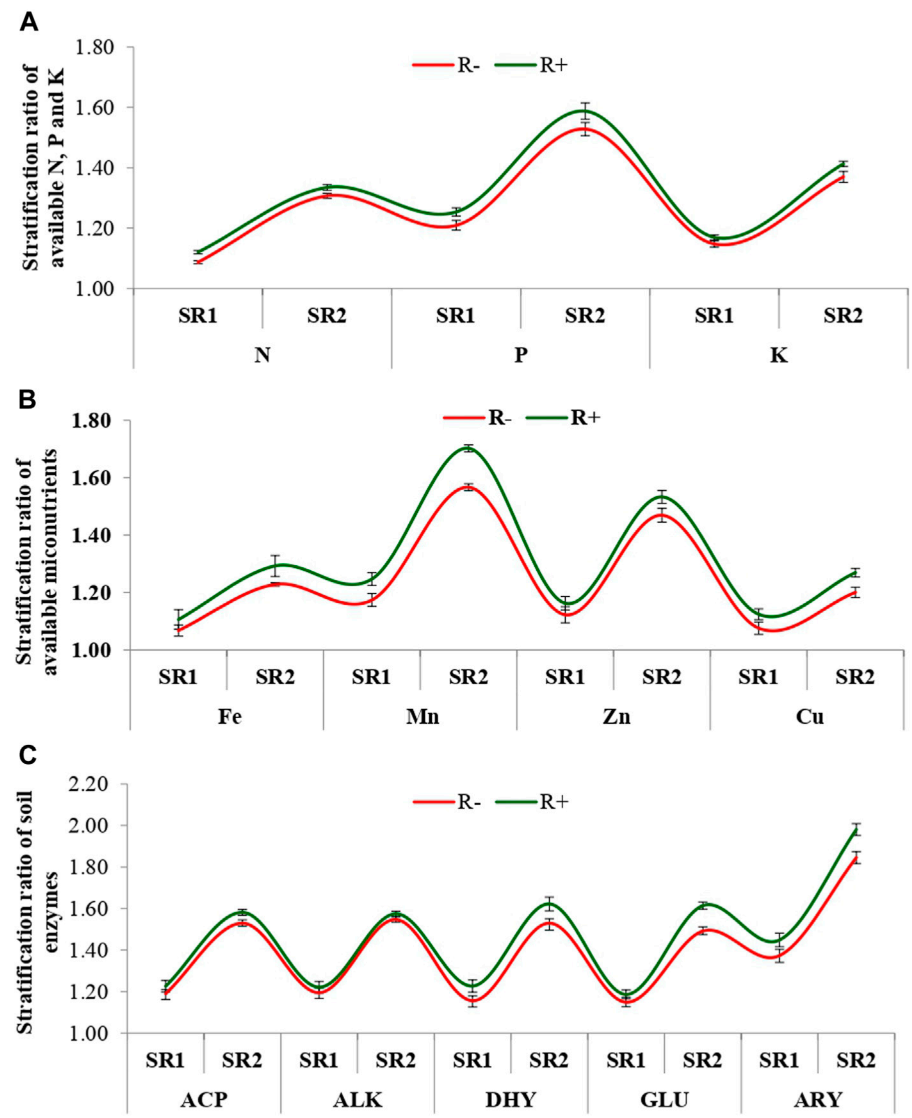

FIGURE 3
Stratification ratios of **(A)**. Available N, P, and K **(B)**. Micronutrients Fe, Mn, Zn, and Cu **(C)**. Soil enzymes as influenced by residue management after five years of experimentation. NGM: No green manuring, GGM: greengram green manuring, CGM: cowpea green manuring, SGM: sesbania green manuring, R-: residue removal, R+: residue retention SRI: stratification ratio (ratio of 0–0.15 and 0.15–0.30 m soil depth), SR2: stratification ratio (ratio of 0–0.15 and 0.15–0.30 m soil depth). ACP: Acid phosphates (u mol pNP g^{-1}), GLU: beta glucosidase (ug g^{-1} of h-[1]), ARY: arylsulfatase activity (ug pNP g^{-1} of soil h^{-1}). Vertical bar (both way) represents the standard error of mean (p<0.05).

the soil, is known to build up SOC accumulation and improve soil biological function (enzymatic activities) (Lungmuana, et al., 2019). Our findings showed that using *Sesbania* green manure along with residues retained from maize + groundnut followed by pea cropping system resulted in the highest overall biomass accumulation (22.84 Mg ha^{-1} $annum^{-1}$) and supplied a significant quantity of C to the soil (>9.58 Mg ha^{-1} $annum^{-1}$). Because of its quick growth behavior, *Sesbania aculeata* and maize along with legumes (groundnut and pea) in the cropping system are known to have increased shoot and root biomass, resulting in a substantial ($p <$ 0.05) increase in SOC stock (Ansari et al., 2022b). Soil nutrients and enzymes are greatly affected by several factors like land-use patterns, type of vegetation, crop residue recycling, green manuring, and soil management practices (Huang et al., 2016). Intensive crop cultivation without proper nutrient application and input addition to the soil reduces SOC stock and nutrient concentrations and imposes adverse effects on the soil physico-chemical and biological properties (Choudhury et al., 2021). In our findings, it is reported that the consecutive 5 years of *Sesbania* green manuring in the maize + groundnut-pea cropping system added

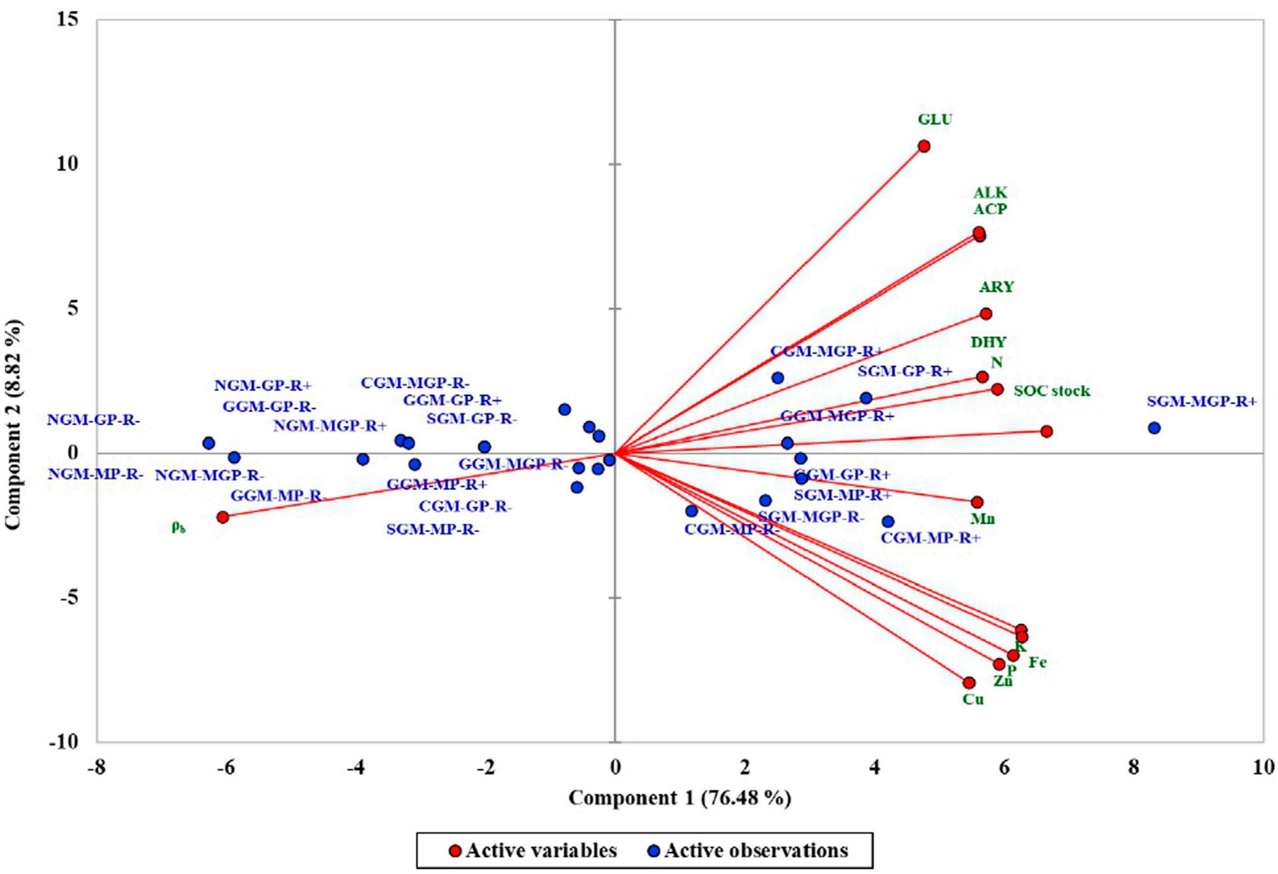

FIGURE 4
Principal component analysis (PCA). of system productivity and soil variables for treatment combinations of green manuring, cropping system, and residue management practices. NGM: No green manuring, GGM: greengram green manuring, CGM: cowpea green manuring, SGM: sesbania green manuring, GP: groundnut–pea, MP: maize–pea, MGP: maize + groundnut–pea, R-: residue removal, R+: Available phosphorus, K: Available potassium, Fe, Mn, Zn, Cu: DTPA-extractable soil micronutrients iron, manganese, zinc, and copper, respectively. ACP: Acid phosphates (u mol pNP g^{-1} of soil h^{-1}), ALK: Alkaline phosphates (ug g^{-1} of soil h^{-1}), DHY: Dehydrogenase (ug TPF g^{-1} of soil h^{-1}) GLU: beta glucosidase (ug g^{-1} of soil h^{-1}), ARY: arylsulfatase activity (ug pNP g^{-1} of soilh^{-1}); SOC stock: soil organic carbon stock.

+210.7, +67.8, +365.2, +3.0, +3.14, +1.39, and +0.17 kg ha^{-1} N, P, K, Fe, Mn, Zn, and Cu, respectively (Figure 1), in an experimental plot. The highest concentration of macro- and micronutrients in surface and subsurface soil under the MGP cropping system coupled with SGM may be attributed to nutrient addition and recycling ultimately improving soil nutrient (macro- and micro) concentrations. The addition of biomass either through green manuring with leguminous crops or residue retention is known to increase SOC build-up, and nutrient concentration in the soils (Nath et al., 2019; Choudhury et al., 2021). Stabilization of soil C and nutrients will help to reduce the CO_2 emission to the atmosphere and can address several SDGs such as climate action (SDG-13), life on land (SDG-15) through maintaining soil microbial diversity, which is an essential component of growing crops for human and livestock on the Earth. *Sesbania* is a leguminous crop that has a narrow C:N ratio (23.5:1.0), thereby enhancing the residue decomposition and release of nutrients and harbors potential enzymatic activities (Babu et al., 2020; Yadav et al., 2021). The retention of moisture and ambient temperature in the surface soil due to crop cover in *Sesbania* incorporated plots may have created a favorable environment for increased microbial decomposition, resulting in faster decomposition and nutrient release. Ma et al. (2021) concluded in their meta-analysis on the effect of green manure on nutrient availability that among different kinds of green manures, leguminous green manure significantly increased nitrate and hydrolysable nitrogen, whereas non-legume green manure significantly improved soil potassium. Amede et al. (2021) obtained an 18–26% increased wheat yield from the plots green manured with vetch and lupin over the fertilizer treatments due to the improved soil water status, improved P availability, notably increased exchangeable K, Ca, and Mg, and increased pH by about 0.5 units. The increase in soil C relies on the balance between the addition of C inputs (root exudates, root biomass, crop residues) and C losses (respiration by soil biota, erosion, etc.). It is also influenced

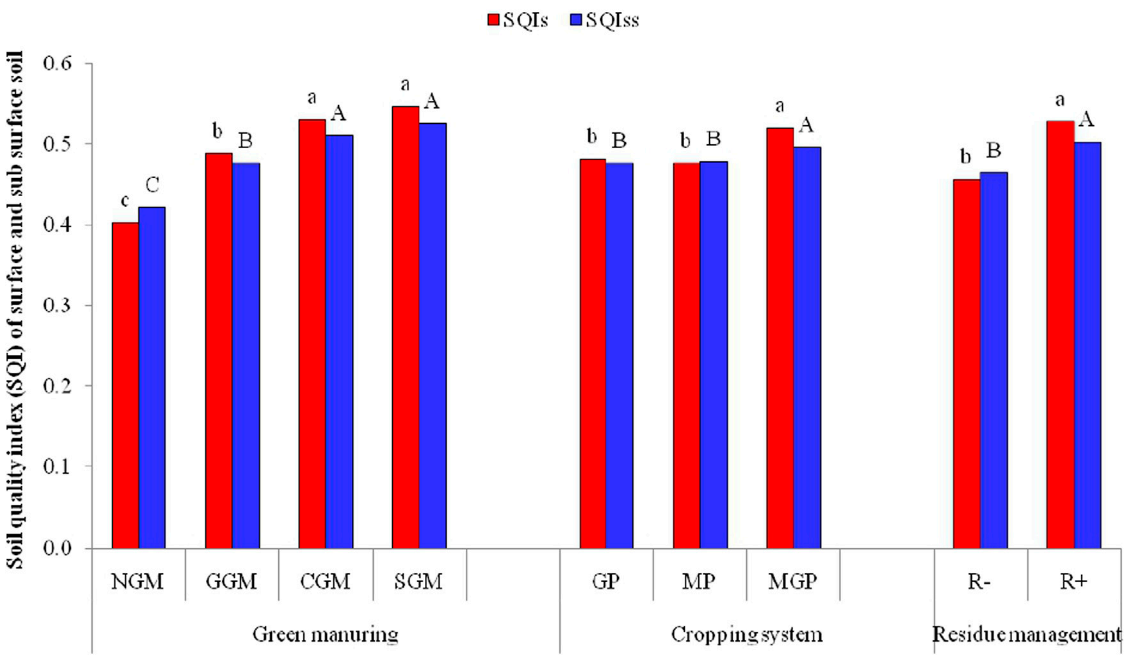

FIGURE 5
Soil quality index of surface (0–0.15 m) and subsurface soil (0.15–0.45 m) as influenced by green manuring, cropping systems, and residue management Green manuring, cropping system, and residue management followed by different letters in surface (a–c) and subsurface **(A–C)** soil is significantly different at (p < 0 .05). (DMRT: Duncan's Multiple Range Test). NGM: No green manuring, GGM: greengram green manuring, CGM: cowpea green manuring, SGM: sesbania green manuring, GP: groundnut–pea, MP: maize–pea, MGP: maize + groundnut-pea, R-: residue removal, R+: residue retention, SQIs: Soil quality index of surface soil, SQIss: Soil quality index of subsurface soil. Different lowercase letters in the same color columns (for each main factor are significantly different at p < 0.05).

by the amount of residue accumulated, the quality of residue, and the rate of decomposition (Chen et al., 2020; Almagro et al., 2021). The incorporation of green manure biomass significantly improves the soil enzymatic activities (Sürücü et al., 2014). The inclusion of nutrient-rich leguminous crops and their incorporation as green manure biomass into the soil under cereal-based cropping systems safeguard nutrients available to subsequent crops, improve the carrying capacity, and make the system viable and sustainable (Ansari et al., 2021). Ma et al. (2021) conducted a meta-analysis of the effect of green manure in China and concluded that green manure significantly improves soil quality by reducing bulk density (approximately by 5.6%) and improving soil enzymatic activities (14–39%). This study notably suggests that the incorporation of *Sesbania* as green manure in the MGP cropping system along with crop residue retention could increase the nutrient concentration in soil and harbor more soil enzymatic activity.

Vertical nutrient distribution, soil enzymes, and stratification ratio

Sesbania aculeata has fast growth behavior, and it is well known for the higher shoot and root biomass, resulting in a significant ($p < 0.05$) improvement in nutrient content and enzymatic activities in surface and subsurface soil (Ansari et al., 2021). Ansari et al. (2016) reported that maize roots were found in 1:3 ratio in the surface (0–0.20 m) and subsurface (0.20–0.40 m) soils, respectively. The significant amount of biomass of *Sesbania aculeata* and residue retention of the MGP cropping system improved the SOC stock, soil available nutrients (macro and micro), and soil enzymatic activities in the surface followed by subsurface soil as compared to no green manuring with residual removal. In another study, Hirte et al. (2018) reported that 186 g m^{-2} root biomass might have stronger influence on soil properties. The fine roots were significantly higher in the subsurface layer as compared to that in the surface layers, which could be explained by the decrease in root diameter and length as the soil depth increased (Zhang et al., 2021). The higher carbon accumulated from higher biomass in surface soil provides the higher energy source for microbes, which improves the enzymatic activities (Das et al., 2021). Higher enzymatic activities indicate the good quality of soil, which is directly related to soil carbon and biomass accumulation (Meetei et al., 2020). The vertical distribution of soil enzymes was also affected due to the quality and quantity of biomass accumulation. Reduction in soil enzymatic activities in the subsurface layer could be due to a decrease

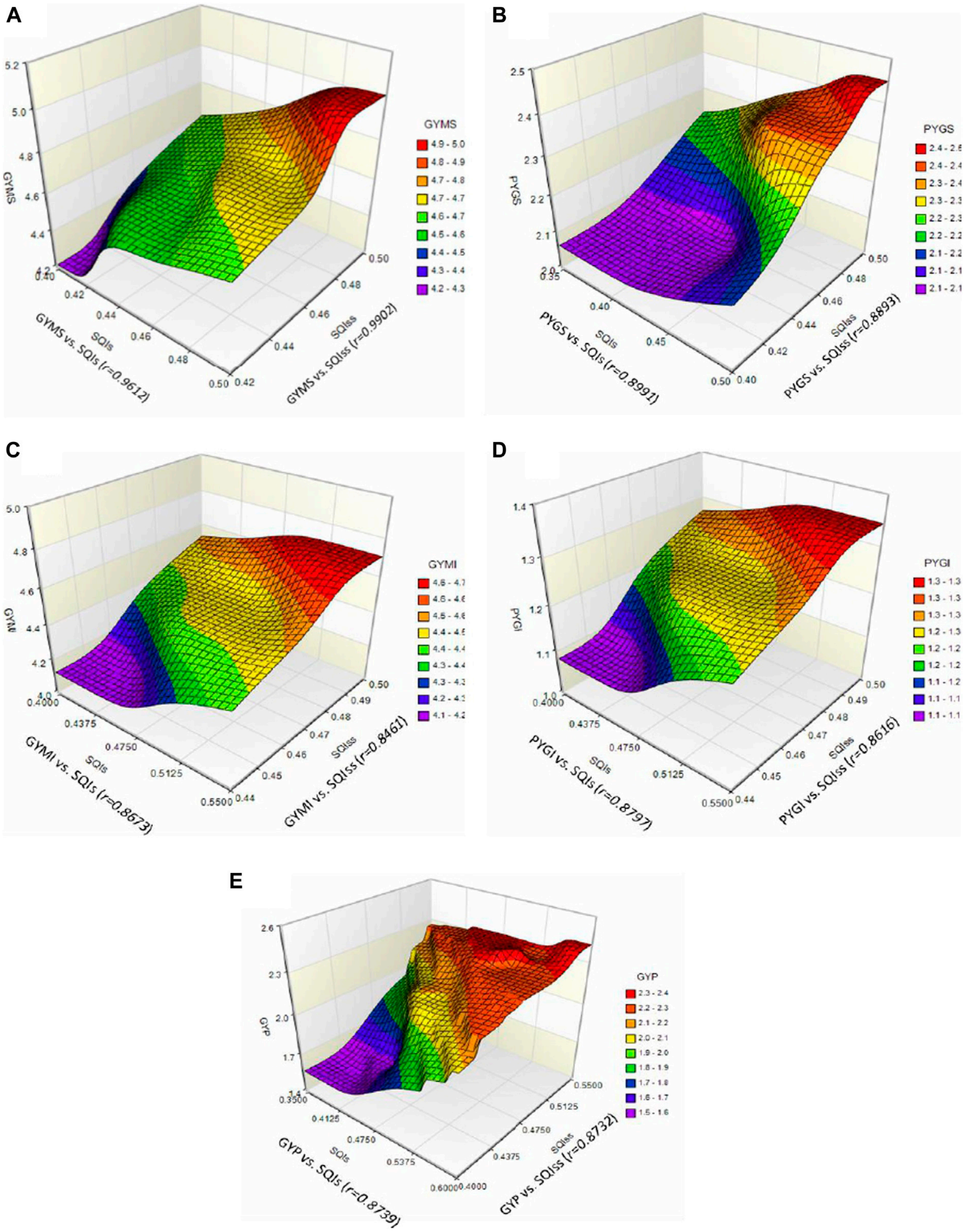

FIGURE 6
3D surface plots of relationship (r) between soil quality index of soil (SQIs, 0–0.15 m) and subsurface soil (SQIss, 0.15–0.45 m) with mean maize/groundnut yield after five years of experimentation, **(A)** grain yield of maize sole crop (GYMS, Mg ha^{-1}), **(B)** pod yield of groundnut sole group (PYGS, Mg ha^{-1}), **(C)** grain yield of intercropped maize (GYMI, Mg ha^{-1}), **(D)** pod yield of intercropped groundnut (PYGI, Mg ha^{-1}), **(E)** grain yield of pea (GYP, Mg ha^{-1}).

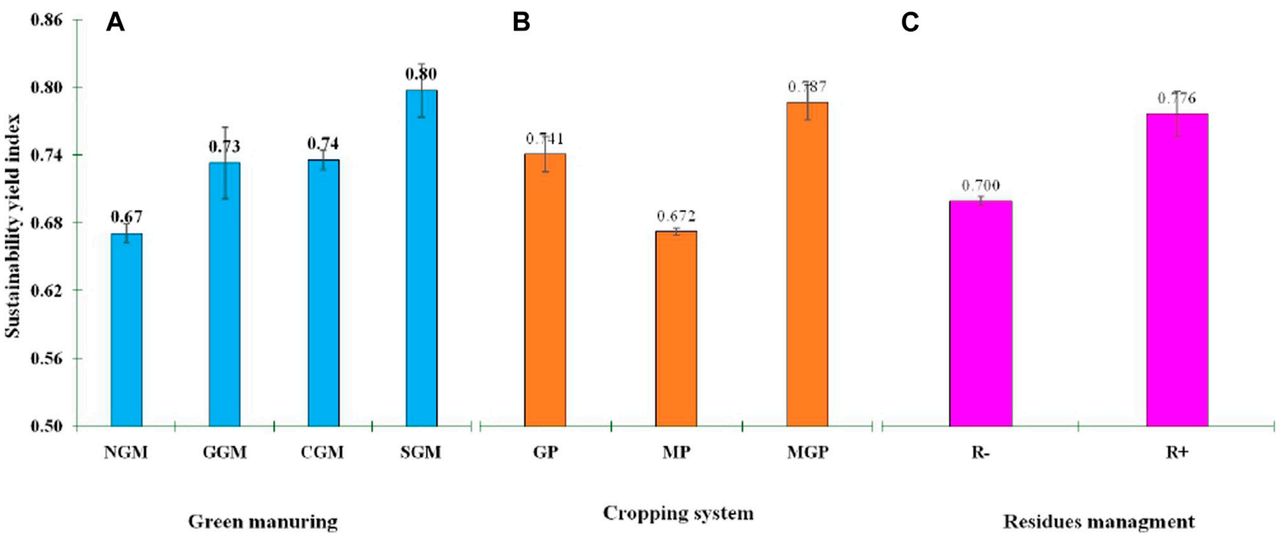

FIGURE 7
Sustainability yield index as influenced by **(A)** green manuring, **(B)** cropping systems, **(C)** residue management NGM: No green manuring, GGM: greengram manuring, CGM: cowpea green manuring, SGM: sesbania green manuring, GP: groundnut–pea, MP: maize–pea, MGP: maize + Groundnut–pea, R-: residue removal, R+: residue retention. The vertical bars represent p<0.05 significant level.

in C input deposition from the land use-mediated addition of plant residues, such as root biomass (Meetei et al., 2020). However, a continuous drop in soil C stocks in deeper soil depths could explain the decrease in soil enzymatic activities and nutrients as soil depth increased (Lungmuana et al., 2019).

In this study, higher SR of nutrients (macro: N, P, K and micro: Fe, Mn, Zn, Cu) and soil enzymes (ACP, ALK, DHY, GLU, and ARY) were observed with SGM > CGM > GGM > NGM. Similarly, residue retention enhanced the SR of nutrients and enzymes as compared to residue removal in the MGP cropping system, which might be attributed to higher biomass and residue-mediated nutrient concentration in soil (Qua et al., 2020). Higher SR of nutrients and soil enzymes improves soil health and indicates that the soil is free from the degradation process (Franzluebbers, 2002). In the sloping uplands of Manipur, India's Eastern Himalayan area, Ansari et al. (2022a) confirmed that degraded soils from unsustainable land-use activities (e.g. hill slope agriculture) produced a reduction in SR, whereas stable land-use techniques (e.g., agroforestry or woody horticulture) improved SRs. The aforesaid findings were validated in the MGP cropping system, which included green manuring and crop residue retention and gave higher nutrient sequestration and harbored more enzymatic activities than other treatments. Almost a two fold increase in SR1 and SR2 corroborated the constant decrease in available nutrients (micro and macro) and enzymatic activities from the surface (L_1) to the subsoil (L_3). Previous studies have also affirmed that the soil nutrients and enzymatic activities decline at varying rates depending on soil depth (Lungmuana et al., 2019). In the studied region, Ansari et al. (2022a) found a substantial increase in SR along with a depth of up to 1.0 m in both cultivated (e.g., upland and lowland agriculture, horticulture, and agroforestry) and uncultivated (dense forest) land uses. Thus, our findings notably reported that the use of green manuring is important in maize/groundnut cropping systems in the subtropical regions for stabilizing soil quality indicators (soil nutrients and enzymatic activities), which is critical for maintaining long-term crop productivity.

Soil quality index

Biomass accumulation through green manuring and crop residue retention in cropping systems is one of the most significant and easily implemented strategies for enhancing, regulating, and supporting ecosystem services and combating soil degradation (Lal, 2017). Soil micro-climate-mediated biomass accumulation creates a favorable soil environment, which improves the nutrient utilization efficiency and leads to higher crop productivity (Lal, 2017; Ansari et al., 2022b). However, an intensive cropping system with inadequate agro-technique and residue removal could lead to soil quality deterioration as well as poor responsive soils (Singh et al., 2021). In 5 years of study, we notably observed that the soil quality indicators like SOC stock, available macro- (N, P, and

K) and micro (Fe, Mn, Zn, and Cu)-nutrients as well as enzymatic activities (ACP, ALK, DHY, GLU, and ARY) improved significantly ($p < 0.05$) in the MGP cropping systems with SGM and residue retention as compared to other cropping systems with residue removal. Across the cropping systems, SYI significantly correlated with available macronutrients (r = +0.65–0.781), available micronutrients (r= +0.782–0.824), and soil enzymatic activities (r = +0.0.570–0.791) (Supplementary Table S3). In this study, soil carbon, nutrients, and potential soil enzyme status improved significantly in MGP cropping system. SGM and crop residue retention resulted in the improvement of SQI. Green manuring and residue retention resulted in the substantial reduction in dependency on fertilizers through improvement in nutrient availability and modified biomass-mediated enzyme activities (Shahid et al., 2013; Nath et al., 2019). Further, higher SQI in surface and subsurface soil suggests for the adoption of MGP with SGM and residue retention in this region as well as similar ecosystems elsewhere.

Yield sustainability

The SYI is used to measure long-term sustainability in terms of yield. Its value varies from zero to unity. Higher values indicate that treatments give constantly higher yields across the years. Higher SYI and system productivity provide the opportunity to achieve the SDGs and especially good health and well-being. Averaged over the years, *Sesbania* green manuring treatment gave a 24.2% higher system productivity in terms of maize equivalent yield (MEY) over no-green manuring treatment (Figure 7). The continuous application of SGM treatment reflected significant ($p <$ 0.05) improvement in the SYI (+18.8%) as compared to that of NGM. Similarly, the maize + groundnut–pea cropping system recorded +16.4 and +39.6% higher system productivities over the groundnut–pea and maize–pea cropping system, respectively. Consequently, the MGP cropping system recorded higher SYI (6.8%–17.6%) as compared to the other two systems. Continuous crop residue retention increased the system productivity by 11.3% averaged over 5 years and consequently recorded higher SYI (+11%) over residue removal. No-green manuring and removal of crop residues from maize + groundnut–pea cropping system resulted in a decline in system productivity and SYI over 5 years of experimentation.

Conclusion

Stabilized soil carbon and nutrient (macro and micro) management efficiency and ecosystem services, as well as maintaining higher yield sustainability and soil quality through sustainable agriculture management practices, are the key aims for sustainable agricultural production. These improvements may contribute a little toward achieving of SDGs viz., reduction of poverty, ensure zero hunger, good health and well-being, climate action, and life on land. Continuous five-year SGM incorporation, MGP cropping system, and residue retention increased the SYI by 19%, 17.0%, and 11.0%, respectively, over NGM, MP, and residue removal. Similarly, the same treatment increased the SQI by 35.7%, 9.5%, and 15.8% in the surface and by 24.4%, 4.4%, and 8.0% in subsurface soils, respectively. Higher available soil macro- and micronutrient content and soil enzymatic activities have resulted from the increase in their SR, SQI, and SYI under groundnut intercropped with maize followed by the pea cropping system. Soil SR and SQI along with SYI have emerged as major sustainability indicators. Augmenting these indicators in the long-term production system is of paramount significance. Hence, a multi-indicator-based approach including crop management under resource conservation along with green manuring, residue retention, and cropping intensification with the improvement of enzymatic activities, availability of macro- and micronutrients, and land productive capacity.

Data availability statement

The datasets presented in this study can be found in online repositories. The names of the repository/repositories and accession number(s) can be found in the article/ Supplementary Material.

Author contributions

Conceptualization, investigation, monitoring, data curation, and writing of original and final draft: MA; review and writing, editing: SB and JC; review and writing, funding acquisition and review: NR and ASP.

Acknowledgments

The authors acknowledge the physical and, scientific equipment facilities and financial support received from the Director, ICAR Research Complex for NEH Region, Meghalaya, India under the ICAR Institute project (Project code: IXX09777). The authors are gratefully acknowledged to the Director, ICAR-IIFSR, Modipuram and All India Network Programme on Organic Farming (AI-NPOF) for financial assistance in publication of research outcome. The authors express their gratitude to the project staff and technical officer for their assistance during the project.

Conflict of interest

The authors declare that the research was conducted in the absence of any commercial or financial relationships that could be construed as a potential conflict of interest.

Publisher's note

All claims expressed in this article are solely those of the authors and do not necessarily represent those of their affiliated organizations, or those of the publisher, the editors, and the reviewers. Any product that may be evaluated in this article, or claim that may be made by its manufacturer, is not guaranteed or endorsed by the publisher.

Supplementary material

The Supplementary Material for this article can be found online at: https://www.frontiersin.org/articles/10.3389/fenvs.2022.940349/full#supplementary-material

References

Almagro, M., Ruiz-Navarro, R. N., Díaz-Pereira, D. P., Albaladejo, A., and Martínez-Mena, M. M. (2021). Plant residue chemical quality modulates the soil microbial response related to decomposition and soil organic carbon and nitrogen stabilization in a rainfed Mediterranean agroecosystem. *Soil Biol. Biochem.* 156, 108198. doi:10.1016/j.soilbio.2021.108198

Amede, T., Legesse, G., Agegnehu, G., Gashaw, T., Degefu, T., Desta, G., et al. (2021). Short term fallow and partitioning effects of green manures on wheat systems in East African highlands. *Field Crops Res.* 269, 108175. doi:10.1016/j.fcr.2021.108175

Amede, T., and Taboge, E. (2007). "Optimizing soil fertility gradients in the enset systems of the Ethiopian highlands: Trade-offs and local innovations," in *Advances in integrated soil fertility management in Sub-Saharan Africa: Challenges and Opportunities* (Dordrecht: Springer), 289–297. Avaliable At: http://hdl.handle.net/10625/38152.

Ansari, M. A., Choudhary, B. U., Prakash, N., Kumar, B., Jat, S. L., Mishra, D., et al. (2016). Genotypic variations in phenology, productivity and heat-use efficiency of rainfed maize (*Zea mays*) in acid soils of north eastern Himalayan region. *Indian J. Agric. Sci.* 86 (6), 796–802. Avaliable At: https://epubs.icar.org.in/ejournal.

Ansari, M. A., Choudhury, B. U., Layek, J., Das, A., Lal, R., and Mishra, V. K. (2022b). Green manuring and crop residue management: Effect on soil organic carbon stock, aggregation, and system productivity in the foothills of eastern himalaya (India). *Soil Tillage Res.* 218, 105318. doi:10.1016/j.still.2022.105318

Ansari, M. A., Choudhury, B. U., MandalJat, S. S. L., and Jat, C. B. (2022a). Converting primary forests to cultivated lands: Long-term effects on the vertical distribution of soil carbon and biological activity in the foothills of Eastern Himalaya. *J. Environ. Manage.* 301, 113886. doi:10.1016/j.jenvman.2021.113886

Ansari, M. A., Choudhury, B. U., Roy, S. S., Sharma, S. K., Singh, I. M., and SinghPrakash, A. L. N. (2020). Performance of groundnut (*Arachis hypogaea*) cultivars for higher productivity in hilly ecosystem. *Indian J. Agric. Sci.* 90 (4), 818–822. Avaliable At: https://epubs.icar.org.in/ejournal.

Ansari, M. A., Saha, S., Das, A., Lal, R., Das, B., Choudhury, B. U., et al. (2021). Energy and carbon budgeting of traditional land use change with groundnut-based cropping system for environmental quality, resilient soil health and farmers income in eastern Indian Himalayas. *J. Environ. Manage.* 293, 112892. doi:10.1016/j.jenvman.2021.112892

Babu, S., Mohapatra, K. P., Das, A., Yadav, G. S., Tahasildar, M., Singh, R., et al. (2020). Designing energy-efficient, economically sustainable and environmentally safe cropping system for the rainfed maize–fallow land of the Eastern Himalayas. *Sci. Total Environ.* 722, 137874. doi:10.1016/j.scitotenv.2020.137874

Banerjee, V., Krishnan, P., Das, B., Verma, A. P. S., and Varghese, E. (2015). Crop status index as an indicator of wheat crop growth condition under abiotic stress situations. *Field Crops Res.* 18, 16–31. doi:10.1016/j.fcr.2015.06.009

Baveye, P. C., Baveye, J., and Gowdy, J. (2016). Soil ecosystem services and natural capital: Critical appraisal of research on uncertain ground. *Front. Environ. Sci.* 4, 1–49. doi:10.3389/fenvs.2016.00041

Blake, G. R., and Hartge, K. H. (1986). "Bulk density," in *Methods of soil analysis, Part I: Physical and mineralogical methods*. Editor A. Klute. second edn. (Madison WI: American Society of Agronomy).

Buragohain, S., Sharma, B., Nath, J. D., Gogaoi, N., Meena, R. S., and Lal, R. (2017). Impact of ten years of bio-fertilizer use on soil quality and rice yield on an inceptisol in Assam, India. *Soil Res.* 56 (1), 49–58. doi:10.1071/SR17001

Casida, L. E., Jr., Klein, D. A., and Santoro, T. (1964). Soil dehydrogenase activity. *Soil Sci.* 98, 371–376. doi:10.1097/00010694-196412000-00004

Chen, A., Wang, Z., Lin, Y., Wang, X., Li, Y., Zhang, Y., et al. (2020). Temporal variation of soil organic carbon pools along a chronosequence of reforested land in Southwest China. *Catena* 194, 104650. doi:10.1016/j.catena.2020.104650

Choudhury, B. U., Ansari, M. A., Chakraborty, M., and Meetei, T. T. (2021). Effect of land-use change along altitudinal gradients on soil micronutrients in the mountain ecosystem of Indian (Eastern) Himalaya. *Sci. Rep.* 11, 14279. doi:10.1038/s41598-021-93788-3

Choudhury, B. U., Nengzouzam, G., Ansari, M. A., and Islam, A. (2022). Causes and consequences of soil erosion in northeastern Himalaya, India. *Cur. Sci.* 122 (7), 772–789. doi:10.18520/cs/v122/i7/772-789

Das, A., Devi, M. T., Babu, S., Ansari, M. A., Layek, J., Bhowmick, S. N., et al. (2018). "Cereal-legume cropping system in Indian himalayan region for food and environmental sustainability," in *Legumes for soil health and sustainable management*. Editors (Springer Nature Singapore Pte Ltd). doi:10.1007/978-981-13-0253-4_2

Das, A., Layek, J., Yadav, G. S., Lal, R., Saha, S., Singh, R., et al. (2021). "Managing soil organic carbon in croplands of the eastern Himalayas, India," in *Soil organic matter and feeding the future*. Editor R. Lal. doi:10.1201/9781003102762-12

Eivazi, F., and Tabatabai, M. A. (1988). Glucosidases and galactosidases in soils. *Soil Biol. biochem.* 20, 601–606. doi:10.1016/0038-0717(88)90141-1

Franzluebbers, A. J. (2002). Soil organic matter stratification ratio as an indicator of soil quality. *Soil Tillage Res.* 66 (2), 95–106. doi:10.1016/S0167-1987(02)0001810.1016/s0167-1987(02)00018-1

Hirte, J., Leifeld, J., Abiven, S., and Mayer, J. (2018). Maize and wheat root biomass, vertical distribution, and size class as affected by fertilization intensity in two long-term field trials. *Field Crops Res.* 216, 197–208. doi:10.1016/j.fcr.2017.11.023

Huang, K., Yangjian, Z., Juntao, Z., Yaojie, L., Jiaxing, Z., and Jing, Z. (2016). The influences of climate change and human activities on vegetation dynamics in the Qinghai-Tibet Plateau. *Remote Sens.* 8 (10), 876. doi:10.3390/rs8100876

Jackson, M. L. (1973). *Soil chemical analysis*. New Delhi: Prentice Hall of India Pvt. Ltd.

Kaiser, H. F. (1960). The application of electronic computers to factor analysis. *Educ. Psychol. Meas.* 20, 141–151. doi:10.1177/001316446002000116

Karlen, D. L., Andrews, S. S., and Doran, J. W. (2001). Soil quality: Current concepts and applications. *Adv. Agron.* 74, 1–40. doi:10.1016/s0065-2113(01)74029-1

Lal, R. (2017). Improving soil health and human protein nutrition by pulses-based cropping systems. *Adv. Agron.* 145, 167–204. doi:10.1016/bs.agron.2017.05.003

Lindsay, W. L., and Norvell, W. A. (1978). Development of a DTPA soil test for zinc, iron, manganese and copper. *Soil Sci. Soc. Am. J.* 42, 421–428. doi:10.2136/sssaj1978.03615995004200030009x

Lungmuana, S., Singh, S. B., Choudhury, B. U., VanthawmlianaSaha, S., and Hnamte, V. (2019). Transforming jhum to plantations: Effect on soil microbiological and biochemical properties in the foot hills of North Eastern Himalayas, India. *Catena* 177, 84–91. doi:10.1016/j.catena.2019.02.008

Ma, D., Lina, Y., Wenliang, J., Xiankun, L., Xiaoxiao, L., Xiping, D., et al. (2021). Meta-analysis of green manure effects on soil properties and crop yield in northern China. *Field Crops Res.* 266, 108146. doi:10.1016/j.fcr.2021.108146

Meena, B. L., Fagodiya, R. K., Prajapat, K., Dotaniya, M. L., Kaledhonkar, M. J., Sharma, P. C., et al. (2018). "Legume green manuring: An option for soil sustainability," in *Legumes for soil health and sustainable management* (Singapore: Springer), 387–408. doi:10.1007/978-981-13-0253-4_12

Meetei, T. T., Choudhury, B. U., Mohapatra, K. P., Singh, N. U., Das, A., and Devi, Y. B. (2020). Effect of 25 years old agroforestry practices on soil quality attributes in the northeastern Himalayan region of India. *Int. J. Chem. Sci.* 8 (1), 2371–2379. doi:10.22271/chemi.2020.v8.i1aj.8623

Melero, S., Juan, C. R. P., Jua, F. H., and Engracia, M. (2006). Chemical and biochemical properties in a silty loam soil under conventional and organic management. *Soil Tillage Res.* 90 (1-2), 162–170. doi:10.1016/j.still.2005.08.016

Nath, C. P., Hazra, K. K., Kumar, N., Praharaj, C. S., Singh, S. S., Singh, U., et al. (2019). Including grain legume in rice-wheat cropping system improves soil organic carbon pools over time. *Ecol. Eng.* 129, 144–153. doi:10.1016/j.ecoleng.2019.02.004

Nelson, D. W., and Sommers, L. E. (1973). Determination of total nitrogen in plant material. *Agron. J.* 65, 109–112. doi:10.2134/agronj1973.00021962006500010033x

Peregrina, F., Pérez-Álvarez, E. P., and García-Escudero, E. (2014). Soil microbiological properties and its stratification ratios for soil quality assessment under different cover crop management systems in a semiarid vineyard. *J. Plant. Nutr. Soil Sci.* 177 (4), 548–559. doi:10.1002/jpln.201300371

Qua, Q., Xub, H., Xuea, S., and Liua, G. (2020). Stratification ratio of rhizosphere soil microbial index as an indicator of soil microbial activity over conversion of cropland to forest. *Catena* 195, 104761. doi:10.1016/j.catena.2020.104761

Ravisankar, N., Ansari, M. A., Shamim, M., Prusty, A. K., Singh, R., Panwar, A. S., et al. (2022). Sustainable livelihood security of small farmers improved through resilient farming systems in the Semi-Arid Region of India. *Land Degrad. Dev.*, 1–13. doi:10.1002/ldr.4358

Sarkar, D., Baishya, L. K., Meitei, C. B., Naorem, G. C., Thokchom, R. C., Singh, J., et al. (2018). Can sustainability of maize-mustard cropping system be achieved through balanced nutrient management? *Field Crops Res.* 225, 9–21. doi:10.1016/j.fcr.2018.05.018

Shahid, M., Nayak, A. K., Shukla, A. K., Tripathi, R., Kumar, A., Mohanty, S., et al. (2013). Long-term effects of fertilizer and manure applications on soil quality and yields in a sub-humid tropical rice-rice system. *Soil Use Manag.* 29, 322–332. doi:10.1111/sum.12050

Singh, R., Babu, S., Avasthe, R. K., Meena, R. S., Yadav, G. S., Das, A., et al. (2021). Conservation tillage and organic nutrients management improve soil properties, productivity, and economics of the maize-vegetable pea system in the Eastern Himalayas. *Land Degrad. Dev.* 32 (16), 4637–4654. doi:10.1002/ldr.4066

Stagnari, F., Maggio, A., Galieni, A., and Pisante, M. (2017). Multiple benefits of legumes for agriculture sustainability: An overview. *Chem. Biol. Technol. Agric.* 4 (2), 1–13. doi:10.1186/s40538-016-0085-1

Subbiah, B. V., and Asija, C. L. (1956). A rapid procedure for estimation of available nitrogen in soils. *Curr. Sci.* 25, 259–260. Avaliable At: https://www.scienceopen.com/document?vid=6fc73f08-2bbf-4ac7-93e5-7f405a35961f.

Sürücü, A., Mehmetm, A. Ö., Betül, B., and Rıdvan, K. (2014). Effects of green manuring on soil enzyme activity. *Fresenius Environ. Bull.* 23 (9), 2126–2132.

Tabatabai, M. A., and Bremmer, J. M. (1969). Use of p–nitrophenyl phosphate for assay of soil phosphatase activity. *Soil Biol. biochem.* 1, 301–307. doi:10.1016/0038-717(69)90012-110.1016/0038-0717(69)90012-1

Tabatabai, M. A., and Bremner, J. M. (1970). Arylsulfatase activity in soils. *Soil Sci. Soc. Am. Proc.* 34, 225–229. doi:10.2136/sssaj1970.03615995003400020016x

Vance, E. D., Brookes, P. C., and Jenkinson, D. S. (1987). An extraction method for measuring soil microbial biomass C. *Soil Biol. biochem.* 19, 703–707. doi:10.1016/0038-0717(87)90052-6

Walkley, A., and Black, I. A. (1934). Estimation of soil organic carbon by the chromic acid titration method. *Soil Sci.* 37, 29–38. doi:10.1097/00010694-193401000-00003

Wander, M. M., Cihacek, L.,J., Coyne, M., Drijber, R. A., Grossman, J. M., Gutknecht, J. L. M., et al. (2019). Developments in agricultural soil quality and health: Reflections by the research committee on soil organic matter management. *Front. Environ. Sci.* 7, 109. doi:10.3389/fenvs.2019.00109

Yadav, G. S., Das, A., Kandpal, B. K., Babu, S., Lal, R., Datta, M., et al. (2021). The food-energy-water-carbon nexus in a maize-maize-mustard cropping sequence of the Indian Himalayas: An impact of tillage-cum-live mulching. *Renew. Sustain. Energy Rev.* 151, 111602. doi:10.1016/j.rser.2021.111602

Yuan, B. C., and Yue, D. X. (2012). Soil microbial and enzymatic activities across a chronosequence of Chinese pine plantation development on the loess plateau of China. *Pedosphere* 22 (1), 1–12. doi:10.1016/S1002-0160(11)60186-0

Zhang, C., Chen, L., and Jiang, J. (2014). Vertical root distribution and root cohesion of typical tree species on the Loess Plateau, China. *J. Arid. Land.* 6 (5), 601–611. doi:10.1007/s40333-014-0004-x

Zhang, G., Meng, W., Pan, W., Han, J., and Liao, Y. (2021). Effect of soil water content changes caused by ridge-furrow plastic film mulching on the root distribution and water use pattern of spring maize in the Loess Plateau. *Agric. Water Manag.* 261, 107338. doi:10.1016/j.agwat.2021.107338

frontiers | Frontiers in Environmental Science

TYPE Original Research
PUBLISHED 08 September 2022
DOI 10.3389/fenvs.2022.964698

OPEN ACCESS

EDITED BY
Thiru Selvan,
Tripura University, India

REVIEWED BY
Manuel Canovas,
Catholic University of the North, Chile
Qingguang Li,
Guizhou University, China

*CORRESPONDENCE
Khalil EL Mejahed,
khalil.elmejahed@um6p.ma

SPECIALTY SECTION
This article was submitted to Soil Processes,
a section of the journal
Frontiers in Environmental Science

RECEIVED 08 June 2022
ACCEPTED 25 July 2022
PUBLISHED 08 September 2022

CITATION
Outbakat MB, Choukr-Allah R,
EL Gharous M, EL Omari K, Soulaimani A and EL Mejahed K (2022), Does phosphogypsum application affect salts, nutrients, and trace elements displacement from saline soils?
Front. Environ. Sci. 10:964698.
doi: 10.3389/fenvs.2022.964698

Does phosphogypsum application affect salts, nutrients, and trace elements displacement from saline soils?

M Barka Outbakat[1], Redouane Choukr-Allah[1], Mohamed EL Gharous[1], Kamal EL Omari[2], Aziz Soulaimani[1] and Khalil EL Mejahed[1]*

[1]Agricultural Innovation and Technology Transfer Center (AITTC), Mohammed VI Polytechnic University, Benguerir, Morocco, [2]OCP Group, OCP Sustainability Platform, Casablanca, Morocco

Salinity and sodicity are the most agricultural challenges in arid and semi-arid regions. A pot experiment was undertaken, to evaluate the effect of Phosphogypsum (PG) and Gypsum (G), to remove salts, nutrients and trace elements in leached water from saline and saline-sodic soils. In order to determine the efficiency and safety of these amendments, as an affordable strategy, for overcoming salinity and sodicity stress. The PG at 0, 15, 30 and 45 t/ha and G at 15 t/ha were mixed with the upper 9 cm soil in the pot before being leached. The soils were collected from Sed El Masjoune and Sidi El Mokhtar areas of morocco with ECe of 140.6 mS/cm and 11.7 mS/cm respectively. The highest doses of PG (≥30 t/ha) removed significant amount of salts and nutrients. Calcium sulfate supplies calcium ions to replace salt ions (sodium, especially). The replaced salts are leached from the soil. The PG was more efficient compared to G in terms of salts leaching. Quantities of trace elements in the leachate, for most analyzed elements, were below the recommended limits of drinking and irrigation water. Because the experiment's alkaline conditions (basic water and soil) reduce the solubility and mobility of trace elements. The amendment application did not affect saturation index (SI) of the main minerals. However, water passing through the soil increased the SI. which could result in groundwater mineral precipitation.

KEYWORDS

soil salinity and sodicity, phosphogypsum, gypsum, leached water, plant nutrients, trace elements, saturation index

Introduction

Soils are fundamental to life on Earth but human and environmental pressures on soil resources are reaching critical limits. Soil is one of the most important natural resources which can be subject to different forms of degradation (salinity, acidity, erosion…). Salinity and sodicity are among the ten threats to soils identified by FAO (FAO, 1999). Salinity is increasingly threatening agricultural production, especially in arid and semi-arid areas.

The human-induced salinity through irrigating soils with salty (brackish/saline) water (2ndry salinity) is great threat to irrigated agriculture, whereby, we are losing 2,000 ha daily of farm land due to only soil salinization (UNU, 2014). Based on the electrical conductivity of saturated soil paste (ECe). The soil is classified as no-saline (0 < Ece (dS/m)≤2) to very strongly saline (Ece (dS/m) > 16) (Figure 1) (Lech et al., 2016). While sodic soil has a percentage of exchangeable sodium (ESP) higher 15% (FAO, 1988). The area of total land impacted by salts is about one billion hectares, and the trend is significantly increasing (Ivushkin et al., 2019). In Morocco, salinization affects 5% of agricultural soils (Antipolis, 2003). Which corresponds to 435,000 ha. In addition to saline soils, most of the groundwater is also saline in fact, 25% of Moroccan groundwater is characterized by a salts content of 1–2 g/L, and 27.5% has a salt concentration greater than 2 g/L (Hssaisoune et al., 2020).

Prolonged drought periods with low and erratic rainfall distribution and extreme temperatures, due to climate changes, cause, the increase of saline soils in arid, semi-arid, and coastal agricultural areas (Corwin, 2021). On the other hand, anthropogenic activities, especially irrigation management and low water quality induce significant soil salinization (Moharana et al., 2019). Salt affected soils usually generate physical, chemical and physiological disorders in soil-plant- water system. The presence of salts leads to the development of osmotic potential of soil water, which reduces plant transpiration thereby affecting crop yield (Lamsal et al., 1999). Whereas sodicity degrades soil structure and destroy its stability (El hasini et al., 2019) which subsequently affect water and air movement and root development. The reclamation of salt affected soils has been subject of numerous studies around the world. Many approaches were evaluated to mitigate soil salinity for example phytoremediation by using halophyte plants which have a capacity to tolerate saline conditions (Okur et al., 2020). Mu et al. (2021) reported that halophytes plants (*Sedum aizoon* L. and *Sesbania cannabina* Pers.) performed better at saline soil remediation. Devi et al. (2016) characterized *Suaeda fruticosa* and *Atriplex lentiformis* as salt hyperaccumulator species. Hirich et al. (2021) reported that the introduction of alternative crops, such as blue panicum, quinoa and sesbania, reduces the impacts of soil and water salinity. Moreover, the reclamation of saline and sodic soils can be achieved using integrated soil reclamation approach including physical, chemical, hydrological and biological methods, based on the scientific diagnostics of both the salinity and sodicity, such as PG (Smaoui-Jardak et al., 2017; El Mejahed et al., 2020), and G (Makoi and Verplancke, 2010; Zaman et al., 2018). The PG is a byproduct of phosphate industry according to the following reaction.

$$\mathrm{Ca10\,(PO_2)6F_2} + \mathrm{10H_2SO_4} + \mathrm{20H_2\,O} \rightarrow 6H_3PO_4 + 2HF + 10\,(CaSO4\,.2H_2O) \tag{1}$$

The world annual production of PG is about 300 Mt (Cuadri et al., 2021). However, only 15% of PG produced at the global level is recycled. The PG has been used in construction industry (Manal et al., 2012) and in agriculture as fertilizer and as amendment for reclamation of degraded soils such as saline, sodic, acidic and alkaline soils (Mesić et al., 2016).

Calcium sulfate can readily furnish soluble calcium (Ca) to substitute exchangeable sodium (Na), the reaction is as follows (FAO, 1988):

$$\mathrm{CaSO_4{+}2Na - clay \rightarrow Ca - clay + Na_2SO_4} \downarrow \tag{2}$$

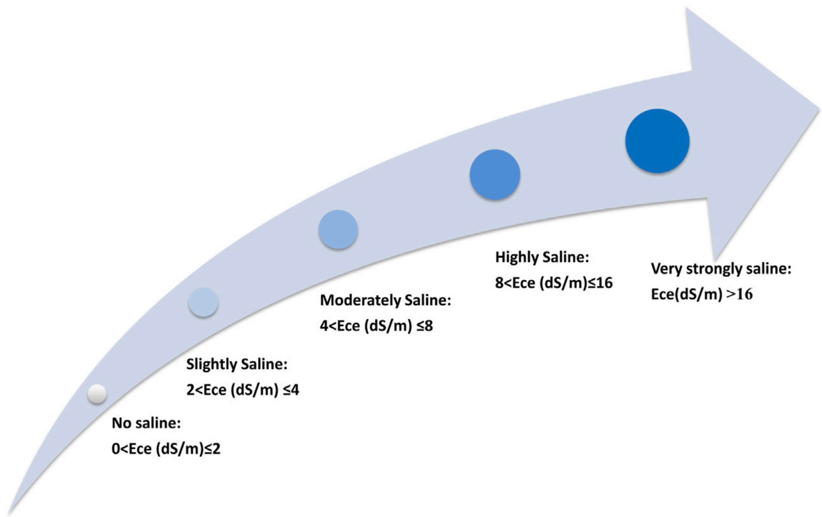

FIGURE 1
Soil salinization classification standards (Lech et al., 2016).

Reclamation process is illustrated in Figure 2.

The use of 40 t/ha of PG for reclamation of a very strongly saline soil (ECe = 52 ds/m and ESP = 35.7%) using moderate saline water (EC = 2.2 ds/m and Sodium adsorption ratio (SAR) = 4.1 Meq/l) increased the relative removal of sodium (Na/Na_0), which was 0.80 in the treated soil leachate compared to 0.42 in the control test (Gharaibeh et al., 2010).

The PG showed its desalinization and desodification abilities by reducing soil EC and exchangeable sodium percentage (ESP) (Abdel-Fattah and EL-Naka, 2015). The application of PG reclaimed the soil which passes from saline-sodic situation to normal (Diop et al., 2019). On the other hand, Makoi and Verplancke (2010) indicated that leaching after gypsum application reduced exchangeable Na, Sodium adsorption ratio (SAR) and subsequently the ESP of the soil.

However PG contains several heavy metals and radioactive elements (Lütke et al., 2020; Qamouche et al., 2020). The agricultural PG use should examine the transferability of these elements to the soil, plant, and water systems. Gypsum has relatively low solubility, especially in saline water (EC > 2.2 dS/m), resulting in its precipitation (Porta, 1998).

Groundwater, a natural water resource, is mainly used for domestic and irrigation purposes (Jiang et al., 2009; Nagarajan et al., 2012). Groundwater quality is very much affected by anthropogenic activities, especially agriculture, which may be considered as one of the most important sources of groundwater contamination, mainly by nitrate (NO_3) and trace elements leaching (Agostini, et al., 2010; Zhao et al., 2011; Adimalla and Qian, 2019), for these reasons, the evaluation of leached water quality is highly important. The use of PG for saline soils shows the tendency of sodium to be leached from the soil, and the accumulation of phosphorus and rare-earth elements in saline soils (Gorbunov et al., 1992). Because of alkaline conditions that decrease the leachability and mobility of the majority of heavy metals (Al-Masri et al., 2004). Several authors (Ismail et al., 2015; Walawalkar et al., 2016; Mashifana et al., 2019) have used different acids, such as nitric, hydrochloric, sulfuric and citric acids to leach rare elements from PG. In addition, Motalane and Strydom (2004) reported that the acidic nature of Phosphogypsum can increase heavy metal mobility and leachability.

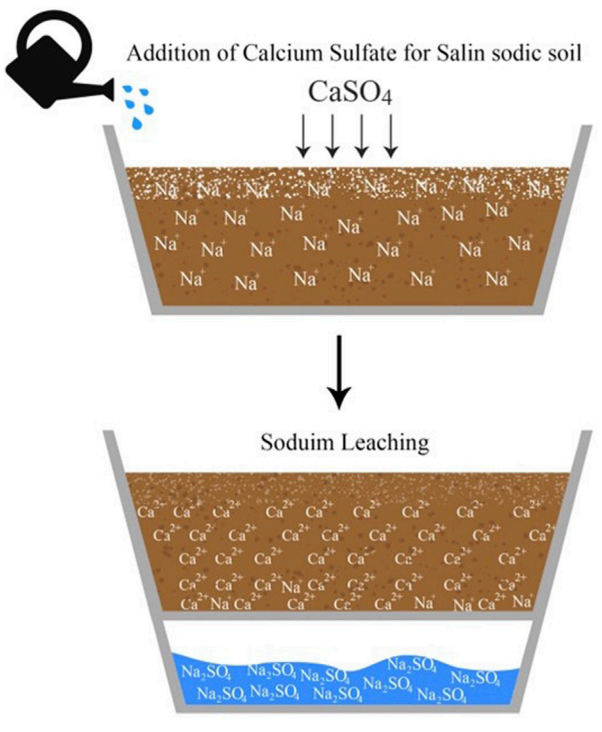

FIGURE 2
Reclamation of saline and sodic soils by using calcium sulfate.

Leaching of PG with distilled water shows that lead (Pb), selenium (Se), silver (Ag), zinc (Zn) and copper (Cu) were retained in soil surface and their contents in leached water were bellow recommended limits for drinking water, while arsenic (As), cadmium (Cd), chromium (Cr) and nickel (Ni) could present transfer risk to groundwater (Hassoune et al., 2017). Al-Hwaiti et al. (2010) concluded that As, Cd, Cr, Cu, uranium (U) and Zn were not leached from the Phosphogypsum in significant amounts, and they were not transferred easily to the aquatic environment. The PG leaching tests showed that Ca, fluoride (F), phosphorus (P), sulfur (S), silicon (Si), As, barium (Ba), Cr, Cu, nickel (Ni), Pb, strontium (Sr), Zn contents in leachate did not exceed the threshold limits. However, Zn, Cd and Se were above the allowed limits (Zmemla et al., 2020).

Soil nutrients losses, such as Ca, magnesium (Mg), potassium (K), and nitrogen (N) has been released by PG (Brien and Sumner, 2008) and gypsum (Alva and Gascho, 1991) applications.

Salinity is a growing threat to food security in arid and semi-arid regions. Phosphogypsum is an affordable saline soil amendment. In fact, Moroccan phosphate industry generates huge quantities of PG (around 25 MT/year) (Harrou et al., 2020). However, limited number of papers focus on the valorization of Moroccan PG in agriculture. The objectives of this study is to evaluate salts, nutrients, and trace elements removal in leachate of salt affected soils treated with G and different rates of PG, and to investigate the environmental impacts of G and PG on groundwater.

Materials and methods

Soil sampling and analysis

The bulk soil samples were collected at 0–20 cm soil depth from Sed El Masjoune (32°06′08.4″N 7°35′10.6″W), a well-known salt-affected region in Morocco (El hasini et al., 2019) and Sidi El Mokhtar (31°34′28.4″N 9°03′26.7 "W) region of Morocco (Figure 3).

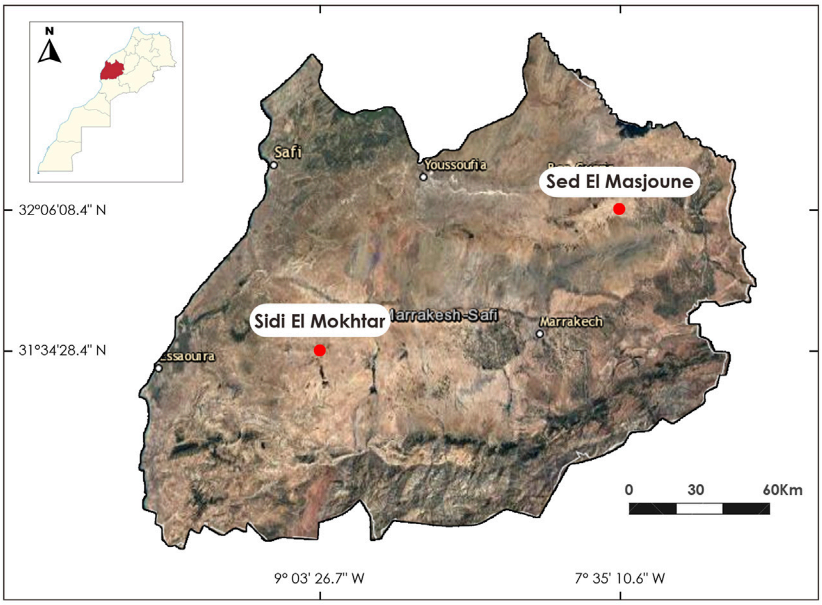

FIGURE 3
Location of collected soils.

Sed el Masjoune is a seasonal lake, and more than 10,000 ha of saline land surround this lake. It corresponds to the final valley, where water runoff stored on the lake's high plateaus evaporates during the hot seasons, causing the soil salinization (El hasini et al., 2019). It has a semiarid climate with an average annual precipitation of 200 mm/year and temperature ranges as min/max values of −3.6°C in winter and 48°C in summer (Zouahri et al., 2018).

Sidi El Mokhtar area is part of the large basin of the Tensift wadi. It is a semi-arid region with annual average precipitation of 180 mm and temperatures ranging from 15 to 20°C (Fathallah et al., 2021).

Soil samples were air dried, ground and passed through a 2 mm sieve to collect fine-earth fraction (<2 mm). Soil pH was measured in the 1:5 soil: water extract (ISO 10390). Soil salinity was determined by measuring EC of the extract (ECe) from saturated soil paste (Richards, 1954) and presented as mS/cm. Phosphorus content was determined by Olsen method (Olsen et al., 1954). Spectrophotometry (Agilent Technologies. Cary 60 UV-Vis) was used to determine, sulfate, ammonium (NH_4), chlorine (Cl) and nitrate contents. The sodium, potassium, calcium and magnesium contents were determined by atomic absorption spectroscopy (Agilent Technologies. 200 Series AA). Total lime was analyzed using the method of Allison. (1960). Heavy metals were determined by ICP (Agilent Technologies. 5110 ICP-OES). The ESP was calculated using standard equation (Qadir et al., 2007)

$$\mathbf{ESP} = \mathbf{Exchangeable}\,\{\mathbf{Na}/((\mathbf{Ca}+\mathbf{Mg}+\mathbf{K}+\mathbf{Na}))\}\mathbf{x\,100} \tag{3}$$

with all the cations expressed as $cmol_c$ kg.$^{-1}$

Soils, PG, G, water used for drainage and leached water analysis were carried out at the soil, plant, and water laboratory of the Agriculture Innovation Transfer Technololgy Center of the University Mohammed six Polytechnic at Ben Guerir, Morocco.

Based on the values of ECe and ESP (Table 1), the soil of Sidi El Mokhtar is classified as moderately saline soil and Sed El Masjoune soil is strongly saline-sodic soil (Qadir et al., 2007; Lech et al., 2016). Both the soils are categorized as moderately alkaline with respect to soil pH. Chemical characteristics of the soils used in this experiment are presented in Table 1.

The pH and EC of amendments were measured in the 1:5 PG or G: water extracts. Nutrients and heavy metals contents were quantified by ICP-OES. The results show (Table 2) that PG is acidic and richer on Ca, S and P than natural gypsum. However, the G is richer in Mg and K relative to PG. In terms of heavy metals content, PG is more charged with Ba, Cd, Cr, Cu, boron (B), molybdenum (Mo), antimony (Sb) and Se, while Gypsum contains more of Zn, cobalt (Co), Iron (Fe), aluminium (Al), lithium (Li), As, manganese (Mn) and Ni.

The pH and EC of water for drainage and leached water were measured by using calibrated pH (InoLab pH 7310) and conductivity meters (Mettler Toledo. SevenCompact) respectively. The Sulfate, Ammonium, Chlorine and Nitrate contents were quantified by Spectrophotometry. ICP-OES was used to determine the Phosphorus, Sodium, Potassium, Calcium, Magnesium and Heavy metals contents.

The SAR is calculated from the following equation (Qadir et al., 2007):

TABLE 1 Chemical characteristics of soils.

Properties	Sidi EL mokhtar	Sed EL masjoune	Properties	Sidi EL mokhtar	Sed EL masjoune
pH (1:5)	8.1	8.1	**Ba (mg/kg)**	92	181
ECe (mS/cm)	11.7	140.6	**Cd (mg/kg)**	2.4	0.2
ESP	7%	62%	**Co (mg/kg)**	7	11
P_2O_5 (mg/kg)	67	43	**Cr (mg/kg)**	30	28
K_2O (mg/kg)	308	697	**Cu (mg/kg)**	11	20
CaO (mg/kg)	7 984	10,923	**Fe (mg/kg)**	9038	14,536
Na_2O (mg/kg)	759	26,628	**Li (mg/kg)**	18	51
MgO (mg/kg)	1 067	2 496	**Mn (mg/kg)**	211	420
$CaCO_3$ (%)	8.4	7.5	**Mo (mg/kg)**	<0.01	<0.01
SO_4 (mg/kg)	3211	2728	**Ni (mg/kg)**	17	20
NO_3 (mg/kg)	40	66	**Pb (mg/kg)**	7.4	8.8
NH_4 (mg/kg)	6	9	**Sb (mg/kg)**	1.3	0.9
Clay (%)	20	26	**Se (mg/kg)**	<0.01	<0.01
Silt (%)	28	28	**Zn (mg/kg)**	50	39
Sand (%)	52	46	As (mg/kg)	6	6
OM (%)	1.86	1.61	B (mg/kg)	20	38

TABLE 2 PG and G chemical characteristics.

Properties	PG	G	Properties	PG	G
pH	5.8	8.1	**Ba** (mg/kg)	54.4	15.6
EC (mS/cm)	2.4	2.3	**Cd** (mg/kg)	4.7	<0.003
Ca (%)	22.8	17.0	**Zn** (mg/kg)	8.5	9.9
S (%)	23.7	13.1	**Co** (mg/kg)	0.1	1.9
P (%)	0.8	0.02	**Cr** (mg/kg)	6.3	4.0
K (mg/kg)	869	969	**Cu** (mg/kg)	2.6	2.4
Mg (mg/kg)	259	7587	**Fe** (mg/kg)	126	2606
Al (mg/kg)	719	1328	**Li** (mg/kg)	0.7	32.8
As (mg/kg)	1.3	1.4	**Mn** (mg/kg)	1.8	50.3
B (mg/kg)	21.5	7.2	**Mo** (mg/kg)	1.0	<0.01
Sb (mg/kg)	0.7	<0.01	**Ni** (mg/kg)	1.8	4.2
Se (mg/kg)	0.4	<0.01	**Pb** (mg/kg)	1.9	1.4

$$\mathbf{SAR} = [\mathbf{Na}+]/\ (([\mathbf{Ca}2+]\ +\ [\mathbf{Mg}2+]))/2)\ 1/2 \tag{4}$$

Na, Ca and Mg expressed as meq/l.

Nutrients and heavy metals contents of the water used for drainage are below the recommended limits for irrigation water, excluding sodium and molybdenum contents (Table 3).

According to (Suarez et al., 2006), Irrigation water with values of SAR higher than 4 Meq/l, represents sodicity risks for the soils. For this reason, we used the PG also for the soil of Sidi El Mokhtar even if it was not initially sodic (sodicity problem prediction).

The saturation index is one of the crucial criteria that affect the thermodynamic stability of groundwater. Saturation index of mineral is calculated by using the following equation (Garrels and Mackenzie, 1967):

$$SI = \log\left(K_{IAP}/K_{sp}\right) \tag{5}$$

K_{IAP} is the ion activity product. It is determined based on the chemical analysis of the water.

K_{SP} is the mineral's solubility product

SI was calculated using the PHREEQC software (Parkhurst and Appelo, 1999).

Trials installation

The pot experiment was conducted at the experimental farm of Mohamed six Polytechnic University (UM6P) in Ben Guerir Morocco. Moroccan PG is the first amendment used. The second one was is the natural Gypsum of agriculture grade commonly used to reclaim sodic and saline-sodic soils in agriculture fields. Different experimental treatments [Control (T1), 15 t/ha of G (T2), 15 (T3), 30 (T4) and 45 (T5) t/ha of PG] were used. Each pot was filled with 10 kg of the processed soil (<2 mm). The PG and G were mixed with the upper 9 cm of the soil. The base of pots was perforated and covered with stones to avoid soil leakage and to ensure water drainage; the leached water was collected in small basins under the pots for analyses.

The thickness and the diameter of the soil column were 19 and 22 cm, respectively (Figure 4). The water replenishment was intermittent.

TABLE 3 Water for drainage chemical properties.

Properties	Water for drainage	Irrigation water guidelines (moroccan ministry of equipment and ministry charged of territorial planning, 2002; FAO, 1985.)	Properties	Water for drainage	Irrigation water guidelines (moroccan ministry of equipment and ministry charged of territorial planning, 2002; FAO, 1985)
pH	7.8	6.5–8.4	**Ba (mg/L)**	0.1	
EC (mS/cm)	1.5		**Cd (mg/L)**	<0.003	0.01
Cl (mg/L)	252	350	**Co (mg/L)**	<0.01	0.05
SO_4 (mg/L)	64	250	**Cr (mg/L)**	<0.01	0.1
NO_3 (mg/L)	24.8	30	**Cu (mg/L)**	<0.01	0.2
PO_4 (mg/L)	0.05		**Fe (mg/L)**	0.03	5
NH_4 (mg/L)	0.04		**Li (mg/L)**	0.09	2.5
K (mg/L)	28.6		**Mn (mg/L)**	<0.01	0.2
Na (mg/L)	215	69	**Mo (mg/L)**	0.05	0.01
Ca (mg/L)	85		**Ni (mg/L)**	<0.01	0.2
Mg (mg/L)	67		**Pb (mg/L)**	<0.01	5
Al (mg/L)	0.03	**5**	**Sb (mg/L)**	0.04	
As (mg/L)	<0.01	0.1	**Se (mg/L)**	<0.01	0.02
Zn (mg/L)	<0.01	**2**	**B (mg/L)**	0.5	3
SAR (Meq/l)	4.2				

Statistical analysis

The experiment was conducted in a complete randomized design (CRD), in which the treatments are entirely assigned randomly; indeed, each experimental unit has an equal probability of obtaining any treatment (FAO, 1999; Alkutubi 2012), with seven replications for Sidi El Mokhtar soil and eight replications for Sed El Masjoune soil. Data were analyzed statistically using IMB SPSS (Version 20, IBM SPSS Inc., Chicago, IL, USA). . One-way analysis of variance (ANOVA), tests were performed to relieve the effect of treatments on pH, Ec, salts, nutrients, heavy metals contents in leached water. If the differences between the treatment were significant ($p < 0.05$), the Student-Newman-keuls Test was used as a post hoc mean separation test to detect mean differences (Kucuk et al., 2016). All data are presented as mean ± standard deviation.

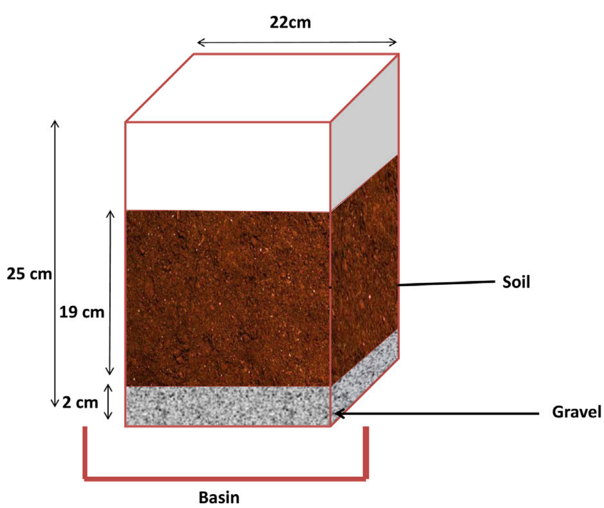

FIGURE 4
Leaching experimental design.

Results and discussion

pH of leached water

The amendment application did not significantly affect the pH of leached water (Figure 5). Several authors confirmed that PG (Gharaibeh et al., 2011) and G (Chaganti et al., 2015) did not influence soil pH after leaching.

Salts and nutrients leaching

Results of salts, and nutrients contents of leachate of Sidi El Mokhtar soil showed that PG application removed significant amounts of Na and Cl. The same trend was observed for EC of leached water. Indeed, the increase in salts concentrations in leachate results in an increase of its EC. Compared to the control, EC of leached water was increased by 23 and 28% with T4 and T5 respectively, and correspondingly, Cl content increased by 27 and 33%, and sodium content by 36 and 33% (Table 4). The increased salts in leachate can be reflected by soil salinity reduction. Diop et al. (2019) concluded that PG offered significant soil salinity reduction that is up to 45%.

In addition to the removal of salts, the PG application contributed to substantial nutrients losses, such as Ca, Mg, K, and N. These elements play key role in plant development and soil fertility. Similar results were reported by (Brien and Sumner, 2008) who affirmed that the use of PG has improved Ca, Mg, K composition of the leachate. Shainberg et al. (1989) reported that the use of PG renders Mg and K prone to leaching and proposed post drainage fertilization to restore balanced nutrition. Because the saline and sodic soils fertility is typically low, the use of PG must be reasoned, mainly if it is applied frequently.

Even though the effect of 15 t/ha of natural gypsum and PG were not statistically different, the latter increased the EC of the leachate by 6% compared to the former. The same trend was observed for Cl, Na and Mg, this finding can be explained by the fact that PG was more acidic than G (Table 2). The acidic conditions favor salts solubilization and ameliorate their leaching (Phung et al., 1979).

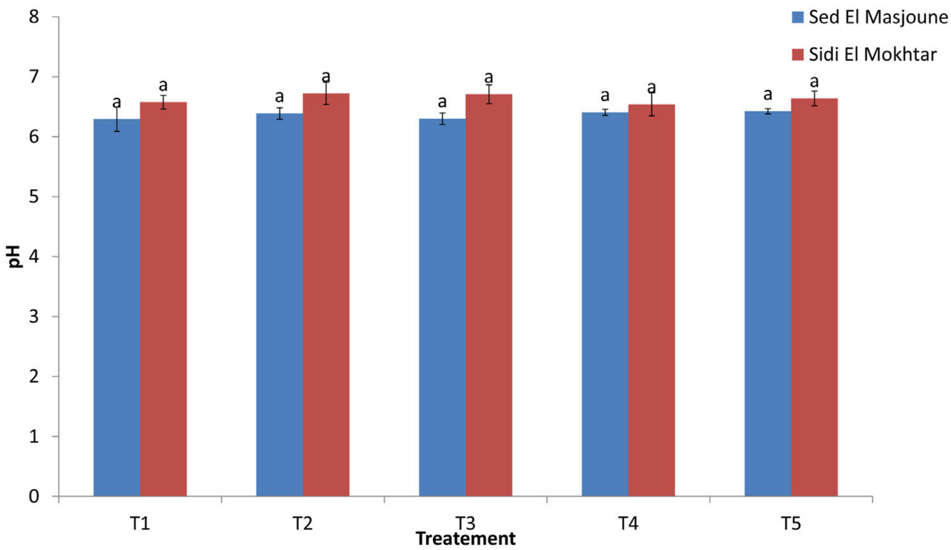

FIGURE 5
pH of leached water for different treatments. In a column series, same letters indicate no significant differences among treatments.

TABLE 4 EC, salts, and nutrients contents of leachate of Sidi El Mokhtar soil for different treatments. In a line series, same letters indicate no significant differences among treatments ($p < 0.05$, S-N-K 's test).

Properties	Treatments				
	T1	T2	T3	T4	T5
EC (mS/cm)	41.2 ± 5.7 b	40.9 ± 3.9 b	43.4 ± 2.0 b	50.6 ± 6.8 a	52.6 ± 3.3 a
Na (g/L)	3.0 ± 0.4 b	2.9 ± 0.4b	3.1 ± 0.2b	4.1 ± 0.7 a	4.0 ± 0.6 a
Mg (g/L)	2.0 ± 0.3 b	2.0 ± 0.4 b	2.1 ± 0.2 b	2.8 ± 0.6 a	2.8 ± 0.4 a
K (mg/L)	65 ± 10 b	81 ± 18 ab	74 ± 5 ab	81 ± 9 ab	87 ± 18 a
SO_4 (g/L)	2.0 ± 0.2 a	2.2 ± 0.4 a	1.9 ± 0.3 a	2.4 ± 0.4 a	2.3 ± 0.4 a
NO_3 (g/L)	2.6 ± 0.6 b	2.7 ± 0.7 b	2.8 ± 0.5 b	3.8 ± 0.7 a	3.7 ± 0.7 a
P_2O_5 (mg/L)	1.21 ± 0.28 a	1.13 ± 0.45 a	1.22 ± 0.36 a	1.54 ± 0.49 a	1.33 ± 0.30 a
NH_4 (mg/L)	7.2 ± 0.7 a	7.4 ± 1.5 a	7.9 ± 0.4 a	8.1 ± 0.7 a	8.7 ± 1.2 a
Ca (g/L)	4.0 ± 0.6 b	4.3 ± 0.6 b	4.3 ± 0.3 b	5.6 ± 1.2 a	5.6 ± 0.7 a
Cl (g/L)	15 ± 2 b	15 ± 2 b	15 ± 1 b	19 ± 3 a	20 ± 2 a

The NH_4, P_2O_5 and SO_4 contents of the leachate were not statistically significant. The ammonium is known as a low mobile element in the soil (Li et al., 2003)and its initial soil content was low (6 ppm). Phosphorus has a limited mobility in the soil and tends to precipitate, particularly, in soils with alkaline pH range (Llanderal et al., 2021). Additionally, P has a high soil matrix fixation rate (Shen et al., 2011) Hence, low concentrations of ammonium and phosphorus in the leached water were recorded.

The EC, salts, and nutrients contents of the leachate from Sed El Masjoune soil are presented in Table 5. All amendments application rates significantly increased sodium concentration in the drainage water. The most significant rise of Na was recorded with T4 and T5 treatments with subsequent increase of EC of the leachates. Calcium sulfate furnishes soluble calcium to substitute exchangeable sodium, which results in sodium leaching from the saline-sodic soil (FAO, 1988). Increasing the PG rate induces the enhancement of soluble calcium in the soil. As a result, a large amount of sodium was substituted.

The same trend was observed for NH_4 content.

The amendments (PG and G) did not produce significant effect in terms of removing Cl, SO_4, NO_3, Mg, Ca, K and P_2O_5. These findings can be explained by the fact that one time drainage was not enough to produce significant effect, especially when the soil is more charged with salts. Sed El Masjoune's soil is strongly saline-sodic, with an ESP of 62%, whereas Sidi El Mokhtar's soil is saline with an ESP of 7% (Table 1). Goncalo Filho et al. (2020) Reported that Calcium ions must eliminate a significant portion of exchangeable sodium to improve sodic soil. Which explains that the PG used rates were more effective for the soil of Sidi El Mokhtar than Sed El Masjoune.

Abdel-Fattah (2012) reported that total soluble salts removal in the leachate was related to increased number of leaching performed. Moreover, Gharaibeh et al. (2010) affirmed that most Na removed was detected after three and four drainage sessions.

For both soils, the highest doses of PG (30 and 45 t/ha) are more efficient for removing the salts. A Similar finding was reported by Gharaibeh et al. (2014) who indicated that effluent sodium levels were higher with rising PG rates.

Heavy metals leaching

For the leachate of Sidi El Mokhtar soil. The amendment application did not result in significant differences on leachate concentrations of B, Co, Li, Ni, Zn, Sb and Mo (Table 6). Zn is a very mobile element in PG (Al-Masri et al., 2004; Al-Hwaiti et al., 2019) but it is affected by pH, indeed under alkaline conditions, Zn can be almost undetected (Zmemla et al., 2016). Arsenic, chromium, lead, and selenium leachate values were <0.01 mg/L regardless of treatments. Hassoune et al. (2017) Indicated that Phosphogypsum leachate had low values of Se and Pb. However, Zmemla et al. (2016) reported a potential release of Se and Cr from PG. The T4 and T5 have caused an increase of Al, Cd and Mn contents in the leached water. In addition, all amendments rates (G and PG) significantly affected Ba content mainly with T4 and T5 treatments. Copper and iron levels in leachate were significantly higher with T4 compared to the other treatments. Al-Hwaiti et al. (2005) reported that Cu had a highest mobility during the PG leaching experiments. While, Al and Fe have shown limited removal (Zmemla et al., 2016).

All heavy metals contents in the leachate of Sed El Masjoune soil have not shown any significant differences between the treatments (Table 7). Al-Masri et al. (2004) attributed the low removal of trace elements to alkaline conditions which strongly decrease their mobility and solubility.

The comparison of leachate trace element contents with irrigation water and drinking water guidelines standards is necessary to reveal the effects of PG and G applications on the

TABLE 5 EC, salts, and nutrients contents of leachate of Sed El Masjoune soil for different treatments. In a line series, same letters indicate no significant differences among treatments (p < 0.05, S-N-K 's test).

Properties	Treatments				
	T1	T2	T3	T4	T5
EC (mS/cm)	218 ± 4 b	218 ± 5 b	220 ± 3 b	222 ± 2 a	222 ± 2 a
Na (g/L)	70 ± 6 b	72 ± 6 ab	74 ± 5 ab	79 ± 5 a	78 ± 5 a
Mg (g/L)	8.2 ± 1.1 a	8.7 ± 1.1 a	8.3 ± 1.1 a	8.3 ± 0.6 a	8.4 ± 0.8 a
K (g/L)	1.8 ± 0.3 a	1.7 ± 0.08 a	1.9 ± 0.2a	1.8 ± 0.09a	1.7 ± 0.1 a
SO_4 (g/L)	2.8 ± 0.5 a	2.4 ± 0.6 a	2.5 ± 0.5a	2.5 ± 0.4 a	2.2 ± 0.4a
NO_3 (g/L)	3.0 ± 0.4 a	3.19 ± 0.4 a	3.0 ± 0.4 a	2.8 ± 0.3a	2.9 ± 0.3 a
P_2O_5 (mg/L)	<0.02	<0.02	<0.02	<0.02	<0.02
NH_4 (mg/L)	28 ± 2 b	27 ± 2 b	29 ± 3 ab	31 ± 2 a	30 ± 3 a
Ca (g/L)	9.8 ± 1.8 a	10.6 ± 0.6 a	9.3 ± 0.3 a	10.3 ± 0.7 a	10.9 ± 1.3 a
Cl (g/L)	154 ± 11 a	158 ± 13 a	165 ± 8 a	165 ± 9 a	164 ± 9 a

TABLE 6 Heavy metals contents of leachate of Sidi El Mokhtar soil for different treatments. Same letters in a line series indicate no significant differences among treatments (p < 0.05, S-N-K's test).

Heavy metals (mg/L)	T1	T2	T3	T4	T5	Irrigation water guidelines (Moroccan Ministry of Equipment and Ministry charged of Territorial Planning 2002; FAO, 1985)	Drinking water guidelines (WHO, 2017)
Al	0.074 ± 0.015 b	0.078 ± 0.015 b	0.076 ± 0.017 b	0.125 ± 0.039 a	0.117 ± 0.044 ab	5	0.2
B	0.625 ± 0.097 a	0.571 ± 0.053 a	0.575 ± 0.039 a	0.555 ± 0.045 a	0.585 ± 0.042 a		2.4
Ba	0.343 ± 0.047 b	0.403 ± 0.053 ab	0.368 ± 0.041 ab	0.430 ± 0.070 a	0.434 ± 0.038 a		1.3
Cd	0.025 ± 0.004 ab	0.023 ± 0.003 b	0.025 ± 0.005 ab	0.029 ± 0.005 a	0.030 ± 0.003 a	0.01	0.003
Co	0.035 ± 0.002 a	0.035 ± 0.004 a	0.034 ± 0.005 a	0.037 ± 0.004 a	0.038 ± 0.003 a		
Cu	0.052 ± 0.013 ab	0.044 ± 0.014 b	0.046 ± 0.01 ab	0.064 ± 0.008 a	0.048 ± 0.018 ab	0.2	2
Fe	0.051 ± 0.012 b	0.026 ± 0.004 c	0.032 ± 0.009 c	0.079 ± 0.012 a	0.051 ± 0.011 b	5	0.3
Li	1.396 ± 0.369 a	1.206 ± 0.265 a	1.174 ± 0.171a	1.360 ± 0.225a	1.368 ± 0.138a	2.5	
Mn	1.135 ± 0.236 b	1.015 ± 0.273 b	1.128 ± 0.072 b	1.323 ± 0.299 a	1.486 ± 0.164 a	0.2	0.1
Mo	0.031 ± 0.009 a	0.026 ± 0.001 a	0.026 ± 0.003 a	0.025 ± 0.003 a	0.025 ± 0.003 a	0.01	
Ni	0.039 ± 0.005 a	0.038 ± 0.005 a	0.043 ± 0.003 a	0.037 ± 0.005 a	0.040 ± 0.007 a	0.2	0.07
Sb	0.029 ± 0.007 a	0.026 ± 0.009 a	0.022 ± 0.007 a	0.025 ± 0.008 a	0.025 ± 0.008 a		
Zn	0.016 ± 0.010 a	0.025 ± 0.012 a	0.028 ± 0.017 a	0.019 ± 0.005 a	0.028 ± 0.009 a	2	3
As	<0.01	<0.01	<0.01	<0.01	<0.01	0.1	
Cr	<0.01	<0.01	<0.01	<0.01	<0.01	0.1	
Pb	<0.01	<0.01	<0.01	<0.01	<0.01	5	0.01
Se	<0.01	<0.01	<0.01	<0.01	<0.01	0.02	0.04

environment. For all treatments, trace elements were conformed to irrigation water standards, except Mn, Cd and Mo for Sidi El Mokhtar and Li and Mn for Sed El Masjoune leachates (Tables 6 and 7). When comparing the drainage water with drinking water guidelines, the results showed that for Sidi El Mokhtar soil Cd and Mn and for Sed El Masjoune Pb and Mn contents exceeded the limits regardless of the treatments.

In the light of findings from the present study, for most heavy metals analyzed, the obtained values remained below the recommended limits of drinking and irrigation waters. Therefore, leachate of soils may not negatively affect groundwater quality. In fact, the alkaline conditions in Morocco for irrigation water and soils (Carle, 1930; El Oumlouki et al., 2014; Touhtouh et al., 2014) could lead to the safe use of PG and G in Morocco, considering, that heavy metals solubility and leachability decrease at high pH.

Saturation index

The saturation index determines the degree of chemical equilibrium between water and mineral in the aquifer matrix, and it identifies the dissolution or precipitation process regarding the water-rock interaction (Aghazadeh et al., 2017).

The mineral is in an equilibrium state when SI = 0. When SI exceeds zero, the mineral is oversaturated and tends to precipitate in order to attain equilibrium. SI less than zero indicates the undersaturation and the mineral will dissolve until the balance achievement (Reyes-Santiago et al., 2021).

In this study, the SI of minerals reveals three distinct groups in the initial water stat (Figures 6, 7):

Group A: Alunite, jarosite-K, halite, anhydrite, and gypsum were undersaturated.

(Bernis), 2015 reported similar findings, in fact halite, anhydrite, and gypsum were undersaturated in the alkaline water.

Group B: Hematite and goethite were oversaturated and tended to precipitate.

Group C: Barite, gibbsite and hydroxyapatite were close to the balanced state.

For Sidi El Mokhtar soil leached (Figure 6), except for hematite, and goethite, soil leaching generates an increase on the mineral's saturation index for all treatment compared to the initial stat of water. Alunite was passed from undersaturation state (SI = -6.94) to saturation stat after drainage applying, especially with 30 and 45 t/ha of PG, respectively SI = 4.96 and 4.48. Anhydrite and gypsum moved from the undersaturated to equilibrium state due to drainage

TABLE 7 Heavy metals contents of leachate of Sed El Masjoune soil for different treatments. Same letters in a line series indicate no significant differences among treatments ($p < 0.05$, S-N-K's test).

Heavy metals (mg/L)	T1	T2	T3	T4	T5	Irrigation water guidelines (Moroccan Ministry of Equipment and Ministry charged of Territorial Planning, 2002; FAO, 1985)	Drinking-water guidelines (WHO, 2017)
Al	0.087 ± 0.067 a	0.079 ± 0.059 a	0.052 ± 0.012 a	0.044 ± 0.013 a	0.059 ± 0.026 a	5	0.2
B	0.602 ± 0.088 a	0.602 ± 0.106 a	0.538 ± 0.106 a	0.482 ± 0.048 a	0.538 ± 0.106 a		2.4
Ba	0.303 ± 0.031 a	0.294 ± 0.033 a	0.281 ± 0.034 a	0.274 ± 0.022 a	0.265 ± 0.017 a		1.3
Li	4.007 ± 0.788 a	4.059 ± 0.553 a	4.008 ± 0.803 a	3.574 ± 0.310 a	4.017 ± 0.300 a	2.5	
Ni	0.016 ± 0.004 a	0.017 ± 0.003 a	0.019 ± 0.002 a	0.019 ± 0.002 a	0.019 ± 0.003 a	0.2	0.07
Zn	0.070 ± 0.011 a	0.065 ± 0.018 a	0.078 ± 0.018 a	0.061 ± 0.010 a	0.063 ± 0.011 a	2	3
Pb	0.026 ± 0.007 a	0.025 ± 0.010 a	0.025 ± 0.009 a	0.018 ± 0.002 a	0.021 ± 0.004 a	5	0.01
Sb	0.023 ± 0.008 a	0.021 ± 0.010 a	0.024 ± 0.007 a	0.019 ± 0.003 a	0.021 ± 0.004 a		
Mn	0.551 ± 0.062 a	0.514 ± 0.117 a	0.522 ± 0.068 a	0.471 ± 0.036 a	0.508 ± 0.027 a	0.2	0.1
As	<0.01	<0.01	<0.01	<0.01	<0.01	0.1	
Cd	<0.003	<0.003	<0.003	<0.003	<0.003	0.01	0.003
Co	<0.01	<0.01	<0.01	<0.01	<0.01	0.05	
Cr	<0.01	<0.01	<0.01	<0.01	<0.01	0.1	
Fe	<0.01	<0.01	<0.01	<0.01	<0.01	5	0.3
Mo	<0.01	<0.01	<0.01	<0.01	<0.01	0.01	
Cu	<0.01	<0.01	<0.01	<0.01	<0.01	0.2	2
Se	<0.01	<0.01	<0.01	<0.01	<0.01	0.02	0.04

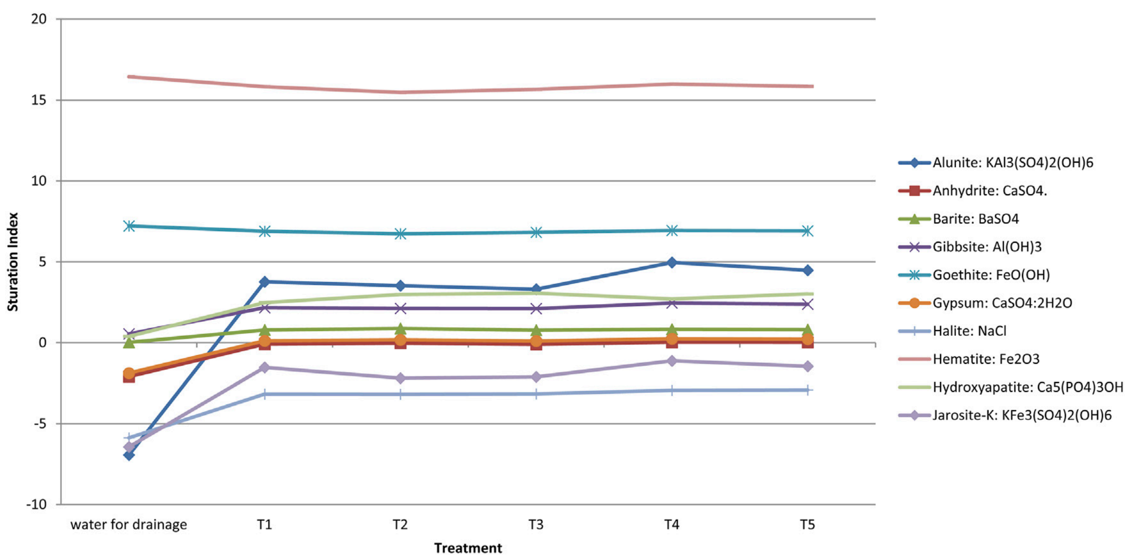

FIGURE 6
Saturation index of Sidi El Mokhtar soil leached water.

application. In addition, because of leaching, the saturation index of barite increased slightly, but it remains close to the balance state. Hydroxyapatite and gibbsite were transferred from the equilibrium to the oversaturation state. Although, Halite and Jarosite-K saturation indices increased after drainage, they remained in the undersaturation range. For goethite and

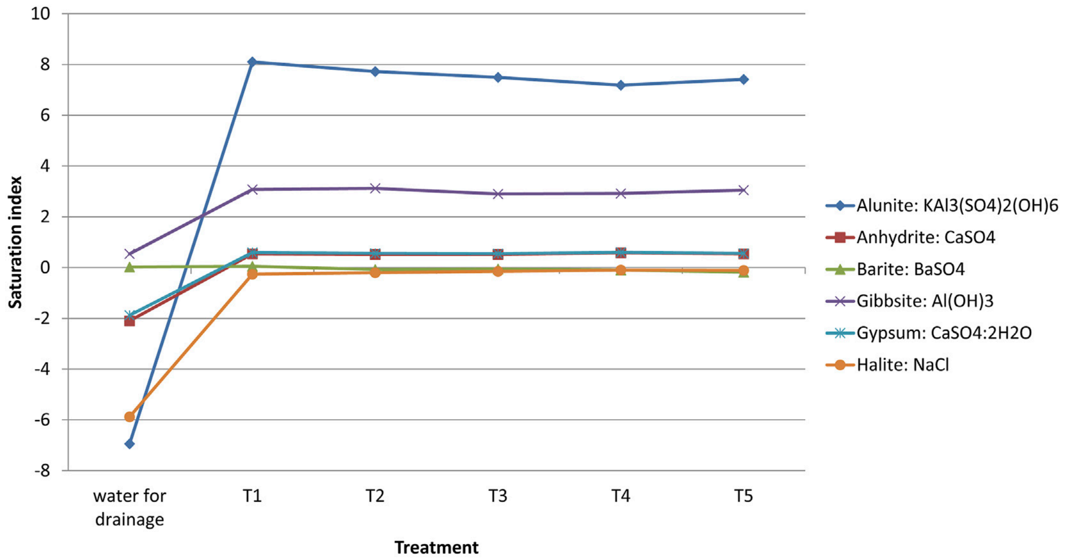

FIGURE 7
Saturation index of Sed El Masjoune soil leached water.

hematite, a slight decrease in SI was observed when drainage was applied.

Halite, gypsum, and anhydrite were moved from an undersaturation, shape in the initial water, to a steady state in the leached water of Sed El Masjoune soil. The gibbsite was converted from equilibrium to oversaturation state whatever treatment. The application of leaching caused an increase in the saturation index of alunite and did not affect the barite SI (Figure 7).

The leaching of the component elements (Ca, SO_4, K, Al, P, Na, Cl, Ba and Fe) of the studied minerals from the soil into the leached water results in minerals precipitation or saturation, which explains the augmentation of the SI (Maia, 2018). Water pH impacts significantly the saturation index (Gitari et al., 2011). We noticed a reduction in the leached water's pH compared to the initial pH (Figure 5). Nordstrom and Ball (1989), reported the gibbsite index saturation increasing following the pH reduction from eight to 6.

The saturation index was not affected by the amendment application. Water passing through the soil has increased the saturation index of the main minerals, which will result in groundwater mineral precipitation (Zhang et al., 2020).

Conclusion

It was concluded that PG application to soil has increased salts significantly in the leachate. Compared to the control, two treatments (T4 and T5) have removed 36 and 33% of sodium in leachate of Sidi El Mokhtar soil, and 13 and 11% in leachate of Sed El Masjoune respectively. The PG application induced losses of beneficial nutrients from the soil, thus fertilization after leaching is recommended. The PG had high ability to leach salts compared to G. The majority of analyzed trace elements in the leachates were below the recommended limits for drinking and irrigation water quality. The saturation index was increased after applying drainage without being affected by amendment application. The present work suggested that PG can be used for reclamation of saline and saline-sodic soils with no negative environmental impacts.

Data availability statement

The raw data supporting the conclusion of this article will be made available by the authors, without undue reservation. Data can be provided upon request from the corresponding author.

Author contributions

MBO: contributed to the study conception and design, investigation, analyzed the data and original draft writing; RC-A: language editing and substantial correction; MEG: co-supervisor and contributed to the study conception and design; KEO: contributed to the study conception and design; AS: contributed to the chemical analysis; KEM: supervisor, contributed to the study conception and design, language editing and substantial correction. All authors have read and agreed to the published version of the manuscript.

Funding

This research was financially supported by the OCP sustainability platform under the specific agreement “AS 49—P1”.

Acknowledgments

Authors would like to impressively acknowledge the AITTC Soil, Water and Plant Analysis Laboratory, the AITTC experimental farm for providing the facilities and OCP for financial support to carry out the present investigation.

Conflict of interest

KEO are employed by the company OCP Group manufacturing company.

The remaining authors declare that the research was conducted in the absence of any commercial or financial relationships that could be construed as a potential conflict of interest.

Publisher's note

All claims expressed in this article are solely those of the authors and do not necessarily represent those of their affiliated organizations, or those of the publisher, the editors and the reviewers. Any product that may be evaluated in this article, or claim that may be made by its manufacturer, is not guaranteed or endorsed by the publisher.

References

Abdel-Fattah, M., and El-Naka, E. S. (2015). Empirical approach of leaching curves for determining the efficiency of reclaiming saline-sodic soils in sahl el-Tina, sinai, Egypt. *Ijpss* 8, 1–9. doi:10.9734/ijpss/2015/18606

Abdel-Fattah, M. K. (2012). Role of gypsum and compost in reclaiming saline-sodic soils. *Iosrjavs* 1, 30–38. doi:10.9790/2380-0133038

Adimalla, N., and Qian, H. (2019). Groundwater quality evaluation using water quality index (WQI) for drinking purposes and human health risk (HHR) assessment in an agricultural region of Nanganur, south India. *Ecotoxicol. Environ. Saf.* 176, 153–161. doi:10.1016/j.ecoenv.2019.03.066

Aghazadeh, N., Chitsazan, M., and Golestan, Y. (2017). Hydrochemistry and quality assessment of groundwater in the ardabil area, Iran. *Appl. Water Sci.* 7, 3599–3616. doi:10.1007/s13201-016-0498-9

Agostini, F. T., Tei, M., Silgram, M., Farneselli, P., Benincasa, M. F., and Aller, M. F. (2010). “Decreasing nitrate leaching in vegetable crops with better N management,” in *Genetic engineering, biofertilisation, soil quality and organic farming* (E. Lichtfouse), 147–200. doi:10.1007/978-90-481-8741-610.1007/978-90-481-8741-6_6

Al-Hwaiti, M., Ibrahim, K. A., and Harrara, M. (2019). Removal of heavy metals from waste phosphogypsum materials using polyethylene glycol and polyvinyl alcohol polymers. *Arabian J. Chem.* 12 (8), 3141–3150. doi:10.1016/j.arabjc.2015.08.006

Al-Hwaiti, M., Carney, V., Ranville, J. F., and Ross, P. E. (2005). Heavy metal assessment of phosphogypsum waste stockpile material from Jordan. *Asmr* 2005, 1–22. doi:10.21000/jasmr05010001

Al-Hwaiti, M. S., Ranville, J. F., and Ross, P. E. (2010). Bioavailability and mobility of trace metals in phosphogypsum from Aqaba and Eshidiya, Jordan. *Geochemistry* 70 (3), 283–291. doi:10.1016/j.chemer.2010.03.001

Al-Masri, M. S., Amin, Y., Ibrahim, S., and Al-Bich, F. (2004). Distribution of some trace metals in Syrian phosphogypsum. *Appl. Geochem.* 19 (5), 747–753. doi:10.1016/j.apgeochem.2003.09.014

Alkutubi, H. (2012). Completely random design and least significant differences for breast cancer in Al-najaf city (2005-2009). *Int. Res. J. Appl. Basic Sci.* 3 (6), 1178–1182.

Allison, L. E. (1960). Wet-combustion apparatus and procedure for organic and inorganic carbon in soil. *Soil Sci. Soc. Am. J.* 24 (1), 36–40. doi:10.2136/sssaj1960.03615995002400010018x

Alva, A. K., and Gascho, G. J. (1991). Differential leaching of cations and sulfate in gypsum amended soils. *Commun. Soil Sci. Plant Analysis* 22 (11–12), 1195–1206. doi:10.1080/00103629109368484

Antipolis, S. (2003). Les menaces sur les sols dans les pays mediterraneens. Plan Bleu, 80. Bernis, NAnalyse Statistique Et Geochimique De La Dynamique Des Parametres Physico-Chimiques Des Eaux Souterraines Du Synclinal De Ghassira Algerie Orientale Brinis. *Larhyss J.* 22, 123–137.

Carle, G. (1930). Étude sur les Sols marocains. *jatba* 10 (101), 15–21. doi:10.3406/jatba.1930.4819

Chaganti, V. N., Crohn, D. M., and Šimůnek, J. (2015). Leaching and reclamation of a biochar and compost amended saline-sodic soil with moderate SAR reclaimed water. *Agric. Water Manag.* 158, 255–265. doi:10.1016/j.agwat.2015.05.016

Corwin, D. L. (2021). Climate change impacts on soil salinity in agricultural areas. *Eur. J. Soil Sci.* 72 (2), 842–862. doi:10.1111/ejss.13010

Cuadri, A. A., Pérez-Moreno, S., Altamar, C. L., Navarro, F. J., and Bolívar, J. P. (2021). Phosphogypsum as additive for foamed bitumen manufacturing used in asphalt paving. *J. Clean. Prod.* 283, 124661. doi:10.1016/j.jclepro.2020.124661

Devi, S., Nandwal, A. S., Angrish, R., Arya, S. S., Kumar, N., and Sharma, S. K. (2016). Phytoremediation potential of some halophytic species for soil salinity. *Int. J. Phytoremediation* 18 (7), 693–696. doi:10.1080/15226514.2015.1131229

Diop, T., Ndiaye, R., Sow, S. A., and Ba, D. D. (2019). Analyse des effets du phophogypse et du fumier sur la salinité de la cuvette de Ndiol dans le Delta du fleuve Sénégal Résumé. *Afrique Sci.* 15 (4), 71–80.

El hasini, S., Iben. HalimaHalima, O., El. Azzouzi, M., Douaik, A., Azim, K., and Zouahri, A. (2019). Organic and inorganic remediation of soils affected by salinity in the sebkha of sed el mesjoune - marrakech (Morocco). *Soil Tillage Res.* 193, 153–160. doi:10.1016/j.still.2019.06.003

El Mejahed, K., Zeroual, Y., and Hiltonno, J. (2020). “Valorisation of phosphogypsum as amendment for the reclamation of saline/sodic soils: Agronomic field trials - Morocco,” in *Phosphogypsum leadership innovation partnership* (IFA Paris), 60–69.

El Oumlouki, K., Moussadek, R., Zouahri, A., Dakak, H., Chati, M., and El Amrani, M. (2014). Étude de la qualité physico-chimique des eaux et des sols de la région Souss Massa, (Cas de périmètre Issen), Maroc (Study of physic-chemical quality of water and soil in the region Souss Massa (Case perimeter Issen), Morocco). *J. Mat. Environ. Sci.* 5 (S2), 2365–2374.

FAO (1999). “A statistical manual for forestry research. Forestry research support programme,” in *Status of the world's soil resources (SWSR) - main report, food and agriculture organization of the united nations and intergovernmental technical panel on soils* (Rome, Italy: FAO and ITPS). Available at: https://www.fao.org/3/x6831e/X6831E00.htm#TOC.

FAO (1988). Salt-affected soils and their management. Available at: http://www.fao.org/3/x5871e/x5871e00.htm.

FAO (1985). Water quality for agriculture. Available at: https://www.fao.org/3/T0234E/T0234E01.htm.

Fathallah, F. E., Algouti, A., and Algouti, A. (2021). Normalized difference vegetation index (NDVI) of the chichaoua watershed-Morocco: Comparison and evolution. *J. Anal.* 3, 65–73. doi:10.48402/IMIST.PRSM/jasab-v3i1.28247

Garrels, R., and Mackenzie, F. (1967). "Origin of the chemical compositions of some springs and lakes," in *Equilibrium concepts in natural water systems*. Editor R. F. Ground (Washington: American Chemical Society Publications). doi:10.1021/ba-1967-0067.ch010

Gharaibeh, M. A., Eltaif, N. I., and Albalasmeh, A. A. (2011). Reclamation of highly calcareous saline sodic soil using Atriplex halimus and by-product gypsum. *Int. J. Phytoremediation* 13 (9), 873–883. doi:10.1080/15226514.2011.573821

Gharaibeh, M. A., Eltaif, N. I., and Shra'ah, S. H. (2010). Reclamation of a calcareous saline-sodic soil using phosphoric acid and by-product gypsum. *Soil Use Manag.* 26 (2), 141–148. doi:10.1111/j.1475-2743.2010.00260.x

Gharaibeh, M. A., Rusan, M. J., Eltaif, N. I., and Shunnar, O. F. (2014). Reclamation of highly calcareous saline-sodic soil using low quality water and phosphogypsum. *Appl. Water Sci.* 4, 223–230. doi:10.1007/s13201-014-0189-3

Gitari, W. M., Leslie, F. P., Key., David L., and Charles, O. (2011). Interaction of acid mine drainage with ordinary portland cement blended solid residues generated from active treatment of acid mine drainage with coal fly ash. *J. Environ. Sci. Health* 46, 37–117. doi:10.1080/10934529.2011.532423

Gonçalo Filho, F. G., da Silva Dias, N., Suddarth, S. R. P., Ferreira, J. F. S., Anderson, R. G., and dos Santos Fernandes, C. (2020). Reclaiming tropical saline-sodic soils with gypsum and cow manure. *WaterSwitzerl.* 12 (1), 57. doi:10.3390/w12010057

Gorbunov, A. V., Frontasyeva, M. V., Gundorina, S. F., Onischenko, T. L., Maksjuta, B. B., and PalSen, C. (1992). Effect of agricultural use of phosphogypsum on trace elements in soils and vegetation. *Sci. Total Environ.* 122 (3), 337–346. doi:10.1016/0048-9697(92)90051-S

Harrou, A., Gharibi, E. K., Taha, Y., Fagel, N., and El Ouahabi, M. (2020). Phosphogypsum and black steel slag as additives for ecological bentonite-based materials: Microstructure and characterization. *Minerals* 10 (12), 1–16. doi:10.3390/min10121067

Hassoune, H., Lahhit, M., Khalid, A., and Lachehab, A. (2017). Application of leaching tests on phosphogypsum by infiltration-percolation. *Water Sci. Technol.* 76 (7), 1844–1851. doi:10.2166/wst.2017.368

Hirich, A., Choukr-Allah, R., Ezzaiar, R., Shabbir, S. A., and Lyamani, A. (2021). Introduction of alternative crops as a solution to groundwater and soil salinization in the Laayoune area, South Morocco. *Euro-Mediterranean J. Environ. Integration* 6 (2), 1–13. doi:10.1007/s41207-021-00262-7

Hssaisoune, M., Bouchaou, L., Sifeddine, A., Bouimetarhan, I., and Chehbouni, A. (2020). Moroccan groundwater resources and evolution with global climate changes. *Geosci. Switz.* 10 (2), 81. doi:10.3390/geosciences10020081

Ismail, Z. H., Elgoud, E. M. A., Hai, F. A., Ali, I. O., and Aly, H. F. (2015). Leaching of some lanthanides from phosphogypsum fertilizers by mineral acids. *Arab J. Nucl. Sci. Appl.* 48 (2), 37–50.

Ivushkin, K., Bartholomeus, H., Bregt, A. K., Pulatov, A., Kempen, B., and de Sousa, L. (2019). Global mapping of soil salinity change. *Remote Sens. Environ.* 231, 111260. doi:10.1016/j.rse.2019.111260

Jiang, Y., Wu, Y., Groves, C., Yuan, D., and Kambesis, P. (2009). Natural and anthropogenic factors affecting the groundwater quality in the Nandong karst underground river system in Yunan, China. *J. Contam. Hydrology* 109, 49–61. doi:10.1016/j.jconhyd.2009.08.001

Kucuk, U., Eyuboglu, M., Kucuk, H. O., and Degirmencioglu, G. (2016). Importance of using proper post hoc test with ANOVA. *Int. J. Cardiol.* 209, 346. doi:10.1016/j.ijcard.2015.11.061

Lamsal, K., Paudyal, G. N., and Saeed, M. (1999). Model for assessing impact of salinity on soil water availability and crop yield. *Agric. Water Manag.* 41 (1), 57–70. doi:10.1016/S0378-3774(98)00116-4

Lech, M., Fronczyk, J., Radziemska, M., Sieczka, A., Garbulewski, K., Koda, E., et al. (2016). Monitoring of total dissolved solids on agricultural lands using electrical conductivity measurements. *Appl. Ecol. Environ. Res.* 14 (4), 285–295. doi:10.15666/aeer/1404_285295

Li, J., Zhang, J., and Ren, L. (2003). Water and nitrogen distribution as affected by fertigation of ammonium nitrate from a point source. *Irrigation Sci.* 22 (1), 19–30. doi:10.1007/s00271-003-0064-8

Llanderal, A., Garcia-Caparros, P., Contreras, J. I., Lao, M. T., and Segura, M. L. (2021). Spatial distribution and mobility of nutrients on sand mulching soil for fertigated green bean crops under greenhouse conditions in southern Spain: (I) macronutrients. *Agronomy* 11 (5), 842. doi:10.3390/agronomy11050842

Lütke, S. F., Oliveira, M. L. S., Silva, L. F. O., Cadaval, T. R. S., and Dotto, G. L. (2020). Nanominerals assemblages and hazardous elements assessment in phosphogypsum from an abandoned phosphate fertilizer industry. *Chemosphere* 256, 127138. doi:10.1016/j.chemosphere.2020.127138

Maia, F. M. S. (2018). Impact of increasing the temperature up to 80 oC on the behav- iour of radionuclides in the callovo-oxfordian formation: Appli- cation to uranium. Report.

Makoi, J. H. J. R., and Verplancke, H. (2010). Effect of gypsum placement on the physical chemical properties of a saline sandy loam soil. *Aust. J. Crop Sci.* 4 (7), 556–563.

Manal, N., Samdi, A., Elabassi, K., Gomina, M., and Moussa, R. (2012). Recyclage de déchets industriels, phosphogypse et cendres volantes, dans des matériaux de construction. *MATEC Web Conf.* 2, 15. doi:10.1051/matecconf/20120201015

Mashifana, T., Ntuli, F., and Okonta, F. (2019). Leaching kinetics on the removal of phosphorus from waste phosphogypsum by application of shrinking core model. *South Afr. J. Chem. Eng.* 27, 1–6. doi:10.1016/j.sajce.2018.11.001

Mesić, M., Brezinščak, L., Zgorelec, Z., Perčin, A., Sestak, I., Bilandžija, D., et al. (2016). The application of phosphogypsum in agriculture. *acs* 81, 7–13.

Moharana, P. C., Singh, R. S., Singh, S. K., Tailor, B. L., Jena, R. K., and Meena, M. D. (2019). Development of secondary salinity and salt migration in the irrigated landscape of hot arid India. *Environ. Earth Sci.* 78 (15), 4. doi:10.1007/s12665-019-8460-4

Moroccan Ministry of Equipment and Ministry charged of Territorial Planning (2002). Normes de qualité des eaux destinées à l ' irrigation. Bulletin officiel n° 5062 du 30 ramadan 1423.

Motalane, M. P., and Strydom, C. A. (2004). Potential groundwater contamination by fluoride from two South African phosphogypsums. *Water sa.* 30 (4), 465–468. doi:10.4314/wsa.v30i4.5098

Mu, Y., Tang, D., Mao, L., Zhang, D., Zhou, P., Zhi, Y., et al. (2021). Phytoremediation of secondary saline soil by halophytes with the enhancement of γ-polyglutamic acid. *Chemosphere* 285, 131450. doi:10.1016/j.chemosphere.2021.131450

Nagarajan, R., Thirumalaisamy, S., and Lakshumanan, E. (2012). Impact of leachate on groundwater pollution due to non-engineered municipal solid waste landfill sites of erode city, Tamil Nadu, India. *J. Environ. Health Sci. Eng.* 9 (1), 1–12. doi:10.1186/1735-2746-9-35

Nordstrom, D. K., and Ball, J,B. (1989). Mineral Saturation States in Natural Waters and Their Sensitivity to Thermodynamic and Analytic Errors. Etat de Saturation Des Minéraux Dans Les Eaux Naturelles et Sensibilité Des Tests Aux Données Thermodynamiques et Aux Erreurs Analytiques. *Sci. Géologiques. Bull.* 42, 80–269. doi:10.3406/sgeol.1989.1828

O'Brien, L. O. O., and Sumner, M. E. (2008). Effects of phosphogypsum on leachate and soil chemical composition. *Commun. Soil Sci. Plant Analysis* 19, 1319–1329. doi:10.1080/00103628809368015

Okur, B ., and Örçen, N. (2020). "Soil salinization and climate change," in *Climate change and soil interactions* (International Journal of Agriculture, Forestry and Plantation), 331–350. doi:10.1016/b978-0-12-818032-7.00012-6

Olsen, S. R., Cole, C. V., Watanabe, F. S., and Dean, L. A. (1954). *Estimation of available phosphorus in soils by extraction with sodium bicarbonate*. USDA Circ, 19. No. 939.

Parkhurst, D. L., and Appelo, C. A. J. (1999). User's guide to PHREEQC (ver. 2): A computer program for speciation batch-reaction one- dimensional transport and inverse geochemical calculations. *U. S. Geo Surv. Water Resour. Invest. Rept* 99, 4259.

Phung, H. T., Lam, L. H., Page, A. L., and Lund, L. J. (1979). The practice of leaching boron and soluble salts from fly ash-amended soils. *Water, Air, AndSoilPollution* 12, 247–254. doi:10.1007/bf01047127

Qadir, M., Oster, J. D., Schubert, S., Noble, A. D., and Sahrawat, K. L. (2007). Phytoremediation of sodic and saline-sodic soils. *Adv. Agron.* 96, 197–247. doi:10.1016/S0065-2113(07)96006-X

Qamouche, K., Chetaine, A., Elyahyaoui, A., Moussaif, A., Touzani, R., Benkdad, E., et al. (2020). Radiological characterization of phosphate rocks, phosphogypsum, phosphoric acid and phosphate fertilizers in Morocco: An assessment of the radiological hazard impact on the environment. *Mater. Today Proc.* 27, 3234–3242. doi:10.1016/j.matpr.2020.04.703

Reyes-Santiago, J. R., García-Villanueva, L. A., Fernández-Villagómez, G., and Guzmán-Guadarrama, P. (2021). Geochemical characterization and saturation index (Si) in the montebello lagunar system liquidamber lagoon, chiapas Mexico. *Nat. Environ. Pollut. Technol.* 20, 1415–1425. doi:10.46488/NEPT.2021.v20i04.004

Richards, L. A. (1954). Diagnosis and improvement of saline and alkaline soils. *Soil Sci. Soc. Am. J.* 18 (3), 348. doi:10.2136/sssaj1954.03615995001800030032x

Shainberg, I., Sumner, M. E., Miller, W. P., Farina, M. P. W., Pavan, M. A., and Fey, M. V. (1989). Use of gypsum on soils: A review. *January* 9, 1–111. doi:10.1007/978-1-4612-3532-3_1

Shen, J., Yuan, L., Zhang, J., Li, H., Bai, Z., Chen, X., et al. (2011). Phosphorus dynamics: From soil to plant. *Plant Physiol.* 156 (3), 997–1005. doi:10.1104/pp.111.175232

Smaoui-Jardak, M., Kriaa, W., Maalej, M., Zouari, M., Kamoun, L., Trabelsi, M., et al. (2017). Effect of the phosphogypsum amendment of saline and agricultural soils on growth, productivity and antioxidant enzyme activities of tomato (Solanum lycopersicum L.). *Ecotoxicology* 26 (8), 1089–1104. doi:10.1007/s10646-017-1836-x

Suarez, D. L., Wood, J. D., and Lesch, S. M. (2006). Effect of SAR on water infiltration under a sequential rain-irrigation management system. *Agric. Water Manag.* 86 (1–2), 150–164. doi:10.1016/j.agwat.2006.07.010

Touhtouh, D., Elfaleh, E. M., and Moujahid, Y. (2014). Caractérisations physico-chimiques et minéralogiques des sols du Saïs, Maroc (Physicochemical and mineralogical characterizations of soils of Saïs, Morocco). *Environ. Sci.* 5, 2534–2539.

UNU (2014). World losing 2,000 hectares of farm soil daily to salt-induced degradation. Available at: https://unu.edu/media-relations/releases/world-losing-2000-hectares-of-farm-soil-daily-to-salt-induced-degradation.html.

Walawalkar, M., Nichol, C. K., and Azimi, G. (2016). Process investigation of the acid leaching of rare Earth elements from phosphogypsum using HCl, HNO3, and H2SO4. *Hydrometallurgy* 166, 195–204. doi:10.1016/j.hydromet.2016.06.008

WHO (2017). *Guidelines for drinking-water quality*. Fourth edition. Incorporating the first addendum.

Zaman, M., Shahid, S. A., and Heng, L. (2018). "Introduction to soil salinity, sodicity and diagnostics techniques," in *Guideline for salinity assessment, mitigation and adaptation using nuclear and related techniques* (International Atomic Energy Agency), 1–38. doi:10.1007/978-3-319-96190-3

Zhao, B. Q., Li, X. Y., Liu, H., Wang, B. R., Zhu, P., Huang, S. M., et al. (2011). Results from long-term fertilizer experiments in China: The risk of groundwater pollution by nitrate. *NJAS - Wageningen J. Life Sci.* 58 (3–4), 177–183. doi:10.1016/j.njas.2011.09.004

Zmemla, R., Chaurand, P., Benjdidia, M., Elleuch, B., and Yves, J. (2016). Characterization and pH dependent leaching behavior of Tunisian phosphogypsum. *Am. Sci. Res. J. Eng. Technol. Sci.* 24 (1), 230–244.

Zmemla, R., Sdiri, A., Naifar, I., Benjdidia, M., and Elleuch, B. (2020). Tunisian phosphogypsum tailings: Assessment of leaching behavior for an integrated management approach. *Environ. Eng. Res.* 25 (3), 345–355. doi:10.4491/eer.2019.046

Zouahri, A., Hasini, S. E. L., Dakak, H., Iben Halima, O., Iaaich, H., Ghanimi, A., et al. (2018). Qualitative assessment of irrigation water in the central bahira plains – El KALÂA - MOROCCO. Report.

frontiers | Frontiers in Environmental Science

TYPE Original Research
PUBLISHED 13 September 2022
DOI 10.3389/fenvs.2022.937147

OPEN ACCESS

EDITED BY
Irene Petrosillo,
University of Salento, Italy

REVIEWED BY
Swapan Talukdar,
Jamia Millia Islamia, India
Solhanlle Bonilla-Duarte,
Santo Domingo Institute of Technology,
Dominican Republic

*CORRESPONDENCE
Nicola Clerici,
nicola.clerici@urosario.edu.co

SPECIALTY SECTION
This article was submitted to Land Use Dynamics,
a section of the journal
Frontiers in Environmental Science

RECEIVED 05 May 2022
ACCEPTED 22 August 2022
PUBLISHED 13 September 2022

CITATION
Toro G, Otero MP, Clerici N, Szantoi Z, González-González A and Escobedo FJ (2022), Interacting municipal-level anthropogenic and ecological disturbances drive changes in Neotropical forest carbon storage.
Front. Environ. Sci. 10:937147.
doi: 10.3389/fenvs.2022.937147

Interacting municipal-level anthropogenic and ecological disturbances drive changes in Neotropical forest carbon storage

Giselle Toro[1], Maria Paula Otero[1,2], Nicola Clerici[1]*, Zoltan Szantoi[3,4,5], Andrés González-González[1] and Francisco J. Escobedo[6]

[1]Department of Biology, Faculty of Natural Sciences, Universidad del Rosario, Bogotá, DC, Colombia, [2]Centro Interdisciplinario de Estudios sobre el Desarrollo, Universidad de Los Andes (CIDER), Bogotá, Colombia, [3]Earth Observation Science, Applications and Climate Department, European Space Agency, Frascati, Italy, [4]Science, Applications and Climate Department, European Space Agency, Frascati, Italy, [5]Department of Geography and Environmental Studies, Stellenbosch University, Stellenbosch, South Africa, [6]Pacific Southwest Research Station, USDA Forest Service, Riverside, CA, United States

Deforestation is a documented driver of biodiversity loss and ecosystem services in the tropics. However, less is known on how interacting regional and local-level anthropogenic and ecological disturbances such as land use activities, human populations, and armed conflict affect carbon storage and emissions in Neotropical forests. Therefore, we explored how local-scale, socio-ecological drivers affect carbon dynamics across space and time in a region in Colombia characterized by deforestation, land use cover (LULC) changes, and armed conflict. Specifically, using available municipal level data from a period of armed conflict (2009–2012), spatiotemporal analyses, and multivariate models, we analyzed the effects of a suite of socio-ecological drivers (e.g., armed conflict, illicit crops, human population, agriculture, etc.) on deforestation and carbon storage-emission dynamics. We found that about 0.4% of the initial forest cover area was converted to other LULC types, particularly pastures and crops. Gross C storage emissions were 4.14 Mt C, while gross carbon sequestration was 1.43 Mt C; primarily due to forest regeneration. We found that livestock ranching, illegal crop cultivation, and rural population were significant drivers of deforestation and carbon storage changes, while the influential role of armed conflict was less clear. However, temporal dynamics affected the magnitude of LULC effects and deforestation on carbon storage and emissions. The approach and findings can be used to better inform medium to long-term local and regional planning and decision-making related to forest conservation and ecosystem service policies in Neotropical forests experiencing disturbances related to global change and socio-political events like armed conflict.

KEYWORDS

Colombia, socio-ecological systems, ecosystem services, armed conflict, deforestation, spatiotemporal analyses

1 Introduction

Anthropogenic disturbances have a profound effect on the structure, composition, and function of global forested ecosystems (Machlis and Hanson, 2008; Perring et al., 2016). In the tropics, deforestation, or the conversion of forests to non-forested land use (LU)- land cover (LC), is a primary cause of biodiversity loss, and a disruption of several provisioning, cultural, and regulating ecosystem services, including carbon dioxide sequestration and emissions due to loss of carbon storage (Sanchez-Cuervo and Aide. 2013). Regionally, such loss of tropical forests and their regulating and cultural ecosystem services also have implicit trade-offs related to local scale provisioning ecosystem services, such as timber and non-timber forest products, crop yields, and cattle production (Murad and Pearse, 2018).

Large-scale tropical deforestation is often driven by LULC conversion agents, such as industrialized agriculture and livestock production activities (Landholm et al., 2019). The effects of ecological disturbance agents such as fire, drought, pests and diseases, and extreme events related to climate change have been well studied (Achard et al., 2014), as well as the dynamic between global and national socioeconomic and political drivers and Neotropical deforestation (González-González et al., 2021). However, tropical deforestation can also be driven by other cross-scale anthropogenic disturbance drivers such as land tenure regimes, inequity and poverty, poor governability, unbalanced power structures, illicit cropping, mining, and even warfare (Hoffmann, et al., 2018). This specific role of regional and local-level anthropogenic disturbance drivers in changing ecosystem functions and services in tropical regions has been less studied (Salazar, 2016; Bautista-Cespedes et al., 2021). Indeed, regional conservation efforts and local use and management of Neotropical forests are important, as they provide multiple types of regional-continental ecosystem services such as climate regulation (e.g., carbon storage and sequestration, temperature regulation; Gibbs et al., 2007) and water regulation and provisioning services for humans settlements (Clerici et al., 2019). They can also provide local-level provisioning services such as timber, non-timber forest products, crops and forage, and cultural ecosystem services such as wildlife viewing opportunities, ecotourism as well as spiritual and educational opportunities (Carriazo et al., 2019; Ocampo-Penuela and Winton 2017). Forest carbon storage is important since deforestation of tropical forests contributes to about 15%–25% of all annual global greenhouse gas emissions (Gibbs, et al., 2007; Phillips et al., 2016). Similarly, carbon storage, sequestration, and offset programs are a key component of many local-regional Payment for Ecosystem Service and REDD+ (Reducing Emissions from Deforestation and forest Degradation in developing countries) programs and instruments.

Although anthropogenic disturbances driving deforestation and carbon storage are complex and context specific, less studied socio-ecological factors, such as: demographics, population density changes and migration, economic activities, actor groups, and factors associated with socio-economic and political factors can provide key insights into these dynamics (Leite et al., 2018; Betancur-Alarcón and Krause, 2020). For example, a less studied anthropogenic disturbance affecting tropical forests and their ecosystem services in countries such as Colombia, Democratic Republic of the Congo (DRC), Sri Lanka, Indonesia, among others, is warfare or armed conflict. Armed conflict and its associated variables such as internal displacement, violence, armed encounters, and casualties is a multi-faceted phenomenon with complex socio-political, socio-economic, and ecological dynamics and effects (Camargo et al., 2020). Armed conflict incorporates the interaction of governments military, civilians, and the environment. Warfare dynamics imply socioecological changes, because warfare requires extraction of natural resources and movement of people, which have often impacts on natural ecosystems. Depending on the relationship among ecosystems and conflict dynamics, either deforestation or “gun-point conservation” of forests will imply changes within the landscape. Although conflict has recently been used with frequency to discuss its role in national and regional tropical deforestation, it can also interact with local-regional level factors driving ecosystem services such as: resource extraction, landscape fragmentation, habitat loss, soil erosion, and socio-economic disruption (Murillo-Sandoval et al., 2020; Bautista-Cespedes et al., 2021; Liévano-Latorre et al., 2021). For a more detailed discussion about conflict and warfare ecology-related concepts, please refer to Machlis and Hanson (2008). Also refer to Schoon and Cox (2012) for an in-depth discussion of socio-ecological disturbance typologies and frameworks for distinguishing between natural and anthropogenic disturbances (i.e., drivers as used in the ecosystem services literature).

As such, forests in tropical countries provide unique opportunities to explore the effects of complex anthropogenic disturbances on the regional and local supply and demand of ecosystem services. Using such disturbances as variables in statistical models can provide context-relevant information about deforestation as well as reforestation and regeneration dynamics (Sanchez-Cuervo and Aide, 2013). In particular, tropical forests that have or are experiencing armed conflict, several factors have been found to be correlated with deforestation: rural and urban population density, agricultural activity (cattle, agro-industrial products included), infrastructure, mining (legal and illegal), and illegal cropping (crops or plants which have been deemed illegal to grow by the government, e.g., coca bush or opium poppy) (Gaveau et al., 2009; Kanninen et al., 2009; Potapov et al., 2012; Yasmi et al., 2013; Butsic et al., 2015; Camisani 2018).

However, *in-situ* measurements and access to such forests is complex and often not possible; thus, remote sensing techniques based on satellite imagery and geospatial analyses are regularly used to measure and monitor tropical deforestation in these contexts (Achard et al., 2014; Murad and Pearse, 2018). Free and open access to satellite imagery (e.g., from Landsat and Sentinel), geospatial datasets (Turner et al., 2015), and recently available socio-economic, commodity production, and armed conflict data can allow for the study of the spatiotemporal dynamics related to these natural and anthropogenic disturbances influencing LULC change in tropical forests, and subsequent changes to ecosystem services (Suárez et al., 2018). We refer to the interaction of natural and anthropogenic disturbances hereafter as *socio-ecological drivers* (Schoon and Cox. 2012).

Accordingly, this study aims to better understand how local-level socio-ecological disturbances affect deforestation and subsequent carbon storage across space and time in a socio-ecologically complex region that experienced conflict in central Colombia. The country is characterized by historic and recent high rates of deforestation due to agriculture, livestock, mining, and armed conflict (Camargo et al., 2020; Prem et al., 2020). Thus, its socio-political and socio-economic dynamics provide a unique opportunity to explore the role of socio-ecological disturbances and drivers on Neotropical forest carbon storage during 2009–2012; a period of active internal armed conflict. Our specific study objectives are three-fold:

1. Spatio-temporally estimate the area of forest conversions to other land use-land covers,
2. Spatio-temporally analyze forest carbon storage changes related to land use-land cover transitions, and
3. Explore the effects of socio-ecological drivers on deforestation and subsequent forest carbon storage-emission dynamics.

In the below study we analyzed a number of direct and indirect drivers of forest and land cover change to better understand the role of municipal-level socio-ecological disturbances on Neotropical Forest carbon. Such approach and information are key to better informing local and regional policies and programs such as Reduced Emission from Deforestation and Degradation (REDD+) and Payments for ecosystem services (Gibbs et al., 2007). The approach, as detailed below, can also be used to assess the sustainable provisioning of agricultural products and promoting opportunities for cultural ecosystem services (Ocampo-Peñuela and Winton, 2017; Phillips et al., 2016).

2 Materials and methods

2.1 Study area

The study area encompasses 12 different municipalities in the Departments of Meta, Guaviare and Caquetá, in central Colombia (Figure 1). The three departments have a mean annual temperature range of 25–30°C and mean annual rainfall of approximately 2,500–3,000 mm (IDEAM, 2020). The main ecosystems in the Departments include fragmented humid forests, savannas, secondary vegetation, agroecosystems and wetlands (Suarez et al., 2018). Elevation ranges from approximately to 125–4,100 m (Eastern Andean Cordillera) above sea level. Several protected areas are present in the study area (Figure 1) and include: Natural National Parks Sierra de la Macarena, Picachos, Tinigua, Serrania de Chiribiquete, and Natural National Reserve Nukak. The main socio-economic activities of the region are related to agricultural production related to coffee cultivation and livestock production, and mining to a lesser extent (DANE, 2020; Castro-Nunez et al., 2017). However, other illicit activities such as coca cultivation, illegal timber harvesting, and illicit mining operation also influence economic activities and supply chains throughout the study area (Rodríguez-de-Francisco et al., 2021). This region is home to an important biological mega-corridor between the Andes and Amazon biogeographical region: the Amazon-Andes Transition Belt (Clerici et al., 2018).

The total 2020 population in the study area's three Departments is approximately: 411,000 in Caquetá; 86,000 in Guaviare, and more than one million people in Meta (Statista Research Department, 2021). The region has historically been characterized by armed conflict and the presence of several armed groups, including the Revolutionary Armed Forces of Colombia (FARC), National Liberation Army (ELN), paramilitaries and other groups associated with illicit crops cultivation and natural resource extraction (Rincón Ruiz et al., 2013; Bautista-Cespedes et al., 2021; Sanchez-Cuervo and Aide 2013). In this study we focus on the time interval 2009–2012, a period characterized by: 1) active and intense armed conflict (i.e., the 2009 *Seguridad Democratica* or Democratic Security period) that coincided with increased military spending and operations against the FARC, and 2) a transition period as of 2012 that was characterized by a lower intensity of armed conflict and a period that eventually led to a post-conflict warfare dynamics (i.e., the FARC Peace Process; Camargo et al., 2020).

2.2 Land use-land cover transitions

Specific Land use-Land cover transitions from 2009 to 2012 were estimated using the ESA Land Cover Climate Change Initiative Copernicus LC land cover products (Copernicus). The data are based on a 22 class LULC system,

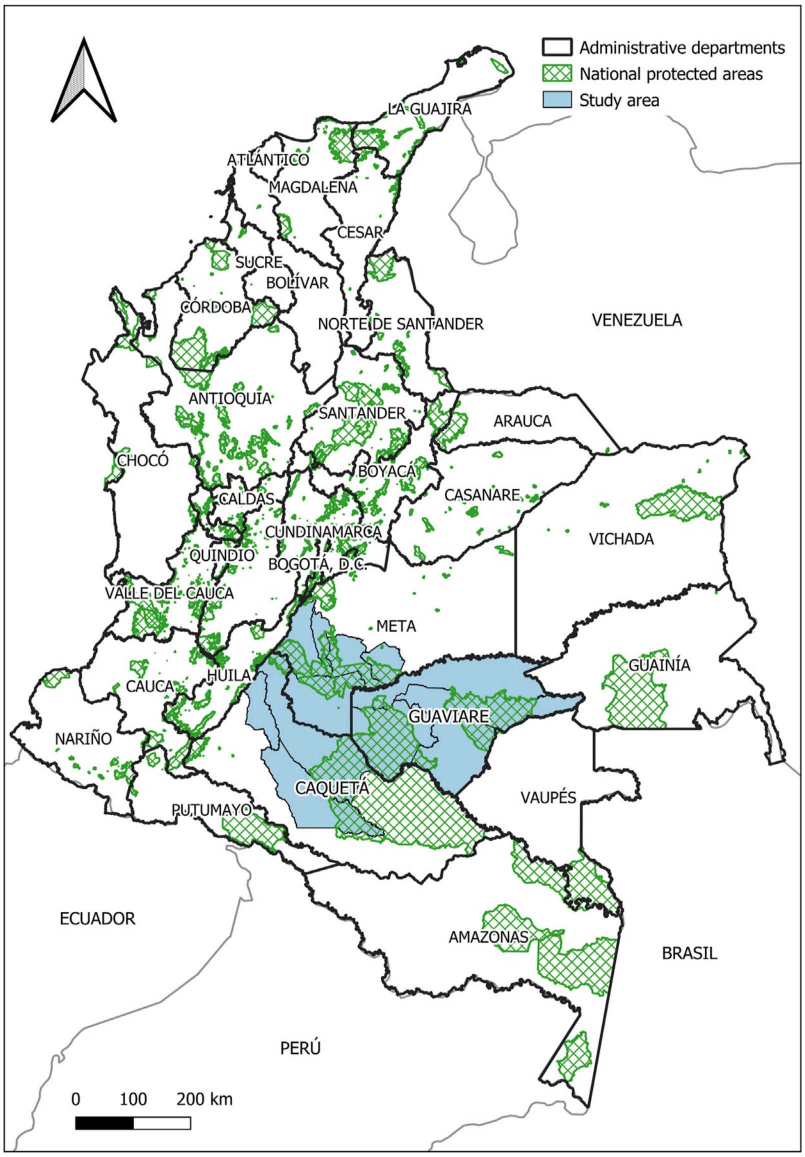

FIGURE 1
Study area (blue polygons) in the departments of Meta, Guaviare and Caquetá, Colombia. Protected areas are shown in green.

defined using the United Nation Food and Agriculture Organization's (UN FAO) Land Cover Classification System (LCCS), and provides annual gridded LULC maps at 300 m resolution from 1992 to 2020. Detailed LULC class descriptions are discussed in Copernicus (2021b). The analyzed products for the years 2009 and 2012 are MERIS based global coverage at 300 m (https://earth.esa.int/eogateway/instruments/meris), generated by ESA from MERIS Full Resolution surface reflectance data. The Coordinate Reference System used for the global land cover database is a geographic coordinate system (GCS) based on the World Geodetic System 84 (WGS84) reference ellipsoid. To ensure the quality and consistency of the LC maps, the sets of annual maps were not produced independently, but they were derived from a unique baseline LC map, which was generated using the entire MERIS Full Resolution and MERIS Reduced Resolution (1,000 m) archive from 2003 to 2012, employing a machine learning spectral classification module (ESA, 2017a). The validation process was ensured through: 1) validation datasets that were not used during the production of the LC maps and 2) carried out by external parties, not involved in the production of the LC maps. The first step in a validation process was to estimate the accuracy of the latest year (2015) using an independent dataset and the process revealed that the overall accuracy of

TABLE 1 ESA LC CCI land use and land cover classes (LULC; left column) and aggregated LULC classes in this work (right column).

Copernicus LULC classes	Aggregated LULC classes
Tree cover, broadleaved, evergreen, closed to open (>15%)	Forest
Tree cover, broadleaved, deciduous, closed to open (>15%)	
Tree cover, flooded, fresh or brackish water	
Tree cover, flooded, saline water	
Water bodies	Water
Cropland, rainfed	Pastures and crops
Cropland, rainfed, herbaceous cover	
Mosaic cropland (>50%)/natural vegetation (tree, shrub, herbaceous cover) (<50%)	
Mosaic natural vegetation (tree, shrub, herbaceous cover) (>50%)/cropland (<50%)	Shrub and herbaceous vegetation
Shrubland	
Grassland	
Shrub or herbaceous cover, flooded, fresh/saline/brackish water	
Mosaic tree and shrub (>50%)/herbaceous cover (<50%)	
Mosaic herbaceous cover (>50%)/tree and shrub (<50%)	
Urban areas	Urban and paved surfaces
Bare areas	Sparse or no vegetation
Sparse vegetation (tree, shrub, herbaceous cover) (<15%)	

TABLE 2 Land use-Land Cover (LULC) classes and reported mean aboveground carbon storage densities used in this study, with bibliographic source.

LULC class	Mean aboveground carbon storage density (Mg C/ha)	Source
Forest	132.1	Yepes et al. (2011); humid tropical forest
Shrubs and herbaceous vegetation[a]	18.95	Yepes et al. (2011)
Urban and paved surfaces	0	Yepes et al. (2011)
Pastures and crops[a]	9.68	Yepes et al. (2011), Rincón and Ligarreto (2007), Arce et al. (2008); crops Fisher et al. (1994); deep-rooted grass Noordwijk et al. (2002); crops IPCC (2003; 2006); grassland and crops
Sparse or no vegetation[a]	3.0	Asner et al. (2012)
Water	0	N/A

[a]Subcomponents of LULC class represented in equal proportions.

the 2015 LC map was 71.45% (ESA, 2017b). While there is no direct evaluation of the overall accuracy of the 2009–2012 products, it was reported in a second step, that there is a reported good agreement (>90%) for croplands, broadleaved evergreen forests, urban areas, bare areas, water bodies, and permanent snow and ice cover with the previous yearly products compared to the 2015 LULC map.

The 17 Copernicus LULC classes present in the study area were aggregated into six general classes (Table 1), that were subsequently used to analyzed forest to other LULC transitions during 2009–2012; (i.e., forest cover was the starting or target class; Szantoi et al., 2021).

2.3 Forest carbon storage changes

Mean aboveground *gross carbon* (*C*) *storage* densities (Mg C/ha) were compiled for the various LULC classes based on context-relevant information from the region (Table 2). These carbon storage densities were used to estimate the carbon storage per LULC class per area for the analysis period and carbon storage changes from the transitions from 2009 to 2012. These changes in *gross carbon storage* were converted to a per year basis, or annualized, during the 3-year period and are reported as *carbon sequestration* in the case of annual carbon storage increases, or conversely *carbon emissions* in the case of annual carbon storage losses.

TABLE 3 Municipal-level socio-ecological drivers (i.e., anthropogenic and ecological disturbances) affecting deforestation and carbon storage change in Neotropical forests in central Colombia.

Municipality-level socio-ecological drivers	Variable name	Unit	Source
Crop yields	Yield_Pro[a]	Ton/ha	DANE (2020)
Total rural population	Rural_Popu	Total population	
Deforestation	Area_Def	Square km	(Copernicus)
Seeded area of annual crops	Annual_SeedCrop	ha	The Amazon Scientific Research Institute SINCHI: https://datos.siatac.co/
Presence of permanent crops	Permanent_Crop	1 (present); 0 (absent)	
Seeded area of transitory crops	Transitory_SeedCrop	ha	
Illegal crops area	Illegal_Crops	ha	
Cattle number	Cattle_N	Number of total cattle in the area	Colombian Federation of Cattle Ranchers: https://www.fedegan.org.co/estadisticas/produccion-0
Number of FARC attacks	Atfarc	Number of armed encounters	Historical Memory Center (2012), Prem et al. (2020)
People that migrated from the municipality due to armed conflict	ACP_Expelled	Number of internally displaced people	Camargo et al. (2020)

[a]Data did not specify the type of crop; a sum of hectares per farm was made and summarized at municipal level.

2.4 Socio-ecological drivers of forest carbon emissions

We analyzed available and relevant socio-ecological drivers associated with deforestation across 12 municipalities (Supplementary Table S1) from Table 3. The data were at the municipal-level to better understand their role as regional-local scale drivers of forest loss and subsequent carbon storage changes (i.e., emissions) in the study area during the study period. We first used an exploratory analysis to identify spatiotemporal dynamics and patterns in the data, as well as data quality issues (Behrens, 1997). Accordingly, we used Pearson correlation analyses and Stepwise Regression to reduce errors associated with redundant variables, identify statistically significant variables, and to address multi-collinearity issues (Harrell, 2013).

The selected variables were also tested for spatial autocorrelation using Moran's I index (Celemín, 2009; Durán and Monsalves, 2020) and a spatial weighted matrix with a first-order queen contiguity matrix to evaluate variable pattern distribution in each municipality (Carracedo and Debón, 2017). To identify spatial changes in our variables we also used a Spatial Delay Analysis with a weighted average of random variables in neighboring locations (Pérez Pineda, 2006). These tests found no spatial auto-correlation issues.

Accordingly, these drivers in Table 3 were then used to statistically analyze the effect of municipal-level socio-ecological drivers on forest loss and its relationship with carbon storage during 2009–2012. First, we developed a mean comparison or variance model (Model 1, hereafter) to account for continuous and categorical data and their independence (Villa et al., 2012). Here we used a factorial design that considers a single factor, i.e., the dependent variable (deforestation) and the levels reported in Table 3 (Palmer Po, 2019). We tested for two different temporal groups, "A" for 2009 and "B" for 2012, respectively, and used the test levels a and b (a, b ≥ 2), with a factorial arrangement or design of a x b treatments, or:

$$Y_{ijk} = \mu + \alpha_i + \beta_j + (\alpha\beta)_{ij} + \varepsilon_{ijk} \tag{1}$$

where $i = 1, 2, \ldots, a$; $j = 1, 2, \ldots, b$; $k = 1, 2, \ldots, n$. a_i is the effect due to the ith level of factor A; b_i is the effect of the jth level of factor B. α, β, μ are the model's estimators.

To better understand the role of year (i.e., time) and a municipality's characteristics on deforestation, we also used a second analysis (Model 2, hereafter) of the form:

$$Are\_def = year + x_{municipality} \tag{2}$$

where Are_def is the deforested area and x varies for each of the 12 municipalities (Appendix A). Model 2 was based on a factorial multivariate analysis of variance (MANOVA) model to account for the temporal nature of deforestation across different years (Warne, 2014). We evaluated a null hypothesis in which the value of the mean in the dependent variable can be statistically dependent on each group of independent variables. We used four conventional statistics to test for variance means in the multivariate model, specifically: Pillai's Trace, Wilk's Lambda, Hotelling's Trace, and Roy's Largest Root (Chen, 2011). All significance tests were obtained with a fixed value of $p = 0.05$. All statistical analyses were performed using R v. 3.6 (R Core Team, 2017).

A resuming flow-chart of all processing steps is reported in Supplementary Figure S1.

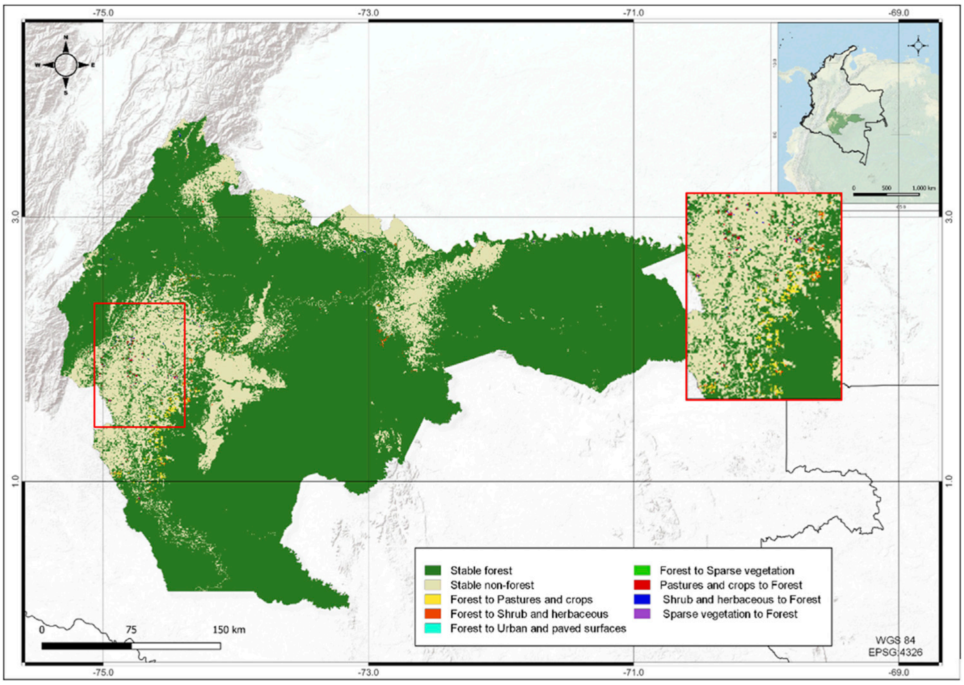

FIGURE 2
Land use land cover transitions in the study area in 2009–2012. Red frame: a zoom western of Sabanas del Yarí region in central Colombia.

TABLE 4 Land use and land cover (LULC) transitions type and extent (ha) in the central Colombian study area during 2009–2012.

LULC transition	Extent (ha)
Stable Forest	8664678.1
Forest to Water	0
Forest to Pastures and crops	23,227.2
Forest to Shrub and herbaceous vegetation	11,413.1
Forest to Urban and paved surfaces	28.7
Forest to Sparse or no vegetation	19.1
Water to Forest	0
Pastures and crops to Forest	7,029.3
Shrub and herbaceous vegetation to Forest	4,889.9
Urban and paved surfaces to Forest	0
Sparse or no vegetation to Forest	114.6

3 Results

3.1 Land use land cover change

Land use and land cover transitions (2009–2012) derived from the Copernicus dataset (Copernicus, 2021a) are shown in Figure 2. The area extent of the LULC transitions involving forests in the study area are shown in Table 4. The main LULC transition is represented by the conversion of Forests to Pastures and Crops (23,227 ha), while the second largest transition is represented by Forest conversion to Shrubs and Herbaceous Vegetation (11,413 ha); the latter indicating a process of deforestation followed by regeneration, and/or forest degradation. A total of 11,918 ha represents areas where forest regeneration has occurred as shown by the areas of pastures, crops, shrubs, and herbaceous LULCs converting to secondary forests (Table 4).

3.2 Forest carbon storage and emission dynamics

Overall, gross carbon emissions in the study period were 4.14 Mt C (average annual C emissions were 1.38 Mt C yr^{-1}), and gross carbon sequestration 1.43 Mt C (average annual C sequestration was 0.48 Mt C yr^{-1}). The non-annualized difference between gross carbon storage and carbon emission was estimated at 2.71 Mt C in the study area during 2009–2012. Figures 3, 4 show municipal-level forest C storage changes (i.e., emissions) for targeted LULC transitions, respectively. Forest carbon emissions and gross carbon storage estimations between 2009 and 2012 are shown in Table 5 and were calculated using the carbon density values presented in Table 2. Table 5 shows that carbon storage increases are overall, lower than carbon emissions. Municipalities with the areas of greatest carbon storage occurred in the municipalities of San

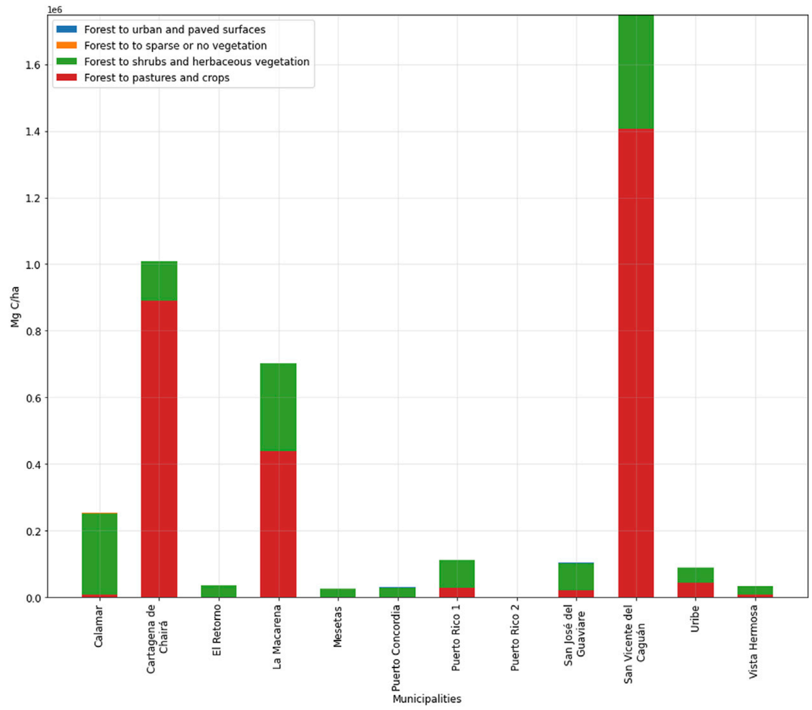

FIGURE 3
Forest carbon emissions (Mg C * 10^6) by municipality and land use land cover transitions in the study area during 2009–2012.

Vicente del Caguán, San José del Guaviare, La Macarena, and Cartagena del Chairá (Figure 4. We note that these estimates were not analyzed as compositional data). The highest carbon emissions occurred in Forests that were converted to pasture and crop areas in the municipalities of San Vicente del Caguán, Cartagena de Chairá and La Macarena (Figure 3). The municipalities of Mesetas and Vistahermosa had the lowest values of carbon emissions and storage, respectively.

3.3 Socio-ecological drivers of forest carbon storage changes

Our factorial design for Model 1 was used to account for the relationships or interactions among the anthropogenic and ecological disturbances in the study area during the analysis period. Accordingly, these socio-ecological drivers comprising the model (Table 3), were analyzed to determine the significance of temporal changes among them (Oehlert, 2010). Again, Model 2 in turn was used to understand the temporal influence of these socio-ecological drivers on deforestation and carbon storage changes. We note that Model 2 is a multivariate model with two dependent variables that avoids the use of "year" as a dependent variable; as used in Model 1 (See Section 3.3.1 below).

3.3.1 Statistical analysis

Model 1 was significant (0.019, $<p = 0.05$), and can explain some of the variation in deforestation observed in the study area. We found that some variables such as illegal crops during both 2009 and 2012 groups were significant. Accordingly, we used both these groups/years as a fixed factor in the model and adopted an H_0 hypothesis where the means are the same. All the variables related to this hypothesis were tested (Table 3) and all were found not be not significant; therefore, the null hypothesis was rejected. We found that permanent crops (variable Permanent_C) was redundant within the model and thus not explanatory. Overall, the model factors explained 86.5% of the variance in deforestation (Area_Def). The limits and significance of the estimators in the variables that have Year as a factor are shown in Table 6. Results show that "Year" when used as a factor was not significant. However illicit crops and number of cattle were found to be significant ($p = 0.05$) and rural population was somewhat significant ($p = 0.07$). The results showing the effects of the model with the factor (Year) and the interaction and intersection for each factor are shown in Table 7.

Using results from Tables 6, 7, an equation was developed to better understand the interactions among the different socio-ecological drivers of deforestation (Area_Def); the variables are explained in Table 8.

 10.3389/fenvs.2022.937147

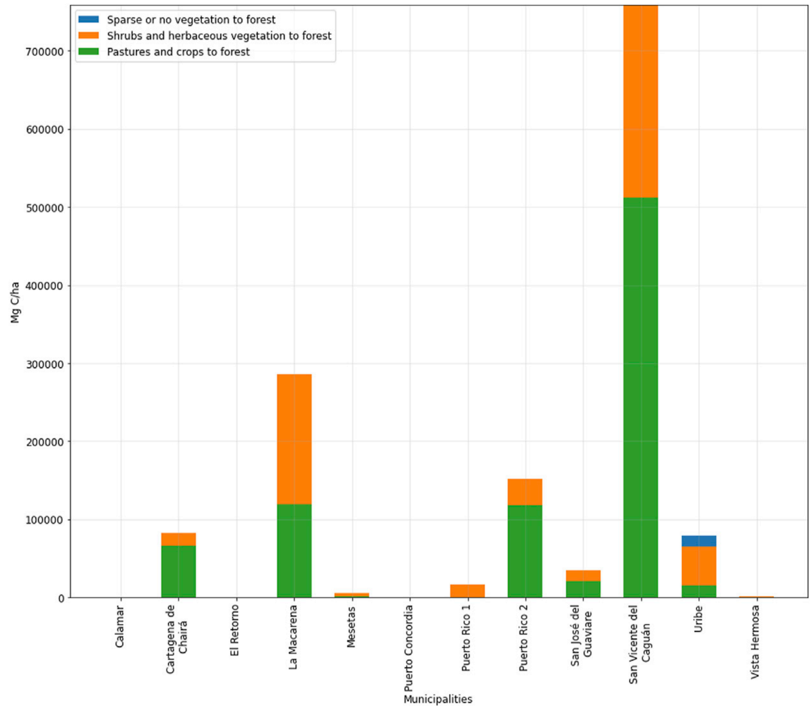

FIGURE 4
Carbon storage due to forest regeneration and/or degradation (Mg C) by municipality and land use and land cover transition in the study area during 2009–2012.

TABLE 5 Forest gross carbon emissions and gross carbon storage between 2009 and 2012 in the study area.

LULC (2009)	LULC (2012)	Transition area (ha)	Mg C
Carbon emissions (Mg C)			
Forest	Pastures and crops	23,227.24	2843473.8
Forest	Shrub and herbaceous vegetation	11,413.06	1291392.3
Forest	Urban and paved surfaces	28.65	3,791.3
Forest	Sparse or no vegetation	19.10	2,465.8
Gross carbon storage (Mg C)			
Pastures and crops	Forest	7,029.30	860526.9
Shrub and herbaceous vegetation	Forest	4,889.95	553292.2
Urban and paved surfaces	Forest	0	0
Sparse or no vegetation	Forest	114.61	14,794.9

[a]Transitions involving Water are not reported being equal to 0 ha in extent.

$$Area_{Def} = -5.41 + 1.9X_1 + 0.95X_2 + 1.23X_3 - 1.25X_5 + 2.95X_6 - 2.55X_7 - 0.01X_8 + 1.13X_9 - 0.46$$

Although results (Tables 5, 6) showed a significant relationship between deforestation and year, cattle numbers ($p < 0.05$) and illegal crops ($p < 0.05$) as well as moderately significant with rural population ($p < 0.07$); interestingly year 2009 showed no statistical significance. To better understand how these interacting variables over time (i.e., year) influenced deforestation, we used multivariate model 2 with municipalities as the fixed effect and removing the variable Permanent C. This corrected model resulted in an acceptable level of significance (adjusted model of 95%) and explained the two dependent variables, deforestation and year, and their spatiotemporal

TABLE 6 Tests of inter-subject effects with a factorial model.

Origin	Sum of Squares Type III	Degrees of freedom.	Square root	F	Significance
Dependent variable: Area_Def (deforestation)					
Corrected Model	13,649.258	10	1,364.926	7.666	0.001*
Intersept	0.000	0			
Rural_Popu	689.969	1	689.969	3.875	0.073**
Yield_Proha	161.632	1	161.632	0.908	0.359
Annual_SeedCrop (ha)	270.801	1	270.801	1.521	0.241
Transitory_Seedcrop (ha)	282.433	1	282.433	1.586	0.232
Illegal_Crops (ha)	1,555.003	1	1,555.003	8.734	0.012*
Cattle_N	1,159.596	1	1,159.596	6.513	0.025*
Atfarc	0.029	1	0.029	0	0.990
ACP_Received	230.063	1	230.063	1.292	0.278
Loss_Carbon	2,584.637	1	2,584.637	14.517	0.002*
Year	364.363	1	364.363	2.046	0.178
Error	2,136.522	12	178.043		
Total	41,463.704	23			
Corrected total	15,785.780	22			

R squared = 0.865; *R* squared adjusted = 0.752; * significant $p < 0.05$; ** significant at $p < 0.10$

TABLE 7 Parameter estimates from the explanatory variables.

Parameter	*B*	Standard deviation	*t*	Significance	95% confidence interval	
					Lower limit	Upper limit
Dependent variable: Area_Def (Area deforestation)						
Intercept	−5.417	11.625	−0.466	0.650	−30.746	19.912
Rural_Popu	0.001	0.001	1.969	0.073	0.000	0.003
Yield_Proha	0.000	0.000	0.953	0.359	−0.001	0.002
Annual_SeedCrop (ha)	0.006	0.005	1.233	0.241	−0.005	0.017
Permanent_C	0[a]					
Transitory_Seedcrop (ha)	−0.004	0.003	−1.259	0.232	−0.011	0.003
Illegal_Crops (ha)	0.013	0.005	2.955	0.012	0.004	0.023
Cattle_N	−0.113	0.044	−2.552	0.025	−0.210	−0.017
Atfarc	−0.037	2.908	−0.013	0.990	−6.373	6.299
ACP_Received	0.012	0.011	1.137	0.278	−0.011	0.036
Loss_Carbon	0.000	0.000	3.810	0.002	0.000	0.001
[Year = 2009]	12.244	8.559	1.431	0.178	−6.404	30.891
[Year = 2012]	0[a]					

[a]This parameter is equal to zero due to redundancy.

relationship with several drivers. We found that Year had a negative adjusted R^2 (−1.09; $R^2 = 0.714$) while Deforestation had a positive Adjusted R^2 (0.954; R^2 = 0.994); indicating that deforestation was not a significant driver with respect to time. However, deforestation was significantly related to other variables such as illegal crops and specific municipal-level dynamics (Table 7).

4 Discussion

This study used available geospatial and socio-ecological data to analyze deforestation, LULC changes, and drivers influencing forest C storage dynamics in a region that experienced armed conflict in central Colombia. We found that forest cover loss (i.e., deforestation) was primarily a function of forest conversion

TABLE 8 Explanatory variables included in Model 1.

Model Variable	Variable	Description
X1	Rural_Popu	Total rural population
X2	Yield_Proha	Crop yield and production
X3	Annual_SeedCrop ha	Seeded area of annual crops
X4	Transitory__SeedCrop ha	Seeded area of seasonal crop
X5	Illegal_Crops ha	Illegal crop area
X6	Cattle_N	Number of cattle
X7	atfarc	Numer of FARC attacks
X8	ACP_Expelled	Number of people displaced from the municipality because of armed conflict
X9	Loss_Carbon	Mean aboveground carbon emission to non- forested LULC (i.e., Pastures and crops, Shrub and herbaceous vegetation, Urban and paved surfaces, Sparse or no vegetation)

to pastures-crops in our study area. This result was likely influenced by the governmental policies and programs related to the promotion of the agricultural production and livestock ranching between 2009-2010 (Suarez et al., 2018; Bautista-Cespedes et al., 2021). Our findings also indicate that some of the socio-ecological drivers behind deforestation and carbon storage changes were related to the amount of rural population, livestock ranching activity, and illicit crop cultivation, however the presence of armed groups such as the FARC was less clear (Camargo et al., 2020; Bautista-Cespedes et al., 2021).

More specifically, our LULC change analyses shows an increase in agriculture and pastures and conversely a decrease in forest cover. We found that almost 347 km^2 of forests, about 0.4% of the initial forest cover extension, were converted to other LULC types between 2009 and 2012 (Table 4). Deforestation in the study region is known to be linked to both "land grabbing" for illegal ranching and land speculation for expected future increases in land value (Rodríguez-de-Francisco et al., 2021). The use of this area by the armed groups is also well known, as these groups strategically used forested areas during the period, for both illicit cultivation of coca and military-related operation operations (Camargo et al., 2020; Castro-Nunez et al., 2017). Previous studies have found that the effect of armed conflict on deforestation in Colombia is complex and varies across regions and time, but in general most literature agrees that deforestation might increase after the cessation of intense armed conflict (Murillo-Sandoval et al., 2021; Reuveny et al., 2010; Clerici et al., 2020; Baker et al., 2003). During 2012, initial discussions that led to the peace agreement with FARC have been reported as another potential factor that could have influenced deforestation and conversion to extensive uncontrolled farming and mining operations. as well as the movements of armed groups (Yu. et al., 2014; Bautista-Cespedes et al., 2021; Salazar, 2016). However, as we will later discuss, there is limited literature regarding how armed conflict directly and indirectly affects ecosystem function and services, particularly carbon storage and climate regulation.

Studies suggest that regions similar to our study area have experienced lower deforestation rates during conflict as compared to post-conflict periods (Castro-Nunez et al., 2017). After the cease-fire period in 2015 many of these forests experienced high rates of deforestation and conversion to land uses related to cattle farming, mining, and licit/illicit cropping (Bautista-Cespedes et al., 2021). Increase in deforestation during post-conflict was facilitated by easier access to pasture areas for cattle and crop farming due to the exit of FARC, and the return of internally displaced peoples (Negret, et al., 2019; Landholm et al., 2019). Nevertheless, studies like Bautista-Cespedes et al. (2021) and Salas-Salazar (2016) document that deforestation dynamics within each municipality can be different due to power-influence dynamics or warfare dynamics as well as the specific history of the rural areas during and after the armed conflict. Castro-Nunez et al. (2017) reports that during Colombia's period of actively armed conflict, there were increases in certain LU activities that resulted in agricultural colonization practices that promote forest loss and thus increased carbon emissions. With respect to protected areas, Liévano-Latorre et al. (2021) found that only areas administered by Colombian natural parks were effective in avoiding deforestation (2000–2017), but that the presence of FARC increased deforestation at the regional level (Liévano-Latorre et al., 2021).

We found that there were specific socio-ecological drivers in addition to armed conflict driving C storage changes. The municipalities in the study area experienced several complex socio-political processes during our analysis period related to unregulated cattle ranching and both legal and illegal mining (UNODC and Ministerio de Justicia y del Derecho, 2015). Such activities have also been associated with deforestation activities and also contribute to explain the increase in carbon emissions (Table 5). Coca production has frequently been linked to deforestation in humid tropical forested ecosystems in Colombia (Rincón-Ruiz and Kallis et al., 2013), however, most of the carbon emissions rates in San Vicente del Caguán can also be related to agroforestry practices such as rubber and cocoa production, infrastructure development (González et al., 2018). In municipalities such as San José del Guaviare and La Macarena, agricultural practices could involve extensive illicit livestock and crop operations. But in other municipalities such as Puerto Rico (Meta), Vistahermosa, Uribe and Mesetas, few changes were observed in regard to forest carbon storage losses (Figure 3). These trends are likely a result of historic ranching and coca crop cultivation activities in recent history and thus no prominent changes in carbon storage losses were found in our study for these municipalities (UNODC and Ministerio de Justicia y del Derecho, 2015).

Our modelling approach accounted for the different and interacting municipal-level socio-ecological drivers affecting deforestation across space and time in the study area. By accounting for these temporal disturbances in Model 2 we also obtained a much higher fit relative to Model 1 (Table 7). The drivers identified by both our statistical models show that many of them are likely interacting (Table 7). Such interacting activities that affect deforestation can include illicit crop cultivation, ranching, internally displaced people, and armed conflict (Sanchez-Cuervo and Aide. 2013; Rincón Ruiz et al., 2013). Such extractive natural resource activities are primarily found in deforested areas in less mountainous and more accessible areas (Sanchez-Cuervo and Aide. 2013; Bautista-Cespedes et al., 2021). Accordingly, our results are in-line with other studies (e.g., González-González et al., 2021; Ganzenmüller et al., 2022) in that different variables drive deforestation differently across space and time. In terms of ecosystem service provision, Castro-Nunez et al. (2017) investigated the spatial associations between carbon in woody biomass and conflict-related variables in Colombia's Amazon region and found an inverse relation between carbon and both armed actions and conflict victims in the Amazon region.

However, we do note some limitations in our study, First, we only used available geospatial data, with a spatial resolution of 300 m × 300 m, without field verification. Second, our armed conflict variable was limited to presence or absence (binary data) of FARC-related armed groups in each municipality. The use of continuous data for armed conflict might have yielded new results and insights. Future research should account for additional anthropogenic and ecological disturbances to better analyse deforestation, such as mining, wood extraction (forest degradation), expansion of infrastructure, and other conflict-related drivers such as type of armed groups, and casualties.

This study's findings shows that using socio-ecological data as proxies for disturbance agents—and their influence on deforestation and carbon storage—can be a viable approach for parsing out socio-political and economically relevant drivers, such as illicit crops, FARC attacks, and local-level land use activities affecting ecosystem service provision. Such dynamics can also depend on issues not addressed in this study, such as those related to governance and associated policies, laws, and events such as the fumigation of illicit crops or even the recent peace processes. Our findings and those from the literature demonstrate in general the need for improved governability as well as governance in remote rural locations in places such as this region in Colombia.

In conclusion, the approach and findings of this study can be used to better inform local-level decision-making related to forest conservation and ecosystem service provision policies and programs in Neotropical forests. Policies and legislation incentivizing the use of conservation instruments such as Payment for Ecosystem Services, for example, are well established in places such as Colombia. Thus, use of available, municipal-level data as used in this study can also be used to monitor and evaluate how socio-economic, political, and ecological indicators can drive not only the sustainable provisioning and regulating ecosystem services, but also opportunities for enhancing cultural ecosystem services in areas that lack data and access to on-site measurements.

Data availability statement

The datasets used in this study can be found in public online repositories; the source of these can be found in the article reference section. Access to the data produced in this research work will be made available upon request to the corresponding author.

Author contributions

FE, NC, and ZS developed the original research proposal; GT, MO, AG-G, and NC performed the calculations. GT and MO wrote the original draft; all authors contributed to the final version of the manuscript and agreed to its submission.

Funding

This research was founded by Universidad del Rosario, Small Grant 2017 "Trayectorias socioeconómicas, ecológicas y políticas de la deforestación en bosques tropicales en transición de postconflicto: lecciones para Colombia".

Acknowledgments

We acknowledge the Dirección de Investigación e Innovación of Universidad del Rosario for granting the funds and for administrative support.

Conflict of interest

The authors declare that the research was conducted in the absence of any commercial or financial relationships that could be construed as a potential conflict of interest.

Publisher's note

All claims expressed in this article are solely those of the authors and do not necessarily represent those of their affiliated organizations, or those of the publisher, the editors and the reviewers. Any product that may be evaluated in this article, or claim that may be made by its manufacturer, is not guaranteed or endorsed by the publisher.

Supplementary material

The Supplementary Material for this article can be found online at: https://www.frontiersin.org/articles/10.3389/fenvs.2022.937147/full#supplementary-material

References

Achard, F., Beuchle, R., Mayaux, P., Stibig, H., Bodart, C., Brink, A., et al. (2014). Determination of tropical deforestation rates and related carbon losses from 1990 to 2010. *Glob. Change Biol.* 20 (8), 2540–2554. doi:10.1111/gcb.12605

Arce, N., Ortiz, E., Villalobos, M., and Cordero, S. (2008). Existencias de carbono en charrales y sistemas agroforestales de cacao y banano de fincas indígenas bribri y cabécar de Talamanca. Costa Rica. *Agroforestería las Américas* 46, 30–33.

Asner, G. P., Clark, J. K., Mascaro, J., Galindo García, G. A., Chadwick, K. D., Navarrete Encinales, D. A., et al. (2012). High-resolution mapping of forest carbon stocks in the Colombian Amazon. *Biogeosciences* 9 (7), 2683–2696. doi:10.5194/bg-9-2683-2012

Baker, M., Clausen, R., Kanaan, R., N'Goma, M., Roule, T., and Thomson, J. (2003). Conflict timber: Dimensions of the problem in Asia and Africa, Volume III, African cases. *Final report submitted to the United States agency for international development* (Burlington, VT, United States: ARD)

Bautista-Cespedes, O. V., Willemen, L., Castro-Nunez, A., and Groen, T. A. (2021). The effects of armed conflict on forest cover changes across temporal and spatial scales in the Colombian Amazon. *Reg. Environ. Change* 22 (3), 70. doi:10.1007/s10113-021-01770-6

Behrens, J. T. (1997). Principles and procedures of exploratory data analysis. *Psychol. Methods* 2 (2), 131–160. doi:10.1037/1082-989x.2.2.131

Betancur-Alarcón, L., and Krause, T. (2020). Reaching for the mountains at the end of a rebelocracy: Changes in land and water access in Colombia's highlands during the post-peace agreement phase. *Front. Environ. Sci.* 8 (2), 29. doi:10.3389/fenvs.2020.546821

Butsic, V., Baumann, M., Shortland, A., Walker, S., and Kuemmerle, T. (2015). Conservation and conflict in the Democratic Republic of Congo: The impacts of warfare, mining, and protected areas on deforestation. *Biol. Conserv.* 191 (191), 266–273. doi:10.1016/j.biocon.2015.06.037

Camargo, G., Sampayo, A. M., Peña Galindo, A., Escobedo, F. J., Carriazo, F., and Feged-Rivadeneira, A. (2020). "Exploring the dynamics of migration, armed conflict, urbanization, and anthropogenic change in Colombia,". Editor B. Xue, 15, e0242266. doi:10.1371/journal.pone.0242266*PLOS ONE*11

Camisani, P. B. (2018). Sri Lanka: A political ecology of socio-environmental conflicts and development projects. *Sustain. Sci.* 13 (3), 693–707. doi:10.1007/s11625-018-0544-7

Carracedo, P., and Debon, A. (2017). Seleccion de modelos espacio-temporales con datos de panel en Matlab y R. *Rect@.* 18 (1), 93–118. doi:10.24309/recta.2017.18.2.01

Carriazo, F., Labarta, R., and Escobedo, F. J. (2019). Incentivizing sustainable rangeland practices and policies in Colombia's Orinoco region. *Land use policy* 95, 104203. doi:10.3390/land10020108

Castro-Nunez, A., Mertz, O., and Sosa, C. C. (2017). Geographic overlaps between priority areas for forest carbon-storage efforts and those for delivering peacebuilding programs: Implications for policy design. *Environ. Res. Lett.* 12 (5), 054014. doi:10.1088/1748-9326/aa6f20

Celemín, J. P. (2009). Autocorrelación espacial e indicadores locales de asociación espacial Importancia. estructura y aplicación [Internet]. Available at: https://www.redalyc.org/pdf/3832/383239099001.pdf.

Chen, C-Y. (2011). Statistical and dynamical analyses of propagation mechanisms of solitary internal waves in a two-layer stratification. *J. Mar. Sci. Technol.* 16 (1), 100–114. doi:10.1007/s00773-010-0112-z

Clerici, N., Armenteras, D., Kareiva, P., Botero, R., Ramírez-Delgado, J. P., Forero-Medina, G., et al. (2020). Deforestation in Colombian protected areas increased during post-conflict periods. *Sci. Rep.* 10 (1), 4971. doi:10.1038/s41598-020-61861-y

Clerici, N., Cote-Navarro, F., Escobedo, F. J., Rubiano, K., and Villegas, J. C. (2019). Spatio-temporal and cumulative effects of land use-land cover and climate change on two ecosystem services in the Colombian Andes. *Sci. Total Environ.* 685 (12594), 1181–1192. doi:10.1016/j.scitotenv.2019.06.275

Clerici, N., Salazar, C., Pardo-Díaz, C., Jiggins, C. D., Richardson, J. E., and Linares, M. (2018). Peace in Colombia is a critical moment for Neotropical connectivity and conservation: Save the northern Andes-Amazon biodiversity bridge. *Conserv. Lett.* 12, e12594. doi:10.1111/conl.12594

Copernicus Copernicus climate change service tutorial CDR land cover (brokered from CCI land cover) [internet]. 2021b. Available at: https://datastore.copernicus-climate.eu/documents/satellite-land-cover/D4.3.3-Tutorial_CDR_LC-CCI_v2.0.7cds_PRODUCTS_v1.0.1.pdf.

Copernicus Copernicus climate data store | Copernicus climate data store [internet]. cds.climate.copernicus.eu 2021a. Available at: https://cds.climate.copernicus.eu/cdsapp#!/dataset/satellite-land-cover?tab=overview.

DANE - Departamento Administrativo Nacional de Estadística (2020). Geoportal DANE - marco geoestadístico nacional (MGN). Accessed at: https://www.dane.gov.co/index.php/estadisticas-por-tema/cuentas-nacionales/cuentas-nacionales-departamentales.

DANE - Departamento Administrativo Nacional de Estadística (2017). Geoportal DANE ANDA. Access to anonymous metadata and microdata. Accessed at: https://sitios.dane.gov.co/anda-index/.

Durán, D., and Monsalves, M. J. (2020). Spatial autocorrelation of breast cancer mortality in the metropolitan region, Chile: An ecological study. *Medwave* 20 (01), e7766. doi:10.5867/medwave.2020.01.7766

IPCC- Intergovernmental Panel on Climate Change (2006). in *IPCC guidelines for national greenhouse gas inventories. Prepared by the national greenhouse gas inventories programme. Published by*. Editors H. S. Eggleston, L. Buendia, K. Miwa, and T. y. Tanabe K. Ngara (Hayama (Japan): IGES). Available at: https://www.ipcc-nggip.iges.or.jp/public/gpglulucf/gpglulucf_files/GPG_LULUCF_FULL.pdf

ESA (2017a). Land cover CCI algorithm theoretical basis document. Part III: Classification. Available at: https://www.esa-landcover-cci.org/?q=webfm_send/139.

ESA (2017b). Land cover CCI product user guide. Available at: https://www.esa-landcover-cci.org/?q=webfm_send/112.

Fisher, M. J., Rao, I. M., Ayarza, M. A., Lascano, C. E., Sanz, J. I., Thomas, R. J., et al. (1994). Carbon storage by introduced deep-rooted grasses in the South American savannas. *Nature* 371, 236. Available at: https://www.nature.com/articles/371236a0.

Ganzenmüller, R., Sylvester, J. M., and Castro-Nunez, A. (2022). What peace means for deforestation: An analysis of local deforestation dynamics in times of conflict and peace in Colombia. *Front. Environ. Sci.* 10 (1), 21. doi:10.3389/fenvs.2022.803368

Gaveau, D. L. A., Wich, S., Epting, J., Juhn, D., Kanninen, M., and Leader-Williams, N. (2009). The future of forests and orangutans (Pongo abelii) in sumatra: Predicting impacts of oil palm plantations, road construction, and mechanisms for reducing carbon emissions from deforestation. *Environ. Res. Lett.* 4 (3), 034013. doi:10.1088/1748-9326/4/3/034013

Gibbs, H. K., Brown, S., Niles, J. O., and Foley, J. A. (2007). Monitoring and estimating tropical forest carbon stocks: Making REDD a reality. *Environ. Res. Lett.* 2 (4), 045023. doi:10.1088/1748-9326/2/4/045023

González, J., Cubillos, A., Chadid, M., Cubillos, A., Arias, M., Zúñiga, E., et al. (2018). *Caracterización de las principales causas y agentes de la deforestación a nivel nacional período 2005-2015*. Bogotá: Instituto de Hidrología. Meteorología y Estudios Ambientales – IDEAM-. Ministerio de Ambiente y Desarrollo Sostenible. Programa ONU-REDD Colombia.

González-González, A., Villegas, J. C., Clerici, N., and Salazar, J. F. (2021). Spatial-temporal dynamics of deforestation and its drivers indicate need for locally-adapted environmental governance in Colombia. *Ecol. Indic.* 126, 107695. doi:10.1016/j.ecolind.2021.107695

Harrell, F. E. (2013). *Regression modeling strategies: With applications to linear models, logistic regression, and survival analysis*. New York: Springer-Verlag.

Hoffmann, C., García Márquez, J. R., and Krueger, T. (2018). A local perspective on drivers and measures to slow deforestation in the Andean-Amazonian foothills of Colombia. *Land Use Policy* 77, 379. Available at: https://www.sciencedirect.com/science/article/pii/S0264837717304179.

IDEAM - Instituto de Hidrología Meteorología y Estudios Ambientales (2020). Atlas climatológico. Available at: http://atlas.ideam.gov.co/visorAtlasClimatologico.html (Accessed May 27, 2021).

IDEAM-Instituto de Hidrología Meteorología y estudios ambientales instituto alexander von Humboldt. (I.Humboldt). Instituto Geográfico Agustín Codazzi (IGAC). Instituto de Investigaciones Marinas y Costeras "José Benito Vives de Andréis" (Invemar) y Ministerio de Ambiente y Desarrollo Sostenible. (2017). Mapa de Ecosistemas Continentales. Costeros y Marinos de Colombia (MEC) [map]. Versión 2.1. escala 1:100.000. URL:Available at: http://www.ideam.gov.co/web/ecosistemas/mapa-ecosistemas-continentales-costeros-marinos.

IPCC-Intergovernmental Panel on Climate Change (2003). *Good practice guidance for land use, land-use change and forestry*. IPCC National Greenhouse Gas Inventories Programme, Institute for Global Environmental Strategies IGES, 610.

Kanninen, M., Juhn, D., Leader-Williams, N., Epting, J., Gaveau, D. L. A., Wich, S., et al. (2009). The future of forests and orangutans (Pongo abelii) in sumatra: Predicting impacts of oil palm plantations. Road construction. And mechanisms for reducing carbon emissions from deforestation. *Environ. Res. Lett.* 4 (3), 034013. doi:10.1088/1748-9326/4/3/034013

Landholm, D. M., Pradhan, P., and Kropp, J. P. (2019). Diverging forest land use dynamics induced by armed conflict across the tropics. *Glob. Environ. Change* 56, 86–94. doi:10.1016/j.gloenvcha.2019.03.006

Leal Martínez, D. L,, E(13)ique Caballero, N. C., and Herrera Acosta, R. (2014). El derecho de las víctimas del conflicto armado frente a la restitución de tierras en Colombia. *criterio juridic. garantista* 5 (10), 3. doi:10.26564/21453381.433

Leite, A., Cáceres, A., Melo, M., Mills, M. S. L., and Monteiro, A. T. (2018). Reducing emissions from Deforestation and forest Degradation in Angola: Insights from the scarp forest conservation "hotspot. *Land Degrad. Dev.* 29 (12), 4291–4300. doi:10.1002/ldr.3178

Liévano-Latorre, L. F., Brum, F. T., and Loyola, R. (2021). How effective have been guerrilla occupation and protected areas in avoiding deforestation in Colombia? *Biol. Conserv.* 253, 108916. doi:10.1016/j.biocon.2020.108916

Machlis, G. E., and Hanson, T. (2008). Warfare ecology. *BioScience* 58 (8), 729–736. doi:10.1641/b580809

Memory Center, Historical (2012). Bases de datos - ¡Basta ya! Colombia: Memorias de guerra y dignidad. [Internet]. Bases de datos - ¡Basta ya! Colombia: Memorias de guerra y dignidad. Available at: http://www.centrodememoriahistorica.gov.co/micrositios/informeGeneral/basesDatos.html.

Murad, C. A., and Pearse, J. (2018). Landsat study of deforestation in the Amazon region of Colombia: Departments of Caquetá and putumayo. Remote sensing applications. *Soc. Environ.* 11, 16. doi:10.26564/21453381.433

Murillo-Sandoval, P. J., Van Dexter, K., Van Den Hoek, J., Wrathall, D., and Kennedy, R. (2020). The end of gunpoint conservation: Forest disturbance after the Colombian peace agreement. *Environ. Res. Lett.* 15 (3), 034033. doi:10.1088/1748-9326/ab6ae3

Negret, P. J., Sonter, L., Watson, J. E. M., Possingham, H. P., Jones, K. R., Suarez, C., et al. (2019). Emerging evidence that armed conflict and coca cultivation influence deforestation patterns. *Biol. Conserv.* 239, 108176. doi:10.1016/j.biocon.2019.07.021

Noordwijk, M., Rahayu, S., Hairiah, K., Wulan, Y. C., Farida, A., and Verbist, B. (2002). Carbon stock assessment for a forest-to-coffee conversion landscape in sumber-jaya (lampung. Indonesia): From allometric equations to land use change analysis. *Sci. China Ser. C Life Sci.* 45, 75–86.

Observatorio de Drogas en Colombia.| Centro de Conocimiento [internet] . Available at: http://www.odc.gov.co

Ocampo-Peñuela, N., and Winton, R. S. (2017). Economic and conservation potential of bird-watching tourism in postconflict Colombia. *Trop. Conservation Sci.* 10, 194008291773386. doi:10.1177/1940082917733862

Oehlert, G. A. (2010). First course in design and analysis of experiments. Available at: http://users.stat.umn.edu/~gary/book/fcdae.pdf.

Palmer Pol, A. L. (2019). *Estadística Aplicada con R 11. Análisis de Diseños Factoriales de Bloqueo con el Package Pblock*. Palma (Illes Balears), España: Edicions U.

Pérez Pineda., J. A. (2006). Spatial econometrics and regional science. *Investig. Económica.* 65 (258), 129–160. doi:10.1111/j.1435-5957.2008.00208.x

Perring, M. P., De Frenne, P., Baeten, L., Maes, S. L., Depauw, L., Blondeel, H., et al. (2016). Global environmental change effects on ecosystems: The importance of land-use legacies. *Glob. Chang. Biol.* 22 (4), 1361–1371. doi:10.1111/gcb.13146

Phillips, J., Duque, Á., Scott, C., Wayson, C., Galindo, G., Cabrera, E., et al. (2016). Live aboveground carbon stocks in natural forests of Colombia. *For. Ecol. Manage.* 374, 119–128. doi:10.1016/j.foreco.2016.05.009

Potapov, P. V., Turubanova, S. A., Hansen, M. C., Adusei, B., Broich, M., Altstatt, A., et al. (2012). Quantifying forest cover loss in Democratic Republic of the Congo, 2000–2010, with Landsat ETM+ data. *Remote Sens. Environ.* 122, 106–116. doi:10.1016/j.rse.2011.08.027

Prem, M., Saavedra, S., and Vargas, J. F. (2020). End-of-conflict deforestation: Evidence from Colombia's peace agreement. *World Dev.* 129 (129), 104852. doi:10.1016/j.worlddev.2019.104852

R Core Team (2017). R: A language and environment for statistical computing. Available at: https://www.R-project.org/.

Reuveny, R., Mihalache-O'Keef, A. S., and Quan, Li (2010). The effect of warfare on the environment. *J. Peace Res.* 47 (6), 749–761. doi:10.1177/0022343310382069

Rincón, A., and Ligarreto, G. (2007). Productividad de la asociación maíz-astos en suelos ácidos del Piedemonte Llanero colombiano. *Revista Corpoica-Ciencia y Tecnología Agropecuaria* 9 (1), 73–80. doi:10.21930/rcta.vol9_num1_art:107

Rincón, Á., and Ligarreto, G. (2008). Productividad de la asociación maíz–pastos en suelos ácidos del Piedemonte Llanero colombiano. *Ciencia Tecnología Agropecuaria* 9 (1), 73–80. doi:10.21930/rcta.vol9_num1_art:107

Rincón-Ruiz, A., and Kallis, G. (2013). Caught in the middle, Colombia's war on drugs and its effects on forest and people. *Geoforum* 46, 60. Available at: https://www.sciencedirect.com/science/article/abs/pii/S0016718512002837.

Rincón-Ruiz, A., Pascual, U., and Flantua, S. (2013). Examining spatially varying relationships between coca crops and associated factors in Colombia, using geographically weight regression. *Appl. Geogr.* 37, 23–33. doi:10.1016/j.apgeog.2012.10.009

Rodríguez-de-Francisco, J. C., del Cairo, C., Ortiz-Gallego, D., Velez-Triana, J. S., Vergara-Gutiérrez, T., and Hein, J. (2021). Post-conflict transition and REDD+ in Colombia: Challenges to reducing deforestation in the Amazon. *For. Policy Econ.* 127, 102450doi:10.1016/j.forpol.2021.102450

Salazar, G. S. (2016). El conflicto armado y su incidencia en la configuración territorial: Reflexiones desde la ciencia geográfica para la consolidación de un periodo de pos negociación del conflicto armado en Colombia. *Bitácora Urbano Territorial* 26 (2), 45. doi:10.15446/bitacora.v26n2.57605

Sanchez-Cuervo, A. M., and Aide, T. M. (2013). Identifying hotspots of deforestation and reforestation in Colombia (2001–2010): Implications for protected areas. *Ecosphere* 4 (11), art143. doi:10.1890/es13-00207.1

Schoon, M. L., and Cox, M. E. (2012). Understanding disturbances and responses in social-ecological systems. *Soc. Nat. Resour.* 25 (2), 141–155. doi:10.1080/08941920.2010.549933

Statista Research Department (2021). Statista research department. Available at: https://es.statista.com/estadisticas/1191612/numero-de-personas-en-colombia-por-departamento (Accessed January 6, 2022).

Suarez, A., Árias-Arévalo, P. A., and Martínez-Mera, E. (2018). Environmental sustainability in post-conflict countries: Insights for rural Colombia. *Environ. Dev. Sustain.* 20 (3), 997–1015. doi:10.1007/s10668-017-9925-9

Szantoi, Z., Jaffrain, G., Gallaun, H., Bielski, C., Ruf, K., Lupi, A., et al. (2021). Quality assurance and assessment framework for land cover maps validation in the Copernicus Hot Spot Monitoring activity. *Eur. J. Remote Sens.* 54 (1), 538–557. doi:10.1080/22797254.2021.1978001

Turner, W., Rondinini, C., Pettorelli, N., Mora, B., Leidner, A. K., Szantoi, Z., et al. (2015). Free and open-access satellite data are key to biodiversity conservation. *Biol.*

Conserv. 182, 173. Available at: https://www.sciencedirect.com/science/article/abs/pii/S000632071400473X.

UNODC y Ministerio de Justicia y del Derecho (2015). Caracterización Regional de la problemática asociada a las drogas ilícitas en el departamento del Meta. Guaviare y Caqueta. Available at http://www.odc.gov.co/TERRITORIOS/Documentos/Caracterizaciones.

Villa, Romero. A. R., Moreno Altamirano, L., and García de la Torre, G. S. (2012). *Epidemiología y estadística en salud pública*. McGraw-Hill Medical.

Warne, R. (2014). A primer on multivariate analysis of variance (MANOVA) for behavioral scientists. *Pract. Assess. Res. Eval.* 1917. doi:10.7275/sm63-7h70

Yasmi, Y., Kelley, L. C., and Enters, T. (2013). Community–outsider conflicts over forests: Perspectives from southeast asia. *For. Policy Econ.* 33, 21–27. doi:10.1016/j.forpol.2012.05.001

Yepes, A., Navarrete, D. A., Phillips, J. F., Duque, A. J., Cabrera, E., and Galindoet, al. (2011). *Estimación de las emisiones de dióxido de carbono generadas por deforestación durante el periodo 2005-2010*. Bogotá (Colombia): Instituto de Hidrología. Available at: http://www.ideam.gov.co/documents/13257/13548/Emisiones.pdf/a86b9bd1-0050-4bb9-a54f-c3ad6b3cda26.

Yu, T., Yu, G., Li, P-Y., and Wang, L. (2014). Citation impact prediction for scientific papers using stepwise regression analysis. *Scientometrics* 101 (2), 1233–1252. doi:10.1007/s11192-014-1279-6

10.3389/fenvs.2022.937147

Appendix A: Factors used in Model 2 to understand the role of a specific year (i.e., time) and a municipality's characteristics on deforestation in Neotropical forests of central Colombia

Municipality	Factor in the model
Calamar	−22.33
Cartagena del Chairá	71.92
El Retorno	−10.38
La Macarena	83.96
Mesetas	−30.47
Puerto Concordia	−4.8
Puerto Rico	1.58
San José del Guaviare	89.22
San Vicente del Caguán	−202.16
Uribe	1.50

frontiers | Frontiers in Environmental Science

TYPE Original Research
PUBLISHED 20 September 2022
DOI 10.3389/fenvs.2022.981608

OPEN ACCESS

EDITED BY
Thiru Selvan,
Tripura University, India

REVIEWED BY
Amit Chawla,
Institute of Himalayan Bioresource Technology (CSIR), India
Pankaj Panwar,
Indian Institute of Soil and Water Conservation (ICAR), India

*CORRESPONDENCE
D. R. Bhardwaj,
bhardwajdr_uhf@rediffmail.com

SPECIALTY SECTION
This article was submitted to Land Use Dynamics,
a section of the journal
Frontiers in Environmental Science

RECEIVED 29 June 2022
ACCEPTED 19 August 2022
PUBLISHED 20 September 2022

CITATION
Kumar D, Thakur CL, Bhardwaj DR, Sharma N, Sharma P and Sankhyan N (2022), Biodiversity conservation and carbon storage of Acacia catechu willd. Dominated northern tropical dry deciduous forest ecosystems in north-western Himalaya: Implications of different forest management regimes. *Front. Environ. Sci.* 10:981608.
doi: 10.3389/fenvs.2022.981608

Biodiversity conservation and carbon storage of *Acacia catechu* willd. Dominated northern tropical dry deciduous forest ecosystems in north-western Himalaya: Implications of different forest management regimes

Dhirender Kumar[1], C. L. Thakur[1], D. R. Bhardwaj[1]*, Nidhi Sharma[2], Prashant Sharma[1] and Neeraj Sankhyan[3]

[1]Department of Silviculture and Agroforestry, Dr YSP University of Horticulture and Forestry, Solan, India, [2]Division of Temperate Animal Husbandry, IVRI, Mukteshwar, India, [3]Department of Basic Sciences, Dr YSP University of Horticulture and Forestry, Solan, India

Sustainable forest management is the key to biodiversity conservation, flow of resources and climate change mitigation. We assessed the impact of various forest management regimes (FMRs): legal felling series [(reserve forest (RF), demarcated protected forest (DPF), un-demarcated protected forest (UPF), co-operative society forest (CSF) and un-classed forest (UF)] on biodiversity conservations and carbon storage in *Acacia catechu* Willd. Dominated northern tropical dry deciduous forest ecosystems in Nurpur Forest Division of north-western Himalaya, India. The study revealed significant variations in floristic composition, biodiversity indices, population structure and C storage potential among different forest management regimes. The RF and DPF were found to be rich in species diversity and richness whereas the Simpson dominance index for trees and shrubs was maximum in UF and UPF, respectively. The diversity of understory herbs were higher in CSF and UF. The maximum density of seedlings, saplings and poles were recorded in RF followed by DPF and UPF, whereas the minimum density was found in CSF. The tree C density (69.15 Mg C ha^{-1}) was maximum in UF closely followed by RF; whereas the minimum was recorded in CSF (33.27 Mg C ha^{-1}). The soil C density was maximum in RF (115.49 Mg C ha^{-1}) and minimum in CSF (90.28 Mg C ha^{-1}). Similarly, the maximum total ecosystem C density was recorded in RF (183.52 Mg C ha^{-1}) followed by DPF (166.61 Mg C ha^{-1}) and minimum in CSF (126.05 Mg C ha^{-1}). Overall, UF management regimes were shown to have a greater capacity for C storage in vegetation, whereas strict FMRs, such as RF and DPF, were found to be more diverse and have a higher soil and ecosystem carbon density. The study established that in the midst of climate and biodiversity emergencies, it is urgent to maintain, protect and strengthen the network of RF and DPF FMRs for biodiversity conservation, climate change adaptation and mitigation.

KEYWORDS

carbon density, reserve forests, protected forest, unclassed forest, community society forest, stand characteristics, natural regeneration, biodiversity conservation

Introduction

Tropical forests once covered over half of the total area of the tropics (Janzen, 1988), but have dwindled to a great extent during the last decennia (Sagar and Singh, 2005). On the global scale, out of the total coverage of forests, 52% are tropical forests (Singh and Singh, 1988). In India, forests cover nearly 21.71% of the country's total geographical area (FSI, 2021) and tropical forests account for 86% of the total forest land (Singh and Singh, 1988). Tropical forests also harbor maximum diversity of plant species found on the earth (WCMC, 1992). Among the different forest types, tropical forests contribute to 25% of the total terrestrial carbon stock and are major sink (Bonan, 2008), playing major roles in regulating climate dynamics on earth (Lewis et al., 2009; Zhou et al., 2013). Thus, tropical forests play a critical role in the global carbon (C) balance, biodiversity conservation and offer several other valuable environmental services. In addition to this, these ecosystems are a stockpile of resources and sustain the lives of millions of people across the globe. Tropical dry deciduous forests (TDFs) are particularly indispensable for sustaining vulnerable households during hardships (Blackie et al., 2014). These forests are rich in medicinal and economically important plants. But TDFs are dwindling at an alarming rate (Blackie et al., 2014) due to excessive exploitation and land-use change, biological invasion (Kumar et al., 2021) and climate change. Thus, a study on species composition and diversity, carbon sink potential, population structure and soil health status of northern TDFs is ecologically significant besides being useful in forest management.

Terrestrial ecosystems, particularly TDFs with their abundant biodiversity and C storage capacity (Kothandaraman, et al., 2020) are major C sinks playing a dynamic role in the mitigation of global warming. In a forest ecosystem, C is stored in vegetation carbon, soil carbon, and detritus pools (Lee et al., 2014; Herault and Piponiot, 2018; Lafleur et al., 2018). Therefore, the estimation of forest ecosystem C storage is of utmost importance to understand global carbon cycle and for framing strategies for mitigating the likely impacts of climate change (Sun and Liu, 2020). The global forests hold 662 Gt C stock of which 300 Gt is in soil organic matter, 295 Gt in living biomass and 68.0 Gt in detritus, which accounts for the sequestration of 2.4 pentagrams of C every year (FAO, 2020). As a result, preserving or restoring standing forest biomass is a relatively low-hanging fruit in terms of reducing human GHG emissions (Seddon et al., 2020). Forest management is thus required which aims at the long-term storage of biomass and soil. Defining the C storage/sequestration capacity of forest ecosystems always remains a major strategy for reducing CO_2 concentrations in the atmosphere (Forster et al., 2021). Particularly, protected forests (PF) are one of the major C sinks in the forest ecosystems, although their efficiency varies with continuance (Collins and Mitchard, 2017).

The type of forest management regimes (FMRs) have a key role in maintaining structural diversity of forests and also helps in protection of forests (Gao et al., 2014; Chazdon et al., 2017; Dieler et al., 2017; Mancosu et al., 2018; Reise et al., 2019). Stand diversity is recognized as a significant aspect of forest ecosystem functioning such as primary production (Paquette and Messier 2010; Liang et al., 2016), stability of wood production (Jucker et al., 2014), resistance to environmental disturbances (Pretzsch et al., 2013; Jactel et al., 2017) and nutrient cycling (Richards et al., 2010; Handa et al., 2014). A forest stand with greater diversity is more efficient in providing a wide range of provisioning services (Gamfeldt et al., 2013; Forrester and Bauhus, 2016), more resistant to various disturbances, holds sufficient soil nutrients and has a considerably greater prediction value for tree C (Liang et al., 2016; Van et al., 2017; Zhang et al., 2017; Liu et al., 2018) than the stand with low species diversity (Wardle, 2001; Lefcheck et al., 2015; Jactel et al., 2017).

The intrinsic role of forests in C management and biodiversity management is an additional service that sustainable forest management can offer leading to earning financial incentives through REDD+ in developing countries. Being a signatory to the UNFCCC, India participates in REDD+ through the Forest Carbon Partnership Facility program. In India, forests cover 21.71% of the land area (FSI 2021), are legally managed under the Indian Forest Act of 1927 and are classified as reserve forest (RF), PF and un-classed forest (UF) based on degree of protection provided for the conservation or restoration. In RF, utilization is generally strictly prohibited, while the PF have a limited degree of protection. The UF is an area recorded as a forest but not included in RF or PF category (IFA, 2016). In India, more than half (57.05%) of the total recorded forest area falls under RF, whereas less than one-third (27.38%) of the forests are designated as PF and 15.57% as UF (FSI, 2021). The PF are further divided into demarcated protected forest (DPF) and un-demarcated protected forest (UPF) based on boundary demarcation. Further, in Himachal Pradesh, a small hill state situated in north-western Himalayas, some other category of forest exists, such as co-operative society forest (CSF) under Kangra Forest Co-operative Scheme, 1938, where local people are involved in management and utilization of certain forest. The recorded forest area of Himachal Pradesh is 37,948 sq km, of which the majority of the forest area (76.12%) is under PF (DPF-33.87% + 42.25% UPF), 18.05% is under UF, 4% under RF, and 0.05% is managed under CSF (FSI, 2021). In Himachal Pradesh, the tropical dry deciduous forest occurs up to an altitude of 1,200 m in the lower hills and accounts for about 14.54% of the total forest cover of state (FSI, 2019).

Acacia catechu, commonly known as Khair, is a multipurpose moderate-sized deciduous tree primarily occurring in the tropical moist deciduous forests, dry tropical forests and tropical thorn forests (Champion and Seth, 1968). In Himachal Pradesh, Khair is widely distributed in Mandi, Hamirpur, Kangra (Nurpur), Solan, Sirmour, Una and Bilaspur districts. However, it is most abundantly found in the Nurpur Forest Division which is maintained under Khair Working Circle because of favorable climatic and edaphic condition. It is an economically significant plant that is commercially exploited for katha (catechin) and cutch (Catechu tannic acid) (Lakshmi and Kumar, 2011). Besides its commercial importance, the rural communities depend on this tree for fulfilling their daily needs of fuel, fodder, building material, etc. Owing to their high commercial and social value, Khair forests are susceptible to a high degree of anthropogenic pressure, especially illicit logging. These disturbances, tend to change/influence the species composition, stand structure, C cycling of the forest ecosystem (Chauhan, 1999; Yohannes et al., 2015) along with biomass loss (Gautam and Mandal, 2016), and a decline in the plant diversity and other associated vegetation (Sapkota et al., 2010; Gautam and Mandal, 2016). Even a minor perturbation in these forest ecosystems could have a substantial impact on biodiversity, species composition and forests C-storage capacity. Studies carried out in various parts of the world have revealed that the stand diversity and C stock of forest ecosystems are influenced by several factors, of which the intensity and frequency of anthropogenic disturbances have been reported to play a significant role in regulating the regeneration dynamics, structure and floristic composition of forest ecosystems (Upadhaya et al., 2008; Mir and Upadhaya, 2017). Hence, the Khair forests in the foothills of Shiwalik of the Nurpur forest division are legally managed under different FMRs i.e., RF, DPF, UPF, CSF, and UF based on the management objectives and location of forests with respect to distance from human habitat (Working Plan, 2013). The level of disturbances in these forest categories varied with their protection status and rights to utilize resources. These FMRs provide varied degree of protection from encroachment to Khair Forest and play a crucial role in the maintenance of species diversity and C stock. Consequently, the occurrence of Khair dominated forests in Nurpur Forest Division makes the region more appropriate for knowing the influence of different FMR's and disturbances which ultimately help to determine the conservation implication (Working Plan, 2013). Further, management and cultural operations in a forest are the most important factors that influence the species diversity, C content, stand characteristics, and regeneration process. However, the lack of monitoring and evaluation of various management regimes is a great hindrance to understanding the effectiveness and impact of FMRs on these ecosystem services. As these forests are continuously subjected to exploitation and anthropogenic pressure, therefore it has become imminent to have an in-depth understanding of the impact of management practices on biodiversity and C storage capacity. Despite their vast ecological and socio-economic significance so far, there has not been any comprehensive study that examines the biodiversity and C stock in relation to various management regimes, thus creating a hindrance to set conservation implications for C management, biodiversity conservation and sustainable utilization that will eventually enhance the ecological health of the forests and increase the flow of ecosystem services (Pearce, 2001; Malhi et al., 2008; Paudel and Sah, 2015). Therefore, this study was carried out with the objectives to 1) quantify the differences in the C stock of the woody biomass and soil, 2) estimate biodiversity conservation and 3) study population distribution and stand structure, under different FMRs in the Nurpur Forest Division of Himachal Pradesh in India.

Materials and methods

Study area

The present study was carried out in the foothills of Shiwalik ranges of Himachal Pradesh that lies between the latitudes 75.77°–76.02° N and longitudes 32.23°–32.40° E with elevation ranges from 500 to 700 m above mean sea level (asl). The area has a hot dry summer from April to June and monsoon season from July to September, followed by a cool and relatively dry winter. The texture of the soil is sandy loam, with sand stones rock type. The scientific management of Khair forests in Himachal Pradesh was initiated in 1879 and was traditionally managed through selection felling, i.e., harvesting of an individual tree above certain diameter and leaving a few mother trees for regeneration. The interval and diameter for harvest varied according to species with no tree less than 10 cm diameter harvested. However, green felling has been banned vide orders of the Hon'ble Supreme Court of India dated 12th

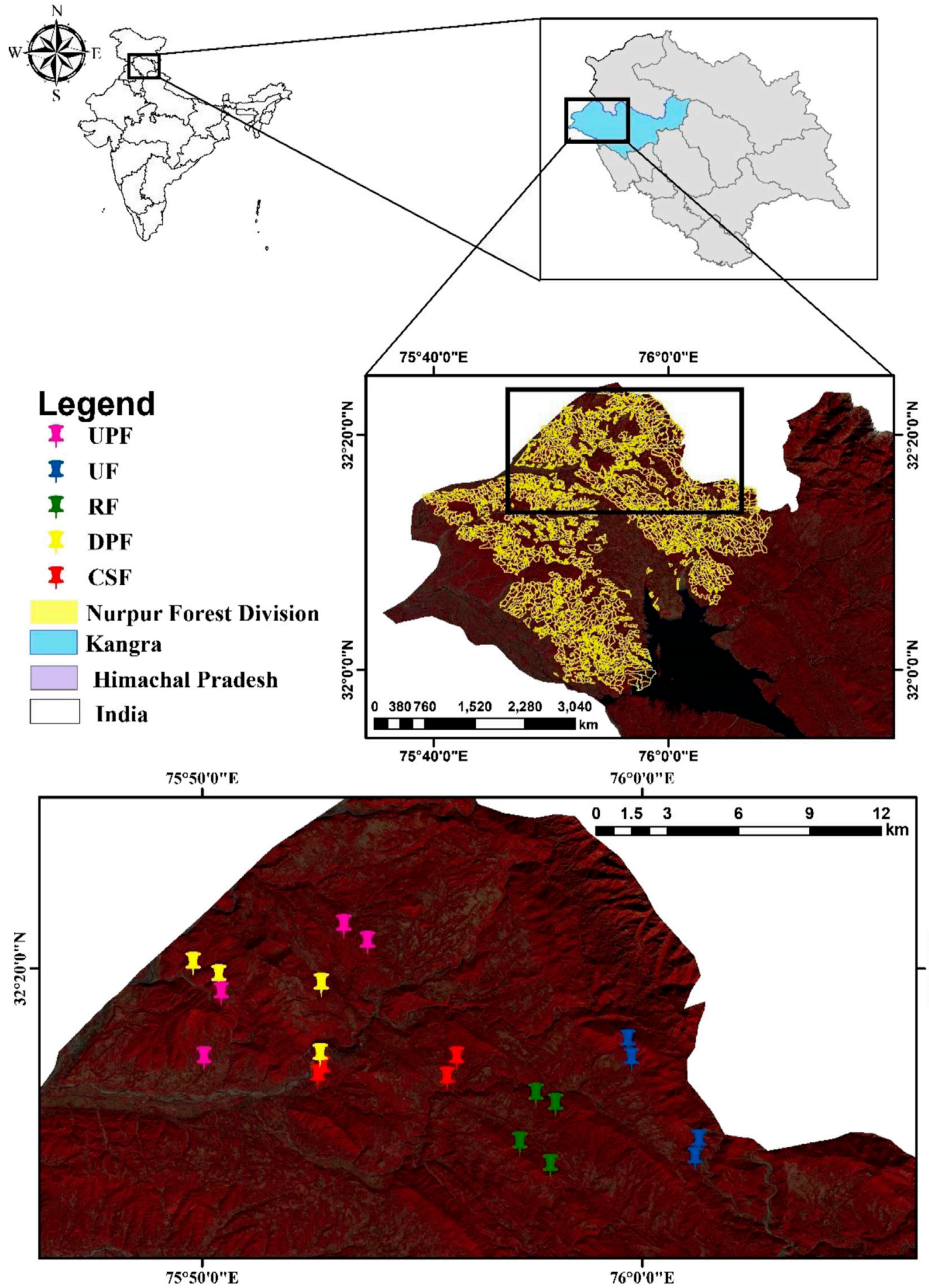

FIGURE 1
Map showing study area under investigation.

December 1996 and February 2000 and reinitiated on experimental basis in the selected forest compartments vide the Hon'ble Supreme court order of 2018 through which it has been proposed that 80% of trees of *A. catechu* of 25 cm diameter and above be felled and the remaining 20% (>20 cm) retained as mother trees. Therefore, five differently

10.3389/fenvs.2022.981608

TABLE 1 Detailed description of each FMRs of Khair Working Circle in Nurpur Forest Division, Himachal Pradesh, India (Source: Working Plan, 2013).

FMRs	Code	Notification number with date	Detail of selected compartments		
			Compartment name	Area (ha)	Silviculture system
Reserved Forest	RF	Notification No.111-F and 112F dated 6th March 1879	C_{3c} R_1 N Tattal	59.08	Chir Shelterwood Working Circle, PB-II with Khair over lapping
			C_{3b} R_1N Tattal	80.52	Chir Shelterwood Working Circle, PB-I with Khair over lapping
			C_1 R_2 N Mehdhar	52.20	Chir Shelterwood, PB-I with Khair overlapping
			C_2 R_2 N Mehdhar	96.29	Chir shelterwood PB-II with Khair overlapping
Un-classed Forest	UF	Notification No.111-F and 112F dated 6th March 1879	C_{10} U_{20} Punder	23.88	Selection system, Plantation Working Circle with Khair overlapping
			C_{15} U_{20} Punder	64.74	Selection system, Plantation Working Circle with Khair overlapping
			C_3 U_{20} Punder	32.78	Selection system, Plantation Working Circle with Aspect
			C_7 U_{20} Punder	36.42	Selection system, Plantation Working Circle with Khair overlapping
Demarcated Protected Forest	DPF	Notification No.57 dated the 26th of January 1897 and No. 56 dated 6th February 1904	C_2 P_{35} N Kopra	9.31	Chir Shelterwood Working Circle, PB-IV with Khair overlapping
			P_{32} N Bharnu	6.72	Chir Shelterwood Working Circle, PB-IV with Khair overlapping
			P_{31} N Mehra	17.01	Chir Shelterwood Working Circle PB-IV with Khair overlapping
			C_{26} Nurpur	16.14	Chir Shelterwood Working Circle PB-IV with Khair overlapping
Un-demarcated Protected Forest	UPF	Notification No 992 dated the 11th January 1919	C_{11} UP_{14} Thora	6.07	Khair overlapping and Plantation working circle
			C_5 UP_{10} Sadwan	26.30	Chir Shelterwood Working Circle, PB- Unalloted
			C_6 UP_{10} Sadwan	10.92	Plantation Working Circle
			UP C_{31} Mehra	29.31	Khair overlapping and Plantation Working Circle
Co-operative Society Forests	CSF	The Co-operative Society Forest were managed under the working plans for other Governments Forests up to 1941 when these societies were created. Each Co-operative Society had a separate working plan/working scheme till 1967–68	P_1 CFS Jachh	4.86	Plantation Working Circle
			P_2 CFS Jachh	9.71	Plantation Working Circle
			U_8 CFS Gahin lagor	18.79	Plantation Working Circle
			U_8 CFS Gahin lagor	22.83	Plantation Working Circle

managed FMRs viz., Reserve Forest (RF), Demarcated Protected Forest (DPF), Un-demarcated Protected Forest (UPF), Co-operative Society Forest (CSF) and Un-class Forest (UF) in Khair Working Circle of Nurpur Forest Division of Himachal Pradesh, India were selected (Figure 1) so as to represent the entire range of canopy conditions and management regimes based on the satellite and field observations. The detailed description of each FMRs is tabulated in Table 1.

Species diversity and stand structure

In each FMRs, four separate compartments were selected for executing the present study. Under each compartment, a plot of 6.25 ha (250 m × 250 m) was demarcated for a detailed study. Thus, there were 20 stands (4 compartments × 5 Forest regimes). In each forest stand, four sample plots of 0.1 ha (31.62 m × 31.62 m) were laid out in the main plot for trees. In each 0.1 ha of sample plot, two subplots of size 5 m × 5 m were laid out. Further, in each shrub plot, two subplots of size 1 m × 1 m were laid out to study the herb-related traits. Standard measurement procedures were followed for taking primary observations, such as tree height and diameter at breast height (DBH). Tree height was measured with a Ravi altimeter (Blue Leiss Hypsometer). The diameter was measured by taking two measurements of stems (major and minor axis) at breast height (1.37 m) with tree callipers, and their mean was calculated as the DBH of a tree. To analyze the tree structure, the individuals were categorized into six diameter classes viz., 10–15, 15–20, 20–25, 25–30, 30–35, >35 cm. A regeneration survey was also carried out in a 2 m × 2 m plot by recording the number of seedlings (<0.5 m) and saplings (0.5–2 m) (Schwab et al., 2022). Trees, saplings and seedlings within each plot were counted to determine their density. The specimens were prepared and identified at Department of Forest Products, Dr. YSP University of Horticulture and Forestry, Nauni, Solan, Himachal Pradesh.

Vegetation indices

Community diversity was assessed using non-parametric measures such as diversity indices (Magurran, 1988). Simpson diversity index (D′) (Simpson, 1949), Margalef index of species richness (MI) (Margalef, 1958), Shannon–Weaver diversity index (H′) (Shannon and Weaver, 1963) and Pielou equitability (Ep) (Pielou, 1966) were calculated using the formulae mentioned below.

Shannon-Weaver Index of diversity (H′) = -∑pi In pi.

Simpson's diversity index (D′) = 1-$\sum pi^2$

Margalef's Index of richness (MI) =(S-1)/lnN.

Pielou equitability (Ep) = $\frac{H'}{H'_{max}} = \frac{H'}{lnS}$

Where,

pi = ni/n (ni = IVI value of *i*th species, n = Total IVI value).

S = total number of species.

N = total density per ha

ln = log natural.

Estimation of tree C density

To determine the tree C stock, the above-ground tree biomass (AGB) and the volume (m^3 ha^{-1}) of each species were first estimated using volumetric equations (Table 2) (FSI, 1996). The estimated growing stock volume of the tree was then converted to AGB (Mg ha^{-1}) by multiplying the growing stock volume with specific wood density (g cm^{-3}) of the respective species (Rajput et al., 1996). Global wood density database was used for wood specific gravity of each species (Chave et al., 2009; Zanne et al., 2009). The below-ground tree biomass (BGB) (fine and coarse roots) was estimated using regression equation (Cairns et al., 1997):

$$\mathrm{BGB}\left(\mathrm{Mg\,ha^{-1}}\right) = \exp\left\{-1.059 + 0.884 \times \ln\left(\mathrm{AGB}\right) + 0.284\right.$$

The total tree biomass (Mg ha^{-1}) is the sum of AGB and BGB. The C density of the tree species was then determined as:

$$\text{Carbon density}\left(\mathrm{Mg\,ha^{-1}}\right) = \text{Biomass}\left(\mathrm{Mg\,ha^{-1}}\right) \times \mathrm{C\%}$$

where C is the carbon concentration of the corresponding vegetation. A universal coefficient of 0.475 was used for tree C estimation (Raghubanshi, 1991; Singh and Chand, 2012), indicating approximately 47.5% of C in dry plant biomass (Westlake, 1963).

Understory C density

The understory biomass, i.e., shrubs (woody species other than trees with less than 1 m height) and herbs, was estimated by randomly laying 5 m × 5 m and 1 m × 1 m quadrat for shrubs and herbs, respectively. The shrub biomass was estimated by harvesting method, where 10% of each species of shrub was harvested and the fresh weight of the harvested sample was measured immediately with an electronic balance in the field. For the herbaceous biomass, all the herbaceous vegetation falling in 1 m × 1 m quadrat was harvested and the fresh weight was measured immediately in the field. The representative samples of both herbs and shrubs were taken to the laboratory, where they were oven-dried at 65°C for 48 h. The dry weight of the sample was then extrapolated to find out the entire biomass of shrub and herb samples. The C stock in the understory (shrubs and herbs) was considered to be 50% of dry weight (Dar and Sundarapandian, 2015). Therefore, the understory C stock was determined by multiplying the dry weight with a coefficient of 0.50.

Soil C density

Soil carbon density (SCD) was then calculated based on the bulk density and soil organic carbon concentration using the following equation:

SCD = [Soil bulk density (g cm^{-3}) × Soil depth (0–40 cm) × soil organic carbon] × 100 (Nelson and Sommers, 1996).Where, the soil organic carbon was calculated using Walkley and Black (1934). For bulk density, undisturbed soil samples were collected with a soil corer of known volume (31.4 cm^3) and oven-dried at 105°C for 72 h to determine the dry weight.

Total vegetation and ecosystem C density (Mg ha^{-1})

The total vegetation C density (VCD) was taken as the sum of C content in trees, shrubs and herbs whereas the total ecosystem C density (ECD) was taken as the sum of VCD and soil pool i.e., SCD.

Statistical analysis

Species diversity matrices were calculated using the software Past 3.1 program (version 3.1; Oyvind Hammer, Natural History

TABLE 2 List of volumetric equations and species-specific gravity, biomass expansion factor used in present study (Source: FSI, 1996).

Scientific name	Volumetric equation	Wood specific gravity	Biomass expansion factor
Acacia catechu	$V = 0.048535–0.183567*SQRT*D+3.787825*D^2$	0.875	2.52
Aegle marmelos	$V = D^2*(0.0697/D^2–1.4597/F16 + 11.79933–2.35397*D)$	0.754	1.5
Albizia lebbeck	$V = 0.27–2.953*D+12.336*D^2$	0.66	1.5
Bombax ceiba	$V = D^2*(0.18573/D^2–2.8541/D+15.03576)$	0.329	1.4
Broussonetia papyrifera	V=SQRT (−0.10185087 + 3.07466775*D)	0.619	1.5
Butea monosperma	$V = D^2*(0.0697/D^2–1.4597/D+11.79933–2.35397*D)$	0.465	1.5
Casearia tomentosa	$V = 0.066 + 0.287*D^2*H$	0.746	1.5
Cassia festula	$V = 0.066 + 0.287*D^2*H$	0.746	1.5
Dalbergia sissoo	$V = -0.013703 + 3.943499*D^2$	0.669	1.5
Eucalyptus globulus	$V = -0.0015 + 0.2401*D^2*H$	0.619	1.5
Ficus benghalensis	V=SQRT (0.03629 + 3.95389*D-0.84421*SQRT(D))	0.385	1.5
Ficus glomerata	V=SQRT (0.3629 + 3.95389*D-0.84421*SQRT(D))	0.619	1.5
Ficus palmata	V=SQRT (0.3629 + 3.95389*D–0.84421*SQRT(D))	0.619	1.5
Flacourtia indica	$V = D^2*(0.0697*D^2–1.4597/D+11.79933–2.35397*D)$	0.619	1.5
Lannea coromandelica	$V = -0.004511 + 0.377131*D^2*H$	0.513	1.5
Leucaena leucocephala	$V = D^2*(−0.00342/D^2–0.0922/D+2.28178 + 9.46641*D)$	0.55	1.5
Mallotus phillippensis	$V = 0.14749–2.87503*D+19.61977*D^2–19.1163*D^3$	0.64	1.5
Morus alba	$V = 0.167174–1.735312*D+12.039017*D^2$	0.622	1.3
Ougeinia oojeinensis	$V = D^2*(0.0697/D^2–1.4597/D+11.79933–2.35397*D)$	0.704	1.5
Phyllanthus embelica	$V = -0.406 + 3.54*D-2.31*D^2$	0.619	1.5
Pinus roxburghii	$V = D^2*(0.167095/D^2–2.085944/D+9.929936)$	0.47	1.5
Pistacia integerrima	$V = D^2*(0.0697/D2–1.4597/D+11.79933–2.35397*D)$	0.619	1.5
Pyrus pashia	$V = D^2*(0.0697/D^2–1.4597/D+11.79933–2.35397*D)$	0.754	1.5
Stephegyne parvifolia	V = D2*(0.0697/D2-1.4597/F30 + 11.79933–2.35397*D)	0.619	1.5
Syzygium cumini	$V = D^2*(0.09809/D^2–1.94468/D+13.36728–6.33263*D)$	0.647	1.5
Terminalia arjuna	V=SQRT (-0.14017 + 3.36423*D)	0.628	1.56
Terminalia bellirica	V=SQRT (−0.14017 + 3.36423*D)	0.628	1.56
Wendlandia exserta	$V = D^2*(0.0697/D^2–1.4597/D+11.79933–2.35397*D)$	0.704	1.51
Xylosma longifolium	$V = D^2*(0.0697/D^2–1.4597/D+11.79933–2.35397*D)$	0.619	1.5

V = volume (m^3), D = diameter at breast height, H = height.

Museum, University of Oslo) (Hammer et al., 2001). SPSS Software package (ver. 20.0; SPSS, Chicago, IL) was used for statistical analysis and the analysis of variance (ANOVA) was performed using Duncan's Multiple Range Test to test the significance of C density of different FMRs.

Results

Biodiversity of Khair dominated forests

The diversity indices of different FMRs of Khair Working Circle is depicted in Table 3. The maximum number of tree species representations was recorded in the RF (17) while the minimum number was found in UPF and UF. Under the shrub category, the maximum number of shrub species (9.0) was recorded in RF; however, its variation with the other forest regime was very less. In the herb category, the maximum number of herbs (6) was recorded in UF while the minimum number of herb species was found in the DPF (3). Similarly, the maximum tree density (399.17 N ha^{-1}) and herb density (43,700.00 N ha^{-1}) among the different FMRs were observed in RF. However, the shrub forms were having the maximum density (3,725.00 N ha^{-1}) under the DPF management regimes. A similar pattern for basal area (m^2 for trees and cm^2 for understory vegetation) was observed under herb, shrub and tree layers among different FMRs.

A cursory look at the tree component (Table 3) of the Khair Working Circle revealed that the different biodiversity indices viz., Simpson's diversity index (D′), Shannon-Weaver Index of diversity (H′), Pielou equitability (Ep), and Margalef's Index of richness (MI) were having their highest values in DPF/RF categories as compared

TABLE 3 Values of various diversity indices in forests under different FMRs in Khair Working Circle of Nurpur Forest Division, Himachal Pradesh, India.

Diversity indices	Trees					Shrubs					Herbs				
	RF	DPF	UPF	CSS	UF	RF	DPF	UPF	CSF	UF	RF	DPF	UPF	CSF	UF
Flora	17	16	11	13	11	9	7	7	6	6	5	3	5	4	6
Density (N ha^{-1})	399	340	308	250	294	3,160	3,725	2,775	3,260	3,440	43,700	33,865	31,000	26,800	32,900
Basal area (m^2 cm^2)[a]	14.53	12.21	9.25	6.64	13.67	92,080.34	102,978.10	84,660.08	101,180.38	97,838.91	722.41	517.81	550.28	472.03	611.17
D′	0.8	0.84	0.8	0.75	0.56	0.65	0.69	0.60	0.63	0.65	0.65	0.5	0.67	0.70	0.67
H′	1.91	2.13	1.85	1.78	1.24	1.45	1.48	1.32	1.30	1.31	1.24	0.85	1.25	1.29	1.29
MI	2.68	2.58	1.75	2.18	1.78	0.99	0.73	0.76	0.62	0.61	0.37	0.19	0.39	0.29	0.48
Ep	0.67	0.77	0.77	0.69	0.52	0.66	0.76	0.68	0.73	0.73	0.77	0.78	0.78	0.93	0.72

[a]Basal area in m^2 for trees whereas cm^2 for shrub and herbs, N = number, D′ = Simpson's diversity index, H′ = Shannon-Weaver Index of diversity, MI = Margalef's Index of richness, Ep = Pielou equitability.

to UPF, CSF and UF. However, D′ (0.56), H′ (1.24) and Ep (0.52) exhibited their minimum values under UF. Ep demonstrated that the tree species are distributed equitably in DPF and UPF categories. For the shrub component (Table 3), not much variation was found for D′ under different FMRs. However, the H′ revealed the highest values under RF (1.45) and DPF (1.48) than under UPF (1.32), CSF (1.30) and UF (1.31). Similarly, MI (0.99) exhibited the maximum species richness under RF management regime. Shrub species in the Khair Working Circle demonstrated maximum value of Ep (0.76) under DPF. For herbs, both D′ and H′ indicated the highest value under CSF and UF. MI also showed its highest value under UF (0.48) and Ep was maximum under CSF (0.93) whereas the other FMRs revealed little or no variability for Ep.

Stand and population structure (N ha^{-1})

Figure 2 depicts the stand structure under the different FMRs. The distribution of trees under different FMRs barring UF exhibited the reverse J-shaped pattern (a characteristic feature of De liocourt's law) from 15–20 cm diameter class onward. Among all the FMRs, the RF had more similarity to De liocourt's law in terms of stem progression from 15–20 cm to >35 cm diameter class. The distribution of stems in the diameter classes viz., 10–15, 20–25, 25–30, and 30–35 cm was the greatest in RF whereas the distribution of stems in the diameter class 15–20 cm was the highest in DPF FMRs. Further, the maximum stem density in the diameter class >35 cm and the minimum in diameter class 10–15 cm were found in UF. CSF had the lowest stem distribution among all diameter classes, except for 10–15 cm diameter class.

The distribution of seedlings, saplings and poles under different FMRs is depicted in Figure 3. A reverse J shape curve can be clearly noticed under RF, DPF and UPF. The maximum number of seedlings, saplings and poles was recorded in RF followed by DPF, UPF, UF, and CSF, respectively in the descending order. Additionally, the proportion of Khair individuals alone in comparison to other species at pole stage was higher in UF than in the other FMRs of Khair Working Circle.

Carbon density (Mg ha^{-1}) of Khair dominated forests

Among different FMRs, UF had the highest AG tree C density (46.03 Mg C ha^{-1}), whereas the lowest AG C density (21.51 Mg C ha^{-1}) was recorded in CSF (Table 4). Similarly, the BG and the total tree C density were highest in UF (23.12 and 69.15 Mg C ha^{-1}). While the lowest value was recorded in CSF (11.76, 33.27 Mg C ha^{-1}). However, the different FMRs i.e., DPF and UPF; UPF and CSF on the other hand remained statistically alike. The C density also varied significantly in shrub component of different FMRs. DPF and CSF displayed maximum AG shrub C density (1.62 Mg C ha^{-1}). The BG shrub C density was maximum in DPF (0.83 Mg C ha^{-1}) and the lowest in UPF (0.52 Mg C ha^{-1}). The minimum value of total shrub C density was recorded in UPF (1.67 Mg C ha^{-1}). The maximum C density for herb components (AG, BG and TC) was found in RF (0.52 Mg C ha^{-1}). Overall, VCD under different FMRs remained highest in UF (71.81 Mg C ha^{-1}). The SCD under different FMRs varied from 90.28–115.49 Mg C ha^{-1} with a mean value of 102.57 Mg C ha^{-1}. The maximum SCD was recorded in RF (115.49 Mg C ha^{-1}) and the minimum in CSF (90.28 Mg C ha^{-1}). Additionally, the variation between UPF and DPF, CSF and UF remained statistically identical. The ECD was estimated to be significantly higher in RF (183.52 Mg C ha^{-1}) than in the other FMRs, whereas CSF (126.05 Mg C ha^{-1}) had the lowest ECD.

10.3389/fenvs.2022.981608

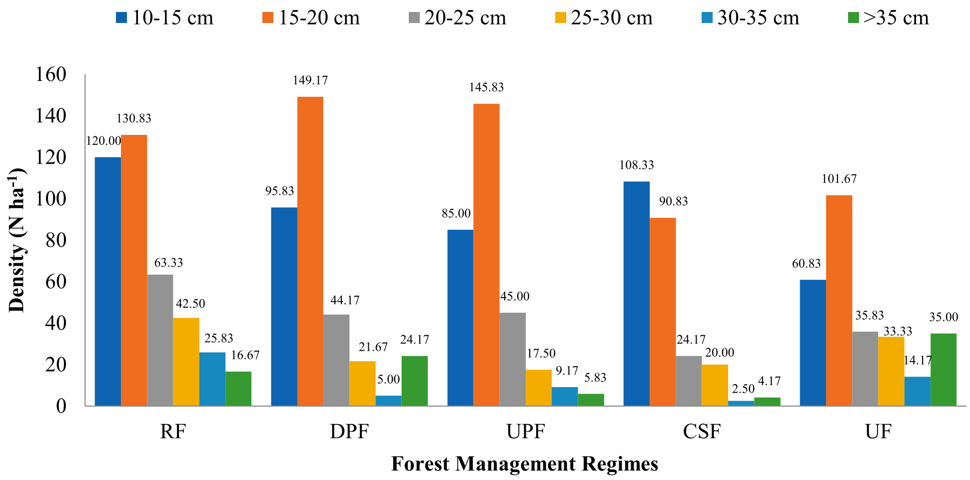

FIGURE 2
Stand structure of Khair Working Circle under different FMRs in Nurpur Forest Division, Himachal Pradesh, India.

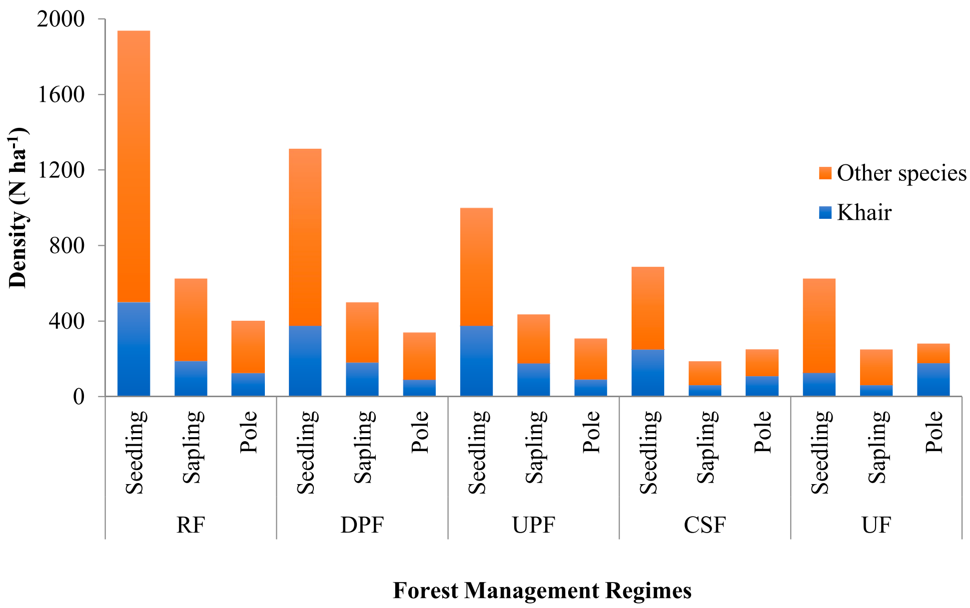

FIGURE 3
Population structure of Khair Working Circle under different FMRs in Nurpur Forest Division, Himachal Pradesh, India.

Species-wise contribution to total biomass

The species-wise contribution to the total tree biomass in each FMR is presented in Table 5. *Acacia catechu* contributed 40.59% to the total tree biomass in RF (137.45 Mg ha^{-1}), followed by *Pinus roxburghii* (14.56%), *Lannea coromandelica* (12.93%) and *Cassia fistula* (11.83%). However, in DPF, *P. roxburghii* contributed the most (31.17%) followed by *A. catechu* (29.56%). The overall tree biomass in UPF was 83.53 Mg ha^{-1}of which *A. catechu* accounted for 49.19% of the total biomass, followed by *L. coromandelica* (17.87%) and *Albizia lebbeck* (10.71%), respectively. In CSF, the total tree biomass was estimated to be 70.04 Mg ha^{-1} of which *A. catechu* contributed 57.02% followed by *L. coromandelica* (12.31%). In UF, out of the total tree biomass of 145.58 Mg ha^{-1}, *A. catechu* contributed the most

TABLE 4 Carbon density (Mg C ha^{-1}) of trees, shrubs and herbs under different FMRs in Khair Working Circle of Nurpur Forest Division, Himachal Pradesh, India.

	RF	DPF	UPF	CSF	UF	Mean
Tree carbon density (Mg C ha^{-1})						
Above-ground	42.62 ± 4.08^{a}	39.06 ± 4.65^{a}	25.49 ± 1.60^{b}	21.51 ± 1.49^{b}	46.03 ± 6.97^{a}	34.94 ± 2.29
Below-ground	22.67 ± 2.06^{a}	17.66 ± 1.48^{ab}	14.19 ± 0.90^{bc}	11.76 ± 0.76^{c}	23.12 ± 3.18^{a}	17.88 ± 1.03
Total	65.29 ± 6.14^{a}	56.72 ± 5.47^{ab}	39.68 ± 2.48^{bc}	33.27 ± 2.24^{c}	69.15 ± 10.14^{a}	52.82 ± 3.25
Shrub carbon density (Mg C ha^{-1})						
Above-ground	1.54 ± 0.06^{a}	1.62 ± 0.04^{a}	1.15 ± 0.06^{b}	1.62 ± 0.04^{a}	1.58 ± 0.03^{a}	1.50 ± 0.05
Below-ground	0.67 ± 0.03^{b}	0.83 ± 0.02^{a}	0.52 ± 0.03^{c}	0.72 ± 0.02^{b}	0.67 ± 0.01^{b}	0.68 ± 0.03
Total	2.21 ± 0.09^{b}	2.45 ± 0.07^{a}	1.67 ± 0.09^{c}	2.32 ± 0.06^{ab}	2.25 ± 0.04^{ab}	2.18 ± 0.07
Herb carbon density (Mg C ha^{-1})						
Above-ground	0.38 ± 0.03^{a}	0.20 ± 0.02^{bc}	0.25 ± 0.01^{b}	0.13 ± 0.03^{c}	0.30 ± 0.05^{ab}	0.25 ± 0.03
Below-ground	0.14 ± 0.01^{a}	0.07 ± 0.01^{bc}	0.09 ± 0.01^{b}	0.05 ± 0.01^{c}	0.11 ± 0.02^{ab}	0.09 ± 0.01
Total	0.52 ± 0.04^{a}	0.27 ± 0.03^{bc}	0.34 ± 0.02^{b}	0.18 ± 0.04^{c}	0.41 ± 0.06^{ab}	0.34 ± 0.04
Total carbon density (Mg C ha^{-1})						
VCD	68.02 ± 6.47^{a}	59.44 ± 6.02^{ab}	41.69 ± 2.56^{bc}	35.77 ± 2.33^{c}	71.81 ± 10.55^{a}	55.35 ± 6.50
SCD	115.49 ± 2.96^{a}	106.49 ± 4.04^{b}	107.64 ± 1.80^{ab}	90.28 ± 0.87^{c}	92.98 ± 2.08^{c}	102.57 ± 2.82
ECD	183.52 ± 6.47^{a}	166.61 ± 6.02^{ab}	149.32 ± 2.56^{b}	126.05 ± 2.33^{c}	164.80 ± 10.55^{b}	156.06 ± 6.49

Mean value ±standard error (SE). Different letters in the same row indicate significant differences at $p \leq 0.05$. VCD, vegetation carbon density; SCD, soil carbon density; ECD, ecosystem carbon density.

biomass (66.07%) followed by *P. roxburghii* (14.54%). The other associated tree species under different FMRs accounted for a low proportion (less than 10%) of the total tree biomass.

Discussion

An enhanced level of protection plays a pivotal role in conserving biodiversity (Hoffmann et al., 2018; Birben, 2019); however, its effectiveness depends upon governance and management (Cazalis et al., 2020). The forests in India are governed by various agencies viz., Government Forest officials, right holders/stakeholders, private individuals and organizations, indigenous people, etc. Each governance type has differentiated strategies depending upon the key actors involved in decision-making and level of their powers resulting in variation in the conservation outcomes (Macura et al., 2015). Strict FMRs are vital for biodiversity conservation and the minimization of loss (Hoffmann et al., 2018; Birben, 2019; Geldmann et al., 2019). However, the efficiency of any FMRs in conserving biodiversity is contingent on the governance or management of a specific forest (Cazalis et al., 2020).

Biodiversity of Khair dominated forests

In the present investigation, the maximum representation of trees and shrubs as recorded in terms of their number, density and basal area was observed in RF and DPF, which can be owed to high level of protection accorded to them. The maximum number of herb species, their density as well as basal area were found in UF, which could be due to the lesser tree density under this management regime, thus offering enough openings for the emergence of herbs on the ground floor. Additionally, the basal area and stem density recorded in response to FMRs can represent the stand structure and is also a useful indicator of human impact on a forest stand (Ingram et al., 2005) and may be ascribed to the species composition, age structure and degree of disturbance (Sundarapandian and Swamy, 1997). For Indian forests, the H′ for tree components varied from 0.83 to 4.1

TABLE 5 Contribution of each species in total biomass (Mg ha⁻¹) under different FMRs in Khair Working Circle of Nurpur Forest Division, Himachal Pradesh, India.

Species	RF	DPF	UPF	CSF	UF
Acacia catechu	55.79 (40.59%)	35.30 (29.56%)	41.09 (49.19%)	39.94 (57.02%)	96.19 (66.07%)
Aegle marmelos	0.25 (0.18%)	—	0.28 (0.34%)	0.07 (0.10%)	—
Albizia lebbeck	—	0.72 (0.60)	8.95 (10.71%)	—	—
Bombax ceiba	0.20 (0.15%)	1.11 (0.93%)	—	—	—
Broussonetia papyrifera	—	—	—	2.20 (3.14%)	—
Butea monosperma	—	0.19 (0.16%)	—	—	—
Casearia tomentosa	0.32 (0.23%)	0.44 (0.37%)	—	—	—
Cassia fIstula	16.25 (11.82%)	8.52 (7.14%)	6.58 (7.88%)	4.61 (6.58%)	11.36 (7.80%)
Dalbergia sissoo	—	2.18 (1.83%)	1.32 (1.58%)	2.83 (4.04%)	—
Eucalyptus globulus	—	—	—	—	0.56 (0.38%)
Ficus benghalensis	0.70 (0.51%)	—	0.35 (0.42%)	—	0.19 (0.13%)
Ficus glomerata	—	—	—	0.93 (1.33%)	—
Ficus palmata	—	—	—	4.97 (7.10%)	—
Flacourtia indica	0.44 (0.32%)	—	0.68 (0.81%)	—	—
Lannea coromandelica	17.77 (12.93%)	11.63 (9.74%)	14.93 (17.87%)	8.62 (12.31%)	7.03 (4.83%)
Leucaena leucocephala	—	—	—	0.75 (1.07%)	—
Mallotus phillippensis	10.59 (7.70%)	10.86 (9.09%)	5.75 (6.88%)	3.65 (5.21%)	8.42 (5.78%)
Morus alba	—	—	—	0.13 (0.19%)	—
Ougeinia oojeinensis	0.72 (0.52%)	2.64 (2.21%)	—	—	—
Phyllanthus embelica	0.68 (0.49%)	0.39 (0.33%)	0.51 (0.61%)	—	—
Pinus roxburghii	20.01 (14.56%)	37.22 (31.17%)	3.11 (3.72%)	—	21.17 (14.54%)
Pistacia integerrima	—	1.95 (1.63%)	—	—	—
Pyrus pashia	0.84 (0.61%)	—	—	—	0.22 (0.15%)
Stephegyne parvifolia	—	—	—	—	0.08 (0.05%)
Syzygium cumini	3.16 (2.30%)	2.41 (2.02%)	—	0.68 (0.97%)	—
Terminalia arjuna	1.58 (1.15%)	—	—	—	—
Terminalia bellirica	7.31 (5.32%)	1.18 (0.99%)	—	—	0.005 (0.003%)
Wendlandia exserta	0.84 (0.61%)	2.68 (2.24%)	—	—	—
Xylosma longifolium	—	—	—	0.66 (0.94%)	0.36 (0.25%)
Total biomass (Mg ha⁻¹)	137.45	119.41	83.53	70.04	145.58

The bold values are the total biomass.
Values in the parenthesis is the relative proportion of each species in particular FMRs.

(Devi and Yadava, 2006), 1.85–5.68 for different tropical forests of the Eastern Ghats of India (Chittibabu and Parthadarathy, 2000; Reddy et al., 2011; Panda et al., 2013; Naidu and Kumar, 2016). The studies undertaken in various parts of the north-western Himalayas in India indicates wide range of tree species diversity. Pokhriyal et al. (2012) recorded a range of 2.42–2.44 H′ in Phakot, Tehri Garhwal at 600–1900 m asl elevation, whereas, Sharma et al. (2010) discovered 1.14 H′ at Fatehpur, Deogadd at 750–1,250 m elevation in the foothills of Garhwal Himalaya. On addition, Sharma and Kala, (2022) reported a range of 2.01–2.11 tree H′ in Dhauladhar mountain of north-western Himalayas. In Kashmir, the average Ep, D′ and H′ was reported to be 1.42, 3.13, and 0.92, respectively (Shaheen et al., 2011). The DPF had the maximum tree H′, followed by RF, UPF, UF and CSF, respectively, which could be attributed to the degree of legal protection accorded to each FMRs. The degree of protection adopted in these FMRs followed the order; RF > DPF > UPF > UF > CSF, respectively. Anthropogenic pressure in UF and CSF FMRs may have led to disturbances, resulting in decreased species diversity and composition. This shows that the forest managed under varied regimes had a substantial effect on the diversity and heterogeneity among different FMRs. Amongst FMRs of Khair Working Circle, *A. catechu* was identified as a highly dispersed tree species followed by *M. phillippensis, C. fistula, L. coromandelica and P. roxburghii;* while, the remaining species exhibited accidental population occurrence. The findings of Biswas and Mukhopadhyay (2016) on phyto-sociology in developing conservation and management strategies for forests reveal that the degree of protection and anthropogenic activities considerably influence the vegetation structure in terms of species dominance and richness. They reported the maximum value for Simpson dominance in the area with the maximum disturbance. However, the richness was higher in the area with the least disturbance. The phyto-sociological attributes and diversity indices of differentially managed forests are comparable to the community-managed forests and government-managed forests of Bangladesh (Shinwari and Khan, 2000). They observed greater floral diversity, species richness and mature trees in the reserve forest as compared to those in the unreserved forest.

Since the anthropogenic disturbances occur in UF and CS, this might be the reason for the low species diversity under these FMRs observed in our study. However, the greater tree diversity in DPF than that of RF may be attributed to complete protection accorded to RF thus allowing the ecological succession to proceed smoothly, which may have resulted in the disappearance of species. However, in UF and CSF, trees of human interest are cultivated which ultimately increases the species dominance in the area. Similarly, Aime et al. (2015) found that PF (5.78) and natural RF (5.06) had a higher H′ than the community forests (4.64). However, Ep did not differ much between the protected (0.81) and community forests (0.83) but it was considerably different in natural voluntary reserve (0.71). In our study, the maximum Ep for trees was reported in DPF and UPF (0.77), whereas the minimum was in UF (0.52). The apparent similarity in Ep distribution in DPF and UPF was most likely due to the spatial patterns of stands that enable them to efficiently utilize the resources, such as sunlight, soil fertility, and species coexistence from the same functional group. Contrary to our findings, Pradhan et al. (2019) reported that the sacred groove forest managed by the local community had greater species richness, density and diversity than the wildlife sanctuary. This may be due to more awareness, religious beliefs and involvement of local people in forest management and conservation activities.

Stand and population structure

The stand structure of different FMRs viz., RF, DPF, UPF and CSF followed a reverse J-shaped curve from 15–20 cm diameter class onward. However, in reserve forests, the distribution of trees in various diameter classes was more balanced than in the other FMRs. A reverse J-shaped curve suggests exploitation in higher diameter classes (Rao et al., 1990) and is a good indicator for sustainable management of forest stands and steady growth of forest. In all FMRs, the lesser number of trees in diameter class 10–15 cm compared to 15–20 cm diameter class indicates concerns related to natural regeneration in the area. According to Philip and Gentry (1993), a reverse “J” shape is common for natural forests with active regeneration and recruitment. In general, trees with larger diameters contribute more basal area, than those with smaller ones (Hailemariam and Temam, 2018). Additionally, the lesser number of trees in bigger diameter classes in CSF compared to other FMRs is attributable to anthropogenic disturbances such as logging, fuel wood extraction and encroachments.

The seedlings and saplings of diverse species can help in forecasting future changes, regeneration, and status of flora biodiversity in any forest (Malik and Bhatt, 2016). The regeneration behavior of species depends on the internal community processes and exogenic disturbances (Barker and Patrik, 1994). In the present study, the lowest seedling and sapling density was found in UF and CSF which can be owed to variations in their management approach and the accessibility of these forests to local communities. According to Saxena and Singh (1984), grazing and trampling by animals affect the seedlings, regenerations, establishment and soil structure by compacting it, and leads to lower moisture content and permeability. This may alter the habitat and render it less suitable for the germination and establishment of seedlings. The enhanced canopy cover in CSF and UF categories had a direct effect on seed production, amount of light reaching the understory vegetation, soil properties and ultimately regenerative capacity of the stand (Vetaas, 2000). The reason for greater numbers of seedlings and saplings in RF and DPF as compared to other FMRs may be due to their higher degree of protection resulting in reduced disturbance and favorable conditions for regeneration to take place (Nagamastu et al., 2002). Traore et al. (2008) studied the regeneration success of *Acacia* spp. In eastern Burkina under two land-use regimes and reported good regeneration rate of *Acacia* spp. In protected areas as compared to the areas with high human impact. Also, Fayiah et al. (2018) recorded a fair regeneration for two forest reserves inventoried in southern Sierra Leone.

Carbon density of Khair dominated forests

Biomass and C stocks under different components-above, below and total (above + below) of trees, shrubs and herbs varied significantly in response to variation in FMRs. Forest C is considered a function of tree size and tree density (Lecina-Diaz et al., 2018; Van De Perreet al., 2018; Yuan et al., 2018; Ali et al., 2019), canopy cover, age, altitude and stand structure, composition, architectural attributes and ecological processes (Panzou et al., 2018) and forest management practices (Poudyal et al., 2019). Thus, this provides critical insights for sustainable forest management, enhancing forest conservation and ecosystem services. We found that RF and DPF have more ECD than the other FMRs. The maximum VCD was recorded in UF, which was mainly due to single species dominance (*A. catechu*) with a large basal area, each containing a disproportionately large C stock (Lung and Espira, 2015;

Srinivas and Sundarapandian, 2019; Damptey et al., 2020) than many small trees as these forests are of plantation origin. Further, the high value of specific gravity (0.874 g cm^{-3}) of Khair trees and biomass expansion factor also play a key role in C stock accumulation. Trees of bigger diameter classes are the main drivers of biomass and C stock variation across the tropics (Slik et al., 2013) and the heterogeneous distribution of large trees is influenced by basal area (Panzou et al., 2018). Our study confirms that RF and protected forest (DPF and UPF) have a favorable impact on biomass and C storage. Structurally, diverse forests were reported to have higher ecosystem productivity than simpler forests (Ali, 2019). In contrast, the smaller trees in CSF accounted for lower values of tree C density. Anthropogenic pressure near settlements altered the forest structure and had negative consequences on vegetation carbon (Vaidyanathan et al., 2010; Sapkota et al., 2018). Similarly, Gogoi et al. (2017) also reported that the total plant biomass and diversity decreased from the least disturbed to the most disturbed site. The difference in C stock values among these FMRs can also be attributed to species variability, tree structure, basal area, heterogeneity in diameter class, soil characteristics, study site conditions as well as anthropogenic factors (Lal, 2008; Becknell et al., 2012; Lewis et al., 2013; Slik et al., 2013; Sundarapandian et al., 2013; Dar and Sundarapandian 2015). The lower values in the less protected FMRs could also be due to unchecked extraction of timber, fuel wood and fodder from these forests, because of their proximity to human settlements (Sagar et al., 2003; Pande, 2005).

Conclusion

Ecosystem-based forest management practices are critical for the maintenance of species biodiversity, C density and forest soil health. In the present study, it was found that under different FMRs of Khair Working Circle, a representative forest of northern tropical deciduous forest, degree of protection and variation in their management approaches considerably influenced the biodiversity and soil C storage. UF management regime was found to be better at storing carbon in vegetation, while RF and DPF management regimes were more diverse and had more carbon in the soil and at ecosystem level. So, our study concluded that the legal framework is a crucial factor explaining much higher biodiversity, SCD and balanced distribution of tree biomass among different diameter classes inside RF and DPF than in UPF, UF and CSF. Although, the value for C density was higher in UF, yet diversity, as well as regeneration also have an important role in bio-resource conservation and sustainable management. Understanding the impact of different FMRs on forest composition, diversity and C storage capacity may offer evidence to support management decisions that will eventually improve the ecological health of the forests, increase the flow of ecosystem services, and support livelihoods in rural societies that are dependent on forest resources. In the present-day scenario, local communities also play a decisive role in conservation and maintenance of forest resources. However, in the present study, the CSF exhibited reduced biodiversity and C storage status. This calls for better coordination between local community and forest department officials in the management of Khair Working Circle forests to ensure their C mitigation potential and biodiversity conservation. Thus, it was clearly demonstrated that legal binding on forest protection would increase the amount of protected habitat for biodiversity conservation and C storage to maintain ecological functions for climate change adaptation. Therefore, in order to ensure biodiversity conservation and maintain large C sinks, it is crucial to fully protect RF and DPF and bring the unprotected FMRs viz., UPF, UF, and CSFs FMRs under REDD + initiative.

Data availability statement

The raw data supporting the conclusions of this article will be made available by the authors, without undue reservation.

Author contributions

Conceptualization, methodology, validation, formal analysis, investigation, DK, DB, and CT; data curation, writing—original draft, DK, DB, and CT; writing—review and editing, software visualization, NSh, PS, and NSa. All authors have read and agreed to the published version of the manuscript.

Acknowledgments

We duly acknowledge the technical guidance and contribution of Sh. V.P. Mohan, Chairman of the committee constituted for monitoring Silviculture Green Felling in Himachal Pradesh by Hon'ble Supreme Court of India, Basu Kaushal (DFO, Nurpur Forest Division), Sh. Sandeep Kohli (ACF, Nurpur Division), Sh. Arun Sharma (ACF, HP State Forest Department) and field staff of the Nurpur Forest Division. The authors are also grateful to the Head of the Department of Silviculture and Agroforestry, Y.S. Parmar, University of Horticulture and Forestry, Solan (HP), India, for providing the necessary facilities and technical support during the study. We are also thankful to two reviewers and Jinniu Wang from the Chinese Academy of Sciences, China for his valuable suggestions and comments on the overall improvement of the manuscript.

Conflict of interest

The authors declare that the research was conducted in the absence of any commercial or financial relationships that could be construed as a potential conflict of interest.

Publisher's note

References

Aime, C. D. V. B. T., Yves, A. Y. C., Djaha, K., Bruno, K. K., Bertin, G. B. Z., and Edouard, N. K. (2015). Trees species diversity and above ground biomass in three tropical forest types in Azaguie area. *Glob. Adv. Res. J. Plant Sci.* 1, 30–38.

Ali, A. (2019). Forest stand structure and functioning: Current knowledge and future challenges. *Ecol. Indic.* 98, 665–677. doi:10.1016/j.ecolind.2018.11.017

Ali, A., Lin, S. L., He, J. K., Kong, F. M., Yu, J. H., and Jiang, H. S. (2019). Big-sized trees overrule remaining trees' attributes and species richness as determinants of aboveground biomass in tropical forests. *Glob. Change Biol.* 25, 2810–2824. doi:10.1111/gcb.14707

Barker, P. C. J., and Patrik, L. B. K. (1994). Phyllocladus aspleniifolius: Variability in the population structure, the regeneration niche and dispersion patterns in tasmanian forests. *Aust. J. Bot.* 42, 163–190. doi:10.1071/bt9940163

Becknell, J. M., Kucek, L. K., and Powers, J. S. (2012). Aboveground biomass in mature and secondary seasonally dry tropical forests: A literature review and global synthesis. *For. Ecol. Manag.* 276, 88–95. doi:10.1016/j.foreco.2012.03.033

Birben, U. (2019). The effectiveness of protected areas in biodiversity conservation: The case of Turkey. *Cerne* 25, 424–438. doi:10.1590/01047760201925042644

Biswas, S., and Mukhopadhyay, S. C. (2016). Plant community structure and carbon stock assessment through phytosociological approach at dry tropics of Banka Forest Division, Bihar. *Indian J. Plant Sci.* 5, 72–82.

Blackie, R., Baldauf, C., Gautier, D., Gumbo, D., Kassa, H., Parthasarathy, N., et al. (2014). *Tropical dry forests: The state of global knowledge and recommendations for future research*. Bogor: CIFOR. Discussion Paper.

Bonan, G. B. (2008). Forests and climate change: Forcings, feedbacks, and the climate benefits of forests. *Science* 320, 1444–1449. doi:10.1126/science.1155121

Cairns, M. A., Brown, S., Helmer, E. H., and Baumgardner, G. A. (1997). Root biomass allocation in the world's upland forests. *Oecologia* 111, 1–11. doi:10.1007/s004420050201

Cazalis, V., Prince, K., Mihoub, J. B., Kelly, J., Butchart, S. H., and Rodrigues, A. S. (2020). Effectiveness of protected areas in conserving tropical forest birds. *Nat. Commun.* 11, 4461–4468. doi:10.1038/s41467-020-18230-0

Champion, H. G., and Seth, S. K. (1968). *A revised survey of the forest types of India*. Manager of Publications, Delhi, India. 404p.

Chauhan, N. S. (1999). *Medicinal and aromatic plants of Himachal Pradesh*. Indus Publishing Company. New Delhi, India. 632p.

Chave, J., Coomes, D. A., Jansen, S., Lewis, S. L., Swenson, N. G., and Zanne, A. E. (2009). Towards a worldwide wood economics spectrum. *Ecol. Lett.* 12, 351–366. doi:10.1111/j.1461-0248.2009.01285.x

Chazdon, R. L., Brancalion, P. H. S., Lamb, D., Laestadius, L., Calmon, M., and Kumar, C. (2017). A policy-driven knowledge agenda for global forest and landscape restoration. *Conserv. Lett.* 10, 125–132. doi:10.1111/conl.12220

Chittibabu, C. V., and Parthasarathy, N. (2000). Attenuated tree species diversity in human-impacted tropical evergreen forest sites at Kolli hills, Eastern Ghats, India. *Biodivers. Conserv.* 9, 1493–1519. doi:10.1023/a:1008971015545

Collins, M. B., and Mitchard, E. T. A. (2017). A small subset of protected areas are a highly significant source of carbon emissions. *Sci. Rep.* 7, 41902. doi:10.1038/srep41902

Damptey, F. G., Birkhofer, K., Nsiah, P. K., and De la Riva, E. G. (2020). Soil properties and biomass attributes in a former gravel mine area after two decades of forest restoration. *Land* 9, 209. doi:10.3390/land9060209

Dar, J. A., and Sundarapandian, S. M. (2015). Variation of biomass and carbon pools with forest type in temperate forests of Kashmir Himalaya, India. *Environ. Monit. Assess.* 187, 55–61. doi:10.1007/s10661-015-4299-7

Devi, L. S., and Yadava, P. S. (2006). Floristic diversity assessment and vegetation analysis of tropical semievergreen forest of Manipur, north east India. *Trop. Ecol.* 47, 89–98.

Dieler, J., Uhl, E., Biber, P., Muller, J., Rotzer, T., and Pretzsch, H. (2017). Effect of forest stand management on species composition, structural diversity, and productivity in the temperate zone of Europe. *Eur. J. For. Res.* 136, 739–766. doi:10.1007/s10342-017-1056-1

FAO (2020). *Global forest resources assessment 2020*. Rome: FAO. doi:10.4060/ca8753en

Fayiah, M., Swarray, M. K., Otesile, A., and Chen, B. (2018). "Comparative study of the regeneration potential of kasewe and taia riverine forests, moyamba district, Sierra Leone," in presented at the 40th Annual Conference of Forestry Association of Nigeria (FAN) (New York: Conscientia Beam).

Forrester, D. I., and Bauhus, J. (2016). A review of processes behind diversity—Productivity relationships in forests. *Curr. For. Rep.* 2, 45–61. doi:10.1007/s40725-016-0031-2

Forster, E. J., Healey, J. R., Dymond, C., and Styles, D. (2021). Commercial afforestation can deliver effective climate change mitigation under multiple decarbonisation pathways. *Nat. Commun.* 12, 3831. doi:10.1038/s41467-021-24084-x

FSI (2019). *India state of forest report 2019*. Dehradun, India: Ministry of Environment, Forest and Climate Change.

FSI (2021). *India state of forest report 2021*. Dehradun, India: Ministry of Environment, Forest and Climate Change.

FSI (1996). *Volume equations for forests of India, Nepal and Bhutan*. India: Forest Survey of India, Ministry of Environment and Forests, Government of India.

Gamfeldt, L., Sneall, T., Bagchi, R., Jonsson, M., Gustafsson, L., Kjellander, P., et al. (2013). Higher levels of multiple ecosystem services are found in forests with more tree species. *Nat. Commun.* 4, 1340–1348. doi:10.1038/ncomms2328

Gao, T., Hedblom, M., Emilsson, T., and Nielsen, A. B. (2014). The role of forest stand structure as biodiversity indicator. *For. Ecol. Manage.* 330, 82–93. doi:10.1016/j.foreco.2014.07.007

Gautam, T. P., and Mandal, T. N. (2016). Effect of disturbance on biomass, production and carbon dynamics in moist tropical forest of eastern Nepal. *For. Ecosyst.* 3, 11–10. doi:10.1186/s40663-016-0070-y

Geldmann, J., Manica, A., Burgess, N. D., Coad, L., and Balmford, A. (2019). A global-level assessment of the effectiveness of protected areas at resisting anthropogenic pressures. *Proc. Natl. Acad. Sci. U. S. A.* 116, 23209–23215. doi:10.1073/pnas.1908221116

Gogoi, A., Sahoo, U. K., and Singh, S. L. (2017). Assessment of biomass and total carbon stock in a tropical wet evergreen rainforest of Eastern Himalaya along a disturbance gradient. *J. Plant. Nutr. Soil Sci.* 4, 1–8.

Hailemariam, M. B., and Temam, T. D. (2018). The vegetation composition, structure and regeneration status of Gole natural forest, West Arsi Zone, Oromia regional state. *Ethiop. J. Agric. Sci.* 2, 10–21. doi:10.35841/2591-7897.2.2.10-21

Hammer, O., Harper, D. A. T., and Ryan, P. D. (2001). Past: Paleontological statistics software package for education and data analysis. *Palaeont. Electron.* 4, 4–9.

Handa, I. T., Aerts, R., Berendse, F., Berg, M. P., Bruder, A., Butenschoen, O., et al. (2014). Consequences of biodiversity loss for litter decomposition across biomes. *Nature* 509, 218–221. doi:10.1038/nature13247

Herault, B., and Piponiot, C. (2018). Key drivers of ecosystem recovery after disturbance in a neotropical forest. *For. Ecosyst.* 5, 2. doi:10.1186/s40663-017-0126-7

Hoffmann, S., Beierkuhnlein, C., Field, R., Provenzale, A., and Chiarucci, A. (2018). Uniqueness of protected areas for conservation strategies in the European Union. *Sci. Rep.* 8, 6445. doi:10.1038/s41598-018-24390-3

IFA. 2016. The Indian forest Act, 1927. State Forest Acts.

Ingram, J. C., Whittaker, R. J., and Dawson, T. P. (2005). Tree structure and diversity in human-impacted littoral forests, Madagascar. *Environ. Manage.* 35, 779–798. doi:10.1007/s00267-004-0079-9

Jactel, H., Bauhus, J., Boberg, J., Bonal, D., Castagneyrol, B., Gardiner, B., et al. (2017). Tree diversity drives forest stand resistance to natural disturbances. *Curr. For. Rep.* 3, 223–243. doi:10.1007/s40725-017-0064-1

Janzen, D. H. (1988). Management of habitat fragments in a tropical dry forest: Growth. *Ann. Mo. Botanical Gard.* 75, 105–116. doi:10.2307/2399468

Jucker, T., Bouriaud, O., Avacaritei, D., Danila, I., Duduman, G., Valladares, F., et al. (2014). Competition for light and water play contrasting roles in driving diversity-productivity relationships in Iberian forests. *J. Ecol.* 102, 1202–1213. doi:10.1111/1365-2745.12276

Kumar, A., Pinto, M. C., Candeias, C., and Dinis, P. A. (2021). Baseline Maps of Potentially Toxic Elements in the Soils of Garhwal Himalayas, India: Assessment of Their Eco-environmental and Human Health Risks. *Land Degrad. Dev.* 32, 3856–3869. doi:10.1002/ldr.3984

Kothandaraman, S., Dar, J. A., Sundarapandian, S., Dayanandan, S., and Khan, M. L. (2020). Ecosystem-level carbon storage and its links to diversity, structural and environmental drivers in tropical forests of Western Ghats, India. *Sci. Rep.* 10, 1–15. doi:10.1038/s41598-020-70313-6

Lafleur, B., Fenton, N. J., Simard, M., Leduc, A., Pare, D., Valeria, O., et al. (2018). Ecosystem management in paludified boreal forests: Enhancing wood production, biodiversity, and carbon sequestration at the landscape level. *For. Ecosyst.* 5, 27. doi:10.1186/s40663-018-0145-z

Lakshmi, T., and Kumar, A. (2011). Preliminary phytochemical analysis & invitro antibacterial activity of *Acacia catechu* Willd Bark against Streptococcus mitis, Streptococcus sanguis & Lactobacillus acidophilus. *Int. J. Phytomedicine* 3, 579.

Lal, R. (2008). Sequestration of atmospheric CO_2 in global carbon pools. *Energy Environ. Sci.* 1, 86–100. doi:10.1039/b80-9492-f

Lecina-Diaz, J., Alvarez, A., Regos, A., Drapeau, P., Paquette, A., Messier, C., et al. (2018). The positive carbon stocks-biodiversity relationship in forests: Co-occurrence and drivers across five subclimates. *Ecol. Appl.* 28, 1481–1493. doi:10.1002/eap.1749

Lee, J., Yoon, T. K., Han, S., Kim, S., Yi, M. J., Park, G. S., et al. (2014). Estimating the carbon dynamics of South Korean forests from 1954 to 2012. *Biogeosciences* 11, 4637–4650. doi:10.5194/bg-11-4637-2014

Lefcheck, J. S., Byrnes, J. E., Isbell, F., Gamfeldt, L., Griffin, J. N., Eisenhauer, N., et al. (2015). Biodiversity enhances ecosystem multifunctionality across trophic levels and habitats. *Nat. Commun.* 6, 6936. doi:10.1038/ncomms7936

Lewis, S. L., Lopez-Gonzalez, G., Sonke, B., Affum-Baffoe, K., Baker, T. R., Ojo, L. O., et al. (2009). Increasing carbon ´ storage in intact African tropical forests. *Nature* 457, 1003–1006. doi:10.1038/nature07771

Lewis, S. L., Sonke, B., Sunderland, T., Begne, S. K., Lopez-Gonzalez, G., van der Heijden, G. M. F., et al. (2013). Above-ground biomass and structure of 260 African tropical forests. *Philos. Trans. R. Soc. Lond. B Biol. Sci.* 368, 20120295. doi:10.1098/rstb.2012.0295

Liang, J., Crowther, T. W., Picard, N., Wiser, S., Reich, P. B., Alberti, G., et al. (2016). Positive biodiversity-productivity relationship predominant in global forests. *Science* 354, 8957. doi:10.1126/science.aaf8957

Liu, B., Liu, Q., Daryanto, S., Guo, S., Huang, Z., Wang, Z., et al. (2018). Responses of Chinese fir and Schima *superba* seedlings to light gradients: Implications for the restoration of mixed broadleaf-conifer forests from Chinese fir monocultures. *For. Ecol. Manage.* 41, 51–57. doi:10.1016/j.foreco.2018.03.033

Lung, M., and Espira, A. (2015). The influence of stand variables and human use on biomass and carbon stocks of a transitional african forest: Implications for forest carbon projects. *For. Ecol. Manage.* 351, 36–46. doi:10.1016/j.foreco.2015.04.032

Macura, B., Secco, L., and Pullin, A. S. (2015). What evidence exists on the impact of governance type on the conservation effectiveness of forest protected areas? Knowledge base and evidence gaps. *Environ. Evid.* 4, 24–29. doi:10.1186/s13750-015-0051-6

Magurran, A. E. (1988). *Ecological diversity and its measurement*. Princeton, New Jersey: Princeton University Press.

Malhi, Y., Roberts, J. T., Betts, R. A., Killeen, T. J., Li, W., and Nobre, C. A. (2008). Climate change, deforestation and the fate of the Amazon. *Science* 319, 169–172. doi:10.1126/science.1146961

Malik, Z. A., and Bhatt, A. B. (2016). Regeneration status of tree species and survival of their seedlings in Kedarnath Wildlife Sanctuary and its adjoining areas in Western Himalaya, India. *Trop. Ecol.* 57, 677–690.

Mancosu, E., Marín, A. I., Malak, D. A., Trombetti, M., and Bastrup-Birk, A. (2018). "Setting priorities for the management of primary forest areas: The importance of a harmonized inventory for supporting regional conservation and restoration efforts," in 5th Forum Carpaticum.

Margalef, D. R. (1958). Information theory in ecology. *Int. J. Gen. Syst.* 3, 36–71.

Mir, A. H., and Upadhaya, K. (2017). Effect of traditional management practices on woody species composition and structure in montane subtropical forests of Meghalaya, Northeast India. *J. Mt. Sci.* 14, 1500–1512. doi:10.1007/s11629-016-4145-6

Nagamastu, D., Seiwa, K., and Sakai, A. (2002). Seedling establishment of deciduous trees in various topographic positions. *J. Veg. Sci.* 13, 35–44. doi:10.1111/j.1654-1103.2002.tb02021.x

Naidu, M. T., and Kumar, O. A. (2016). Tree diversity, stand structure, and community composition of tropical forests in Eastern Ghats of Andhra Pradesh, India. *J. Asia. Pac. Biodivers.* 9, 328–334. doi:10.1016/j.japb.2016.03.019

Nelson, D. W., and Sommers, L. E. (1996). Total carbon, organic matter. In: *Method of soil analysis. Part 3. Chemical methods* (D. L. Sparks eds). Soil Science Society of America, Madison, Wisconsin. 961–1010pp.

Panda, P. C., Mahapatra, A. K., Acharya, P. K., and Debata, A. K. (2013). Plant diversity in tropical deciduous forests of eastern Ghats, India: A landscape level assessment. *Int. J. Biodivers. Conserv.* 5, 625–639. doi:10.5897/IJBC2013.0581x

Pande, P. K. (2005). Biomass and productivity in some disturbed tropical dry deciduous teak forests of Satpura plateau. *Madhya Pradesh. Trop. Ecol.* 46, 229–240.

Panzou, G. J. L., Fayolle, A., Feldpausch, T. R., Ligot, G., Doucet, J. L., Forni, E., et al. (2018). What controls local-scale aboveground biomass variation in central africa? Testing structural, composition and architectural attributes. *For. Ecol. Manage.* 429, 570–578. doi:10.1016/j.foreco.2018.07.056

Paquette, A., and Messier, C. (2010). The role of plantations in managing the world's forests in the Anthropocene. *Front. Ecol. Environ.* 8, 27–34. doi:10.1890/080116

Paudel, S., and Sah, P. J. (2015). Effects of different management practices on stand composition and species diversity in subtropical forests in Nepal: Implications of community participation in biodiversity conservation. *J. Sustain. For.* 34, 738–760. doi:10.1080/10549811.2015.1036298

Pearce, D. W. (2001). The economic value of forest ecosystems. *Ecosyst. Health* 7, 284–296. doi:10.1046/j.1526-0992.2001.01037.x

Philip, O., and Gentry, A. H. (1993). The useful plants of tambopata, Peru: Statistical hypothesis tests with a new quantitative technique. *Econ. Bot.* 47, 15–32.

Pielou, E. C. (1966). The measurement of diversity in different types of biological collections. *J. Theor. Biol.* 13, 131–144. doi:10.1016/0022-5193(66)90013-0

Pokhriyal, P., Chauhan, D. S., and Todaria, N. P. (2012). Effect of altitude and disturbance on structure and species diversity of forest vegetation in a watershed of central Himalaya. *Trop. Ecol.* 53, 307–315.

Poudyal, B. H., Maraseni, T., and Cockfield, G. (2019). Impacts of forest management on tree species richness and composition: Assessment of forest management regimes in Tarai landscape Nepal. *Appl. Geogr.* 111, 102078. doi:10.1016/j.apgeog.2019.102078

Pradhan, A., Ormsby, A. A., and Behera, N. (2019). A comparative assessment of tree diversity, biomass and biomass carbon stock between a protected area and a sacred forest of Western Odisha, India. *Ecoscience* 26, 195–204. doi:10.1080/11956860.2019.1586118

Pretzsch, H., Schutze, G., and Uhl, E. (2013). Resistance of European tree € species to drought stress in mixed versus pure forests: Evidence of stress release by inter-specific facilitation. *Plant Biol. (Stuttg).* 15, 483–495. doi:10.1111/j.1438-8677.2012.00670.x

Raghubanshi, A. S. (1991). Dynamics of soil biomass C, N, and P in a dry tropical forest in India. *Biol. Fertil. Soils* 12, 55–59. doi:10.1007/bf00369388

Rajput, S. S., Shukla, N. K., Gupta, V. K., and Jain, J. D. (1996). *Timber mechanics: Strength classification and grading of timber*. New Forest, Dehradun: Indian Council of Forestry Research and Education, 189.

Rao, P., Barik, S. K., Pandey, H. N., and Tripathi, R. S. (1990). Community composition and tree population structure in a sub-tropical broad-leaved forest along a disturbance gradient. *Vegetatio* 88, 151–162. doi:10.1007/bf00044832

Reddy, C. S., Babar, S., Amarnath, G., and Pattanaik, C. (2011). Structure and floristic composition of tree stand in tropical forest in the Eastern Ghats of northern Andhra Pradesh. *Indian J. For.* 22, 491. doi:10.1007/s11676-011-0193-5

Reise, J., Kukulka, F., Flade, M., and Winter, S. (2019). Characterising the richness and diversity of forest bird species using National Forest Inventory data in Germany. *For. Ecol. Manage.* 432, 799–811. doi:10.1016/j.foreco.2018.10.012

Richards, A. E., Forrester, D. I., Bauhus, J., and Scherer-Lorenzen, M. (2010). The influence of mixed tree plantations on the nutrition of individual species: A review. *Tree Physiol.* 30, 1192–1208. doi:10.1093/treephys/tpq035

Sagar, R., Raghubanshi, A. S., and Singh, J. S. (2003). Tree species composition, dispersion and diversity along a disturbance gradient in a dry tropical forest region of India. *For. Ecol. Manage.* 186, 61–71. doi:10.1016/s0378-1127(03)00235-4

Sagar, R., and Singh, J. S. (2005). Structure, diversity, and regeneration of tropical dry deciduous forest of northern India. *Biodivers. Conserv.* 14, 935–959. doi:10.1007/s10531-004-0671-6

Sapkota, I. P., Tigabu, M., and Oden, P. C. (2010). Changes in tree species diversity and dominance across a disturbance gradient in Nepalese Sal (Shorea robusta Gaertn. f.) forests. *J. For. Res.* 21, 25–32. doi:10.1007/s11676-010-0004-4

Sapkota, R. P., Stahl, P. D., Hengaju, K., and Rijal, K. (2018). Changes in the ecological parameters of mixed forests of sal (*Shorea robusta* gaertn.) are a function of distance from the human settlements. *Int. J. Ecol.* 2018, 1–29. doi:10.1155/2018/1394814

Saxena, A. K., and Singh, J. S. (1984). Tree population structure of certain Himalayan Forest associations and implications concerning their future composition. *Vegetatio* 58, 61–69. doi:10.1007/bf00044928

Schwab, N., Burzle, B., Bobrowski, M., Bohner, J., Chaudhary, R. P., Scholten, T., et al. (2022). Predictors of the success of natural regeneration in a himalayan treeline ecotone. *Forests* 13, 454. doi:10.3390/f13030454

Seddon, N., Chausson, A., Berry, P., Girardin, C. A. J., Smith, A., and Turner, B. (2020). Understanding the value and limits of nature-based solutions to climate change and other global challenges. *Phil. Trans. R. Soc. B* 375, 20190120. doi:10.1098/rstb.2019.0120

Shaheen, H., Khan, S. M., Harper, D. M., Ullah, Z., and Qureshi, R. A. (2011). Species diversity, community structure, and distribution patterns in Western Himalayan alpine pastures of Kashmir, Pakistan. *Mt. Res. Dev.* 31, 153–159. doi:10.1659/mrd-journal-d-10-00091.1

Shannon, C. E., and Weaver, W. (1963). *The mathematical theory of communication*. Urbana, USA: University Illinois Press, 117p.

Sharma, C. M., Baduni, N. P., Gairola, S., Ghildiyal, S. K., and Suyal, S. (2010). Tree diversity and carbon stocks of some major forest types of Garhwal Himalaya. India. *For. Ecol. Manage.* 260, 2170–2179. doi:10.1016/j.foreco.2010.09.014

Sharma, N., and Kala, C. P. (2022). Patterns in plant species diversity along the altitudinal gradient in Dhauladhar mountain range of the North-West Himalaya in India. *Trees, For. People* 1, 100196. doi:10.1016/j.tfp.2022.100196

Shinwari, M. I., and Khan, M. A. (2000). Folk use of medicinal herbs of margalla hills national park, islamabad. *J. Ethnopharmacol.* 69, 45–56. doi:10.1016/s0378-8741(99)00135-x

Simpson, E. H. (1949). Measurement of diversity. *Nature* 163, 688. doi:10.1038/163688a0

Singh, K., and Chand, P. (2012). Above-ground tree outside forest (TOF) phytomass and carbon estimation in the semi-arid region of southern Haryana: A synthesis approach of remote sensing and field data. *J. Earth Syst. Sci.* 121, 1469–1482. doi:10.1007/s12040-012-0237-z

Singh, K. P., and Singh, J. S. (1988). Certain structural and functional aspects of dry tropical forests and savanna. *Int. J. Ecol. Environ. Sci.* 14, 31–45.

Slik, J. W. F., Paoli, G., McGuire, K., Amaral, I., Barroso, J., Bastian, M., et al. (2013). Large trees drive forest aboveground biomass variation in moist lowland forests across the tropics. *Glob. Ecol. Biogeogr.* 22, 1261–1271. doi:10.1111/geb.12092

Srinivas, K., and Sundarapandian, S. (2019). Biomass and carbon stocks of trees in tropical dry forest of East Godavari region, Andhra Pradesh, India. *Geol. Ecol. Landscapes* 3, 114–122. doi:10.1080/24749508.2018.1522837

Sun, W., and Liu, X. (2020). Review on carbon storage estimation of forest ecosystem and applications in China. *For. Ecosyst.* 7, 4. doi:10.1186/s40663-019-0210-2

Sundarapandian, S. M., and Swamy, P. S. (1997). Plant biodiversity at low-elevation evergreen and moist deciduous forests at Kodayar (W. Ghats, India). *Int. J. Ecol. Environ. Sci.* 23, 363–379.

Sundarapandian, S. M., Dar, J. A., and Gandhi, D. S. (2013). Estimation of biomass and carbon stocks in tropical dry forests in Sivagangai district, Tamil Nadu, India. *Int. J. Environ. Sci. Eng. Res.* 4, 66–76.

Traore, S., Kabore, O., Rasolodimby, J. M., Thiombiano, L., and Guinko, S. (2008). Impact of protected areas and land use on regeneration of Acacia woodlands in eastern Burkina Faso. *Flora Veg. Sudano-Sambesica* 11, 17–24. doi:10.21248/fvss.11.3

Upadhaya, K., Barik, S. K., and Pandey, H. N. (2008). Response of woody species to anthropogenic disturbances in sacred forests of northeast India. *Inter. J. Ecol. Environ. Sci.* 34, 245–257.

Vaidyanathan, S., Krishnaswamy, J., Samba, K. N., Dhanwatey, H., Dhanwatey, P., and Karanth, K. U. (2010). Patterns of tropical forest dynamics and human impacts: Views from above and below the canopy. *Biol. Conserv.* 143, 2881–2890. doi:10.1016/j.biocon.2010.04.027

Van, P. F., Ratcliffe, S., Ruiz-Benito, P., Allan, E., Verheyen, K., Wirth, C., et al. (2017). Continental mapping of forest ecosystem functions reveals a high but unrealised potential for forest multifunctionality. *Ecol. Lett.* 21, 31–42. doi:10.1111/ele.12868

Van De Perre, F., Willig, M. R., Presley, S. J., Andemwana, F. B., Beeckman, H., Boeckx, P., et al. (2018). Reconciling biodiversity and carbon stock conservation in tropical forest landscape. *Sci. Adv.* 4, 1–9. doi:10.1126/sciadv.aar6603

Vetaas, O. R. (2000). The effect of environmental factors on the regeneration of *Quercus semecarpifolia* Sm. in Central Himalaya, Nepal. *Plant Ecol.* 146, 137–144. doi:10.1023/a:1009860227886

Walkley, A., and Black, J. A. (1934). Estimation of soil organic carbon by chromic acid filtration method. *Soil Sci.* 37, 38–39.

Wardle, D. A. (2001). Experimental demonstration that plant diversity reduces invasibility–evidence of a biological mechanism or a consequence of sampling effect? *Oikos* 95, 161–170. doi:10.1034/j.1600-0706.2001.950119.x

WCMC (1992). *Global biodiversity: Status of the earth's living resources*. London: Chapman and Hall.

Westlake, D. F. (1963). Comparison of plant productivity. *Biol. Rev.* 38, 385–425. doi:10.1111/j.1469-185x.1963.tb00788.x

Working Plan (2013). *Nurpur forest division - working plan 2012-13*. Himachal Pradesh, India: Himachal Pradesh State Forest Department.

Yohannes, H., Soromessa, T., and Argaw, M. (2015). Carbon stock analysis along forest disturbance gradient in gedo forest: Implications of managing forest for climate change mitigation. *J. Ecosyst. Ecogr.* 5, 1–5. doi:10.4172/2157-7625.1000170

Yuan, Z., Wang, S., Ali, A., Gazol, A., Ruiz-Benito, P., Wang, X., et al. (2018). Aboveground carbon storage is driven by functional trait composition and stand structural attributes rather than biodiversity in temperate mixed forests recovering from disturbances. *Ann. For. Sci.* 75, 67–71. doi:10.1007/s13595-018-0745-3

Zanne, A. E., Lopez Gonzalez, G., Comes, D. A., Ilic, J., Janson, S., Lewis, S. L., et al. (2009). *Global wood density database*. Dryad digital repository. Available at: http://hdl.handle.net/10255/dryad.235.

Zhang, Z. Z., Zhou, J., Zhao, X. H., Zhao, P., Zhu, L. W., Ouyang, L., et al. (2017). Maximised photosynthetic capacity and decreased hydraulic failure risk during aging in the clump bamboo, *Bambusa chungii*. *Funct. Plant Biol.* 44, 785–794. doi:10.1071/FP16381

Zhou, X., Fu, Y., Zhou, L., Li, B., and Luo, Y. (2013). An imperative need for global change research in tropical forests. *Tree Physiol.* 33, 903–912. doi:10.1093/treephys/tpt064

frontiers | Frontiers in Environmental Science

TYPE Original Research
PUBLISHED 28 September 2022
DOI 10.3389/fenvs.2022.955876

Check for updates

EDITED BY
Donatella Valente,
University of Salento, Italy

REVIEWED BY
Ziyi Wang,
Nanjing University, China
Muhammad Ikram,
Al Akhawayn University, Morocco

*CORRESPONDENCE
Xiaoqin Cheng,
cxq_200074@163.com

SPECIALTY SECTION
This article was submitted to Land Use Dynamics,
a section of the journal
Frontiers in Environmental Science

RECEIVED 29 May 2022
ACCEPTED 23 August 2022
PUBLISHED 28 September 2022

CITATION
Li ZZ, Hu B, Qin Y and Cheng X (2022), Drivers of spatiotemporal disparities in the supply-demand budget of ecosystem services: A case study in the Beijing-Tianjin-Hebei urban agglomeration, China.
Front. Environ. Sci. 10:955876.
doi: 10.3389/fenvs.2022.955876

Drivers of spatiotemporal disparities in the supply-demand budget of ecosystem services: A case study in the Beijing-Tianjin-Hebei urban agglomeration, China

Zu Zheng Li[1], Baoan Hu[2], Yangyi Qin[2] and Xiaoqin Cheng[2]*

[1]State Key Laboratory of Urban and Regional Ecology, Research Center for Eco-environmental Sciences (CAS), Beijing, China, [2]School of Ecology and Nature Conservation, Beijing Forestry University, Beijing, China

Assessing the spatiotemporal patterns of ecosystem services (ESs) supply and demand, as well as the drivers thereof during specific time periods, is critical for regional policy making and sustainable management. Taking the Beijing-Tianjin-Hebei (BTH) urban agglomeration of China as an example, we studied four ES supply-demand budgets: carbon storage, water provision, food provision and soil conservation from 2000 to 2015. Through the geodetector model, canonical analysis and Multiscale Geographically Weighted Regression (MGWR) model, the drivers of the ES supply-demand budget were explored. The results showed that the areas supplying high amounts of ESs in the northern region usually did not overlap those areas consuming intensive ESs, which were mainly distributed in metropolitan areas. The anthropological factors, including per capita gross domestic product (Per.GDP) and population density (POP.Den), were the dominant influencing factors for the imbalance between the supply and demand of carbon storage, water provision and food provision, which were mainly distributed in the central and southern regions of the study area. Geomorphological factors (ELE and SLO) were the key driving factors of soil conservation, which was mainly distributed in the eastern regions. In all, our findings could provide comprehensive information for decision-making and ES management.

KEYWORDS

ecosystem services (ESs), mismatch, BTH urban agglomeration, MGWR, spatiotemporal patterns

Introduction

Ecosystem services (ESs) are defined as the various benefits that people obtain from ecosystems, which helps maintain global life support systems (Costanza et al., 1997; Daily et al., 2009; Raoet al., 2018). They are necessary for human well-being as they provide multiple functions including food, water, timber, minerals, climate regulation, water purification, soil erosion prevention, and recreation (Nelson et al., 2009; Cruz-Garcia et al., 2017). Over the past three decades, global changes such as climate change, population increase, rapid urbanization, technological development and policy making have threatened and affected large-scale natural ecosystem structures and functions as never before, causing severe modifications in ESs and threatening human well-being (Mooney et al., 2009; Nelson et al., 2009). In response to this background, a growing number of scientists have been working on mapping and analyzing ES supply (Minin et al., 2017; Wilkerson et al., 2018). Landscapes are geospatially heterogeneous, socioeconomically driven, regionally coupled systems of human-environment interaction (Sun et al., 2019). Most of these prior studies have focused mainly on exploring ES supply changes under the effects of climate, land-use changes and topographical factors (Peng et al., 2017; Borrelli et al., 2020; Li et al., 2021).

Nevertheless, the status of ESs is not only influenced by the supply capacity of ecosystems, but also driven by human demands and desires for different kinds of ESs (Wei et al., 2017; Yu et al., 2021). On the one hand, ES supply is generally defined as the ecological products and services provided by eco-systems to human society based on biophysical characteristics, ecological functions and social characteristics (de Groot et al., 2010). ES demand, on the other hand, can be described as the actual use or consumption of ESs by stakeholders in a particular area within a given time, which is affected by socioeconomic system and has received increased attention in the last 10 years (Burkhard et al., 2012; Schirpke et al., 2019). However, because of the complex coupling between social systems and natural ecosystems, focusing on only one side of ESs will lead to an imbalance between ES supply and demand, causing unexpected ecological concerns and social equity issues (Baró et al., 2016; Delphin et al., 2016). Therefore, incorporating ES demand side into ES assessments can help decision makers identify ES supply and demand surplus and deficit and provide a scientific basis for achieving regional sustainable development goals (Costanza et al., 2017; Schirpke et al., 2019).

Previous studies have assessed spatial dynamic variations in ES supply and demand (Burkhard et al., 2012; Chen et al., 2019; Xu et al., 2021); clarified the spatial matching of ES supply and demand, such as the ratio of supply to demand (Boithias et al., 2014; Bryan et al., 2018); and evaluated the mismatch between ES supply and demand to inform regional management (Larondelle and Lauf, 2016). These studies help us understand the mismatch between ES supply and demand in different contexts (Ahmad et al., 2020; Yao et al., 2021). However, improving the matching of ES supply and demand is still a significant challenge in the crusade to meet human needs and demands (Mehring et al., 2018). To attain a balance, it is necessary to comprehensively manage land use and other social resources to avoid ES deficit–defined as the ES supply cannot meet ES demand (the value of ES gap is lower than 0) (Cui et al., 2019). Although it has been proven that land use, climate, topographical and socio-economic factors significantly influence ES supply and demand, few studies have comprehensively explored the drivers of ES supply and demand as a whole (Costanza et al., 2017; Chaplin-Kramer et al., 2019). Furthermore, current studies lack discussions on the scale dependence in the spatially non-stationary relationships between driving factors and ES supply and demand.

The Beijing-Tianjin-Hebei (BTH) urban agglomeration is densely populated, and is one of the regions with the most rapid economic and urbanization development in the world. It suffers from serious environmental problems, such as air pollution, water and soil loss, water scarcity and biodiversity loss (Li et al., 2017; Yang et al., 2019), which leads to the losses of regional ESs (Zhang et al., 2017). Therefore, this study chose the BTH urban agglomeration as a case to evaluate the supply, demand, and gap of ESs and their drivers the spatial scale, which can enrich researches in this field. This study has three specific objectives: *1*) to quantify the spatial and temporal variations of four critical ES supply and demand from 2000 to 2015, including carbon storage (CS), water provision (WP), food provision (FP), and soil conservation (SC); *2*) to examine the spatiotemporal patterns of the mismatches between ES supply and demand at the county or district scale; and *3*) to explore the key drivers of the mismatches between ES supply and demand and analyze the spatial heterogeneity of these effects. This study aims to propose several land-use strategies and socioeconomic and ecological management measures that can alleviate ES mismatches, supporting regional ecological security and sustainable development.

Materials and methods

This study proposed a framework to assess the effects of anthropological, climate factors, and geomorphological factors on ESDRs and support regional ES management in the Beijing-Tianjin-Hebei urban agglomeration (Figure 1). Firstly, relevant data were collected and three comprehensive factors was measured. Secondly, the spatio-temporal variations of comprehensive factors and four ES supply-demand ratio (ESDRs) were evaluated from 2000 to 2015. Thirdly, relationships between ESDRs and anthropological, climate

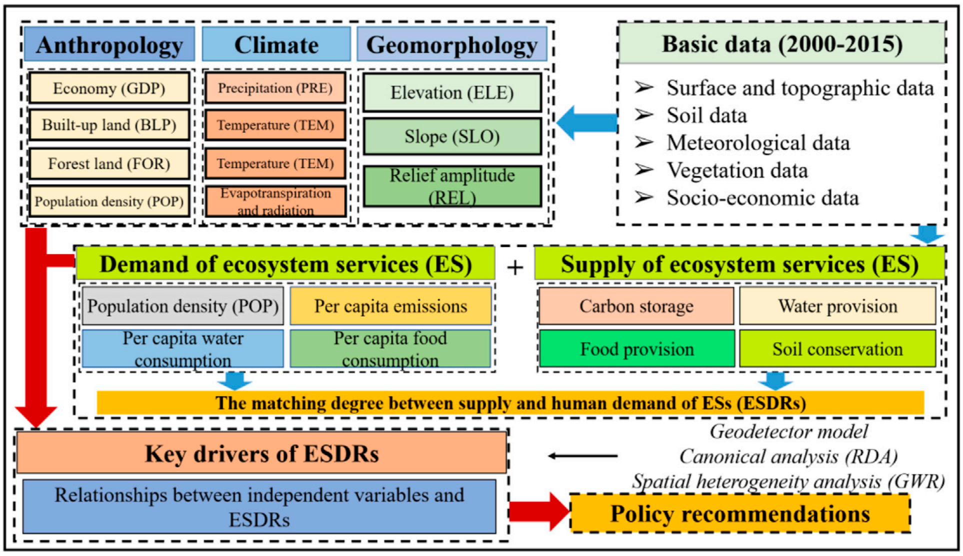

FIGURE 1
The framework and procedures of this study.

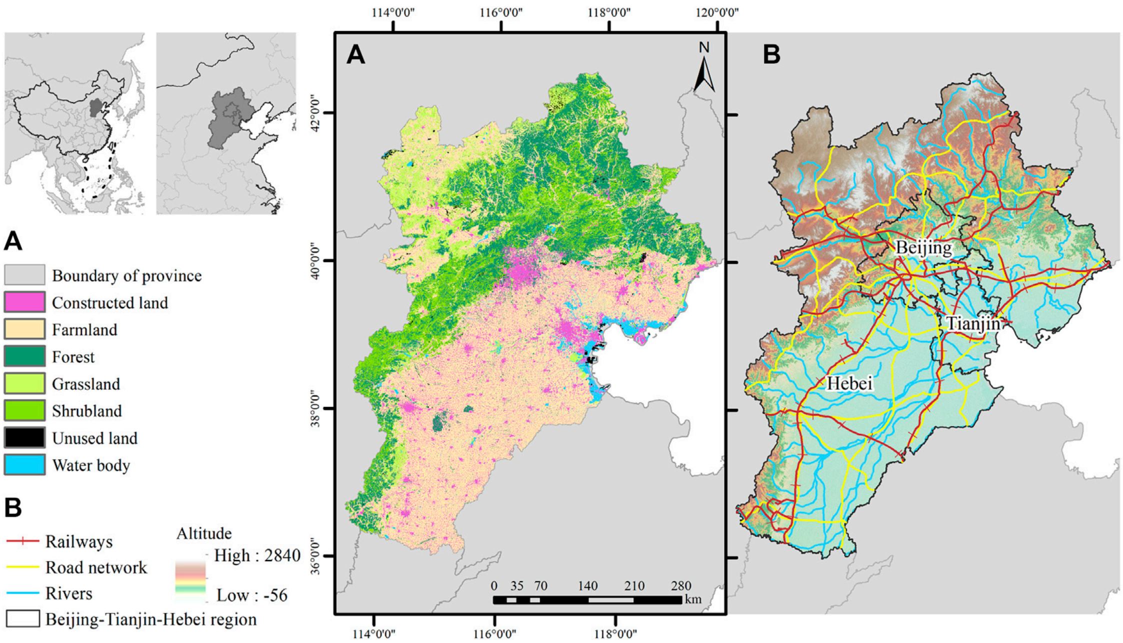

FIGURE 2
Study area. **(A)** LULC distribution of cover-types. **(B)** Map of major rivers and urban and peri-urban infrastructure, including roads, railway, and municipal boundaries.

factors, and geomorphological factors was analyzed by using geodetector model, RDA, and GWR model. Finally, some relevant policy recommendations and measures were put forward.

Study area

The BTH urban agglomeration, located in Northern China (35°03′–42°40′N, 113°27′–119°50′E, Figure 2), borders the

Taihang Mountain, Yanshan Mountain and Bohai Bay. It covers an area of 212,962 km^2, including two municipalities (Beijing and Tianjin city), as well as Hebei province with 11 prefectural-level cities, amounting to 173 counties. The northwestern part of this region has a higher elevation and is mostly hilly, while the southeast is relatively flat with an elevation of less than 100 m. The BTH urban agglomeration has a temperate continental climate, with an annual mean precipitation of 420–550 mm and an annual mean temperature of −3.5° to 24.5°C (Shen, J et al., 2020). The southeastern plain is an important grain production area in China, growing corn, wheat, and peanuts.

The BTH urban agglomeration is a political, cultural, and economic center in China. In 2019, BTH created a GDP of 8.46 trillion yuan, accounting for 8.5% of the country's GDP. From 2000 to 2019, the urbanization of this region developed rapidly. The urbanization rate increased from 38.50% in 2000 to 66.70% in 2019. The urban population of the BTH urban agglomeration increased from 70.91 million to 113.07 million. With its high-density population and high rate of urbanization, the region has experienced long-term water resource shortages and unbalanced development between the sown area and grain yield (Li et al., 2017). Moreover, the imbalance between resource supply and demand has triggered a series of regional problems, including surface runoff decrease, land desertification, groundwater over-extraction, air quality deterioration, biodiversity reduction, and eco-system degradation (Zhang et al., 2017; Yang et al., 2019). Therefore, a comprehensive diagnosis of ESs from the sup-ply-demand perspective is highly significant for BTH's sustainable ES management.

Data sources

Five types of data were used in this study: land-use, statistical, meteorological, geomorphological, and soil (Supplementary Table S1). Land use data were obtained from the Resource and Environ-mental Science Data Center of the Chinese Academy of Sciences (http://www.resdc.cn/). We adopted the classification system proposed in the "Current Land Use Classification" formulated by the Ministry of Natural Resources of China (Ministry of Natural and Re-sources of R.P.C) as the basic classification system (Ministry of Natural and Resources of R.P.C, 2017). Land use was classified into seven types: grassland, water body, cultivated land, artificial surface, unused land, forest land, and shrub land. All vector and raster data were converted to the same projection coordinate system (Bei-jing_1954_3_Degree_GK_CM_ 114E), and the spatial accuracy of all raster data was modified to 30 m by resampling in ArcGIS 10.3.

Quantification of ecosystem services supply and demand

In this work, four key ESs were selected according to the latest version of the Common International Classification of ES (CICES). The selected ESs are very important for the sustainable development of the BTH urban agglomeration and are sensitive to global climate changes, land use changes and significantly increased human activities (CICES, https://cices.eu/resources/). Table 1 provides an overview of the ESs evaluated in the study area and the reasons for their selections by literature reviews.

Carbon storage

(1) Supply

Carbon storage (CS) refers to the capacity of vegetation to store carbon, which is essential for climate change mitigation (Onaindia et al., 2013). Here, the "InVEST carbon storage model" was used to quantify carbon storage based on land use maps and four carbon pools: *1*) above-ground biomass (CS_a); *2*) below-ground biomass (CS_b); *3*) soil organic matter (CS_s); and *4*) dead organic matter (CS_d) (Sharp et al., 2020). The carbon stocks per unit area for each land use type were derived from literature based on local studies (Tallis and Polasky, 2009). The total carbon stored SCS for each pixel (Mg) was calculated as:

$$SCS = PA\left(CS_A + CS_b + CS_c + CS_d\right) \quad (1)$$

where PA is the pixel area (30 × 30 m = 900 m^2 or 0.09 ha), CS_a is the above-ground carbon density ($Mg\ C{\cdot}ha^{-1}$); CS_b is the below-ground carbon density ($Mg\ C{\cdot}ha^{-1}$); CS_s is the soil organic carbon density ($Mg\ C{\cdot}ha^{-1}$); and CS_d is the dead organic matter carbon density ($Mg\ C{\cdot}ha^{-1}$).

(2) Demand

The total amount of carbon emissions was used as the demand for carbon storage in this study, as the changes of per capita emissions will lead to an increase or decrease of the demand for carbon sequestration (Bateman et al., 2013). The total amount of carbon emission is calculated by multiplying the total energy consumption by the standard carbon emission coefficient according to the data provided by CO_2 emission inventory of BTH (*e.g.* residential, industry, and agriculture) (BMBS, 2015; HMBS, 2015; TMBS, 2015). The amount of carbon contained in CO_2 was estimated to be about 27% of total carbon. We multipled the average value of emissions per capita by the population density to obtain the total carbon emitted per pixel (González-García et al., 2020). The calculation of total amount of carbon emissions is as follow:

$$D_{CP} = D_{pcfc} \times D_{pop} \quad (2)$$

where *DCP* is the demand for carbon sequestration (t), *Dpcfc* is the per capita carbon emissions (t); and *Ppop* is the population

TABLE 1 Ecosystem services evaluated in the Beijing-Tianjin-Hebei urban agglomeration.

Ecosystem services	Selection reasons
Carbon storage (CS)	Absorption of CO_2 by vegetation is of great significance to regional climate change, and directly affects human health
Water provision (WP)	Water resources re recharged by terrestrial and aquatic ecosystems, affecting the growth of vegetation
Food provision (FP)	Food production is mainly provided by cultivated land, and is the basic material for human survival
Soil conservation (SC)	Reduction of soil erosion caused by storm runoff and topography is important in the BTH urban agglomeration

density (person·km^2). For details, please refer to Supplementary Table S2.

Water provision

(1) Supply

Water provision (WP) refers to the annual quantity of water yield available to humans within a given region (Boithias et al., 2014). The "Hydropower Water Yield module" of InVEST was used to quantify water provision based on the Budyko curve, with the data including average annual precipitation, root restricting layer depth (mm), plant available water content, annual reference evapotranspiration (mm), and land use maps (Sharp et al., 2020). The calculation of annual water provision Y for each pixel is as follows:

$$Y = (1 - AET/P).P \tag{3}$$

$$AET/P = (1 + PET/P) - [1 + (PET/P)^{\omega}]^{1/\omega} \tag{4}$$

$$PET = K.ET_0/P \tag{5}$$

$$\omega = Z.AWC/P + 1.25 \tag{6}$$

$$AWC = Min\,(Rest.layer.Soil\,Depth,\ Root.Depth).PAWC \tag{7}$$

where AET is the annual actual evapotranspiration (mm); P is the annual precipitation (mm); AET/P is based on an expression of the Budyko curve proposed by (Fu, 1981; Zhang et al., 2004); PET is the potential evapotranspiration, ω is an empirical parameter that characterizes the natural climatic-soil properties; $ET0$ is the reference evapotranspiration; K is the vegetation evapotranspiration coefficient associated with the land use (Sharp et al., 2020); AWC is the volumetric plant available water content; Z is the empirical constant, and sometimes referred to as "seasonality factor" (1–30); and $PAWC$ is the Plant Available Water Content fraction (0–1) (Sharp et al., 2020).

(2) Demand

Water demand (D_{WY}) refers to the total amount of water consumption for agricultural and industrial production, inhabitants, and ecological purposes (Burkhard et al., 2013; Chen et al., 2019). For this estimate, we collected the population density map and the water resource bulletins from each county which provides the water consumption per inhabitant per studied year (BMBS, 2015; HMBS, 2015; TMBS, 2015). The calculations of water demand D_{WY} is as follows:

$$D_{WY} = D_{pcwc} \times P_{pop} \tag{8}$$

where D_{pcwc} is the per capita water consumption; and P_{pop} is the population density (person·km^2). For details, please refer to Supplementary Table S3.

Food provision

Both the supply and demand for food provision (FP) were estimated through statistical data. Here, for FP supply, we first added up each county's production of grain, vegetables, and fruit products, which were the three main types of foods produced in cropland (https://data.cnki.net/Yearbook/Navi?type=type&code=A). Then, we estimated the demand for FP by multiplying the per capita food consumption by the population density. According to (Tang and Li, 2012), the per capita food demand was 322.07 kg·a-1, which can basically meet China's per capita food security. For counties without per capita food consumption data, city or provincial-scale per capita food consumption was used as an alternative. Food provision supply and demand can be calculated using the following equations:

$$S_i^{FP} = \sum_j^n P_{(i,j)}\,(j = 1, 2, 3\ldots, n) \tag{9}$$

$$D_i^{FP} = D_{pcfp} \times P_{pop} \tag{10}$$

where $S_i^{FP}$is the FP supply for county I; P (i, j) is the annual provision of j type food for each county, including grains, vegetables and fruits; D_i^{FP} is the FP demand for county I; D_{pcfp} is the per capita food demand; and P_{pop} is the population density (person·km^2).

Soil conservation

(1) Supply

The "Sediment Delivery Ratio module" of InVEST was used to map and calculate the total amount of soil conservation per pixel based on the universal soil loss equation ($RUSLE$) (Sharp et al., 2020). Soil conservation equals the difference between the actual amount of soil erosion ($USLE$) and the maximum potential amount of soil erosion ($RKLS$), assuming the original land cover without the C or P factors (Kareiva et al., 2011; Ouyang et al., 2016), and is calculated as:

$$SC = RKLS - usle \tag{11}$$

10.3389/fenvs.2022.955876

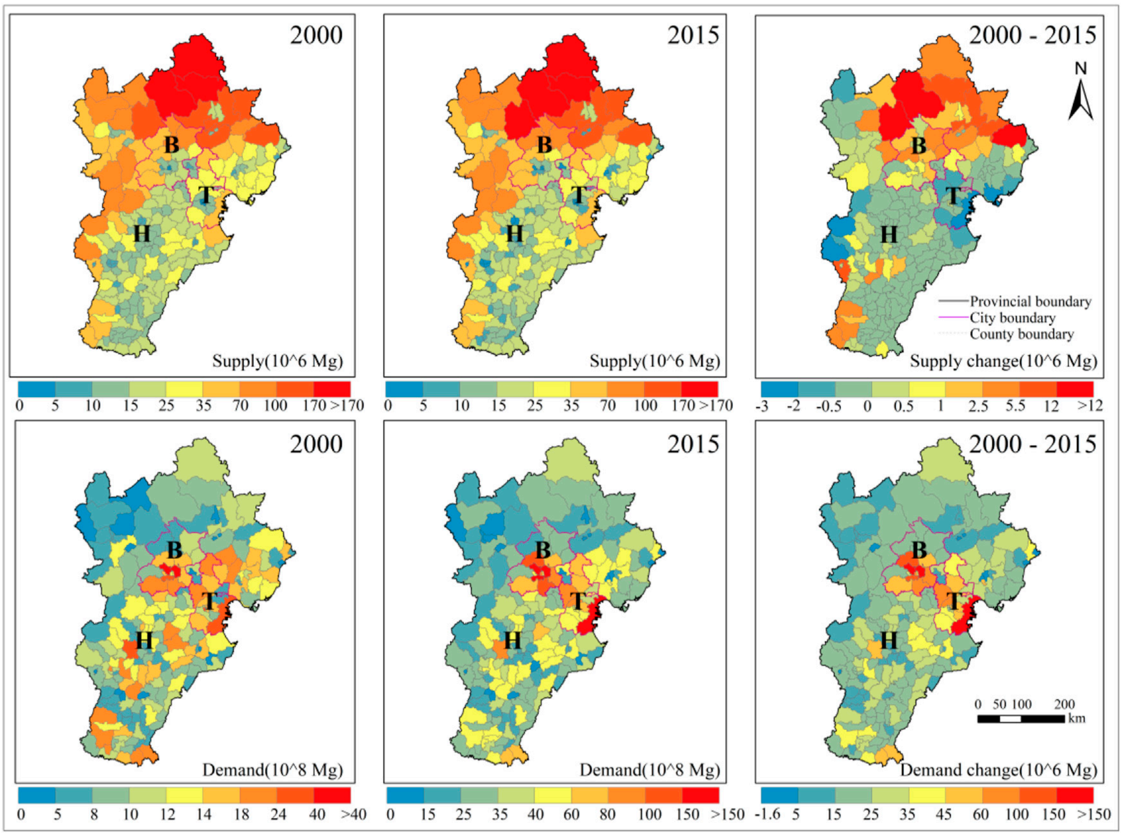

FIGURE 3
Distribution of carbon storage supply, demand and their changes from 2000 to 2015. B: Beijing city; T: Tianjin city; H: Hebei province.

$$usle = R.K.LS.C.P \tag{12}$$

$$RKLS = R.K.LS \tag{13}$$

where SC is the amount of soil conservation ($tons \cdot ha{-}1 \cdot yr{-}1$); $usle$ is the amount of actual soil loss ($tons \cdot ha{-}1 \cdot yr{-}1$); $RKLS$ is the amount of potential soil loss ($tons \cdot ha{-}1 \cdot yr{-}1$); R is rainfall erosivity (MJ · mm ($ha \cdot hr$)−1); K is the soil erodibility factor for each pixel (MJ · mm ($ha \cdot hr$)−1); LS is the slope length-gradient factor (dimensionless); and C and P are the crop management and support practice factors for each pixel (dimensionless), respectively.

(2) Demand

The amount of actual soil loss was used to define demand for soil conservation, which is based on the quantity of actual soil erosion that human beings are expected to deal with (Liu et al., 2019). The calculation of the amount of actual soil loss is below:

$$usle = R.K.LS.C.P \tag{14}$$

where $usle$ is the amount of actual soil loss ($tons \cdot ha{-}1 \cdot yr{-}1$). For details, please refer to Supplementary Table S4.

Relationship between ES supply and demand

Ecosystem service supply-demand ratio (ESDR)

The ecosystem service supply-demand ratio ($ESDR$) index was used to quantify the relationship between the actual ES supply and human demand, identifying ES supply-demand shortages and mismatches (Chen et al., 2019). The ESDR index is calculated as follows:

$$ESDR_i = \frac{S_i - D_i}{(S_{max} + D_{max})/2} \tag{15}$$

where $\boldsymbol{S_i}$ and $\boldsymbol{D_i}$ refer to the actual ES supply and demand for pixel i, respectively; and S_{max} and D_{max} indicate the maximum value of actual ES supply and human demand in the county, respectively. A value greater than 0 indicates an ES surplus, meaning that supply can meet demand, a value of 0 indicates ES supply-demand balance, and a value lower than 0 indicates a deficit—supply cannot meet demand.

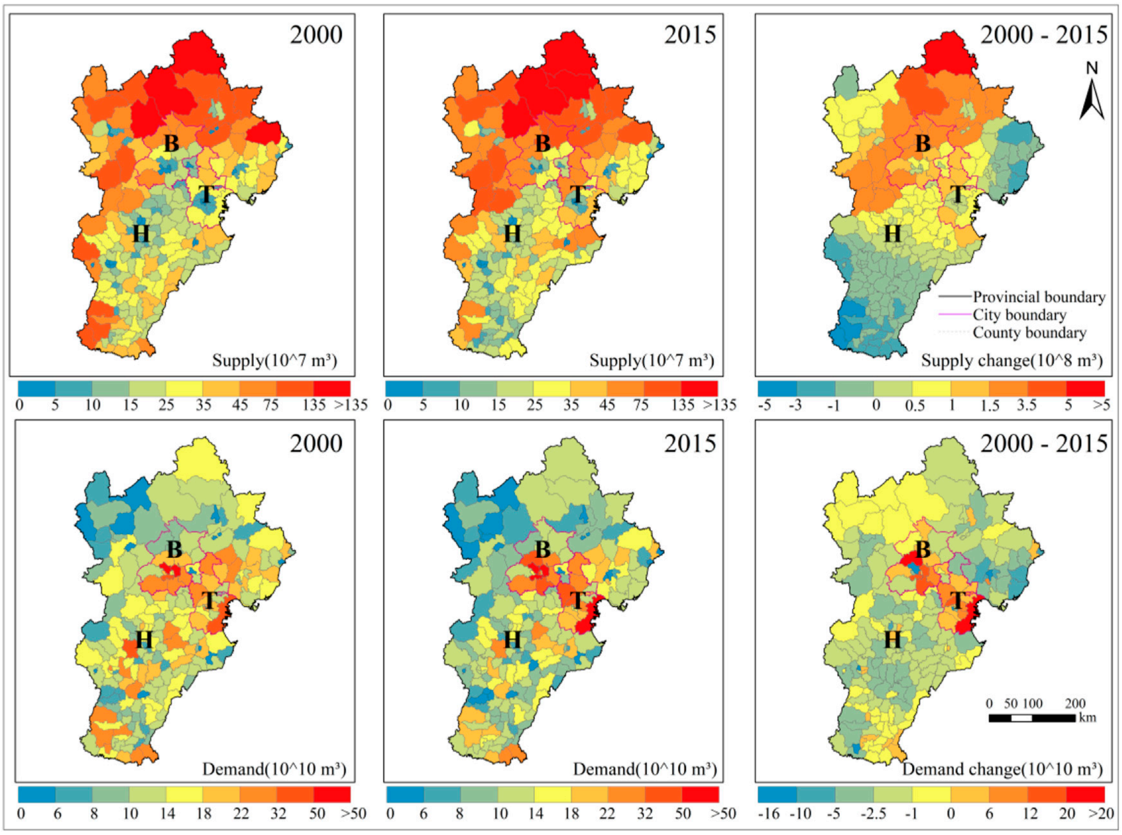

FIGURE 4
Distribution of water provision supply, demand and their changes from 2000 to 2015. B: Beijing city; T: Tianjin city; H: Hebei province.

Global spatial autocorrelation

Global spatial autocorrelation can describe the overall distribution of ESDER spatial correlation (aggregation characteristics) in the BTH urban agglomeration by calculating Moran's I in the GeoDA software, which ranges from −1 to 1 (Anselin, 1996). Moran's $I > 0$ indicates that a variable appeared in a spatial aggregation pattern. Moran's $I < 0$ indicates that a variable presented a discrete pattern. Moran's $I = 0$ indicates no autocorrelation; the spatial units are randomly distributed. The closer the Moran's I is to +1, the more significant the spatial autocorrelation occurs. It is calculated as follows:

$$Moran's\, I = \frac{n\sum_{i=1}^{n}\sum_{j\neq 1}^{n} w_{ij}(x_i-\bar{x})(x_j-\bar{x})}{\left(\sum_{i=1}^{n}\sum_{j=1}^{n} w_{ij}\right)\sum_{i=1}^{n}(x_i-\bar{x})^2} \tag{16}$$

where n is the total number of spatial units; x_i and x_j are ESDR values of the spatial units i and j, respectively; W_{ij} is the spatial matrix of units i and j obtained through the rook adjacency matrix; and $\bar{x}$ is the mean value of *ESDR*.

Local spatial autocorrelation

The Moran scatterplot and local indicators of spatial association (LISA) were used to measure the correlation between individual observation and neighboring objects (local spatial autocorrelation) (Anselin, L, 1995). The local Moran's I, includes positive and negative values, which can reflect the local patterns of spatial clustering and the spatial outliers in the maps. It can be classified into clusters of high values (HH), which are high values in a high value neighborhood, and clusters of low values (LL), which are low values in a low value neighborhood. Spatial outliers include high–low outliers (HL) and low–high outliers (LH), which are a high value in a low value neighborhood and a low value in a high value neighborhood, respectively. It is calculated as follows:

$$Moran's\, I = \frac{n(x_i-\bar{x})\sum_j w_{ij}(x_j-\bar{x})}{\sum_i (x_i-\bar{x})^2} \tag{17}$$

where the meanings of all parameters are consistent with those in formula (16).

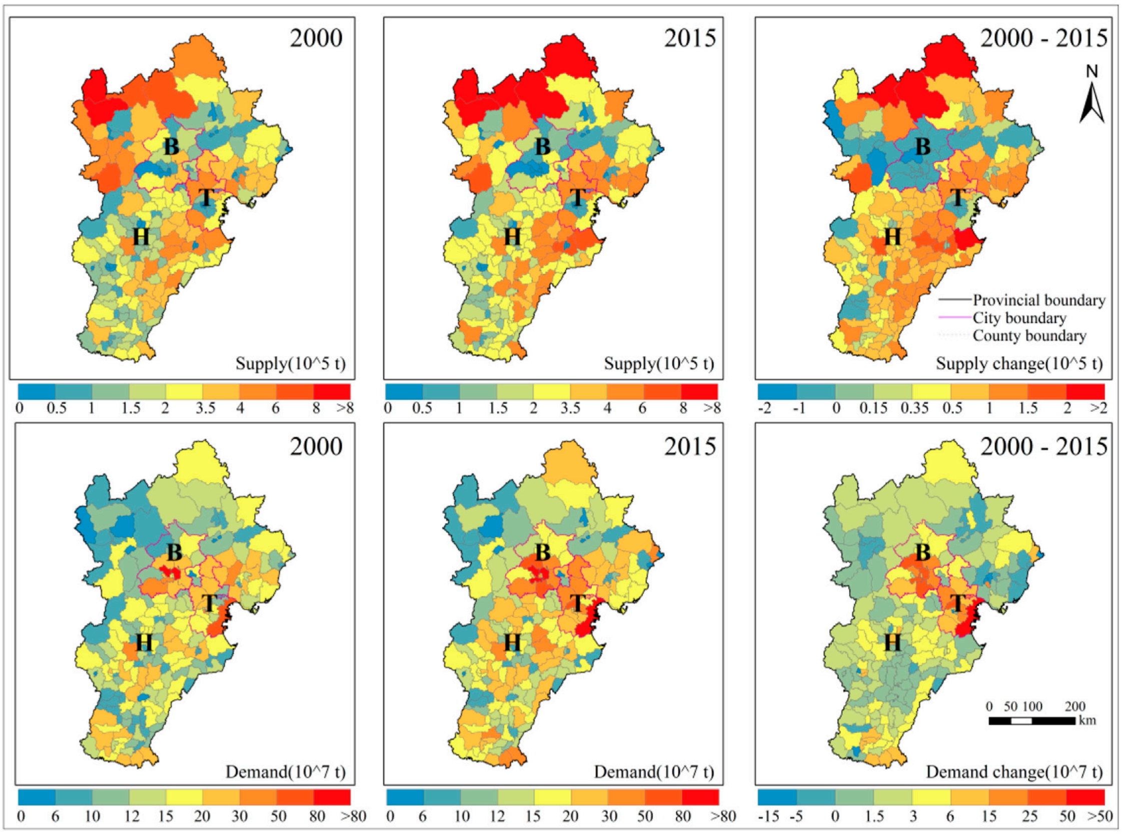

FIGURE 5
Distribution of food provision supply, demand and their changes from 2000 to 2015. B: Beijing city; T: Tianjin city; H: Hebei province.

Drivers analysis

Indicator selection

The ESDR is influenced by anthropological and climate factors as well as geomorphology (Peng et al., 2020; Deng et al., 2021; Zhang et al., 2021), and eleven potentially relevant factors were selected based on the following criteria: *1*) these factors should be measurable and independent; *2*) these factors should include the three aspects of anthropology, climate and geomorphology; and *3*) these data should be readily available (Sannigrahi et al., 2020). Therefore, the drivers used in this study included anthropological influence (changes of per capita gross domestic product (Per.GDP), changes of percentage of built-up land (BLP), changes of percentage of forest land (FOR), changes of population density (POP.Den)); climate influence (changes of average annual precipitation (PRE), changes of annual average temperature (TEM), changes of actual evapotranspiration (EVA), changes of annual average solar radiation (SRD)); and geomorphological influence (mean elevation (ELE), mean slope (SLO), mean relief amplitude (REL)).

Geodetector model

Geodetector model is a statistical tool used to measure spatial heterogeneity and to explore the determinants of spatial heterogeneity (Wang et al., 2010). The basic principle of this model is that if an independent variable has an important influence on a dependent variable, the spatial distribution of the independent variable and the dependent variable should be consistent. The functions of Geodetector model include: *1*) measure the spatial heterogeneity among data; *2*) test the coupling relationship between two variables Y and X, according to their spatial heterogeneity, without assuming the linearity of the association; and *3*) investigate interactions between two explanatory variables X_1 and X_2 to a response variable Y, without any specific form of interaction as the assumed product in econometrics (Wang et al., 2016). Each of the functions can be accomplished by the factor detector q-statistic. Therefore, the Geodetector model is used to identify the invalid and dominant factors among the 11 independent variables affecting the *ESDR*s. The q-statistic is calculated as follows:

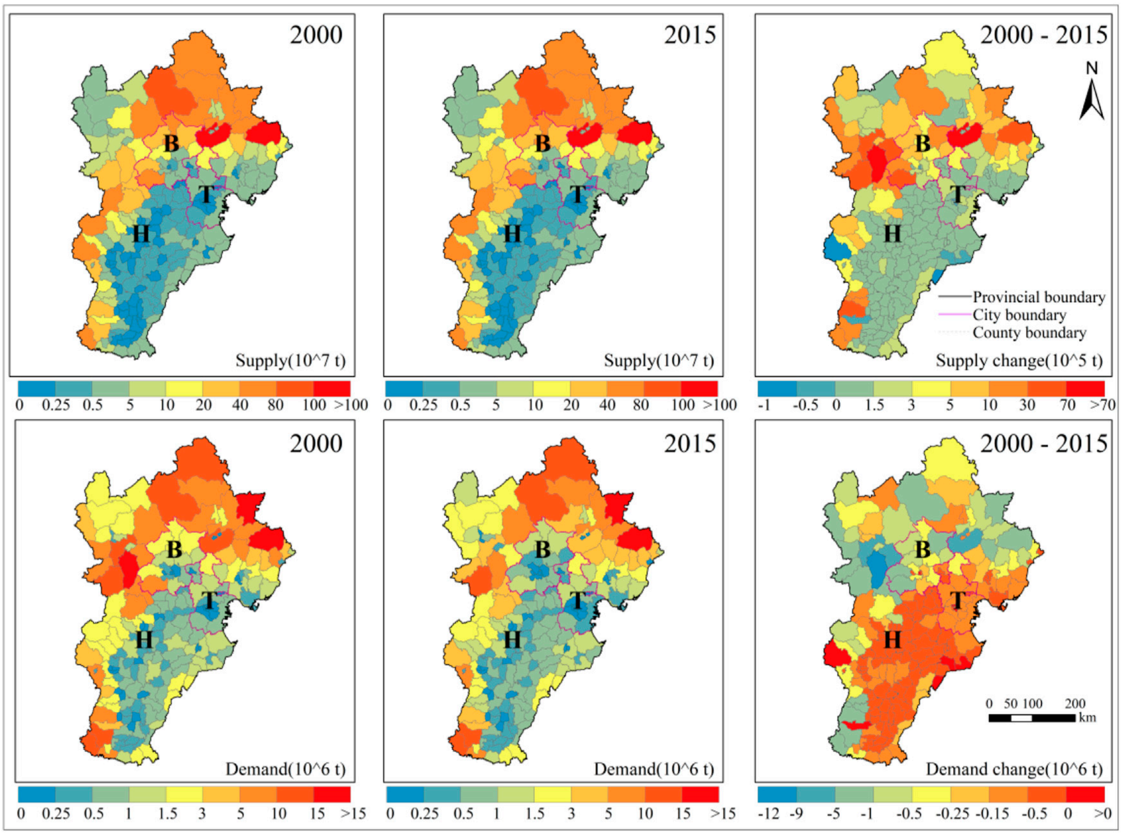

FIGURE 6
Distribution of soil conservation supply, demand and their changes from 2000 to 2015. B: Beijing city; T: Tianjin city; H: Hebei province.

$$q = 1 - \frac{1}{N\sigma^2}\sum_{h=1}^{L} N_h\sigma_h^2 \qquad (18)$$

where q the determinant power of an explanatory variable X of response variable Y; N and σ^2 represent the number of units and the variance of response variable Y in a study area, respectively; h is the partition of variable Y or factor X; σ_h^2 is the discrete variance of the sub-level region; and N_h is the number of secondary units. The value of q ranges from 0 to 1. If Y is stratified by an explanatory variable X, then $q = 0$ indicates that there is no coupling between Y and X; $q = 1$ indicates that Y is completely determined by X; X explains $100q\%$ of Y.

Canonical analysis

Canonical analysis was applied to analyze the strength and direction of correlations between dependent variables (i.e., ES supply, demand, and mismatch) and independent variables (i.e., natural and socio-economic factors) at the county scale (Schmidt et al., 2019). We first standardized all variables. Then, to reduce the dimension of independent variables, the forward stepwise regression was conducted to select the model with the highest R^2 and smallest p value in SPSS 23.0 (Legendre et al., 2011). Multicollinearity among independent variables was tested using the VIF (Variation Inflation Factors), and variables with VIF values larger than 5, indicating collinearity problems were removed from this model (Zuur et al., 2009). Finally, redundancy analysis (RDA) was selected because the gradient length values of DCA were less than 3, and RDA can identify the most relevant driving factors (Legendre et al., 2011; Mouchet et al., 2014). The RDA was performed in the Canoco software (Version 5.0) (Mouchet et al., 2014; Šmilauer and Leps, 2014).

Spatial heterogeneity analysis model

The multi-scale geographically weighted regression (MGWR) model was performed to explore the spatial characteristics and relative contribution of each main factor (MGWR 2.2: https://mgwr.readthedocs.io/en/v2.0.2/index.html) (Fotheringham et al., 2017). The model is an application software for calibrating multi-scale geographically weighted regression (GWR) models based on Microsoft Windows & MacOS platform. GWR can be used to analyze the spatial heterogeneity of the process and the geographical change relationship between the response variables and independent variables at multiple scales, allowing us to generate local R^2, local parameters and model residuals

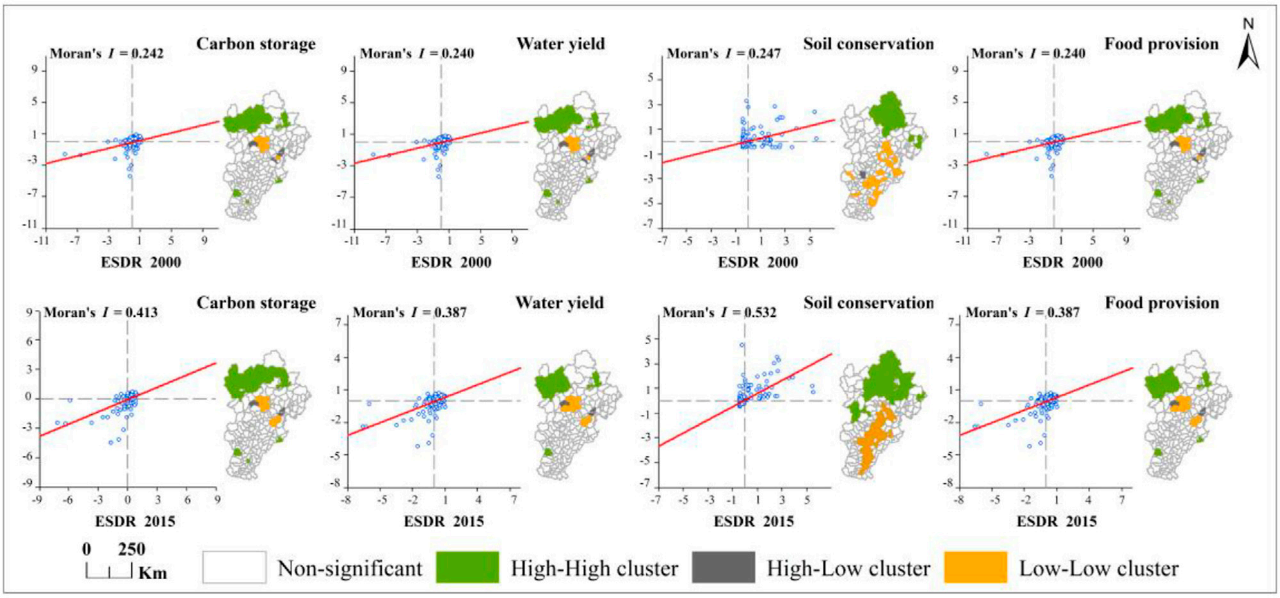

FIGURE 7
The Moran scatterplot and LISA cluster graphs of the ESDRs of four ESs in the BTH from 2000 to 2015.

TABLE 2 The *q* statistics for the explanatory variables derived from Geographic Detector Model.

	GDP	BLP	FOR	POP	PRE	TEM	EVA	ELE	SLO	REL	SRD
CS	0.206*	0.161*	0.063	0.186*	0.112*	0.076*	0.055	0.021	0.023	0.019	0.091
WY	0.234*	0.150*	0.066	0.159*	0.108*	0.059	0.086*	0.060	0.022	0.058	0.075*
FP	0.235*	0.150*	0.067	0.159*	0.109*	0.059	0.086*	0.060	0.022	0.058	0.075*
SC	0.051	0.081*	0.019	0.048	0.017	0.008	0.051	0.149*	0.214*	0.141*	0.032

*** means $p < 0.001$; ** means $0.001 < p < 0.01$; * means $0.01 < p < 0.05$. Per.GDP, changes of per capita gross domestic product; BLP, changes of percentage of built-up land; FOR, changes of percentage of forest land; POP.Den, changes of population density; PRE, changes of average annual precipitation; TEM, changes of annual average temperature; EVA, changes of actual evapotranspiration; SRD, changes of annual average solar radiation; SLO, mean slope; ELE, mean elevation; REL, mean relief amplitude.

(Fotheringham et al., 2017). The dependent variable refers to the change of the ESDR value at a specific location from 2000 to 2015. The change of each driving factor during the corresponding time period is selected as the potential explanatory variable. The MGWR model equation is as follows:

$$Y_i = \beta_0 (U_i, V_i) + \sum j\beta_{bwj} (U_i, V_i) X_{ij} + \varepsilon_{ij} \tag{19}$$

Results

Spatiotemporal dynamics of ES supply and demand

Carbon storage

Carbon storage supply increased from 6.13 billion tons in 2000 to 6.26 billion tons in 2015, with a slight 2.14% increase (Supplementary Table S5). In the same period, the demand increased by 35.2%, from 233.35 billion tons in 2000 to 774.71 billion tons in 2015—an increase of 232% (Supplementary Table S6). There are significant differences in the spatial distribution between the supply and demand (Figure 3). Among them, high carbon storage supply is mostly distributed in the western and northern parts of the study area, while areas with high demand are more concentrated in the urban centers. From 2000 to 2015, supply increases occurred mainly in the northern area, while decreases happened mainly in the east and west of the study area. In addition, the demand for carbon storage increased throughout the whole area, especially in Beijing and Tianjin cities.

Water provision

The water provision supply grew from 62.02 billion m^3 in 2000 to 66.05 billion m^3 in 2015—an increase of 6.49%

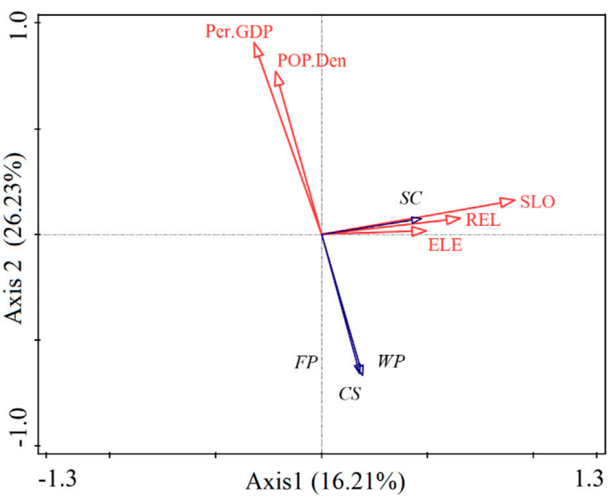

FIGURE 8
RDA results for the explanatory variables of ES ESDRs. The solid blue lines represent the ESDRs changes of ESs. The solid red lines represent the main drivers. Per.GDP, changes of per capita gross domestic product; POP.Den, changes of population density; SLO, mean slope; ELE, mean elevation; REL, mean relief amplitude.

(Supplementary Table S5). In the meantime, the demand for water decreased by 5.31%, from 2.98 × 10^4 billion m^3 in 2000 to 2.83 × 10^4 billion m^3 in 2015 (Supplementary Table S6). The area with the largest supply mainly occurs in the northern parts of the study area, followed by the western area. Areas with high demand are more concentrated in the urban built-up areas (Figure 4). From 2000 to 2015, the increases in supply mainly occurred in the northern part of the study area, while the decrease mainly occurred in the southern part. The increase in water provision service demand was mainly located in Beijing and Tianjin cities.

Food provision

Food provision supply increased by 23.7%, from 4.02 million tons in 2000 to 4.97 million tons in 2015 (Supplementary Table S5). In the same period, food demand showed an increase of 25.44%, from 32.33 billion tons consumed in 2000 to 40.55 billion tons consumed in 2015 (Supplementary Table S6). The area with higher supply was Hebei Province, especially in the northwestern and southeastern parts. Beijing and Tianjin had a lower supply in 2000 and 2015 (Figure 5). From 2000 to 2015, the increases in supply mainly occurred in more counties of Hebei Province, while the food provision supply decreased sharply in Beijing and Tianjin. In terms of demand, most county scale units in Beijing and Tianjin had a markedly higher consumption than that of the counties in Hebei Province. The distribution of the increase in food provision demand was mainly located in Beijing and Tianjin cities.

Soil conservation

Soil conservation supply increased by 0.54% from 17.20 billion tons in 2000 to 17.29 billion tons in 2015 (Supplementary Table S5). In the same period, the demand for soil conservation showed a decrease of 22.01%, from 42.82 million tons to 33.40 million tons (Supplementary Table S6). Higher supply was mainly located in the northeastern parts of the study area, while areas with high demand were more concentrated in the southeast regions (Figure 6). From 2000 to 2015, the increases in supply mainly occurred in the northwest and northeast of Hebei Province and north and west of Beijing, while the southeast of the study area experienced a slight

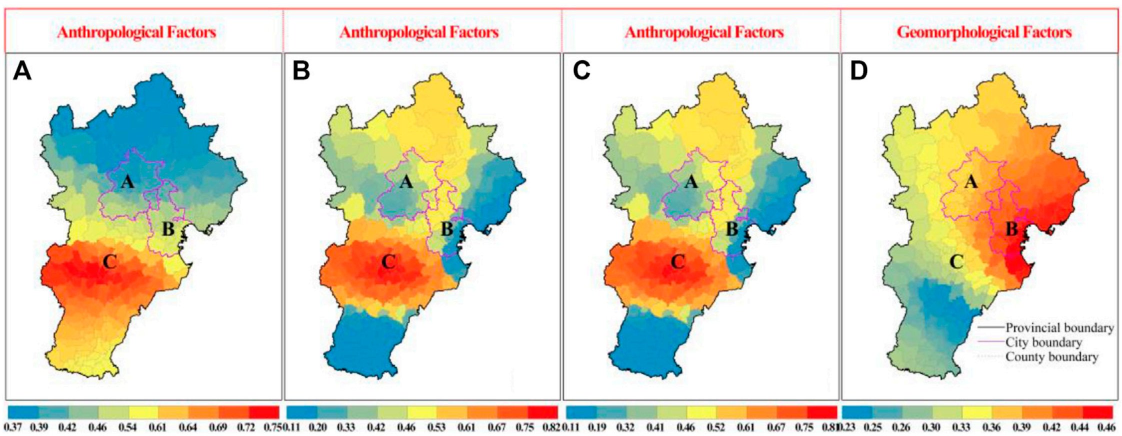

FIGURE 9
The spatial interaction between the driving factors and ESDR of **(A)** carbon storage, **(B)** water provision **(C)** food provision and **(D)** soil conservation. B: Beijing city; T: Tianjin city; H: Hebei province.

TABLE 3 MGWR statistics based on six explanatory factors, VIF based filtered factors, and all explanatory factors for different ecosystem services.

Driving factors	R^2	Adj. R^2	Classic AIC	AICc	BIC/MDL	Intercept
ESDR of CS						
Anthropological factors	0.508	0.486	442.002	442.978	472.011	−1.500
ESDR of WY						
Anthropological factors	0.563	0.536	425.074	426.883	466.122	0.672
ESDR of FP						
Anthropological factors	0.563	0.537	424.712	426.521	465.760	0.692
ESDR of SC						
Geomorphological factors	0.320	0.268	518.085	520.722	567.611	−0.911

decrease. The distribution of the higher demand is more concentrated in the northern part of Hebei Province in 2000 and 2015. The distribution of the increase in soil conservation demand was mainly located in the southeast regions.

Spatiotemporal changes of the ES ESDRs

Sub-area statistical analysis showed that supply-demand ESs of carbon storage, water provision and food provision services in all administrative counties and districts showed negative balances. All sub-areas were at a serious deficit over time in the BTH urban agglomeration (ESDRs <0, detailed mismatch results can be seen in Supplementary Table S7). Soil conservation was the exception; the ESDR was over 0, and showed an upward trend from 2000 to 2015. This indicates that the supply and demand of soil conservation are nearly balanced (Supplementary Table S7).

The spatial correlation of the ESDRs of ESs can be expressed by the global Moran's I at the county or district scale using GeoDA software (Zhang et al., 2017) (Figure 7). The results showed that the global Moran's I values increased from 2000 to 2015 for all the ES ESDRs, with their values all exceeded 0.24. High-value areas tend to be concentrated and low-value areas tend to be adjacent, indicating that the ESDRs generally present significant positive spatial correlation (Moran's I value >0; p-value < 0.01). According to the Moran's I scatterplot, the values for the ESDRs of carbon storage, water provision and food provision services were mainly distributed in the third quadrant, while the values for soil conservation were mainly distributed in the first quadrant (Figure 7). According to the LISA map of the ESDRs, the northern part (mainly in Hebei province) and central part (mainly in Beijing and Tianjin Municipalities) of the BTH showed a diametrically opposite spatial distribution, with the ESDRs in the northern parts showing "High-High" clustering, and the central and southeastern parts showing "Low-Low" clustering.

Associating ESDR with driving factors

Effects the driving factors on ESDRs of ESs

The joint and individual effects of driving factors on ESDRs were analyzed using the Geodetector model (Supplementary Table S8). The results showed that the interaction effect (q) of annual average temperature (TEM) and actual evapotranspiration (EVA) changes on carbon storage, water provision and food provision was the greatest from 2000 to 2015. The next most relevant factors were average annual precipitation (PRE) and population density (POP.Den). Per capita gross domestic product (Per.GDP) interacted strongly with changes in PRE, percentage of forest land (FOR), and POP.Den. In addition, the interaction between mean slope (SLO) and TEM exhibited the largest effect on soil conservation. Soil conservation was also impacted, though not as strongly, by changes in the percentage of built-up land (BLP), changes in average annual precipitation (PRE), and changes in per capita gross domestic product (Per.GDP). The q statistics between the 11 independent variables and the ESDRs of four ESs were estimated (Table 2). Per capita gross domestic product (Per.GDP) had the largest effects on ESDR changes in carbon storage, water provision and food provision. Population density (POP.Den), percentage of built-up land (BLP), and average annual precipitation (PRE), respectively, had the next most significant effect on these ESs. The mean slope (SLO) was the most able to explain the ESDR of soil conservation, followed by mean relief amplitude (REL) and mean elevation (ELE) (Table 2).

To examine the directional associations between the driving variables and the ESDRs, redundancy analysis (RDA) was performed (Figure 8). The results showed that the first two axes explained 42.44% of the total variation. The ESDR changes of the carbon storage, water provision and food provision services were negatively influenced by socio-economic factors, including the changes in per capita gross domestic product (Per.GDP) and population density (POP.Den). Soil conservation was positively affected by geomorphological factors, of which mean slope (SLO) was the most relevant, followed by mean relief amplitude (REL) and mean elevation (ELE).

Spatial regression between driving factors and ESDR

The spatial regression between the driving factors and ESDRs of carbon storage, water provision, food provision and soil conservation were analyzed using the MGWR model and presented in Figure 9. Anthropological factors were correlated with the ESDR changes of carbon storage, water provision and food provision, with local R^2 values of 0.61–0.75, 0.53–0.82, and 0.52–0.81, respectively. The low local R^2 value of the correlation between anthropological factors and ESDR of carbon storage was mainly distributed in the north, ranging from 0.37 to 0.46. Additionally, there is overlap in low-value areas related to water provision and food provision. These are mainly distributed in the south and east of the study area, and range from 0.11 to 0.33. While examining the spatial association between the geomorphological factors and ESDR change of soil conservation, high local R^2 values (R^2 = 0.42–0.46) were found in the eastern areas, while very low regression values (R^2 = 0.23–0.26) were estimated in the southern areas (Table 3). The MGWR estimates revealed that among the 11 driving factors, the anthropological factors produced were the most closely associated with the ESDR change of food provision, characterized by a maximum local R^2 value ($R_{Adj.}{}^2$ = 0.537).

Discussion

Influencing factors of the imbalance between ES supply and demand

The BTH urban agglomeration is composed of two municipalities under the central government and 11 prefecture-level cities. The patterns of the supply and demand of ESs and ESDRs present different spatial distribution characteristics; ES supply and demand has obvious negative spatial correlations, and the spatial imbalance is prominent. This finding is inconsistent with the results discerned by (Wu et al., 2018). (Wu et al., 2018) adopted the scoring matrix method proposed by (Zhang et al., 2004) to quantify the relationship between ES supply and demand, making the scale more detailed. Areas with the lower ESDR values indicate that the ES supply and demand are extremely mismatched, and are mainly distributed in the central urban areas of Beijing and Tianjin. This is because these areas have high levels of urban economic development, high population density, and increasing demand for natural resources (Ou et al., 2018). In addition, the northern region is a key ecological area, and it is also the core of ES supply for carbon storage, water provision and soil conservation in the whole urban agglomeration. Demand in the north is, however, very low.

The shortages and mismatches of ES supply and demand are a result of the complex interaction and comprehensive influence of multiple factors including socioeconomic development and natural occurrences (Sun et al., 2019; Peng et al., 2020; Zhang et al., 2021). Geodetector model results showed that the interaction between the changes of annual average temperature (TEM) and changes of actual evapotranspiration (EVA) has the greatest influence on the ESDR changes of carbon storage, water provision and food provision, although their individual influence is very weak. Studies have shown that several climatic factors (e.g. temperature, precipitation, evapotranspiration) can have significant impacts on multiple ESs, which is illustrated also in our study (Bryan et al., 2018; Chiabai et al., 2018; Chaplin-Kramer et al., 2019; Sannigrahi et al., 2020). (Nelson et al., 2013) suggested that climate change will modify the capability of different key ecosystem functions, including food production, wildfire regulation, hazard reduction, coastal flood protection, water supply, nature-based tourism, and other recreational services. When it comes to the individual influence of factors, strong associations between anthropological factors and carbon storage, water provision and food provision were observed, which is consistent with several previous studies (Yahdjian et al., 2015; Zhang et al., 2021). This indicates that anthropological factors are important in influencing the mismatch between ES supply and demand, even though natural factors determine the mismatch from the supply side to some extent.

The mismatch of soil conservation was mainly affected by the mean slope (SLO), indicating that geomorphological factors played the dominant role; that is, supply determines the mismatch of soil conservation. This is mainly due to the calculation of ESDR of soil conservation service, which does not consider social and economic factors such as population density. Furthermore, the MGWR model was performed to evaluate the spatial interaction between the driving factors and ESDRs of carbon storage, water provision, food provision and soil conservation in the BTH region. The result showed that the anthropological influences on the ESDR of carbon storage varies with geographical space. The corresponding anthropological factors produced very high local R^2 values in the south-central region while they displayed lower regression estimates in the northern region. This suggests that the area near the northern forest is less vulnerable to human activities than the southern plain area.

Suggestions to balance the supply and demand for ESs

Four suggestions were put forward for the BTH urban agglomeration based on our results, which would alleviate the continuous imbalance between ES supply and demand and contribute to the sustainable development of the human-environment system. First, we recommend coordinating the spatial mismatches from both the supply and the demand sides of ESs. More attentions should be paid to alleviating the population pressure, as our study indicated that ESDRs of carbon storage, water provision and food provision are most strongly correlated with anthropological factors (Per.GDP and POP.Den) (Zhang et al., 2021). Second, from the perspective of increasing the supply of carbon storage and water provision, ecological protection and restoration should be carried out on the natural land (Yang et al., 2019). Policies aimed at reducing ES demand are unavoidable, because it is unrealistic to increase vegetated areas to meet the human demand for carbon storage. For instance, energy efficiency should be improved, and energy-saving measures should be implemented, so as to mitigate the imbalance between the supply and demand of carbon storage. Third, the spatial imbalance between ES supply and demand may trigger a series of unintended environmental concerns and social equity issues. Maintaining and improving the original ecosystem supply capacity could alleviate the contradiction between ES supply and demand (Verhagen et al., 2017; Sun et al., 2019), but it may not be the best solution, as the ecosystem has a limited capacity. On the other hand, the shortage of ESs can also be solved through trade, transportation and other measures (Cumming Cramon, 2018). For instance, food and water resources may be transferred from places further away to the urban agglomeration city center, as the area of nearby cultivated land declines and the population within the cities increases (Yu et al., 2021). In addition, implementing the consumption reduction mechanism is a more promising way to meet human demand (Kehoe and Rhodes, 2013).

Limitations and future research directions

Within the background of this study, it is difficult to comprehensively analyze all types and processes of ecosystem supply and demand, as the coupled system integrating human and natural factors is very complicated. Therefore, there are some limitations in our evaluation of ES supply and demand that need to be further explored in future studies. First, the evaluation method of ES supply is based on the land use classifications and the biophysical table, which contains the model information corresponding to each land use type and is revised according to the actual situation in BTH urban agglomeration. However, the classification standards of land use types may be different; some minor lands are considered homogeneous (Li et al., 2020; Sharp et al., 2020). Thus, the calculation of ES supply was considered inaccurate, and the regional difference characteristics of the ES supply pattern cannot be precisely described. Second, this study mainly used the socioeconomic data at the county scale to quantify the demand for ESs, which reflects spatial differences on a coarse scale. This study did not consider the conditions of different ES characteristics and local stakeholders, who may have short-term or long-term interests in ESs (Zhang et al., 2021). Therefore, in the future, we could comprehensively explore the quantification of ESs supply and demand from multiple scales and multiple stakeholders. Third, in addition to accounting for the ES supply and demand, it is important to identify who provides these ESs, which areas have the right to consume, and whether the scope of supply and consumption is available only within an area or extends to other regions (Xu et al., 2021). Even with a study that analyzes those factors, the reality of ES circulation within the regional socioeconomic system is likely more complicated than we can capture. Thus, future research is suggested to incorporate ES flow identifications into ES assessment, which will reveal more details about the interactions between the natural and social systems and provide more information on ES management (Syrbe and Walz, 2012; Schirpke et al., 2019).

Conclusion

This study explored spatiotemporal changes of ES supply and demand, as well as their mismatches in the BTH urban agglomeration of China from 2000 to 2015. Then, we focused on exploring the spatial effects of anthropological, climatic, and geomorphological factors. We further proposed several strategies to offset ES deficits. The results showed that ES supply decreased from 2000 to 2015, while ES demand increased, leading to mismatches spatially, especially in highly urbanized metropolises. To offset the ES deficits, alleviating the population pressure, protecting natural land, and implementing the energy-saving measures would be useful strategies. The anthropological factors, including Per.GDP and POP.Den, are the key drivers in the imbalance of carbon storage, water provision and food provision. Geomorphological factors, including mean elevation (ELE) and mean slope (SLO), are the key drivers for soil conservation. In addition, the drivers of ESs exhibited spatial heterogeneity. The high local R^2 values for ESDR changes of carbon storage, water provision and food provision are mainly distributed in the central and southern region, while a strong association for soil conservation is mainly obtained in the eastern regions. In order to alleviate ES deficits and support ES sustainability, corresponding land-use strategies and socioeconomic and ecological management measures should be adopted. Overall, more localized and efficient land-use decisions and ES management strategies should be implemented to achieve regional sustainability.

Data availability statement

The raw data supporting the conclusions of this article will be made available by the authors, without undue reservation.

Ethics statement

Ethical review and approval was not required for the study on human participants in accordance with the local legislation and institutional requirements. Written informed consent for participation was not required for this study in accordance with the national legislation and the institutional requirements.

Author contributions

Conceptualization, Methodology, and Writing-original draft, ZL; Formal analysis, BH; Valida-tion and Resources, YQ; Software and Data curation, ZL; Project administration and Supervision, BH; Visualization, YQ.

Funding

This research was funded by the Special fund project of Development Planning Office of Beijing Forestry University (2019SHFWYL02).

Acknowledgments

We would like to thank Elizabeth Tokarz at Yale University for her assistance with English language and grammatical editing.

Conflict of interest

The authors declare that the research was conducted in the absence of any commercial or financial relationships that could be construed as a potential conflict of interest.

Publisher's note

All claims expressed in this article are solely those of the authors and do not necessarily represent those of their affiliated organizations, or those of the publisher, the editors and the reviewers. Any product that may be evaluated in this article, or claim that may be made by its manufacturer, is not guaranteed or endorsed by the publisher.

Supplementary material

The Supplementary Material for this article can be found online at: https://www.frontiersin.org/articles/10.3389/fenvs.2022.955876/full#supplementary-material

References

Ahmad, M. A., Waqar, I., Muhammad, S., Ashfaq, R., Abdul, C., Chandio, A. A., et al. (2020). Estimating dynamic interactive linkages among urban agglomeration, economic performance, carbon emissions, and health expenditures across developmental disparities. *Sustain. Prod. Consum.* 26, 239–255. doi:10.1016/j.spc.2020.10.006

Anselin, L. (1995). Local indicators of spatial association-LISA. *Geogr. Anal.* 27, 93–115. doi:10.1111/j.1538-4632.1995.tb00338.x

Anselin, L. (1996). "The Moran scatterplot as an ESDA tool to assess local instability in spatial association," in *Spatial analytical perspectives on GIS in environmental and socio-economic Sciences*. Editors M. Fischer, H. Scholten, and D. Unwin. 1st ed. (London, UK: Taylor & Francis), 4, 111–125.

Baró, F., Palomo, I., Zulian, G., Vizcaino, P., Haase, D., and Gómez-Baggethun, E. (2016). Mapping ecosystem service capacity, flow and demand for landscape and urban planning: A case study in the barcelona metropolitan region. *Land Use Policy* 57, 405–417. doi:10.1016/j.landusepol.2016.06.006

Bateman, I. J., Harwood, A. R., Mace, G. M., Watson, R. T., Abson, D. J., Andrews, B., et al. (2013). Bringing ecosystem services into economic decision-making: Land use in the United Kingdom. *Science* 341, 45–50. doi:10.1126/science.1234379

Beijing Municipal Bureau Statistics (2015). *From january to july, the total revenue of zhongguancun demonstration zone increased by 1.2% year-on-year*. Available online: http://tjj.beijing.gov.cn/ (Accessed on July 8, 2021).

Boithias, L., Acuña, V., Vergoñós, L., Ziv, G., Marcé, R., and Sabater, S. (2014). Assessment of the water supply: Demand ratios in a mediterranean basin under different global change scenarios and mitigation alternatives. *Sci. Total Environ.* 470, 567–577. doi:10.1016/j.scitotenv.2013.10.003

Borrelli, P., Robinson, D. A., Panagos, P., Lugato, E., Yang, J. E., Alewell, C., et al. (2020). Land use and climate change impacts on global soil erosion by water (2015-2070). *Proc. Natl. Acad. Sci. U. S. A.* 117, 21994–22001. doi:10.1073/pnas.2001403117

Bryan, B. A., Ye, Y., Zhang, J. E., and Connor, J. D. (2018). Land-use change impacts on ecosystem services value: Incorporating the scarcity effects of supply and demand dynamics. *Ecosyst. Serv.* 32, 144–157. doi:10.1016/j.ecoser.2018.07.002

Burkhard, B., Crossman, N., Nedkov, S., Petz, K., and Alkemade, R. (2013). Mapping and modelling ecosystem services for science, policy and practice. *Ecosyst. Serv.* 4, 1–3. doi:10.1016/j.ecoser.2013.04.005

Burkhard, B., Kroll, F., Nedkov, S., and Müller, F. (2012). Mapping ecosystem service supply, demand and budgets. *Ecol. Indic.* 21, 17–29. doi:10.1016/j.ecolind.2011.06.019

Chaplin-Kramer, R., Sharp, R. P., Weil, C., Bennett, E. M., Pascual, U., Arkema, K. K., et al. (2019). Global modeling of nature's contributions to people. *Science* 366, 255–258. doi:10.1126/science.aaw3372

Chen, J. Y., Jiang, B., Bai, Y., Xu, X. B., and Alatalo, J. M. (2019). Quantifying ecosystem services supply and demand shortfalls and mismatches for management optimisation. *Sci. Total Environ.* 650, 1426–1439. doi:10.1016/j.scitotenv.2018.09.126

Chiabai, A., Quiroga, S., Martinez-Juarez, P., Higgins, S., and Taylor, T. (2018). The nexus between climate change, ecosystem services and human health: Towards a conceptual framework. *Sci. Total Environ.* 635, 1191–1204. doi:10.1016/j.scitotenv.2018.03.323

Costanza, R., Arge, R., De Groot, R., Farber, S., Hannon, B., Limburg, K., et al. (1997). The value of the world's ecosystem services and natural capital. *Nature* 387, 253–260. doi:10.1038/387253a0

Costanza, R., de Groot, R., Braat, L., Kubiszewski, I., Fioramonti, L., Sutton, P., et al. (2017). Twenty years of ecosystem services: How far have we come and how far do we still need to go? *Ecosyst. Serv.* 28, 1–16. doi:10.1016/j.ecoser.2017.09.008

Cruz-Garcia, G., Sachet, E., Blundo-Canto, G., Vanegas, M., and Quintero, M. (2017). To what extent have the links between ecosystem services and human well-being been researched in Africa, Asia, and Latin America? *Ecosyst. Serv.* 25, 201–212. doi:10.1016/j.ecoser.2017.04.005

Cui, F. Q., Tang, H. P., Zhang, Q., Wang, B. J., and Dai, L. W. (2019). Integrating ecosystem services supply and demand into optimized management at different scales: A case study in hulunbuir, China. *Ecosyst. Serv.* 39, 100984. doi:10.1016/j.ecoser.2019.100984

Cumming, G. S., and Cramon-Taubadel, S. V. (2018). Linking economic growth pathways and environmental sustainability by understanding development as alternate social–ecological regimes. *Proc. Natl. Acad. Sci. U. S. A.* 115, 9533–9538. doi:10.1073/pnas.1807026115

Daily, G. C., Polasky, S., Goldstein, J., Kareiva, P. M., Mooney, H. A., Pejchar, L., et al. (2009). Ecosystem services in decision making: Time to deliver. *Front. Ecol. Environ.* 7, 21–28. doi:10.1890/080025 de Groot, R. S., Alkemade, R., Braat, L., Hein, L., and Willemen, L. (2010). Challenges in integrating the concept of ecosystem services and values in landscape planning, management and decision making. *Ecol. Complex.* 7, 260–272. doi:10.1016/j.ecocom.2009.10.006

Delphin, S., Escobedo, F. J., Abd-Elrahman, A., and Cropper, W. P. (2016). Urbanization as a land use change driver of forest ecosystem services. *Land Use Policy* 54, 188–199. doi:10.1016/j.landusepol.2016.02.006

Deng, C. X., Liu, J. Y., Liu, Y. J., Li, Z. W., Nie, X. D., Hu, X. Q., et al. (2021). Spatiotemporal dislocation of urbanization and ecological construction increased the ecosystem service supply and demand imbalance. *J. Environ. Manag.* 288, 112478. doi:10.1016/j.jenvman.2021.112478

Fotheringham, A. S., Yang, W. B., and Kang, W. (2017). Multiscale geographically weighted regression (mgwr). *Ann. Am. Assoc. Geogr.* 107, 1247–1265. doi:10.1080/24694452.2017.1352480

Fu, B. P. (1981). On the calculation of the evaporation from land surface (in Chinese). *Chin. J. Atmos. Sci.* 5, 23–31.

González-García, A., Palomo, I., González, J. A., López, C. A., and Montes, C. (2020). Quantifying spatial supply-demand mismatches in ecosystem services provides insights for land-use planning. *Land Use Policy* 94, 104493. doi:10.1016/j.landusepol.2020.104493

Hebei Municipal Bureau Statistics (2015). *hebei.gov*. Available online: http://tjj.hebei.gov.cn/hetj/tjsj/ (Accessed on July 6, 2021).

Kareiva, P., Tallis, H., Ricketts, T. H., Daily, G. C., and Polasky, S. (2011). *Natural capital: Theory and practice of mapping ecosystem services*. 1st ed. Oxford, UK: Oxford University, 3–128.

Kehoe, P., and Rhodes, S. (2013). Pushing the conservation envelope through the use of alternate water sources. *J. Am. Water Works Assoc.* 105, 46–50. doi:10.5942/jawwa.2013.105.0026

Larondelle, N., and Lauf, S. (2016). Balancing demand and supply of multiple urban ecosystem services on different spatial scales. *Ecosyst. Serv.* 22, 18–31. doi:10.1016/j.ecoser.2016.09.008

Legendre, P., and Legendre, L. F. (2012). "Multiscale analysis: Spatial eigenfunctions," in *Numerical ecology*. Editors P. Legendre and L. F. Legendre. 2nd ed. (Amsterdam, Netherlands: Elsevier), Vol. 24, 859–906.

Legendre, P., Oksanen, J., and ter Braak, C. J. F. (2011). Testing the significance of canonical axes in redundancy analysis. *Methods Ecol. Evol.* 2, 269–277. doi:10.1111/j.2041-210x.2010.00078.x

Li, D., Wu, S., Liu, L., Liang, Z., and Li, S. (2017). Evaluating regional water security through a freshwater ecosystem service flow model: A case study in beijing-tianjian-hebei region, China. *Ecol. Indic.* 81, 159–170. doi:10.1016/j.ecolind.2017.05.034

Li, J., Zhang, C., and Zhu, S. (2021). Relative contributions of climate and land-use change to ecosystem services in arid inland basins. *J. Clean. Prod.* 298, 126844. doi:10.1016/j.jclepro.2021.126844

Li, Z. Z., Cheng, X. Q., and Han, H. R. (2020). Future impacts of land use change on ecosystem services under different scenarios in the ecological conservation area, beijing, China. *Forests* 11, 584. doi:10.3390/f11050584

Liu, L., Liu, C., Wang, C., and Li, P. (2019). Supply and demand matching of ecosystem services in loess hilly region: A case study of lanzhou. *Acta Geogr. Sin.* 74, 1921–1937.

Mehring, M., Ott, E., and Hummel, D. (2018). Ecosystem services supply and demand assessment: Why social-ecological dynamics matter. *Ecosyst. Serv.* 30, 124–125. doi:10.1016/j.ecoser.2018.02.009

Minin, E. D., Soutullo, A., Bartesaghi, L., Rios, M., Szephegyi, M. N., and Moilanen, A. (2017). Integrating biodiversity, ecosystem services and socio-economic data to identify priority areas and landowners for conservation actions at the national scale. *Biol. Conserv.* 206, 56–64. doi:10.1016/j.biocon.2016.11.037

Ministry of Natural and Resources of R.P.C (MNRC) (2021). *Current land use classification*. GB/T21010-2017. Available online (Accessed on June 8, 2021).

Mooney, H., Larigauderie, A., Cesario, M., Elmquist, T., Hoegh-Guldberg, O., Lavorel, S., et al. (2009). Biodiversity, climate change, and ecosystem services. *Curr. Opin. Environ. Sustain.* 1, 46–54. doi:10.1016/j.cosust.2009.07.006

Mouchet, M. A., Lamarque, P., Martı´n-Lo´pez, B., Crouzat, E., Gos, P., Byczek, C., et al. (2014). An interdisciplinary methodological guide for quantifying associations between ecosystem services. *Glob. Environ. Change* 28, 298–308. doi:10.1016/j.gloenvcha.2014.07.012

Nelson, E. J., Kareiva, P., Ruckelshaus, M., Arkema, K., Geller, G., Girvetz, E., et al. (2013). Climate change's impact on key ecosystem services and the human well-being they support in the US. *Front. Ecol. Environ.* 11, 483–893. doi:10.1890/120312

Nelson, E., Mendoza, G., Regetz, J., Polasky, S., Tallis, H., Cameron, D. R., et al. (2009). Modeling multiple ecosystem services, biodiversity conservation, commodity production, and tradeoffs at landscape scales. *Front. Ecol. Environ.* 7, 4–11. doi:10.1890/080023

Onaindia, M., de Manuel, M. I., Madariaga, I., and Rodríguez-Loinaz, G. (2013). Co-benefits and trade-offs between biodiversity, carbon storage and water flow regulation. *For. Ecol. Manag.* 289, 1–9. doi:10.1016/j.foreco.2012.10.010

Ou, W. X., Wang, H. N., and Tao, Y. (2018). A land cover-based assessment of ecosystem services supply and demand dynamics in the Yangtze River Delta region. *Acta eco. Sin.* 38, 6337e6347. (In Chinese). doi:10.5846/stxb201707061225

Ouyang, Z., Fan, P., and Chen, J. (2016). Urban built-up areas in transitional economies of southeast asia: Spatial extent and dynamics. *Remote Sens.* 8, 819. doi:10.3390/rs8100819

Peng, J., Tian, L., Liu, Y., Zhao, M., Hu, Y., and Wu, J. (2017). Ecosystem services response to urbanization in metropolitan areas: Thresholds identification. *Sci. Total Environ.* 607-608, 706–714. doi:10.1016/j.scitotenv.2017.06.218

Peng, J., Wang, X., Liu, Y., Zhao, Y., Xu, Z. H., Zhao, M. Y., et al. (2020). Urbanization impact on the supply-demand budget of ecosystem services: Decoupling analysis. *Ecosyst. Serv.* 44, 101139. doi:10.1016/j.ecoser.2020.101139

Rao, Y., Zhou, M., Ou, G., Dai, D., Zhang, L., Zhang, Z., et al. (2018). Integrating ecosystem services value for sustainable land-use management in semi-arid region. *J. Clean. Prod.* 186, 662–672. doi:10.1016/j.jclepro.2018.03.119

Sannigrahi, S., Zhang, Q., Pilla, F., Joshi, P. K., Basu, B., Keesstra, S., et al. (2020). Responses of ecosystem services to natural and anthropogenic forcings: A spatial regression based assessment in the world's largest mangrove ecosystem. *Sci. Total Environ.* 715, 137004. doi:10.1016/j.scitotenv.2020.137004

Schirpke, U., Candiago, S., Egarter Vigl, L., Jäger, H., Labadini, A., Marsoner, T., et al. (2019). Integrating supply, flow and demand to enhance the understanding of interactions among multiple ecosystem servicesow and demand to enhance the understanding of interactions among multiple ecosystem services. *Sci. Total Environ.* 651, 928–941. doi:10.1016/j.scitotenv.2018.09.235

Schmidt, K., Martín-López, B., Phillips, P. M., Julius, E., Makan, N., and Walz, A. (2019). Key landscape features in the provision of ecosystem services: Insights for management. *Land Use Policy* 82, 353–366. doi:10.1016/j.landusepol.2018.12.022

Sharp, R., Tallis, H. T., Ricketts, T., Guerry, A. D., Wood, S. A., Chaplin-Kramer, R., et al. (2020). *InVEST 3.8.0 user's guide. The natural capital project*. Stanford University, University of Minnesota. The Nature Conservancy, and World Wildlife FundAvailable online: http://releases.naturalcapitalproject.org/invest-userguide/latest/#supporting-tools.

Shen, J., Li, S., Liang, Z., Liu, L., Li, D., and Wu, S. (2020). Exploring the heterogeneity and nonlinearity of trade-offs and synergies among ecosystem services bundles in the Beijing-Tianjin-Hebei urban agglomeration. *Ecosyst. Serv.* 43, 101103. doi:10.1016/j.ecoser.2020.101103

Šmilauer, P., and Lepš, J. (2014). *Multivariate analysis of ecological data using Canoco 5*. 2nd ed. Cambridge, UK: Cambridge University, 15–38.

Sun, X., Tang, H., Yang, P., Hu, G., Liu, Z. H., and Wu, J. G. (2019). Spatiotemporal patterns and drivers of ecosystem service supply and demand across the conterminous United States: A multiscale analysis. *Sci. Total Environ.* 703, 135005. doi:10.1016/j.scitotenv.2019.135005

Syrbe, R. U., and Walz, U. (2012). Spatial indicators for the assessment of ecosystem services: Providing, benefiting and connecting areas and landscape metrics. *Ecol. Indic.* 21, 80–88. doi:10.1016/j.ecolind.2012.02.013

Tallis, H., and Polasky, S. (2009). Mapping and valuing ecosystem services as an approach for conservation and natural-resource management. *Ann. N. Y. Acad. Sci.* 1162, 265–283. doi:10.1111/j.1749-6632.2009.04152.x

Tang, H. J., and Li, Z. M. (2012). Study on per capita grain demand based on Chinese reasonable dietary pattern. *Sci. Agric. Sin.* 45, 2315–2327.

The Common International Classification of Ecosystem Services (2021). *cices.eu*. Available online: https://cices.eu/resources/ (accessed on March 6, 2021).

Tianjin Municipal Bureau Statistics (2015). *State council information*. Available online: http://stats.tj.gov.cn/ (Accessed on July 9, 2021).

Verhagen, W., Kukkala, A. S., Moilanen, A., van Teeffelen, A. J. A., and Verburg, P. H. (2017). Use of demand for and spatial flow of ecosystem services to identify priority areas. *Conserv. Biol.* 31, 860–871. doi:10.1111/cobi.12872

Wang, J. F., Li, X. H., Christakos, G., Liao, Y. L., Zhang, T., Gu, X., et al. (2010). Geographical detectors-based health risk assessment and its application in the neural tube defects study of the Heshun region, China. *Int. J. Geogr. Inf. Sci.* 24, 107–127. doi:10.1080/13658810802443457

Wang, J. F., Zhang, T. L., and Fu, B. J. (2016). A measure of spatial stratified heterogeneity. *Ecol. Indic.* 67, 250–256. doi:10.1016/j.ecolind.2016.02.052

Wei, H., Fan, W., Wang, X., Lu, N., Dong, X., Zhao, Y., et al. (2017). Integrating supply and social demand in ecosystem services assessment: A review. *Ecosyst. Serv.* 25, 15–27. doi:10.1016/j.ecoser.2017.03.017

Wilkerson, M. L., Mitchell, M. G. E., Shanahan, D., Wilson, K. A., Ives, C. D., Lovelock, C. E., et al. (2018). The role of socio-economic factors in planning and managing urban ecosystem services. *Ecosyst. Serv.* 31, 102–110. doi:10.1016/j.ecoser.2018.02.017

Wu, A., Zhao, Y., Shen, H., Qin, Y., and Liu, X. (2018). Spatio-temporal pattern evolution of ecosystem service supply and demand in beijing-tianjin-hebei region. *J. Ecol. Rural Environ.* 34, 968–975. (In Chinese).

Xu, Q., Yang, R., Zhuang, D., and Lu, Z. L. (2021). Spatial gradient differences of ecosystem services supply and demand in the Pearl River Delta region. *J. Clean. Prod.* 279, 123849. doi:10.1016/j.jclepro.2020.123849

Yahdjian, L., Sala, O. E., and Havstad, K. M. (2015). Rangeland ecosystem services: Shifting focus from supply to reconciling supply and demand. *Front. Ecol. Environ.* 13, 44–51. doi:10.1890/140156

Yang, Y., Zheng, H., Kong, L., Huang, B., Xu, W., and Ouyang, Z. (2019). Mapping ecosystem services bundles to detect high- and low-value ecosystem services areas for land use management. *J. Clean. Prod.* 225, 11–17. doi:10.1016/j.jclepro.2019.03.242

Yu, H. J., Xie, W., Sun, L., and Wang, Y. T. (2021). Identifying the regional disparities of ecosystem services from a supply-demand perspective. *Resour. Conservation Recycl.* 169, 105557. doi:10.1016/j.resconrec.2021.105557

Zhang, D., Huang, Q., He, C., and Wu, J. (2017). Impacts of urban expansion on ecosystem services in the beijing-tianjin-hebei urban agglomeration, China: A scenario analysis based on the shared socioeconomic pathways. *Resour. Conservation Recycl.* 125, 115–130. doi:10.1016/j.resconrec.2017.06.003

Zhang, L., Hickel, K., Dawes, W. R., Chiew, F. H. S., Western, A. W., and Briggs, P. R. (2004). A rational function approach for estimating mean annual evapotranspiration. *Water Resour. Res.* 40, 2. doi:10.1029/2003wr002710

Zhang, Z., Peng, J., Xu, Z. H., Wang, X. Y., and Meersmans, J. (2021). *Ecosystem services supply and demand response to urbanization: A case study of the pearl river delta*, 49. China: Ecosystem Services, 101274.

Zuur, A. F., Ieno, E. N., Walker, N. J., Saveliev, A. A., and Smith, G. (2009). *Mixed effects models and extensions in ecology with R*. 1st ed. New York, USA: Springer, 323–341.

frontiers | Frontiers in Environmental Science

TYPE Original Research
PUBLISHED 10 October 2022
DOI 10.3389/fenvs.2022.972394

Check for updates

OPEN ACCESS

EDITED BY
Irene Petrosillo,
University of Salento, Italy

REVIEWED BY
Rana Singh,
Babasaheb Bhimrao Ambedkar University, India
Thiru Selvan,
Tripura University, India

*CORRESPONDENCE
Meraj A. Ansari,
merajiari@gmail.com
Natesan Ravisankar,
n.ravisankar@icar.gov.in

SPECIALTY SECTION
This article was submitted to Land Use Dynamics,
a section of the journal
Frontiers in Environmental Science

RECEIVED 18 June 2022
ACCEPTED 20 September 2022
PUBLISHED 10 October 2022

CITATION
Panwar AS, Ansari MA, Ravisankar N, Babu S, Prusty AK, Ghasal PC, Choudhary J, Shamim M, Singh R, Raghavendra KJ, Dutta D, Meena AL, Chauhan GV, Ansari MH, Singh R, Aulakh CS, Singh DK and Sharma PB (2022), Effect of organic farming on the restoration of soil quality, ecosystem services, and productivity in rice–wheat agro-ecosystems.
Front. Environ. Sci. 10:972394.
doi: 10.3389/fenvs.2022.972394

Effect of organic farming on the restoration of soil quality, ecosystem services, and productivity in rice–wheat agro-ecosystems

Azad S. Panwar[1], Meraj A. Ansari[1]*, Natesan Ravisankar[1]*, Subhash Babu[2], Ashisa K. Prusty[1], Prakash C. Ghasal[1], Jairam Choudhary[1], Mohammad Shamim[1], Raghuveer Singh[1], K. J. Raghavendra[1], Debashis Dutta[1], Amrit L. Meena[1], Gautam V. Chauhan[1], Majhrool H. Ansari[3], Raghavendra Singh[4], C. S. Aulakh[5], D. K. Singh[6] and P. B. Sharma[7]

[1]ICAR-Indian Institute of Farming System Research, Meerut, India, [2]ICAR-Indian Agricultural Research Institute, Pusa, New Delhi, India, [3]Faculty of Agricultural Sciences, AMU, Aligarh, India, [4]ICAR-Indian Institute of Pulses Research, Kanpur, India, [5]AINP-OF, Punjab Agricultural University, Ludhiana, India, [6]AINP-OF, GB Pant University of Agriculture and Technology, Pantnagar, India, [7]AINP-OF, Jawaharlal Nehru University of Agriculture and Technology, Jabalpur, India

Excess use of hazardous agrochemicals and inorganic fertilizers resulted negative impact on environmental outcomes and degraded soil function, biological diversity, and ecosystem services. A 15-year long-term (2004–05 to 2017–18) field experiment was conducted to improve the ecosystem services with soil quality restoration and stabilization of yield through agronomic manipulation in the rice (*Oryza sativa*)–wheat (*Triticum aestivum*) system under Indo-Gangetic Plains (IGP). Three crop management practices (i) organic crop management, (ii) inorganic crop management, and (iii) integrated crop management were evaluated at four locations (i) Jabalpur, (ii) Ludhiana, (iii) Pantnagar, and (iv) Modipuram in a factorial randomized block design and replicated thrice at each location. Among the spatial variation, the highest soil quality indicators like soil microbial biomass carbon (0.52 mg g^{-1}), fungal (46.2 CFU × 10^4 CFU), bacterial (54.2 CFU × 10^6 CFU), and actinomycetes viable cells (23.0 CFU × 10^6 CFU), and nutrients (available N and available P) were observed at Pantnagar than other location. The soil *p*H varied from 7.2 to 8.3, and the lowest bulk density (ρb) was recorded at Jabalpur and Modipuram. Subsequently, higher system productivity (8,196.7 kg ha^{-1}) and net returns were obtained in Pantnagar > Ludhiana, and it was 44.1–63.4% higher than in Modipuram and Jabalpur. Among the crop management, organic crop management significantly improved ($p < 0.05$) ρb, soil organic carbon, available N, available P, and available K by 3.7%, 33.3%, 16.4%, 37.8%, and 20.3% over inorganic crop management, respectively. Similarly, the highest bacterial, fungal, and actinomycetes viable cell counts were found under the organic plots, followed by integrated plots. In terms of productivity, integrated crop management (ICM) had increased the system productivity by 4.7%–6.7%

and net returns by 22.2% and 23.5% over inorganic and organic crop management. Similarly, the highest sustainability yield index (SYI) was recorded in integrated crop management (0.77) as compared to inorganic (0.74) and organic management (0.75). The soil quality index was estimated as 0.60, 0.53, and 0.54 in organic, inorganic, and ICM, respectively. Hence, the study indicated that the application of organic amendments under organic or integrated crop management improves the system's resiliency and sustainability. Therefore, the study concludes that towards organic approach (integrated application of organic amendments with a gradual reduction in mineral fertilizers) is better suitable for keeping the rice–wheat system productivity and sustainable in the long term.

KEYWORDS

crop management, soil quality and health, system productivity, economics, ecosystem services (ES), yield sustainability

1 Introduction

The Green Revolution's (GR) future is centered on technologies that ensure food security for the burgeoning population without harming the environment (Phillips, 2014). The glory of GR in India was based on the use of high-yielding varieties (HYVs), chemical fertilizers, pesticides, and farm mechanization that led to unprecedented pressure on our natural resource base, including the natural way of controlling pests and diseases (Tripathi et al., 2020). Land degradation is primarily caused by an over-reliance on agrochemicals in agri-food production systems, which has accelerated the loss of regulating and supporting ecosystem services and deteriorated environmental sustainability (Suárez et al., 2021), making it more difficult to achieve sustainable development goals (SDGs). Indiscriminate use of inorganic fertilizers and chemicals also polluted the groundwater resources, contributing to land degradation and unsustainable farming in the long term (Panwar et al., 2021). An intensive cropping system without nature-oriented crop management and a lack of nutrient recycling through crop biomass enhanced nutrient mining and deteriorated the soil health, as well as daunted the physical, chemical, and biological properties of soil (Yadav et al., 2021; Ansari et al., 2022b). In India, 97.85 m ha (29.7%) of the total geographical area underwent land degradation in one or other forms due to conventional farming practices (Sengupta, 2021). The survey conducted by the National Sample Survey Organization (NSSO, 2013) indicates that the dependency of farmers on seeds, fertilizers, and pesticides from outside farms makes farming costlier. However, maintaining soil fertility has become a major concern in India. To ensure sustainable food security and reduce the environmental cost of agriculture, soil health management is critical. Utilizing organic manures, green manuring, and crop residue recycling is necessary to simultaneously improve the regulating, supporting, and provisioning ecosystem services in order to increase the effectiveness of chemical fertilizers and to improve crop responsiveness to the applied fertilizers. Under integrated crop management, the combination of synthetic and natural inputs was tested where in addition of organic inputs helps increase the use efficiency of synthetic inputs due to the betterment of soil physical properties and thereby water retention and absorption. This integrated crop management (ICM) practice involving integrated nutrient, weed, pest, and water management can also be referred to as toward organic approach where a successive reduction in the chemical inputs such as mineral fertilizers and pesticides is possible.

Organic crop management is more of a description of the nature-oriented agricultural practices used on a farm, and these methods combine tradition, innovation, and science. Organic crop management, in simple terms, requires a shift from intensive use of synthetic chemical fertilizers, insecticides, fungicides, herbicides, plant growth regulators (PGRs), and genetically engineered plants to extensive use of animal manures, beneficial soil microbes, bio-pesticides, bio-agents, and indigenous technological knowledge, based on scientific principles of agricultural systems (Ravisankar et al., 2021, 2022). With the increasing awareness about the safety and quality of foods, long-term sustainability of the system, and accumulating evidence of being equally productive, the integrated and organic crop management approach has emerged as an alternative system of farming that addresses little towards the sustainable development goals (SDGs) *viz.* good health and well-being (SDG–3), clean water and sanitation (SDG–6), affordable and clean energy (SDG–7), responsible consumption and production (SDG–12), climate action (SDG–13), life below water (SDG–14), and life on land (SDG–15) toward achieving sustainability and ensuring profitable livelihood option. According to Bhattacharya and Chakraborty (2005), integrating organic and inorganic agriculture would be the optimal approach after observing a number of issues with conventional farming in India. Based on their results, the industrial nitrogen fixation (INF) is 40 mt year^{-1} which accounts for only 15.3% of total nitrogen fixation. On the other hand, the quantity of biological nitrogen fixation (BNF) is 175 mt annum^{-1} contributing to 67.3% of the total amount. The plant also uses nutrients from organic sources through mineralization, and billions of microorganisms are available in the soil for this job. India is endowed with various types of naturally available organic forms of nutrients in different parts of the country and which will help for organic crop management.

Globally, cereal-based systems share 74% in terms of providing calories. Rice–wheat is a major cereal system in India and is being practiced in about ~13.5 m ha (Mahajan and Gupta, 2009), but there is a temporal decline in the response of nutrients, and across the systems, it has been observed that the response of 13.4 kg yield kg^{-1} of NPK in 1960 has come down to 2.7 kg kg^{-1} (Gangwar et al., 2013). The Intergovernmental Panel on Climate Change (IPCC) realized that agriculture as it is practiced today (conventional agriculture, modern agriculture, or GR agriculture) accounts for about one-fifth of the anthropogenic greenhouse effect and generates roughly 50% and 70% of all anthropogenic methane and nitrogen oxide emissions, respectively (Charyulu and Biswas, 2010; Yadav et al., 2020).

Therefore, soil quality stabilization has emerged as a major challenge to sustain soil fertility with agronomic manipulation of crop management practices (Ansari et al., 2022b). Legumes used as green manuring are quickly decomposable and have the added benefit of fixing atmospheric nitrogen. Fast-growing legumes with high nitrogen-fixing prolificacy, such as *Sesbania* green manuring, can be included in rice–wheat cropping systems as sustainable alternative nutrient management and for restoring soil land productive capacity (Meena et al., 2018). After growing green manure crops or incorporating them, crop productivity is improved by nutrient pumping from deeper soil horizons to the furrow soil layer (Stagnari et al., 2017). *Sesbania* green manure crops have the ability of quick growth, deep roots, strong nitrogen fixation, and little lignin, which is effective at recycling nutrients (Dwivedi et al., 2017). The probability of incorporating *Sesbania* green manures into the system increased as a result of the stabilization of soil quality becoming necessary when nutrient imbalances and nutrient mining increased due to inadequate sustainable management practices. The absence of legumes in the cereal-based system would diminish the potential niche that is accessible in these cropping systems. As a result of the enhancement of soil's biological, physical, and chemical properties, biomass recycling has become crucial to control and sustain soil quality.

Sustainable crop management approaches can improve soil carbon storage, nitrogen availability, biological features of soil, and yield stability. Restoration of soil organic C and maintenance of agronomic productivity are difficult due to inadequate soil and crop management practices (Ansari et al., 2022a). Organic manure and green manure are employed to improve and sustain soil organic carbon (SOC), soil biological activity, soil microbial diversity, and chemical characteristics throughout (Yuan and Yue, 2012). However, using organic manure and growing fast with high nitrogen-fixing fecundity as green manure in cereal-based cropping systems has been deemed a viable and long-term solution for restoring soil fertility and system productivity (Yadav et al., 2021). *Sesbania*, as fast-growing, deep-rooted, high nitrogen-fixing, and low lignin-containing crops, are effective in capturing and recycling nutrients (Meena et al., 2018).

Thus, modern agriculture is more marketized and has both advantages and disadvantages. Meeting the SDGs by 2030 is very important, and the agriculture sector will play a vital role in achieving the same. The government of India is implementing National Mission on Sustainable Agriculture involving integrated and organic management approaches covering all the states and union territories (Panwar et al., 2020). India is the largest country in terms of the number of organic producers worldwide and the ninth largest country in terms of the total amount of arable land used for organic farming. The Sikkim state of India has been brought under complete organic certification and production since 2016 (Aulakh and Ravisankar, 2017). By March 2021, 2.66 million hectares of land had been converted to organic farming and was third-party certified, while 0.73 million ha was brought under the Participatory Guarantee System (PGS) of certification. At the moment, about 2.4 percent of the net cultivated land is either under-certified or transitioning to organic farming. In the past 6 years, the area under organic farming has grown at an annual growth rate of 22% (Ravisankar et al., 2021). A better option for national food security, higher household income, and climate resilience is the "toward organic" (integrated crop management) approach for input-intensive areas (food hubs) and the "certified organic" approach by integrating tradition, innovation, and science in the *de facto* organic areas (hill and rainfed/dryland regions), which will further enhance safe food production and meet the social values. Continuous practice of raising the crops organically shows good potential to sequester C (up to 63% higher C stock in 10 years), higher soil organic carbon (22% increase in 6 years), reduction in energy requirement (by about 10%–15%), and increase in water-holding capacity (by 15%–20%), thereby promoting climate resilience farming and addressing SDGs (Sharma et al., 2021).

However, systematic research on agronomic manipulation of crop management coupled with green manuring in the rice–wheat system under different agroecosystems was evaluated to find the changes in soil quality, microbial diversity, ecosystem services, and yield sustainability. Therefore, a field experiment was executed for 15 successive years (2004–05 to 2017–18) at Jabalpur (Madhya Pradesh), Ludhiana (Punjab), Pantnagar (Uttarakhand), and Modipuram (Uttar Pradesh) under the All India Network Programme on Organic Farming (flagship program of the Indian Council of Agricultural Research) to assess the effect of agronomic manipulation on soil quality, ecosystem services, and productivity in the rice–wheat system. The sites represent the various agro-ecosystems in which the rice–wheat cropping system is practiced. Findings from the study will aid in the development and implementation of appropriate agronomic management practices and policies in the rice–wheat system in Indo-Gangetic Plains.

2 Materials and methods

2.1 Description of the site, soil characteristics, and weather

This study was conducted on a research farm at four locations *viz.* ICAR-Indian Institute of Farming Systems Research, Modipuram (29.84′°N, 77.46′°E), Uttar Pradesh; Punjab Agricultural University, Ludhiana (24.35′°N, 74.42′°E), Punjab; GB Pant University of Agriculture and Technology, Pantnagar (29.00′°N, 79.30′°E),Uttarakhand; and Jawaharlal Nehru Krishi Vishwavidyalaya, Jabalpur (24.30′°N, 80.15′°E), Madhya Pradesh. The experimental site is presented in Figure 1. The experimental sites of Modipuram and Pantnagar are representing the part of the Upper Gangetic Plain region, having sandy loam texture soil (52.5% sand, 30.9% clay, and 16.6% silt) of Gangetic alluvial origin, very deep (> 20 m), well-drained, and with flat (1% slope) topography. Similarly, the sites of Ludhiana and Jabalpur are part of the Trans-Gangetic Plain region and Central Plateau and Hill region, respectively. Initial soil parameters for all the locations were (0 cm–15 cm depth) analyzed at the onset of the experiment and are presented in Supplementary Table S1. According to Köppen's climate classification, the sites of Modipuram, Ludhiana, and Pantnagar are humid subtropical. However, the climate of Jabalpur is classified as Mediterranean with hot summer. The average annual minimum temperature of Jabalpur, Ludhiana, Pantnagar, and Modipuram varied from 6.0°C to 19.6°C, 16.9°C to 18.6°C, 11.5°C to 20.1°C, and 16.2°C to 23°C, and the maximum temperature varied from 27.8°C to 40.0°C, 29.3°C to 30.6°C, 27.2°C to 31.9°C, and 29.9°C to 37.8°C, respectively. Similarly, the total annual rainfall during the study period (2004–05 to 2017–18) varied from 1,038.0 mm annum^{-1} to 1857.9 mm annum^{-1}, 505.1 mm annum^{-1} to 1,248.4 mm annum^{-1}, 844.6 mm annum^{-1} to 2,247.6 mm annum^{-1}, and 244.8 mm annum^{-1} to 1,012.2 mm annum^{-1}, respectively. Around 75% of this is received through the southwest monsoon during July–September. The year-wise weather data are presented in Figure 2. The soil of all the experimental sites was neutral to mild alkaline and non-saline conditions.

2.2 Treatment detail

Long-term field experiments were conducted under the All India Network Programme on Organic Farming (AINP–OF) for successive fifteen years during 2004–05 to 2017–18 in rice–wheat cropping systems under various agro-ecosystems. The field experiment was conducted at four locations, namely, Jabalpur, Pantnagar, Ludhiana, and Modipuram, under the Upper, Trans Indo-Gangetic Plains (IGP), and Central Plateau regions. At all the locations, a field experiment was conducted under three crop management practices (i) organic crop management, (ii) inorganic crop management, and (iii) integrated crop management, which were evaluated in larger plots of 150 m^2. The treatment-wise crop management practices are presented in Supplementary Table S2. National Standards for Organic Production (NSOP) were followed under organic management while choosing the inputs for application. In the present investigation, soil quality parameters of rice–wheat cropping systems were studied from Modipuram, Ludhiana, Pantnagar, and Jabalpur locations.

2.3 Crop management

The rice field was ploughed twice by a disc harrow, puddled twice by a puddler in standing water (5 –7 cm), and leveled. Under organic crop management, 7.84 t ha^{-1} farm yard manure (FYM), 3.13 t ha^{-1} vermicompost, and 853 kg non-edible oilcake (neem cake) were added at final field preparation. Under inorganic crop management, 26.2 kg P ha^{-1} through DAP, 50 kg K ha^{-1} through muriate of potash, and 29.2 kg N ha^{-1} through urea (46% N) were added at the time of final puddling. The remaining 80 kg N ha^{-1} was

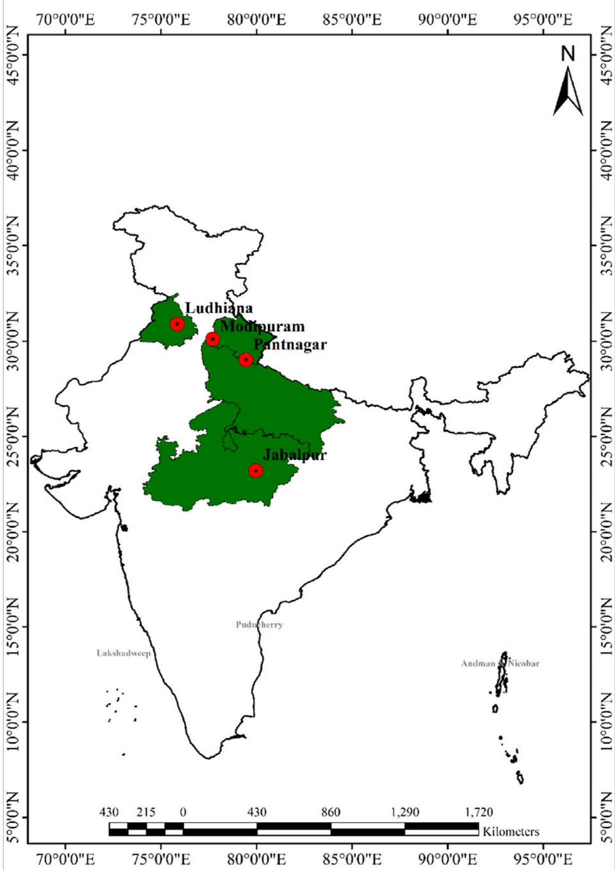

FIGURE 1
Location of the experimental sites.

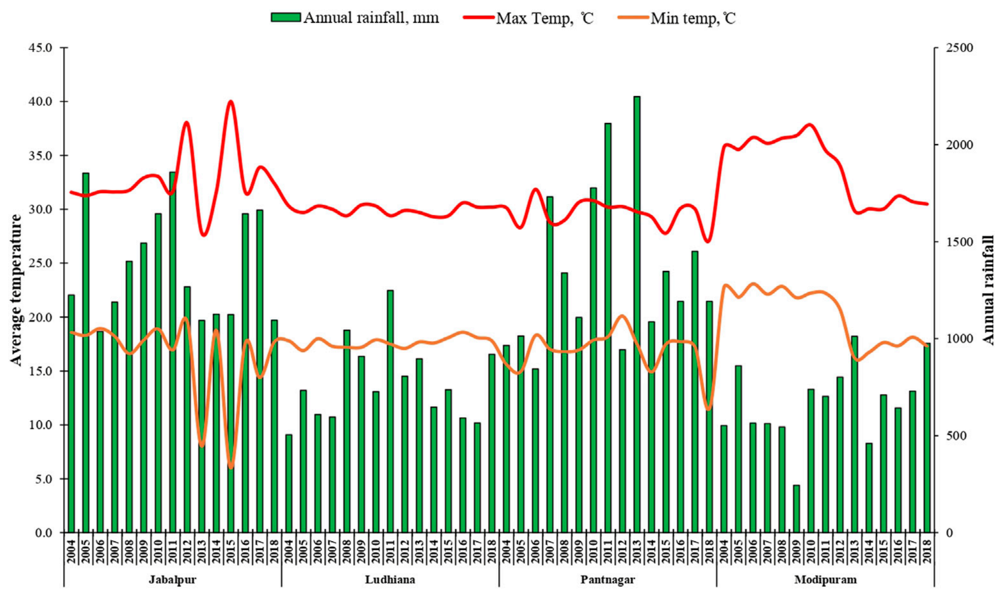

FIGURE 2
Weather data on the experimental site.

top-dressed in two equal splits at 20 days after transplanting (DAT) and 45 DAT. Similarly, under integrated crop management treatment (ICM), 5.88 t ha^{-1} FYM, 2.34 Mg ha^{-1} vermicompost, 13.1 kg P ha^{-1} through DAP, and 25 kg K ha^{-1} through muriate of potash were added during the final puddling. Nitrogen at 55 kg ha^{-1} through urea was top-dressed in two equal splits at 20 DAT and 45 DAT. 25-day-old seedlings of rice cv. Pusa Basmati–1 (Modipuram), Punjab Basmati-3 (Ludhiana), Pusa Basmati-1 (Pantnagar), and Pusa Basmati–1 (Jabalpur) at 20 cm × 15 cm spacing (2 seedlings $hill^{-1}$) were transplanted during the first fortnight of July. In wheat, organic manure (FYM, vermicompost, and oilcake) and chemical fertilizers for P and K were basally applied at the time of field preparation in respective treatments. Top dressing of N at 80 kg ha^{-1} and 55 kg ha^{-1} in two equal splits was performed at 21 days after sowing (DAS) and 45 DAS. Wheat cv HI 8713 (Modipuram), PBW–725 (Ludhiana), UP–2572 (Pantnagar), and MPO–1106 (Jabalpur) were sown at 22.5 cm row spacing using at 100 kg ha^{-1} seed rate during the third week of November. In rice and wheat, weeds were managed by two-hand weeding at 25 and 50 DAT/DAS. The rice and wheat crops were harvested in the second fortnight of October and the second fortnight of April, respectively. The crops were raised as per the recommended standard package of practices.

2.4 Soil sampling and analysis

Soil samples were collected at the initial stage and analyzed for initial soil properties in 2004–05 from 0 to 15 cm soil depth. After completion of 15 successive rice–wheat cycles in 2017–18 at Jabalpur, Ludhiana, Pantnagar, and Modipuram under each treatment (organic, inorganic, and integrated crop management), soil bulk density (ρb) was determined *in situ* using the core method (5.15 cm height and 4.7 cm diameter) after oven drying at 105°C ± 1°C (Blake and Hartge, 1986). Soil *p*H was determined using a 1:2.5 soil:water suspension (pH meter; Eutech pH 700-Eutech Instruments, Singapore). The available N (AvN) was determined using the $KMnO_4$ oxidation method (Subbiah and Asija, 1956), and the SOC content was determined using the $K_2Cr_2O_7$ wet oxidation method (Walkley and Black, 1934). The available P (AvP) was extracted using the Olsen and Sommers method (Olsen and Sommers, 1982). The available K (AvK) of NH_4OAc was determined using a flame photometer (ESICO-1382, India).

Soil samples from 0 to 15 cm depth were collected after last harvest (2018) from different crop management plots in four locations, namely, Jabalpur (Madhya Pradesh), Ludhiana (Punjab), Pantnagar (Uttarakhand), and Modipuram (Uttar Pradesh), to study the effect of different crop management practices on the soil microbial population. The total viable count of bacteria, fungi, and actinomycetes was estimated by serial dilution and plating methods. Nutrient agar (NA), Martin's Rose Bengal agar (MRBA), and Kenknight and Munaier's medium (KM) were used for bacteria, fungi, and actinomycetes, respectively. The plates of NA and MRBA were kept at 28°C ± 2°C and KM media plates at 35°C. The viable counts were taken after 24 h, 48 h, and 120 h for bacteria, fungi, and actinomycetes, respectively. The microbial biomass carbon was estimated by the fumigation extraction method given by Vance et al. (1987).

2.5 Soil quality index

The soil quality index (SQI) was calculated by using the approach given by Banerjee et al. (2015). To summarize, all of the soil indicators studied (soil *p*H, ρb, SOC, MBC, AvN, AvP, AvK, fungi, bacteria, and actinomycetes) were treated with principal component analysis (PCA) to reduce dimensionality while maintaining the most variation in the dataset. The first PC accounted for the largest variability, while the remaining PCs explained the residual variability. Based on factor loading values, the essential underlying variables for each PC were discovered. Under each PC, variables with absolute values of less than 20% of the maximum weighted factor were kept. The correlation matrix was used to verify the interlinkage of the extracted variables under respective PCs, and the most prominent variables from each PC were chosen for SQI development. After homothetic translation of each value within a mutual scale ranging from 0.1 to 1.0, the weighted addition for the final computation of index SQI for location and crop management was computed individually. All other indicators, except for ρb and pH, were treated as 'more is better' for all treatment combinations.

2.6 Computation of carbon stocks, system productivity, and the sustainability index

Carbon stocks, system productivity in terms of rice equivalent yield, and the sustainability yield index (SYI) were computed by using Eqs. (1,3)

$$\mathrm{REY}\ (kg/ha) = rice\ grain\ yield + \frac{(wheat\ grain\ yield\ (kg/ha) x\ market\ price\ of\ wheat)}{market\ price\ of\ rice\ (INR)}, \tag{1}$$

$$\mathrm{SYI} = \frac{(y-\sigma)}{ymax}, \tag{2}$$

where, y, σ, and ymax represents the average yield of treatment over the years, standard deviation, and observed maximum yield over the years.

$$\text{Carbon stock} = \rho b(\text{g cm}^{-3}) * \text{C concentration}(\%) * \text{soil depth(cm), Mg ha}^{-1}. \tag{3}$$

2.7 Data analysis

The data from soil analysis and grain yield measurement were processed for analysis of variance (ANOVA) in a factorial RBD using R version 9.2 to examine the statistical significance of the treatments (location and agronomic manipulation in crop management). Using R, the LSD of the mean was calculated using Duncan's multiple-range test (DMRT) ($p < 0.05$). At the $p < 0.05$ level of significance in DMRT, values in a column that are followed by a comparable letter in lowercase are not substantially different. By examining data on soil quality indicators (soil physical, chemical, and biological qualities) from various treatments, principal component analysis (PCA) was utilized to reduce dimensionality while maintaining the maximum variance in the studied dataset. Variables with factor loadings and PCs with multiple eigenvalues were determined to be the best variables for describing system properties. As a result, PCs with eigenvalues greater than 1.0 were chosen for further investigation since they were thought to be more informative than the rest (Kaiser, 1960). The first PC described the most variability, while the remaining PCs explained the majority of the leftover variability (Table 1).

TABLE 1 Details of the rotated component matrix–eigenvalues and rotated sums of squared loadings in our present study.

Principal component	PC1	PC2	PC3
Eigenvalues	4.52	3.24	1.85
% of variance	45.2	32.4	18.5
Cumulative variability (%)	45.2	77.6	96.1
Factor loading			
Soil pH	−0.679	−0.627	0.135
Pb	0.839	0.538	0.045
SOC	−0.299	0.807	0.506
AvN	0.918	0.384	0.068
AvP	0.593	0.168	0.778
AvK	−0.841	0.34	−0.386
MBC	−0.317	0.817	0.473
Fungi	0.702	0.552	−0.448
Bacteria	0.017	0.80	−0.592
Actinomycetes	0.879	−0.049	−0.192

Pb: bulk density, SOC: soil organic carbon, AvN: available nitrogen, AvP: available phosphorus, AvK: available potassium, MBC: microbial biomass carbon (mg g−1).

3 Result

3.1 Spatial and crop management amendment variability on soil pH, ρb, and nutrients

The spatial variability influenced the soil parameters. The soil *p*H varied from 7.2 (Jabalpur) to 8.3 (Modipuram). Similarly, ρb varied from 1.33 g cm^{-3} to 1.57 g cm^{-3}. The highest was recorded at Ludhiana, and the minimum was recorded at the rest of the locations, which are statistically on par with each other. The highest SOC (10.6 g kg^{-1} of soil) and AvP (58.2 kg ha^{-1}) were recorded at Pantnagar, while minimum SOC and AvP were recorded at Ludhiana (5.1 g kg^{-1} of soil) and Jabalpur (16.2 kg ha^{-1}), respectively. The highest AvN was recorded at Ludhiana (338.9 kg ha^{-1}), followed by Pantnagar (318.8 kg ha^{-1}). The highest AvK was recorded at Jabalpur (282.8 kg ha^{-1}), followed by Modipuram (273.7 kg ha^{-1}). Among the crop management practices, 0.2 unit of soil pH was optimized under ICM as compared to the rest of the treatments. Soil ρb was lower with the application of organic amendments under organic crop management (1.36 g cm^{-3}), followed by ICM (1.41 g cm^{-3}), as compared to inorganic crop management (1.41 g cm^{-3}). The enforcement of organic matter in organic crop management significantly improved ($p < 0.05$) SOC, AvN, AvP, and AvK by 33.3%, 16.4%, 37.8%, and 20.3% over inorganic crop management. Similarly, integration of organic and inorganic crop management improved ($p < 0.05$) regulating ecosystem services like SOC, AvN, AvP, and AvK by 14.3%, 3.9%, 5.4%, and 9.9%, respectively, over inorganic crop management (Table 2).

3.2 Spatial and crop management amendment variability on microbial diversity

Among the different locations, the highest microbial biomass carbon was found at Pantnagar (0.52 mg g^{-1} soil), followed by Jabalpur (0.39 mg g^{-1} soil). The lowest microbial biomass carbon was found at Ludhiana (0.25 mg g^{-1} soil). The highest bacterial, fungal, and actinomycetes counts were also found to be highest at Pantnagar, followed by Jabalpur. The lowest microbial population was found in Ludhiana (Table 3). Among the different nutrient management plots of rice–wheat cropping systems, across the different locations, the highest bacterial, fungal, and actinomycetes viable cell counts were found under the pure organic plots, followed by integrated plots. The highest microbial biomass carbon was found under organic plots, followed by integrated plots. The lowest microbial biomass carbon was found in Ludhiana (Table 3).

3.3 Spatial and crop management amendment variability on yield sustainability

Averaged over the years (2004–05 to 2017–18), rice grain yield (RGY) varied from 3,543.0 kg ha^{-1} to 3,791.4 kg ha^{-1} across the location. Similarly, wheat grain yield (WGY) varied from 3,406.4 kg ha^{-1} to 4,416.1 kg ha^{-1}. The system productivity expressed in terms of rice equivalent yield (REY) varied from 7,035.6 kg ha^{-1} to 8,223.0 kg ha^{-1} across the location (Table 4). However, no significant difference was recorded between Ludhiana and Pantnagar in terms of RGY, WGY, and REY. However, both the locations had 5.2%–6.2%, 27.5%–14.3%, and 16.5%–10.7% significantly ($p < 0.05$) higher RGY, WGY, and REY over Jabalpur and Modipuram, respectively. Consequently, Ludhiana (0.82) and Pantnagar (0.83) had a significantly ($p < 0.05$) higher sustainability yield index (SYI) than Jabalpur (0.64) and Modipuram (0.72) (Figure 3). Among the crop management practices, the highest grain yield of rice (3,746.3 kg ha^{-1}) and wheat (4,190.4 kg ha^{-1}) was recorded in integrated crop management (ICM) as compared to organic and inorganic crop management. Hence, ICM had increased the system productivity (REY) by 4.7%–6.7%

TABLE 2 Effect of spatial and cop management on soil pH, bulk density, soil organic carbon, and nutrients in the rice–wheat system.

Treatment/location	Soil pH	Pb (g cm^{-3})	SOC, g kg^{-1}	AvN, kg ha^{-1}	AvP, kg ha^{-1}	AvK, kg ha^{-1}
Location						
Jabalpur	7.2	1.33	7.8	276.9	16.5	282.8
Ludhiana	7.4	1.57	5.1	338.9	46.5	154.5
Pantnagar	7.2	1.38	10.6	318.8	58.2	201.1
Modipuram	8.3	1.33	7.4	169.8	24.3	273.7
LSD ($p < 0.05$)	0.12	0.05	0.39	20.6	2.4	17.0
Crop management						
Organic crop management	7.6	1.36	8.8	293.5	40.8	249.6
Inorganic crop management	7.6	1.44	6.6	252.1	29.6	207.4
Integrated crop management	7.4	1.41	7.7	282.6	38.7	227.1
LSD ($p < 0.05$)	0.10	0.02	0.34	7.8	2.1	14.7
Interaction						
LSD ($p < 0.05$)	0.21	0.03	0.68	15.7	4.2	29.4

Pb: bulk density, SOC: soil organic carbon, AvN: available nitrogen, AvP: available phosphorus, AvK: available potassium.

TABLE 3 Effect of spatial and crop management on microbial diversity in the rice–wheat system.

Treatment/location	MBC, mg g^{-1}	Total fungi, x10^4 CFU	Total bacteria, x10^6 CFU	Total actinomycetes, x10^6 CFU
Location				
Jabalpur	0.39	39.8	30.5	12.4
Ludhiana	0.25	5.2	17.7	5.8
Pantnagar	0.52	46.2	54.2	23.0
Modipuram	0.37	32.1	22.3	11.7
LSD ($p < 0.05$)	0.02	3.8	3.7	1.9
Crop management				
Organic crop management	0.45	36.2	40.6	17.5
Inorganic crop management	0.32	25.8	25.4	12.4
Integrated crop management	0.38	30.3	27.6	9.8
LSD ($p < 0.05$)	0.02	3.3	3.2	1.7
Interaction				
LSD ($p < 0.05$)	0.04	6.6	6.4	3.4

MBC: microbial biomass carbon.

TABLE 4 Effect of spatial and crop management on grain yield and system productivity of the rice–wheat system.

Treatment/location	Rice grain yield (kg ha^{-1})	Wheat grain yield (kg ha^{-1})	Rice equivalent yield (kg ha^{-1})
Location			
Jabalpur	3,576.9	3,406.4	7,035.6
Ludhiana	3,734.5	4,416.1	8,223.0
Pantnagar	3,791.4	4,341.4	8,196.7
Modipuram	3,543.0	3,796.9	7,404.2
LSD ($p < 0.05$)	142.4	209.1	572.7
Crop management			
Organic crop management	3,740.1	3,702.0	7,499.4
Inorganic crop management	3,498.0	4,078.2	7,643.1
Integrated crop management	3,746.3	4,190.4	8,002.1
LSD ($p < 0.05$)	123.4	181.1	496.0
Interaction (location × crop management)			
LSD ($p < 0.05$)	246.7	362.1	991.9

over inorganic and organic crop management. Similarly, the highest SYI was recorded in ICM (0.77) as compared to inorganic (0.74) and organic management (0.75) (Figure 3).

3.4 Spatial and crop management amendment variability in economics

Spatial variability significantly influences the farm net returns of the long-term (15 years) rice–wheat cropping system. Among the location, net returns and B:C ratio varied from Indian rupees (INR) 7.4×10^4 to 12.8×10^4 and 2.02 to 2.95, respectively. The highest net return was obtained in Pantnagar > Ludhiana, and it was 44.1%–63.4% higher than those in Modipuram and Jabalpur. Similarly, on an average, the B:C ratio was increased by 21.0%–35.3% in Pantnagar > Ludhiana over Modipuram and Jabalpur, respectively (Figure 4). Crop management practices had significantly ($p < 0.05$) different net returns and B:C ratio. The ICM gave 22.2% and 23.5% higher net returns over organic and inorganic crop management practices.

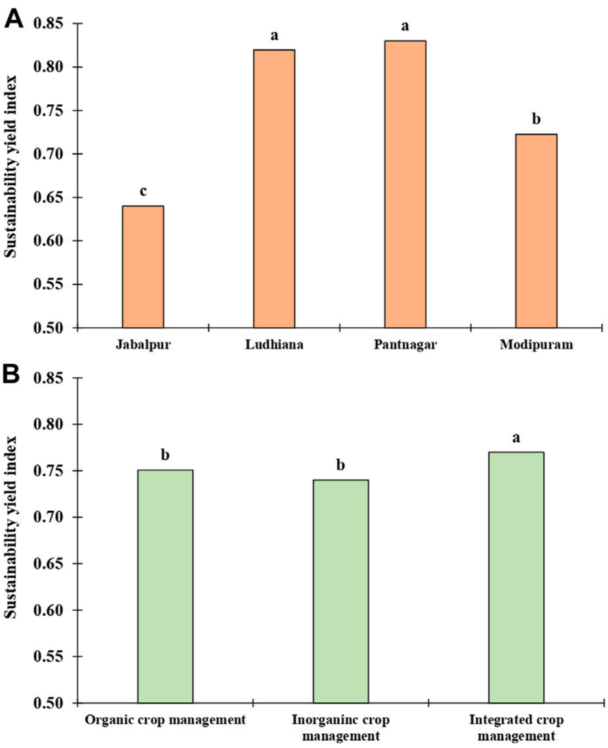

FIGURE 3
Sustainability yield index influenced by **(A)** spatial variation and **(B)** crop management in the rice–wheat system. Different lowercase letters in the same color columns (for each factor) are significantly different at $p < 0.05$.

Similarly, a higher benefit-cost ratio was recorded in ICM (2.52) as compared to organic (1.84) and inorganic (2.45) crop management practices (Figure 4).

3.5 Spatial and crop management amendment variability on the soil quality index

For deriving SQI, soil *p*H, ρb, SOC, AvN, AvP, AvK, MBC, total fungi, total bacteria, and total actinomycetes were included in the data for principal component analysis. In Table 1, the first, second, and third PCs explained 45.2%, 32.4%, and 18.5% of variability with eigenvalues of 4.52, 3.24, and 1.85, respectively. Therefore, the eigenvalues of three PCs (principal components) were ≥ 1 which explained 96.1% of the cumulative variability. The calculated weights for PC 1, PC 2, and PC 3 were 0.47, 0.34, and 0.19, respectively. Soil *p*H, ρb, AvK, fungi, and actinomycetes have the highest factor loading in the first PC1. As AvN has a strong positive correlation with other indicators, AvN was retained in PC1 as the minimum dataset (MDS). In PC2, MBC was selected with the highest loading factor. In PC3, AvP with the highest weighted factor was selected for MDS. The highly weighted factors that were taken for deriving the SQI were AvN (factor loading: 0.918), MBC (factor loading: 0.817), and AvP (factor loading: 0.778) from PC1, PC2, and PC3, respectively. Thus, AvN, MBC, and AvP were selected as MDS for deriving the SQI. Spatial variation influenced the SQI, and it varied from 0.53 to 0.61. The highest SQI was recorded in Pantnagar (0.63) as compared to other locations (0.53–0.55). Similarly, the SQI for crop management practices were estimated as 0.60, 0.53, and 0.54 in organic, inorganic, and ICM, respectively (Figure 5).

3.6 Interaction and correlation

Spatial variation (Jabalpur, Ludhiana, Pantnagar, and Modipuram) and crop management practices (organic, inorganic, and ICM) having a significant ($p < 0.05$) interaction with productivity, economics, and soil quality indicators (soil *p*H, ρb, SOC, AvN, AvP, AvK, MBC, total fungi, total bacteria, and total actinomycetes) were studied. The interaction between spatial variation and crop management practices is presented in Tables 1–4; Figure 6 revealed a strong relationship between soil quality indicators like SOC (r = +0.84, $p < 0.01$) and MBC (r = +0.72, $p < 0.01$) with SQI. Soil microbial diversity like actinomycetes was also strongly correlated with soil quality indicators like ρb (r = 0.92, $p < 0.001$), AvN (r = +0.90, $p < 0.01$), and total fungi (r = +0.77, $p < 0.01$). Similarly, MBC was strongly correlated with soil physical indicators *viz.* ρb (r = −0.88, $p < 0.01$) (Figure 6). The favorable relationship between soil quality indicators and SQI has a significant impact on soil ecosystem services.

4 Discussion

4.1 Current and future importance of organic and toward organic approaches in the IGP

Many districts in the IGPs have large tracts of chaur (waterlogged soils), tal (active flood plains), and diara (lamp-shaped depressions/shifting river course) which are flooded during monsoon, and fields get vacated very late for wheat. Furthermore, ρb of trans and upper IGPs are higher than in middle and lower areas indicating soil compaction, leading to a reduction in long-term soil productivity, especially under the rice–wheat system. However, results indicate that the addition of organic manures, especially FYM, helps improve the soil condition, especially the physical properties of soil (Patil et al., 2014). Therefore, the present investigation of organic and toward organic (integrated crop management) approaches aims to reverse the soil's physical property degradation in addition to

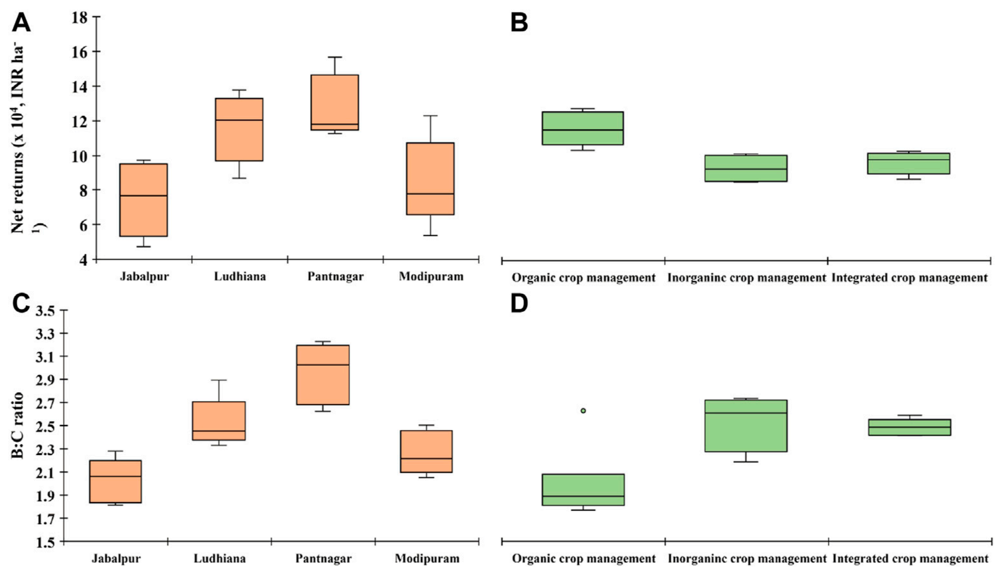

FIGURE 4
Economics **(A,B)**. Net returns **(C,D)**. Benefit: cost (B: C) ratio of the rice–wheat system influenced by spatial variation and crop management.

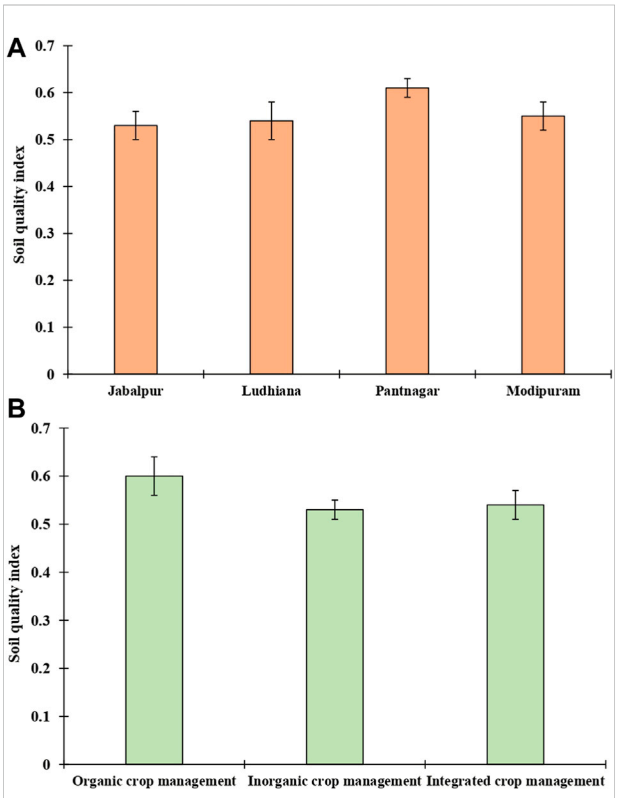

FIGURE 5
Soil quality index influenced by **(A)** spatial variation and **(B)** crop management in the rice–wheat system. Vertical bar represents a standard error (SE) of mean.

maintaining the comparable productivity of the rice–wheat system with that of synthetic-oriented conventional farming.

Crop residues (straws) are a by-product (241 million tonnes of crop residues, including 85 million tonnes from wheat and 21 million tonnes from sorghum, pearl millet, and maize in IGP) of crop production and in the majority of the IGP areas, the residues of rice, wheat and maize are not being utilized as livestock feed; rather, it is burnt, causing pollution, especially air.

Ruminant population in IGP includes 69.86 million (34%) cattle, 36.72 million (44%) buffalo, 46 million (40%) goats, and 6.80 million (13%), thereby cattle and buffalo contributing to a major manure supply for farming. However, progressive replacement of draught animals by electrical and mechanical sources of power, diminishing reliance on crop residues as ruminant fodder, large-scale burning of straw, and a progressive decline in the recycling of farmyard manure for enriching soils have all upset the traditional symbiotic interactions between crops and livestock in the small-holder, mixed farming systems in the IGP (Rao, 2002). Only a few parts of IGP, namely, the middle and lower areas continue to utilize crop residues for livestock feed. Therefore, it again provides great opportunities to utilize the crop residues in the Trans and Upper Gangetic Plains to promote organic and toward organic approaches there by which the long-term soil productivity could be maintained as evidenced from the current study.

Deteriorating water quality in the IGPs is a major concern, especially in the intensively cultivated areas with synthetic inputs. A study conducted by Sihi et al. (2020) points out that the quality parameters of water (nitrate, NO_3; total dissolved solids (TDS); electrical conductivity (EC)), *p*H, and irrigation (sodium

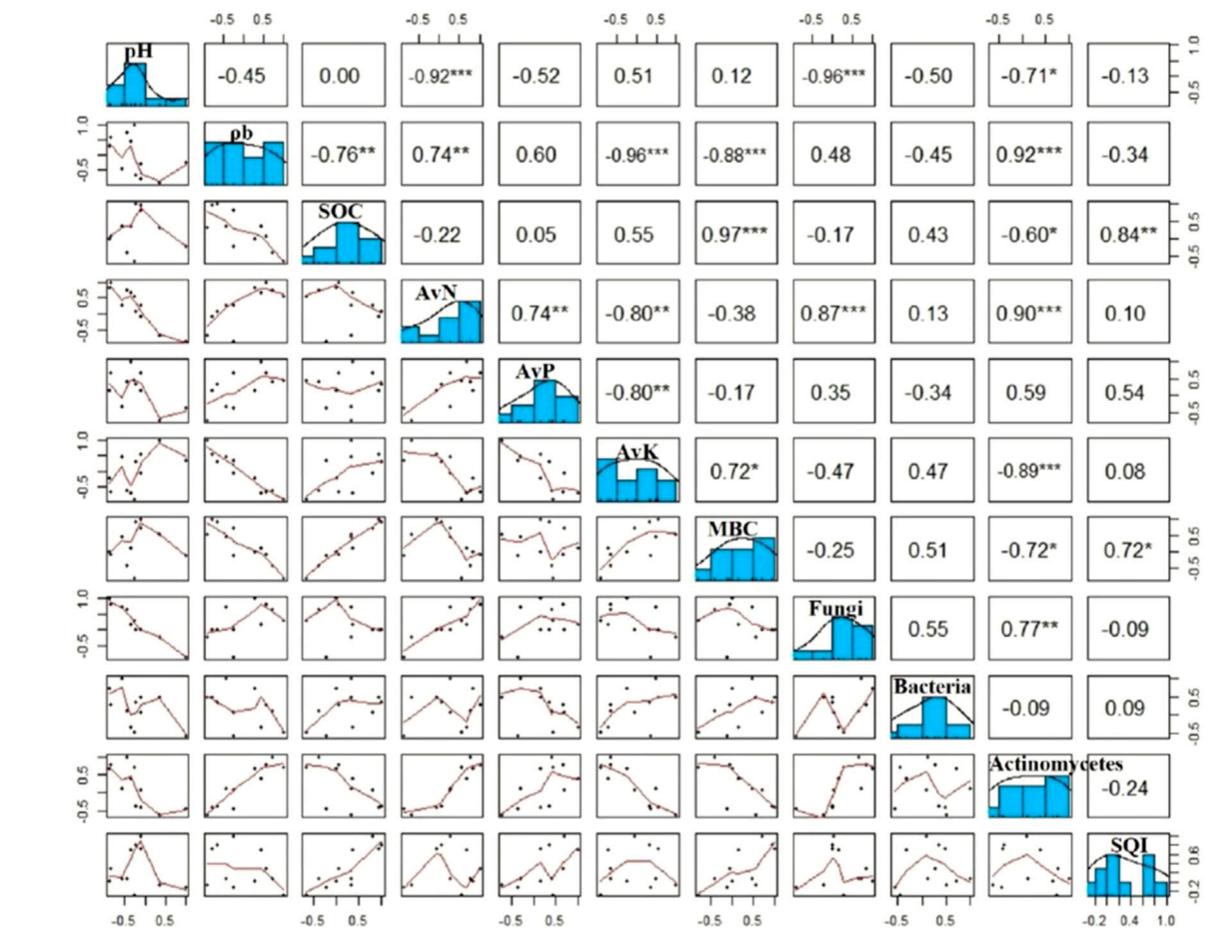

FIGURE 6
Correlations between soil quality indicators as influenced by spatial variation and crop management in the rice–wheat cropping system. pb: bulk density, SOC: soil organic carbon; AvN: available nitrogen, AvP: available phosphorus, AvK: available potassium, microbial biomass carbon, SQI: soil quality index.

adsorption ratio (SAR) and residual sodium carbonate (RSC)) used for drinking purposes were below permissible limits for all samples collected from organic fields and those from conventional fields over the long term (~15 and ~20 years). The magnitude of water NO_3 contamination in conventionally farmed fields was approximately double that of organic fields in the IGP in South-Eastern Asia. Therefore, the current study on the long-term effect of organic and toward organic approaches is more relevant in reducing the water pollution in the Gangetic areas in addition to sustaining the crop productivity and its interaction with livestock systems in the region.

Furthermore, the Government of India has been focusing on the promotion of organic and natural farming on either side of the Ganga River up to 5 km stretches in order to reduce the agriculturally induced water pollution in the river. Schemes such as Paramparagat Krishi Vikas Yojana (PKVY; Traditional Agricultural Development Plan), Namami Ganga, and Rashtriya Krishi Vikas Yojana (RKVY; National Agricultural Development Plan) are being implemented to promote organic farming practices in the IGP areas. It is aimed to bring 10% of the area under organic farming by 2030 by using available organic resources such as livestock manures, cropping system diversification including green manuring, crop residue utilization for soil health restoration, sustaining the crop-livestock interactions, and crop productivity, reducing the water and air pollution. Therefore, findings from the current study on the long-term (15 years) impact on organic and toward organic (integrated crop management) approaches will enable the policymakers to implement the eco-system restoration farming practices in the IGPs.

4.2 Spatial variability and crop management on yield sustainability and economics

In IGPs, the rice–wheat cropping system is the life-supporting and most prevalent production system, occupying about ~13.5 million ha of productive land (~10 m ha in India). The land degradation and soil fertility depletion were reported across different states, especially on account of the non-application of organic amendments to the system and without the inclusion of leguminous green manure crops/crop residue recycling. Inclusion of legumes and green manure crops like *Sesbania* increased the system productivity and stabilized the yield sustainability in saline-alkaline soils (Parihar et al., 2018) of the IGP and acidic soils of the Eastern Himalayan region (Ansari et al., 2022b). In this study, SYI varied from 0.64 to 0.73 due to spatial variability and 0.74 to 0.77 due to manipulation in crop management practices. Across the location and treatment, the SYI value is higher than 0.50 of the critical limits. This indicates long-term enforcement of organic amendments either in organic crop management or ICM, enhancing the system productivity and stabilizing the yield sustainability as compared to inorganic crop management. Therefore, this study notably suggests that enforcement of organic inputs along with the inclusion of green manuring in the system could stabilize the system's productivity and sustainability in the IGP. Due to an improvement in the physical, biological, and chemical characteristics of the soil, the addition of green manure crops and the enforcement of organic amendments have emerged as potential options to increase economic production (grain yield) (Babu et al., 2020a; Ansari et al., 2021). The nutrient availability and microbial diversity are directly related to the improvement in soil productivity. The increased grain production of rice and wheat in this study, compared to the organic and inorganic nutrient additions and crop management, led to higher net returns and the benefit-cost ratio being obtained under ICM. Due to the changes occurring in the soil health and climate as a result of the continuous and expanded use of synthetics in farming, policy planners are placing a greater emphasis on food security, safety, and sustainability. Therefore, results clearly bring out that organic amendment integration in the existing conventional system (synthetic-based) is important and needs to be promoted for the long-term sustainability of the rice–wheat system.

4.3 Spatial variability and crop management on soil quality indicators and ecosystem services

Long-term data generated in this study under the national level scheme, namely, the All India Network Programme on Organic Farming indicates that the crop productivity of selected crops in identified regions having better soil health can be sustained without an external supply of synthetic fertilizers and pesticides. However, soil quality parameters are better under organic management, which will again be helpful for improved water and nutrient use efficiency of the cropping system, leading to the long-term sustainability of the cropping system. Maintaining supporting, and regulating ecosystem services require ecologically feasible and socially acceptable agriculture management technologies (Baveye et al., 2016). Soil quality refers to a set of specific soil factors that are crucial for long-term agricultural production and ecosystem (vegetation and soil) health (Karlen et al., 2001). Organic matter enforcement, either through green manuring (leguminous) or organic nutrient amendments in the soil, is known to increase soil organic C accumulation and improve soil biological function (diversity in soil microbial population) in tropical and subtropical soils (Ansari et al., 2022a). This study revealed that enforcement of organic manure provided a large amount of C into the soil (8.21 Mg C ha^{-1} annum^{-1}) through FYM/oilcake/biofertilizers and (> 9.58 Mg C ha^{-1} annum^{-1}) through green manuring under organically crop management treatment. Similarly, the integration of organic manure provided 5.88 Mg C ha^{-1} annum^{-1} and > 9.58 Mg C ha^{-1} annum^{-1} through green manuring under ICM. Therefore, all these enforcements significantly ($p < 0.05$) increased the C stock in the soil under organic and ICM as compared to inorganic crop management. Several factors, such as spatial variation, land-use patterns, vegetation types, organic manure enforcement, green manuring, and soil management strategies, have a significant impact on soil nutrients (Choudhury et al., 2021). Intensive crop cultivation without sufficient nutrient application and input addition to the soil lowers soil carbon stock and nutrient concentrations and has negative consequences for soil physicochemical and biological qualities (Choudhury et al., 2021).

In this study, it is reported that organic enforcement improved by +41.4, +11.2, and +42.2 and ICM improved by +30.5, +9.1, and 19.7 kg AvN, AvP, and AvK kg ha^{-1}, respectively, as compared to inorganic crop management. Under organic crop management combined with *Sesbania* green manuring, the highest concentration of N, P, and K can be attributed to nutrient addition and recycling, which improves soil nutrient concentrations and microbial diversity (Choudhury et al., 2021). Stabilization of soil C and nutrients will help reduce CO_2 emissions into the atmosphere and can address several SDGs, including climate action (SDG–13) and life on land (SDG–15), by preserving soil microbial diversity, which is an important component of growing crops for humans and livestock on the planet. *Sesbania* is a leguminous crop with a low C:N ratio (23.5: 1.0), which aids in residue decomposition and nutrient release, as well as having potential microbial diversity (Babu et al., 2020a; Ansari et al., 2022c). In *Sesbania* integrated sites, the crop cover may have generated a conducive environment for greater microbial breakdown, resulting in faster decomposition and nutrient release. The balance between the addition of C inputs (root exudates, root biomass, and crop wastes) and C losses is critical for increasing soil C (respiration by soil biota and erosion). The amount of residue accumulated, the quality of the residue, and the rate of decomposition all play a role (Almagro et al., 2021). The inclusion of green manure biomass boosts microbial activities substantially. Under cereal-based cropping systems, including nutrient-rich leguminous crops and incorporating them as green manure biomass into the soil protects nutrients for succeeding crops, improves carrying capacity, and makes the system feasible and sustainable (Babu et al., 2020b; Ansari et al., 2021). In this study, green manure and organic manure enforcement greatly improve the soil quality by reducing the bulk density (about +5.9%) and enhancing the soil microbial population (+40%–60%). Green manuring and organic manure enforcement resulted from a significant reduction in fertilizer dependency due to increased nutrient availability and altered biomass-mediated soil ecological functions and ecosystem services (Shahid et al., 2013). Soil organic matter is the storehouse of different nutrients required for plant growth and development. It plays a crucial role in maintaining the soil health and sustainable crop production. Excessive application of agrochemicals during the last few decades for intensive agriculture has resulted in the severe degradation of different soil properties. Long-term management of soil in different ways for nutrient, insect, and disease management has a significant impact on soil physic-chemical and biological properties. Biological diversity, especially bacteria, fungi, and actinomycetes, has been crucial to understanding the structure and function of soil ecology, and diversity plays a key role in the resilience and adaptability of complex systems (Bebber and Richards, 2022). The highest number of bacterial, fungal, and actinomycetes viable counts found under organic management plots may be due to the greater availability of soil organic carbon (SOC) and nutrients due to the application of different organic inputs/practices like FYM, vermicompost, and green manuring that might have favored the growth and proliferation of microbes. Growth and colonization of soil microorganisms can be affected by the physico-chemical properties of soil. Naher et al. (2021) found a greater microbial population under the long-term PL (poultry litter)-INM and CD (cow dung)-INM (balance chemical fertilizer + decomposed poultry litter/cow dung) plots as compared to chemically managed plots. They also found higher enzymatic activities and a greater population of nitrogen-fixing and phosphate-solubilizing bacteria under PL-INM and CD-INM plots. Naher et al. (2021) also found a significant increase (18%) in soil organic matter with the application of poultry litter (at 2.0 t ha^{-1}). Similarly, Adeleye et al. (2010) reported a 37.8% increase in SOC with the application of poultry litter (at 10 t ha^{-1}). The greater microbial population is directly related to the microbial biomass carbon present in the soil.

The plant biomass and amendments of organic manure influence changes in microbial populations (Naher et al., 2021). Previous studies also affirmed that soil's physical, chemical, and biological properties influence the soil community structure and ecosystem services (Pang et al., 2017). It is also reported that the cropping system, soil fertility, and soil microbial community structure are all interrelated and can be adjusted at the same time, as confirmed experimentally (Song et al., 2018). Apart from the treatment effect, the varying population of microbes under different locations is governed by soil and environmental factors. The greater amount of microbial biomass at Pantnagar as compared to others may be due to the availability of more vegetation cover and comparatively cooler climate which might have favored the proliferation of microbes. The results of regulating and supporting ecosystem services from long-term organic and integrated crop management will further strengthen and pave way for more such studies to precisely estimate and value these benefits which can be passed on to farm households by the policymakers.

4.4 Spatial variability and crop management on the soil quality index

One of the most important and easily adopted strategies for improving, regulating, and supporting ecosystem services and fighting soil degradation is quality biomass inversion through green manuring in cropping systems (Lal, 2017). Biomass accumulation and retention, as well as organic amendment enforcement-mediated soil microclimate, generates a favorable soil environment that promotes nutrient pumping from the sub-surface to the surface for plant uptake, and improvement of the nutrient utilization efficiency leads to increased crop output (Lal, 2017). However, an intensive cropping system in IGP with unsustainable agro-techniques could result in land degradation, which leads to deterioration in the soil quality (Kumar et al., 2019). In this long-term study (15 years), we notably observed that enforcement of organic amendments in organic crop management, followed by ICM, improved the soil quality indicators like SOC, MBC, AvN, AvP, and AvK, as well as enriched the microbial diversity (fungi, actinomycetes, and bacteria). The microbial diversity improved due to the abundant energy obtained from the organic substrates and drives the biological processes like nutrient/microbial decomposition, nutrient transformation/mobilization, and physical property optimization. All the organic enforcements act as a major source of nutrients and improve resilience. Furthermore, higher SQI across the crop management and location affirmed that green manuring and organic amendments under organic crop management and ICM resulted in a substantial reduction in dependency on fertilizers through improvement in nutrient storage in soil and their availability for plant uptake in long term.

Conclusion

The essential goals for agriculture's sustainable production are to reduce gas emissions and optimize carbon, as well as nutrient management efficiency with restoring the soil quality. Organic manure enforcement along with green manuring improves the soil's biological function and ecosystem services. Continuous enforcement of green manuring and organic manure through different sources improved the soil's biological properties like soil organic carbon (14.3%–33.3%), available N (4.0%–16.4%), available P (5.4%–37.8%), and available K (9.9%–20.3%) in organic and integrated crop management, respectively, over inorganic crop management. Similarly, these practices also improve the biological diversity in soil *viz.*, microbial biomass carbon (18.4%–40.6%), fungi (19.5%–40.3%), bacteria (47.1%–59.8%), and actinomycetes (41.1%–78.6%) in organic and integrated crop management, respectively, over inorganic crop management. Hence, higher SYI was recorded in ICM (0.77) followed by organic (0.75) than in inorganic crop management (0.74). With the improvement in soil biological functions and availability of nutrients, the SQI was estimated to be higher in organic (0.60), followed by ICM (0.54) than inorganic crop management (0.53). Hence, enforcement of organic manure along with green manuring, either as fully organically managed or in integration, yield sustainability, soil quality, nutrient availability, and biological function leads to improving the ecosystem services and restoring land productive capacity in the Indo-Gangetic Plains of India.

Policy implication

Rice–wheat (RWS) is the life–supporting and pre-dominant production system spread over ~10.0 M ha in the Indian Indo-Gangetic Plains, meeting 60% of the calorie intake of the population. Contemporary soil and crop management practices are capital, energy, water, and external input-intensive upsetting the ecological balance and depleting ground water and soil organic carbon, thereby affecting the long-term sustainability of the RWS. The result of the present study indicates that integrated crop management otherwise can be referred to as the toward organic approach and organic management as National Standard for Organic Products (NSOP) standards are able to sustain the system with better soil quality and yield stability with supporting and regulating ecosystem services. Overall, our estimates suggested that the adoption of ICM in rice–wheat systems increases system farm productivity by ~5% and soil organic carbon by 2.46 Mg ha^{-1} over traditional rice–wheat systems (business as usual of the region). The Indian government is promoting organic and natural farming along both banks of the Ganges River up to 5 km lengths. To encourage the use of organic farming methods in the IGP regions, programs like the Rashtriya Krishi Vikas Yojana (RKVY; National Agricultural Development Plan), Namami Ganga, and Paramparagat Krishi Vikas Yojana (PKVY; Traditional Agricultural Development Plan) are being implemented. By utilizing readily available organic resources like livestock manures, cropping system diversification, including green manuring, crop residue utilization for soil health restoration, sustaining crop–livestock interactions and crop productivity, and lowering water and air pollution, it is intended to convert 10% of the agricultural land to organic farming by 2030. Hence, it is presumed that if a 10% area of RWS brings under integrated organic nutrient management that will add ~5% in food grain in addition to ~3.32 × 10^6 Mg C ha^{-1} storage in soil carbon over traditional production practices. Therefore, findings from the study will help the policymakers to realize the benefits of long-term organic and integrated crop management practices and devise appropriate policies for incentivization including extending carbon credit benefits *in lieu* of contributing to ecosystem services for the adoption of the toward organic approach. The findings of the present study will also reinforce India's commitments toward COP-26 and Bonn challenges.

Data availability statement

The datasets presented in this study can be found in online repositories. The names of the repository/repositories and accession number(s) can be found in the article/Supplementary Material.

Author contributions

ASP: Visualization, supervision and project administration, MAA: conceptualization, data analysis, writing of original and first draft, and review and editing of the final draft; NR: data curation, review and editing, visualization, and supervision; SB: review and editing; AKP: statistical analysis, and review and editing; PCG: data curation and editing of materials and method: JC: data curation, and review and editing; MS: meteorological data analysis; RS: review and editing; RKJ: review and editing; DD: review and editing; ALM: review and editing; GVC: data compilation; MHA: review and editing of the first and final draft; RS: review and editing; CSA, DKS, and PBS: data curation.

Acknowledgments

The authors are grateful for financial assistance from the Indian Council of Agricultural Research through the All-India Network Programme on Organic Farming (AI–NPOF), Indian Institute of Farming Systems Research, Modipuram. The authors express their gratitude to the other scientists and project staff of respective AI–NPOF centers for their support.

Conflict of interest

The authors declare that the research was conducted in the absence of any commercial or financial relationships that could be construed as a potential conflict of interest.

The handling editor IP declared a past co-authorship with the authors SB and RS.

Publisher's note

All claims expressed in this article are solely those of the authors and do not necessarily represent those of their affiliated organizations, or those of the publisher, the editors, and the reviewers. Any product that may be evaluated in this article, or claim that may be made by its manufacturer, is not guaranteed or endorsed by the publisher.

Supplementary material

The Supplementary Material for this article can be found online at: https://www.frontiersin.org/articles/10.3389/fenvs.2022.972394/full#supplementary-material

References

Adeleye, E. O., Ayeni, L. S., and Ojeniyi, S. O. (2010). Effect of poultry manure on soil physico- chemical properties, leaf nutrient contents and yield of yam (*Dioscorea rotundata*) on alfisol in southwestern Nigeria. *Am. J. Sci.* 6 (10), 871–878. https://www.researchgate.net/publication/259999743.

Almagro, M., Antonio, R. N., Elvira, D. P., Juan, A., and María, M. M. (2021). Plant residue chemical quality modulates the soil microbial response related to decomposition and soil organic carbon and nitrogen stabilization in a rainfed Mediterranean agroecosystem. *Soil Biol. Biochem.* 156, 108198. doi:10.1016/j.soilbio.2021.108198

Ansari, M. A., Babu, S., Choudhury, J., Ravisankar, N., and Panwar, A. S. (2022c). Soil quality restoration and yield stabilization in acidic soils of northeastern Himalayas: Five years impact of green manuring and crop residue management. *Front. Environ. Sci.* 10 (940349), 1–18. doi:10.3389/fenvs.2022.940349

Ansari, M. A., Choudhury, B. U., Layek, J., Das, A., Lal, R., and Mishra, V. K. (2022b). Green manuring and crop residue management: Effect on soil organic carbon stock, aggregation, and system productivity in the foothills of eastern himalaya (India). *Soil Tillage Res.* 218, 105318. doi:10.1016/j.still.2022.105318

Ansari, M. A., Choudhury, B. U., MandalJat, S. S. L., and Meitei, C. (2022a). BungbungchaConverting primary forests to cultivated lands: Long-term effects on the vertical distribution of soil carbon and biological activity in the foothills of Eastern Himalaya. *J. Environ. Manage.* 301, 113886. doi:10.1016/j.jenvman.2021.113886

Ansari, M. A., Saha, S., Das, A., Lal, R., Das, B., Choudhury, B. U., et al. (2021). Energy and carbon budgeting of traditional land use change with groundnut-based cropping system for environmental quality, resilient soil health and farmers income in eastern Indian Himalayas. *J. Environ. Manage.* 293, 112892. doi:10.1016/j.jenvman.2021.112892

Aulakh, C. S., and Ravisankar, N. (2017). Organic farming in Indian context: A perspective. *Agricul. Res. Jour.* 54 (2), 149–164. doi:10.5958/2395-146x.2017.00031.x

Babu, S., Mohapatra, K. P., Das, A., Yadav, G. S., Tahasildar, M., Singh, R., et al. (2020b). Designing energy-efficient, economically sustainable and environmentally safe cropping system for the rainfed maize–fallow land of the Eastern Himalayas. *Sci. Total Environ.* 722, 137874. doi:10.1016/j.scitotenv.2020.137874

Babu, S., Singh, R., Avasthe, R. K., Yadav, G. S., Das, A., Singh, V. K., et al. (2020a). Impact of land configuration and organic nutrient management on productivity, quality and soil properties under baby corn in Eastern Himalayas. *Sci. Rep.* 10 (1), 16129–16214. doi:10.1038/s41598-020-73072-6

Banerjee, V., Krishnan, P., Das, B., Verma, A. P. S., and Varghese, E. (2015). Crop status index as an indicator of wheat crop growth condition under abiotic stress situations. *Field Crops Res.* 18, 16–31. doi:10.1016/j.fcr.2015.06.009

Baveye, P. C., Baveye, J., and Gowdy, J. (2016). Soil ecosystem services and natural capital: Critical appraisal of research on uncertain ground. *Front. Environ. Sci.* 4, 1–49. doi:10.3389/fenvs.2016.00041

Bebber, D. P., and Richards, V. R. (2022). A meta-analysis of the effect of organic and mineral fertilizers on soil microbial diversity. *Appl. Soil Ecol.* 175, 104450. doi:10.1016/j.apsoil.2022.104450

Bhattacharyya, P., and Chakraborty, G. (2005). Current status of organic farming in India and other countries. *Indian J. Fert.* 1 (9), 11–123.

Blake, G. R., and Hartge, K. H. (1986). *Bulk density in: Methods of soil analysis, Part I: Physical and mineralogical methods*. Editor A. Klute. second ed. (Madison WI: American Society of Agronomy).

Charyulu, K., and Biswas, S. (2010). *Organic input production and marketing in India : Efficiency, issues and policies*. IIMA, Ahmedabad: CMA Publication, 239.

Choudhury, B. U., Ansari, M. A., Chakraborty, M., and Meetei, T. T. (2021). Effect of land-use change along altitudinal gradients on soil micronutrients in the mountain ecosystem of Indian (Eastern) Himalaya. *Sci. Rep.* 11, 14279. doi:10.1038/s41598-021-93788-3

Dwivedi, B. S., Singh, V. K., and Meena, M. C. (2017). Efficient nitrogen management under predominant cropping systems of India. *Indian Nitrogen Assess.* 2017, 95–115. doi:10.1016/B978-0-12-811836-8.00007-0

Gangwar, B., Singh, V. K., and Ravisankar, N. (2013). Fertilizer best management practices in important cropping systems. *Indian J. Fert.* 9 (4), 34–51. https://krishi.icar.gov.in/jspui/bitstream/123456789.

Kaiser, H. F. (1960). The application of electronic computers to factor analysis. *Educ. Psychol. Meas.* 20, 141–151. doi:10.1177/001316446002000116

Karlen, D. L., Andrews, S. S., and Doran, J. W. (2001). Soil quality: Current concepts and applications. *Adv. Agron.* 74, 1–40. doi:10.1016/S0065-2113(01)74029-1

Kumar, N., Nath, C. P., Hazra, K. K., Das, K., Venkatesh, M. K., Singh, S. S., et al. (2019). Impact of zero-till residue management and crop diversification with legumes on soil aggregation and carbon sequestration. *Soil Tillage Res.* 189, 158–167. doi:10.1016/j.still.2019.02.001

Lal, R. (2017). Improving soil health and human protein nutrition by pulses-based cropping systems. *Adv. Agron.* 145, 167–204. doi:10.1016/bs.agron.2017.05.003

Mahajan, A., and Gupta, R. D. (2009). *Balanced use of plant nutrients: Integrated nutrient management (INM) in a sustainable rice–wheat cropping system*. Dordrecht: Springer. doi:10.1007/978-1-4020-9875-8_8

Meena, B. L., Fagodiya, R. K., Prajapat, K., Dotaniya, M. L., Kaledhonkar, M. J., Sharma, P. C., et al. (2018). "Legume green manuring: An option for soil sustainability," in *Legumes for soil health and sustainable management* (Singapore: Springer), 387–408. doi:10.1007/978-981-13-0253-4_12

Naher, U. A., Haque, M. M., Khan, F. H., Sarkar, M. I. U., Ansari, T. H., Hossain, M. B., et al. (2021). Effect of long-term nutrient management practices on soil health and paddy yield of rice-rice-fallow cropping system in tropic humid climate. *Eur. J. Soil Biol.* 107, 103362. doi:10.1016/j.ejsobi.2021.103362

NSSO (2013). *India - situation assessment survey of agricultural households, january - december 2013, NSS 70th round*. New Delhi: National Sample Survey Organization - Ministry of Statistics and Programme Implementation (MOSPI), Government of India.

Olsen, S. R., and Sommers, L. E. (1982). "Phosphorus," in *Methods of soil analysis: Part 2. Chemical and microbiological properties*. 2nd ed (Madison, WI: ASA and SSSA), 403–430.

Pang, G., Cai, F., Li, R., Zhao, Z., Li, R., Gu, X., et al. (2017). Trichoderma-enriched organic fertilizer can mitigate microbiome degeneration of monocropped soil to maintain better plant growth. *Plant Soil* 416, 181–192. doi:10.1007/s11104-017-3178-0

Panwar, A. S., Ravisankar, N., Sharma, S. K., and Suja, G. (2020). "Organic and low input agriculture: Gandhian Way," in *Mahatma gandhi's vision of agriculture: Achievements of ICAR*. Editors H. Pathak, Suresh Pal, and T. Mohapatra (New Delhi: Indian Council of Agricultural Research), 86–96.

Panwar, A. S., Shamim, M., Ravisankar, N., Ansari, M. A., Singh, R., Prusty, A. K., et al. (2021). Influence of long-term fertilization with organic sources on crop productivity and soil quality in rice-wheat system under arid and sub humid conditions. *Indian J. Fert.* 16 (6), 544–554. https://scholar.google.com/citations.

Parihar, C. M., Parihar, M. D., Sapkota, T. B., Nanwal, R. K., Singh, A. K., Jat, S. L., et al. (2018). Long-term impact of conservation agriculture and diversified maize rotations on carbon pools and stocks, mineral nitrogen fractions and nitrous oxide fluxes in inceptisol of India. *Sci. Total Environ.* 604-641, 1382–1392. doi:10.1016/j.scitotenv.2018.05.405

Patil, N. G., Tiwary, P., Bhattacharyya, T., Chandran, P., Sarkar, D., Pal, D. K., et al. (2014). Natural resources of the indo-gangetic plains: A land-use planning perspective. *Curr. Sci.* 107 (9), 1537–1549. https://www.researchgate.net/publication/268212008.

Phillips, R. L. (2014). "Green revolution: Past, present, and future," in *Neal K. Van alfen. Encyclopedia of agriculture and food systems* (Amsterdam, Netherlands: Academic Press), 529–538. doi:10.1016/B978-0-444-52512-3.00208-4

Rao, P. P. (2002). "Role of livestock subsystem in sustaining the mixed crop-livestock farming systems in the Indo-Gangetic plains in India," in *Rice-wheat consortium regional technical coordination committee meeting. 10–13 February 2002* (New Delhi, India: Rice–Wheat Consortium for the Indo-Gangetic Plains).

Ravisankar, N., Ansari, M. A., Panwar, A. S., Aulakh, C. S., Sharma, S. K., Suganthy, M., et al. (2021). Organic farming research in India: Potential technologies and way forward. *Indian J. Agron.* 66, S142–S162. https://www.researchgate.net/publication/356000991.

Ravisankar, N., Ansari, M. A., Shamim, M., Prusty, A. K., Singh, R., Panwar, A. S., et al. (2022). Sustainable livelihood security of small farmers improved through a resilient farming system in the semiarid region of India. *Land Degrad. Dev.* 33, 2830–2842. doi:10.1002/ldr.4358

Sengupta, R. (2021). Land degradation in India hurts farmers and forest dwellers the most. Avaliable At: https://www.downtoearth.org.in/news/environment/land-degradation-in-india-hurts-farmers-and-forest-dwellers-the-most-78701.

Shahid, M., Nayak, A. K., Shukla, A. K., Tripathi, R., Kumar, A., Mohanty, S., et al. (2013). Long-term effects of fertilizer and manure applications on soil quality and yields in a sub-humid tropical rice-rice system. *Soil Use Manag.* 29, 322–332. doi:10.1111/sum.12050

Sharma, S. K., Ravisankar, N., Chander, M., Jat, G., Choudhary, R., Kumar Fagodiya, R., et al. (2021). Organic agriculture under changing climate scenario. *Indian J. Agron.* 66, S82–S94. https://www.researchgate.net/publication/362491232.

Sihi, D., Dari, B., Yan, Z., Sharma, D. K., Pathak, H., Sharma, O. P., et al. (2020). Assessment of water quality in Indo-Gangetic Plain of South-Eastern Asia under organic vs. conventional rice farming. *Water* 12, 960. doi:10.3390/w12040960

Song, X., Tao, B., Guo, J., Li, J., and Chen, G. (2018). Changes in the microbial community structure and soil chemical properties of Vertisols under different cropping systems in Northern China. *Front. Environ. Sci.* 6, 132. doi:10.3389/fenvs.2018.00132

Stagnari, F., Maggio, A., Galieni, A., and Pisante, M. (2017). Multiple benefits of legumes for agriculture sustainability: An overview. *Chem. Biol. Technol. Agric.* 4, 2. doi:10.1186/s40538-016-0085-1

Suárez, R. P., Goijman, A. P., Cappelletti, S., Solari, L. M., Cristos, D., Rojas, D., et al. (2021). Combined effects of agrochemical contamination and forest loss on anuran diversity in agroecosystems of east-central Argentina. *Sci. Total Environ.* 759, 143435. doi:10.1016/j.scitotenv.2020.143435

Subbiah, B. V., and Asija, C. L. (1956). A rapid procedure for estimation of available nitrogen in soils. *Curr. Sci.* 25, 259–260.

Tripathi, S., Srivastava, P., Devi, R. S., and Bhadouria, R. (2020). "Influence of synthetic fertilizers and pesticides on soil health and soil microbiology," in *Agrochemicals detection, treatment and remediation pesticides and chemical fertilizers* Editor M. N. V. Prasad. (Oxford, United Kingdom: Butterworth Heinemann, Elsevier Ltd), 25–54. doi:10.1016/B978-0-08-103017-2.00002-7

Vance, E. D., Brookes, P. C., and Jenkinson, D. S. (1987). An extraction method for measuring soil microbial biomass C. *Soil Biol. Biochem.* 19 (6), 703–707. doi:10.1016/0038-0717(87)90052-6

Walkley, A., and Black, I. A. (1934). An examination of the Degtjareff method for determining soil organic matter and a proposed modification of the chromic acid titration method. *Soil Sci.* 37, 29–38. doi:10.1097/00010694-193401000-00003

Yadav, G. S., Babu, S., Das, A., Mohapatra, K. P., Singh, R., Avasthe, R. K., et al. (2020). No till and mulching enhance energy use efficiency and reduce carbon footprint of a direct-seeded upland rice production system. *J. Clean. Prod.* 271, 122700. doi:10.1016/j.jclepro.122700

Yadav, G. S., Das, A., Kandpal, B. K., Babu, S., Lal, R., Datta, M., et al. (2021). The food-energy-water-carbon nexus in a maize-maize-mustard cropping sequence of the Indian Himalayas: An impact of tillage-cum-live mulching. *Renew. Sustain. Energy Rev.* 151, 111602. doi:10.1016/j.rser.2021.111602

Yuan, B. C., and Yue, D. X. (2012). Soil microbial and enzymatic activities across a chronosequence of Chinese pine plantation development on the Loess Plateau of China. *Pedosphere* 22 (1), 1–12. doi:10.1016/S1002-0160(11)60186-0

frontiers | Frontiers in Environmental Science

TYPE Original Research
PUBLISHED 13 October 2022
DOI 10.3389/fenvs.2022.1002902

OPEN ACCESS

EDITED BY
Carlos Marcelo Scavuzzo,
National Space Activities Commission, *Argentina*

REVIEWED BY
Hao Liu,
Shandong University, China
Yuanyuan Zhao,
Beijing Forestry University, China

*CORRESPONDENCE
Ji Yang,
yangji@gdas.ac.cn
Wumeng Huang,
huangwumeng@gdas.ac.cn

†These authors have contributed equally to this work and share first authorship

SPECIALTY SECTION
This article was submitted to Land Use Dynamics,
a section of the journal
Frontiers in Environmental Science

RECEIVED 25 July 2022
ACCEPTED 26 September 2022
PUBLISHED 13 October 2022

CITATION
Chen W, Jiang C, Wang Y, Liu X, Dong B, Yang J and Huang W (2022), Landscape patterns and their spatial associations with ecosystem service balance: Insights from a rapidly urbanizing coastal region of southeastern China. *Front. Environ. Sci.* 10:1002902.
doi: 10.3389/fenvs.2022.1002902

Landscape patterns and their spatial associations with ecosystem service balance: Insights from a rapidly urbanizing coastal region of southeastern China

Weilian Chen[1†], Chong Jiang[1,2†], Yixin Wang[3], Xiaoding Liu[4], Binbin Dong[4], Ji Yang[1,2]* and Wumeng Huang[1,2]*

[1]Guangzhou Institute of Geography, Guangdong Academy of Sciences, Guangzhou, China, [2]Southern Marine Science and Engineering Guangdong Laboratory (Guangzhou), Guangzhou, China, [3]State Key Laboratory of Hydrology-Water Resources and Hydraulic Engineering, Hohai University, Nanjing, China, [4]Surveying and Mapping Institute, Lands and Resource Department of Guangdong Province, Guangzhou, China

Abstract: Assessing ecosystem service (ES) balance and exploring critical drivers are crucial for landscape management. However, a lack of understanding of the determinants of the ecosystem service supply–demand budget, their spillover effects, and spatial variabilities offsets the efficacy of landscape planning and ecosystem conservation. This novel study attempted to close this gap by quantifying ecosystem service budget using an expert knowledge-based supply–demand matrix and explored its dependencies through spatial econometrics and geographically weighted regression approaches instead of using ordinary model simulation and conventional statistical analysis. The overall patterns of ecosystem service balance in the southeastern coast were found to have remained stable in 1980, 2000, and 2017, although remarkable ecosystem service deficits were identified in hotspots of rapid urbanization. The ecosystem service balance was negatively associated with the proportions of built-up land and cropland ($p < 0.0001$) and exhibited positive associations with the proportions of woodland and grassland ($p < 0.0001$). Landscape structure and population density were identified as the primary determinants of ecosystem service balance and exhibited spatial variability and spillover effects (i.e., determining ecosystem service balance in both individual and adjacent units). These findings demonstrate the significance of spatial disparities and external effects of determinants of the supply–demand budget in integrative landscape governance. Consequently, localized and targeted strategies for landscape planning are increasingly needed to optimize landscape configuration and alleviate ecosystem service imbalance according to individual socioeconomic conditions and landscape structures. In addition, the spillover effects demonstrate that the maintenance of regional ecosystem service balance and ecosystem sustainability depends not only on individual areas but also on cross-regional collaborations with neighboring regions. These findings have critical implications on strategy formulation for coastal landscape management and ecosystem sustainability.

KEYWORDS

ecosystem service, supply-demand balance, spatial determinant, spillover effect, coastal area

1 Introduction

Ecosystem services (ESs) link social systems and natural ecosystems and play extremely important roles in sustaining human survival and well-being and achieving sustainable development goals through optimized environmental management (Costanza et al., 2017; Mandle et al., 2020). An integrated ES assessment involves the supply and demand of ESs, which reflect the supply capacity of natural ecosystems and the actual demands required or desired by human society, respectively (Burkhard et al., 2012, 2014). Existing studies have mostly focused on quantifying and mapping the supply potential of natural ecosystems through multiple indicators, frameworks, biophysical models, and economic valuation approaches (e.g., Chaplin-Kramer et al., 2019; Ouyang et al., 2020; Zhang et al., 2021) and identifying the climatic, topographical, vegetation, socioeconomic, and landscape variables that determine the ES supply capacity (e.g., Turpie et al., 2017; Wilkerson et al., 2018). However, in comparison with the supply side, ES demand has not received sufficient attention, and the quantification framework is not well established (Costanza et al., 2017; Tao et al., 2018; Mandle et al., 2020).

An integrated ES assessment that incorporates the demand aspect into assessment can effectively identify the mismatch between supply and demand, support policy formulation and decisions regarding ES management, and balance the spatial and temporal disparities in the supply–demand budget (Castillo-Eguskitza et al., 2018; Chaplin-Kramer et al., 2019). In the past decade, a series of studies have attempted to integrate the demand aspect into ES assessment by quantifying and comparing specific indicators, including carbon sequestration, soil erosion control, hydrological regulation, food provision, and cultural services, in a particular ecosystem category (e.g., Campagne et al., 2018; Ma et al., 2019; Liu et al., 2020). Multiple approaches, including expert knowledge (Sun et al., 2020; Jiang et al., 2021a), questionnaire surveys (Castillo-Eguskitza et al., 2018), monetary value (Liu et al., 2021; Wang et al., 2021), and model simulation (Larondelle and Lauf, 2016; Yu et al., 2021; Zhang et al., 2021), have been adopted to quantify both sides of ESs. In particular, the level of demand for ESs by communities and residents in Spain was quantified through a questionnaire survey (Castillo-Eguskitza et al., 2018). Peng et al. (2020) investigated the spatial disparities in supply–demand balance based on the land use and land cover (LULC) category and expert knowledge in rapidly expanding city clusters in southern China. Chaplin-Kramer et al. (2019) projected the future supply and demand of ESs on a global scale based on model simulation and scenario analysis. The applicability of these methods varies in different cases according to data requirements and parameter settings. The model simulation approach largely relies on input parameters and spatially explicit data; thus, it is normally limited by data accessibility (Blanco et al., 2017). Although theoretically feasible for community- and county-scale studies, a questionnaire survey is not practically suitable for regional or continental assessments (Burkhard et al., 2014). The monetary value approach normally reflects the total value of ESs without a good spatially explicit representation that can reveal the spatial mismatches of supply and demand sides (Liu et al., 2021; Wang et al., 2021).

Additionally, ES supply generally reflects the beneficial function supplied by natural ecosystems through a combination of biophysical indicators, whereas ES demand is normally indicated by preferences, perceptions, market values, and actual consumption; thus, different measurement units constrain the direct comparison of both sides (Burkhard et al., 2014; Peng et al., 2020). The empirical knowledge method assumes that landscape patterns (i.e., LULC categories) determine ecological functions and ESs and then alter the supply–demand relationship. A proposed supply–demand matrix model takes the LULC category as a proxy and utilizes (semi-)empirical expert knowledge to quantify the supply–demand balance (Burkhard et al., 2014). Although this approach does not establish complete quantification methodologies, it can quickly obtain relatively reliable results without relying on complex models and input parameters, particularly for the assessment of cultural services (Sun et al., 2020).

For the optimization of landscape configuration and maintenance and enhancement of ecosystem sustainability, revealing the driving factors and influencing mechanisms of the ES supply–demand budget is as crucial as that of ES budget quantification (Sun et al., 2020; Jiang et al., 2021a). The formation, delivery, and circulation of matter and energy within a certain space (e.g., coenobium, ecosystem, watershed, and administrative unit) exhibit spillover effects on neighboring regions because the landscape compositions and biophysical/biogeochemical processes are interconnected (Li et al., 2019a; Li et al., 2019b; Zhang et al., 2022). Thereby, spatial attributes and spillover effects are supposed to be sufficiently revealed and integrated into landscape conservation and environmental governance (Wang et al., 2021; Zhang et al., 2021). However, previous literature lack sufficient understanding of geographic variations in the determinants of ES budgets and their spatial dependences and spillover effects (Chi and Ho, 2018). These findings have largely focused on individual units or local scales and neglected the spatial variability of important determinative factors from a regional perspective (Wang et al., 2021; Zhang et al., 2021). Moreover, the spillover effects of determinants have not been examined by commonly adopted statistical approaches, such as the least squares approach (Li et al., 2019a; Li et al., 2019b), random forest model (Liu et al., 2021), structural equation simulation (Jiang et al., 2021b), linear regression analysis (Wang et al., 2021), and other conventional econometric models (LeSage et al., 2009), because the spatial information is not taken into account in these models (Chi and Ho, 2018). Consequently, the external effects of determinants on strategy formulation in terms of landscape management have rarely been revealed (Jiang et al., 2021a; Zhang et al., 2022).

The southeastern coastal area of China has been characterized by rapid economic development, urban sprawl, and population expansion over the past 4 decades, which has led to inappropriate agricultural reclamation, deforestation, and other development and construction practices (Jia et al., 2018). This region suffers from the degradation of ecological function and resource scarcity as well as a severe mismatch and imbalance between the supply and demand of ESs (Zhang et al., 2021). We selected coastal areas as a case study to reveal the spatiotemporal evolution of the ES budget and identify the determinants and their spillover effects. Considering the limitations and knowledge gaps in existing literature, the main objectives of the current study were 1) to identify the spatial disparities of ES budgets for three important time nodes (1980, 2000, and 2018) based on the supply–demand matrix proposed according to expert knowledge, and discuss their responses to human disturbance and policy intervention-induced changes in landscape compositions; 2) to determine the critical dependences of the ES budget and their spatial disparities and spillover effects using spatial econometrics and geographically weighted regression (GWR) approaches; 3) to probe the implications of spatial dependencies of ES balance on the optimization of landscape configuration. The novelty of this study is in revealing the spatial associations of determinants of ES balance, in particular, in terms of their spillover effect and spatial variability, which distinguishes this study from previous studies that use ordinary model simulation and conventional statistical analysis. The research findings are expected to reconcile the mismatch between supply and demand sides of ESs, further improve the efficacy of landscape management, thereby supporting ecosystem conservation and contributing to coastal sustainable development.

2 Materials and methods

2.1 Study site

The study site (Figure 1A) is situated in the southeastern coastal region of China (19° 52′–28° 41′ N, 105° 38′–120° 39′ E), with a rough area of 578,000 km^2 encompassing three provinces (Fujian, Guangdong, and Hainan) and one autonomous region (Guangxi) from Guangxi in the west to Fujian in the east. Most areas within the study region belong to the southern subtropics, and a small part of Fujian province belongs to the middle subtropics. The subtropical monsoon climate, characterized by a warm climate and sufficient rainfall, breeds a large number of valuable animal and plant resources, and the forest coverage rate in the region is the highest in China (Jia et al., 2018; Chen J et al., 2020; Li et al., 2020). The dominant LULC categories are woodland, cropland, wetland/waterbody, and built-up areas, which are distributed according to topography and landform conditions (Figure 1B). The woodlands and croplands are concentrated around mountainous areas and flatlands, respectively, whereas large urban agglomerations are primarily distributed along the coastal area (Liu et al., 2021; Wang et al., 2021). As one of the dominant ecosystem categories, coastal wetland encompasses two second-level categories including swampland and bottom land, which are comprised of mangrove, coral reef, beach, and intertidal zone, and exhibit important ecological benefits (Liu et al., 2014; Jia et al., 2018). The geographic location of the study region is adjacent to Hong Kong, Macao, and Taiwan; thus, it is the gateway to China's policy of reform and opening up, and its economic development occupies a leading position in the country (Lin et al., 2019; Zhang et al., 2021).

In this important agricultural production and economic development region, intensive or even excessive anthropogenic pressure (e.g., agricultural reclamation, urbanization, and deforestation), along with extreme rainfall and heterogeneous landscapes has led to severe soil erosion, which is the primary cause of land degradation (Chen Y et al., 2020; Li et al., 2020). In the past 4 decades from 1978 to 2017, the southeastern coastal area has experienced rapid economic and population growth, urban expansion, and ecosystem conservation and restoration. Furthermore, land-use transformation has been accelerated by intensive human disturbances and policy interventions, such as wetland reclamation, deforestation, revegetation projects, ecosystem restoration efforts, soil and water conservation measures, and urban landscape projects (Mao et al., 2018a; Mao et al., 2018b; Li et al., 2020; Yu et al., 2021). Land-use transitions, particularly among cropland, woodland, and built-up areas, directly alter ecosystem patterns, ES provision capacity, and potential demand (Peng et al., 2020; Wang et al., 2021; Zhang et al., 2021). In particular, urban expansions around southeastern Guangdong and Fujian provinces have degraded cropland and wetland resources, thereby threatening food and ecological security (Zhang et al., 2018; Chen et al., 2019b). Moreover, regional disparities in economic development and population growth have led to significant differentiation and spatial mismatches between the supply and demand of ESs (Peng et al., 2020; Yu et al., 2021).

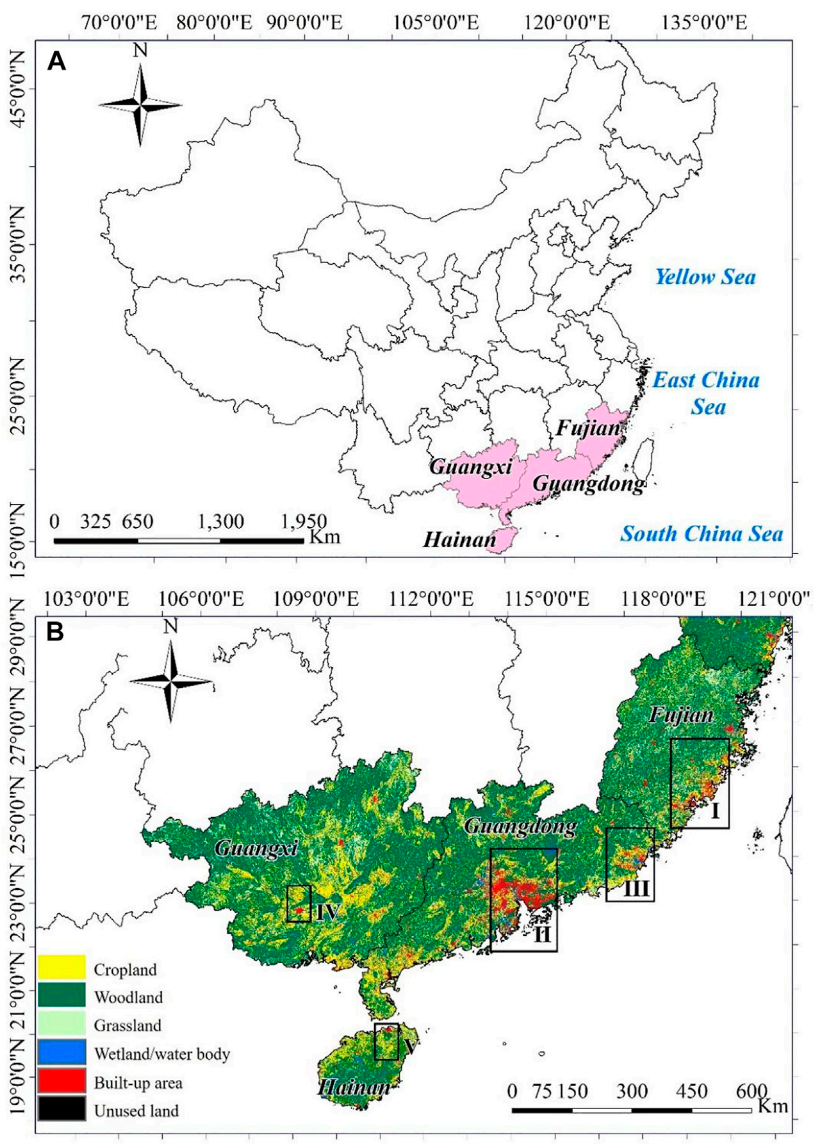

FIGURE 1
(A) Geographic situation of southeastern coastal areas in China and **(B)** LULC compositions in 2017. The five hotspots experiencing rapid urban expansion are identified in **(B)**: (I) Fujian province coastal city cluster (i.e., Xiamen, Zhangzhou, and Quanzhou cities), (II) the Pearl River Delta city cluster (i.e., Guangzhou, Shenzhen, Dongguan, and Foshan cities), (III) Chao-Shan city cluster (i.e., Chaozhou, Shantou, and Jieyang cities), (IV) Nanning city in Guangxi province, and (V) Haikou city in Hainan province.

2.2 Study framework and workflow

Landscape structure is closely associated with ecological processes and functions (Jean et al., 2021), and landscape composition and configuration directly alter ecological processes encompassing material and energy circulation, species migration, hydrological processes, carbon stock, and biodiversity maintenance, eventually resulting in changes in the provision capacity of ESs (Chen et al., 2019a; Chen W et al., 2020; Jean et al., 2021). In addition, human disturbances and policy interventions profoundly alter landscape composition and result in an ES imbalance (Figure 2A). For instance, population migration leads to urban expansion and increases in food and energy demands, thereby further accelerating land-use transformation among woodland, cropland, and urban areas through agricultural reclamation and deforestation practices and ultimately exacerbating the imbalance of ESs and resource scarcity. In contrast, positive policy interventions, such as ecosystem restoration projects, revegetation practices, urban landscape,

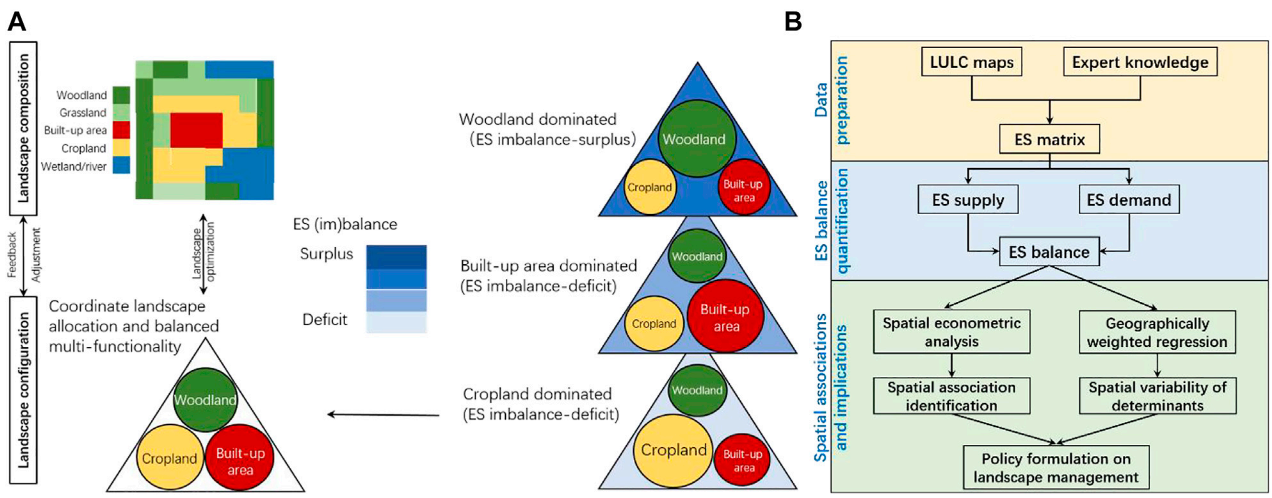

FIGURE 2
(A) Diagram of linkages between the ES balance and landscape composition and **(B)** study workflow. Woodlands, croplands, and built-up areas in the left column were the three dominant landscape categories, accounting for more than 90% of the total area, and were closely associated with ES supply, demand, and balance. The evolution of landscape composition and the associated ES balance are illustrated in **(A)** and Supplementary Figure S1.

and catchment management projects cause vegetation restoration and considerable changes in ecosystems, which maintain the supply capacity and enhance landscape sustainability (Yuan et al., 2019; Jiang et al., 2021a). Different landscape structures (Supplementary Figure S1) have been demonstrated to profoundly influence the material transportation, formation, and delivery of ESs (Lee et al., 2015). Specifically, the structures that are centralized, uniform, monotonous, closed, and lacking in connectivity and diversity have adverse effects on the formation and accessibility of ESs, whereas complex and diverse shapes are beneficial for biodiversity maintenance (Jean et al., 2021).

Landscape metrics encompassing patch density (PD), landscape shape index (LSI), aggregation index, and Shannon's diversity index (SHDI), are effective and critical indicators that reflect landscape composition, structure, shape, and fragmentation, and diversity, respectively, and have been applied worldwide in landscape planning and related fields (Mitchell et al., 2015; Ayinuer et al., 2018). For definitions and calculation formulas of landscape metrics, refer to McGarigal et al. (2012). In addition, socioeconomic variables, including population density (POPD) and gross domestic product, which indicate the intensity of human activities in the social system, also directly and indirectly respond to ESs and represent the promotion or restriction impacts of ecosystems on socioeconomic development (Wang et al., 2021; Yu et al., 2021). Thereby, we selected a group of landscape and socioeconomic variables as explanatory variables to explain the evolution of the ES balance and explore the spillover effects of spatial determinants, as presented in Figure 2B.

2.3 Datasets and methodologies

2.3.1 Data preparation

LULC datasets with a resolution of 30 × 30 m for three periods (1980, 2000, and 2017), interpreted from moderate-resolution satellite images, were derived from the Resource and Environment Data Cloud Platform (Liu et al., 2014). These datasets were produced by combining visual interpretation and machine learning techniques based on relatively high-quality images obtained from Landsat Multispectral Scanner, Thematic Mapper, Enhanced Thematic Mapper Plus, and Operational Land Imager sensors. Cross-validation through pixel checking and field validation showed that the overall accuracy for interpretation reached 92%, which is capable of capturing landscape pattern changes for regional-scale studies and has been widely applied for ecosystem assessment and ES quantification as well as in other research fields (Liu et al., 2014; Jiang et al., 2021a; Wang et al., 2021). In southeastern coastal areas as shown in Figure 1B, the first-level LULC categories encompass cropland, woodland, grassland, wetland/waterbodies, artificial surface/built-up areas, and unused land/bare land, and the second-level categories include more than 20 sub-categories; for more details on the definitions of each category and technical details for interpretation, refer to Liu et al. (2014). In addition, spatial datasets on demographic and economic attributes, with a resolution of 1 × 1 km, were derived and applied to reflect POPD and economic development changes from 1980 to 2017 (i.e., 1980, 2000, and 2017). These datasets were generated based on the significant spatial regression relationship between statistical records and nighttime stable light data derived by the Defense Meteorological Satellite Program Operational Line-scan System sensor for the years 1980–2015 (Liu et al., 2005). To avoid inconsistencies and uncertainties arising from different projection systems and spatial resolutions of LULC maps and socioeconomic indicator datasets, this study unified the coordinate and projection systems and spatial resolution (i.e., 1 × 1 km) via projection transformation and resampling tools, respectively, on ArcMap Platform (Version 10.3).

2.3.2 Quantification of ecosystem service supply–demand budget

This study applied the supply–demand budget matrix to derive the ES supply, demand, and budget indexes (ESSI, ESDI, and ESBI, respectively) of regulating, provisioning, and cultural ESs for the three time nodes over the past 4 decades. Supply and demand matrices for eighteen LULC categories and twenty-three ES categories were created on the basis of the matrix proposed and developed by Burkhard et al. (2012), Burkhard et al. (2014), with the original matrix adjusted according to expert knowledge for a specific research area (Supplementary Figure S2). The detailed process was as follows: First, because of the different LULC classification systems, we integrated the ESSI, ESDI, and ESBI proposed by Burkhard et al. (2012) by consolidating similar LULC categories. Second, more than thirty papers involving ES matrix, in particular on southern China, were collected and reviewed (e.g., Cai et al., 2017; Ou et al., 2018; Tao et al., 2018; Chen J et al., 2020; Peng et al., 2020; Jiang et al., 2021a), and the scores for entries were assigned according to these studies. The score for each entry indicates supply/demand level of individual ES, the greater is the ESSI/ESDI, the higher is the supply/demand. Then, a group of experts holding doctoral degrees, including more than 25 scholars from related fields, such as ecology, environment, hydrology, biology, and botany, of different research institutions, communities, and non-governmental organizations were requested to score matrix entries individually based on their understanding of the definitions involved in the matrix. Allowing for the relatively extensive disciplinary background, we specifically invited ten additional experts from different fields of ES research, including carbon sequestration, soil and water conservation, biodiversity conservation, climate regulation, water and soil purification, and cultural services (e.g., cultural education and recreation) for scoring. All these experts had good background knowledge and research experience in ecological, geographical, and environmental sciences in southeastern China, which guaranteed an objective and fair evaluation of criteria (Peng et al., 2020). Finally, we organized three rounds of panel discussions to reach an agreement on the final scores for the matrices. Three ES balance indexes were calculated according to the following equations:

$$ESSI = \sum_{v=1}^{o}\sum_{u=1}^{p}(A_u \times S_{uv}) \Big/ \sum_{u=1}^{p} A_u \tag{1}$$

$$ESDI = \sum_{v=1}^{o}\sum_{u=1}^{p}(A_u \times D_{uv}) \Big/ \sum_{u=1}^{p} A_u \tag{2}$$

$$ESBI = \sum_{v=1}^{o}\sum_{u=1}^{p}(A_u \times B_{uv}) \Big/ \sum_{u=1}^{p} A_u \tag{3}$$

where S_{uv}, D_{uv}, and B_{uv} are the supply, demand, and budget matrices, respectively, of the *vth* ES category of the *uth* LULC category; A_u represents the area of the *uth* LULC type; and *p* and *o* denote the number of LULC and ES categories, respectively.

2.3.3 Model for spatial spillover effects of the determinants of ecosystem service balance

We applied spatial econometric models (SECMs) to determine the associations, including spillover effects, between ESBI and drivers. Conventional econometric models (such as logistic regression and multiple regression approaches) are completely dependent on the over-idealized assumptions that suggest all involved variables are independent, stationary, and structurally stable (LeSage et al., 2009). Moreover, conventional econometric analyses rarely take the spatial correlations of independent variables into account, which results in inaccurate conclusions (Chaurasia et al., 2020). By contrast, SECMs consider the spatial associations between individual and other variables, under the premise that many socioeconomic and biophysical variables (e.g., population, trade, infrastructure, carbon emission, resource consumption, ESs, and biomass) are spatially related and closely interconnected (Cai et al., 2021). As presented in Fig. S3, the Moran's I scatterplots of the ESBI in four provinces/region and three periods presented close correlations with the values of Moran's I larger than 0.55, featured by spatial aggregations of ESBIs. A majority of the ESBIs concentrated in the first and third quadrants, implying that the distributions of ES deficit/surplus tend to be adjacent and spatially autocorrelated; thereby, conventional econometric analyses cannot be applied in this case. Consequently, multiple SECMs, encompassing the spatial lag model (SLM), spatial error model (SEM), and spatial Durbin model (SDM) (LeSage et al., 2009), were applied to identify the spillover effects of determinants on the ESBI. The primary formulas are expressed as follows:

$$Ln\,ESBI_{it} = \alpha\beta\, Ln\,ESBI_{it} + \gamma_i LnX + \gamma_0 + \sigma_{it} \tag{4}$$

$$Ln\,ESBI_{it} = \gamma_0 + \gamma_i LnX + \sigma_{it}, \sigma_{it} = \mu\beta\sigma + \epsilon_{it} \tag{5}$$

$$Ln\,ESBI_{it} = \alpha\beta\, Ln\,ESBI_{it} + \gamma_0 + \gamma_i LnX + \theta_i\beta LnX + \sigma_{it} \tag{6}$$

where α means the significance of the autocorrelation of the ESBI between individual and adjacent units; LnX represents the socioeconomic and landscape variables that determine the ESBI; β $LnESBI_{it}$ and β LnX denotes the spatial lag terms of the observation and explanatory variables, respectively (i.e., the external effect from adjacent units); μ, ϵ_{it}, and σ_{it} are the autocorrelation, random error, and disturbance terms, respectively; θ_i indicates the coefficient of $\beta\ LnX$ that needs to be derived; β represents the weight matrix.

Specifically, the partial differential approach (Elhorst, 2014) was utilized to quantify the direct and indirect effects (i.e., spatial spillover effects) of the associated variables on the ESBI. Thus, the SDM is written as follows:

$$ESBI_t = (I_n - \alpha W)^{-1}(X_t\gamma + WX_t\theta) + (I_n - \alpha W)^{-1}\sigma_t^* \quad (7)$$

where I_n indicates the Moran's I index (Dall'erba, 2009) and σ_t^* is the error term. The partial differential formula of the observation variable to the kth explanatory variable in different spatial units (X_{jk} for $j = 1, \ldots, M$) at an individual time is written as below:

$$\left[\frac{\partial ESBI}{\partial X_{1k}} \cdots \frac{\partial ESBI}{\partial X_{Nk}}\right]_t = (I - \alpha W)^{-1}\begin{bmatrix} \gamma_k & \beta_{12}\theta_k & \cdots & \beta_{1N}\theta_k \\ \beta_{21}\theta_k & \gamma_k & \cdots & \beta_{2N}\theta_k \\ \beta_{N1}\theta_k & \beta_{N2}\theta_k & \cdots & \gamma_k \end{bmatrix} \quad (8)$$

The diagonal and the row or column of the non-diagonal terms reflect the direct and indirect effects of the explanatory variables on the ESBI, respectively. The former and latter represent the effects of changes in an explanatory variable on the ESBI in individual and adjacent units, respectively (Meng et al., 2021).

2.3.4 Model comparison and validation

To examine the effects of spatiotemporal variation (i.e., heterogeneity) of independent variables on dependent variables, the geographically and temporally weighted regression (GTWR) approach (Fotheringham et al., 1998; He and Huang, 2018) was used to identify the spatiotemporal associations between the ES supply–demand budget and socioeconomic and landscape variables (Cai et al., 2021). The fundamental formulas are as follows:

$$Y_i = \alpha_0(u_i, v_i) + \sum_{j=1}^{m}\alpha_j(u_i, v_i)x_{ij} + \delta_i \quad (9)$$

$$\alpha_j(u_i, v_i) = \left(M^T V(u_i, v_i)M\right)^{-1} M^T V(u_i, v_i)y_i \quad (10)$$

where $Y_i$denotes the dependent variable (i.e., ESBI); $\alpha_0(u_i, v_i)$ and α_j denote the intercept and regression coefficient for variable j in county i, respectively; (u_i, v_i) represents the coordinates of the geographic center of gravity; m is the number of explanatory variables; δ_i is a residual term; M and M^T are the independent variables and transposed matrixes, respectively; $V(u_i, v_i)$ is the spatial weight matrix. As shown in Supplementary Table S1, in contrast to ordinary least squares and GWR, GTWR performs better in capturing the effects of spatiotemporal heterogeneity in independent variables, because the overall assessment results, indicated by R^2, of GTWR for three periods are larger than those of the other two models.

To minimize the effect of the multicollinearity of independent variables (i.e., landscape metrics and socioeconomic variables) on spatial econometric analyses, this study tested the multicollinearity before linear regression through the variance inflation factor (VIF; Zheng, 1995), which denotes the possibility of collinearity between explanatory variables. The calculation formula for VIF is expressed as follows:

$$VIF = \frac{1}{1 - r_i^2} \quad (11)$$

where r_i represents the coefficient of correlation between the independent variable i and the other explanatory variables. When the VIF is less than 10, multicollinearity does not significantly influence the performance of the regression model. As shown in Table 1, the VIF values were less than 10, indicating that multicollinearity did not exist between the explanatory variables.

3 Results

3.1 Landscape dynamics and evolution of the ecosystem service supply–demand budget

In the three time nodes of 1980, 2000, and 2017, the overall patterns of landscape composition in the four provinces/region remained stable, except for some hotspots of rapid urban expansion (Figure 3). The narrow coastal zone of Fujian province experienced rapid land-use transformation from croplands, including agricultural ponds and wetlands, to urban areas (Figure 3A). In Guangdong province, the two large urban agglomerations around the northeast and southeast along the coastal area (Chao-Shan and the Pearl River Delta city clusters in Figure 1B) also expanded rapidly, which accelerated the loss of wetlands and agricultural ponds, particularly of mangrove, coral reef, beach, and intertidal zone in the Pearl River Delta city cluster (Figure 3B). In contrast to those in Fujian and Guangdong, the urbanizing trends of Zones III and IV were not as significant as those of Zones I and II, and Nanning city and Haikou city were situated in the inland and coastal regions, respectively (Figures 3C,D). Similarly, the landscape metrics remained stable for the overall patterns of the three periods (Fig. S4), and substantial landscape changes were identified in coastal hotspots of urbanization.

The ES balance patterns, including the ESSI, ESDI, and ESBI, presented similar patterns as that of landscape composition (Figure 4): the high ESSIs were mainly spatially concentrated in woodlands and grasslands in inland areas, whereas the coastal areas were characterized by strong ES demands (i.e., ESDIs), particularly for rapidly expanding areas. Accordingly, the high and low ESBI values (i.e., ES surplus and deficit, respectively) were situated in the inland and coastal regions, respectively. Specifically, this study focused on the four hotspots of rapid expansion and investigated the temporal changes in the three ES balance indexes (Figure 5). All the ESBIs in the four zones declined substantially, and the different categories of ESs and

TABLE 1 Summaries of the ESBI and explanatory variables for 1980, 2000, and 2017.

Dependent and explanatory variables	Unit	Mean value	Standard deviation	Minimum	Maximum	VIF	Moran's I
ESBI	–	41.682	24.533	−60.618	79.000		0.672***
PD	#/100 ha	0.669	0.260	0.208	1.586	9.978	0.572***
SHAPE	–	1.830	0.153	0.788	2.253	3.563	0.459***
ENN	m	470.509	145.521	186.325	2,175.438	1.541	0.201***
IJI	%	57.568	12.579	21.480	89.978	3.061	0.468***
DIVISION	%	0.741	0.178	0.242	0.968	3.953	0.308***
SPLIT	%	6.687	5.407	1.320	39.190	2.661	0.195***
SHDI	–	0.987	0.228	0.441	1.593	6.430	0.536***
'POPD	Persons km^{-2}	875.764	1876.189	42.011	17,636.999	1.571	0.628***

Notes: ***$p \le 0.01$, **$p \le 0.05$, *$p \le 0.1$, the same below. PD: patch density, SHAPE: mean shape index, ENN: mean Euclidian nearest-neighbor distance, IJI: interspersion and juxtaposition index, DIVISION: landscape division index, SPLIT: splitting index, and SHDI: Shannon's diversity index.

total ESs presented increasingly strong demands and weak supply capacity (i.e., high ESDIs and low ESSIs, respectively).

3.2 Spatial associations between the ecosystem service supply–demand budget and landscape structure

As shown in Figure 6, the ES balance indexes were significantly correlated with landscape composition ($p < 0.0001$). The proportions of woodlands and grasslands were positively correlated with ESSI and ESBI but negatively correlated with ESDI. In contrast, both ESSIs and ESDIs in cropland and urban areas presented downward and upward trends, respectively, with increasing proportions, reflecting that woodland and grassland had relatively high ES supply capacities, whereas urban area and cropland presented strong ES demands.

In addition to landscape composition, landscape metrics were also significantly related to ES balance indexes (Figures 7, 8). The number of patches (NP), landscape shape index (LSI), and patch cohesion index (COHESION) were positively correlated with the ESSI, whereas the other metrics presented negative correlations, all of which reached the $p = 0.0001$ significance level. The ESBI also showed a similar correlation with landscape metrics, and positive correlations were observed only in NP, LSI, and COHESION. Both ESSI and ESBI were negatively correlated with POPD, which indicated that population growth weakened ES supply and exacerbated ES imbalance.

SECMs revealed that observation and explanatory variables (i.e., ESBI and associated variables) were significantly correlated, but the regression coefficients in the different models with spatial and time-period fixed effects (STFEs) were different (Table 2). For example, in the SLM and SEM with STFEs and SDM with spatial fixed effects (SFEs), PD, ENN, and SHDI made positive contributions to the ESBI, whereas SHAPE, IJI, and DIVISION negatively contributed to the ESBI; almost all the regressions reached a significance level of $p = 0.01$. In the SDM with time-period fixed effects (TFEs), the regression coefficients of PD, SHAPE, ENN, and SHDI were opposite to those in the other models, including SLM, SEM, and SDM with SFEs and SDM with STFEs. In addition, the GTWR revealed that the spatial determinants of ESBI showed strong variability (Supplementary Figure S5), which depended on the dominant effects of the landscape metrics for specific regions.

The direct, indirect, and total effects of the explanatory variables on ESBIs in local and adjacent locations are listed in Table 3. Direct and indirect effects mean the impact of explanatory variables from local and adjacent locations, respectively. In the SDM, almost all explanatory variables were statistically significant in the regression analyses. For example, the direct and indirect effects (spillover effects) of SHDI were 15.340 and 10.274, respectively, indicating that an increase in SHDI in individual areas resulted in an increase in the ESBI in local and adjacent locations.

4 Discussion

4.1 Spatial determinants of the ecosystem service supply–demand budget

Significant spatial associations between ES balance and explanatory variables embody the importance of landscape metrics in describing spatial composition and configuration, which are associated with ecological, hydrological, and other biophysical and biogeochemical processes (Mitchell et al., 2015; Jean et al., 2021). Specifically, landscape dynamics driven by human disturbances and policy interventions, for instance, urbanization, terrain reconstruction, revegetation projects, and soil and water conservation measures, might prevent or disturb

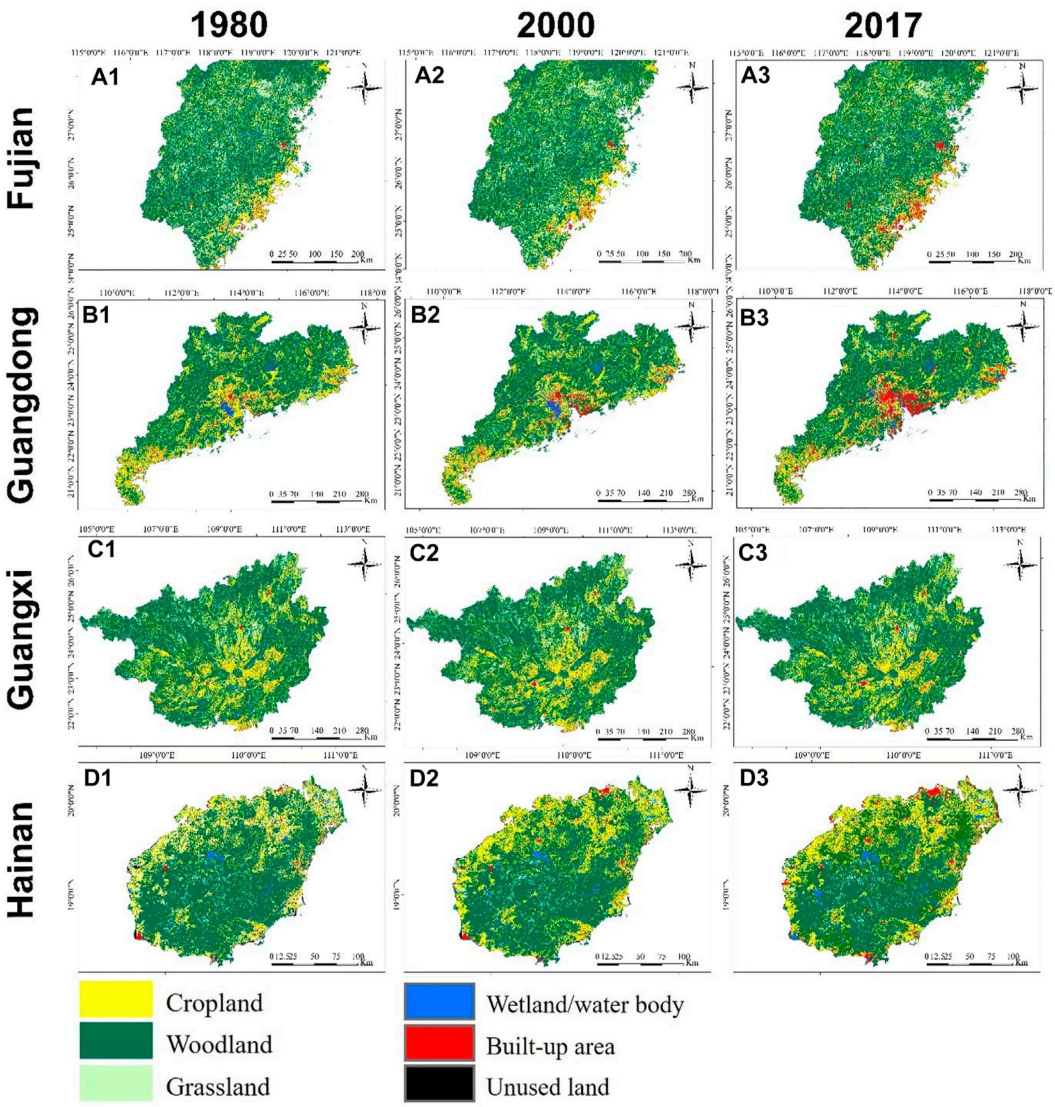

FIGURE 3
Spatial disparities of landscape composition for four provinces/region in the three periods of 1980, 2000, and 2017: **(A)** Fujian, **(B)** Guangdong, **(C)** Guangxi, and **(D)** Hainan.

material circulation and energy transportation and further influence the formation of ESs, such as soil erosion control, hydrological and climatic regulations, and species migration (Jean et al., 2021). For instance, PD reflects landscape fragmentation and intensity of human interventions (McGarigal et al., 2012; Ayinuer et al., 2018). Normally, the areas that feature high human activities are located in urban areas, which have strong demands and low provision capacity of ESs (Peng et al., 2020; Zhang et al., 2021); thus, PD negatively correlates with the ESSI and ESBI (Figures 7, 8). The LSI represents the complexity of patches, and the positive correlation between LSI and ESSI (ESBI) demonstrates that the more irregular the patches are, the smaller the ESBI is. Identifying the spatial relationship between landscape structure and the ES supply–demand balance deepens our understanding of the impact of landscape composition and structure on this balance, which further supports landscape planning and management by monitoring landscape dynamics and optimizing the critical landscape composition and configuration (Mitchell et al., 2015; Chen et al., 2019a; Chen W et al., 2020).

In addition, spatial econometric analyses concluded that neither landscape metrics nor socioeconomic variables are the sole driving factors of ES balance; thus, these factors should be concurrently considered as critical determinants in landscape planning and ES management (Jiang et al., 2020; Yu et al., 2021). The significantly negative correlations ($p < 0.0001$) between ESBI and POPD demonstrated that population growth resulted in a rapid increase in the demand for food, water, energy, and land resources, and ESs, which further promoted land-use transitions, altered supply and demand patterns, and challenged the ES balance (Wang et al., 2021).

Traditional econometric models assume that observation and explanatory variables are spatially independent, whereas geographic location-based variables are typically spatially correlated, and that this spatial characteristic should be carefully considered in regression analyses to reduce inaccurate results (Meng et al., 2021). Spatial econometric analyses consider spatial dependence and spillover effects, which improves the interpretability of spatial autocorrelations and demonstrates that SECMs can be adopted as useful tools to identify the determinative variables of ES budgets (Chen W et al., 2020; Cai et al., 2021; Meng et al., 2021). In addition, GTWR analysis revealed that the primary determinants presented strong spatial heterogeneity in influencing the patterns of supply–demand balance (Supplementary Figure S5), which has also been proved in existing literatures (e.g., Ayinuer et al., 2018; Funes et al., 2019). Landscape planning should allow for spatial variations in critical landscape metrics according to specific locations and formulation of localized and flexible, but not monotonous, policy interventions to optimize the regional landscape and ensure ES balance.

4.2 Implications of research findings for landscape planning and ecosystem service management

Incorporating ES supply and demand perspectives into ES assessment provides a complete and clear understanding of ecosystem evolution and ES dynamics and supports practical benefits for landscape optimization, ES management, and ecosystem conservation (Chen W et al., 2020). Revealing the ES surplus and deficit enables us to understand the impacts of human activity-driven landscape changes on ESs and identify regions that suffer from ES scarcity, and therefore, are not suitable for future exploitation. Furthermore, ES balance indexes can be used as effective indicators or policy tools to direct landscape planning and decisions (Yuan et al., 2019; Jiang et al., 2021a; Zhang et al., 2021).

SECMs identified the primary determinants of ES supply–demand balance and found that landscape composition, fragmentation, shape, and complexity were closely correlated with the ES balance. These determinants

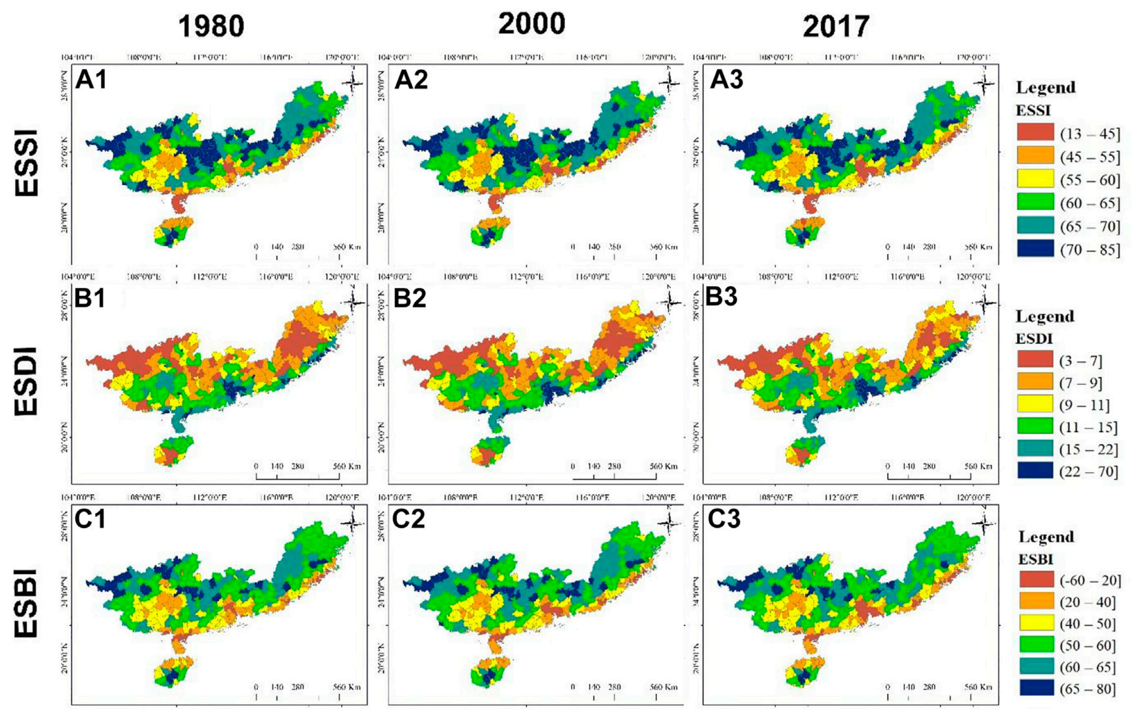

FIGURE 4
Spatial evolution of the **(A)** ESSI, **(B)** ESDI, and **(C)** ESBI of the south-eastern coastal region of China for the three periods of 1980, 2000, and 2017.

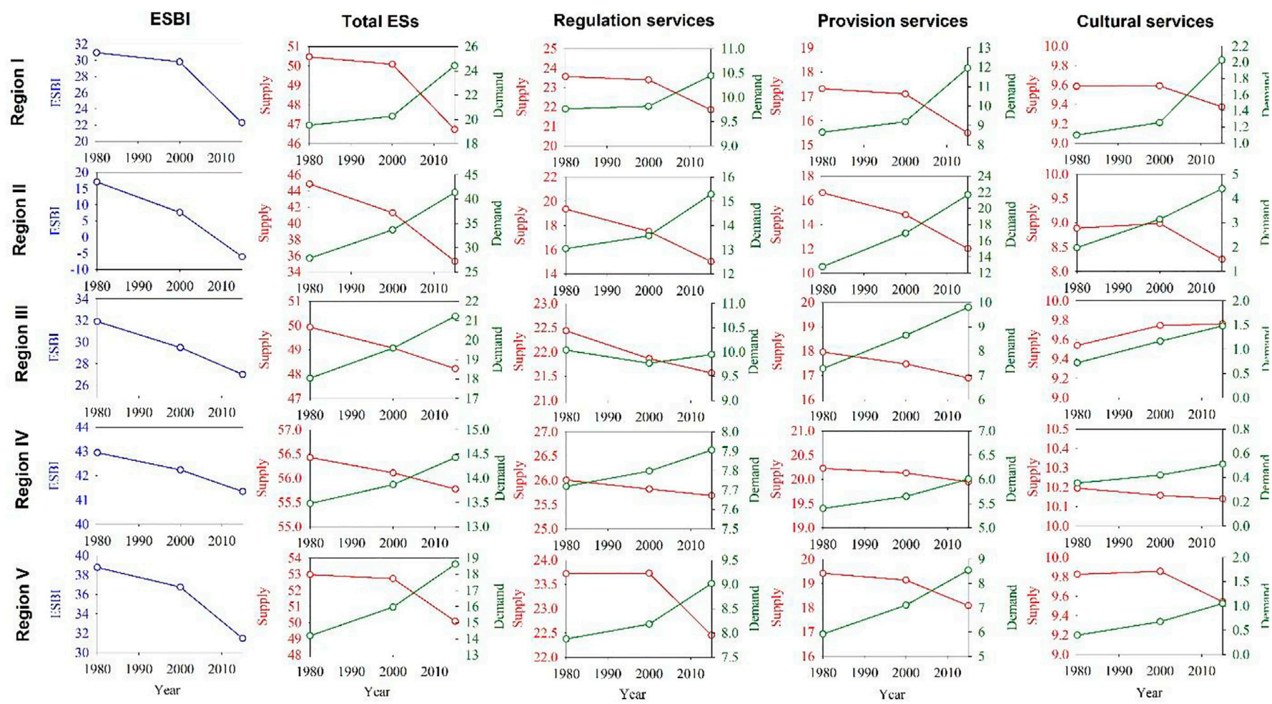

FIGURE 5
Temporal changes in the ESBI and supply and demand of total ESs and different categories of ESs in five hotspots of rapid urbanization. Blue, green, and red lines represent the budget index, supply, and demand of ESs, respectively. For geographic locations of rapidly urbanizing regions, refer to Figure 1B.

should be considered in landscape planning and land-use allocation, particularly for green and blue infrastructure in rapidly expanding urban agglomerations and coastal areas experiencing intensive exploitation. For instance, as shown in Figures 9A–D, the case of Guangzhou city (i.e., one of the city clusters in Zone II of Figure 1B) demonstrated that local environmental management and landscape planning already considered green and blue spaces as important components of urban ecosystems and reserved some spaces for rivers, lakes, forests, grasslands, and wetlands (Mao et al., 2018a; Mao et al., 2018b). These components generate crucial ESs such as air and water purification, climatic regulation, and cultural services, including education, tourism, and recreation (Zhang et al., 2021). However, the spatial allocation of these landscape patches is still not completely appropriate. For instance, one of the most important functions of green and blue spaces in urban agglomerations is to mitigate the heat island effect through the cooling effect of woodlands, grasslands, and wetlands (Liu et al., 2021). However, the parallel distribution of different landscape categories shown in Supplementary Figure S1A4–A5 is not beneficial for heat transportation and air temperature regulation (Zhang et al., 2021). In addition, the concentration and distribution of urban areas (Supplementray Figure S1A1–A3) do not sufficiently allow for the connectivity and diversity of landscape patches and constitute adverse conditions for material transportation, species migration, and delivery of other ESs (Mitchell et al., 2015). Therefore, the diversity, connectivity, and appropriate combination of different landscape categories should be maintained, reallocated, and optimized from the perspective of ES balance and landscape multifunctionality (Supplementray Figure S1A6); Chen W et al., 2020; Sun et al., 2020). However, considering the negative correlations between landscape fragmentation and the ESBI (Figure 8), the patches should be maintained as relatively complete because excessive fragmentation cannot facilitate the maintenance of ES balance.

Specifically, considering the distinctive environmental, socioeconomic, and industrial features of coastal cities, landscape planning and regional development for these areas should conserve and appropriately allocate important landscape elements according to their ecological benefits to maintain regional ES balance and enhance ecosystem sustainability. For instance, coastal mangroves and coral reefs typically have important ecological functions, such as the mitigation of geological and meteorological disasters caused by tsunamis and typhoons (Ren et al., 2019). In addition, the wetland and mangrove ecosystems in urban–rural transition zones primarily support material

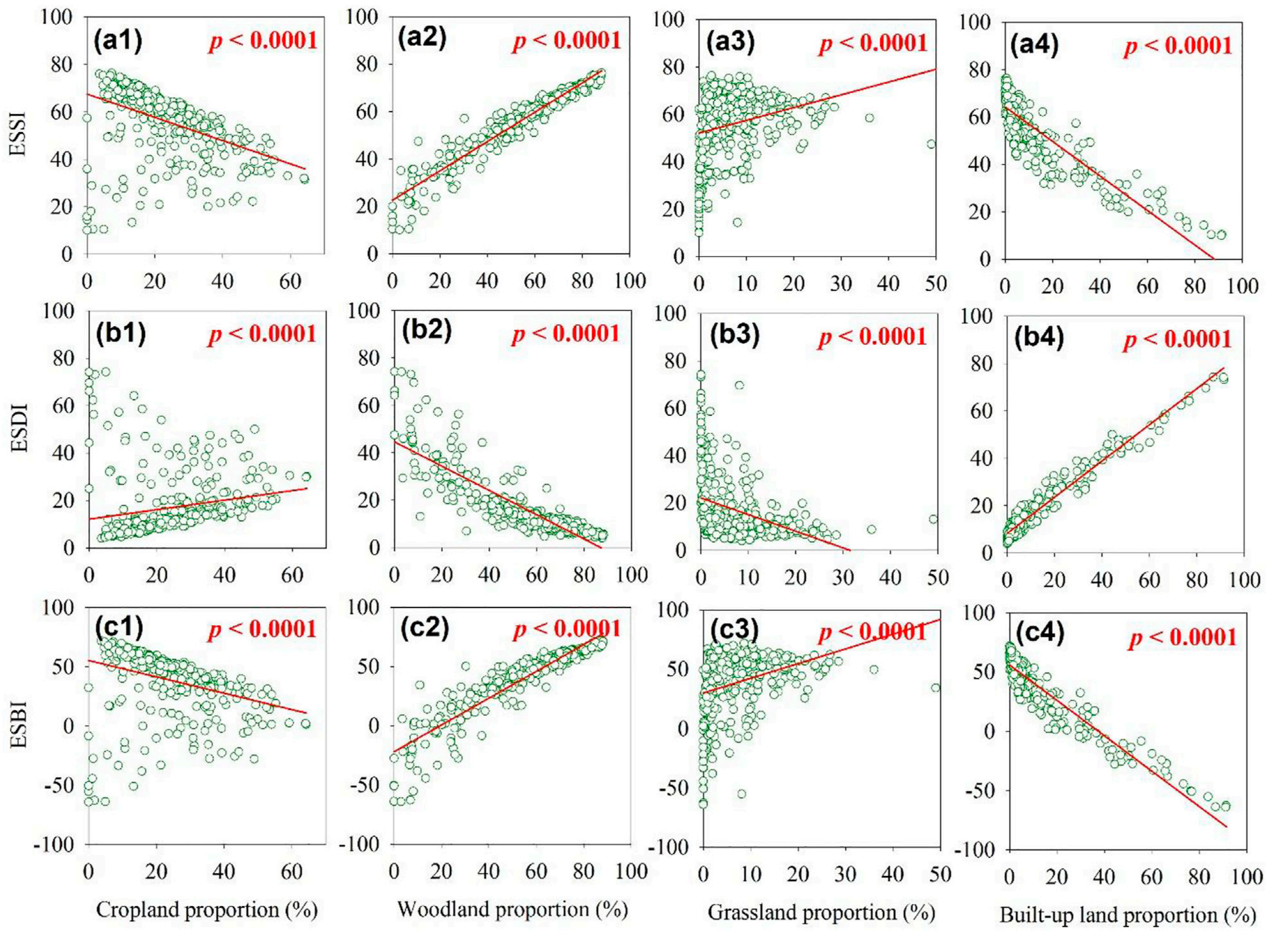

FIGURE 6
Associations between **(A)** ESSI, **(B)** ESDI, and **(C)** ESBI and dominant landscape compositions.

and energy cycles and exhibit important ESs, such as heat island effect mitigation and aquatic purification (Jia et al., 2018). However, commercial exploitation and other inappropriate practices such as mangrove deforestation for aquaculture ponds as well as agricultural pond and wetland losses caused by urbanization and development of tourism industry normally destroy ecosystems, which further weakens ESs and might lead to irreversible damage (Mao et al., 2018a; Mao et al., 2018b; Ren et al., 2019). Therefore, coastal wetlands, mangroves, and coral reefs should be carefully conserved from the perspective of ecosystem connectivity, diversity, and functionality, and their excessive exploitation for commercial purposes and economic benefits, such as by tourism and real estate industries, should be avoided.

Results of the spatial regression analysis shown in Table 3 indicate that the ES balance in specific locations is associated with the ES balance in adjacent regions because of the existence of spatial spillover effects. The underlying explanation is that a specific landscape category is more likely to be converted to another category if it is adjacent to a location that has been converted (Jiang et al., 2020; Cai et al., 2021). Similarly, population growth and economic development in developed regions tend to provide economic benefits and environmental pressures to neighboring regions (Chi and Ho, 2018; Jiang et al., 2020). Urban sprawl and population pressure result in increased energy, resource, and ES demands, which in turn lead to the degradation of the ecosystem and deterioration of the ES balance (Baró et al., 2016; Zhang et al., 2021). To expand the production scale, increase economic profits, and fulfill the requirements of resources and ESs, industries and enterprises that have high resources and ES demands tend to shift from local counties with considerable environmental constraints to adjacent regions with sufficient ES supplies and fewer resource constraints. Thus, the landscape and socioeconomic variables in local areas not only determine the ES balance in local areas but also influence the ES balance in their surrounding regions (Chen et al., 2019a; Chen W et al., 2020). Specifically, spillover effects are clearly presented in urban landscape projects, including catchment governance and soil erosion control

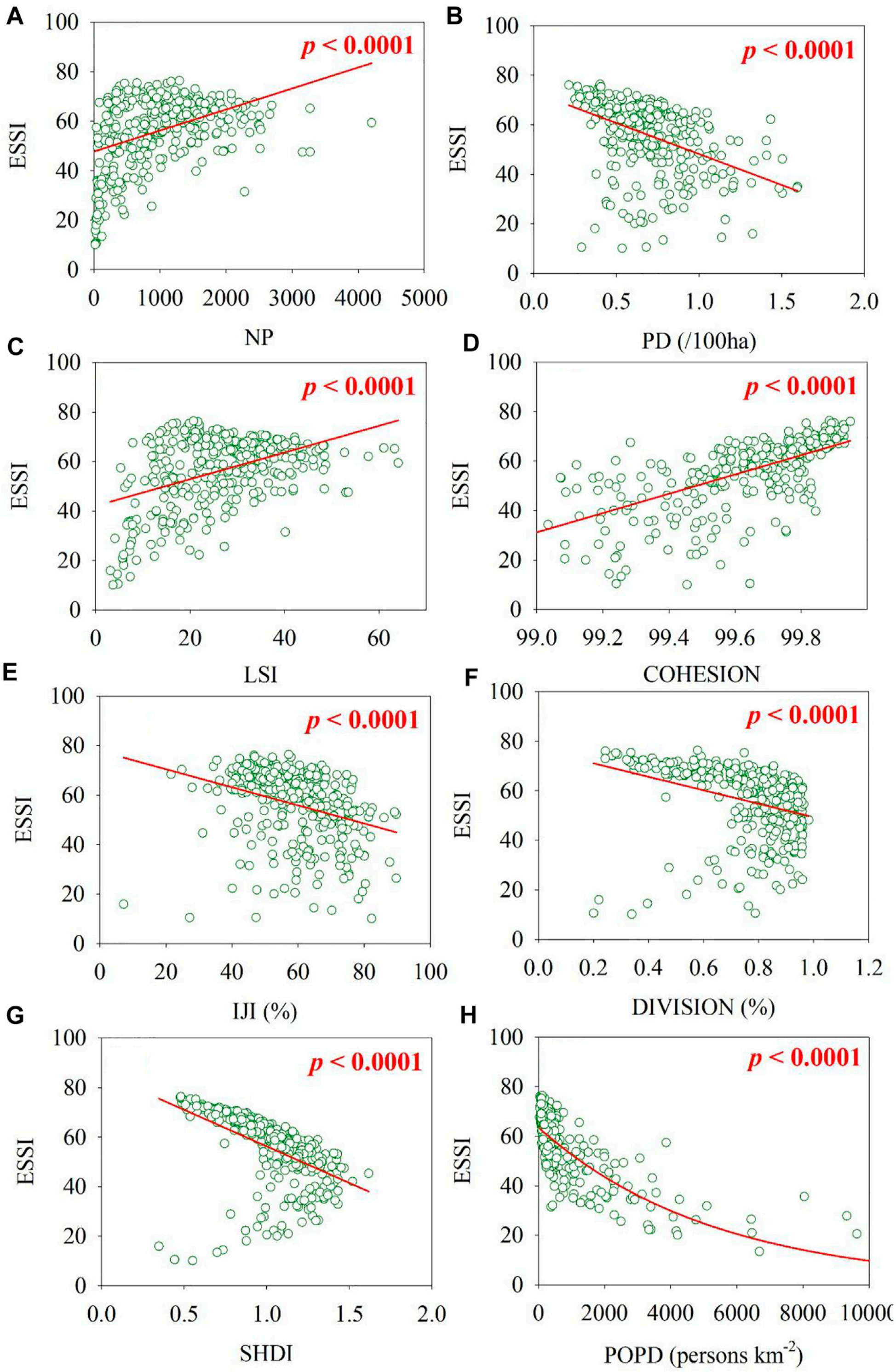

FIGURE 7
Associations between the ESSI and landscape and socioeconomic variables: **(A)** NP, **(B)** PD, **(C)** LSI, **(D)** COHESION, **(E)** IJI, **(F)** DIVISION, **(G)** SHDI, and **(H)** POPD.

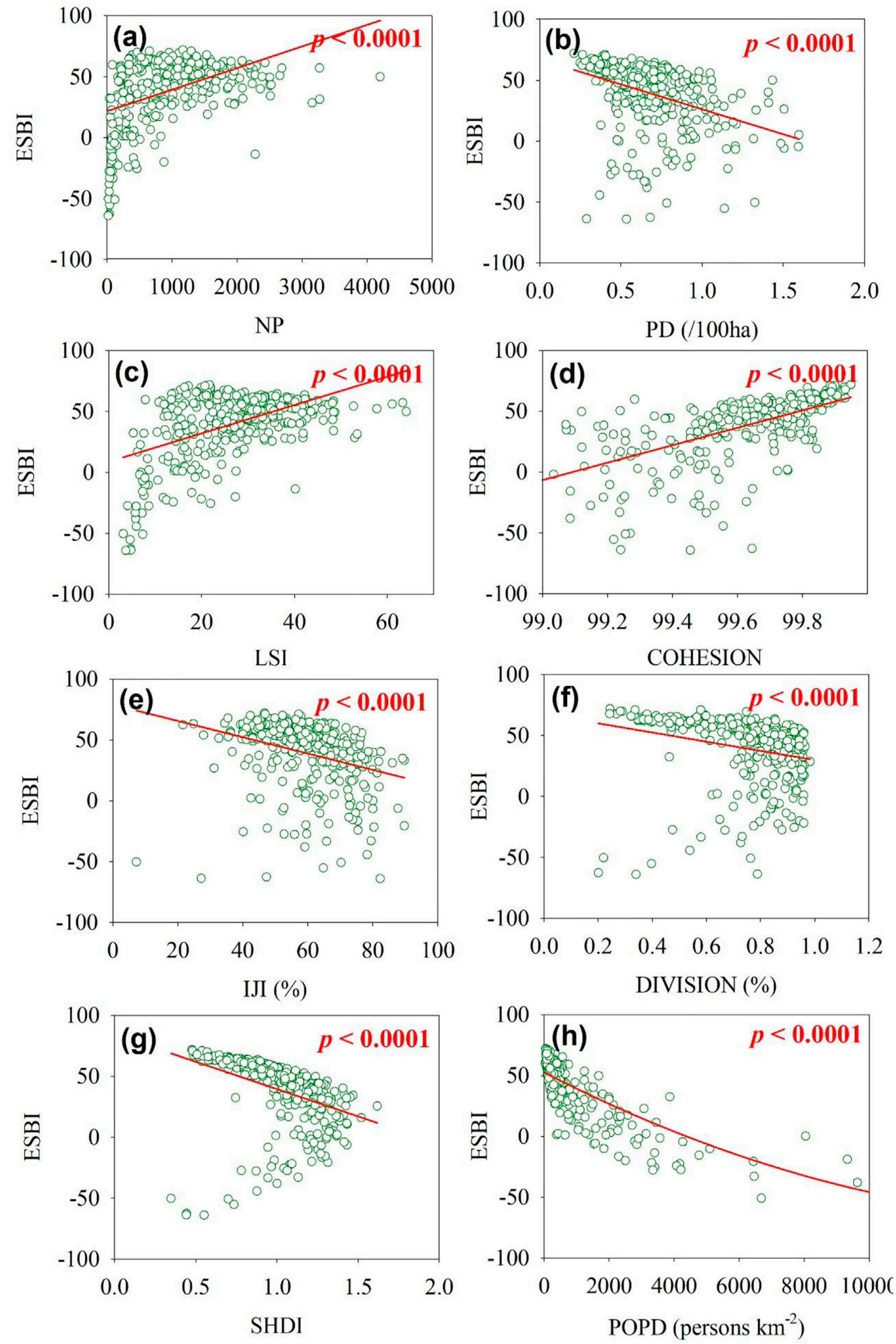

FIGURE 8
Associations between the ESBI and landscape and socioeconomic variables: **(A)** NP, **(B)** PD, **(C)** LSI, **(D)** COHESION, **(E)** IJI, **(F)** DIVISION, **(G)** SHDI, and **(H)** POPD.

TABLE 2 Spatial associations between the ESBI and explanatory variables quantified using the SECMs.

Explanatory variables	SLM (STFEs)	SEM (STFEs)	SDM (SFEs)	SDM (TFEs)	SDM (STFE)
PD	24.298***	27.218***	24.638***	−16.164***	25.191***
SHAPE	−10.973***	−20.209***	−8.346***	20.479***	−6.835**
ENN	0.005***	0.006***	0.006***	−0.0108***	0.006***
IJI	−0.154***	−0.168***	−0.214***	−0.039	−0.196***
DIVISION	−15.438***	−6.288	−12.227***	−3.427	−13.151***
SPLIT	−0.071	0.043	0.010	0.218**	0.013
SHDI	15.331***	18.437***	13.973***	−19.797***	14.629***
POPD	−0.0002**	0.00004	0.0002	−0.0044384	0.0002*
*W**PD			−9.732*	1.103	−12.588**
*W**SHAPE			41.416***	−14.309***	41.248***
*W**ENN			−0.003	−0.015**	−0.003
*W**IJI			0.088	−0.005	0.179**
*W**DIVISION			−23.882***	4.485	−27.256***
*W**SPLIT			−0.26817***	−0.401**	−0.267***
*W**SHDI			−30.296***	0.740	−24.809***
*W**POPD			−0.0026247***	0.002***	−0.002***
*W**ESBI	0.611***		0.449***	0.594***	0.429***
*W**μ		0.728***			
R^2	0.835	0.975	0.925	0.654	0.933
Adjusted R^2	0.833	0.975	0.924	0.646	0.931
σ^2	7.884	7.077	6.243	120.311	6.161
Log-likelihood	−1705.727	−2,944.99	−1,608.933	−2,632.778	−1,602.870

TABLE 3 Direct and indirect effects of explanatory variables on the ESBI quantified using the SDM.

Explanatory variables	Direct effects	Indirect effects	Total effects
PD	26.416***	17.692***	44.108***
SHAPE	−7.168**	−4.801**	−11.968**
ENN	0.007***	0.004***	0.011***
IJI	−0.206***	−0.138***	−0.343***
DIVISION	−13.791***	−9.236***	−23.027***
SPLIT	0.013	0.009	0.022
SHDI	15.340***	10.274***	25.614***
POPD	0.0002*	0.0002*	0.0004*

(Figures 9F–H). Although landscape projects in downstream ecosystems have improved land surface vegetation cover (Figure 9G), the soil loss-induced water pollution in upstream regions has not been effectively mitigated; thus, river channel sedimentation downstream is still severe (Figures 9F,H).

This study revealed the determinants of ES balance and their spillover effects, implying that, in addition to effective efforts by individual local communities to conserve ecosystems and maintain ES balance, strengthening coordination and collaborative efforts are also required from adjacent areas for them to move from being ES supply sources to beneficiaries (Chen et al., 2019a; Jiang et al., 2021a; Jean et al., 2021).

4.3 Uncertainties, limitations, and future perspectives

Some uncertainties and limitations remain in the current study. The current supply–demand matrix proposed by Burkhard et al. (2012), Burkhard et al. (2014) and adapted

FIGURE 9
(A–D) Pictures of urban landscape compositions coordinating blue and green infrastructures (i.e., wetlands, rivers, lakes, woodlands, and grasslands) and urban development, **(E)** coastal exploitation, and **(F–H)** inappropriate urban landscape and catchment management projects that damage surface vegetation cover and exacerbate soil loss and water pollution. **(A and B)**, **(C and D)**, and **(E)** are from the Haizhu and Liwan districts of Guangzhou city and Jieyang city of Guangdong province, respectively. **(F and H)** Are from the Nanshan District of Shenzhen city, Guangdong province.

based on semi-quantitative local expert knowledge might not completely reflect the actual conditions of the research areas, and hence, it should be further refined and adapted according to other natural environmental conditions and socioeconomic features, including climate, terrain, vegetation species, and industrial and economic levels (e.g., Lorencová et al., 2016; Carli et al., 2018; Barbieri and Consoli, 2019; Raza et al., 2019). Existing studies have adopted an expert knowledge approach to quantify social demands for the assessment of ES balance, particularly for the demand aspect (e.g., Campagne et al., 2018; Tao et al., 2018; Sun et al., 2020). As the scoring method is based on subjective experience and it largely does not rely on accurate input parameters and complex data requirements, it can only reflect the relative levels of supply and demand (Burkhard et al., 2014). In addition, the ES demands of each era are different, and their values also differ over decades with the development of socioeconomic conditions (Carli et al., 2018; Barbieri and Consoli, 2019), and thus, it is not completely reasonable to apply the present assessment standards (as shown in Fig. S2) to assess the ES balance in previous decades. Therefore, in future studies, more input data from various sources, such as statistical records and spatially explicit data, should be incorporated into the assessment to obtain more accurate results and absolute values of ES demand (Schirpke et al., 2019; Yuan et al., 2019; Wang et al., 2021). Allowing for the low data accessibility of county-scale socioeconomic and environmental variables (Blanco et al., 2017), this study recommends exploring the possibilities of applying various emerging spatial mobile data to assess sub-county, site, and pixel-scale ES demands (Funes et al., 2019; Liu et al., 2020).

The GTWR and Moran's I scatterplots showed that the supply–demand balance and its determinants exhibited significant spatial autocorrelations and heterogeneity and might largely rely on research scales. Some studies also show that interactions among ESs are complicated because of scale effects (Kim and Arnhold, 2018; Wilkerson et al., 2018). Therefore, the current county-scale analysis and its conclusions might not be applicable to land-use management at different levels of governments, and hence, further studies should be conducted to reveal the impacts of landscape structure on ES balance at different spatial scales and to practically support strategy formulation and implementation for combating ecosystem degradation. In terms of spillover effects, this study only obtained the direct and indirect effects of explanatory variables through SECMs (Table 3), and therefore, the effects of LULC transformation and socioeconomic indicator change in specific units on the ES balance at a regional scale is still not clear. The mechanisms of influence on the ES balance can be revealed by spatially explicit models, such as Integrated Valuation of Ecosystem Services and Trade-offs (Sharp et al., 2018) and Artificial Intelligence for Ecosystem Services (Villa et al., 2009) that couple landscape composition and structure with ESs in an integrated manner. The driving mechanisms, delivery process, and spatial variation of ES supply and demand must be investigated by including more involved socioeconomic indicators (e.g., transport network and road density) for the formulation of practical solutions toward sustainable landscape management (Wilkerson et al., 2018; Schirpke et al., 2019).

5 Conclusion

A coastal area in southeastern China was selected as a case study to reveal the spatial patterns of ES supply–demand budget in 1980, 2000, and 2017 by applying the supply–demand matrix. We identified the spatial determinants and heterogeneity of the ES budget using SECMs and GWR approaches. The overall patterns of ES balance in three time nodes were stable, whereas ES deficits typically existed in rapidly urbanizing areas. ESSI and ESBI closely correlated with landscape proportions because cropland and built-up areas exhibited week ES supply and strong ES demand, while woodland and grassland had strong ES supply and week ES demand. Landscape variables and POPD were identified as the primary spatial determinants of the ES balance and they were closely associated with the ESBI and exhibited remarkable spatial variability and external effects.

The spatial heterogeneity of determinants implies that regional landscape management strategies should account for the spatial dependencies of independent variables and provide an important reference for decision-making for regional landscape planning and ecosystem conservation. In addition, localized biophysical and socioeconomic variables, such as landscape composition, environmental conditions, economic levels, and localized management practices, which are designed according to actual conditions, should be considered to accurately assess and effectively reconcile ES imbalance (i.e., ES deficits) through targeted policy regulations, landscape optimizations, and other human interventions. Considering the existence of spatial spillover effects of determinants, the strategy formulation and solution implementation for landscape planning and ES management should not completely rely on individual governments or organizations but rather require collaborative efforts from different levels of communities in both local and adjacent districts (i.e., cross-border regions), particularly for the rapidly expanding coastal urban agglomerations.

Data availability statement

The original contributions presented in the study are included in the article/Supplementary Material, further inquiries can be directed to the corresponding author.

Author contributions

WC and CJ: Conceptualization, Methodology, Writing "original draft, Writing" review and editing. YW: Investigation, Methodology, Data curation. XL, BD, JY, and WH: Funding acquisition, Project administration, Resources.

Acknowledgments

Guangdong Academy of Sciences Project of Science and Technology Development (2020GDASYL-20200103010), National Natural Science Foundation of China (41901258;

41976189; 42006170; 42101084), Guangdong Forestry Science and Technology Project (2020KJCX003), Provincial Science and Technology Program of Guangdong Province (2019B020208002), Marine Economy Development Foundation of Guangdong Province (No. GDNRC[2020]051), Natural Science Foundation of Guangdong Province (2022A1515011898), and National Park Construction Project (2021GJGY029).

Conflict of interest

The authors declare that the research was conducted in the absence of any commercial or financial relationships that could be construed as a potential conflict of interest.

Publisher's note

All claims expressed in this article are solely those of the authors and do not necessarily represent those of their affiliated organizations, or those of the publisher, the editors and the reviewers. Any product that may be evaluated in this article, or claim that may be made by its manufacturer, is not guaranteed or endorsed by the publisher.

Supplementary material

The Supplementary Material for this article can be found online at: https://www.frontiersin.org/articles/10.3389/fenvs.2022.1002902/full#supplementary-material

References

Ayinuer, Y., Zhang, F., Yu, H., and Kung, H. (2018). Quantifying the spatial correlations between landscape pattern and ecosystem service value: a case study in ebinur lake basin, xinjiang, China. *Ecol. Eng.* 113, 94–104. doi:10.1016/j.ecoleng.2018.02.005

Barbieri, N., and Consoli, D. (2019). Regional diversification and green employment in US metropolitan areas. *Res. Policy* 48, 693–705. doi:10.1016/j.respol.2018.11.001

Baró, F., Palomo, I., Zulian, G., Vizcaino, P., Haase, D., and Gómez-Baggethun, E. (2016). Mapping ecosystem service capacity, flow and demand for landscape and urban planning: a case study in the barcelona metropolitan region. *Land Use Policy* 57, 405–417. doi:10.1016/j.landusepol.2016.06.006

Blanco, V., Holzhauer, S., Brown, C., Lagergren, F., Vulturius, J., Lindeskog, M., et al. (2017). The effect of forest owner decision-making, climatic change and societal demands on land-use change and ecosystem service provision in Sweden. *Ecosyst. Serv.* 23, 174–208. doi:10.1016/j.ecoser.2016.12.003

Burkhard, B., Kroll, F., Nedkov, S., and Müller, F. (2012). Mapping ecosystem service supply, demand and budgets. *Ecol. Indic.* 21, 17–29. doi:10.1016/j.ecolind.2011.06.019

Burkhard, B., Kandziora, M., Hou, Y., and Müller, F. (2014). Ecosystem service potentials, flows and demands concepts for spatial localisation, indication and quantification. *Landsc. Online* 34, 1–32. doi:10.3097/lo.201434

Cai, W., Gibbs, D., Zhang, L., Ferrier, G., and Cai, Y. (2017). Identifying hotspots and management of critical ecosystem services in rapidly urbanizing Yangtze River Delta Region, China. *J. Environ. Manage.* 191, 258–267. doi:10.1016/j.jenvman.2017.01.003

Cai, Z., Li, W., and Cao, S. (2021). Driving factors for coordinating urbanization with conservation of the ecological environment in China. *Ambio* 50, 1269–1280. doi:10.1007/s13280-020-01458-x

Campagne, C. S., Roche, P. K., and Salles, J.-M. (2018). Looking into pandora's box: ecosystem disservices assessment and correlations with ecosystem services. *Ecosyst. Serv.* 30, 126–136. doi:10.1016/j.ecoser.2018.02.005

Carli, R., Dotoli, M., and Pellegrino, R. (2018). Multi-criteria decision-making for sustainable metropolitan cities assessment. *J. Environ. Manage.* 226, 46–61. doi:10.1016/j.jenvman.2018.07.075

Castillo-Eguskitza, N., Martín-Lopez, ´ B., and Onaindia, M. (2018). A comprehensive assessment of ecosystem services: integrating supply, demand and interest in the urdaibai biosphere reserve. *Ecol. Indic.* 93, 1176–1189. doi:10.1016/j.ecolind.2018.06.004

Chaplin-Kramer, R., Sharp, R. P., Weil, C., Bennett, E. M., Pascual, U., Arkema, K. K., et al. (2019). Global modeling of nature's contributions to people. *Science* 366 (6462), 255–258. doi:10.1126/science.aaw3372

Chaurasia, H., Srivastava, S., and Singh, J. K. (2020). Does seasonal variation affect diarrhoea prevalence among children in India? An analysis based on spatial regression models. *Child. Youth Serv. Rev.* 118, 105453. doi:10.1016/j.childyouth.2020.105453

Chen, W., Chi, G., and Li, J. (2019a). The spatial association of ecosystem services with land use and land cover change at the county level in China, 1995–2015. *Sci. Total Environ.* 669, 459–470. doi:10.1016/j.scitotenv.2019.03.139

Chen, W., He, B., Nover, D., Lu, H., Liu, J., Sun, W., et al. (2019b). Farm ponds in southern China: Challenges and solutions for conserving a neglected wetland ecosystem. *Sci. Total Environ.* 659, 1322–1334. doi:10.1016/j.scitotenv.2018.12.394

Chen, J., Xiao, H., Li, Z., Liu, C., Ning, K., and Tang, C. (2020). How effective are soil and water conservation measures (SWCMs) in reducing soil and water losses in the red soil hilly region of China? A meta-analysis of field plot data. *Sci. Total Environ.* 735, 139517. doi:10.1016/j.scitotenv.2020.139517

Chen, W., Chi, G., and Li, J. (2020). The spatial aspect of ecosystem services balance and its determinants. *Land Use Policy* 90, 104263. doi:10.1016/j.landusepol.2019.104263

Chen, Y., Dong, J., Xiao, X., Ma, Z., Tan, K., Melville, D., et al. (2020). Effects of reclamation and natural changes on coastal wetlands bordering China's Yellow Sea from 1984 to 2015. *Land Degrad. Dev.* 30, 1533–1544. doi:10.1002/ldr.3322

Chi, G., and Ho, H. C. (2018). Population stress: a spatiotemporal analysis of population change and land development at the county level in the contiguous United States, 2001-2011. *Land Use Policy* 70, 128–137. doi:10.1016/j.landusepol.2017.10.008

Costanza, R., de Groot, R., Braat, L., Kubiszewski, I., Fioramonti, L., Sutton, P., et al. (2017). Twenty years of ecosystem services: how far have we come and how far do we still need to go? *Ecosyst. Serv.* 28, 1–16. doi:10.1016/j.ecoser.2017.09.008

Dall'erba, S. (2009). "Exploratory spatial data analysis," in *International encyclopedia of human geography* (Cham: Springer), 683–690. doi:10.1016/B978-008044910-4.00433-8

Elhorst, J. P. (2014). MATLAB software for spatial panels. *Int. Reg. Sci. Rev.* 37 (3), 389–405. doi:10.1177/0160017612452429

Fotheringham, A. S., Brundson, C., and Charlton, M. (1998). Geographically weighted regression: A natural evolution of the expansion method for spatial data analysis. *Environ. Plan. A* 30, 1905–1927. doi:10.1068/a301905

Funes, I., Savé, R., Rovira, P., Molowny-Horas, R., Alcañiz, J. M., Ascaso, E., et al. (2019). Agricultural soil organic carbon stocks in the north-eastern iberian peninsula: drivers and spatial variability. *Sci. Total Environ.* 668, 283–294. doi:10.1016/j.scitotenv.2019.02.317

He, Q. Q., and Huang, B. (2018). Satellite-based mapping of daily high-resolution ground PM2.5 in China via space-time regression modeling. *Remote Sens. Environ.* 206, 72–83. doi:10.1016/j.rse.2017.12.018

Jean, P. M., Jaramar, V. R., Andrés, F. S. C., Sofía, L. C., Adrian, G. C., Rebecca, K. R., et al. (2021). Considering landscape-level processes in ecosystem service assessments. *Sci. Total Environ.* 796, 149028. doi:10.1016/j.scitotenv.2021.149028

Jia, M., Wang, Z., Zhang, Y., Mao, D., and Wang, C. (2018). Monitoring loss and recovery of mangrove forests during 42 years: The achievements of mangrove conservation in China. *Int. J. Appl. Earth Obs. Geoinf.* 73, 535–545. doi:10.1016/j.jag.2018.07.025

Jiang, C., Zhao, L., Dai, J., Liu, H., Lie, Z., Wang, X., et al. (2020). Examining the soil erosion responses to ecological restoration programs and landscape drivers: A spatial econometric perspective. *J. Arid. Environ.* 183, 104255. doi:10.1016/j.jaridenv.2020.104255

Jiang, C., Yang, Z., Wen, M., Huang, L., Liu, H., Wang, J., et al. (2021a). Identifying the spatial disparities and determinants of ecosystem service balance and their implications on land use optimization. *Sci. Total Environ.* 793, 148472. doi:10.1016/j.scitotenv.2021.148472

Jiang, C., Yang, Z., Wang, X., Dong, X., Li, Z., and Li, C. (2021b). Examining the reversal of soil erosion decline in the hotspots of sandstorms: A non-linear ecosystem dynamic perspective. *J. Arid. Environ.* 186, 104421. doi:10.1016/j.jaridenv.2020.104421

Kim, I., and Arnhold, S. (2018). Mapping environmental land use conflict potentials and ecosystem services in agricultural watersheds. *Sci. Total Environ.* 630, 827–838. doi:10.1016/j.scitotenv.2018.02.176

Larondelle, N., and Lauf, S. (2016). Balancing demand and supply of multiple urban ecosystem services on different spatial scales. *Ecosyst. Serv.* 22, 18–31. doi:10.1016/j.ecoser.2016.09.008

Lee, Y., Ahern, J., and Yeh, C. (2015). Ecosystem services in peri-urban landscapes: the effects of agricultural landscape change on ecosystem services in taiwan's Western coastal plain. *Landsc. Urban Plan.* 139, 137–148. doi:10.1016/j.landurbplan.2015.02.023

LeSage, J., Pace, R., Schucany, W., Schilling, E., and Balakrishnan, N. (2009). *Introduction to spatial econometrics*. New York: Chapman and Hall/CRC.

Li, Z., Xu, X., Zhu, J., Xu, C., and Wang, K. (2019a). Sediment yield is closely related to lithology and landscape properties in heterogeneous karst watersheds. *J. Hydrol. X.* 568, 437–446. doi:10.1016/j.jhydrol.2018.10.076

Li, Z., Xu, X., Zhu, J., Xu, C., and Wang, K. (2019b). Effects of lithology and geomorphology on sediment yield in karst mountainous catchments. *Geomorphology* 343, 119–128. doi:10.1016/j.geomorph.2019.07.001

Li, Z., Ning, K., Chen, J., Liu, C., Wang, D., Nie, X., et al. (2020). Soil and water conservation effects driven by the implementation of ecological restoration projects: Evidence from the red soil hilly region of China in the last three decades. *J. Clean. Prod.* 260, 121109. doi:10.1016/j.jclepro.2020.121109

Lin, W., Xu, D., Guo, P., Wang, D., Li, L., and Gao, J. (2019). Exploring variations of ecosystem service value in hangzhou bay wetland, eastern China. *Ecosyst. Serv.* 37, 100944. doi:10.1016/j.ecoser.2019.100944

Liu, H., Jiang, D., and Yang, X. (2005). Spatialization approach to 1km grid GDP supported by remote sensing. *Geo-information Sci.* 7 (2), 120–123. (in Chinese with English abstract). http://www.dqxxkx.cn/CN/Y2005/V7/I2/120.

Liu, J., Kuang, W., Zhang, Z., Xu, X., Qin, Y., Ning, J., et al. (2014). Spatio-temporal characteristics, patterns and causes of land-use changes in China since the late 1980s. *J. Geogr. Sci.* 24 (2), 195–210. doi:10.1007/s11442-014-1082-6

Liu, H., Remme, R. P., Hamel, P., Nong, H., and Ren, H. (2020). Supply and demand assessment of urban recreation service and its implication for greenspace planning-A case study on Guangzhou. *Landsc. Urban Plan.* 203, 103898. doi:10.1016/j.landurbplan.2020.103898

Liu, Z., Wu, R., Chen, Y., Fang, C., and Wang, S. (2021). Factors of ecosystem service values in a fast-developing region in China: Insights from the joint impacts of human activities and natural conditions. *J. Clean. Prod.* 297, 126588. doi:10.1016/j.jclepro.2021.126588

Lorencová, E. K., Harmácŏková, Z. V., Landová, L., Pártl, A., and Vacŏkárŏ, D. (2016). Assessing impact of land use and climate change on regulating ecosystem services in the Czech Republic. *Ecosyst. Health Sustain.* 2 (3), e01210. doi:10.1002/ehs2.1210

Ma, S., Smailes, M., Zheng, H., and Robinson, B. E. (2019). Who is vulnerable to ecosystem service change? Reconciling locally disaggregated ecosystem service supply and demand. *Ecol. Econ.* 157, 312–320. doi:10.1016/j.ecolecon.2018.11.026

Mandle, L., Shields-Estrada, A., Chaplin-Kramer, R., Mitchell, M. G., Bremer, L. L., Gourevitch, J. D., et al. (2020). Increasing decision relevance of ecosystem service science. *Nat. Sustain.* 1–9, 161–169. doi:10.1038/s41893-020-00625-y

Mao, D., Wang, Z., Wu, J., Wu, B., Zeng, Y., Song, K., et al. (2018a). China's wetlands loss to urban expansion. *Land Degrad. Dev.* 29, 2644–2657. doi:10.1002/ldr.2939

Mao, D., Luo, L., Wang, Z., Wilson, M. C., Zeng, Y., Wu, B., et al. (2018b). Conversions between natural wetlands and farmland in China: A multiscale geospatial analysis. *Sci. Total Environ.* 634, 550–560. doi:10.1016/j.scitotenv.2018.04.009

McGarigal, K., Cushman, S. A., and Ene, E., 2012. Fragstats: Spatial pattern analysis Program for categorical and continuous maps. Computer Software Program Produced by the Authors at the University of Massachusetts, Amherst. Available at the following web site: http://www.umass.edu/landeco/research/fragstats/fragstats.html.

Meng, X., Cao, J., Wang, X., Zhang, C., and Lv, J. (2021). Spatial characteristics of the human factors of soil erosion at the boundary of political divisions: A spatial approach. *Catena* 201, 105278. doi:10.1016/j.catena.2021.105278

Mitchell, M. G. E., Suarez-Castro, A. F., Martinez-Harms, M., Maron, M., McAlpine, C., Gaston, K. J., et al. (2015). Reframing landscape fragmentation's effects on ecosystem services. *Trends Ecol. Evol. (Amst.)* 30, 190–198. doi:10.1016/j.tree.2015.01.011

Ou, W. X., Wang, H. N., and Tao, N. (2018). A land cover-based assessment of ecosystem services supply and demand dynamics in the Yangtze River Delta region. *Acta Ecol. Sin.* 38 (17), 6337–6347.

Ouyang, Z., Song, C., Zheng, H., Polasky, S., Xiao, Y., Bateman, I. J., et al. (2020). Using gross ecosystem product (GEP) to value nature in decision making. *Proc. Natl. Acad. Sci. U. S. A.* 117 (25), 14593–14601. doi:10.1073/pnas.1911439117

Peng, J., Wang, X., Liu, Y., Zhao, Y., Xu, Z., Zhao, M., et al. (2020). Urbanization impact on the supply-demand budget of ecosystem services: Decoupling analysis. *Ecosyst. Serv.* 44, 101139. doi:10.1016/j.ecoser.2020.101139

Raza, S. A., Shah, N., and Sharif, A. (2019). Time frequency relationship between energy consumption, economic growth and environmental degradation in the United States: evidence from transportation sector. *Energy* 173, 706–720. doi:10.1016/j.energy.2019.01.077

Ren, C., Wang, Z., Zhang, Y., Zhang, B., Chen, L., Xia, Y., et al. (2019). Rapid expansion of coastal aquaculture ponds in China from Landsat observations during 1984–2016. *Int. J. Appl. Earth Obs. Geoinf.* 82, 101902. doi:10.1016/j.jag.2019.101902

Schirpke, U., Candiago, S., Vigl, L. E., J¨ ager, H., Labadini, A., Marsoner, T., et al. (2019). Integrating supply, flow and demand to enhance the understanding of interactions among multiple ecosystem services. *Sci. Total Environ.* 651, 928–941. doi:10.1016/j.scitotenv.2018.09.235

Sharp, R., Tallis, H. T., Ricketts, T., Guerry, A. D., Wood, S. A., Chaplin-Kramer, R., et al. (2018). *InVEST 3.6.0 user's guide. The natural capital project*. Stanford: Stanford University, University of Minnesota. The Nature Conservancy, and World Wildlife Fundthe United States of America.

Sun, X., Tang, H., Yang, P., Hu, G., Liu, Z., and Wu, J. (2020). Spatiotemporal patterns and drivers of ecosystem service supply and demand across the conterminous United States: A multiscale analysis. *Sci. Total Environ.* 703, 135005. doi:10.1016/j.scitotenv.2019.135005

Tao, Y., Wang, H., Ou, W., and Guo, J. (2018). A land-cover-based approach to assessing ecosystem services supply and demand dynamics in the rapidly urbanizing Yangtze River Delta region. *Land Use Policy* 72, 250–258. doi:10.1016/j.landusepol.2017.12.051

Turpie, J. K., Forsythe, K. J., Knowles, A., Blignaut, J., and Letley, G. (2017). Mapping and valuation of South Africa's ecosystem services: a local perspective. *Ecosyst. Serv.* 27, 179–192. doi:10.1016/j.ecoser.2017.07.008

Villa, F., Ceroni, M., Bagstad, K., Johnson, G., and Krivovet, S. (2009). "ARIES (ARtificial intelligence for ecosystem services): A new tool for ecosystem services assessment, planning, and valuation," in Proceedings of the 11 the Annual BIOECON Conference on Economic Instruments to Enhance the Conservation and Sustainable Use of B. BioEcon, Venezia, Sept 21, 1–10.

Wang, S., Liu, Z., Chen, Y., and Fang, C. (2021). Factors influencing ecosystem services in the Pearl River Delta, China: Spatiotemporal differentiation and varying importance. *Resour. Conserv. Recycl.* 168, 105477. doi:10.1016/j.resconrec.2021.105477

Wilkerson, M. L., Mitchell, M. G. E., Shanahan, D., Wilson, K. A., Ives, C. D., Lovelock, C. E., et al. (2018). The role of socio-economic factors in planning and managing urban ecosystem services. *Ecosyst. Serv.* 31, 102–110. doi:10.1016/j.ecoser.2018.02.017

Yu, H., Xie, W., Sun, L., and Wang, Y. (2021). Identifying the regional disparities of ecosystem services from a supply-demand perspective. *Resour. Conserv. Recycl.* 169, 105557. doi:10.1016/j.resconrec.2021.105557

Yuan, Y., Chen, D., Wu, S., Mo, L., Tong, G., and Yan, D. (2019). Urban sprawl decreases the value of ecosystem services and intensifies the supply scarcity of ecosystem services in China. *Sci. Total Environ.* 697, 134170. doi:10.1016/j.scitotenv.2019.134170

Zhang, J., He, C., Chen, L., and Cao, S. (2018). Improving food security in China by taking advantage of marginal and degraded lands. *J. Clean. Prod.* 171, 1020–1030. doi:10.1016/j.jclepro.2017.10.110

Zhang, Z., Peng, J., Xu, Z., Wang, X., and Meersmans, J. (2021). Ecosystem services supply and demand response to urbanization: A case study of the Pearl River Delta, China. *Ecosyst. Serv.* 49, 101274. doi:10.1016/j.ecoser.2021.101274

Zhang, H., Jiang, C., Wang, Y., Zhao, Y., Gong, Q., Wang, J., et al. (2022). Linking land degradation and restoration to ecosystem services balance by identifying landscape drivers: insights from the globally largest loess deposit area. *Environ. Sci. Pollut. Res. Int.* doi:10.1007/s11356-022-21707-8

Zheng, J. H. (1995). *Statistical dictionary*. Beijing: China Statistics Press, 190. (in Chinese).

frontiers | Frontiers in Environmental Science

TYPE Original Research
PUBLISHED 02 November 2022
DOI 10.3389/fenvs.2022.985516

Check for updates

OPEN ACCESS

EDITED BY
Donatella Valente,
University of Salento, Italy

REVIEWED BY
Ngoc Vinh Tran,
College of Engineering, University of Michigan, United States
Lei Liu,
National University of Defense Technology, China

*CORRESPONDENCE
Giha Lee,
leegiha@knu.ac.kr

SPECIALTY SECTION
This article was submitted to Soil Processes,
a section of the journal
Frontiers in Environmental Science

RECEIVED 04 July 2022
ACCEPTED 18 October 2022
PUBLISHED 02 November 2022

CITATION
Van LN, Le X-H, Nguyen GV, Yeon M, May DTT and Lee G (2022), Comprehensive relationships between kinetic energy and rainfall intensity based on precipitation measurements from an OTT Parsivel[2] optical disdrometer.
Front. Environ. Sci. 10:985516.
doi: 10.3389/fenvs.2022.985516

Comprehensive relationships between kinetic energy and rainfall intensity based on precipitation measurements from an OTT Parsivel^2 optical disdrometer

Linh Nguyen Van[1], Xuan-Hien Le[2,3], Giang V. Nguyen[1], Minho Yeon[1], Do Thi Tuyet May[1] and Giha Lee[1]*

[1]Department of Advanced Science and Technology Convergence, Kyungpook National University, Sangju-si, South Korea, [2]Disaster Prevention Emergency Management Institute, Kyungpook National University, Sangju-si, South Korea, [3]Faculty of Water Resources Engineering, Thuyloi University, Hanoi, Vietnam

When raindrops collide with the topsoil surface, they cause soil detachment, which can be estimated by measuring the kinetic energy (KE) of the raindrops. Considering their direct measurements on terrestrial surfaces are challenging, empirical equations are commonly utilized for estimating the KE from rainfall intensity (I_r), which has a great influence on soil loss and can be easily obtained. However, establishing the optimal relationship between KE and I_r is difficult. In this study, we used a laser-based instrument (OTT Parsivel^2 Optical disdrometer) to collect datasets in Sangju City (South Korea) between June 2020 and December 2021 to examine the characteristics of KE−I_r relationships. We derived two different expressions for KE−I_r: KE expenditure (KE_{exp}; J m^{-2}h^{-1}) and KE content (KE_{con}; J m^{-2}mm^{-1}), using 37 rainfall events. Subsequently, the 37 rainfall events were categorized into three groups based on the magnitude of the mean rainfall intensity of each event. Overall, the KE values estimated through the equations derived based on 37 events were higher than those estimated by the equations derived based on the three rainfall event groups. Our findings should facilitate the development of more suitable physics-based soil erosion models at event scales.

KEYWORDS

disdrometer, rainfall kinetic energy, rainfall intensity, South Korea, Sangju

1 Introduction

Soil is an essential element for sustaining life on Earth and largely determines the function of any ecological system. It influences the biogeochemical (Basu et al., 2021) and carbon dynamics (Majumder et al., 2018)–as well as climate change (Bonfante and Bouma, 2015)–by controlling the movement of minerals, energy, and water in the

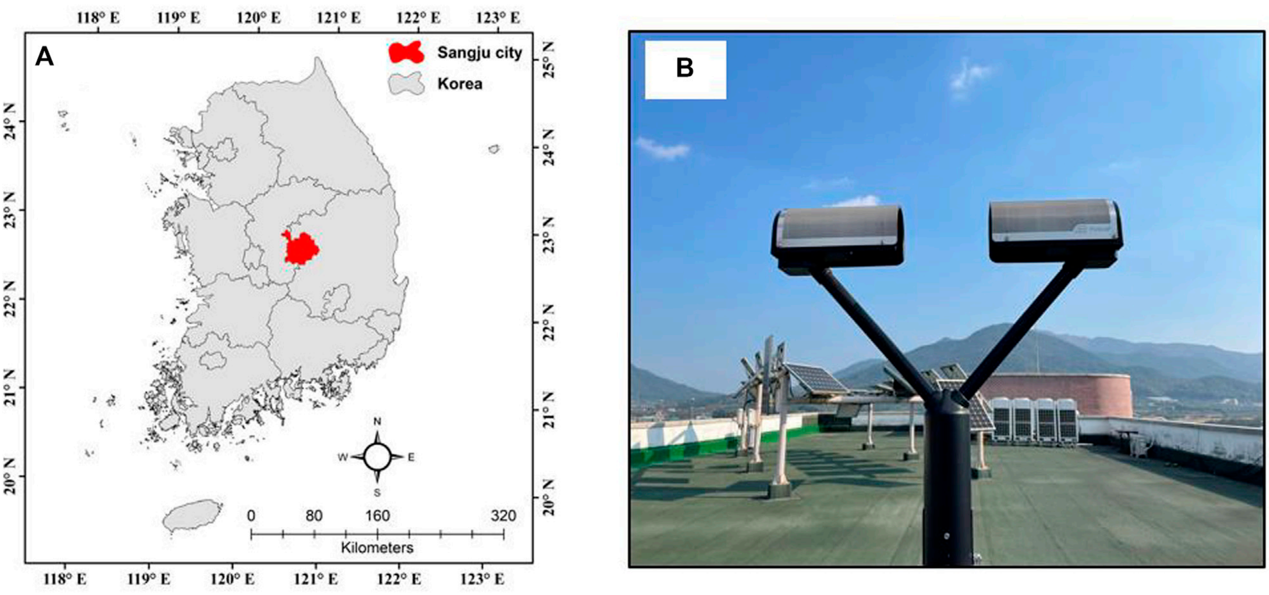

FIGURE 1
(A) Location of Sangju city and **(B)** the Parsivel² disdrometer located inside the Kyungpook National University campus.

environment (Osman, 2014). The loss of millions of hectares of agriculture due to water-induced soil erosion is a global concern, with more than 36 billion tons of soil being eroded annually (Pimentel, 2006). Therefore, understanding the processes that contribute to soil loss is essential.

Water-induced soil erosion is a two-stage process that begins with rainsplash detaching soil particles from the topsoil surface and continues with surface runoff transporting the detached particles (Morgan, 2005). When raindrops impact the soil, they release their kinetic energy (KE), causing soil particles to be airborne and resulting in rainsplash erosion (Torres et al., 1992). The KE of raindrops is a function of their mass and velocity (Eq. 1) and the KE of a single raindrop, assuming it is spherical, is calculated as follows:

$$\mathbf{KE_{raindrop}} = \frac{1}{2}\mathbf{mv^2} = \frac{1}{12}\mathbf{10^{-3}\pi\rho v^2 D^3} \quad (1)$$

where m denotes the raindrop mass (g), ρ denotes the density of raindrop (i.e., 1 g cm^{-3}), v denotes raindrop velocity (m s^{-1}), and D denotes raindrop diameter (mm).

Researchers have differing views on the effectiveness of the KE and momentum for estimating soil detachment by raindrops. According to Rose (1960) and Paringit and Nadaoka (2003), momentum of rainfall substantially outperforms KE in calculating soil detachment; Lim et al. (2015) corroborated these findings. In contrast, Al-Durrah and Bradford (1982) employed KE to forecast the quantity of soil removed. van Dijk et al. (2002) assumed that the amount of energy available for separation and transmission by rain-splash is expressed by KE. Morgan (2005) concluded that rainfall erosivity is best expressed in terms of KE. In addition, KE is an essential parameter in numerous erosion models (e. g., the Universal Soil Loss Equation (Wischmeier and Smith, 1958), SLEMSA (Elwell, 1978), WaTEM/SEDEM (Verstraeten et al., 2002), and Surface Soil Erosion Model (Lee et al., 2013)) for characterizing the erosivity of raindrops.

In recent decades, numerous researchers have developed various approaches for determining the KE of rainfall. Attempts have been tried to directly measure raindrop impact (Madden et al., 1998); however, the instruments involved are both expensive and difficult to operate. Consequently, empirical equations are an alternative for estimating KE from rainfall intensity (I_r), which has a great influence on soil erosion and can be easily obtained. Raindrop size and velocity may be recorded using a number of ways, including the stain-paper methods (Wischmeier and Smith, 1958), video recorders with high frame rates (Kinnell, 1981), as well as more diverse approaches (Kathiravelu et al., 2016). With the advent of technological and electrical improvements, using laser-based instruments, we can more precisely measure the characteristics of raindrops than previous methods.

Several types of KE–I_r equations exist: Polynomial (Carter et al., 1974), power-law (Park et al., 1980), exponential (Brown and Foster, 1987), linear (Sempere-Torres et al., 1998), or logarithmic (Davison et al., 2005). KE of rainfall includes two distinct types, both of which are connected to I_r (Kinnell, 1981). Kinetic energy expenditure (KE_{exp}; J $m^{-2}h^{-1}$) is the rate at which KE is spent per unit area over a certain period of time, and kinetic

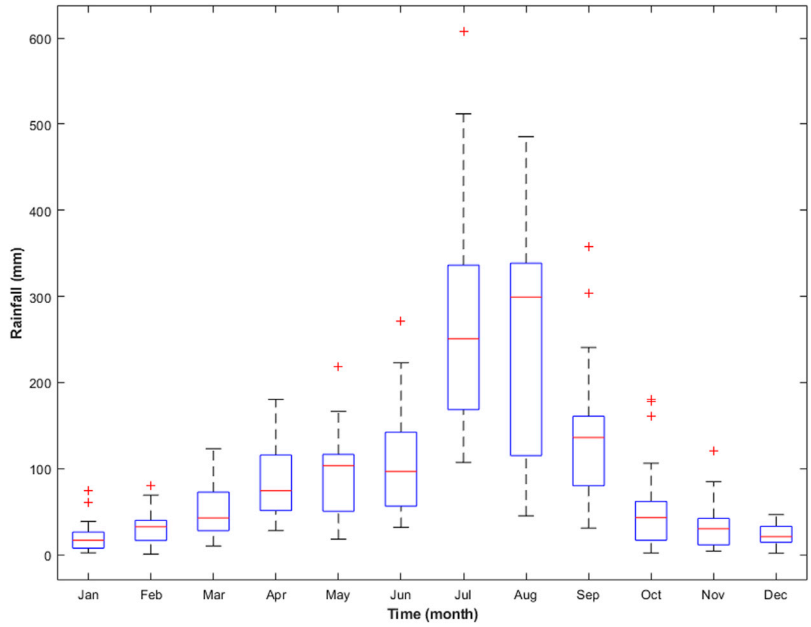

FIGURE 2
Rainfall characteristics recorded at Sangju City illustrated by boxplots. The 25th and 75th percentiles are indicated by the outside borders of the boxes; the median is shown as a red line in the middle of each boxplot. The whiskers at the top and bottom indicate the maximum and lowest values, respectively.

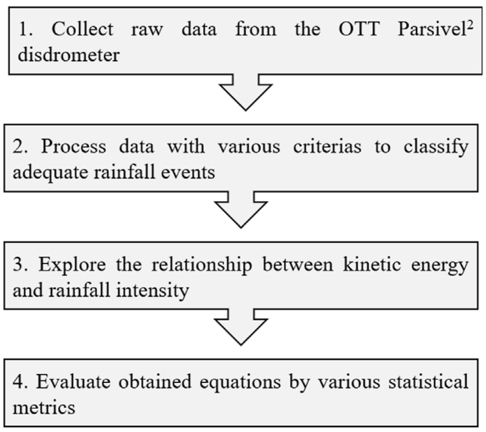

FIGURE 3
Flow chart of the methodology.

energy content (KE_{con}; J $m^{-2}mm^{-1}$) is defined as the KE per unit area per unit depth. KE_{con} stands for the mean squared velocity of raindrops arriving to the ground. Linear (Torres et al., 1992) and power-law (Park et al., 1980) relationships (Eqs 2, 3, respectively) are used for connecting KE_{exp} to I_r; logarithmic (Wischmeier and Smith, 1958) and exponential (Kinnell, 1981) relationships (Eqs 4, 5, respectively) are used for connecting KE_{con} to I_r.

$$\mathbf{KE}_{\mathbf{exp}} = \boldsymbol{a} \times \mathbf{I_r} + \boldsymbol{b} \tag{2}$$

$$\mathbf{KE}_{\mathbf{exp}} = \boldsymbol{c} \times \mathbf{I_r^{\boldsymbol{d}}} \tag{3}$$

$$\mathbf{KE}_{\mathbf{con}} = \boldsymbol{e} + \boldsymbol{f} \times \mathbf{log I_r} \tag{4}$$

$$\mathbf{KE}_{\mathbf{con}} = \boldsymbol{g} \times \left(\mathbf{1} - \boldsymbol{h} \times \mathbf{exp}\left(-\boldsymbol{k} \times \mathbf{I_r}\right)\right) \tag{5}$$

where *a*, *b*, *c*, *d*, *e*, *f*, *g*, *h*, and *k* denote empirical values.

Many scholars have recommended different values in their empirical equations depending on the geographic areas, i.e., the empirical constants vary from one region to another. Differences in measuring methods, the range of I_r, or difficulties in interpretation may all contribute to this discrepancy (van Dijk et al., 2002). In South Korea, numerous studies have been conducted in different locations to obtain the KE–I_r equations, such as in Daejeon (Lim et al., 2015), Seoul (Lee, 2020), Ansung (Kim et al., 2010), and Daegwanryung (Lee and Won, 2013). However, each study produced different results. The precision of KE–I_r connection varies spatially (Fornis et al., 2005); thus, our primary aim is to establish the most appropriate KE–I_r connection in Sangju City (South Korea) and possibly in other parts of the Sangju region with similar climatic conditions. Specifically, we derived two different expressions of the KE–I_r, i.e., KE expenditure (KE_{exp}; J $m^{-2}h^{-1}$) and KE content (KE_{con}; J $m^{-2}mm^{-1}$), based on a dataset of raindrop sizes and terminal velocities complied using a laser optical disdrometer (constructed inside the

TABLE 1 Statistical information on the selected rainfall events.

Event	Date (dd/mm/yy hh:mm)	Duration	No. of raindrops	No. of outliers	Rain depth (mm)	Intensity (mm/h)				
						Max	Mean	Median	St.dev	Skewness
1	10/06/2020 20:51	09 h 30 min	307,808	119	50.46	17.87	4.70	4.00	4.26	0.87
2	13/06/2020 19:54	13 h 42 min	385,208	431	29.75	7.4	1.36	0.21	1.85	1.49
3	24/06/2020 12:45	26 h 31 min	347,936	1573	14.91	1.22	0.20	0.10	0.24	2.37
4	12/03/2021 10:40	06 h 01 min	95,761	93	9.69	3.95	1.44	1.31	0.87	0.65
5	27/03/2021 13:25	14 h 04 min	359,840	117	24.08	5.01	1.61	1.47	1.14	0.60
6	03/04/2021 10:20	21 h 06 min	714,019	314	34.15	5.20	1.35	0.98	1.24	1.02
7	12/04/2021 11:53	13 h 36 min	223,265	202	20.18	4.73	1.30	1.08	1.12	0.92
8	01/05/2021 12:32	17 h 09 min	61,303	1088	4.02	0.5	0.13	0.10	0.08	2.89
9	04/05/2021 16:31	09 h 32 min	182,322	326	9.56	3.07	0.65	0.39	0.69	1.41
10	10/05/2021 07:26	25 h 33 min	188,754	1156	18.36	2.05	0.35	0.10	0.47	1.94
11	16/05/2021 18:15	13 h 23 min	512,393	525	14.46	2.55	0.51	0.24	0.57	1.50
12	20/05/2021 09:37	14 h 49 min	743,031	188	20.28	4.38	1.19	0.96	1.04	0.90
13	28/05/2021 11:49	2 h 39 min	92,003	68	19.92	18.24	5.96	4.75	3.92	1.02
14	30/05/2021 22:25	7 h 04 min	51,022	151	9.90	4.71	0.94	0.10	1.22	1.37
15	03/06/2021 10:01	16 h 13 min	484,004	251	25.25	5.68	1.31	0.90	1.31	1.03
16	10/06/2021 20:06	11 h 45 min	149,679	131	14.6	4.34	1.13	0.83	1.04	0.98
17	22/06/2021 19:45	52 min	17,647	22	8.46	32.48	7.37	3.37	8.29	1.35
18	03/07/2021 13:17	15 h	371,419	305	33.4	7.65	1.66	0.76	1.90	1.28
19	05/07/2021 19:18	9 h 04 min	196,799	75	11.95	4.75	1.23	0.82	1.17	1.05
20	06/07/2021 17:13	24 h 40 min	210,285	1704	12.39	0.37	0.12	0.10	0.05	3.15
21	08/07/2021 01:29	4 h 16 min	149,756	99	32.22	19.50	5.71	4.42	4.71	1.05
22	10/07/2021 19:08	03 h 58 min	52,814	208	16.36	4.93	0.70	0.10	1.13	2.06
23	11/07/2021 19:06	40 min	43,737	36	18.97	53.55	14.22	12.40	11.54	1.28
24	27/07/2021 19:33	01 h 01 min	81,024	7	30.5	92.52	26.08	21.43	23.14	0.82
25	01/08/2021 15:47	07 h 15 min	167,090	318	43.74	10.04	1.90	1.15	2.14	1.45
26	08/08/2021 13:55	01 h 21 min	36,583	78	16.12	30.97	4.29	1.24	7.25	2.32
27	10/08/2021 09:54	01 h 13 min	31,325	30	11.09	36.20	6.31	0.78	9.59	1.52
28	23/08/2021 09:09	27 h 49 min	578,908	659	81.07	8.47	1.99	1.40	1.98	1.16
29	25/08/2021 16:20	07 h 34 min	137,149	339	12.84	2.87	0.47	0.1	0.69	2.00
30	27/08/2021 08:59	8 h 17 min	118,828	138	16.63	8.33	1.55	0.19	2.22	1.41
31	01/09/2021 02:48	13 h 21 min	286,138	404	51.13	11.05	2.09	0.73	2.59	1.34
32	06/09/2021 16:38	21 h 54 min	290,235	837	30.94	3.72	0.65	0.11	0.88	1.66
33	16/09/2021 23:06	13 h 25 min	320,541	173	39.3	11.13	2.45	1.23	2.72	1.11
34	21/09/2021 07:01	4 h 06 min	86,537	38	10.47	9.40	2.32	1.58	2.25	0.94
35	11/10/2021 02:20	40 h 37 min	695,308	561	22.78	2.20	0.50	0.29	0.49	1.15
36	15/10/2021 16:26	14 h 19 min	210,792	419	14.26	2.79	0.75	0.57	0.64	1.19
37	30/11/2021 07:22	16 h 04 min	158,070	406	13.98	3.07	0.62	0.17	0.76	1.43

Kyungpook National University) between June 2020 and December 2021. Our findings should facilitate the development of more suitable physics-based soil erosion models.

The remaining sections of the article are structured as follows. Section 2 presents the features of the study site and measuring equipment. Section 3 presents the methodology. Section 4 provides a comprehensive analysis and discussion of the findings. Finally, the results are summarized in Section 5.

2 Area description and measurement instruments

Rainfall intensity and raindrop size distribution observations were conducted at Kyungpook National University in Sangju City, South Korea. Sangju is located in the North Gyeongsang Province, central South Korea (Figure 1) and has an inland climate. In August, the

10.3389/fenvs.2022.985516

TABLE 2 Information on the assessment criteria used in this study. (x_j: observation, y_j: prediction, $\bar{x}$: mean of observed values, $\bar{y}$: mean of predicted values, n: number of samples).

Indicator	Equation	Range	Optimal value
RMSE	$\sqrt{\frac{1}{n}\sum_{j=1}^{n}(x_j - y_j)^2}$	0.0 to +∞	0.0
MAE	$\frac{1}{n}\sum_{j=1}^{n}\lvert x_j - y_j\rvert$	0.0 to +∞	0.0
R^2	$\frac{[\sum_{j=1}^{n}(x_j-\bar{x})(y_j-\bar{y})]^2}{\sum_{j=1}^{n}(x_j-\bar{x})^2\sum_{j=1}^{n}(y_j-\bar{y})^2}$	0.0 to 1.0	1.0

average air temperature reaches 26°C (79°F), while in January, it drops to 3°C (27°F). There is a significant difference in air temperature between the north and south. This area receives an average of 1,050 mm of rainfall annually. Figure 2 depicts the 20-year average monthly rainfall depth (mm) throughout the 2002–2021 period at Sangju City.

The OTT Parsivel² disdrometer is an optical sensor that generates a 30-mm wide, 180-mm long, and 1-mm high laser beam, and the principle of the measurements is as follows. 1) The maximum voltage is produced at the receiver if no raindrop intersects the laser beam. 2) Raindrops block a section of the laser beam corresponding to their diameter as they pass across the beam; the corresponding lower output voltage dictates the particle size. 3) Particle speed is determined by the duration of the signal. When a raindrop enters the light strip, a signal is generated; it terminates when the raindrop fully exits the light strip.

The disdrometer classifies particles into relevant classes after obtaining the volume equivalent diameter (D) and the particle speed (V). It has measurement ranges of 0.2–8.0 mm for liquid precipitation particles and 0.2–25 mm for solid precipitation particles. Precipitation particles may travel at speeds ranging from 0.2 to 20.0 m/s and this categorization has a smaller scale for tiny, sluggish particles than it does for big, fast particles. Observed particles in a two-dimensional field are divided into 32 D-classes, with ten classes in the 0.00–1.25 mm range, five in the 1.25–2.25 mm range, five in the 2.5–5.0 mm range, five in the 10.0–20.0 mm range, and two in the 20.0–25.0 mm range. Similarly, particle velocity is classified into 32 V-classes: 0.0–1.0 m/s, 1.0–2.0 m/s, 2.0–4.0 m/s, 4.0–8.0 m/s, 8.0–16.0 m/s, and 16.0–20.0 m/s.

3 Methodology

The steps below outlines how we investigated the relationship between KE and I_r from a dataset measured by the OTT Parsivel² disdrometer. Figure 3 is a schematic that depicts our approach.

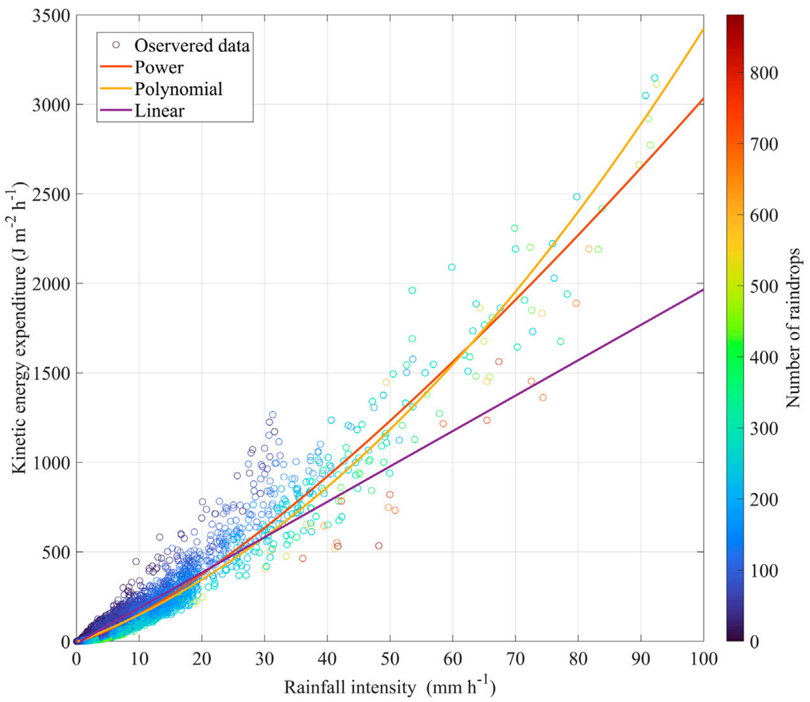

FIGURE 4
Scatter plots of 151,852 KE_{exp}–I_r points, which were analyzed and described by three different models, i.e., the power-law (Eq. 9), polynomial (Eq. 10), and linear (Eq. 11) relationships.

TABLE 3 Statistical analysis of the relationship between KE_{exp} and I_r.

Function	R2	RMSE ($J\ m^{-2}h^{-1}$)	MAE ($J\ m^{-2}h^{-1}$)
Power	0.945	13.52	3.90
Polynomial	0.936	14.57	5.74
Linear	0.866	21.10	10.95

Firstly, the OTT Parsivel^2 (PARticle SIze and VELocity) disdrometer was erected on the roof of a building inside the Kyungpook National University an elevation of 80 m above sea level. Rainfall properties, such as rainfall depth and intensity, as well as raindrop size and velocity were measured using a disdrometer at a 10-s interval starting in June 2020. This devide was then connected to a laptop to automatically save the measured data.

Secondly, individual rainfall events were classified according to the criteria followed by (Fornis et al., 2005; Petan et al., 2010; Lim et al., 2015): 1) Two distinct events should be separated by at least 6 h without rainfall; 2) total rainfall accumulated should amount more than 3 mm, and 3) rainfall event duration and average intensity should be longer than 30 min and higher than 0.1 mm/h, respectively. Table 1 presents detailed information on the selected rainfall events. After processing, the data were thoroughly reviewed for outliers in the rainfall intensity distribution. According to Lim et al. (2015), raindrops interacting with the safety covers of the disdrometer and merging with other drops may generate interference in the lazer zone, resulting in thicker drops. It is possible for two raindrops to travel through the sensor simultaneously during storm events, resulting in an overestimated, abnormally high intensity (Petan et al., 2010). Thus, records with unusually high intensity values were considered outliners and were discarded.

Thirdly, we established a relationship between I_r and KE using 37 rainfall events, which consisted of 151,852 KE–I_r points. The required empirical parameters (Eqs 2–5) were calculated using the least square method in MATLAB to reduce the estimation standard error. To handle the challenges in nonlinear regression, we utilized the Levenberg-Marquardt technique, which is a form of iteration process that terminates iterative computations when the decreasing residual sum of squares is less than the stated convergence threshold (Lim et al., 2015).

The most essential parameter for soil erosion, Ir (mm/h), was determined using the following equation:

$$\mathbf{I_r = 3.6 \times 10^{-3}\left(\frac{\pi}{6}\right)\left(\frac{1}{\Delta t \times A_b}\right)\sum_{i}^{32} N_{D_i} D_i^3} \tag{6}$$

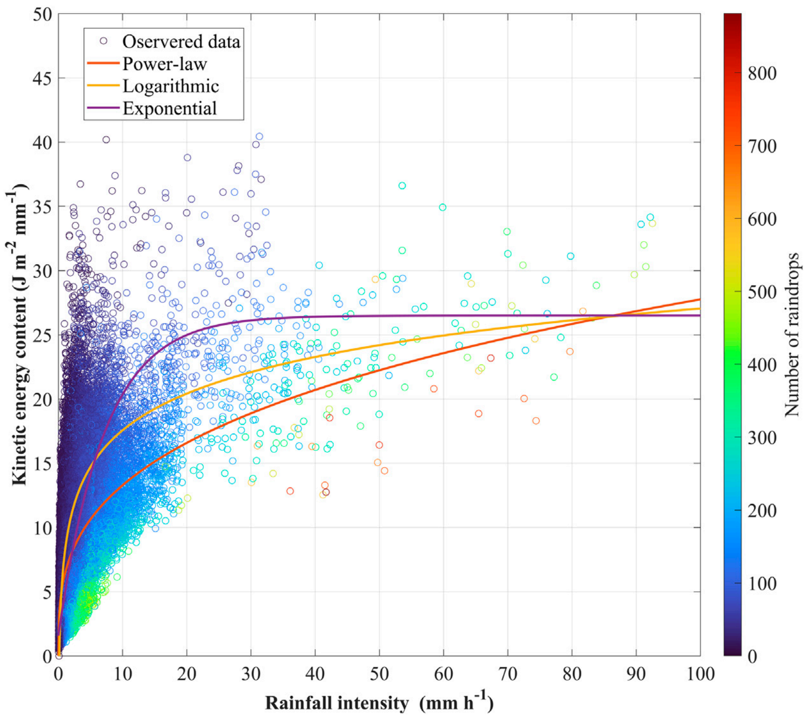

FIGURE 5
Scatter plots of 151,852 KE_{con}–I_r points were analyzed and described by three different models, i.e., the power-law (Eq. 12), logarithmic (Eq. 13), and exponential (Eq. 14) relationships.

TABLE 4 Statistical analysis of the relationship between KE_{con} and I_r.

Function	R2	RMSE (J m^{-2}mm^{-1})	MAE (J m^{-2}mm^{-1})
Power	0.61	3.13	2.58
Logarithmic	0.59	3.20	2.51
Exponential	0.62	3.08	2.38

where A_b denotes the laser beam area (i.e., 0.0054 m^2), Δt denotes the time interval (i.e., 10 s), and N_{D_i} denotes the number of raindrops corresponding to diameter D_i.

Equations 7, 8 constitute two rainfall erosivity indices that were employed in this investigation, including time-related kinetic energy (KE_{exp}; J m^{-2}h^{-1}) and volume-related kinetic energy (KE_{con}; J m^{-2}mm^{-1}), respectively.

$$\mathbf{KE_{exp} = 3.6 \times 10^3 \left(\frac{\pi}{12}\right)\left(\frac{\rho}{\Delta t \times A_b}\right)\sum_{i}^{32} N_{D_i} D_i^3 V_i^2} \tag{7}$$

$$\mathbf{KE_{con} = \frac{KE_{exp}}{I_r}} \tag{8}$$

where V_i denotes the terminal velocity of the raindrops (m/s), corresponding to diameter D_i.

Finally, several statistical metrics [namely, Root Mean Square Error (RMSE), Mean Absolute Error (MAE), and the coefficient of determination (R^2)] were used for evaluating the observed and estimated KE values, which were predicted by KE–I_r relationships. The specifications of the assessment criteria are presented in Table 2. The validity of the empirical models was assessed visually using goodness-of-fit plots.

4 Results and discussion

4.1 KE–I_r relationships: Formation

4.1.1 Kinetic energy expenditure (KE_{exp}; J m^{-2}h^{-1})

The power-law (Eq. 9), polynomial (Eq. 10), and linear (Eq. 11) equations provide the best fits for the KE_{exp}–I_r connection. The scatter plot in Figure 4 depicts the correlations between KE_{exp} and I_r, and Table 3 summarizes the statistical analysis results.

$$\mathbf{KE_{exp} = 7.62 \times I_r^{1.3}} \tag{9}$$

$$\mathbf{KE_{exp} = 0.21 \times I_r^2 + 13.27 \times I_r - 4.56} \tag{10}$$

$$\mathbf{KE_{exp} = 19.77 \times I_r - 11.11} \tag{11}$$

Among the three equations, the power-law equation yields the highest R^2 (i.e., 0.945) and lowest RMSE and MAE (i.e., 13.52 J m^{-2}h^{-1} and 3.90 J m^{-2}h^{-1}, respectively). These three equations provide a statistically equivalent estimation of KE_{exp} with an I_r less than 30 mm/h; however, the disparities become more pronounced with increasing rainfall intensity. The linear equation tends to underestimate the KE_{exp} at I_r levels higher than 30 mm/h. The two remaining equations provide more accurate estimates at higher intensities, with the regression curve nearly crossing the points in the central. The polynomial equation better predicts KE_{exp}, whereas the power-law equation tends to underestimate KE_{exp} at I_r values higher than 90 mm/h. We note that when I_r is zero, the resulting KE_{exp} given by the polynomial and linear equations is negative, which is implausible. At this stage, the power-law equation provides a realistic output.

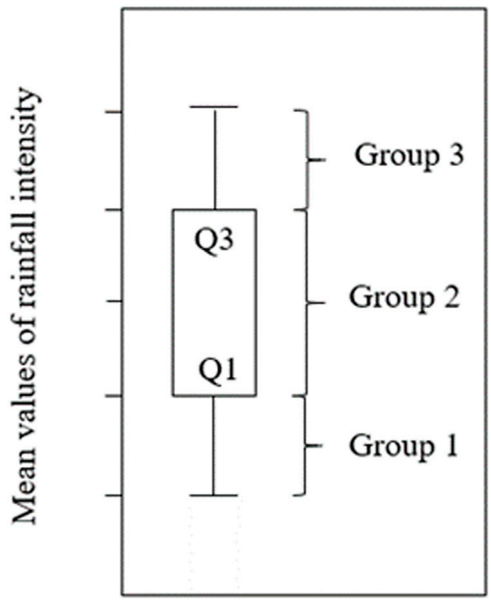

FIGURE 6
Information on the criteria classification of each rainfall event group. Group 1 includes nine rainfall events that having lowest mean rainfall intensity values (namely, events 3, 8, 9, 10, 11, 20, 29, 35, and 37), while group 3 contains nine rainfall events that having highest mean of rainfall intensity values (namely, event 1, 13, 17, 21, 23, 24, 26, 27, and 33). The remaining 19 rainfall events are classified into group 2.

4.1.2 Kinetic energy content (KE_{con}, J m^{-2}h^{-1})

The fitted power-law (Eq. 12), logarithmic (Eq. 13), and exponential (Eq. 14) equations are as follows:

$$\mathbf{KE_{con} = 6.36 \times I_r^{0.32}} \tag{12}$$

$$\mathbf{KE_{con} = 8.08 + 4.12 \times \log(I_r)} \tag{13}$$

$$\mathbf{KE_{con} = 26.5 \times (1 - 0.94 \times \exp(-0.14 \times I_r))} \tag{14}$$

Figure 5 shows a scatter plot of the measured KE_{con} data with the fitted models. We note that KE_{con} exhibits an extreme variation, contrary to KE_{exp}. The equations initially exhibit firm slopes at low intensity (i.e., $I_r < 5$ mm/h). The exponential equation tends to remain steady at I_r values greater than 26.5 mm/h, whereas other equations follow upward trends as I_r increases. The observed KE_{con} values increase with increasing rainfall

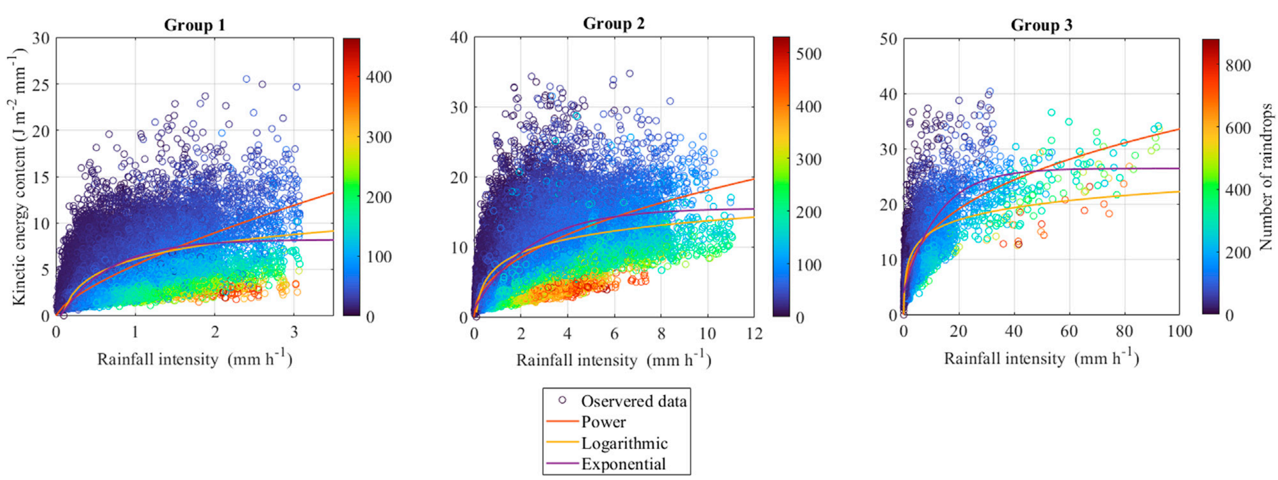

FIGURE 7
Scatter plots of KE_{con}–I_r points, which were analyzed and described by different equations corresponding to each rainfall event group.

TABLE 5 KE_{con}–I_r equations corresponding to the three different rainfall event groups.

	Power-law	Logarithmic	Exponential
Group 1	$5.46 \times I_r^{0.71}$	$6.10 + 2.42 \times \log(I_r)$	$8.5 \times (1 - 1.1 \times \exp(-1.59 \times I_r))$
Group 2	$6.12 \times I_r^{0.47}$	$7.16 + 2.84 \times \log(I_r)$	$15.5 \times (1 - 0.93 \times \exp(-0.41 \times I_r))$
Group 3	$6.71 \times I_r^{0.35}$	$7.65 + 3.18 \times \log(I_r)$	$26.5 \times (1 - 0.85 \times \exp(-0.08 \times I_r))$

intensity in low rainfall intensity zones, but they start to stabilize at rainfall intensities exceeding 30 mm/h.

According to the statistical results in Table 4, the exponential equation outperforms others by yielding the highest R^2 (i.e., 0.62) and lowest RMSE and MAE (i.e., 3.08 and 2.38 J m^{-2} mm^{-1}, respectively). At low rainfall intensities (i.e., $I_r < 5$ mm/h), the regression line for the logarithmic equation increases rapidly with increasing I_r. In comparison to the others, the power-law equation underestimates KE_{con} at high rainfall intensity. The KE_{con} estimates using the power-law and logarithmic equations suggest that KE_{con} has no upper limit, although various studies have suggested otherwise (Kinnell, 1981; Rosewell, 1986; Brown and Foster, 1987). The exponential equation achieves a maximum KE_{con} value and then remains stable regardless of the rainfall intensity; because KE_{con} has a maximum value, defined as the parameter *g* in Eq. 5, the exponential equation is more suitable for forecasting KE_{con} values than the others. This result is consistent with the findings of (Kinnell, 1981).

4.2 KE_{con}–I_r relationship: Revision

The KE_{con}–I_r data points are highly dispersed in the low range in the scatter plot, and this similar phenomena have also been documented by previous research (Fornis et al., 2005; Petan et al., 2010; Sanchez-Moreno et al., 2012; Lim et al., 2015). Consequently, a small number of points with high I_r has a minor impact on the fitted equations, resulting in significant uncertainty and incorrect forecasts (Salles et al., 2002). Thus, this section concentrates on the development of KE_{con}–I_r equations based on magnitudes of the mean rainfall intensity of each event. Figure 6 shows information on the three rainfall event groups.

Figure 7 shows the correlations between KE_{con} and I_r corresponding to the three rainfall event groups. Table 5 contains the fitted equations for each rainfall event group, and Table 6 summarizes the statistical findings compared to observational data. We note that the KE_{con}–I_r points in group 1 exhibit minor dispersion compared to the others, resulting in identical trends of the three equations; however, the R^2 values in group 1 (i.e., 0.59–0.64) are smaller than those in group 2 (i.e., 0.6–0.65) and group 3 (i.e., 0.63–0.72). The exponential equations outperformed the others in every rainfall event group, while yielding the highest R^2 and lowest MAE and RMSE.

Figure 8 shows the uncertainties of KE_{con} estimations from the equations derived from the total 37 rainfall events and grouped rainfall events. We note that the equations obtained

TABLE 6 Statistical analysis of the relationship between KE_{con} and I_r corresponding to the three rainfall event groups.

	Function	R^2	RMSE ($J\ m^{-2}mm^{-1}$)	MAE ($J\ m^{-2}mm^{-1}$)
Group 1	Power	0.59	2.01	1.52
	Logarithmic	0.64	1.89	1.31
	Exponential	0.64	1.89	1.28
Group 2	Power	0.62	3.05	2.36
	Logarithmic	0.61	3.08	2.35
	Exponential	0.65	2.90	2.07
Group 3	Power	0.70	3.45	2.62
	Logarithmic	0.63	3.85	3.01
	Exponential	0.72	3.35	2.33

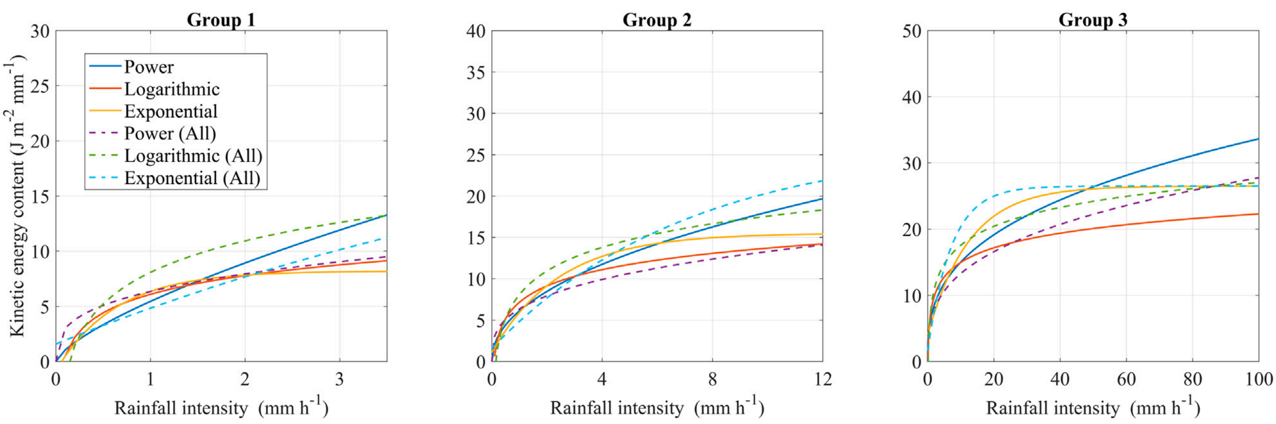

FIGURE 8
Comparison of KE_{con} estimations from equations derived from 37 events (dotted lines) and grouped rainfall events (solid lines). The position of dotted lines higher than that of solid lines indicates the uncertainty of KE_{con} estimation between the two approaches. The equations from group 1 are appropriate for low rainfall intensity, whereas those from group 2 are suitable for high rainfall intensity.

from the total 37 rainfall events tended to overestimate KE_{con}, particularly in rainfall events with low intensity (i.e., group 1).

4.3 KE–I_r relationships: A comment

Both KE_{exp} and KE_{con} are valid representations of the KE of rainfall and can be correlated to I_r. It is possible to discover an empirical connection using KE_{con} versus I_r, although this does not conform to stringent requirements. In terms of statistics, linking KE_{con} to I_r leads to erroneous findings.

According to Kenney (1982), this is a frequent problem in spurious self-correlation. The statistical relationship between KE_{con} and I_r is identical to the relationship between KE_{exp}/I_r and I_r, because KE_{con} is the quotient function of KE_{exp} divided by I_r over a given period, as demonstrated in Eq. 8. This procedure intentionally alters the correlation coefficient between the two variables. As a result, spurious self-correlation coefficients tend to be substantially higher than the actual correlation coefficients between variables. When ratios such as KE_{exp}/I_r were displayed against I_r, they exhibit spurious self-correlation. The correlation coefficient was lowered once the initial variables KE_{exp} and I_r were highly connected, and their coefficients of variation are identical (Lim et al., 2015). This explained why the KE_{exp}–I_r relationship provided a better representation of KE of rainfall than the KE_{con}–I_r relationship; this was also proven by the fact that the former had a higher R^2 than the latter.

Rainfall characteristics, such as raindrop size distribution, which may impact the raindrop terminal velocity, may influence the results (Fornis et al., 2005). Figure 5 illustrates that high KE_{con} values occurred at a low rainfall intensity period, whereas lower KE_{con} values occurred at a higher rainfall intensity zone. This implies that large, quick raindrops form at a low rainfall intensity period, whereas smaller, slower droplets arrive at a higher rainfall intensity zone. According to Blanchard (1953), the onset of a rainfall event signaled by the arrival of a few huge and fast raindrops and followed by a sequence of smaller ones is known as the "sorting phenomenon," leading to significant KE even when the rainfall intensity is modest. Moreover, the effects of wind and turbulence were neglected in this research; wind currents may impact the velocity of raindrops due to contact of air masses with the mountainous geography of South Korea, leading to high KE_{con} values for low intensity.

In this study, the maximum of KE_{con} value given by Eq. 14 is equal to 26.5 J m^{-2} mm^{-1}. This value is substantially lower than those reported in other countries, such as in Spain [i.e., 38.4 J m^{-2} mm^{-1}, (Cerro et al., 1998)], Portugal [i.e., 35.9 J m^{-2} mm^{-1}, (Coutinho and Tomás, 1995)], and Hong Kong [i.e., 36.8 J m^{-2} mm^{-1}, (Jayawardena and Rezaur, 2000)] but is relatively close to that in Korean sites, such as in Daejeon [i.e., 25.75 J m^{-2} mm^{-1}, (Lim et al., 2015)] and Daegwanryung [i.e., 30.03 J m^{-2} mm^{-1}; (Lee and Won, 2013)]. As Rosewell (1986) noted, the maximum of KE_{con} may vary between sites because of alterations in storm energy. Additionally, Angulo-Martínez et al. (2016) investigated these $KE_{con\text{-}max}$ variations and linked them to topographical, meteorological, and experimental characteristics. The evaporation of tiny droplets that fall at great distances from the cloud may modify the raindrop size distribution and liquid water content, according to Blanchard (1953); this modification may have influenced the amount of energy released during rainfall events. The stochasticity of rainfall controls the KE variability can be seen in Figures 4, 5, 7, since a single value of I_r can generate various KE outputs. This could also witness in recent studies (Fornis et al., 2005; Petan et al., 2010; Sanchez-Moreno et al., 2012; Lim et al., 2015).

5 Conclusion

Soil erosion models that employ the KE of rainfall as an erosivity parameter are the most common; however, direct KE measurements are uncommon. Empirical connections between I_r and KE are an alternative.

Raindrop distribution and rainfall intensity were measured using an OTT Parsivel² disdrometer deployed from June 2020 to December 2021 in Sangju City, Korea. Two rainfall erosivity indicators, i.e., KE_{exp} and KE_{con}, were derived using data collected at 10s intervals. The KE_{exp}–I_r and KE_{con}–I_r relationships were established using various mathematical equations. Our key findings are as follows:

1) The KE_{exp}–I_r relationships generated higher R^2 and less dispersion than the KE_{con}–I_r relationships. At low to medium rainfall intensities, the KE_{con} data points are widely spread, whereas the KE_{exp} values tend to follow into a narrow range. The power-law equation provided the best fit between KE_{exp} and I_r, whereas the best match between KE_{con} and I_r was found using an exponential equation.
2) Thirty-seven rainfall events were classified into three rainfall event groups based on the magnitude of the mean rainfall intensity in each event to establish the KE_{con}–I_r relationships. The results from equations derived from all of the 37 events tended to exceed the KE_{con} values, contrary to those derived from the classified groups.

Further research should collect data at multiple geographical and temporal scales to develop more precise equations for calculating raindrop-induced soil erosion.

Data availability statement

The raw data supporting the conclusion of this article will be made available by the authors, without undue reservation.

Author contributions

LV: Conceptualization, methodology, formal analysis, visualization, writing–original draft, and writing–review and editing. X-HL: Methodology, formal analysis, and writing–review and editing. GN: Visualization and writing–review and editing. MY: Data curation and writing–review and editing. DM: Writing–review and editing. GL: Conceptualization, methodology, and writing–review and editing.

Funding

This subject is supported by Korea Ministry of Environment as "The SS projects; 2019002830001."

Conflict of interest

The authors declare that the research was conducted in the absence of any commercial or financial relationships that could be construed as a potential conflict of interest.

Publisher's note

All claims expressed in this article are solely those of the authors and do not necessarily represent those of their affiliated organizations, or those of the publisher, the editors and the reviewers. Any product that may be evaluated in this article, or claim that may be made by its manufacturer, is not guaranteed or endorsed by the publisher.

References

Al-Durrah, M. M., and Bradford, J. M. (1982). Parameters for describing soil detachment due to single waterdrop impact. *Soil Sci. Soc. Am. J.* 46, 836–840. doi:10.2136/sssaj1982.03615995004600040034x

Angulo-Martínez, M., Beguería, S., and Kyselý, J. (2016). Use of disdrometer data to evaluate the relationship of rainfall kinetic energy and intensity (KE-I). *Sci. Total Environ.* 568, 83–94. doi:10.1016/j.scitotenv.2016.05.223

Basu, S., Kumar, G., Chhabra, S., and Prasad, R. (2021). "Chapter 13 - role of soil microbes in biogeochemical cycle for enhancing soil fertility," in *New and future developments in microbial biotechnology and bioengineering*. Editors J. P. Verma, C. A. Macdonald, V. K. Gupta, and A. R. Podile (Amsterdam, Netherlands: Elsevier), 149–157. doi:10.1016/B978-0-444-64325-4.00013-4

Blanchard, Duncan. C. (1953). Raindop size-distribution in Hawaiian rains. *J. Meteor.* 10, 457–473. doi:10.1175/1520-0469(1953)010<0457:rsdihr>2.0.co;2

Bonfante, A., and Bouma, J. (2015). The role of soil series in quantitative land evaluation when expressing effects of climate change and crop breeding on future land use. *Geoderma* 259, 187–195. doi:10.1016/j.geoderma.2015.06.010

Brown, L. C., and Foster, G. R. (1987). Storm erosivity using idealized intensity distributions. *Trans. ASAE* 30, 0379–0386. doi:10.13031/2013.31957

Carter, C. E., Greer, J. D., Braud, H. J., and Floyd, J. M. (1974). Raindrop characteristics in south central United States. *Trans. ASAE* 17, 1033–1037. doi:10.13031/2013.37021

Cerro, C., Bech, J., Codina, B., and Lorente, J. (1998). Modeling rain erosivity using disdrometric techniques. *Soil Sci. Soc. Am. J.* 62, 731–735. doi:10.2136/sssaj1998.03615995006200030027x

Coutinho, M. A., and Tomás, P. P. (1995). Characterization of raindrop size distributions at the vale formoso experimental erosion center. *CATENA* 25, 187–197. doi:10.1016/0341-8162(95)00009-H

Davison, P., Hutchins, M. G., Anthony, S. G., Betson, M., Johnson, C., and Lord, E. I. (2005). The relationship between potentially erosive storm energy and daily rainfall quantity in England and wales. *Sci. Total Environ.* 344, 15–25. doi:10.1016/j.scitotenv.2005.02.002

Elwell, H. A. (1978). Modelling soil losses in southern Africa. *J. Agric. Eng. Res.* 23, 117–127. doi:10.1016/0021-8634(78)90043-4

Fornis, R. L., Vermeulen, H. R., and Nieuwenhuis, J. D. (2005). Kinetic energy–rainfall intensity relationship for central cebu, Philippines for soil erosion studies. *J. Hydrology* 300, 20–32. doi:10.1016/j.jhydrol.2004.04.027

Jayawardena, A. W., and Rezaur, R. B. (2000). Drop size distribution and kinetic energy load of rainstorms in Hong Kong. *Hydrol. Process.* 14, 1069–1082. doi:10.1002/(SICI)1099-1085(20000430)14:6<1069:AID-HYP997>3.0.CO;2-Q

Kathiravelu, G., Lucke, T., and Nichols, P. (2016). Rain drop measurement techniques: A review. *Water* 8, 29. doi:10.3390/w8010029

Kenney, B. C. (1982). Beware of spurious self-correlations. *Water Resour. Res.* 18, 1041–1048. doi:10.1029/WR018i004p01041

Kim, J. G., Yang, D. Y., and Kim, M. S. (2010). Evaluation physical characteristics of raindrop in Anseung, Gyeonggi province. *J. Korean Geomorphol. Assoc.* 17, 49–57.

Kinnell, P. I. A. (1981). Rainfall Intensity-kinetic energy relationships for soil loss prediction1. *Soil Sci. Soc. Am. J.* 45, 153. doi:10.2136/sssaj1981.03615995004500010033x

Lee, G., Yu, W., and Jung, K.APIP (2013). Catchment-scale soil erosion and sediment yield simulation using a spatially distributed erosion model. *Environ. Earth Sci.* 70, 33–47. doi:10.1007/s12665-012-2101-5

Lee, J.-H. (2020). Characterization of rainfall kinetic energy in seoul. *KSCE J. Civ. Environ. Eng. Res.* 40, 111–118. doi:10.12652/KSCE.2020.40.1.0111

Lee, J. S., and Won, J. Y. (2013). Analysis of the characteristic of monthly rainfall erosivity in Korea with derivation of rainfall energy equation. *J. korean Soc. hazard Mitig.* 13, 177–184. doi:10.9798/kosham.2013.13.3.177

Lim, Y. S., Kim, J. K., Kim, J. W., Park, B. I., and Kim, M. S. (2015). Analysis of the relationship between the kinetic energy and intensity of rainfall in daejeon, Korea. *Quat. Int.* 384, 107–117. doi:10.1016/j.quaint.2015.03.021

Madden, L. V., Wilson, L. L., and Ntahimpera, N. (1998). Calibration and evaluation of an electronic sensor for rainfall kinetic energy. *Phytopathology®* 88, 950–959. doi:10.1094/PHYTO.1998.88.9.950

Majumder, S. P., Krishna Chaitanya, A., Datta, A., Padhan, D., Badole, S., and Mandal, B. (2018). "Chapter 11 - dynamics of carbon and nitrogen in agricultural soils: Role of organic and inorganic sources," in *Soil management and climate change*. Editors M. Á. Muñoz and R. Zornoza (Cambridge, Massachusetts, USA: Academic Press), 151–169. doi:10.1016/B978-0-12-812128-3.00011-2

Morgan, R. P. C. (2005). *Soil erosion and conservation*. 3rd ed. Malden, MA: Blackwell Pub.

Osman, K. T. (2014). *Soil degradation, conservation and remediation*. Berlin/Heidelberg, Germany: Springer Dordrecht.

Paringit, E. C., and Nadaoka, K. (2003). Sediment yield modelling for small agricultural catchments: Land-cover parameterization based on remote sensing data analysis. *Hydrol. Process.* 17, 1845–1866. doi:10.1002/hyp.1222

Park, S. W., Mitcell, J. K., and Bubenzer, G. D. (1980). "*An analysis of splash erosion mechanics. ASAE Paper No 80-2502*," in 1980 Winter Meeting, Chicago, IL (St. Joseph, MI: ASAE).

Petan, S., Rusjan, S., Vidmar, A., and Mikoš, M. (2010). The rainfall kinetic energy–intensity relationship for rainfall erosivity estimation in the mediterranean part of Slovenia. *J. Hydrology* 391, 314–321. doi:10.1016/j.jhydrol.2010.07.031

Pimentel, D. (2006). Soil erosion: A food and environmental threat. *Environ. Dev. Sustain.* 8, 119–137. doi:10.1007/s10668-005-1262-8

Rose, C. W. (1960). Soil detachment caused by rainfall. *Soil Sci.* 89, 28–35. doi:10.1097/00010694-196001000-00005

Rosewell, C. J. (1986). Rainfall kinetic energy in eastern Australia. *J. Appl. Meteorology Climatol.* 25, 1695–1701. doi:10.1175/1520-0450(1986)025<1695:RKEIEA>2.0.CO;2

Salles, C., Poesen, J., and Sempere-Torres, D. (2002). Kinetic energy of rain and its functional relationship with intensity. *J. Hydrology* 257, 256–270. doi:10.1016/S0022-1694(01)00555-8

Sanchez-Moreno, J. F., Mannaerts, C. M., Jetten, V., and Löffler-Mang, M. (2012). Rainfall kinetic energy–intensity and rainfall momentum–intensity relationships for Cape Verde. *J. Hydrology* 454 (455), 131–140. doi:10.1016/j.jhydrol.2012.06.007

Sempere-Torres, D., Porrà, J. M., and Creutin, J.-D. (1998). Experimental evidence of a general description for raindrop size distribution properties. *J. Geophys. Res.* 103, 1785–1797. doi:10.1029/97JD02065

Torres, D. S., Salle, S. C., Creutin, J. D., and Delrieu, G. (1992). Quantification of soil detachment by raindrop impact: Performance of classical formulae of kinetic energy in mediterranean storms. *IAHS Publ.* 210, 115–122.

van Dijk, A. I. J. M., Bruijnzeel, L. A., and Rosewell, C. J. (2002). Rainfall intensity–kinetic energy relationships: A critical literature appraisal. *J. Hydrology* 261, 1–23. doi:10.1016/S0022-1694(02)00020-3

Verstraeten, G., Oost, K., Rompaey, A., Poesen, J., and Govers, G. (2002). Evaluating an integrated approach to catchment management to reduce soil loss and sediment pollution through modelling. *Soil Use Manag.* 18, 386–394. doi:10.1111/j.1475-2743.2002.tb00257.x

Wischmeier, W. H., and Smith, D. D. (1958). Rainfall energy and its relationship to soil loss. *Trans. AGU.* 39, 285. doi:10.1029/TR039i002p00285

frontiers | Frontiers in Environmental Science

TYPE Original Research
PUBLISHED 30 November 2022
DOI 10.3389/fenvs.2022.1011755

OPEN ACCESS

EDITED BY
Donatella Valente,
University of Salento, Italy

REVIEWED BY
Kai Liu,
Shandong Normal University, China
Fengtai Zhang,
Chongqing University of Technology, China

*CORRESPONDENCE
Shiliang Liu,
shiliangliu@bnu.edu.cn
Yuhong Dong,
yhongdong@163.com

SPECIALTY SECTION
This article was submitted to Land Use Dynamics, a section of the journal Frontiers in Environmental Science

RECEIVED 04 August 2022
ACCEPTED 10 November 2022
PUBLISHED 30 November 2022

CITATION
Liu S, Dong Y, Wang F and Liu H (2022), Priority area identification of ecological restoration based on land use trajectory approach—Case study in a typical karst watershed.
Front. Environ. Sci. 10:1011755.
doi: 10.3389/fenvs.2022.1011755

Priority area identification of ecological restoration based on land use trajectory approach—Case study in a typical karst watershed

Shiliang Liu[1]*, Yuhong Dong[2]*, Fangfang Wang[1] and Hua Liu[1]

[1]State Key Laboratory of Water Environment Simulation, School of Environment, Beijing Normal University, Beijing, China, [2]Research Institute of Forestry, Chinese Academy of Forestry, Beijing, China

In the planning and restoration of land ecological space, the ecological restoration priority area has attracted more and more attention, especially in the regions with great vulnerability. As a typical area of karst ecological region in Southwest China, Wujiang River Basin experienced human disturbance and land uses which had great impacts on the ecological environment. Based on the land use evolution from 1985 to 2019, the change of ecological-production-living land in Wujiang River Basin was analyzed by transfer matrix, intensity analysis and long-time series trajectory approaches. The results showed that from 1985 to 2019, the ecological land in Wujiang River Basin significantly decreased, the production land increased first then decreased, and living land increased significantly. The reduced ecological land was mainly transformed to cropland. After 1990, the change intensity of land use in Wujiang River Basin gradually increased. At the category level, the intensity of forest land change was the most stable, and while that of barren land, shrub land and grassland were active. At the transition level, the increased impervious land was mainly from cropland, and the reduced forest land was mainly transformed into cropland. Trajectory analysis from 1985 to 2019 showed that the stable land use type of Wujiang River accounted for 67.36% of the total area of the basin and forest land was the main stable land use type. Our research spatially identified the land use change from different aspects which could be a new approach for ecological restoration. Also, our study can provide decision-making basis for the sustainable use of land resources in the study area.

KEYWORDS

land use change, ecological-production-living land, spatial-temporal variation, land use change trajectory, Wujiang River Basin

1 Introduction

Land use changes are one of the world-wide issues which have the most significant effects on the natural environment and ecosystem processes (Bryan et al., 2018; Hasan et al., 2020; Chu et al., 2022). The spatial-temporal change of land use provides basic data for other studies (Tang et al., 2020; Chen et al., 2021; Zhang et al., 2021; Chatterjee et al., 2022). In order to optimize and coordinate the leading functions of land use, the concept of ecological-production-living spaces is put forward, which is an effective integration and supplement for detailed land use classification (Yang et al., 2018). Many researches on ecological land have been carried out from different types (Guo et al., 2018), in different regions (Zheng and He, 2021) and at different scales (Zhao et al., 2022).

For quantitative methods on land use change, many approaches measuring the dynamics, pattern and process are gradually developed with different conceptual approaches. Usually, land use change was analyzed by transfer matrix method in different periods (Meyer and Früh-Müller, 2020), utilizing different land use data for various data sources (Chen et al., 2021). The land use transfer matrix can comprehensively and specifically analyze the quantitative and structural characteristics of regional land use change and the change direction of each category (Takada et al., 2010). Land use matrix was used to analyzed the ecological effects by ecosystem services value (Niu et al., 2018; Qiu et al., 2019). This method is simple and widely used which is effective for describing historical land use change and simulation analysis. However, the direct transformation information on different land use type change cannot reveal the inherent interaction process between human and environment. Also, it cannot be systematically conducted in-depth research on the multiple consecutive time intervals. The matrix method do not show the interval's rate of change, the change of each category's relative to the its size and specific transitions form one category to another category (Huang et al., 2012). Therefore, the intensity analysis method is proposed to calculate the intensity of land use change from the interval level, the category level and the transition level, respectively (Aldwaik and Pontius, 2012). The intensity analysis method can systematically study the transfer matrix of land use in multiple continuous time intervals (Mallinis et al., 2014). Land use intensity has been defined as an effective means of quantifying the intensity of human interference with land development and use, management and conservation, and the corresponding land outputs that result (Huang et al., 2012). Intensity analysis was used to identify systematic and stationary processes to analysis its relation with socioeconomic changes and policies (Mallinis et al., 2014). This concept and its methodology are commonly promoted in ecology, land science and socio-economic fields, where demand pressures on different land use types and land management approaches become the basis for constructing a land use intensity indicator system. However, both the two above methods are based on the comparison of adjacent land use data to reveal the spatio-temporal patterns of two or more periods. To acquire more information of land use evolution, trajectory method has been brought out to obtain not only the spatial and temporal characteristics of land use change, but also its transfer and flow direction (Swetnam, 2007). The method was used to reveal the effect of human activities and environmental factors (Zhou et al., 2008), reveal the relationships between change patterns and natural factors (Wang et al., 2012), the impact of land use trajectories on ground water (Zomlot et al., 2017), and the impacts of historical trajectories of land use on soil properties (Libessart et al., 2022). The spatial pattern of land use change trajectories can provide data support for land use policy and protection of ecological environment (Wang et al., 2020).

Karst land is an important and unique terrain on the earth's surface because of its high ecological fragility. Wujiang River Basin is located in the typical karst area of Southwest China. The special geological background, coupled with the impact of human activities, has led to the continuous degradation of the ecological environment, which has evolved into a typical ecological fragile area (Wang and Li, 2007; Xu et al., 2021). Land use is the most important manifestation of human action on karst environment. The research on land use change in Wujiang River Basin mainly includes the impact of land use on soil erosion intensity (Wang et al., 2013b), analysis on the evolution of ecosystem service value based on land use (Niu et al., 2018), spatial and temporal evolution of land use based on topographic gradient (Liu et al., 2020), evaluation of eco-environmental effect of karst mountain basin based on land use transformation (Liu et al., 2021). Based on this, this study used the transformation matrix, the intensity analysis and the change trajectory analysis method to analyze the land use change in Wujiang River Basin. The objectives of this study were to 1) reveal the change of ecological-production-living land based on the land use matrix method; 2) evaluate the intensity and stability of land use change; 3) identify the spatio-temporal land use change trajectories, so provide basis for identification of priority areas for ecological restoration. Our study provided an integrated application of land use change trajectory method with traditional land use change analysis methods. The research can provide data support and decision-making basis for the sustainable use of land resources and ecological environment protection.

2 Material and methods

2.1 Study area

The Wujiang River Basin is located in Southwest China (26°06′–30°22′N, 104°10′–109°22′E), (Figure 1), with an area of 87,900 km^2 and a total length of 1,037 km. The region is characterized by the subtropical temperate and humid monsoon climate, with an average annual temperature of 13–18°C, an annual

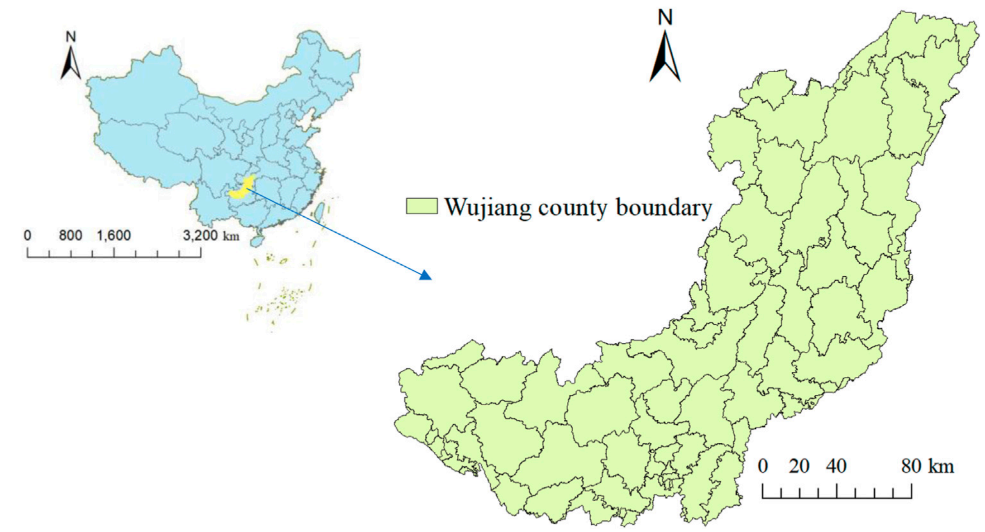

FIGURE 1
The position of Wujiang River Basin.

TABLE 1 Code table of land use types.

Land use code	Type
1	Cropland
2	Forest land
3	Shrub land
4	Grassland
5	Water area
6	Impervious land
7	Barren land

average precipitation of 1,130 mm. It is a typical karst area and rocky desertification area, as well as an important water conservation area and soil conservation area designated by National Ecological Function Zoning. Irrational land use has led to ecological degradation of this fragile karst systems.

2.2 Data sources

The land use data from 1985 to 2019 were derived from https://zenodo.org/record/4417810#.YuqLFc7YuUl, with a spatial resolution of 30 m and eight period. The land use in the study area is classified into 7 types, including cropland, forest land, shrub land, grassland, water area, barren land, impervious land. The land use codes used for trajectory analysis were shown in Table 1. The ecological lands include forest land, shrub land, grass land, water area and barren land. Cropland is classified as production land and impervious land is classified as living land.

2.3 Research methods

2.3.1 Land use transfer matrix

The land use transfer matrix was used to analyze the transformation of various land use types during one certain period, which can describe the changing area and direction of different land use types (Cai et al., 2017).

2.3.2 Analysis of land use intensity change and stability

Intensity analysis includes three levels: time interval level, category level and transition level (Aldwaik and Pontius, 2012). The change area and change intensity of each time interval and each land type were calculated, and the observed change intensity was compared with the uniform change intensity to reveal the change characteristics of different levels.

2.3.3 Land use change trajectory method

The trajectory of land use change refers to successions of land use types over the eight periods. The trajectory codes was calculated using formula as below (Wang et al., 2013a):

$$T_i = (G1)_i \times 10^{n-1} + (G2)_i \times 10^{n-2} + \cdots + (Gn)_i \times 10^{n-n}$$

where T_i is the trajectory code of land use change at the give gird; n is the number of time nodes; $(G1)_i$, $(G2)_i$, and $(Gn)_i$ are the codes of the land use type of each time node at the given grid.

A GIS database of the land use change trajectory of Wujiang River Basin was obtained using the formula. The database file of the change trajectory were processed further to extract three indices, namely: similarity (T), turnover (T) and diversity (D) (Swetnam,

TABLE 2 Classification principle of land use change trajectory.

Turover	Diversity	Similarity	Class	Example	Notes
0	1	6	Stable	11111111	No changes
2	2	7	Metastable	11111211	One dominant category and changes once in a certain period
1	2	7	Metastable	12222222, 11111117	
1	2	4, 5, 6	Stepped	11111122, 55511111	One change between two dominant categories
2	2	4, 5, 6	Discontinuous	11112211	Elements exhibits different trends
2	3	3, 4, 5, 6	Discontinuous	11111552	
3–6	2/3	4, 5, 6/5, 6	Cyclical	21211212	Frequent change has occurred
7	2	4	Cyclical	12121212	
3, 4/5, 6	3	3, 4	Dynamic	13212331	A high turnover between many different classes
3–6	4	2, 3, 4, 5	Dynamic	11212143	
4, 5	5	2, 3, 4	Dynamic	11233455	
6	5	3	Dynamic	15765411	
7	3, 4	3, 4	Dynamic	12313414	

1, cropland; 2, forest land; 3, shrub land; 4, grassland; 5, water area; 6, impervious land; 7, barren land.

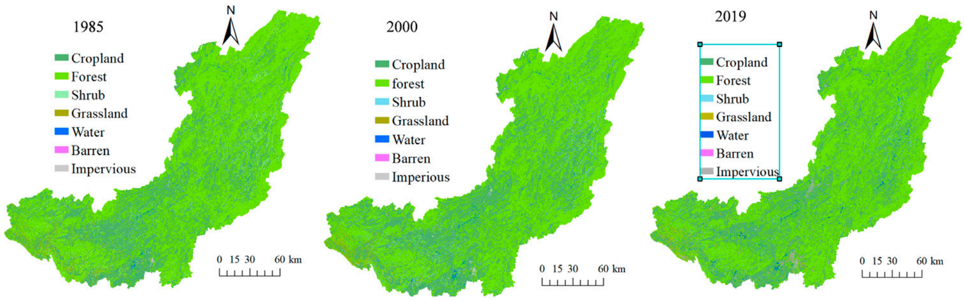

FIGURE 2
The land use in Wujiang River Basin in 1985, 2000 and 2019.

2007; Wang et al., 2020). The STD method was used to determined land use change trajectory. The three indices were combined into one of six groups: stable, metastable, stepped, discontinuous, cyclical and dynamic (Table 2). These six groups were then linked back to the GIS database to map the spatial trajectory of land use change.

3 Results

3.1 Land use transfer matrix

The land use in Wujiang River Basin was mainly cropland and forest land, followed by shrub land and grassland. From 1985 to 2000, the area of shrub land, grassland and barren land decreased, and the area of other land use types increased (Figure 2). The policy of returning farmland to forests from 2000 had an important impact on the land use change pattern of the Wujiang River basin. From 2000 to 2019, the area of shrub land, grassland and cropland decreased, and the area of other land use types increased. The ecological land decreased and the living land increased in the two time interval, while the production land increased in the first time interval and decreased in the second time interval.

As seen from Figure 3, the land use change in Wujiang River Basin in various periods was mainly the conversion between cropland and forest land, followed by the conversion from shrub land to forest land and cropland, forest land to shrub land, cropland to shrub land and grassland, and grassland to cropland. The main land use change showed different trends. From 1985 to 1995, shrub land decreased and cropland increased. From 1995 to 2000, cropland decreased and forest land increased. From 2000 to 2005, cropland and grassland decreased and shrub land increased. From 2005 to 2010, shrub land and grass land decreased and cropland increased. From 2010 to 2015, shrub land decreased and cropland and forest land increased. From

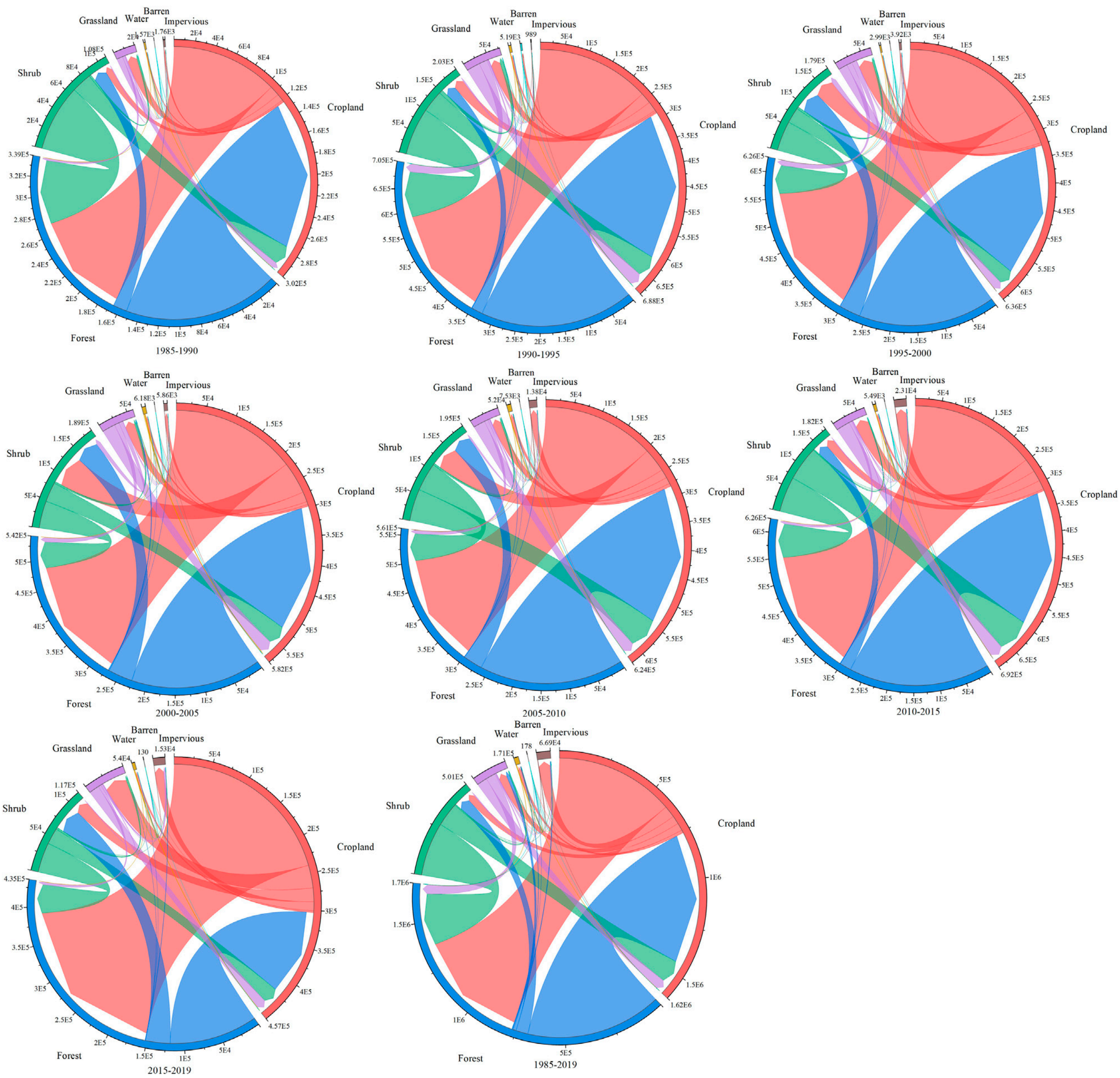

FIGURE 3
The change area of land use in different periods (The outer circle is the changed land type, the inner circle links the conversion direction and area between land types, the transfer line is the flow direction of a certain land type, and the line thickness indicates the conversion area).

2015 to 2019, cropland decreased and forest land increased. The area of impervious land continued to increase, significantly increasing after 2005. The land use change was closely related to socio-economic factors and policy factors. The pilot project of returning farmland to forests was completed in 2000 and launched in 2002. In 2008, comprehensive desertification control was launched, and the water and soil conservation plan were implemented in 2017.

3.2 Intensity and stability of land use change

3.2.1 Land use change in the time interval level

The annual intensity of land use change in the time interval level is shown in Figure 4. The annual intensity in 1990–1995, 1995–2000, 2005–2010 and 2010–2015 was greater than the uniform annual change, indicating the rapidly change in these periods. The change

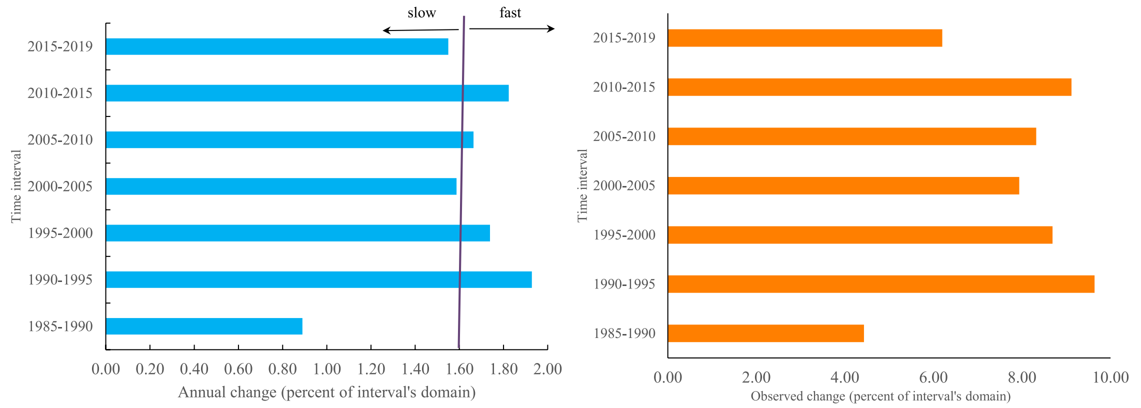

FIGURE 4
The interval level change of land use in Wujiang River Basin.

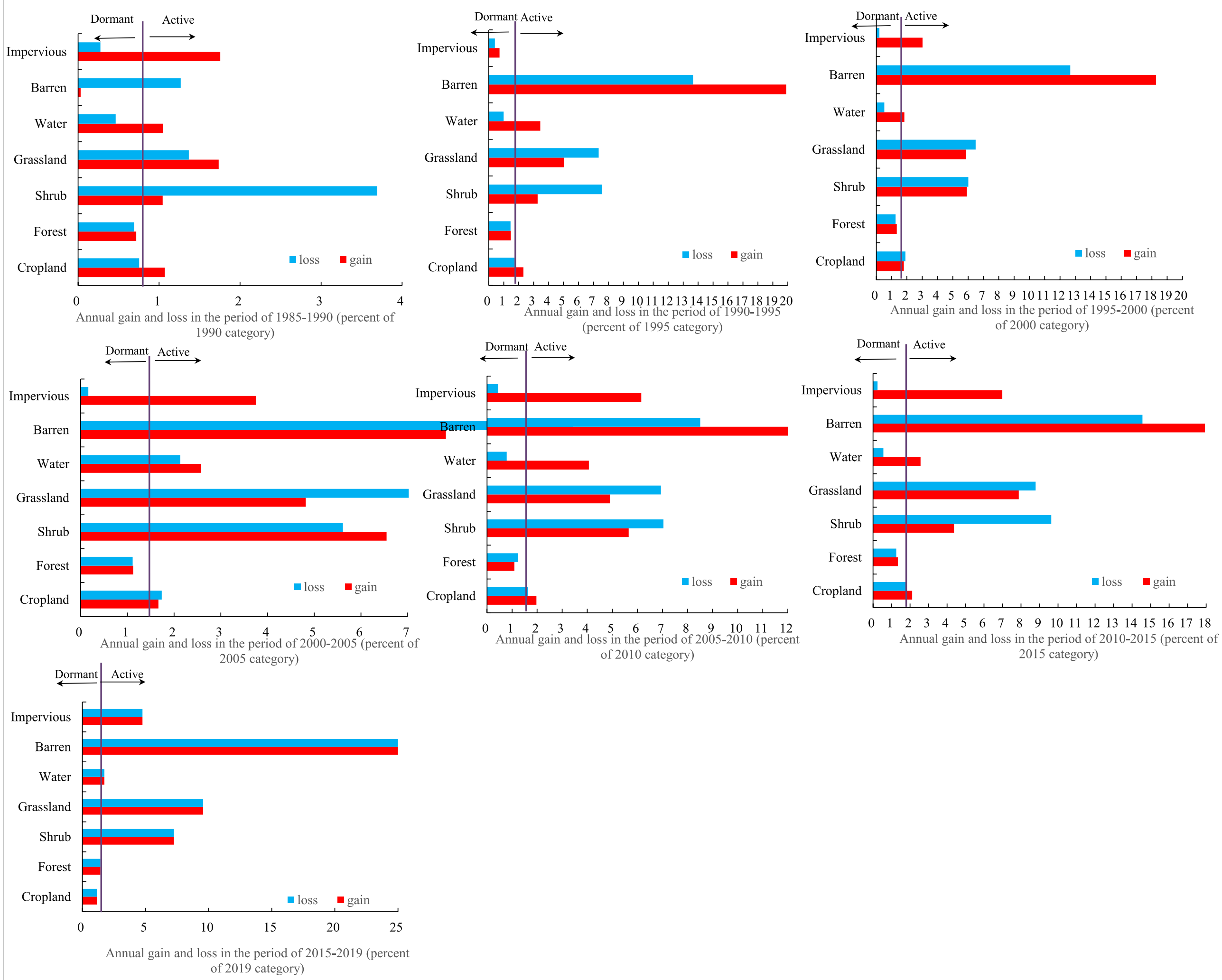

FIGURE 5
Intensity changes of land use in category level in Wujiang River Basin.

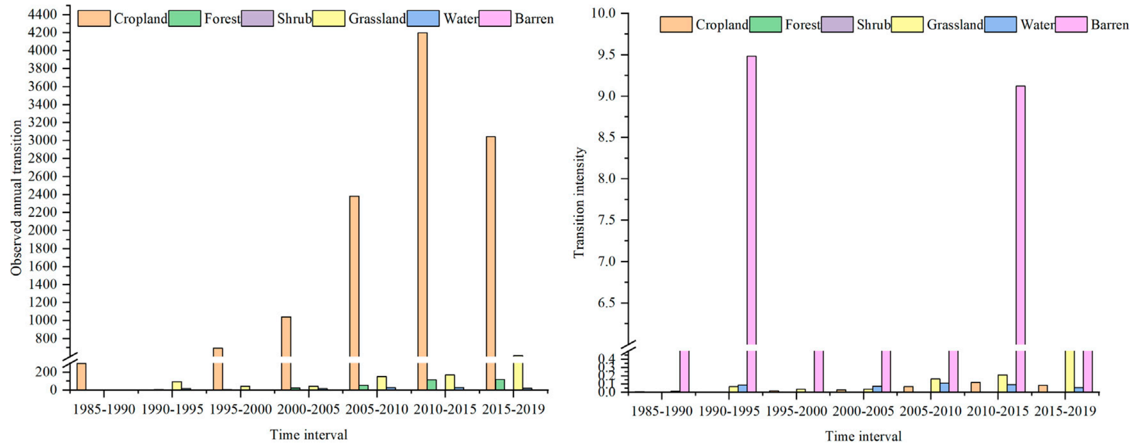

FIGURE 6
Transition from other land use types to impervious land in the transition level.

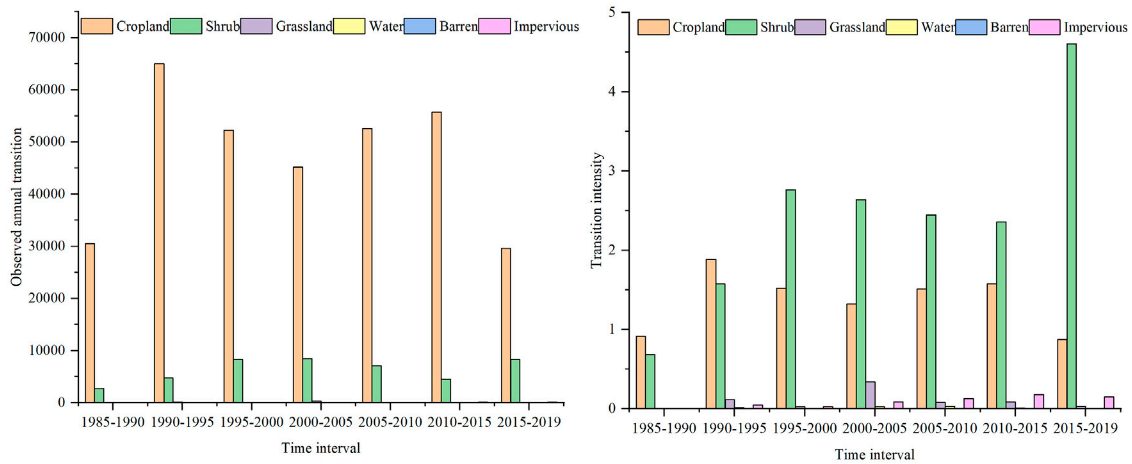

FIGURE 7
Transition from forest land to other land use types in the transition level.

intensity in 1985–1995, 2000–2005 and 2015–2019 was less than the uniform annual change, indicating that the annual intensity in these periods was slow. The trend of area change is consistent with the annual intensity change. The change area in 1990–1995 and 2010–2015 was the largest, accounting for 9.64% and 9.12% of the study area respectively. The change area in 1985–1990 was the smallest, accounting for 4.43% of the study area.

3.2.2 Land use changes in the category level

The change intensity of the land use in the category level is shown in Figure 5. The increase and decrease intensity of the forest land were less than the uniform intensity, and the forest land was stable in the whole period. The increasing intensity and decreasing intensity of shrub land and grassland were greater than the uniform intensity, and they are active in the whole period. Except that the increase intensity of barren land in the period of 1985–1990 was less than the average value, the increase and decrease intensity in other time intervals were greater than the uniform intensity, which was basically active in the whole period. Cropland, water area and impervious land showed different intensity change trends in different time intervals.

3.2.3 Land use change in the transition level

The transition level to impervious land in the seven time intervals is shown in Figure 6. The transition intensity of barren

10.3389/fenvs.2022.1011755

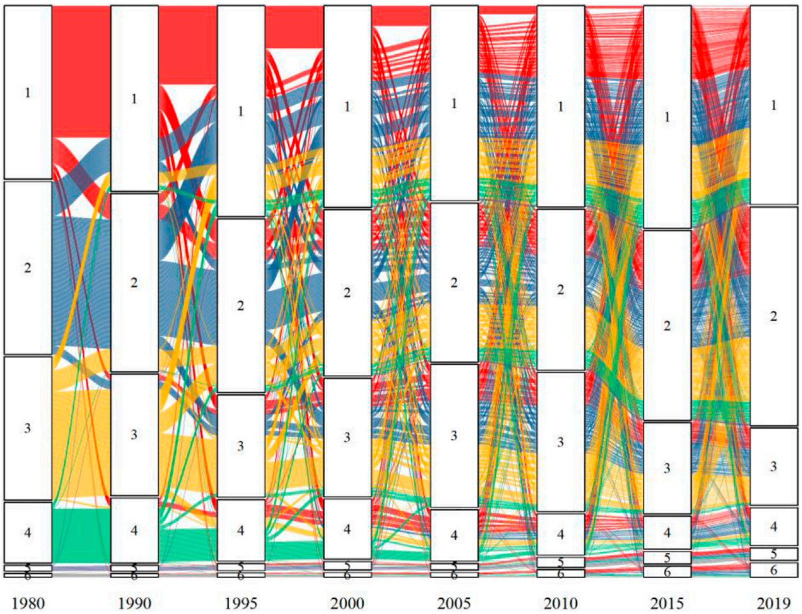

FIGURE 8
Land use change trajectory of Wujiang River Basin from 1985 to 2019 (1, Cropland; 2, Forest land; 3, Shrub land; 4, Grassland; 5, Water area; 6, Impervious land; area > 1 km^2).

land, water area and cropland were greater than the uniform intensity in 1985–1990. The transition intensity of barren land, grassland and water area was greater than the uniform intensity in 1990–1995. The transition intensity of barren land, grassland land and cropland were greater than the uniform intensity in 1995–2000. In all periods after 2000, transition intensity of barren land, water area, grassland and cropland were greater than the average change intensity. The increase of impervious land was mainly from cropland, followed by grassland and forest land.

The annual transition and transition intensity from forest land to other land use types in transition level in seven time intervals are shown in Figure 7. The transition intensity of forest land into cropland from 1985 to 1990, from 1990 to 1995 and from 2010 to 2015 were greater than the uniform intensity, and the reduction from forest land into shrub land in the period from 1995 to 2019 were greater than the uniform intensity. The observed annual transition of forest land was mainly to cropland and shrub land.

3.3 Spatio-temporal trajectory change

The change trajectory with an area greater than 1 km^2 is shown in Figure 8. The trajectory changes of different land use types in different periods were obvious. The change track was stable in the early stage, and changed drastically after 2000. From 1985 to 2019, cropland mainly flowed to forest land and shrub land, followed by grassland, water area and impervious land. Forest land mainly flowed to cropland and shrub land, followed by grassland, and shrub mainly flowed to cropland, forest land, followed by grassland.

From 1985 to 2019, the land use change trajectories in Wujiang River Basin are shown in Figure 9. The stable type accounted for 67.36% of the total area and was the largest type. The metastable type, stepped type, discontinuous type, cyclical type and dynamic type accounts for 8.40%, 13.11%, 5.90%, 4.22% and 0.92% of the total area respectively. The discontinuous type, cyclical type and dynamic type of land use change trajectories are sporadically distributed in the whole Wujiang River Basin, of which the distribution in the high-altitude areas is affected by the karst landforms and mines, while in other regions, these three change trajectories changes are more distributed in the lower altitude areas.

4 Discussion

4.1 The changes of ecological-production-living land and the priority area identification of regional ecological restoration

Understanding the ecological effects of land use based on the ecological-production-life function is an important issue of land use/land cover change (Zhang et al., 2019). The eco-environmental effects and spatial heterogeneity of

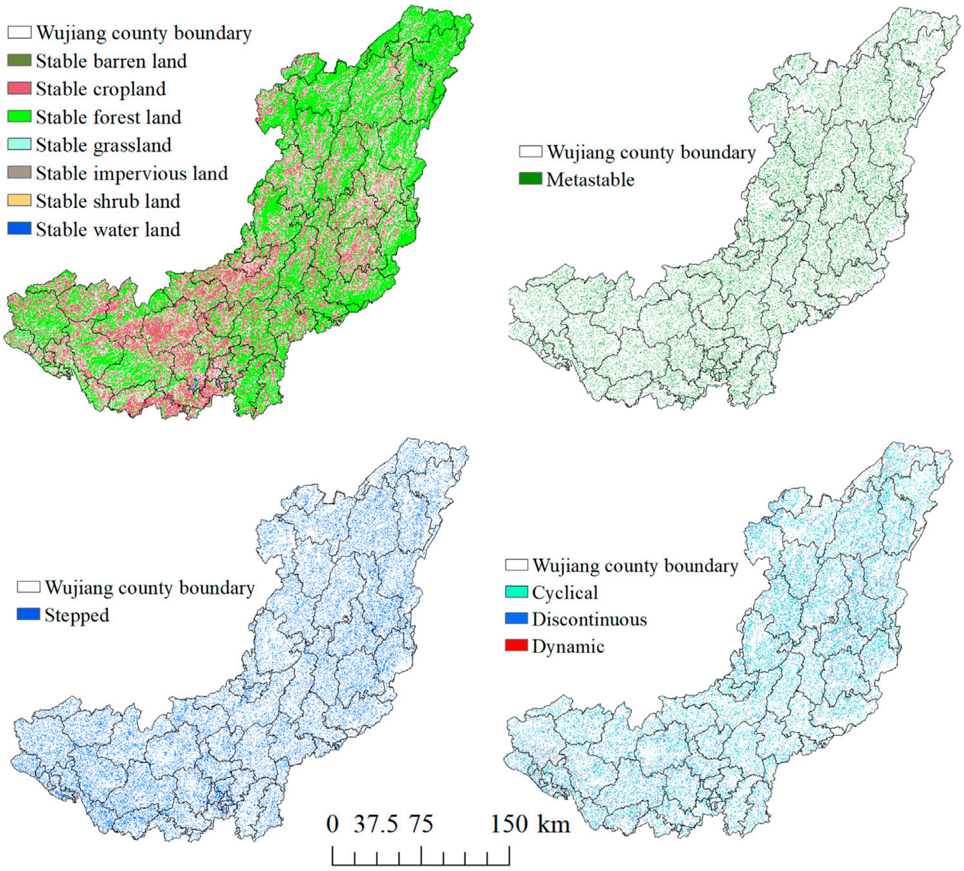

FIGURE 9
The land use change trajectory from 1985 to 2019.

ecological-productive-living land is an important basis for regional territorial development planning and eco-environment protection (Han et al., 2021). In this study, the ecological land decreased from 1985 to 2000 and from 2000 to 2019, the production increased first then decreased, and living land increased in Wujiang River Basin, and the reduction of ecological land is mainly due to the reduction of shrub land and grassland. The land use change based on land use matrix method is mainly between cropland, forest land and shrub land. The land use change in Wujiang River Basin is closely related to terrain gradient, and also influenced by socioeconomic factors, and policy factors (Liu et al., 2020). Since 2000, the increase of ecological land area of forest land and water area in the Wujiang River basin is due to the ecological quality control projects such as the comprehensive control project of rocky desertification, the project of returning farmland to forest and grassland, and the construction of water conservancy facilities (Liu et al., 2021). Other research using land use transfer matrix showed that ecological land was decreasing continuously and living land expanded rapidly (Cai et al., 2017). The rapid increase of farmland and construction land has damaged the ecosystem, including grasslands, forest lands and aquatic regions, thus decreasing the ecosystem services value (Wang et al., 2017). The result of this study showed the most stable land was forest land, while baren land, shrub land and grassland were the most active in the category level. Other research showed that agriculture land and built land are active categories and the transition from agriculture land to built land is intensively systematic (Huang et al., 2012).

In this study, the land use change trajectory method was used to reveal the stability and change area of the ecological-production-living land during in the long-time series of Wujiang River Basin. As shown in Figure 8, the flow of land use type was obvious during the long-term time series. By classification of the land use change trajectory into six groups as shown in Table 2, the spatial distribution was shown if Figure 9. The results showed the most stable land was forest land. And the distribution of dynamic trajectory zone was affected by the karst landforms and mines in the higher altitude region, which may be identified as priority area in regional ecological restoration.

4.2 Limitations of the three different methods

In this study, land use dynamics is revealed based on three methods, which is useful for ecological restoration priority identification. Intensity analysis is a top-down hierarchical interpretive mathematical framework, which is important for systematic and in-depth understanding of the land use change process. The complex land use in the study area is more suitable for using different levels of intensity analysis. However, intensity analysis cannot reveal the change trajectory. The trajectory method can accurately extract land use change trajectories to exhibit the transfer, flow and pattern of land use types, thus the spatial and temporal evolution characteristics of land can be derived from time series aspect. However, the main problem is that with the increase of study time series, the trajectories of land use change become more complicated and the trajectories are more difficult to extract.

The shortcomings of this study are that the driving force mechanism of land use change is not deeply elaborated and the future change trend is not predicted. In addition, the study of landscape fragmentation, spatial heterogeneity trends, and evaluation of the risk of human activities on ecosystem stability need to be further explored in depth.

5 Conclusion

The study area has undergone dramatic land use change in the past 34 years. The goal of this study was to quantify the spatial and temporal changes of ecological space and analyze its stability. The results showed that from 1985 to 2019, ecological land reduced, the production land increased first then decreased, and living land increased, and the conversion between production land and living land was frequent. The stable trajectory area accounted for the largest proportion of the study area, indicating that land use situation in the study area was stable on the whole. It is necessary to further investigate the ecological space that needs to be repaired from the aspects of ecosystem service function and ecological vulnerability.

Data availability statement

The original contributions presented in the study are included in the article/Supplementary Materials, further inquiries can be directed to the corresponding authors.

Author contributions

SL: research design, review and editing; YD: drafting the article and revising; FW and HL: the methods and the reference.

Funding

This work was supported by National Key Research and Development Project (No. 2022YFF1303204) and National Natural Sciences Fund Project (No. 42271097).

Conflict of interest

The authors declare that the research was conducted in the absence of any commercial or financial relationships that could be construed as a potential conflict of interest.

References

Aldwaik, S. Z., and Pontius, R. G. (2012). Intensity analysis to unify measurements of size and stationarity of land changes by interval, category, and transition. *Landsc. Urban Plan.* 106 (1), 103–114. doi:10.1016/j.landurbplan.2012.02.010

Bryan, B. A., Ye, Y., Zhang, J. e., and Connor, J. D. (2018). Land-use change impacts on ecosystem services value: Incorporating the scarcity effects of supply and demand dynamics. *Ecosyst. Serv.* 32, 144–157. doi:10.1016/j.ecoser.2018.07.002

Cai, E., Jing, Y., Liu, Y., Yin, C., Gao, Y., and Wei, J. (2017). Spatial–temporal patterns and driving forces of ecological-living-production land in Hubei Province, Central China. *Sustainability* 10 (1), 66. doi:10.3390/su10010066

Chatterjee, S., Dutta, S., Dutta, I., and Das, A. (2022). Ecosystem services change in response to land use land cover dynamics in Paschim Bardhaman District of West Bengal, India. *Remote Sens. Appl. Soc. Environ.* 27, 100793. doi:10.1016/j.rsase.2022.100793

Chen, H., Chen, C., Zhang, Z., Lu, C., Wang, L., He, X., et al. (2021). Changes of the spatial and temporal characteristics of land-use landscape patterns using multi-temporal landsat satellite data: A case study of zhoushan island, China. *Ocean Coast. Manag.* 213, 105842. doi:10.1016/j.ocecoaman.2021.105842

Chu, X., Lu, Z., Wei, D., and Lei, G. (2022). Effects of land use/cover change (LUCC) on the spatiotemporal variability of precipitation and temperature in the Songnen Plain, China. *J. Integr. Agric.* 21 (1), 235–248. doi:10.1016/s2095-3119(20)63495-5

Guo, X., Chang, Q., Liu, X., Bao, H., Zhang, Y., Tu, X., et al. (2018). Multi-dimensional eco-land classification and management for implementing the ecological redline policy in China. *Land Use Policy* 74, 15–31. doi:10.1016/j.landusepol.2017.09.033

Han, M., Kong, X., Li, Y., Wei, F., Kong, F., and Huang, S. (2021). Eco-environmental effects and its spatial heterogeneity of 'ecological-production-living' land use transformation in the Yellow River Delta. *Sci. Geogr. Sinia* 41 (6), 1009–1018. doi:10.13249/j.cnki.sgs.2021.06.010

Hasan, S. S., Zhen, L., Miah, M. G., Ahamed, T., and Samie, A. (2020). Impact of land use change on ecosystem services: A review. *Environ. Dev.* 34, 100527. doi:10.1016/j.envdev.2020.100527

Huang, J., Pontius, R. G., Li, Q., and Zhang, Y. (2012). Use of intensity analysis to link patterns with processes of land change from 1986 to 2007 in a coastal watershed of southeast China. *Appl. Geogr.* 34 (3), 371–384. doi:10.1016/j.apgeog.2012.01.001

Libessart, G., Franck-Néel, C., Branchu, P., and Schwartz, C. (2022). The human factor of pedogenesis described by historical trajectories of land use: The case of Paris. *Landsc. Urban Plan.* 222, 104393. doi:10.1016/j.landurbplan.2022.104393

Liu, C. J., Zhou, G. F., Huang, Q. F., Lei, C., Zhou, Y., and Zhang, N. (2020). Spatial-temporal evolution of land use in Wujiang River Basin in Guizhou Province based on the terrain gradient. *J. Guizhou Normal Univ. (Nat. Sci.* 38 (6), 45–54. doi:10.1088/1755-1315/108/4/042066

Liu, C., Zhou, G., Huang, Q., Zhou, Y., and Zhang, D. (2021). Ecological environment effect on the karst mountain watershed based on land use transition. *Ecol. Sci.* 40 (3), 102–111. doi:10.14108/j.cnki.1008-8873.2021.03.013

Mallinis, G., Koutsias, N., and Arianoutsou, M. (2014). Monitoring land use/land cover transformations from 1945 to 2007 in two peri-urban mountainous areas of Athens metropolitan area, Greece. *Sci. Total Environ.* 490, 262–278. doi:10.1016/j.scitotenv.2014.04.129

Meyer, M. A., and Früh-Müller, A. (2020). Patterns and drivers of recent agricultural land-use change in Southern Germany. *Land Use Policy* 99, 104959. doi:10.1016/j.landusepol.2020.104959

Niu, Q., Zhou, X., Xu, Y., Yang, J., and Zhang, J. (2018). Analysis of ecosystem service value evolution of Wujiang River basin of Guizhou Province based on land use. *Ecol. Sci.* 37 (5), 165–173. doi:10.14108/j.cnki.1008-8873.2018.05.022

Qiu, L., Pan, Y., Zhu, J., Amable, G. S., and Xu, B. (2019). Integrated analysis of urbanization-triggered land use change trajectory and implications for ecological land management: A case study in Fuyang, China. *Sci. Total Environ.* 660, 209–217. doi:10.1016/j.scitotenv.2018.12.320

Swetnam, R. D. (2007). Rural land use in England and Wales between 1930 and 1998: Mapping trajectories of change with a high resolution spatio-temporal dataset. *Landsc. Urban Plan.* 81 (2), 91–103. doi:10.1016/j.landurbplan.2006.10.013

Takada, T., Miyamoto, A., and Hasegawa, S. F. (2010). Derivation of a yearly transition probability matrix for land-use dynamics and its applications. *Landsc. Ecol.* 25 (4), 561–572. doi:10.1007/s10980-009-9433-x

Tang, J., Li, Y., Cui, S., Xu, L., Ding, S., and Nie, W. (2020). Linking land-use change, landscape patterns, and ecosystem services in a coastal watershed of southeastern China. *Glob. Ecol. Conservation* 23, e01177. doi:10.1016/j.gecco.2020.e01177

Wang, D., Gong, J., Chen, L., Zhang, L., Song, Y., and Yue, Y. (2012). Spatio-temporal pattern analysis of land use/cover change trajectories in Xihe watershed. *Int. J. Appl. Earth Obs. Geoinf.* 14 (1), 12–21. doi:10.1016/j.jag.2011.08.007

Wang, D., Gong, J., Chen, L., Zhang, L., Song, Y., and Yue, Y. (2013a). Comparative analysis of land use/cover change trajectories and their driving forces in two small watersheds in the Western Loess Plateau of China. *Int. J. Appl. Earth Obs. Geoinf.* 21, 241–252. doi:10.1016/j.jag.2012.08.009

Wang, S., Feng, Z., Yu, Y., and Zhang, H. (2020). Land use/cover change trajectory analysis based on improved stable mapping method. *China Acad. J. Electron. Publ. House* 51 (8), 152–162. doi:10.6041/j.issn.1000-1298.2020.08.017

Wang, S., and Li, Y. (2007). Problems and development trends about researches on karst rocky desertification. *Adv. Earth Sci.* 22 (6), 573–582. doi:10.3321/j.issn:1001-8166.2007.06.003

Wang, X., Dong, X., Liu, H., Wei, H., Fan, W., Lu, N., et al. (2017). Linking land use change, ecosystem services and human well-being: A case study of the manas River Basin of xinjiang, China. *Ecosyst. Serv.* 27, 113–123. doi:10.1016/j.ecoser.2017.08.013

Wang, Y., Cai, Y. L., and Pan, M. (2013b). Analysis on the relationship between soil erosion and land use in Wujiang River Basin in Guizhou Province. *Res. Soil Water Conservation* 20 (3), 11–18.

Xu, G., Xiao, J., Oliver, D. M., Yang, Z., Xiong, K., Zhao, Z., et al. (2021). Spatio-temporal characteristics and determinants of anthropogenic nitrogen and phosphorus inputs in an ecologically fragile karst basin: Environmental responses and management strategies. *Ecol. Indic.* 133, 108453. doi:10.1016/j.ecolind.2021.108453

Yang, Q. K., Duan, X. J., and Wang, L. (2018). Land use transformation based on ecological-production-living spaces and associated eco-environment effects: A case study in the yangtze river Delta. *Sci. Geogr. Sin.* 38 (1), 97–106. doi:10.3390/land11071076

Zhang, L., Liu, G., Liu, Y., and Wei, J. (2019). The effects of "ecological-production-living" land use transformation on associated ecological service value: A case study of yingkou city. *Chin. J. Ecol.* 38 (3), 838–846. doi:10.13292/j.1000-4890.201903.024

Zhang, Y., Li, Y., Lv, J., Wang, J., and Wu, Y. (2021). Scenario simulation of ecological risk based on land use/cover change – a case study of the Jinghe county, China. *Ecol. Indic.* 131, 1–12. doi:10.1016/j.ecolind.2021.108176

Zhao, H. L., Xu, Y., Zhou, Y., Zhang, G. L., and Chen, X. (2022). Quantitative identification and analysis of spatiotemporal evolution characteristics of ecological space: Case study of Hulun Buir citys. *J. Nat. Resour.* 37 (8), 2153–2168. doi:10.31497/zrzyxb.20220815

Zheng, Z., and He, Q. (2021). Spatio-temporal evaluation of the urban agglomeration expansion in the middle reaches of the Yangtze River and its impact on ecological lands. *Sci. Total Environ.* 790, 148150. doi:10.1016/j.scitotenv.2021.148150

Zhou, Q., Li, B., and Kurban, A. (2008). Spatial pattern analysis of land cover change trajectories in Tarim Basin, northwest China. *Int. J. Remote Sens.* 29 (19), 5495–5509. doi:10.1080/01431160802060938

Zomlot, Z., Verbeiren, B., Huysmans, M., and Batelaan, O. (2017). Trajectory analysis of land use and land cover maps to improve spatial-temporal patterns, and impact assessment on groundwater recharge. *J. Hydrology* 554 (554), 558–569. doi:10.1016/j.jhydrol.2017.09.032

frontiers | Frontiers in Environmental Science

TYPE Original Research
PUBLISHED 09 December 2022
DOI 10.3389/fenvs.2022.1009660

Check for updates

OPEN ACCESS

EDITED BY
Donatella Valente,
University of Salento, Italy

REVIEWED BY
Meraj Alam Ansari,
ICAR-Indian Institute of farming system research, Modipuram, India
Bilal Ahmad,
Northwest University, China

*CORRESPONDENCE
Owais Ali Wani,
owaisaliwani@skuastkashmir.ac.in
Subhash Babu,
subhiari@gmail.com

†These authors share first authorship

SPECIALTY SECTION
This article was submitted to Land Use Dynamics,
a section of the journal
Frontiers in Environmental Science

RECEIVED 02 August 2022
ACCEPTED 22 November 2022
PUBLISHED 09 December 2022

CITATION
Kumar SS, Wani OA, Mir SA, Babu S, Sharma V, Chesti MUH, Baba ZA, Sofi PA, Wani FJ, Dar SR, Singh R and Yadav D (2022), Soil carbon dynamics in the temperate Himalayas: Impact of land use management.
Front. Environ. Sci. 10:1009660.
doi: 10.3389/fenvs.2022.1009660

Soil carbon dynamics in the temperate Himalayas: Impact of land use management

Shamal Shasang Kumar[1†], Owais Ali Wani[1*†], Shakeel Ahmad Mir[1], Subhash Babu[2*], Vikas Sharma[3], Majeed Ul Hassan Chesti[1], Zahoor Ahmad Baba[1], Parvaze Ahmad Sofi[1], Fehim Jeelani Wani[1], Shahnawaz Rasool Dar[1], Raghavendra Singh[4] and Devideen Yadav[5]

[1]Sher-e-Kashmir University of Agricultural Sciences and Technology of Kashmir, Srinagar, India, [2]Division of Agronomy, ICAR, Indian Agricultural Research Institute, New Delhi, India, [3]Sher-e-Kashmir University of Agricultural Sciences and Technology of Jammu, Jammu, India, [4]ICAR, Indian Institute of Pulses Research, Kanpur, India, [5]ICAR, Indian Institute of Soil and Water Conservation (ICAR), Dehradun, India

Food security and environmental health are directly linked with soil carbon (C). Soil C plays a crucial role in securing food and livelihood security for the Himalayan population besides maintaining the ecological balance in the Indian Himalayas. However, soil C is being severely depleted due to anthropogenic activities. It is well known that land use management strongly impacted the soil organic carbon (SOC) dynamics and also regulates the atmospheric C chemistry. Different types of cultivation practices, i.e., forest, plantations, and crops in the Kashmir Himalayas, India, has different abilities to conserve SOC and emit C in the form of carbon dioxide (CO_2). Hence, five prominent land use systems (LUC) (e.g., natural forest, natural grassland, maize-field-converted from the forest, plantation, and paddy crop) of Kashmir Himalaya were evaluated to conserve SOC, reduce C emissions, improve soil properties and develop understanding SOC pools and its fractions variations under different land use management practices. The results revealed that at 0–20 cm and 20–40 cm profile, the soil under natural forest conserved the highest total organic carbon (TOC, 24.24 g kg^{-1} and 18.76 g kg^{-1}), Walkley-black carbon (WBC, 18.23 g kg^{-1} and 14.10 g kg^{-1}), very-labile-carbon (VLC, 8.65 g kg^{-1}, and 6.30 g kg^{-1}), labile-carbon (LC, 3.58 g kg^{-1} and 3.14 g kg^{-1}), less-labile-carbon (VLC, 2.59 g kg^{-1}, and 2.00 g kg^{-1}), non-labile-carbon (NLC, 3.41 g kg^{-1} and 2.66 g kg-1), TOC stock (45.88 Mg ha^{-1} and 41.16 Mg ha^{-1}), WBC stock (34.50 Mg ha^{-1} and 30.94 Mg ha^{-1}), active carbon pools (AC, 23.14 Mg ha^{-1} and 20.66 Mg ha^{-1}), passive carbon pools (PC, 11.40 Mg ha^{-1} and 10.26 Mg ha^{-1}) and carbon management index (CMI, 100), followed by the natural grassland. However, the lowest C storage was reported in paddy cropland. The soils under natural forest and natural grassland systems had a greater amount of VLC, LC, LLC, and NLC fraction than other land uses at both depths. On the other hand, maize-field-converted-from-forest-land-use soils had a higher proportion of NLC fraction than paddy soils; nonetheless, the NLC pool was maximum in natural forest soil. LUS based on forest crops maintains more SOC, while agricultural crops, such as paddy and maize, tend to emit more C in the Himalayan region. Therefore, research findings suggest that SOC under the Kashmir Himalayas can be protected by adopting suitable LUS, namely forest soil protection, and by placing some areas under plantations. The areas under the rice and maize fields emit more CO_2, hence, there is a need to adopt the conservation effective measure to conserve the SOC without compromising farm productivity.

KEYWORDS

carbon geochemistry, carbon management index, fragile ecosystem, functional land restoration, climate change

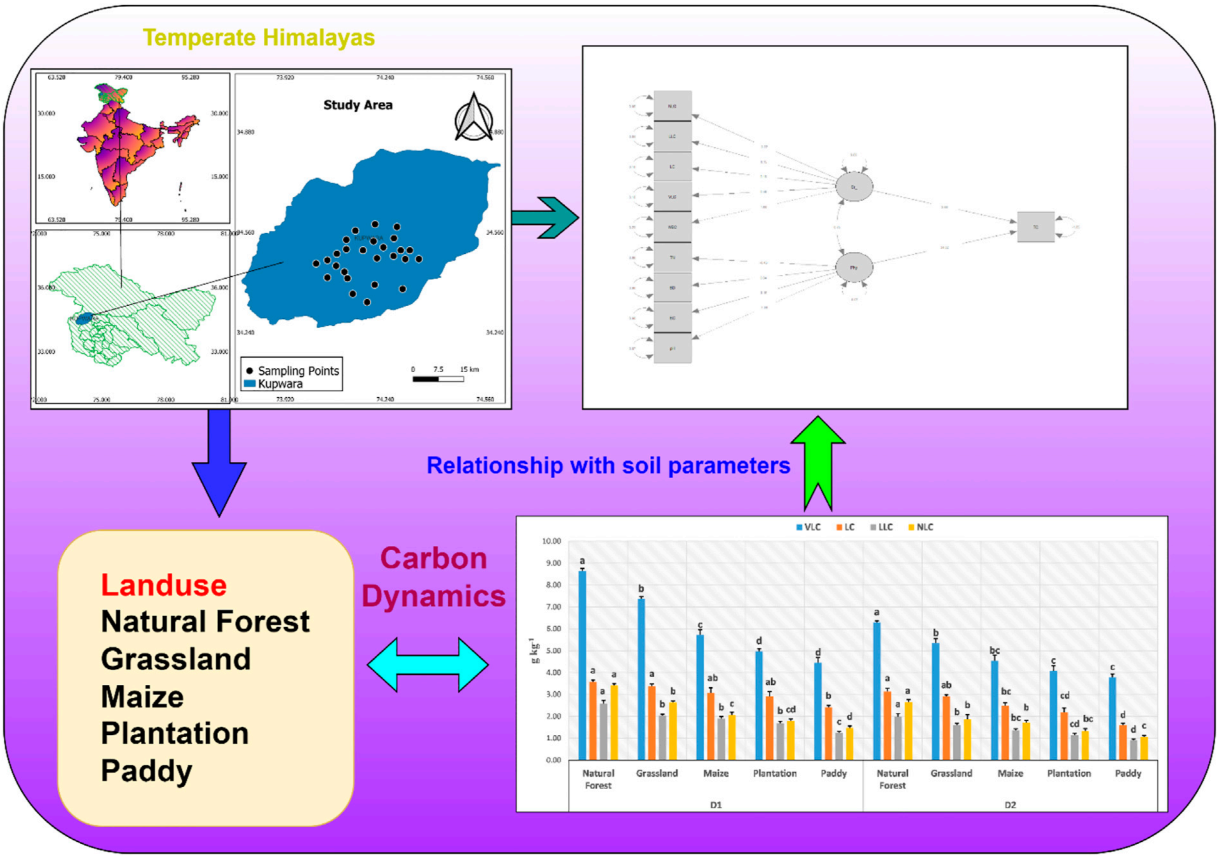

GRAPHICAL ABSTRACT

Introduction

Soil organic carbon (SOC) strongly impacts the global C cycle and regulates ecosystem functionality (Yadav et al., 2021; Yadav et al., 2022). SOC is also critical for the preservation of soil fertility and has a significant impact on various soil characteristics and processes (Pan et al., 2009). SOC consists of multiple compounds, from simple to more complex molecules, which can have different stability (Babu et al., 2020; Gerzabek et al., 2022). It is advisable that measuring rapidly changing SOC pools (labile pools) might be more informative in assessing soil quality (Anantha et al., 2022). Labile carbon (LC) mainly originates from the decomposition of plant and faunal biomass, root exudates, and deceased microbial biomass (Ahmed et al., 2022). The LC pool is directly available for microbial activity and, hence, is considered the primary energy source for microorganisms (Bei et al., 2022). Therefore, LC has the potential to act as an indicator of soil functions, in particular: nutrient cycling, soil aggregate formation, carbon sequestration, and habitat provision for biodiversity (Yadav et al., 2019; Singh R. et al., 2021; Yadav et al., 2021). Particulate organic matter carbon is very important for soil aggregate stability, nutrient cycling, etc., and microbial biomass carbon (MBC) and mineralizable C are also considered labile organic carbon fractions (Yadav et al., 2021). Whereas, the passive pool of SOC, also known as the non-labile pool (NLC), is more stable, as it is made up of refractory SOC fractions that form organic-mineral complexes with soil minerals and are slowly broken down by microbial activity (Wiesenberg et al., 2010). The labile SOC pool is critical for the immediate flow of CO_2, which is a better measure of the quality of the soil to evaluate variations caused by changes in land use (Vieira et al., 2007), whereas the non-labile SOC pool adds on to the TOC stock. SOC comprises of organic material except coasrse roots and that pool of biomass which is below surface. Key indicator for soil fertility and soil soility is SOC it also determines CO_2 fixation. Soil biological and chemical properties are greatly influenced by SOC.

Land use change and the associated management practices exert a strong impact on SOC dynamics (Babu et al., 2020). Land-use change currently contributes to a net emission of 1.4 Pg C yr^{-1} (Arneth et al., 2019). Anthropogenic factors, such as the management practices associated with agricultural activity, has a more tenacious impact on SOC stock than climate change (Kumar et al., 2020; Wu et al., 2022). Transitions in land utilization/land cover patterns are considered the crucial factor that affects the SOC pools. Land-use changes have resulted in a decrease in the cumulative SOC content by approximately 55 ± 78 Gt since 1750 (Lal, 2004). Misplacing in input (e.g., plant litter) and output rates (e.g., SOC mineralization) of SOM as a result of alterations in plant community and land management practice is the major cause of SOC depletion (Dawson and Smith, 2007). Several studies have shown the decrease in SOC storage by changes from natural land-use systems to artificial land use, and the transition of an artificial land-use pattern to a natural soil-use pattern ultimately causes an increment in SOC reservoirs (Guo and Gifford, 2002; Wei et al., 2014; Hobley et al., 2015).

The hill and mountain environment covers 54 Mha of the total geographical area of 329 Mha of India (Kumar, 2018). The Indian Himalayas are a mountain range characterized by varying altitudes, slopes, aspects, and climate resulting in wide ecological diversity. The northwest Himalayas (NWH) spread over Jammu & Kashmir, Himachal Pradesh, and Uttarakhand and cover 17.7 Mha of the land of India (Arora and Bhatt, 2016). The valleys of NWH receive ~1,600–2000 mm of precipitation and have fertile soil (Bhardwaj et al., 2021). While soil properties, including SOC, is decreased over the years due to improper land use practices (Singh et al., 2019), the adoption of improved land use practices (cropping systems, conservation tillage, nutrient management, etc.) has been reported to enhance the SOC, microbial carbon, and available N, P and K contents of Himalayan soils (Gogoi et al., 2021). The C status of the Himalayan soil varies according to the land use pattern followed, i.e., forests, plantation crops, and grasses are major C sinks because of their high storage potential and low decomposition processes compared to other agricultural crops (Babu et al., 2021; Yadav et al., 2021; WANI et al., 2022). Numerous studies also suggested that agricultural soils or intensively cultivated soils have lower labile C than forest and grassland soils (Geraei et al., 2016; Kumar et al., 2022). However, the magnitude of the reduction of soil C depends on the soil types, management practices adopted, and climatic conditions. The distribution of SOC into labile and non-labile or recalcitrant pools under different land uses varied significantly in most studies (Sainepo et al., 2018; Yeasmin et al., 2020). Because labile SOC fractions have faster turnover rates than recalcitrant fractions and are more responsive to anthropogenic and management-driven changes than total SOC, they are given higher priority as an indicator. (Mikha et al., 2013; Shao et al., 2015; Yu et al., 2017). In undisturbed soils, accumulation of more labile C occurs within aggregates that lead to enhanced protection, and thus there are differences found in the chemical composition of unprotected and protected SOM (Aduhene-Chinbuah et al., 2022). Since the types of land use systems influence the quantity and quality of litter inputs, decomposition, and organic matter stabilization/protection processes in soils, it is essential to control SOM storage (Qafoku, 2015; von Haden et al., 2019).

Increasing population pressure with growing food demand causes a rampant land-use change in the ecologically and environmentally fragile region of the Himalayas. In addition, the glaciers melting due to increasing temperature affects the natural vegetation and land use practices in the region, thus causing depletion in the soil C content. As a result, identifying more vulnerable SOM fractions can broaden the understanding and trajectories of SOC during the early stages of land use and management changes. Various studies regarding different SOC pools have been conducted in different parts of the hilly ecosystems like the eastern Himalayas (Yadav et al., 2019; Babu et al., 2020) and western Himalayas (Yadav et al., 2019). However, very few studies on changes in SOC due to land use practices i.e., forest, plantation, agricultural cropland, etc., in the Kashmir Himalayas have so far been conducted. Hence, a comprehensive study on the effects of land use management on soil C stocks is needed to identify viable land-use systems for C buildup in Kashmir Himalaya in face of changing climatic parameters. Furthermore, C- stock measurement is also required by an international agreement between 192 countries in the world that have joined to form a treaty (Mathew et al., 2020).

The Kashmir Himalaya is very rich in natural vegetation and plantation crops and has fertile land to cultivate various crops. This study is conducted to estimate C loss while shifting one land use system to others and also to find a suitable land use pattern for Kashmir Himalayas. Certainly, the findings of this study can help in choosing appropriate land use patterns by the farmers of the region to achieve sustainable crop productivity and income while conserving the soil resources of the region. The study also aims to

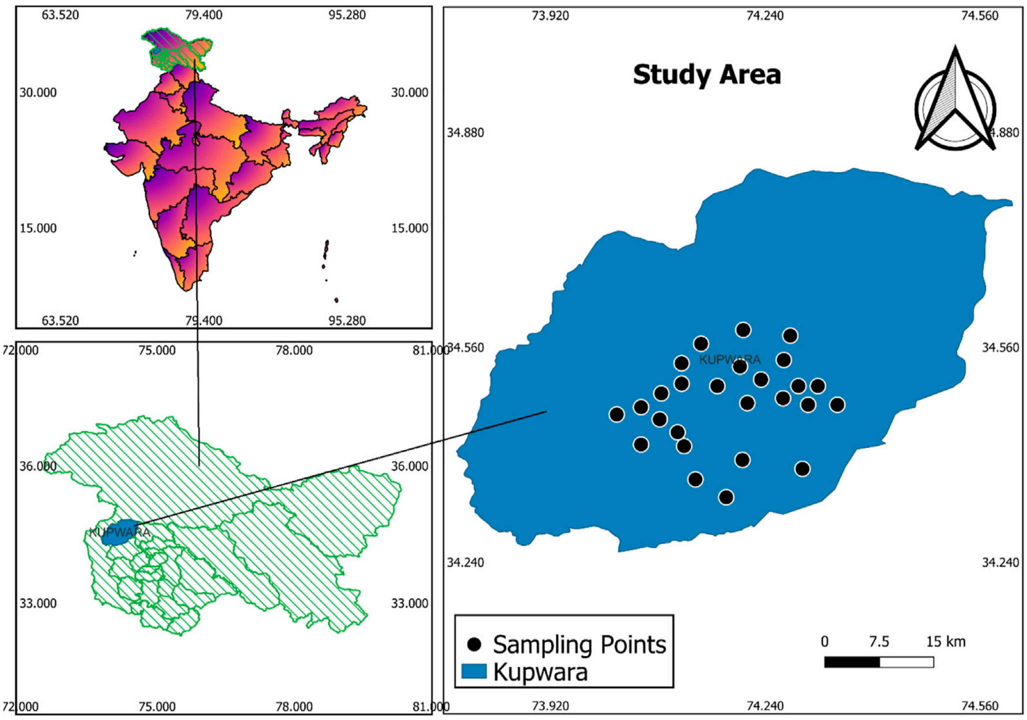

FIGURE 1
Land use systems of the study site.

identify the most stable and quickly depleting form of SOC due to practicing various land use management practices in the Himalayan region. The findings of the current study will assist policymakers in planning soil-supportive and environmentally robust land use policy for sustainable land management and livelihood security of the Himalayas population.

Materials and methods

Study site

The present study was conducted in the Kupwara District of North Kashmir, India. The study site is located in an environmental hotspot in the temperate Himalayas of India. The study site lies between 34°31′32.8544 ″N and 74°15′19.4653 ″E with an elevation ranging from 1,500 to 3,500 m above sea level (Figure 1). Soils of the region are mainly Inceptisols and Entisols which are primarily composed of sandy loam to clayey in texture. Valley has flat to slightly undulating topography. The climate of the study site is Mediterranean-type-temperate-cum with a minimum and maximum temperature of -15°C–35°C. The winter season starts in November, and extreme winter conditions continue until March. The average maximum temperature of the study site was 35°C, while the average minimum temperature was −10°C. The annual rainfall is about 869 mm over about 60 days in the form of rain and snow. Kupwara District is hilly and mountainous in the north, west, and east regions, consisting of Lesser Himalayan Pir-Panjal ranges with wide intermountain valleys. The valley has a diverse range of flora, wildlife, and domesticated species in its forest lands. Plant diversity is critical for the survival of practically all terrestrial ecologies, as humans and animals rely on plants directly and indirectly. The district's forest types range in altitude from low to high (1,500–3,500 m). The forests are dominated by broadleaved trees such as *Populus deltoides*, *Salix* species, *Pinus wallichiana*, *Abies pindrow*, and *Betula utilis*. Farmers in the valley grow paddy, maize, and wheat, as well as apples, walnuts, and other leafy greens.

Soil sampling and sample preparation

Soil samples were collected from five land uses, viz., natural forest, natural grassland, maize-field-converted-from-forest, plantation, and paddy land, during 2020. The natural forests mainly comprise pine plants, with minimal felling in the lower boundaries. Natural grassland had a moderate to severe grazing use pattern. Under maize-field-converted-from-forest; farmers follow a subsistence level of cultivation of local maize genotypes with minimum inputs (basically organic manures) and tillage on the forest margins. Concerning plantation land use, apple orchards were considered. Farmers mainly use moderate quantities of inorganic fertilizers and plant protection chemicals in apple orchards. Under paddy land use; farmers adopted traditional tillage practices for the cultivation of local genotypes. A total of twenty-five sites were selected (five sites for each land use) for the study. Composite soil samples were collected using a soil auger for 0–20 cm (surface/D_1) and 20–40 cm (sub-surface/D_2) depth, with three replicates, and every replicate sample was composited from six randomly selected sub-samples. The stratified random sampling method was followed. After removal of all stubbles, residues, and undesirable substances, the soil samples collected from each site and depth were homogenized and air-dried at room temperature, ground in a mortar, sieved with a 2 mm sieve, and a 0.5 mm sieve (for SOC), thereafter carefully kept in airtight plastic bags for laboratory analysis.

Analysis of soil organic carbon and pools

The method described by (Walkley and Black, 1934) was used to determine the concentration of soil organic carbon/ walkley-black carbon. Organic matter was first oxidized using chromic acid (potassium dichromate + concentrated sulphuric acid), and the unconsumed potassium dichromate was back-titrated against ferrous sulfate (redox titration). Total organic carbon (TOC) was estimated using a modified Mebius-based method (Yeomans and Bremner, 1988). The soil samples were digested at 150°C for 30 min with $K_2Cr_2O_7$ and H_2SO_4, following titration by using 0.2 mol (Fe^{2+}) L^{-1} Mohr salt.

The functional pools of organic carbon (OC) were estimated through a modified (Walkley and Black, 1934) as described by (Chen et al., 2019) using 12.0 N, 18.0 N, and 24.0 N of H_2SO_4, respectively. The very labile carbon was estimated using organic C oxidizable by 12.0 N H_2SO_4. The labile carbon was estimated by the differences in SOC oxidizable by 18.0 N and that under 12.0 N H_2SO_4. The less labile carbon was estimated by the differences in SOC oxidizable under 24.0 N and that under 18.0 N, H_2SO_4. The non-labile carbon was estimated by the differences between SOC oxidizable under 36.8 N and that under 24.0 N H_2SO_4.

Analysis of organic carbon stocks and carbon management index

The SOC stocks were calculated as follows, (Jones et al., 2005).

$$\text{SOC stocks}\ (\text{Mg ha}^{-1}) = \text{SOC x } \rho \text{ x d x } 10{,}000$$

Where; SOC is the soil organic carbon measured in g g^{-1}; ρ is the soil bulk density (g cm^{-3}), and d is the depth of the soil layer (m). The value of 10,000 indicates the stock for 1 ha^{-1} of land.

The CMI was calculated using the formulae;

CMI = CPI x LI x 100, where CPI is the carbon pool index and LI is the lability index of the soil under a particular land use (Blair et al., 1995).

$$\text{CPI} = \text{Total organic carbon in the treatment}\ (\text{g kg}^{-1}) \times /\text{Total organic carbon in the reference}\ (\text{g kg}^{-1})$$

LI = L in the treatment/L in the reference where L is the carbon lability of the soil

$$\text{L} = \text{Content of labile C/Content on non} - \text{labile C}$$

Analysis of soil physico-chemical properties

The soil pH was determined with the help of a glass electrode pH meter (Jackson et al., 1973). The EC of the soil samples was determined using a conductivity bridge in 1:2.5 soil-water suspensions after equilibration for 24 h, using a Solu-bridge conductivity meter (Jackson et al., 1973). The bulk density (ρb) was estimated using the core method (Blake and Hartge, 1986). The modified Kjeldahl digestion method was used to estimate TN in soil. A known weight of soil sample was taken in the presence of concentrated H_2SO_4 and catalyst mixture under high temperature (420°C) and digested to break down complicated structures into simple structures, thereby releasing N in the form of ammoniacal radicles (NH_4^+). The digested samples were then distilled by steam with concentrated NaOH (40%), the released NH_3 is condensed and absorbed in a known volume (20 ml) of boric acid (4%) with a mixed indicator to form ammonium borate, and the excess of which is titrated with 0.1N HCL (Bremner, 1982).

Statistical analysis

The results on different parameters under laboratory conditions were statistically evaluated according to the procedure outlined by (Gomez and Gomez, 1984). The descriptive statistics-one factor analysis was done by using OPSTAT software. The correlation coefficients were computed using SPSS software version 27.0 (Morgan et al., 1988).

Results and discussion

Effect of land use systems on distribution of TOC and WBC

The total organic carbon (TOC) in surface and sub-surface soil under various land uses ranged from 9.81 to 24.24 g kg^{-1}. The

TABLE 1 Soil pH, EC, BD, TN, and TOC in surface and sub-surface soil under diverse land-use systems.

Land use systems	pH		EC (dS m^{-1})		BD (Mg m^{-3})		TN (%)		TOC (g kg^{-1})	
	0–20 cm	20–40 cm	0–20 cm	20–40 cm	0–20 cm	20–40 cm	0–20 cm	20–40 cm	0–20 cm	20–40 cm
Natural Forest	6.55 ± 0.10c	6.97 ± 0.09b	0.13 ± 0.01c	0.17 ± 0.01c	0.94 ± 0.06c	1.09 ± 0.06d	0.49 ± 0.05a	0.38 ± 0.03a	24.24 ± 0.31a	18.76 ± 0.21a
Natural Grassland	6.65 ± 0.07bc	7.12 ± 0.12ab	0.15 ± 0.02bc	0.19 ± 0.02bc	1.07 ± 0.01c	1.18 ± 0.01cd	0.36 ± 0.03b	0.29 ± 0.03b	20.52 ± 0.21b	15.60 ± 0.06b
Maize Field converted from Forest	7.05 ± 0.14ab	7.26 ± 0.13ab	0.20 ± 0.02ab	0.24 ± 0.01ab	1.22 ± 0.01b	1.29 ± 0.01bc	0.26 ± 0.02bc	0.19 ± 0.02c	16.98 ± 0.27c	13.44 ± 0.32c
Plantation	6.83 ± 0.09bc	7.20 ± 0.08ab	0.16 ± 0.02bc	0.23 ± 0.01abc	1.32 ± 0.03ab	1.36 ± 0.03ab	0.20 ± 0.01c	0.15 ± 0.01c	15.13 ± 0.38d	11.60 ± 0.31d
Paddy	7.42 ± 0.10a	7.56 ± 0.08a	0.26 ± 0.02a	0.29 ± 0.02a	1.43 ± 0.01a	1.45 ± 0.01a	0.18 ± 0.01c	0.12 ± 0.01c	12.76 ± 0.30e	9.81 ± 0.30e

EC: electrical conductivity; BD: bulk density; TN: total nitrogen; TOC: total organic carbon; Mean values with the same letters don't differ significantly.

TABLE 2 Functional organic carbon pools in surface and sub-surface soil layers under diverse land-use systems.

Land use systems	WBC (g kg^{-1})		VLC (g kg^{-1})		LC (g kg^{-1})		LLC (g kg^{-1})		NLC (g kg^{-1})	
	0–20 cm	20–40 cm	0–20 cm	20–40 cm	0–20 cm	20–40 cm	0–20 cm	20–40 cm	0–20 cm	20–40 cm
Natural Forest	18.23 ± 0.24a	14.10 ± 0.16a	8.65 ± 0.12a	6.30 ± 0.07a	3.58 ± 0.08a	3.14 ± 0.15a	2.59 ± 0.14a	2.00 ± 0.13a	3.41 ± 0.09a	2.66 ± 0.11a
Natural Grassland	15.42 ± 0.16b	11.73 ± 0.05b	7.37 ± 0.11b	5.35 ± 0.21b	3.38 ± 0.10a	2.91 ± 0.09ab	2.04 ± 0.06b	1.60 ± 0.08b	2.63 ± 0.07b	1.87 ± 0.21b
Maize Field converted from Forest	12.77 ± 0.20c	10.11 ± 0.24c	5.73 ± 0.24c	4.54 ± 0.26bc	3.07 ± 0.24ab	2.49 ± 0.14bc	1.90 ± 0.09b	1.37 ± 0.06bc	2.07 ± 0.12c	1.71 ± 0.11b
Plantation	11.38 ± 0.29d	8.72 ± 0.24d	4.98 ± 0.11d	4.09 ± 0.23c	2.92 ± 0.22ab	2.18 ± 0.20cd	1.69 ± 0.07b	1.13 ± 0.09cd	1.79 ± 0.09cd	1.32 ± 0.12bc
Paddy	9.59 ± 0.23e	7.37 ± 0.22e	4.45 ± 0.24d	3.79 ± 0.15c	2.42 ± 0.08b	1.59 ± 0.09d	1.25 ± 0.07c	0.92 ± 0.05d	1.47 ± 0.09d	1.07 ± 0.07c

WBC: walkley-black carbon; VLC: very-labile-carbon; LC: labile-carbon; LLC: less-labile-carbon; NLC: non-labile-carbon; Mean values with same letters don't differ significantly.

10.3389/fenvs.2022.1009660

mean values of TOC (g kg^{-1}) in surface and sub-surface depths were 24.24 and 18.76 in the natural forest; 20.52 and 15.60 in natural grassland; 16.98 and 13.44 under maize-field-converted-from-forest; 15.13 and 11.60 in the plantation; 12.76 and 9.81 in soils under paddy land use (Table 1). Among surface soils, the highest TOC mean value was found in natural forest soil, which was 90% higher than in paddy soils (12.76 g kg^{-1}). A similar trend was found in the sub-surface soils, with mean TOC content of 18.76 g kg^{-1} in natural forests and 9.81 g kg^{-1} in paddy soils. The natural grassland land use system at both the soil depths also had a significantly higher amount of TOC (20.52 and 15.30 g kg^{-1}) than the maize-field-converted-from-forest system (16.98 and 13.44 g kg^{-1}) and plantation land use (15.13 and 11.60 g kg^{-1}). The Walkley-Black carbon (WBC) in both soil depths was significantly affected by different land-use patterns (Table 2). Natural forests had the highest WBC (18.23 g kg^{-1} and 14.10 g kg^{-1}) among the different land use types, followed by natural grassland land use (15.42 g kg^{-1} and 11.73 g kg^{-1}), maize fields converted from forests (12.77 g kg^{-1} and 10.11 g kg^{-1}), plantations (11.38 g kg^{-1} and 8.72 g kg^{-1}) and paddy soils (9.59 g kg^{-1} in and 7.37 g kg^{-1}) at 0–20 and 20–40 cm soil depths respectively.

The WBC decreased with soil depth. When compared to other land uses, natural forests have a greater TOC due to minimal soil disturbance, and higher levels of C inputs, such as leaf litter and root biomass from natural systems, as well as its recalcitrant characteristic, which limits complete microbial breakdown (Vezzani et al., 2018). The higher carbon under the forest field might be due to the higher soil binding ability of forest trees, which protected soil C from being degraded and lost in the form of CO_2 to the atmosphere. The leaf litter is an important part that transports the carbon from plant to soil (Giweta, 2020). Low TOC contents in cropland use other than natural forests imply a significant reduction in TOC from plant species variations, C loss from the soil due to residue removal, soil perturbation, and a small quantity of added biomass to the soil (Raiesi, 2021). Similar findings have been reported by (Sharma et al., 2018) and (Bahadori et al., 2021). The amount of TOC in the soil decreased with depth, possibly due to an increase in OM at the soil surface (Jobbágy and Jackson, 2000). This is supported by the finding of (Sreekanth et al., 2013). Under various land uses in the temperate Himalayan Region, SOC content and OC stocks have ranged from 4.27 to 27.00 g kg^{-1} and 6.57–54.10 Mg ha^{-1}, respectively (Dar and Sahu, 2018). WBC concentration was substantially greater in natural forest and natural grassland land-use soils than in the other land-use systems investigated.

The WBC content varied greatly among the different land uses in both the surface and sub-surface soil depths. Natural woods had the highest levels of WBC, while paddy soils had the lowest. Higher WBC under natural forest systems under different ecoregions of the world was recorded by many researchers (Prasad et al., 2019; Mourya et al., 2021; WANI et al., 2022). The addition of high levels of inputs, such as leaf litter and root biomass, as well as its recalcitrant nature, high altitude, low temperature, slow rate of mineralization, and role in the augmentation of soil aggregates and ultimately increasing soil OC content, all, contribute to high WBC in natural forests (Nath et al., 2018). Rapid mineralization and C loss from soil-by-soil disturbance and management techniques are to blame for paddy soils' low WBC content (Chauhan et al., 2014). Furthermore, low WBC content in paddy may be due to long-term cultivation under submerged conditions and mineral fertilizer application, puddling, crop removal during harvesting, breakdown of stable aggregates, and deterioration of soil organic matter, resulting in a degradation of overall soil quality (Yang et al., 2005). The results are further supported by the findings of (Kaur and Bhat, 2017). A consistent decrease in WBC content with depth was noticed in all cultivated lands. That might be due to the addition of animal wastes and plant residues to surface soils (Chibsa and Ta'a, 2009). Also, with an increase in soil depth, a decline in fine roots returned, aeration, and soil microbial activity may have resulted in a comparable reduction in WBC content (Sheng et al., 2015; Kaushal et al., 2020).

Effect of land use systems on functional carbon pools

Across both the soil depths, there was a significant difference in C pools among the different land uses. Data about mean values of VLC under different land uses are presented in Table 2. In both the surface and sub-surface soil depth, VLC was observed to be in the order of; natural forest > natural grassland > maize-field-converted-from-forest > plantation > paddy (Figure 2). A decreasing trend with depth was observed for all the land-use systems having the highest values in the surface layer of soil. Among the different land uses, the natural forest and natural grassland land-use systems had the highest VLC, i.e., 8.65 g kg^{-1} and 7.37 g kg^{-1} in 0–20 cm and 6.30 g kg^{-1} and 5.35 g kg^{-1} in 20–40 cm depth, respectively. Natural forests had the highest VLC in surface and subsurface (8.65 and 6.30 g kg^{-1}), followed by natural grassland (7.35 and 5.35 g kg^{-1}), maize-field-converted-from-forest (5.73 and 4.54 g kg^{-1}), and plantation (4.98 and 4.09 g kg^{-1}) and paddy soils (4.45 and 3.79 g kg^{-1}). Among the different land uses, the natural forest had the highest LC, i.e., 3.58 g kg^{-1} in 0–20 cm and 3.14 g kg^{-1} in 20–40 cm depth. Natural forests had 3.58 and 3.14 g kg^{-1} labile carbon content at 0–20 cm and 20–40 cm soil depths, respectively, followed by natural grasslands (3.38 and 2.91 g kg^{-1}), maize-field-converted-from-forest (3.07 and 2.49 g kg^{-1}), plantations (2.92 and 2.18 g kg^{-1}), and paddy (2.42 and 1.59 g kg^{-1}) (Table 2). A perusal of the data reveals that the labile carbon content in natural forests at both depths was higher than the other land uses. The plantation-based land-use system had higher labile carbon content than the paddy system at both soil depths. A decreasing trend in labile carbon content with depth was observed under all the land uses, and it followed the order; natural forest > natural grassland > maize-field-converted-from-forest > plantation > paddy (Figure 2). The less labile carbon (LLC) content at 0–20 cm and 20–40 cm soil depth in the natural forest was 2.59 and 2.00 g kg^{-1}, respectively; natural grassland had 2.04 and 1.60 g kg^{-1}, respectively; maize-field-converted-from-forest 1.90 and 1.37 g kg^{-1}, respectively; plantations had 1.69 and 1.13 g kg^{-1}, and paddy soils had 1.25 and 0.92 g kg^{-1}, respectively (Table 2). It was found that the highest LLC content at the surface and sub-surface soil layers was recorded in natural forests, followed by natural grassland and maize-field-converted-from-forests, whereas the lowest was recorded under paddy soils. A decreasing trend in LLC content with depth was observed under all land uses, with the highest value observed in the surface layer. The LLC had the following order at both the soil depths; natural forest > natural grassland > maize-field-converted-from-forest > plantation > paddy, respectively (Figure 2). A decreasing trend in non-labile carbon (NLC) content with depth was observed under all land uses, with the highest value observed in the surface layer. The NLC followed the order; natural forest > natural grassland > maize-field-converted-from-forest > plantation > paddy (Figure 2). The NLC content in surface and the sub-surface soil was 3.41 and 2.66 g kg^{-1} in the natural forest; 2.63 and 1.87 g kg^{-1} under natural grassland; 2.07 and 1.71 g kg^{-1} in maize-field-converted-from-forest; 1.79 and 1.32 g kg^{-1} in plantations and 1.47 and 1.07 g kg^{-1} in paddy fields (Table 2). The relationship between C fractions and soil properties is shown in Figure 3 using a structural modeling equation (SEM). The mean values of NLC content in natural forest land use at both soil depths were higher than the other land uses, with the lowest recorded in paddy soils. SOC pools such as VLC, LC, LLC, and NLC are influenced by differences in C inputs, litter/crop residue composition, and species richness among land-use regimes. Natural forests had the most VLC and LC in the surface and subsurface layers, followed by natural grassland, and paddy soils had the least. High VLC and LC fractions in natural forest and natural grassland land use compared to other land uses could be attributed to continuous addition (retention) of easily decomposable plant/leaf litter, high microbial biomass, and mechanisms for protecting added C, all of which contribute to significantly increased soil microbial functions and corresponding increases in VLC and LC fractions. Furthermore, tree spices like *Pinus wallichiana* and *Cedrus deodara* have a lot of litterfall. Leaves with a high nitrogen concentration have a greater ability to improve soil LC (Sharma et al., 2014). High concentrations of VLC and LC have been reported by (Benbi et al., 2015) and (Babu et al., 2020) in forests adjacent to other land uses. The low values of VLC and LC in other land-use systems other than native vegetation could be associated with aggregate disruption and more organic matter oxidation in conventional farming systems based on intensive management practices like plowing and harrowing (Bayer et al., 2006). The LLC fraction followed the order as natural forest > natural grassland > maize-field-converted-from-forest > plantation > paddy in both soil depths. The higher LLC in natural forests and low content in paddy soils is due to variations in the plant/tree species found; above-below ground biomass, and its nature of decomposition; and other variables such as climate, which have an intrinsic effect on its decomposition and loss. Natural forests had a significantly higher NLC content than cultivated lands. Higher NLC content in natural forests has also been recorded by (Nath et al., 2018). Usually, forest litters are rich in sources of tannin and wax that are resistant to degradation. This enhances the levels of NLC in natural forests compared to cultivated lands (Nath et al., 2018). The NLC fraction is usually resistant to field management operations and microbial decomposition due to its sorption on fine particles (Sherrod et al., 2005; Sainepo et al., 2018). In general, all the lability-based OC fractions showed a decreasing trend with soil depth (Babu et al., 2021; Xie et al., 2021).

Effect of land use systems on carbon stocks

The TOC stock in natural forest land use (surface soil) was recorded as the highest among the different land uses with a mean of 45.88 Mg ha^{-1}; in the sub-surface, it was 41.16 Mg ha^{-1} (Table 3). In the natural grassland system (surface soil), the mean TOC stock was 43.93 Mg ha^{-1}; in the sub-surface, it was 36.82 Mg ha^{-1}. The mean TOC stock value in maize-field-converted-from-forest (surface and sub-surface soil) was 41.75 Mg ha^{-1} and 34.80 Mg ha^{-1}. In the surface layer, the TOC stock under the plantation was 39.73 Mg ha^{-1}, with the sub-surface having a mean of 31.37 Mg ha^{-1}. In paddy soils, TOC stock in surface and sub-surface soil was 36.45 Mg ha^{-1} and 28.42 Mg ha^{-1}, respectively. The highest TOC stocks (surface and sub-surface) were recorded in natural forests, followed by natural grassland, with the lowest recorded under paddy soils (Figure 4).

Natural forest land-use systems had the highest WBC stock in surface, and sub-surface soil depth, followed by natural grasslands, and paddy soils had the lowest (Figure 4). The WBC stock in the natural forest land-use system was 34.50 Mg ha^{-1} and 30.94 Mg ha^{-1} at the surface and sub-surface, respectively; in the natural grassland system, it was 33.03 Mg ha^{-1} and 27.68 Mg ha^{-1}; in the maize-field-converted-from-forest system, it was 31.26 Mg ha^{-1} and 26.16 Mg ha^{-1}; in plantations, it was 29.87 Mg ha^{-1} and 23.0. The WBC stock had the following order at both the soil depths; natural forest > natural grassland > maize-field-converted-from-forest > plantation > paddy, respectively. The active organic stock (AOC) stocks in the surface and sub-surface layers were 23.14 and 20.66 Mg ha^{-1} in the natural forest; 23.02 and 19.47 Mg ha^{-1} under natural grassland; 21.54 and 18.20 Mg ha^{-1} in maize-field -converted-from-forest; 20.78 and

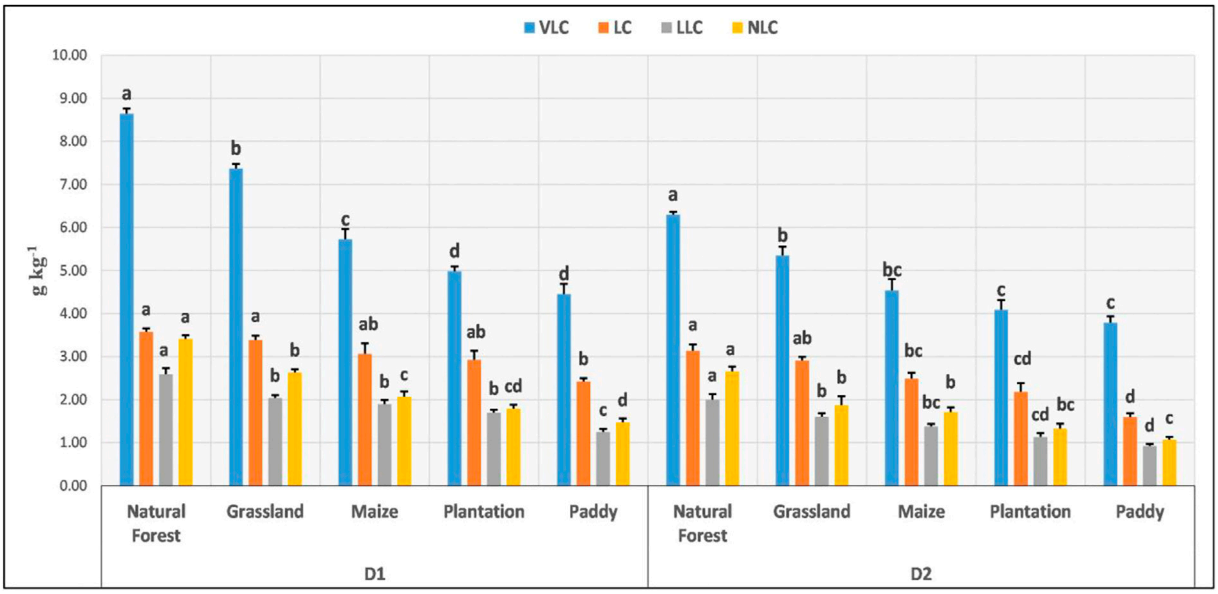

FIGURE 2
Effect of land use on functional organic carbon pools (g kg^{-1}) in 0–20 cm and 20–40 cm soil depth. Error bars indicate the least significant difference (LSD) values at p = 0.05. Mean values with the same letters don't differ significantly.

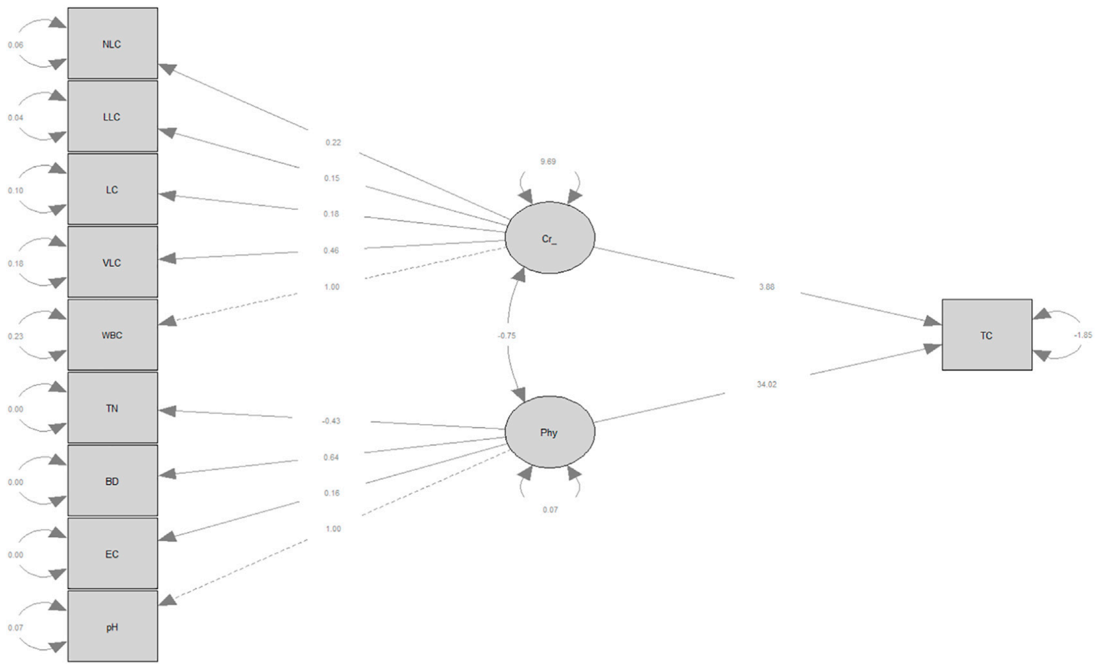

FIGURE 3
Structural equation modeling plot between soil properties and C fractions.

16.95 Mg ha^{-1} in plantations and 19.63 and 15.60 Mg ha^{-1} found in paddy soils (Table 3). The highest AOC stocks were recorded under natural forest land use at both soil depths, followed by natural grasslands, whereas the lowest was recorded in paddy soils (). The AOC stock had the following order at both the soil depths; natural forest > natural grassland > maize-field-

10.3389/fenvs.2022.1009660

TABLE 3 Organic carbon stocks in surface and sub-surface layers under diverse land use systems.

Land use systems	TOC stock (Mg ha^{-1})		WBC stock (Mg ha^{-1})		AOC stock (Mg ha^{-1})		POC stock (Mg ha^{-1})	
	0–20 cm	20–40 cm	0–20 cm	20–40 cm	0–20 cm	20–40 cm	0–20 cm	20–40 cm
Natural Forest	45.88 ± 3.51a	41.16 ± 2.84a	34.50 ± 2.64a	30.94 ± 2.13a	23.14 ± 1.76a	20.66 ± 1.33a	11.40 ± 1.05a	10.26 ± 0.94a
Natural Grassland	43.93 ± 0.92a	36.81 ± 0.40ab	33.03 ± 0.69a	27.68 ± 0.30ab	23.02 ± 0.35a	19.47 ± 0.57ab	10.00 ± 0.25ab	8.21 ± 0.55ab
Maize Field converted from Forest	41.57 ± 0.83ab	34.80 ± 0.91b	31.26 ± 0.62ab	26.16 ± 0.68b	21.54 ± 1.03a	18.20 ± 0.79abc	9.71 ± 0.51ab	7.98 ± 0.23abc
Plantation	39.73 ± 0.55ab	31.37 ± 0.41bc	29.87 ± 0.41ab	23.59 ± 0.31bc	20.78 ± 0.77a	16.95 ± 0.55bc	9.18 ± 0.45ab	6.68 ± 0.60bc
Paddy	36.45 ± 1.02b	28.42 ± 0.99c	27.40 ± 0.76b	21.37 ± 0.74c	19.63 ± 0.78a	15.60 ± 0.48c	7.77 ± 0.241b	5.76 ± 0.16c

TOC: total organic carbon; WBC: walkley and black carbon; AOC: active carbon stock; POC: passive C stock; Mean values with the same letters don't differ significantly.

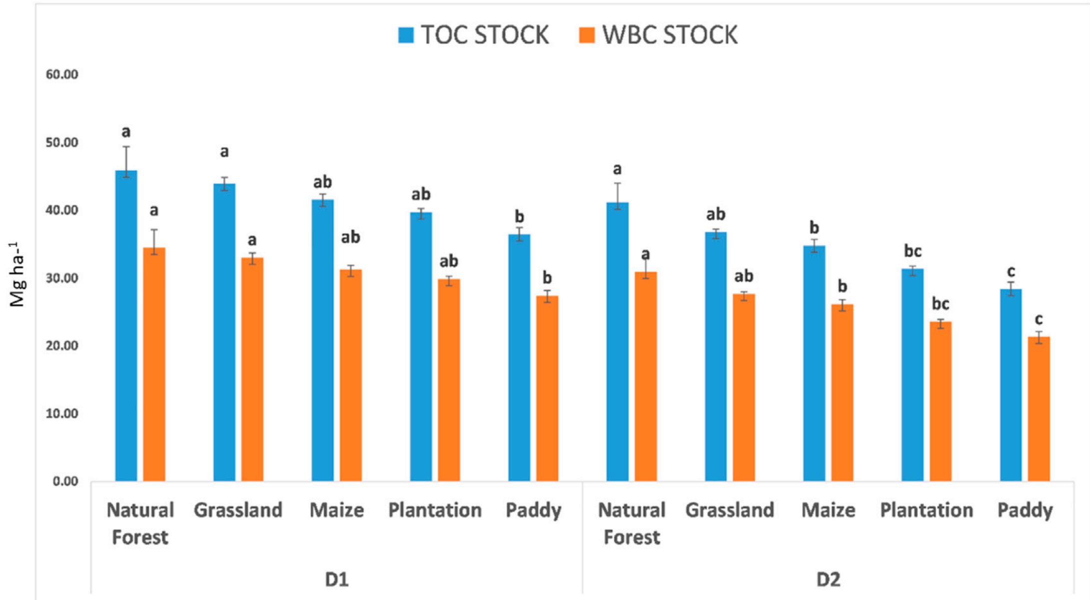

FIGURE 4
Effect of land use on TOC and WBC stocks (g kg^{-1}) in 0–20 cm and 20–40 cm soil depth. Error bars indicate the least significant difference (LSD) values at $p = 0.05$. Mean values with the same letters don't differ significantly.

converted-from-forest > plantation > paddy, respectively. The POC stocks under different land uses are presented in Table 3. The highest POC stocks at both soil depths were recorded under natural forests, followed by natural grasslands, and the lowest was recorded in paddy soils (Figure 5). The POC stocks in surface and sub-surface layers were 11.40 and 10.26 Mg ha^{-1} in the natural forest; 10.00 and 8.21 Mg ha^{-1} under natural grassland; 9.71 and 7.98 Mg ha^{-1} in maize-field-converted-from-forest; 9.18 and 6.68 Mg ha^{-1} in plantations; and 7.77 and 5.76 Mg ha^{-1} in paddy soils. The POC stock had the following order at both the soil depths; natural forest > natural grassland > maize-field-converted-from-forest > plantation > paddy, respectively. The highest TOC stock in surface and sub-surface soil depth was recorded in natural forests, followed by natural grassland, and the lowest in paddy fields. Higher TOC stock in natural forests due to high concentrations of OC, as recorded by (Valbrun et al., 2018) and (Singh R. et al., 2021), due to high leaf litter, less soil disturbance, the presence of a high number of heterogeneous plants with different root structures and less organic matter decomposition as compared to other cultivated lands (Nicodemo et al., 2018). Horticultural land use (plantations) recorded higher TOC stocks as compared to agricultural (paddy) soils since plantations add more litter and input of animal manures, whereas, in agricultural lands, removal of biomass and intensive tillage practices reduce the OC (Hu et al., 2020). Similar results were reported by (Toru and Kibret, 2019). WBC

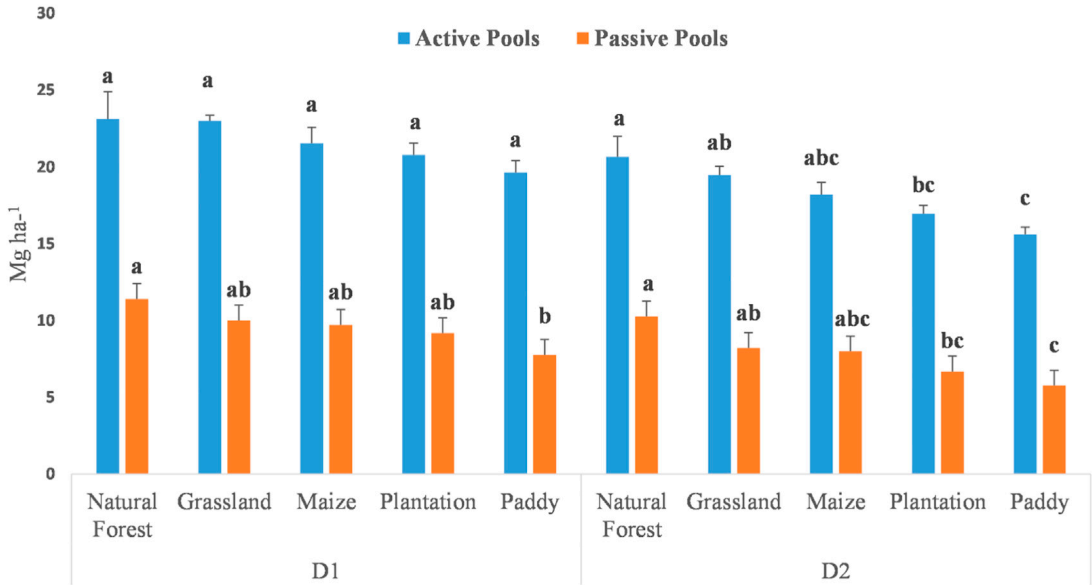

FIGURE 5
Effect of land use systems on active and passive organic carbon stocks (Mg ha^{-1}) in 0–20 cm and 20–40 cm soil depth. Error bars indicate the least significant difference (LSD) values at p = 0.05. Mean values with the same letters don't differ significantly.

stock is mostly attributed to physiography, altitude, bulk density, organic matter additions, tree proportions, and land disturbances (Turner et al., 2005; Wang et al., 2012). The highest WBC stock was found in natural forest land use, followed by natural grasslands, and the lowest in the surface and subsurface of paddy soils, according to the study. Natural forest land use recorded higher WBC stock due to the above-mentioned reasons and is further supported by (Dhakal et al., 2010) and (Yitbarek et al., 2013). The WBC stock varied with soil depth, and with an increase in soil depth, the WBC stock distribution showed a decreasing trend in all land-use systems, which has been observed in many studies (Sahoo et al., 2019). Similar findings of higher WBC stocks in natural forests as compared to agricultural land uses have been reported by (Ali et al., 2019), (Begum et al., 2020), and (Mir et al., 2020). The active OC pool is a chief source of essential plant nutrients (Mandal et al., 2008) and is involved in crop production and soil quality. This particular pool (active OC) of TOC is more easily and readily influenced by management practices when compared to the passive C pool (Biederbeck et al., 1994) and is regarded as an early indicator of soil quality (Duval et al., 2013) (Duval et al., 2013). The active C pool comprises the VLC and the LC pool (Sainepo et al., 2018) and (Bhattacharjya et al., 2017). Converting carbon-rich forests to croplands depletes carbon stocks quickly (Pan et al., 2009) and jeopardizes ecosystem functioning (Isbell et al., 2011). The maximum AOC stock was recorded in natural forests, and the lowest was found in paddy soils in both soil depths. Similar results have been reported by (Sharma et al., 2018) and (Babu et al., 2020), where the high content of the active C pool was due to the availability of readily decomposable organic matter found throughout the year in forests. Also, the root systems of trees are liable as they exude labile C compounds (Conteh et al., 1997). The passive OC pool in the soil is more stable and recalcitrant (Choudhury et al., 2018), and is made up of the LLC and NLC pools (Wiesenberg et al., 2010). A higher POC stock in natural forests and natural grasslands is attributed to the input of high quantities and quality of plant/leaf litter as compared to cultivated lands. Along a successional gradient (Xiang et al., 2015), reported a significant increase in passive C fractions with increasing litterfall. This implies that the OC retrieved in natural grasslands and natural forests are more stable than that retrieved in other land uses. Physical and chemical conservation of C in undisturbed soils may also account for high POC storage in natural forests and grasslands. The variation in AOC and POC stocks among the different land uses might be explained by wide changes in vegetation type, litter input (Yao et al., 2010), and soil perturbation intensity (Yadav et al., 2022).

Effect of land use systems on carbon management index

The natural forests were used as the reference soil to compute the carbon management index (CMI) for various land-use systems. Table 4 represents the CMI of different land-use types. The CMI differed significantly between different land

TABLE 4 Carbon Management Index under diverse land-use systems (0–40 cm).

Land use system	CPI	CPI (g kg^{-1})	L	LI	CMI
Natural Forest	43.00	1.00	4.33	1.00	100
Natural Grassland	36.11	0.84	5.08	1.18	98.71
Maize Field converted from Forest	30.42	0.71	5.10	1.18	83.33
Plantation	26.73	0.62	5.52	1.28	79.39
Paddy	22.57	0.53	5.78	1.34	70.08
CD ($p < 0.05$)					13.45

CPI: carbon pool index; L: lability; LI: labile index; CMI: carbon management index.

uses and varied in response to labile OC concentration patterns. The CMI at 0–40 cm soil depth in different land-use types were as follows; 100.00 in the natural forest; 98.71 in natural grassland; 83.33 in maize-field-converted-from-forest; 79.39 under plantation, and 70.08 in paddy soils. The highest CMI was recorded under natural forest, followed by natural grassland, and the lowest was in paddy soils. The CMI values had the following order; natural forest > natural grassland > maize-field-converted-from-forest > plantation > paddy, respectively (Figure 6).

CMI measures the quality and quantity of soil organic matter in a system (Reddy, 2010). Since the CMI is linked to the carbon pool index (CPI) and the lability index (LI), it may be used as a soil C rehabilitation measure to illustrate how soil C dynamics change as a result of changes in land use and management (de Assis et al., 2010). In reality, higher values indicate soil C rehabilitation, while lower values indicate C compound degradation (Blair et al., 1995). The CMI among the different land-use systems in this study was significantly different. The highest CMI was recorded in natural forests, which were used as a reference due to less anthropogenic disturbance, and the lowest was observed in paddy soils. The CPI is also one of the two indices that make up the CMI, which is also regarded as being more susceptible to the impact of land-use change on soil organic C dynamics (Geraei et al., 2016). Compared to cultivated land uses, adding organic matter regularly improves the ability to boost the CMI by increasing inputs and minimizing losses in natural forests and grasslands. This has also been reported by (Kalambukattu et al., 2013) and (Musinguzi et al., 2015), where cultivated soils had lower CMI values than uncultivated soils (forests).

Effect of land use systems on soil pH, electrical conductivity (EC), bulk density (ρb), and total nitrogen (TN)

Across the land-use systems, soil pH, EC, and ρb increased as soil depth was increased to 40 cm (Table 1). Across all land uses, the lowest pH, EC, and ρb values were found in the surface soil depth, whereas the highest was found in the sub-surface layer. Land-use systems significantly affected soil pH at the surface and sub-surface soil layers. The soil pH at 0–20 cm and 20–40 cm soil depth was 6.55 and 6.97 in the natural forest; 6.65 and 7.12 under natural grassland; 7.05 and 7.26 in maize-field-converted-from-forest; 6.83 and 7.20 under plantation; and 7.42 and 7.56 in paddy soils, respectively. The highest pH values at 0–20 cm and 20–40 cm depth were recorded in paddy land use, and the lowest was recorded in natural forests (Figure 7). At 0–20 cm and 20–40 cm depth, the pH under maize-field-converted-from-forest land use was higher as compared to natural forest, natural grassland, and plantation. The pH values in all land-use systems increased with increased soil depth. The result concerning pH indicates that the soil varied from slightly acidic to mildly alkaline. The overall EC varied among all land use, with the lowest value in the surface soils of natural grasslands and the

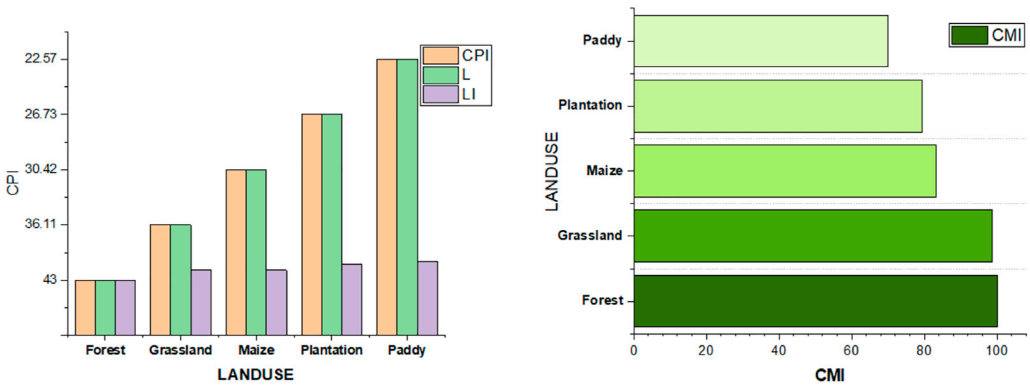

FIGURE 6
Effect of land use on carbon management index in 0–40 cm soil depth. Error bars indicate the least significant difference (LSD) values at p = 0.05.

highest in the sub-surface of paddy soils. The EC at 0–20 cm and 20–40 cm was 0.13 and 0.17 dS m^{-1} in natural forest, 0.15 and 0.19 dS m^{-1} in natural grassland, 0.20 and 0.24 dS m^{-1} in maize-field-converted-from-forest, 0.16 and 0.23 dS m^{-1} in plantation, and 0.26 and 0.29 dS m^{-1} in paddy soils, respectively (Table 1). The highest EC in surface and sub-surface soils was under paddy soil, and the lowest was under natural forest soil (Figure 7). Across the soil depth and land use pattern, land use had a considerable impact on ρb. It is evident from data that paddy soils recorded the highest ρb, i.e., 1.43 and 1.45 Mg m^{-3} at 0–20 and 20–40 cm soil depth, which was followed by plantation land use, viz., 1.32 and 1.36 Mg m^{-3}, and the least was recorded in natural forest, viz., 0.94 and 1.09 Mg m^{-3} in surface and sub-surface layers (Figure 7). The ρb in the surface and subsurface soil layers of natural forest, natural grassland, maize-field-converted-from-forest, plantation and paddy soils was 0.94 and 1.09 Mg m^{-3}, 1.07 and 1.18 Mg m^{-3}, 1.22 and 1.29 Mg m^{-3}, 1.32 and 1.36 Mg m^{-3} and 1.43 and 1.45 Mg m^{-3}, respectively (Table 1). Natural forest land-use type recorded the highest total nitrogen content at the surface and sub-surface soil depths, followed by natural grassland, and the least was recorded in paddy soils. The TN content in 0–20 cm and 20–40 cm soil depth were 0.49 and 0.38% in natural forest; 0.36 and 0.29% under natural grassland; 0.26 and 0.19% in maize-field-converted-from-forest; 0.20 and 0.15% under plantation and 0.18 and 0.12% in soils under paddy land use (Table 1). In general, the total nitrogen content was found in the order of: natural forest > natural grassland > maize-field-converted-from-forest > plantation > paddy (Figure 7). Soils of natural forests and natural grasslands had significantly lower soil pH, EC, and higher ρb and TN than the other land-use systems. The highest soil pH was reported in paddy land use, and the lowest was recorded in the soils of natural forests. Natural forests had low pH, which could be attributed to extensive root systems producing more root exudates, high organic matter content, and leaching of soluble salts from surface soil layers (Perie and Ouimet, 2008). Moreover, soil pH increased with soil depth in the different land uses. Similar findings were reported by (Bhuyan et al., 2013). The quantity of organic matter available in a particular land use system significantly influences the pH of the soil, and the decomposition of this organic matter releases chemicals such as organic acids that cause the lowering of soil pH (Shao et al., 2015). Since the paddy soils contain less organic matter, their pH was the highest among all the land-use systems. Other researchers have also documented variations in soil pH due to different management practices used in diverse land-use types (Orgill et al., 2018). Our study shows that among the various land-use systems, the EC of the soils was the lowest in natural grasslands and the highest in paddy soils. The low EC of natural forest land-use systems can be attributed to the leaching of salts and base-forming cations into the sub-surface layers and translocating them out of the soil profile (Tufa et al., 2019). Higher EC in paddy soils due to the accumulation of salts, usage of fertilizers, and management practices (Kiflu and Beyene, 2013). In the sub-surface soil layer, the EC values are higher than the surface layers, which could be due to the leaching of ions (Kalambukattu et al., 2013). also reported EC values below 1 dS m^{-1} while studying the soils of Jammu and Kashmir. The soil ρb had lower natural forest land use, which could be due to high clay content, less soil disturbance, higher root biomass, and the presence of high amounts of organic matter. Several researchers have revealed lower ρb in natural forest soils (Emadi et al., 2008). The high ρb in paddy lands could also be due to intrinsic soil properties like texture and intensive tillage operations and practices like plowing and puddling that break soil aggregates, increase soil compaction, and reduce the amount of organic matter in the particular land use through direct exposure in the surface soil layer to raindrops and climatic factors (Bennett et al., 2017). The increase in ρb with depth could be attributed to the weight of the overlying soil layers, and the decrease in SOC content (Abad et al., 2014; Gull et al., 2020; Jan et al., 2020). Correspondence increase in ρb with soil depth was also reported by other researchers (Chhagan et al., 2019; Singh G. et al., 2021). Nitrogen has an immense role to play in plant nutrition as it is linked with essential living processes of life. TN content was higher in the natural forest land-use system in both depths than in the other land uses. The high TN of natural forest systems is due to their high organic matter content, which is the biggest and most credible source of total soil nitrogen. Several researchers (Ufot et al., 2016; Wani, 2016) have also revealed that TN is higher in the forest than in cultivated lands. The lowest TN was found in paddy soils, which could be due to higher decomposition rates and oxidation processes, influenced by intensive cultivation practices that, reduce the total nitrogen content. Also, low TN in paddy land could be attributed to the addition of smaller quantities of organic matter, leaching loss of nitrate-nitrogen, and loss of nitrogen through the denitrification process back into the atmosphere. Similarly (Gull et al., 2020; Mansoor et al., 2021), have reported that soils under cultivation tend to have lower TN concentrations as compared to uncultivated lands. A decreasing trend with an increase in soil depth was observed in all the studied land uses, usually due to a decrease in soil organic matter relative to soil depth. Our results are in close conformity with the findings of (Jan et al., 2020), who reported that the TN decreases gradually from the surface to the sub-surface layers.

Policy recommendation and future research perspectives

Our study indicated that the conversion of forest land to cropland has a negative impact on soil carbon storage both in surface (0–20 cm) and subsurface soil layers (20–40 cm) in the temperate region. Hence, to reduce the global temperature rise, we must reduce C emission from the soil by preserving or

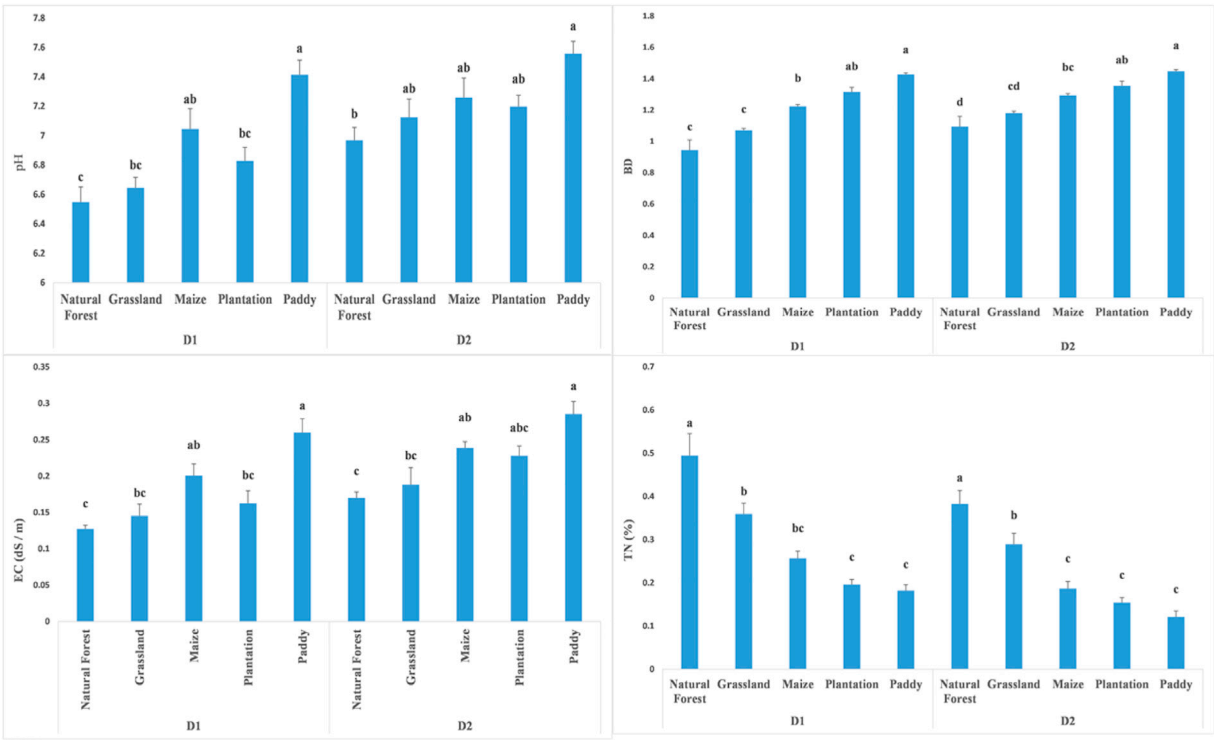

FIGURE 7
Effect of land use on pH, electrical conductivity, bulk density, and total nitrogen in 0–20 cm and 20–40 cm soil depth. Error bars indicate the least significant difference (LSD) values at *p* = 0.05. Mean values with the same letters don't differ significantly.

capturing more CO_2 from the atmosphere and storing it in deep soil. The global temperature had negative consequences on snow cover in the temperate region, which may further amplify the flood problem in the mainland (Nie et al., 2021; Talukder et al., 2021). But at the same time, we cannot compromise the food security of our resource-poor population who lives in a remote location in the Himalayas. Temperate Himalayas is a major source of livelihood and habitat for many plant species, wildlife, and million populations globally (Sharma et al., 2018; Mugloo et al., 2021; Mehmood et al., 2021; Rahman et al., 2022). So it is a social responsibility to ensure the food and livelihood security of the temperate populace. Therefore, current agricultural land must be bought under conservation effective adequate soil and crop management practices. Conservation of effective agricultural practices like diversified farming, organic farming, integrated production systems, no-tilling, mulching, intercropping, etc can satisfy the food demand besides conserving soil C in the long run. Conservation agricultural practices improve food production and soil C levels over conventional farming practices in the Himalayan region (Ngangom et al., 2020; Babu et al., 2021; Singh G. et al., 2021). Fewer C losses in agricultural systems can be achieved through conservation tillage, reduced soil disturbance, and a steady supply of high-quality organic amendments. Hence, the adoption of conservation effective management practices and halting of forest land conversion to agricultural cropland must be a focal recommendation of the policy planners. Future research should concentrate on new and improved methods for increasing the C sequestration potential of agricultural systems in the region to improve soil C besides ensuring food security. According to COP 26 Article 6 of the Paris Agreement, which describes rules for an international carbon market, it layed emphasis on CO2 emissionsand innovative methods to copeup with reduction of emissions from production systems.

Conclusion

The study proved the hypothesis that the land-use changes had a tenacious impact on the different functional carbon pools under the Kashmir Himalaya of India, where the carbon pools are being severely depleted due to climatic and anthropogenic factors. Under all of the studied land-use systems, various carbon fractions were maximum under natural forests followed by plantation crop fields, while there was a lower amount of soil carbon fractions observed under the maize and paddy field. The main differences in soil carbon in different land use systems were due to differences in their soil conservation capacity through root and canopy proliferation, the recyclable biomass produced, and the reduction of CO_2 emissions from the soil. Results from the current experimentation are useful for developing soil carbon status and improving soil properties under the Indian Himalayas. The results are also useful for understanding the transformation behavior of different carbon pools in different Himalayan land use systems. Based on the results of the study, it is possible to develop suitable land use practices for the Kashmir Himalayas. The study also suggests that areas of land in this region, which have already been converted from forest to cropland, should be treated with soil conservation measures to restore soil productivity. As a result, policymakers can think of developing policies to protect forest land and its conversion to agricultural land.

Data availability statement

The raw data supporting the conclusions of this article will be made available by the authors, without undue reservation.

Author contributions

SK Writing Analysis OW Drafting, statistical analysis and review SM Methodology, Writing SB Writing Editing and Review. VS Review Editing, FW Statistical analysis Gobinder Singh writing MA Bhat, MHC, PS and ZB Editing Writing SRD Writing and editing RS Writing Editing and DY Writing Editing.

Conflict of interest

The authors declare that the research was conducted in the absence of any commercial or financial relationships that could be construed as a potential conflict of interest.

Publisher's note

All claims expressed in this article are solely those of the authors and do not necessarily represent those of their affiliated organizations, or those of the publisher, the editors and the reviewers. Any product that may be evaluated in this article, or claim that may be made by its manufacturer, is not guaranteed or endorsed by the publisher.

References

Abad, J. R. S., Khosravi, H., and Alamdarlou, E. H. (2014). Assessment the effects of land use changes on soil physicochemical properties in Jafarabad of Golestan province, Iran. *Bull. Environ. Pharmacol. Life Sci.* 3 (3), 296–300.

Aduhene-Chinbuah, J., Sugihara, S., Komatsuzaki, M., Nishizawa, T., and Tanaka, H. (2022). No tillage increases SOM in labile fraction but not stable fraction of andosols from a long-term experiment in Japan. *Agronomy* 12 (2), 479. doi:10.3390/agronomy12020479

Ahmed, I. U., Assefa, D., and Godbold, D. L. (2022). Land-use change depletes quantity and quality of soil organic matter fractions in Ethiopian highlands. *Forests* 13 (1), 69. doi:10.3390/f13010069

Ali, A., Lin, S-L., He, J-K., Kong, F-M., Yu, J-H., and Jiang, H-S. (2019). Climatic water availability is the main limiting factor of biotic attributes across large-scale elevational gradients in tropical forests. *Sci. Total Environ.* 647, 1211–1221. doi:10.1016/j.scitotenv.2018.08.072

Anantha, K. C., Mandal, B., Badole, S., Majumder, S. P., Datta, A., Padhan, D., et al. (2022). Distribution of sequestered carbon in different pools in Alfisols under long-term groundnut system of hot arid region of India. *Eur. J. Agron.* 135, 126467.

Arneth, A., Barbosa, H., Benton, T. G., Calvin, K., Calvo, E., Connors, S., et al. (2019). *Climate change and land — IPCC*, 41. Intergovernmental Panel on Climate Change.

Arora, S., and Bhatt, R. (2016). "Resource conservation technologies (RCTs) for climate-resilient agriculture in the foothill of northwest Himalayas," in *Conservation agriculture* (Singapore: Springer), 71–111.

Babu, S., Mohapatra, K., Das, A., Yadav, G., Singh, R., Chandra, P., et al. (2021). *Exploring synergies and trade-offs between climate change and the sustainable development goals.* Springer, 119–143.

Babu, S., Mohapatra, K., Yadav, G. S., Lal, R., Singh, R., Avasthe, R., et al. (2020). Soil carbon dynamics in diverse organic land use systems in North Eastern Himalayan ecosystem of India. *Catena* 194, 104785. doi:10.1016/j.catena.2020.104785

Bahadori, M., Chen, C., Lewis, S., Boyd, S., Rashti, M. R., Esfandbod, M., et al. (2021). Soil organic matter formation is controlled by the chemistry and bioavailability of organic carbon inputs across different land uses. *Sci. Total Environ.* 770, 145307. doi:10.1016/j.scitotenv.2021.145307

Bayer, C., Martin-Neto, L., Mielniczuk, J., Pavinato, A., and Dieckow, J. (2006). Carbon sequestration in two Brazilian Cerrado soils under no-till. *Soil Tillage Res.* 86 (2), 237–245. doi:10.1016/j.still.2005.02.023

Begum, F., Abbas, H., Ali, S., Ali, D., Mumtaz, S., Khan, M. Z., et al. (2020). Soil quality and organic carbon stock across the different land use in a mountainous landscape of Karakoram region, Gilgit, Pakistan. *FEB-Fresenius Environ. Bull.* 29 (01), 503.

Bei, S., Li, X., Kuyper, T. W., Chadwick, D. R., and Zhang, J. (2022). Nitrogen availability mediates the priming effect of soil organic matter by preferentially altering the straw carbon-assimilating microbial community. *Sci. Total Environ.* 815, 152882. doi:10.1016/j.scitotenv.2021.152882

Benbi, D. K., Brar, K., Toor, A. S., and Singh, P. (2015). Total and labile pools of soil organic carbon in cultivated and undisturbed soils in northern India. *Geoderma* 237, 149–158. doi:10.1016/j.geoderma.2014.09.002

Bennett, J. M., Roberton, S. D., Jensen, T. A., Antille, D. L., and Hall, J. (2017). A comparative study of conventional and controlled traffic in irrigated cotton: I. Heavy machinery impact on the soil resource. *Soil Tillage Res.* 168, 143–154. doi:10.1016/j.still.2016.12.012

Bhardwaj, D. R., Tahiry, H., Sharma, P., Pala, N. A., Kumar, D., Kumar, A., et al. (2021). Influence of aspect and elevational gradient on vegetation pattern, tree characteristics and ecosystem carbon density in Northwestern Himalayas. *Land* 10 (11), 1109. doi:10.3390/land10111109

Bhattacharjya, S., Bhaduri, D., Chauhan, S., Chandra, R., Raverkar, K., and Pareek, N. (2017). Comparative evaluation of three contrasting land use systems for soil carbon, microbial and biochemical indicators in North-Western Himalaya. *Ecol. Eng.* 103, 21–30. doi:10.1016/j.ecoleng.2017.03.001

Bhuyan, S., Tripathi, O., and Khan, M. (2013). Soil nutrients status in prominent agro-ecosystems of East Siang district, Arunachal Pradesh. *Int. J. Environ. Sci.* 3 (6), 1957.

Biederbeck, V., Janzen, H., Campbell, C., and Zentner, R. (1994). Labile soil organic matter as influenced by cropping practices in an arid environment. *Soil Biol. Biochem.* 26 (12), 1647–1656. doi:10.1016/0038-0717(94)90317-4

Blair, G. J., Lefroy, R. D., and Lisle, L. (1995). Soil carbon fractions based on their degree of oxidation, and the development of a carbon management index for agricultural systems. *Aust. J. Agric. Res.* 46 (7), 1459–1466. doi:10.1071/ar9951459

Blake, G. R., and Hartge, K. (1986). Bulk density. *Methods soil analysis Part 1 Phys. mineralogical methods* 5, 363–375.

Bremner, J. (1982). Total nitrogen. Methods of soil analysis. *Am. Soc. Agron. Mongrn* 10 (2), 594–624.

Chauhan, R., Pande, K., and Thakur, S. (2014). Soil properties affected by land use systems in Western Chitwan, Nepal. *Int. J. Appl. Sci. Biotechnol.* 2 (3), 265–269. doi:10.3126/ijasbt.v2i3.10660

Chen, Z., Yu, G., and Wang, Q. (2019). Magnitude, pattern and controls of carbon flux and carbon use efficiency in China's typical forests. *Glob. Planet. Change* 172, 464–473. doi:10.1016/j.gloplacha.2018.11.004

Chhagan, B. R., Sharma, M., Sharma, K., Samanta, A., Wani, O. A., Kachroo, D., et al. (2019). Impact of organic, inorganic and biofertilizers on crop yield and N, P and K uptake under rainfed maize-wheat cropping system. *Int. J. Curr. Microbiol. Appl. Sci.* 8 (4), 2546–2564. doi:10.20546/ijcmas.2019.804.297

Chibsa, T., and Ta'a, A. (2009). Assessment of soil organic matter under four land use systems in bale highlands, southeast Ethiopia. A. Soil organic matter contents in four land use systems: Forestland, grassland, fallow land and cultivated land. *World Appl. Sci. J.* 6 (9), 1231–1246.

Choudhury, B., Saha, S., Singh, S., Das, A., Buragohain, J., Dayal, V., et al. (2018). Impact of postburn jhum agriculture on soil carbon pools in the north-eastern Himalayan region of India. *Soil Res.* 56 (6), 615–622. doi:10.1071/sr18031

Conteh, A., Lefroy, R., and Blair, G. (1997). Dynamics of organic matter in soil as determined by variations in 13C/12C isotopic ratios and fractionation by ease of oxidation. *Soil Res.* 35 (4), 881–890. doi:10.1071/s96107

Dar, D. A., and Sahu, P. (2018). *Assessment of soil organic carbon stock in five forest types of northern Kashmir and Himalaya*.

Dawson, J. J., and Smith, P. (2007). Carbon losses from soil and its consequences for land-use management. *Sci. Total Environ.* 382 (2-3), 165–190. doi:10.1016/j.scitotenv.2007.03.023

De Assis, C. P., De Oliveira, T. S., Da Nóbrega Dantas, J. D. A., and De Sá Mendonça, E. (2010). Organic matter and phosphorus fractions in irrigated agroecosystems in a semi-arid region of Northeastern Brazil. *Agric. Ecosyst. Environ.* 138 (1-2), 74–82. doi:10.1016/j.agee.2010.04.002

Dhakal, S., Koirala, M., Sharma, E., and Subedi, N. R. (2010). Effect of land use change on soil organic carbon stock in Balkhu Khola watershed southwestern part of Kathmandu valley, central Nepal. *World Acad. Sci. Eng. Technol.* 66.

Duval, M. E., Galantini, J. A., Iglesias, J. O., Canelo, S., Martinez, J. M., and Wall, L. (2013). Analysis of organic fractions as indicators of soil quality under natural and cultivated systems. *Soil Tillage Res.* 131, 11–19. doi:10.1016/j.still.2013.03.001

Emadi, M., Emadi, M., Baghernejad, M., Fathi, H., and Saffari, M. (2008). Effect of land use change on selected soil physical and chemical properties in North Highlands of Iran. *J. Appl. Sci.* 8 (3), 496–502. doi:10.3923/jas.2008.496.502

Geraei, D. S., Hojati, S., Landi, A., and Cano, A. F. (2016). Total and labile forms of soil organic carbon as affected by land use change in southwestern Iran. *Geoderma Reg.* 7 (1), 29–37. doi:10.1016/j.geodrs.2016.01.001

Gerzabek, M. H., Aquino, A. J. A., Balboa, Y. I. E., Galicia-Andrés, E., Grančič, P., Oostenbrink, C., et al. (2022). A contribution of molecular modeling to supramolecular structures in soil organic matter. *J. Plant Nutr. Soil Sci.* 185 (1), 44–59.

Gogoi, B., Borah, N., Baishya, A., Dutta, S., Nath, D. J., Das, R., et al. (2021). Yield trends, soil carbon fractions and sequestration in a rice-rice system of North-East India: Effect of 32 years of INM practices. *Field Crops Res.* 272, 108289. doi:10.1016/j.fcr.2021.108289

Gomez, K. A., and Gomez, A. A. (1984). *Statistical procedures for agricultural research*. John Wiley & Sons.

Gull, R., Bhat, T. A., Sheikh, T. A., Wani, O. A., Fayaz, S., Nazir, A., et al. (2020). Climate change impact on pulse in India-A. *J. Pharmacogn. Phytochemistry* 9 (4), 3159–3166.

Guo, L. B., and Gifford, R. M. (2002). Soil carbon stocks and land use change: A meta analysis. *Glob. change Biol.* 8 (4), 345–360. doi:10.1046/j.1354-1013.2002.00486.x

Hobley, E., Wilson, B., Wilkie, A., Gray, J., and Koen, T. (2015). Drivers of soil organic carbon storage and vertical distribution in Eastern Australia. *Plant Soil* 390 (1), 111–127. doi:10.1007/s11104-015-2380-1

Hu, Y., Wang, S., Niu, B., Chen, Q., Wang, J., Zhao, J., et al. (2020). Effect of increasing precipitation and warming on microbial community in Tibetan alpine steppe. *Environ. Res.* 189, 109917. doi:10.1016/j.envres.2020.109917

Isbell, F., Calcagno, V., Hector, A., Connolly, J., Harpole, W. S., Reich, P. B., et al. (2011). High plant diversity is needed to maintain ecosystem services. *Nature* 477 (7363), 199–202. doi:10.1038/nature10282

Jackson, W., Flesher, D., and Hageman, R. (1973). Nitrate uptake by dark-grown corn seedlings: Some characteristics of apparent induction. *Plant Physiol.* 51 (1), 120–127. doi:10.1104/pp.51.1.120

Jan, B., Bhat, T. A., Sheikh, T. A., Wani, O. A., Bhat, M. A., Nazir, A., et al. (2020). Agronomic bio-fortification of rice and maize with iron and zinc: A review. *Int. Res. J. Pure Appl. Chem.*, 28–37. doi:10.9734/irjpac/2020/v21i1630257

Jobbágy, E. G., and Jackson, R. B. (2000). The vertical distribution of soil organic carbon and its relation to climate and vegetation. *Ecol. Appl.* 10 (2), 423–436. doi:10.1890/1051-0761(2000)010[0423:tvdoso]2.0.co;2

Jones, R. J., Hiederer, R., Rusco, E., and Montanarella, L. (2005). Estimating organic carbon in the soils of Europe for policy support. *Eur. J. Soil Sci.* 56 (5), 655–671. doi:10.1111/j.1365-2389.2005.00728.x

Kalambukattu, J. G., Singh, R., Patra, A. K., and Arunkumar, K. (2013). Soil carbon pools and carbon management index under different land use systems in the Central Himalayan region. *Acta Agric. Scand. Sect. B - Soil & Plant Sci.* 63 (3), 200–205. doi:10.1080/09064710.2012.749940

Kaur, R., and Bhat, Z. (2017). Effect of different agricultural land use systems on physico-chemical properties of soil in sub-mountainous districts of Punjab, North-West India. *J. Pharmacogn. Phytochemistry* 6 (3), 226–233.

Kaushal, R., Singh, I., Thapliyal, S., Gupta, A., Mandal, D., Tomar, J., et al. (2020). Rooting behaviour and soil properties in different bamboo species of Western Himalayan Foothills, India. *Sci. Rep.* 10 (1), 4966–5017. doi:10.1038/s41598-020-61418-z

Kiflu, A., and Beyene, S. (2013). Effects of different land use systems on selected soil properties in South Ethiopia. *J. Soil Sci. Environ. Manage.* 4 (5), 100–107. doi:10.5897/jssem2013.0380

Kumar, S. (2018). Geospatial approach in modeling soil erosion processes in predicting soil erosion. *Remote Sens. Northwest Himal. Ecosyst.* 355.

Kumar, S. S., Mahale, A. G., and Patil, A. C. (2020). Mitigation of climate change through approached agriculture-soil carbon sequestration (A review). *Curr. J. Appl. Sci. Technol.*, 47–64. doi:10.9734/cjast/2020/v39i3331017

Kumar, S. S., Mir, S. A., Wani, O. A., Babu, S., Yeasin, M., Bhat, M. A., et al. (2022). Land-use systems regulate carbon geochemistry in the temperate Himalayas, India. *J. Environ. Manage.* 320, 115811. doi:10.1016/j.jenvman.2022.115811

Lal, R. (2004). Soil carbon sequestration to mitigate climate change. *Geoderma* 123 (1-2), 1–22. doi:10.1016/j.geoderma.2004.01.032

Mansoor, S., Kour, N., Manhas, S., Zahid, S., Wani, O. A., Sharma, V., et al. (2021). Biochar as a tool for effective management of drought and heavy metal toxicity. *Chemosphere* 271, 129458. doi:10.1016/j.chemosphere.2020.129458

Mikha, M. M., Vigil, M. F., and Benjamin, J. G. (2013). Long-term tillage impacts on soil aggregation and carbon dynamics under wheat-fallow in the central Great Plains. *Soil Sci. Soc. Am. J.* 77 (2), 594–605. doi:10.2136/sssaj2012.0125

Mir, S., Wani, J., Sofi, J., Chesti, M., Mir, A., Khan, I., et al. (2020). Soil organic carbon pools and stocks in different land uses of a temperate Himalayan region. *J. Indian Soc. Soil Sci.* 68 (2), 162–169. doi:10.5958/0974-0228.2020.00018.3

Morgan, G. A., Leech, N. L., Barrett, K. C., Brace, N., Snelgar, R., Griego, O. V., et al. (1988). *1. SPSS: Statistical package for the social sciences by norman H nie*.

Mourya, K., Jena, R., Ray, P., Ramachandran, S., Sharma, G., Hota, S., et al. (2021). Profile distribution of soil organic carbon fractions under different landforms in the Meghalaya plateau of India. *Environ. Conserv. J.* 22 (3), 9–16. doi:10.36953/ecj.2021.22302

Musinguzi, P., Tenywa, J. S., Ebanyat, P., Basamba, T. A., Tenywa, M. M., Mubiru, D. N., et al. (2015). Soil organic fractions in cultivated and uncultivated Ferralsols in Uganda. *Geoderma Reg.* 4, 108–113. doi:10.1016/j.geodrs.2015.01.003

Nath, A. J., Brahma, B., Sileshi, G. W., and Das, A. K. (2018). Impact of land use changes on the storage of soil organic carbon in active and recalcitrant pools in a humid tropical region of India. *Sci. Total Environ.* 624, 908–917. doi:10.1016/j.scitotenv.2017.12.199

Nicodemo, M. L. F., Borges, W. L. B., and De Souza, I. M. D. (2018). Atributos físicos do solo em quatro sistemas de uso da terra em São Carlos, SP. *Agraria.* 13 (2), 1–7. doi:10.5039/agraria.v13i2a5524

Orgill, S. E., Condon, J. R., Conyers, M. K., Morris, S. G., Alcock, D. J., Murphy, B. W., et al. (2018). Removing grazing pressure from a native pasture decreases soil organic carbon in southern New South Wales, Australia. *Land Degrad. Dev.* 29 (2), 274–283. doi:10.1002/ldr.2560

Pan, G., Zhou, P., Li, Z., Smith, P., Li, L., Qiu, D., et al. (2009). Combined inorganic/organic fertilization enhances N efficiency and increases rice productivity through organic carbon accumulation in a rice paddy from the Tai Lake region, China. *Agric. Ecosyst. Environ.* 131 (3-4), 274–280. doi:10.1016/j.agee.2009.01.020

Perie, C., and Ouimet, R. (2008). Organic carbon, organic matter and bulk density relationships in boreal forest soils. *Can. J. Soil Sci.* 88 (3), 315–325. doi:10.4141/cjss06008

Prasad, K. K., Veerendra, M., Mahajan, N., Mrunalini, K., Sirisha, L., Reddy, T., et al. (2019). Water-stable aggregates and soil organic carbon fractions in a sub-tropical RWCS under variable tillage and precision nutrient management: A. *IJCS* 7 (3), 2228–2240.

Qafoku, N. P. (2015). *Climate-change effects on soils*.

Raiesi, F. (2021). The quantity and quality of soil organic matter and humic substances following dry-farming and subsequent restoration in an upland pasture. *Catena* 202, 105249. doi:10.1016/j.catena.2021.105249

Reddy, D. (2010). *Determination of labile SOC by KMnO4 oxidation technique and its use in carbon management index*, 66–69. Farmers Resource based site specific integrated nutrient management and on line fertilizer recommendations using GPS and GIS tools.

Sahoo, U. K., Singh, S. L., Gogoi, A., Kenye, A., and Sahoo, S. S. (2019). Active and passive soil organic carbon pools as affected by different land use types in Mizoram, Northeast India. *PLoS One* 14 (7), e0219969. doi:10.1371/journal.pone.0219969

Sainepo, B. M., Gachene, C. K., and Karuma, A. (2018). Assessment of soil organic carbon fractions and carbon management index under different land use types in Olesharo Catchment, Narok County, Kenya. *Carbon Balance Manag.* 13 (1), 4–9. doi:10.1186/s13021-018-0091-7

Shao, X., Yang, W., and Wu, M. (2015). Seasonal dynamics of soil labile organic carbon and enzyme activities in relation to vegetation types in Hangzhou Bay tidal flat wetland. *PLoS One* 10 (11), e0142677. doi:10.1371/journal.pone.0142677

Sharma, O. R., Arya, D., Goel, S., Vyas, K., and Shinde, P. (2018). Trillium govanianum wall. Ex D. Don (nagchatri): An important ethno medicinal plant of himalayan region (Himachal Pradesh). *J. Med. Plants Stud.* 6 (1), 11–13.

Sharma, V., Hussain, S., Sharma, K., and Arya, V. M. (2014). Labile carbon pools and soil organic carbon stocks in the foothill Himalayas under different land use systems. *Geoderma* 232, 81–87. doi:10.1016/j.geoderma.2014.04.039

Sheng, H., Zhou, P., Zhang, Y., Kuzyakov, Y., Zhou, Q., Ge, T., et al. (2015). Loss of labile organic carbon from subsoil due to land-use changes in subtropical China. *Soil Biol. Biochem.* 88, 148–157. doi:10.1016/j.soilbio.2015.05.015

Sherrod, L. A., Peterson, G. A., Westfall, D. G., and Ahuja, L. R. (2005). *Soil organic carbon pools after 12 years in no-till dryland agroecosystems*.

Singh, G., Batra, N., Salaria, A., Wani, O. A., and Singh, J. (2021a). Groundwater quality assessment in Kapurthala district of central plain zone of Punjab using hydrochemical characteristics. *J. Soil Water Conservation* 20 (1), 43–51. doi:10.5958/2455-7145.2021.00008.4

Singh, R., Babu, S., Avasthe, R. K., Meena, R. S., Yadav, G. S., Das, A., et al. (2021b). Conservation tillage and organic nutrients management improve soil properties, productivity, and economics of a maize-vegetable pea system in the Eastern Himalayas. *Land Degrad. Dev.* 32 (16), 4637–4654. doi:10.1002/ldr.4066

Singh, S. B., Choudhury, B. U., Saha, S., Hnamte, V., and Hnamte, V. (2019). Transforming jhum to plantations: Effect on soil microbiological and biochemical properties in the foot hills of North Eastern Himalayas, India. *Catena* 177, 84–91. doi:10.1016/j.catena.2019.02.008

Sreekanth, N., Prabha, S. V., Padmakumar, B., and Thomas, A. (2013). Soil carbon alterations of selected forest types as an environmental feedback to climate change. *Int. J. Environ. Sci.* 3 (5), 1516.

Toru, T., and Kibret, K. (2019). Carbon stock under major land use/land cover types of Hades sub-watershed, eastern Ethiopia. *Carbon Balance Manag.* 14 (1), 7–14. doi:10.1186/s13021-019-0122-z

Tufa, M., Melese, A., and Tena, W. (2019). Effects of land use types on selected soil physical and chemical properties: The case of kuyu district, Ethiopia. *Eurasian J. soil Sci.* 8 (2), 94–109. doi:10.18393/ejss.510744

Turner, J., Lambert, M. J., and Johnson, D. W. (2005). Experience with patterns of change in soil carbon resulting from forest plantation establishment in eastern Australia. *For. Ecol. Manag.* 220 (1-3), 259–269. doi:10.1016/j.foreco.2005.08.025

Ufot, U., Iren, O., and Chikere Njoku, C. (2016). Effects of land use on soil physical and chemical properties in Akokwa area of Imo State, Nigeria. *Int. J. Life Sci. Sci. Res.* 2 (3), 273–278.

Valbrun, W., De Andrade, E., De Almeida, A., and De Almeida, E. (2018). Carbon and nitrogen stock under different types of land use in a seasonally Dry Tropical Forest. *J. Agric. Sci. (Tor).* 10 (12), 479. doi:10.5539/jas.v10n12p479

Vezzani, F. M., Anderson, C., Meenken, E., Gillespie, R., Peterson, M., and Beare, M. H. (2018). The importance of plants to development and maintenance of soil structure, microbial communities and ecosystem functions. *Soil Tillage Res.* 175, 139–149. doi:10.1016/j.still.2017.09.002

Vieira, F. C. B., Bayer, C., Zanatta, J. A., Dieckow, J., Mielniczuk, J., and He, Z. L. (2007). Carbon management index based on physical fractionation of soil organic matter in an Acrisol under long-term no-till cropping systems. *Soil Tillage Res.* 96 (1-2), 195–204. doi:10.1016/j.still.2007.06.007

Walkley, A., and Black, I. A. (1934). An examination of the Degtjareff method for determining soil organic matter, and a proposed modification of the chromic acid titration method. *Soil Sci.* 37 (1), 29–38. doi:10.1097/00010694-193401000-00003

Wang, X., Wang, J., and Zhang, J. (2012). *Comparisons of three methods for organic and inorganic carbon in calcareous soils of northwestern China*.

Wani, O. A., Kumar, S., Hussain, N., Wani, A. I. A., Subhash, B., Parvej, A., et al. (2022). *Multi-scale processes influencing global carbon storage and land-carbon-climate nexus: A critical review*. Pedosphere.

Wani, O. A. (2016). *Mapping of nutrients status in soils of Kishtwar and Ramban districts of J&K using geographic information system (GIS)*. Jammu: Sher-e-Kashmir University of Agricultural Sciences & Technology of Jammu.

Wei, X., Shao, M., Gale, W., and Li, L. (2014). Global pattern of soil carbon losses due to the conversion of forests to agricultural land. *Sci. Rep.* 4 (1), 1–6. doi:10.1038/srep04062

Wiesenberg, G. L., Dorodnikov, M., and Kuzyakov, Y. (2010). Source determination of lipids in bulk soil and soil density fractions after four years of wheat cropping. *Geoderma* 156 (3-4), 267–277. doi:10.1016/j.geoderma.2010.02.026

Wu, L., Adebayo, T. S., Yue, X. G., and Umut, A. (2022). The role of renewable energy consumption and financial development in environmental sustainability: Implications for the Nordic Countries. *Int. J. Sustain. Dev. World Ecol.*, 1–16. doi:10.1080/13504509.2022.2115577

Xiang, H., Zhang, L., and Wen, D. (2015). Change of soil carbon fractions and water-stable aggregates in a forest ecosystem succession in South China. *Forests* 6 (8), 2703–2718. doi:10.3390/f6082703

Xie, X., Wu, T., Zhu, M., Jiang, G., Xu, Y., Wang, X., et al. (2021). Comparison of random forest and multiple linear regression models for estimation of soil extracellular enzyme activities in agricultural reclaimed coastal saline land. *Ecol. Indic.* 120, 106925. doi:10.1016/j.ecolind.2020.106925

Yadav, G. S., Lal, R., Meena, R. S., Babu, S., Das, A., Bhowmik, S., et al. (2019). Conservation tillage and nutrient management effects on productivity and soil carbon sequestration under double cropping of rice in north eastern region of India. *Ecol. Indic.* 105, 303–315. doi:10.1016/j.ecolind.2017.08.071

Yadav, G. S., Das, A., Kandpal, B., Babu, S., Lal, R., Datta, M., et al. (2021). The food-energy-water-carbon nexus in a maize-maize-mustard cropping sequence of the Indian Himalayas: An impact of tillage-cum-live mulching. *Renew. Sustain. Energy Rev.* 151, 111602. doi:10.1016/j.rser.2021.111602

Yadav, V. S., Yadav, S. S., Gupta, S. R., Meena, R. S., Lal, R., Sheoran, N. S., et al. (2022). Carbon sequestration potential and CO2 fluxes in a tropical forest ecosystem. *Ecol. Eng.* 176, 106541. doi:10.1016/j.ecoleng.2022.106541

Yang, C., Yang, L., and Ouyang, Z. (2005). Organic carbon and its fractions in paddy soil as affected by different nutrient and water regimes. *Geoderma* 124 (1-2), 133–142. doi:10.1016/j.geoderma.2004.04.008

Yao, M. K., Angui, P. K., Konaté, S., Tondoh, J. E., Tano, Y., Abbadie, L., et al. (2010). Effects of land use types on soil organic carbon and nitrogen dynamics in Mid-West Cote d'Ivoire. *Eur. J. Sci. Res.* 40 (2), 211–222.

Yeasmin, S., Jahan, E., Molla, M., Islam, A. K. M., Anwar, M., Or Rashid, M., et al. (2020). *Effect of land use on organic carbon storage potential of soils with contrasting native organic matter content*. International Journal of Agronomy.

Yeomans, J. C., and Bremner, J. M. (1988). A rapid and precise method for routine determination of organic carbon in soil. *Commun. soil Sci. plant analysis* 19 (13), 1467–1476. doi:10.1080/00103628809368027

Yitbarek, T., Gebrekidan, H., Kibret, K., and Beyene, S. (2013). Impacts of land use on selected physicochemical properties of soils of Abobo area, Western Ethiopia. *Agric. For. Fish.* 2 (5), 177–183. doi:10.11648/j.aff.20130205.11

Yu, P., Han, K., Li, Q., and Zhou, D. (2017). Soil organic carbon fractions are affected by different land uses in an agro-pastoral transitional zone in Northeastern China. *Ecol. Indic.* 73, 331–337. doi:10.1016/j.ecolind.2016.10.002

Frontiers in Environmental Science

Explores the anthropogenic impact on our natural world

An innovative journal that advances knowledge of the natural world and its intersections with human society. It supports the formulation of policies that lead to a more inhabitable and sustainable world.

Discover the latest Research Topics

See more →

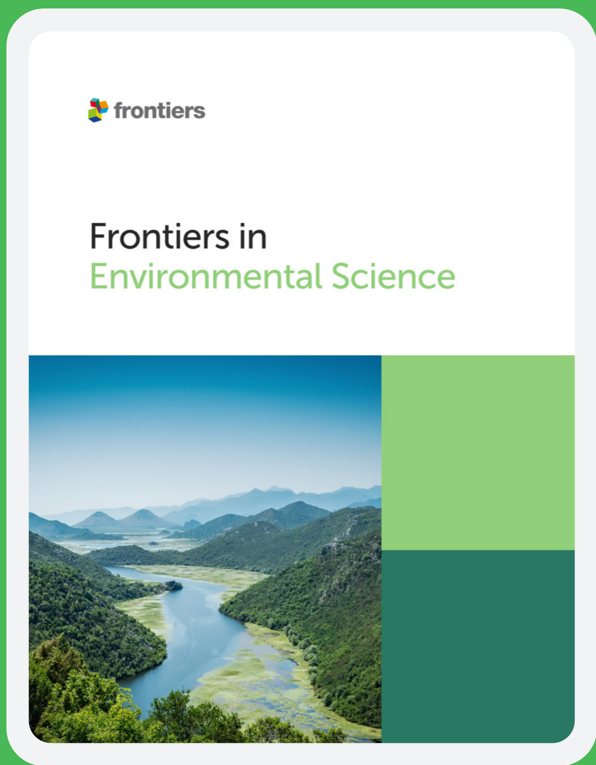

Frontiers

Avenue du Tribunal-Fédéral 34
1005 Lausanne, Switzerland
frontiersin.org

Contact us

+41 (0)21 510 17 00
frontiersin.org/about/contact